Systematic Revision of the Ant Subfamily Leptanillinae (Hymenoptera: Formicidae) based on Reciprocal Illumination from Phylogenomics & Morphology

By

ZACHARY H. GRIEBENOW

DISSERTATION

Submitted in partial satisfaction of the requirements for the degree of

DOCTOR OF PHILOSOPHY

in

ENTOMOLOGY

in the

OFFICE OF GRADUATE STUDIES

of the

UNIVERSITY OF CALIFORNIA

DAVIS

Approved:

Philip S. Ward, Chair

Jason Bond

Marek Borowiec

Committee in Charge

2023

Table of Contents

Abstract

The subfamily Leptanillinae (Hymenoptera: Formicidae) consists of miniscule subterranean ants, most diverse in Southeast Asia, but known throughout the Old World tropics and subtropics. Phylogenomic inference demonstrates that the Leptanillinae are sister to all, or nearly all, other extant Formicidae. Little is known of leptanilline behavior, with the few observations that exist indicating that these ants are specialist predators of geophilomorph centipedes or forcepstails (Diplura: Japygidae), with *Leptanilla* displaying a legionary biology reminiscent of army ants of the subfamily Dorylinae, along with larval hemolymph feeding (LHF) like that observed in the vampire ants (Amblyoponinae). Contrary to the collecting bias observed in most ants, male leptanilline specimens are acquired more easily than workers or queens. The sexes are almost never collected in association, and many subclades within the Leptanillinae are known from male specimens only. These restrictions plague our understanding of the Leptanillinae with probable taxonomic redundancy. My dissertation constitutes a systematic revision of the Leptanillinae that is informed by phylogeny inferred from both genotype and phenotype and integrates morphological data from both sexes. Chapter 1 presents the results of total-evidence Bayesian inference from 11 nuclear loci and 33 binary male morphological characters, which unequivocally support the synonymy of the monotypic genus *Phaulomyrma* Wheeler & Wheeler, known only from a single male specimen, with *Leptanilla* Emery. Chapter 2 describes *Yavnella laventa* Griebenow *et al.*, the first species belonging to the genus *Yavnella* Kugler for which the worker caste is known, identified as *Yavnella* by maximum-likelihood (ML) and Bayesian phylogenomic inference from ultra-conserved elements (UCEs). Chapter 3 provides detailed descriptions of the male genital skeletomusculature of 9 leptanilline morphospecies and 3 outgroups across the Formicidae, based on scans acquired by micro-computed tomography, and

using a novel nomenclature for male genital musculature compatible with topographical main-group nomenclature already created for other anatomical regions and extensible across the whole of the Hymenoptera. Chapter 4 is a comprehensive revision of generic and tribal boundaries in the Leptanillinae, reciprocally illuminated by the results of phylogenetic inference presented in Chapter 5, and worker and male phenotypes; this chapter also includes worker- and male-based dichotomous keys to all described leptanilline species. Finally, Chapter 5 presents the results of phylogenomic inference, including examples of all major leptanilline clades, under frequentist and Bayesian statistical frameworks, along with a coalescent-based approach to accommodate discordant phylogenetic signal among gene trees; plus the results of Bayesian total-evidence (from 58 UCE loci and 64 binary male morphological characters) to resolve the phylogenetic positions of aberrant lineages for which only male morphology is known, including *Scyphodon* Brues.

Acknowledgements

The extreme difficulty in collecting leptanilline ants in the field meant that this project would be unfeasible without many loans or gifts of specimens. For this, I thank (in no particular order) Jadranka Rota (MZLU), Debbie Jennings (ANIC), Masashi Yoshimura (OIST), Kevin Williams (CSCA), Jeremy Frank (BPBM), Crystal Maier (MCZC), Lars Vilhelmsen (ZMUC), Suzanne Ryder (BMNH), Bonnie Blaimer (ZMHB), Brian Fisher (CASC), Chris Darling (ROME), Benoit Guénard (HKUBM), Po-Wei Hsu (NCUE), Majid Moradmand (ZMUI), Christine Sosiak, Alberto Tinaut, Yu Hisasue, and José María Gómez-Durán. Beyond the provision of specimens, the following persons also deserve my gratitude for often indefatigable assistance and collaboration in matters ranging from the conceptual to logistical, across all methodological facets of my research program—Antoine Abrieux, Michael Branstetter, Perry Buenavente, Evan Economo, Tomáš Faragó, Joshua Gibson, Alireza Ghahremani, Dave General, Elias Hamann, Steve Heydon, Mathias Hurst, Marco Isaia, Adam Khalife, Mia Lippey, Dilworth Parkinson, Adrian Richter, Douglas Rowland, and Xavier Zahnle. My systematic revision of the Leptanillinae could not have attained the theoretical rigor that it did without the expertise and critiques of Marek Borowiec, Jason Bond, and especially Ziad Khouri, and for that I am grateful. I also thank my fellow "Wardites" past and present (Brendon Boudinot, Ziv Lieberman, Jill Oberski, and Matthew Prebus) for providing a stimulating and rich environment for my growth as a myrmecologist and scientist. Last (but most important of all), I thank my adviser Phil Ward for his vast expertise and generosity as a person and systematist, and for being the best mentor I could reasonably ask for. This project was supported in part by NSF grant DEB-1932405 to P. S. Ward; UC Davis Jastro-Shields; Ernst Mayr Travel Grant; Systematics, Evolution & Biodiversity (Entomological Society of America) Travel Grant; the UC-Davis Dept. of Entomology; the

Helmsley Charitable Trust; and Smithsonian Institution Global Genome Initiative. This research used resources of the Advanced Light Source, which is a DOE Office of Science User Facility under contract no. DE-AC02-05CH11231. I also acknowledge the KIT Light Source and the Institute for Beam Physics and Technology (IBPT) for allowing operation of the Karlsruhe Research Accelerator (KARA).

Chapter 1. **Synonymisation of the male-based ant genus *Phaulomyrma* (Hymenoptera: Formicidae) with *Leptanilla* based upon Bayesian total-evidence phylogenetic inference**[1]

Over the past three decades, DNA sequences have provided great insight into phylogenetic relationships across the Metazoa, including the insects (Kjer *et al*. 2016). The application of maximum-likelihood (ML) and Bayesian statistical methods to analysis of genetic data has robustly resolved many problems that were intractable when using morphological data alone (e.g. Niehuis *et al*. 2012; Wipfler *et al*. 2019). However, DNA sequences may be unavailable for some taxa, necessitating the integration of morphological and molecular data under the same inferential framework. Fossils are the most obvious example of this: these are valuable for calibration of phylogenies in absolute time under a Bayesian approach, preferably with their topological position being inferred from the data (Ronquist *et al*. 2012; O'Reilly *et al*. 2015; Bapst *et al*. 2016; Matzke and Wright 2016). Although the inclusion of fossils for the purposes of 'tip-dating' has received the bulk of attention in Bayesian total-evidence phylogenetic inference, the lack of molecular data may afflict rare extant taxa as well (Sánchez *et al*. 2016; Robertson and Moore 2017). This is problematic if the affinities of these taxa are not immediately clear from morphology alone.

The ant subfamily Leptanillinae (Hymenoptera: Formicidae) is an apt test case for methods to resolve this problem. A group of small, hypogaeic ants largely restricted to the Old World tropics and subtropics, the Leptanillinae are understood to be one of the earliest-diverging lineages in

[1]This chapter was previously published in *Invertebrate Systematics*, 2021, 35(6), 603–636, https://doi.org/10.1071/IS20059. Note that much of the information presented herein is superseded by Chapters 4-5.

the ant crown-group (Rabeling *et al*. 2008; Kück *et al*. 2011; Borowiec *et al*. 2019). Three out of eight described genera are known from both workers and males: *Opamyrma* Yamane, Bui & Eguchi, 2008 (Yamada *et al*. 2020), *Protanilla* Taylor, 1990 (Griebenow 2020), and *Leptanilla* Emery, 1870 (e.g. Ogata *et al*. 1995). Males of *Anomalomyrma* Taylor, 1990 are unknown. Four leptanilline genera – *Scyphodon* Brues, 1925; *Phaulomyrma* Wheeler & Wheeler, 1930; *Noonilla* Petersen, 1968; and *Yavnella* Kugler, 1987 – have been described solely from males, as have many species of *Leptanilla* (cf. Bolton 1990). Recent molecular data indicate that the type species of *Yavnella* and a specimen provisionally assigned to *Phaulomyrma* are nested within a clade of putative *Leptanilla* morphospecies (Borowiec *et al*. 2019). Moreover, although *Scyphodon anomalum* Brues, 1925 and *Noonilla copiosa* Petersen, 1968 exhibit respective bizarre autapomorphies such as hypertrophied mandibles (Brues 1925) and a ventromedian genital 'trigger' (Petersen 1968), these ants are otherwise similar to males attributed to *Leptanilla* (Boudinot 2015).

This indicates a need for a systematic revision of the Leptanillinae, but almost all published taxonomic studies of the group have been descriptive without recourse to molecular phylogeny, with the exceptions being revisions to our concept of the subfamily. Multilocus DNA datasets demonstrated that the enigmatic Afrotropical genus *Apomyrma* Gotwald, Brown & Lévieux, 1971 is closely related to the Amblyoponinae rather than the Leptanillinae (Brady *et al*. 2006; Moreau *et al*. 2006), and that the superficially similar Asian genus *Opamyrma* is in fact sister to the remaining Leptanillinae (Ward and Fisher 2016). None of these studies focused upon the Leptanillinae or the internal phylogeny of this clade. Such a study must confront two challenges: first, the lack of DNA sequences for certain critical taxa across the Leptanillinae (e.g. *Scyphodon*), which hampers any attempt to confidently resolve relationships among these;

second, the definition of genera based only upon males, which prevents an integrated phylogenetic classification of the Leptanillinae, since phenotypes of only one sex are considered.

The dissociation of leptanilline castes results from collecting bias. Subterranean workers have been largely collected with *lavage de terre* methodology (López et al. 1994; Wong and Guénard 2016), Winkler trapping (Belshaw and Bolton 1994; Leong et al. 2018), and subterranean pitfall traps (Wong and Guénard 2016; Man et al. 2017), whereas male leptanillines are typically collected by sweeping foliage or by deploying Malaise or pan traps (Robertson 2000). None of these methods are likely to collect males in association with workers, nor is the queen caste often collected in association with conspecifics. Contrasting with the alate condition observed in most ants, queens described from the tribe Leptanillini are completely wingless and blind (Emery 1870; Kutter 1948; Masuko 1990; López et al. 1994; Ogata et al. 1995), meaning that these are no more likely to be collected than corresponding workers. Queens belonging to other leptanilline lineages (Opamyrma and the Anomalomyrmini) are alate so far as is known (Bolton 1990; Baroni Urbani and de Andrade 2006; Borowiec et al. 2011; Chen et al. 2017; Hsu et al. 2017; Man et al. 2017), save for ergatoid queens reported in an undescribed Protanilla (Billen et al. 2013), but are infrequently collected.

Therefore, the bulk of known leptanilline diversity, most of it undescribed, is represented by exclusively male material. In some cases, molecular data are inaccessible for male morphotaxa due to paucity of suitably recent specimens, obliging a total-evidence approach to infer the phylogeny of these lineages. This study uses such an approach to resolve the position of the male-based species *Phaulomyrma javana* Wheeler & Wheeler, 1930, the sole species included in this genus. Here, the phylogeny of the Leptanillinae is inferred jointly from 10 protein-coding

genes, *28S* rDNA, and 41 discrete male morphological characters under a Bayesian statistical framework. This is the first combined-evidence Bayesian analysis to include the Leptanillinae and is novel among studies of ant phylogeny in its inclusion of exclusively male morphological characters (Barden *et al*. (2017) used both worker and male morphology in their Bayesian total-evidence inference). Despite the absence of nucleotide sequences for *P. javana* a Bayesian total-evidence approach facilitates the inclusion of this terminal and its confident phylogenetic placement. Based upon the results of these joint molecular and morphological phylogenetic analyses, a revised male-based definition of *Leptanilla* is provided, and *Phaulomyrma* is synonymised with that genus.

Materials & Methods

Taxon sampling

Thirty-five terminals were included in total (Tables 1, 2). Discrete morphological data were scored for those 33 terminals for which male material was known. *Anomalomyrma boltoni* Borowiec, Schulz, Alpert & Baňar, 2011 and Leptanilla revelierii Emery, 1870 were represented in this study by workers alone. The latter was included on account of its status as the type species of that genus: regardless of future systematic revision to the Leptanillinae, the concept of the genus Leptanilla will not exclude this species. DNA sequences for the outgroup *Martialis heureka* Rabeling & Verhaagh, 2008 were obtained from a worker, as published in Borowiec et al. (2019). Most putative morphospecies were represented by singletons (Table 1), but phenotypic variation within those morphospecies for which material was abundant (e.g. *Leptanilla* zhg-my02) is minimal, and so gives no reason to suspect heterospecificity among the

specimens referred to these morphospecies.

Taxon	Designation in Borowiec *et al.* (2019)	Caste or sex	Identifier of sequenced specimen	Percentage missing	AT content	χ^2 test of nucleotide homogeneity (%, *P*-value)	–	?	Number of specimens physically examined
Anomalomyrma boltoni	*Anomalomyrma boltoni*	Worker	CASENT0217032	18.682	0.526	57.33, passed	1747	0	–
Leptanilla GR01	*Leptanilla* GR01	Male	CASENT0106236	19.474	0.536	2.23, failed	1821	0	5
Leptanilla GR02	*Leptanilla* GR02	Male	CASENT0106060	18.939	0.539	0.95, failed	1771	0	9
Leptanilla GR03	–	Male	CASENT0106058	9.817	0.529	10.55, passed	918	0	9
Leptanilla TH01	*Leptanilla* TH01	Male	CASENT0119792	19.731	0.523	59.55, passed	1845	0	1
Yavnella TH02	*Leptanilla* TH02	Male	CASENT0119531	18.629	0.512	42.16, passed	1742	0	1
Yavnella TH03	*Leptanilla* TH03	Male	CASENT0129721	18.747	0.521	73.57, passed	1753	0	1
Yavnella TH04	*Leptanilla* TH04	Male	CASENT0129695	18.768	0.512	46.39, passed	1755	0	1
Yavnella TH05	*Leptanilla* TH05	Male	CASENT0134656	18.811	0.516	58.31, passed	1759	0	1
Yavnella TH06	*Leptanilla* TH06	Male	CASENT0179537	18.918	0.511	41.26, passed	1769	0	1
Yavnella TH08	*Leptanilla* TH08	Male	CASENT0227555	18.961	0.514	60.05, passed	1773	0	1
Leptanilla TH09	*Leptanilla* TH09	Male	CASENT0227556	18.822	0.542	0.01, failed	1760	0	1
Leptanilla ZA01	*Leptanilla* ZA01	Male	CASENT0106354	18.886	0.545	0.01, failed	1766	0	1
Leptanilla zhg-au02	–	Male	CASENT0758864	60.924	0.545	0.51, failed	777	4920	1
Leptanilla zhg-th01	–	Male	CASENT0842614	46.99	0.518	34.54, passed	1942	2452	2
Leptanilla revelierii	–	Worker	CASENT0842627	29.537	0.516	25.57, passed	629	2133	4
Leptanilla zhg-bt01	–	Male	CASENT0842617	51.92	0.552	0.00, failed	518	4337	1
Leptanilla zhg-my02	–	Male	CASENT0106451	65.715	0.517	2.89, failed	928	5217	49
Leptanilla zhg-my03	–	Male	CASENT0842618	51.845	0.538	1.04, failed	511	4337	4
Leptanilla zhg-my04	–	Male	CASENT0842553	43.985	0.532	11.36, passed	1980	2133	21
Leptanilla zhg-my05	–	Male	CASENT0842568	44.188	0.526	19.01, passed	1999	2133	7
Martialis heureka	*Martialis heureka*	Worker	CASENT0106181	16.308	0.474	0.00, failed	1525	0	–
Noonilla zhg-my02	–	Male	CASENT0842599	58.956	0.523	6.76, passed	2216	3297	12
Noonilla zhg-my06	–	Male	CASENT0106373	42.552	0.53	14.61, passed	1846	2133	3
Opamyrma hungvuong	*Opamyrma hungvuong*	Worker	CASENT0178347	18.426	0.477	0.00, failed	1723	0	–
Yavnella MM01	*Phaulomyrma* MM01	Male	CASENT0179537	19.014	0.514	72.37, passed	1778	0	1
Phaulomyrma javana	–	Male	MCZ:Ent:31142	100	–	–	–	–	1
Protanilla TH01	*Protanilla* TH01	Male	CASENT0119776	18.34	0.529	29.55, passed	1715	0	1
Protanilla TH02	*Protanilla* TH02	Male	CASENT0128922	18.362	0.529	30.49, passed	1717	0	1
Protanilla TH03	*Protanilla* TH03	Male	CASENT0119791	18.95	0.497	0.08, failed	1772	0	1
Protanilla zhg-vn01	–	Male	CASENT0842613	58.208	0.512	3.27, failed	2146	3297	5
Yavnella argamani	*Yavnella argamani*	Male	CASENT0235253	18.789	0.52	61.37, passed	1757	0	1
Yavnella cf. *indica*	–	Male	CASENT0106375	52.989	0.502	6.42, passed	2503	2452	8
Yavnella zhg-bt01	–	Male	CASENT0842616	49.054	0.514	47.75, passed	2454	2133	5
Yavnella zhg-th01	–	Male	CASENT0842615	51.706	0.522	7.42, passed	498	4337	2

Table 1.1. Summary statistics for full 9351-bp DNA legacy-locus alignment. –, absent base; ?, unknown base. Chi-Square test of nucleotide homogeneity was executed with IQ-Tree (ver. 1.6.10, see http://www.iqtree.org/; Nguyen et al. 2015) on the CIPRES Science Gateway (ver. 3.3; Miller et al. 2010).

Representatives of all male-based genera were included in total-evidence analyses, except for *Scyphodon*. These include both *Yavnella argamani* Kugler, 1987 and *Yavnella* cf. *indica*, along with two undescribed *Yavnella* morphospecies from Bhutan and Thailand respectively; *Phaulomyrma javana*; and two morphospecies of *Noonilla* identified as such according to the definition given by Petersen (1968). *Leptanilla* TH02-6 and -8, along with *Phaulomyrma* MM01, were placed in those genera by Borowiec et al. (2019) and Boudinot (2015), but are here

identified as *Yavnella* (Table 1) according to the definition of Kugler (1987) (cf. Griebenow 2020).

Material is deposited in the following repositories: the Bohart Museum of Entomology, University of California, Davis, CA, USA (UCDC); the California Academy of Sciences, San Francisco, CA, USA (CASC); the California State Collection of Arthropods, Sacramento, CA, USA (CSCA); the Lund Museum of Zoology, Lund, Sweden (MZLU); and the Australian National Insect Collection, Canberra, Australia (ANIC).

Molecular dataset

Total-evidence phylogenetic inference was based upon 11 nuclear loci: 28S rDNA (28S), abdominal-A (abdA), arginine kinase (argK), antennapedia (Antp), elongation factor 1-α F2 copy (EF1αF2), long wavelength rhodopsin (LW Rh), NaK ATPase (NaK), DNA pol-delta (POLD1), topoisomerase I (Top1), ultrabithorax (Ubx), and wingless (Wg). For 19 terminals, these 'legacy loci' were derived from the alignment of Borowiec et al. (2019) (doi:10.5281/zenodo.2549806) but expanded to include autapomorphic indels and introns, and constituting 11 090 bp. Legacy loci for *Leptanilla* GR03 were derived from Ward and Sumnicht (2012). For further detail on the protocols for the extraction and amplification of these genetic data, refer to Ward et al. (2010) and Ward and Fisher (2016). Fourteen terminals were added to this 'legacy-locus' intron-inclusive dataset by retrieving orthologous loci from phylogenomic data acquired with the ultraconserved element (UCE) probe set hym-v2 (see https://datadryad.org/stash/dataset/doi:10.5061/dryad.89n87; Branstetter et al. 2017). Phaulomyrma javana was the only terminal for which molecular data were not obtained: this species is known only from two slide-mounted syntypes collected in 1907.

DNA was extracted non-destructively using a DNeasy Blood and Tissue Kit (Qiagen Inc., Valencia, CA) according to manufacturer's instructions. DNA was quantified for each sample with a Qubit 2.0 fluorometer (Life Technologies Inc., Carlsbad, CA, USA). Phylogenomic data were obtained from these taxa using the hym-v2 probe set, with libraries being prepared and target loci enriched using the protocol of Branstetter et al. (2017). Enrichment success and size-adjusted DNA concentrations of pools were assessed using the SYBR FAST qPCR kit (Kapa Biosystems, Wilmington, MA, USA) and all pools were combined into an equimolar final pool. The contents of this final pool were sequenced by an Illumina HiSeq 2500 at the University of Utah's High Throughput Genomics Facility or an Illumina HiSeq 4000 at Novogene, Sacramento, CA, USA. The FASTQ output was demultiplexed and cleansed of adaptor contamination and low-quality reads using illumiprocessor (B. C. Faircloth, see https://github.com/faircloth-lab/illumiprocessor) in the PHYLUCE package. Raw reads were then assembled with trinity (ver. 2013-02-25, see https://github.com/trinityrnaseq/trinityrnaseq/releases; Grabherr et al. 2011) or SPAdes (ver. 3.12.0, see https://github.com/ablab/spades; Bankevich et al. 2012). The possibility of genetic contamination, misassembly or both in the UCE samples was tested by inferring a phylogeny from a concatenated UCE alignment, unpartitioned, using IQ-Tree (ver. 1.6.10, see http://www.iqtree.org/; Nguyen et al. 2015) on the CIPRES Science Gateway (ver. 3.3, see https://www.phylo.org/; Miller et al. 2010) with the GTR+G model of substitution for 1000 ultrafast bootstrap replicates (Hoang et al. 2018): this phylogeny was plausible given preliminary hypotheses, providing no positive evidence of sequence contamination or misassembly. Summary statistics for these UCE assemblies were computed using statswrapper.sh in BBMap

(ver. 38.87, B. Bushnell, see https://sourceforge.net/projects/bbmap/files/, accessed 13 November 2020) and are provided in Table S1 of the Supplementary material.

In the cases of the 14 terminals not included in Ward and Sumnicht (2012) or Borowiec et al. (2019) for which molecular data could be obtained, legacy loci orthologous with those used by Borowiec et al. (2019) were then recovered from genome-scale data using PHYLUCE (ver. 1.6.7, see https://github.com/faircloth-lab/phyluce; Faircloth 2016), as follows. Sequences representing each locus for Leptanilla GR02 were derived from the alignment ANT-exon-sequences-40-taxa-reduced.fasta published by Branstetter et al. (2017), given the comparative completeness of the matrix for that species, and its phylogenetic position nested well within the Leptanillinae. These sequences were then used analogously to probes. Species-specific contig assemblies were obtained using the command phyluce_assembly_match_contigs_to_probes.py (min_coverage = 50, min_identity = 85), a list of legacy loci shared across all taxa was generated using phyluce_assembly_get_match_counts.py, and separate FASTA files for each locus were created using these outputs. Sequences were aligned separately by locus using MAFFT (ver. 7.407, see https://mafft.cbrc.jp/alignment/software/ubuntu_on_windows.html; Katoh et al. 2009) implemented with the command phyluce_assembly_seqcap_align.py, and these sequences were then trimmed with Gblocks (ver. 0.91b, see http://molevol.cmima.csic.es/castresana/Gblocks.html; Castresana 2000) as implemented by the wrapper script phyluce_assembly_get_gblocks_trimmed_alignment_from_untrimmed.py (settings: b1 = 0.5, b2 = 0.5, b3 = 12, b4 = 7). Alignment statistics for the output FASTA files were calculated with phyluce_align_get_align_summary_data.py. Finally, a matrix that was 80% complete with respect to locus coverage was generated using the script phyluce_align_get_only_loci_with_min_taxa.py. This contained 7 out of the 10 protein-coding

loci that were recovered using the exon-based bioinformatic protocol of Branstetter et al. (2017), in addition to 28S rDNA. Legacy loci recovered from UCE assemblies often included non-coding sequences adjacent to the regions included in Borowiec et al. (2019), which were trimmed manually in AliView. In whichever cases those loci had been recovered, sequences for the taxa represented only in the dataset of Borowiec et al. (2019) were then aligned with the recovered legacy loci using the online MAFFT interface (Katoh et al. 2019) with default settings. In cases where legacy loci were not successfully recovered or were incomplete relative to preexisting Sanger-derived sequences, these loci were derived from the datasets of Borowiec et al. (2019) or, in the case of *Leptanilla* GR03, Ward and Sumnicht (2012). These data were concatenated with UCE-derived sequences across all FASTA files, in as much as all sequences for each morphospecies were derived from the same specimen; and all loci were concatenated to produce a final alignment, which was 9351 bp in length. Further summary statistics for this final alignment are provided in Table 1 and Table S2 of the Supplementary material. Alignment was unambiguous once all loci were brought into their respective reading frames. GenBank accession

numbers for all loci used in this study are provided in Table 2.

Taxon	CASENT number	SRA	*28S*	*AbdA*	*EF2*	*LwRh*	*Wg*	*AP*	*ArgK*	*NaK*	*POLD1*	*Top1*	*Ubx*
Anomalomyrma boltoni	CASENT0217032	SRR11742957	KU671445	KU672069	KU671496	KU671547	KU671598	KU671848	KU671656	KU672002	KU671925	KU671719	KU671782
Leptanilla GR01	CASENT0106236	SRR11881502	EF012999	JN967847	JN967830	JN967890	JN967854	MF625736	JN967880	MF626276	MF625821	JN967820	JN967809
Leptanilla GR02	CASENT0106060	SRR11881501	JN967864	JN967848	JN967831	JN967891	JN967856	MF625737[A]	JN967883	MF626277[A]	MF625822[A]	JN967823	JN967812
Leptanilla GR03	CASENT0106058	SRR11793843	JN967868	JN967851	JN967834	JN967894	JN967859	MT603718	JN967885	MT603718	MT526730	JN967826	JN967815
Leptanilla TH01	CASENT0119792	SRR11881509	KU671447	JN967845	JN967836	KU671549	JN967853	KU671856	KU671660	KU672010	KU671933	KU671723	KU671786
Leptanilla TH09	CASENT0227556	–	MF626114	MF625683	MF625896	MF626223	MF626005	MF625744	MF626167	MF626284	MF625829	MF626058	MF625949
Leptanilla ZA01	CASENT0106354	–	AY867452	AY867468	EF013432	AY867483	AY867421	MF625745	JN967878	MF626285	MF625830	JN967818	JN967807
Leptanilla zhg-au02	CASENT0758864	SRR11793848	–	–	–	–	–	MT526744	MT526685	MT526759	–	MT526717	MT526699
Leptanilla zhg-th01	CASENT0842614	SRR11793854	MW325217	–	–	–	–	MT526745	MT526687	MT526761	MT526731	MT526722	MT526705
Leptanilla revelierii	CASENT0842627	SRR11881510	MW325220	–	–	–	–	MW209695	MW209698	MW197678	MW197679	MW209696	MW209697
Leptanilla zhg-bt01	CASENT0842617	SRR11793849	–	–	–	–	–	MT526746	MT526684	MT526760	MT526729	MT526718	MT526697
Leptanilla zhg-my02	CASENT0106451	SRR11793840	–	–	–	–	–	MT526747	MT526688	MT526762	MT526732	–	MT526706
Leptanilla zhg-my03	CASENT0842618	SRR11793851	–	–	–	–	–	MT526748	MT526690	MT526765	MT526734	MT526723	MT526707
Leptanilla zhg-my04	CASENT0842553	SRR11793838	MW325213	–	–	–	–	MT526749	MT526691	MT526764	MT526735	MT526724	MT526709
Leptanilla zhg-my05	CASENT0842568	SRR11793837	MW325214	–	–	–	–	MT526750	MT526689	MT526763	MT526733	MT526725	MT526708
Martialis heureka	CASENT0106181	SRR11881511	KU671448	KU672072	KU671499	KU671550	KU671601	KU671858	KU671661	KU672012	KU671935	KU671724	KU671787
Noonilla zhg-my02	CASENT0842599	SRR11793856	MW325215	–	–	–	–	MT526751	–	MT526767	MT526736	MT526727	MT526712
Noonilla zhg-my06	CASENT0106373	SRR11793842	MW325216	–	–	–	–	MT526753	MT526693	MT526768	MT526737	MT526728	MT526711
Opamyrma hungvuong	CASENT0178347	SRR11742960	KU671407	KU672031	KU671458	KU671509	KU671560	KU671806	KU671616	KU671960	KU671883	KU671679	KU671742
Protanilla TH01	CASENT0119776	SRR12006305	MF626129	MF625698	MF625911	MF626238	MF626020	MF625776	MF626191	MF626316	MF625861	MF626082	MF625973
Protanilla TH02	CASENT0128922	SRR11742959	MF626130	MF625699	MF625912	MF626239	MF626021	MF625777	MF626192	MF626317	MF625862	MF626083	MF625974
Protanilla TH03	CASENT0119791	SRR11742954	MF626131	MF625700	MF625913	MF626240	MF626022	MF625778	MF626193	MF626318	MF625863	MF626084	MF625975
Protanilla zhg-vn01	CASENT0842613	SRR11793859	MW325221	–	–	–	–	MT526754	–	MT526772	MT526742	MT526714	MT526704
Yavnella argamani	CASENT0235253	SRR11793861	KU671449	KU672073	KU671500	KU671551	KU671602	KU671868	KU671665	KU672022	KU671945	KU671728	KU671791
Yavnella cf. *indica*	CASENT0106375	SRR11793841	MW325218	–	–	–	–	MT526755	MT526696	MT526771	MT526741	MT526720	MT526701
Yavnella MM01	CASENT0179537	SRR11742953	MF626120	MF625689	MF625902	MF626229	MF626011	MF625762	MF626178	MF626302	MF625847	MF626069	MF625960
Yavnella TH02	CASENT0119531	SRR11881508	MF626108	MF625677	MF625890	MF626217	MF625999	MF625738	MF626161	MF626278	MF625823	MF626052	MF625943
Yavnella TH03	CASENT0129721	SRR11742956	MF626109	MF625678	MF625891	MF626218	MF626000	MF625739	MF626162	MF626279	MF625824	MF626053	MF625944
Yavnella TH04	CASENT0129695	SRR11742958	MF626110	MF625679	MF625892	MF626219	MF626001	MF625740	MF626163	MF626280	MF625825	MF626054	MF625945
Yavnella TH05	CASENT0134656	SRR11881507	MF626111	MF625680	MF625893	MF626220	MF626002	MF625741	MF626164	MF626281	MF625826	MF626055	MF625946
Yavnella TH06	CASENT0179537	SRR11742955	MF626112	MF625681	MF625894	MF626221	MF626003	MF625742	MF626165	MF626282	MF625827	MF626056	MF625947
Yavnella TH08	CASENT0227555	SRR11881506	MF626113	MF625682	MF625895	MF626222	MF626004	MF625743	MF626166	MF626283	MF625828	MF626057	MF625948
Yavnella zhg-bt01	CASENT0842616	SRR11793850	MW325219	–	–	–	–	MT526756	MT526695	MT526770	MT526740	MT526721	MT526702
Yavnella zhg-th01	CASENT0842615	SRR11793853	–	–	–	–	–	MT526757	MT526694	MT526769	MT526739	MT526719	MT526700

[A]These accession numbers are erroneously attributed to CASENT0106067 (*Leptanilla* GR02) on GenBank as of 13 March 2021.

Table 1.2. NCBI and SRA accession numbers for DNA sequences used in Bayesian total-evidence inference.

Those terminals for which loci were obtained using the 11 nuclear loci from Leptanilla GR02 as 'probes', according to the modified PHYLUCE protocol cited above ('Molecular dataset') (Faircloth 2016), with 80% locus coverage implemented in phyluce_align_get_only_loci_with_min_taxa.py, exhibit low coverage relative to those that were sequenced before this study (Table 1). Therefore, a 9062-bp legacy-locus alignment was created that includes only those data published before this study (Ward and Sumnicht 2012; Borowiec et al. 2019), with 20 terminals. These sequences can be used to test the possibility that missing data would have an appreciable effect on phylogenetic inference.

Morphological dataset

Forty-one discrete binary morphological characters were coded for all 33 morphospecies known from males. In total, 6 were cephalic characters, 11 mesosomal (including the legs and wings), 8

metasomal, and 16 genital. All specimens were examined with a Leica MZ75 compound microscope or by reference to images on AntWeb, except for the males of M. heureka and Opamyrma hungvuong Yamane, Bui & Eguchi, 2008, in the cases of which observations were derived from Boudinot (2015, fig. 11, 12) and Yamada et al. (2020, fig. 11–13) respectively or from the textual descriptions by those authors. Specimens were imaged when necessary using a JVC KY-F75 digital camera, with colour photographs compiled from these with the Syncroscopy AutoMontage Program (ver. 5.0). Scanning electron microscopy was undertaken using a Hitachi TM4000 tabletop microscope. Morphological terminology follows the Hymenoptera Anatomy Ontology (Yoder et al. 2010), with some exceptions being derived from Bolton (2003) and Boudinot (2018). The character coding scheme was binary and non-additive (Pleijel 1995). Missing data were scored as '?'. Autapomorphic characters were included. Numerical scores for all morphological characters are presented in Table S3 of the Supplementary material.

Non-additive binary coding has been criticised for its susceptibility to redundancy (Strong and Lipscomb 1999), stipulation of compound characters, and the inadvertent conflation of morphological absences that are not hierarchically equivalent (Brazeau 2011). These problems largely result from careless character delimitation. These potential flaws were compensated for by defining and using only characters that do not logically depend upon other characters.

Definition of morphological characters

Note that all non-genital morphological data are missing in Leptanilla ZA01, since all that remained of this specimen after destructive DNA extraction was the male genitalia. Missing observations are noted for other terminals where relevant. Males of Protanilla lini Terayama, 2009 were identified as such by molecular data (Griebenow 2020).

1. Mesal protibial margin carinate. A sclerotised carina (Fig. 1.1*A*) is present (1) on the mesal margin of the ventral protibial surface in *Noonilla*. This character could not be scored in *Leptanilla* TH01. Under the alternative character state (0) the mesal protibial face is convex (Fig. 1.1*B*) to carinate.

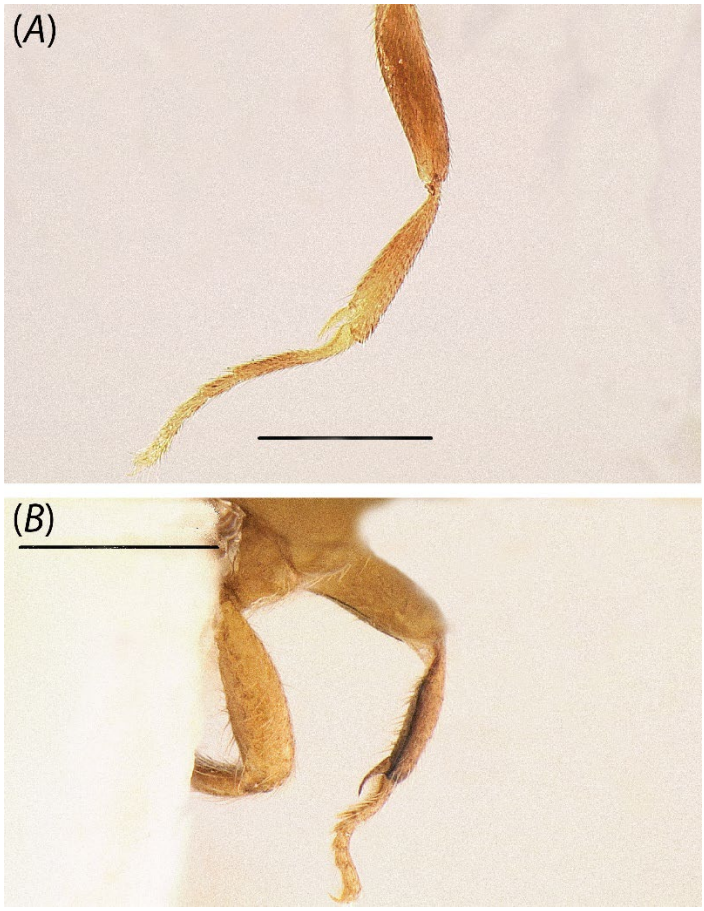

Figure 1.1. Mesal view of protibia of (A) *Protanilla* zhg-vn01 (CASENT0106382) and (B) *Noonilla* zhg-my01 (CASENT0842587; not sequenced in this study). Scale bar: 0.3 mm.

2. Ventral cuticular hook present on profemur. The lateral margin of the ventral profemoral surface is ventrally produced into a hook-like structure (Fig. 1.2*B*, 1.3*B*) (1) in *Leptanilla* ('Bornean morphospecies-group') zhg-my02 and -my05. The morphospecies imaged in 1.2*B*, 1.3*B* is closely related to these (Griebenow 2020). Under the alternative character

state (0) there are no cuticular extensions of the profemur (Fig. 1.2*A*). This character could not be scored in *Leptanilla* TH01.

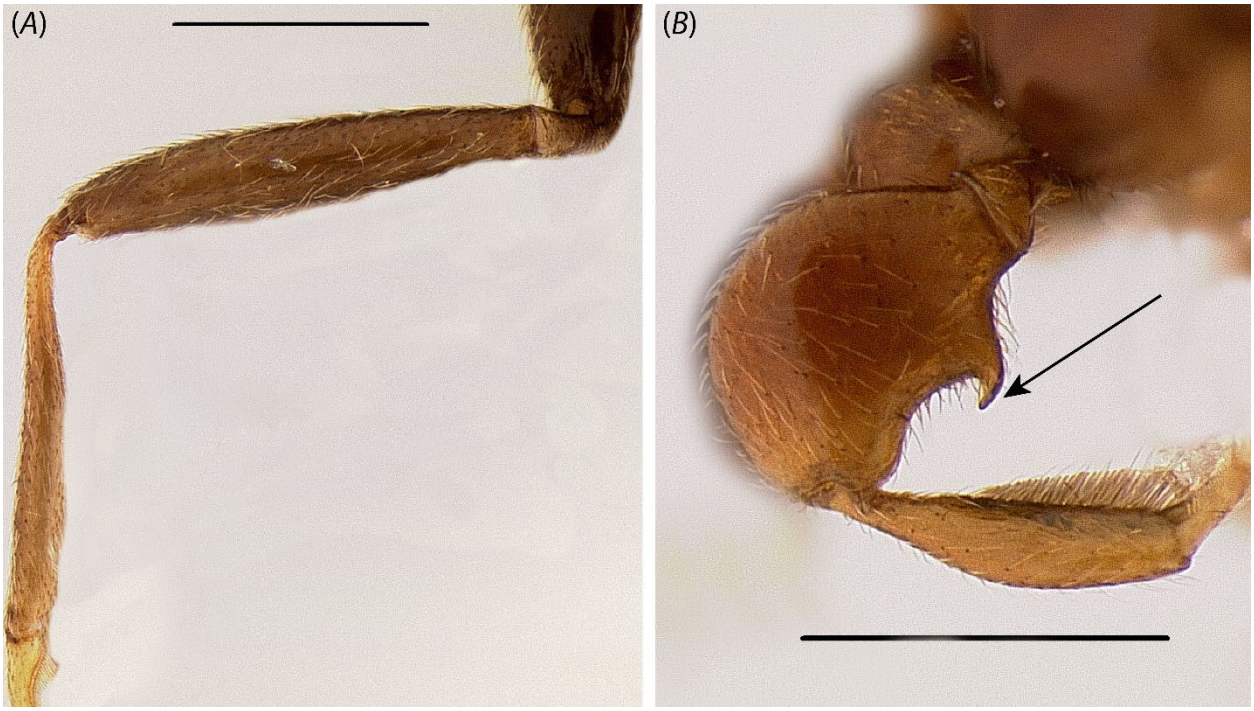

Figure 1.2. Foreleg of (A) *Yavnella argamani* (CASENT0235253) and (B) *Leptanilla* zhg-id01 (CASENT0842626; not sequenced in this study). Scale bar: 0.3 mm.

3. Row of ventral protibial bristles present. A single median row of parallel-sided setae is present (1) on the ventral protibial surface only in the Bornean morphospecies-group (Fig. 1.3*B*). These are robust by comparison with adjacent unmodified setae. Under the alternative character state (0) setae on the protibial venter are not robust, parallel-sided, and arranged in a single medial row (Fig. 1.3*A*). This character could not be scored in *Leptanilla* TH01.

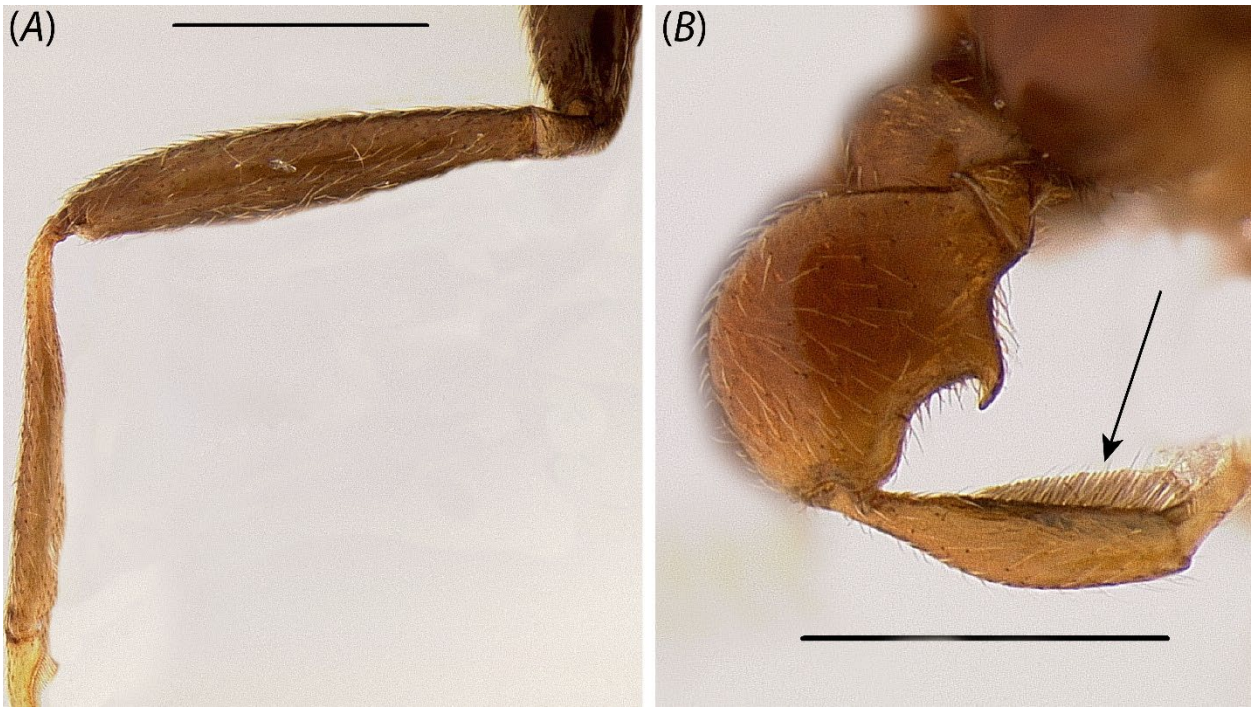

Figure 1.3. Foreleg of (A) *Yavnella argamani* (CASENT0235253) and (B) *Leptanilla* zhg-id01 (CASENT0842626; not sequenced in this study). Scale bar: 0.3 mm.

4. Head inclusive of compound eyes as wide or wider than long. This character state is observed (1) in *O. hungvuong*; all male Anomalomyrmini sampled herein; all *Yavnella s. l.* except for *Yavnella* TH05, -8, and MM01; *Leptanilla* (Bornean morphospecies-group) zhg-my04; and *Noonilla* zhg-my06 (Fig. 1.4*B*). Under the alternative character state (0) the head inclusive of the compound eyes is narrower than long in full-face view (Fig. 1.4*A*).

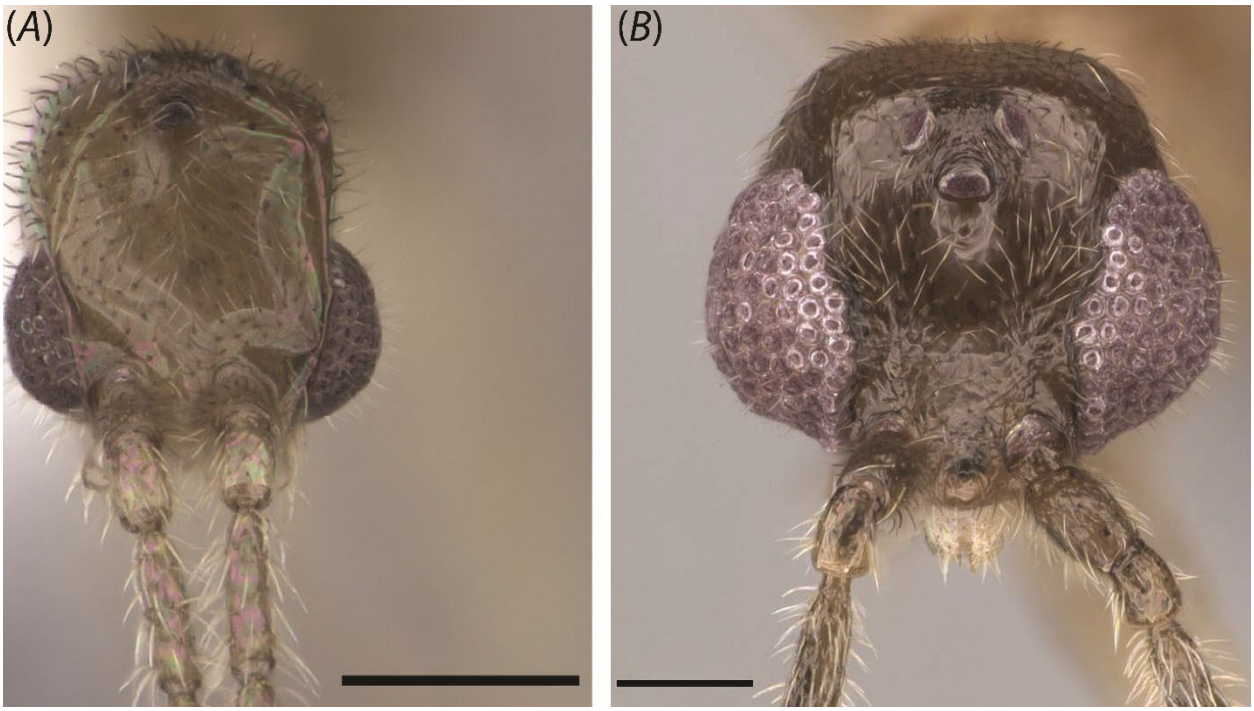

Figure 1.4. Full-face views of (A) *Yavnella* TH08 (CASENT0227555; Michele Esposito) and (B) *Yavnella* TH02 (CASENT0119531; Shannon Hartman). Scale bar: 0.1 mm.

5. Clypeus broader than torular diameter along medial axis. This character state is observed (1) in *M. heureka*; *O. hungvuong*; in all Anomalomyrmini sampled herein; and in all *Yavnella s. l.* for which observations are available (Fig. 1.5*B*). Clypeus narrower than torular diameter along medial axis (0) (Fig. 1.5*A*) may therefore be diagnostic for *Leptanilla s. l.* This character could not be scored in *Yavnella* TH03, -5, -8, zhg-bt01, and MM01; *Leptanilla* zhg-th01; and *Leptanilla* GR01-3, zhg-au02 and zhg-bt01.

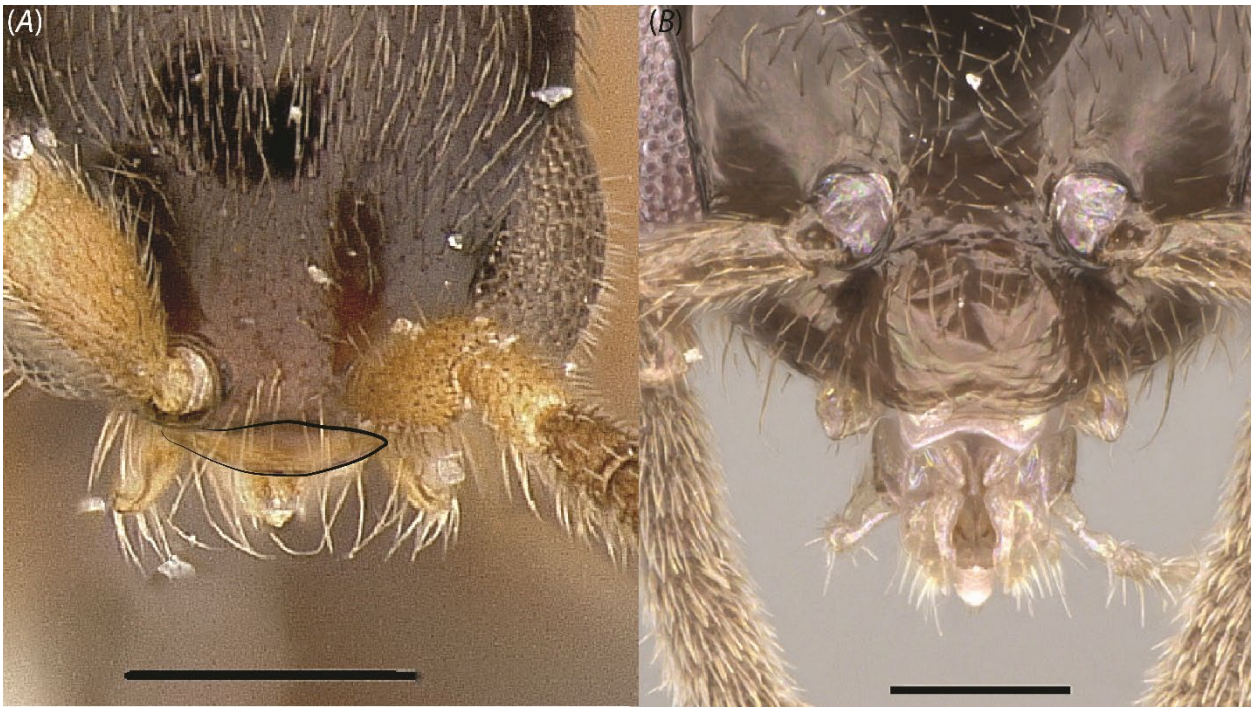

Figure 1.5. Full-face views of (A) *Leptanilla* zhg-my04 (CASENT0842558) and (B) *Protanilla* TH01 (CASENT0119776; Michele Esposito). Scale bars: A, 0.1 mm; B, 0.2 mm.

6. Anterior tentorial pit situated directly anterior to torulus. The anterior tentorial pits are situated directly anterior to the toruli, in whole (Fig. 1.6*B*) or in part (1) so that at least some portion of the anterior tentorial pit intersects an anteroposterior axis drawn through the torulus, in *M. heureka*, *O. hungvuong*, all Anomalomyrmini save *Protanilla* TH01, and all *Yavnella s. l.* save *Yavnella* TH05 and MM01. Under the alternative character state (0), the anterior tentorial pits are situated anterolaterad the toruli or may not be readily discernible (Fig. 1.6*A*), so that no part of the anterior tentorial pit intersects an anteroposterior axis drawn through the torulus. This character could not be scored in *Yavnella* TH03 and -8, *Leptanilla* (Bornean morphospecies-group) zhg-my02, *Leptanilla* zhg-au02, and *P. javana*.

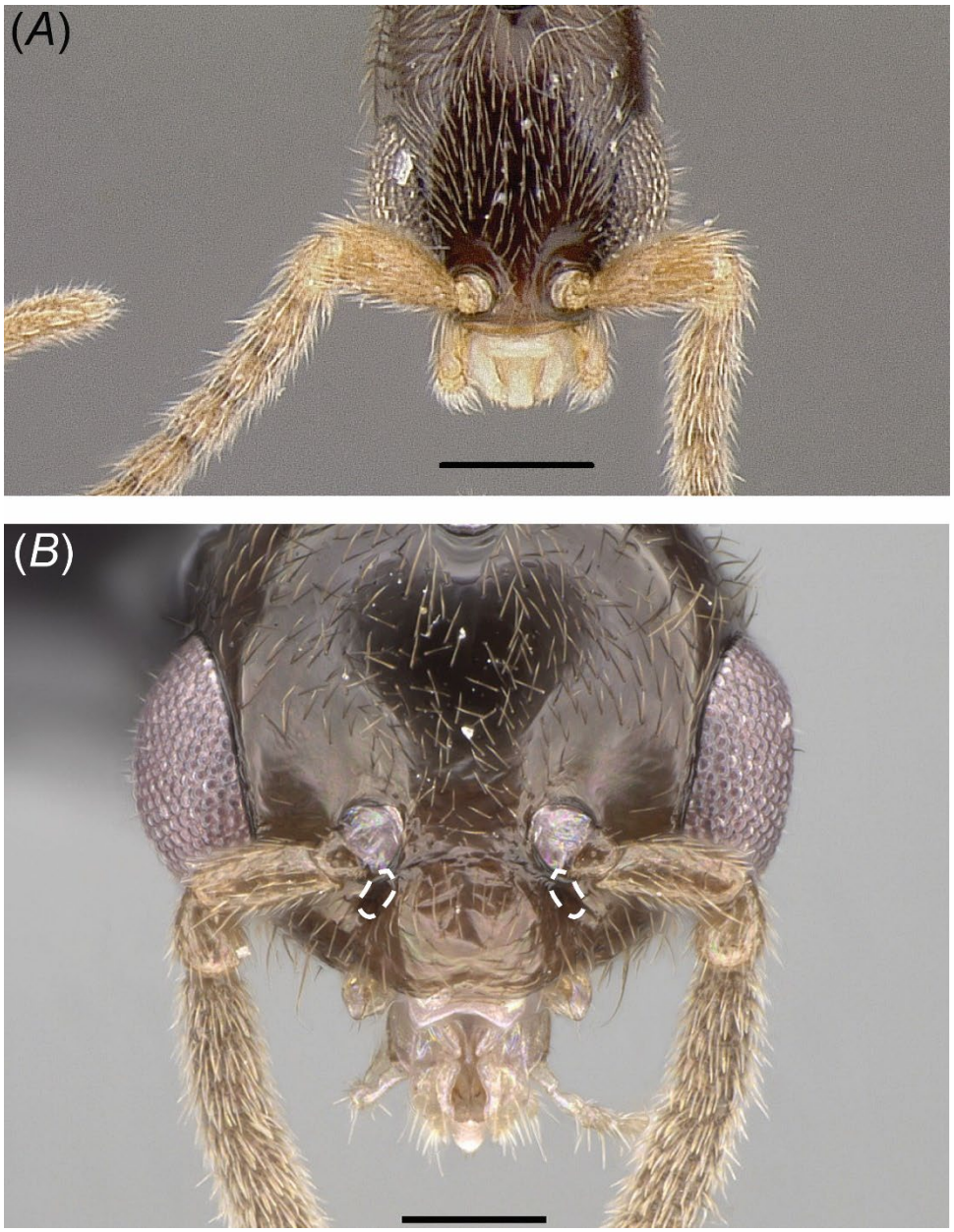

Figure 1.6. Full-face views of (A) *Leptanilla* zhg-my03 (CASENT084545) and (B) *Protanilla* TH01 (CASENT0119776; Michele Esposito). Scale bars: A, 0.1 mm; B, 0.2 mm.

7. Antennomere 3 longer than scape. This character state (1) (Fig. 1.7*B*) is observed in *Protanilla* TH03 and all *Yavnella s. l.* except for *Yavnella* TH05. Under the alternative character state (0) the scape is shorter than (Fig. 1.7*A*) or subequal in length to antennomere 3. This character could not be scored in *O. hungvuong* or *Leptanilla* zhg-au02.

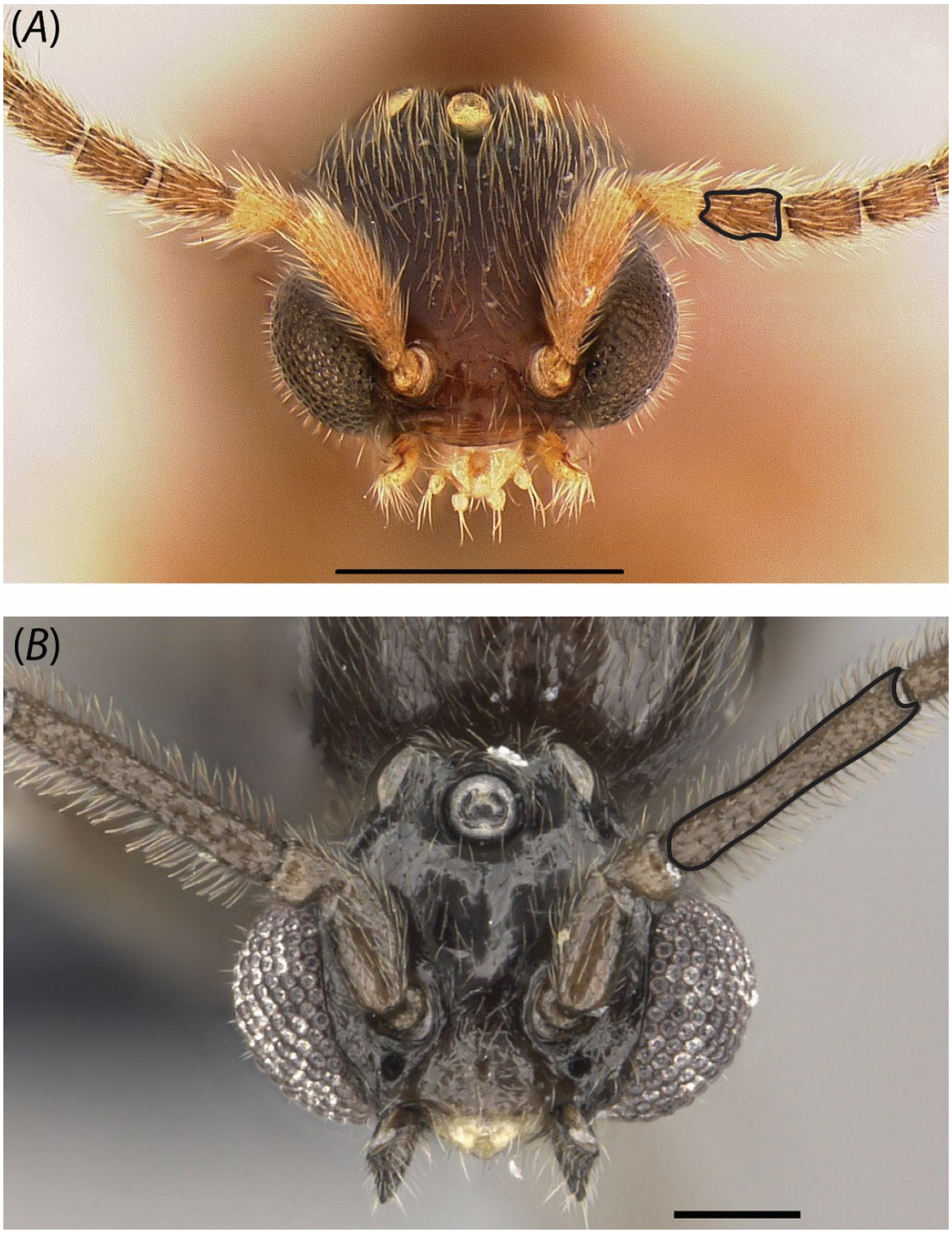

Figure 1.7. Full-face views of (A) *Leptanilla* zhg-my04 (CASENT0842548) and (B) *Yavnella argamani* (CASENT0235253; Shannon Hartman). Scale bars: A, 0.3 mm; B, 0.1 mm.

8. Mandible articulated to gena. The base of the male mandible is visibly fused to the gena (0) in all *Yavnella s. l.* for which observations are available (Fig. 1.8*A*), except for Yavnella TH04. In all other terminals in which this character can be assessed a complete point of articulation to the gena is visible (1) (Fig. 1.8*B*). This character could not be scored in *Yavnella* TH03 and MM01, *Leptanilla* zhg-au02 and -TH09, and *P. javana*.

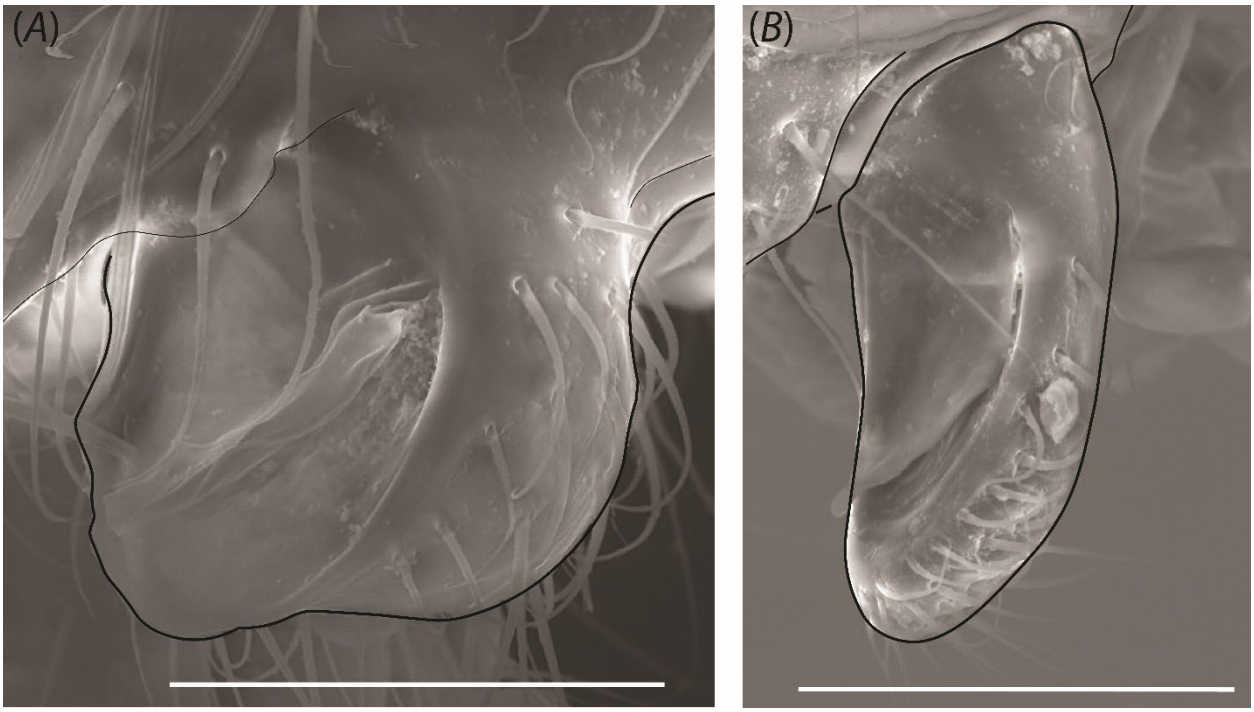

Figure 1.8. Mandible of (A) *Yavnella* cf. *indica* (CASENT0106377) and (B) *Leptanilla* zhg-my03 (CASENT0842618). Scale bars: A, 0.03 mm; B, 0.05 mm.

9. Occipital margin angularly emarginate in dorsal view. The occiput is coded as angularly emarginate in dorsal view (1) if the posterolateral corners of the occipital margin are produced; this character state is observed in *Leptanilla* TH01 (Fig. 1.9*B*) and zhg-th01, and the Bornean morphospecies-group except for *Leptanilla* (Bornean morphospecies-group) zhg-my03. Under the alternative character state (0) the occiput is linear to shallowly emarginate (Fig. 1.9*A*).

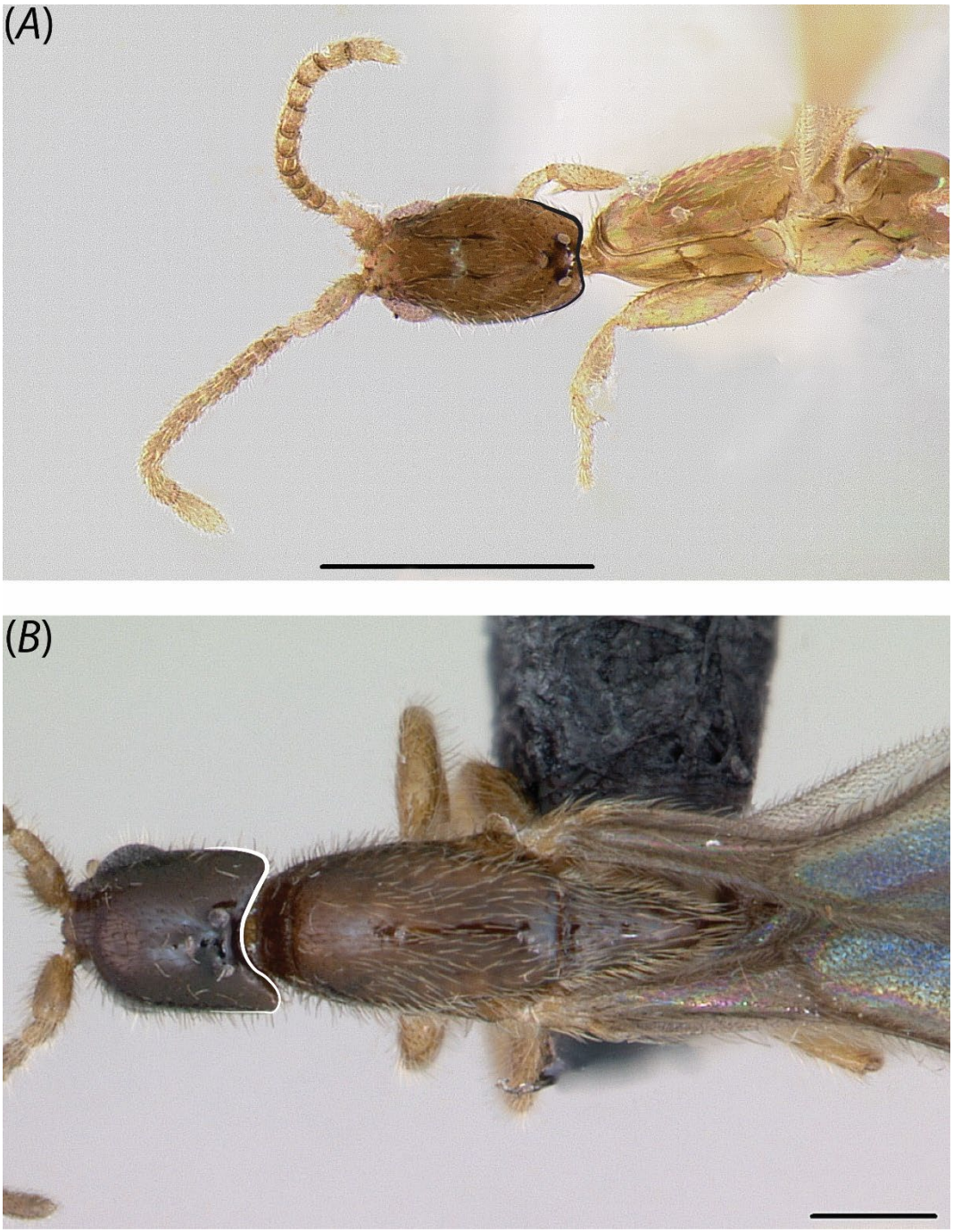

Figure 1.9. Dorsal view of occipital margin in (A) *Leptanilla* TH09 (CASENT0842664) and (B) *Leptanilla* TH01 (CASENT0119792; April Nobile). Scale bars: A, 0.3 mm; B, 0.2 mm.

10. Mesoscutum convex in profile view. The mesoscutum is scored as convex (1) if not planar to shallowly convex (0) (Fig. 1.10*A*). Mesoscutal convexity (1) (Fig. 1.10*B*) is

present in *M. heureka*, *O. hungvuong*, the Anomalomyrmini, *Yavnella s. l.*, and *Leptanilla* (Bornean morphospecies-group) zhg-my04.

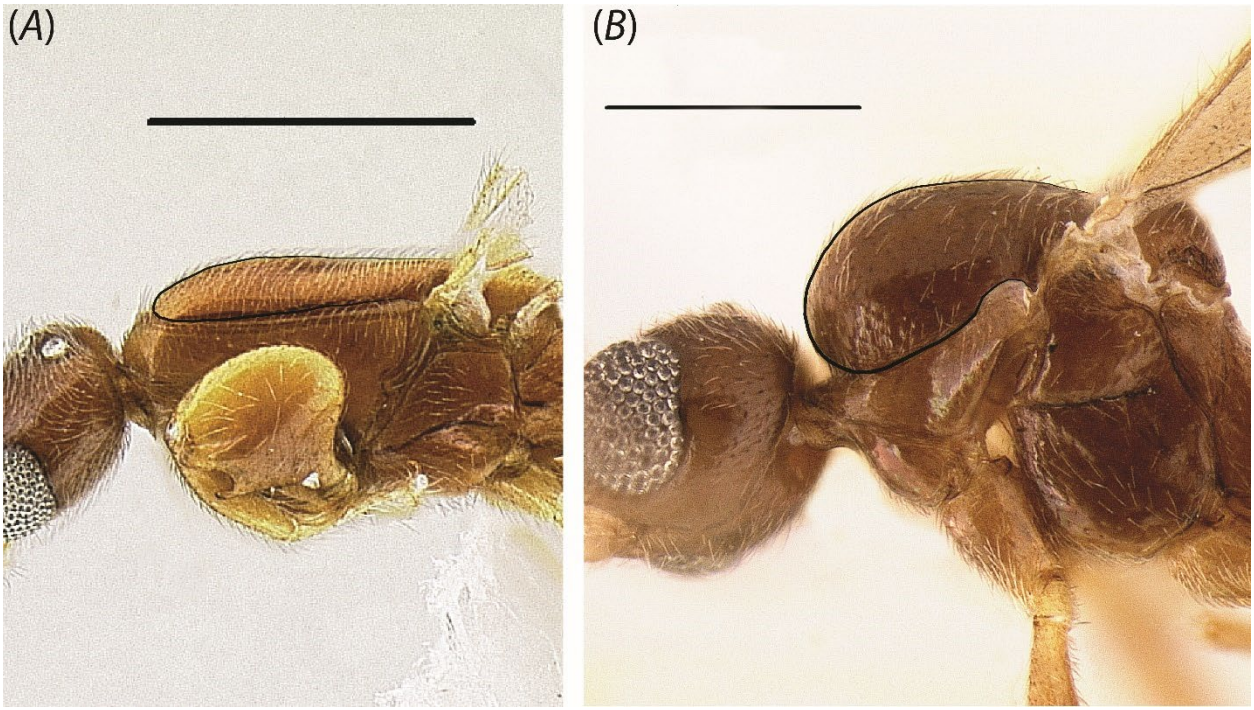

Figure 1.10. Profile view of mesosoma in (A) *Leptanilla* zhg-my02 (CASENT0106416) and (B) *Yavnella* zhg-th01 (CASENT0842620). Scale bars: A, 0.5 mm; B, 0.3 mm.

11. Notauli present. The presence (1) or absence (0) (Fig. 1.11*A*) of notauli is always unambiguous. These are observed only in *M. heureka*, *Protanilla* TH01 and -3 (Fig. 1.11*B*).

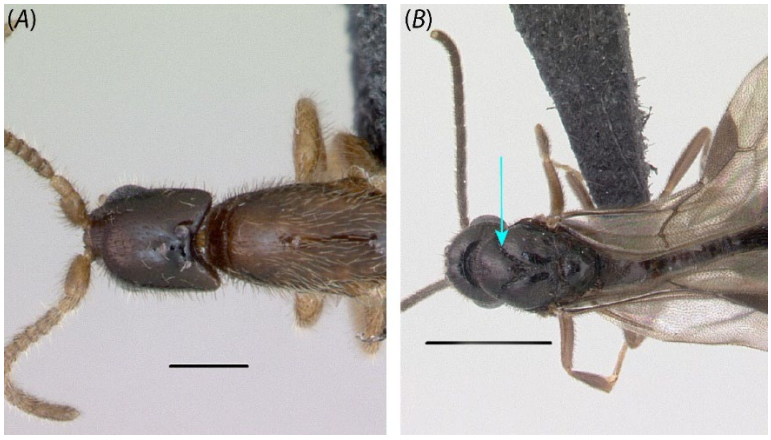

Figure 1.11. Dorsal view of (A) *Leptanilla* TH01 (CASENT0119776; April Nobile) and (B) Protanilla TH03 (CASENT0119791; Erin Prado). Scale bars: A, 0.2 mm; B, 1 mm.

12. Parapsidal signa present. The presence (1) (Fig. 1.12*B*) or absence (0) (Fig. 1.12*A*) of the parapsidal signa can be difficult to discern, varying from a distinct impressed signum to a stripe of glabrous cuticle. Some form of parapsidal signum is present in *M. heureka*; *O. hungvuong*; *Protanilla* zhg-vn01; *Yavnella* cf. *indica*, *Yavnella argamani*, *Yavnella* zhg-th01, TH02, -4, -6 and MM01; *Leptanilla* TH01; *Noonilla* zhg-my06; the Bornean morphospecies-group; and *Leptanilla* GR01. This character could not be scored in *Leptanilla* zhg-au02.

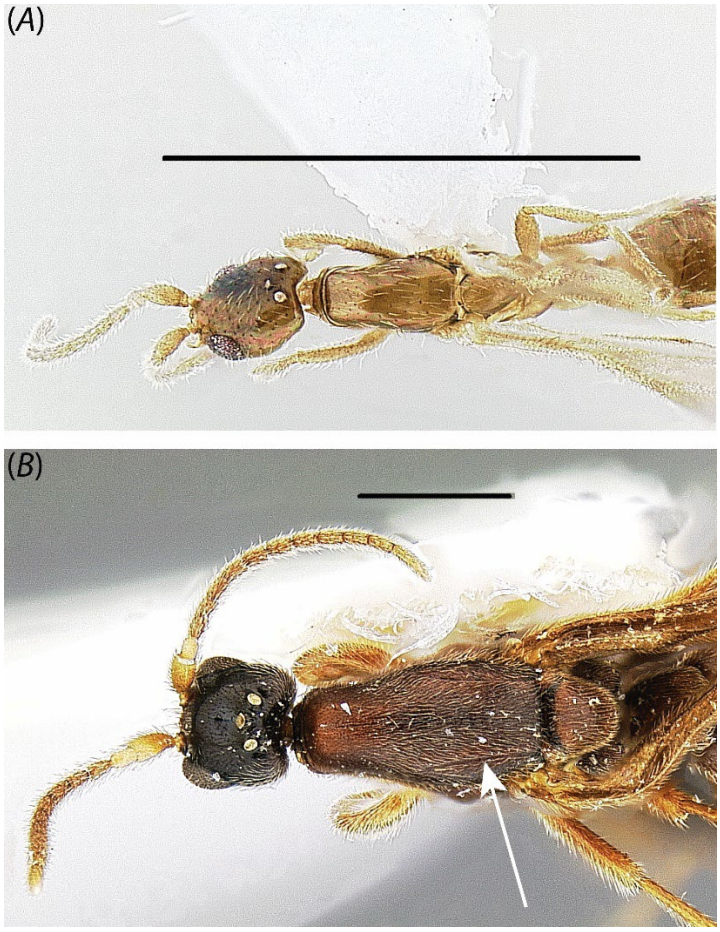

Figure 1.12. Dorsal view of (A) *Leptanilla* zhg-au01 (CASENT0758873; not sequenced in this study) and (B) *Leptanilla* zhg-my04 (CASENT0842558). Scale bars: A, 1 mm; B, 0.5 mm.

13. Oblique mesopleural sulcus adjoining posterior mesopectal margin. This character state is observed (1) in *O. hungvuong*, all Anomalomyrmini (Fig. 1.13*B*) and some *Leptanilla s.*

str. for which this character can be scored, except for *Leptanilla* GR01, -3, TH09, and *Leptanilla* zhg-bt01. Complete bisection of the mesopectus by the oblique mesopleural sulcus is seen in the Anomalomyrmini. The alternative character state (0) encompasses a morphocline from the near-complete loss of the oblique mesopleural sulcus (as in *Leptanilla* zhg-bt01) to the termination of this feature immediately anterior to the upper metapleuron (e.g. *Yavnella* TH02: Fig. 1.13*A*) or propodeum (as in the Bornean morphospecies-group). This character could not be scored in *Leptanilla* zhg-au02.

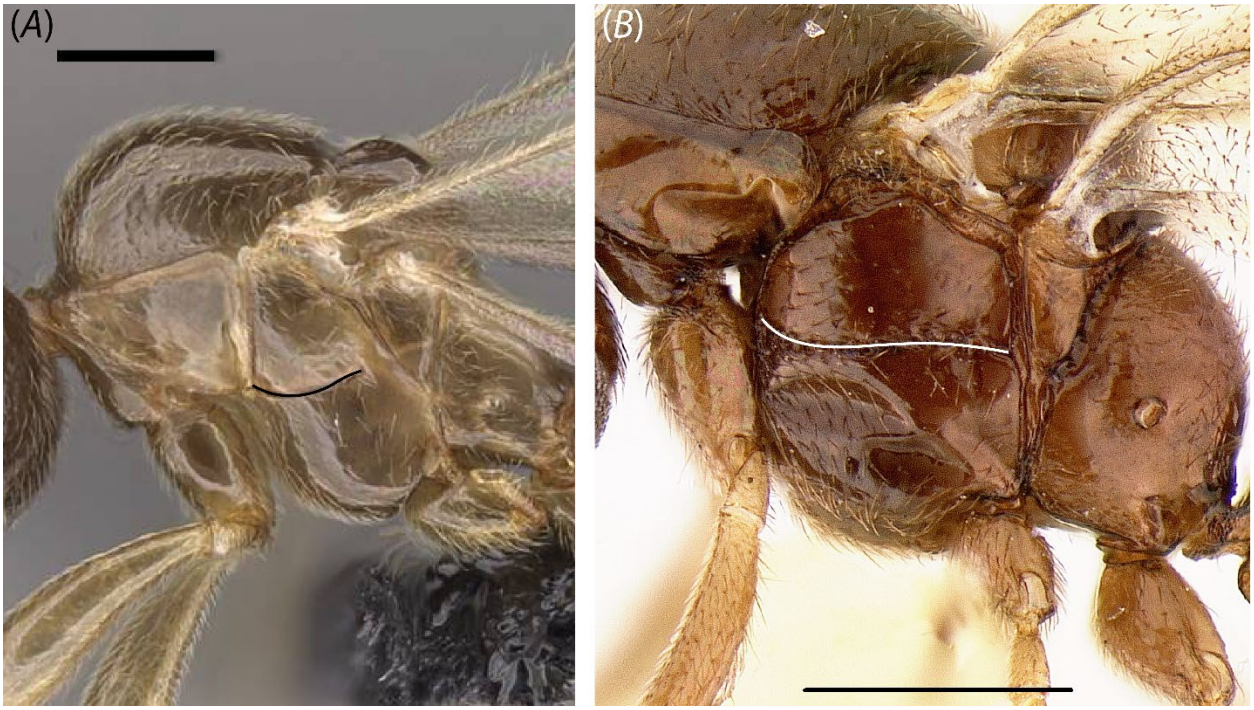

Figure 1.13. Profile view of mesosoma in (A) *Yavnella* TH02 (CASENT0119531; Michele Esposito) and (B) *Protanilla* zhg-vn01 (CASENT0842656). Scale bars: A, 0.2 mm; B, 0.3 mm.

14. Pterostigma present. This character state is observed (1) only in *M. heureka*, *O. hungvuong*, and the Anomalomyrmini (Fig. 1.14*B*). Rf and 2s-rs+Rs+4-6 are confluent in the Bornean morphospecies-group and in *Noonilla* zhg-my06, producing an infuscation of the wing membrane that resembles a pterostigma (0). No infuscation or pterostigma (0) is observed in all other terminals scored (Fig. 1.14*A*). Wings are lost in all available

specimens of *Noonilla* zhg-my02, *Leptanilla* zhg-th01, and *Leptanilla* GR03; therefore, this character could not be scored in these terminals.

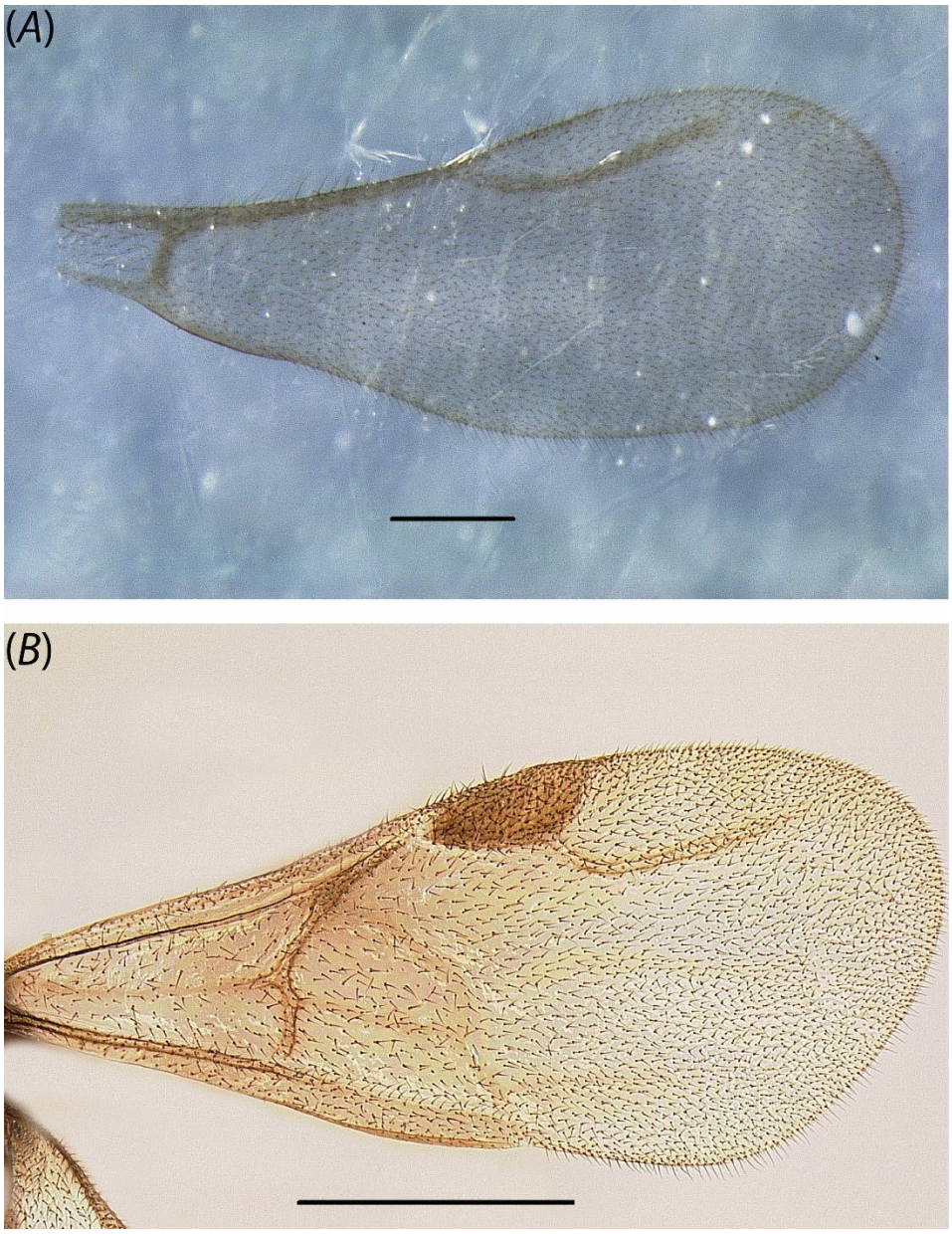

Figure 1.14. Forewing of (A) *Phaulomyrma javana* (MCZ:Ent:31142) and (B) *Protanilla* zhg-vn01 (CASENT0842613). Scale bars: A, 0.2 mm;B, 0.5 mm.

15. Mesoscutellum densely pubescent. The mesoscutellum is covered with sparse setae (0) in all leptanilline males sampled herein except for *Leptanilla* TH01 and zhg-th01, and the

Bornean morphospecies-group (Fig. 1.15*B*); in these cases, the mesoscutellar vestiture is densely pubescent (1) (Fig. 1.15*A*). This character could not be scored in *Yavnella* TH04.

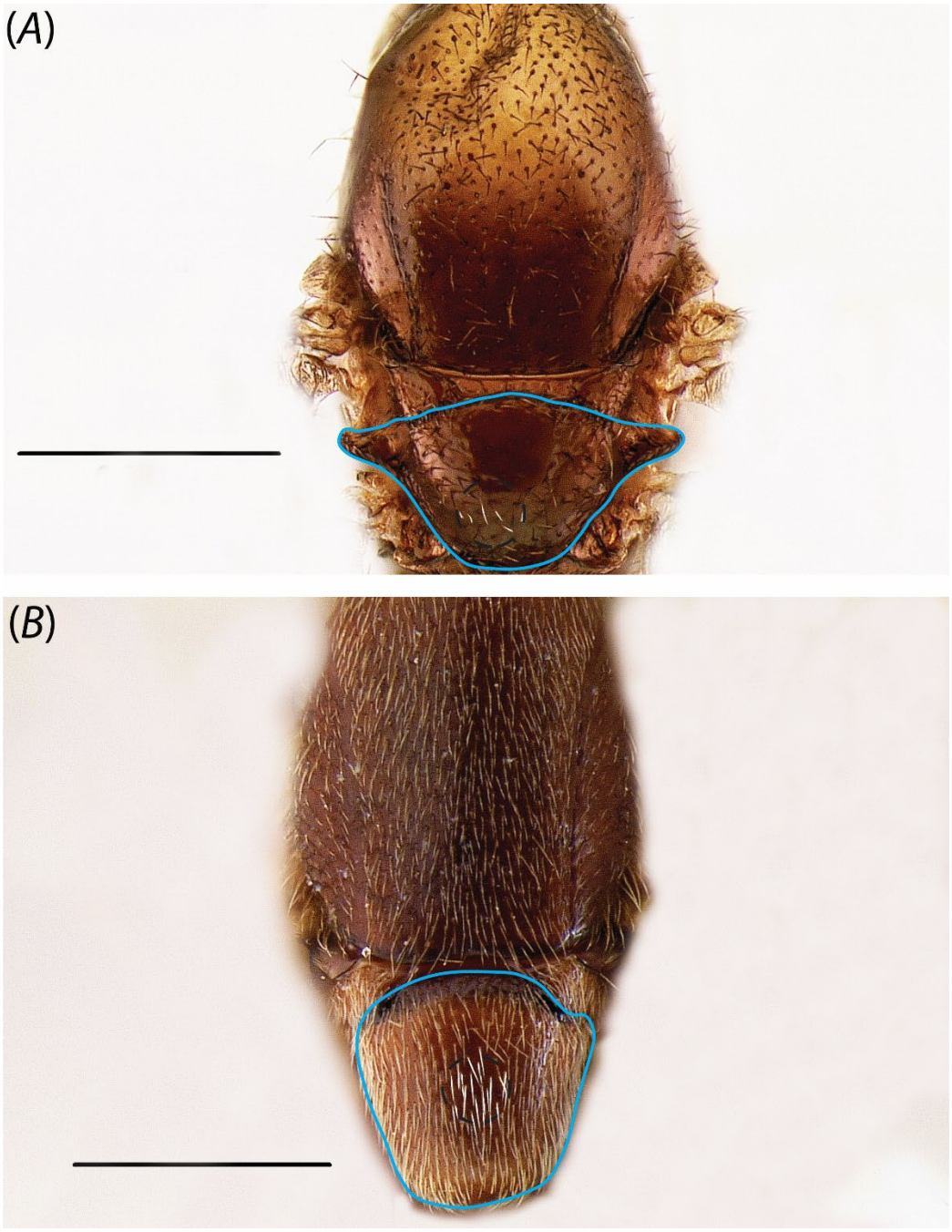

Figure 1.15. Dorsal view of mesosoma in (A) *Protanilla* zhg-vn01 (CASENT0842613) and (B) *Leptanilla* zhg-my04 (CASENT0842548). Scale bar: 0.3 mm

16. Mesoscutellar disc projecting posteriorly in profile view. This character state is observed (1) either as a dorsoventrally robust cuneiform process (*Leptanilla* TH01) or as a

recurved spine (*Leptanilla* zhg-th01) (Fig. 1.16*B*). Under the alternative character state, the posterior margin of the mesoscutellum is rounded (0) (Fig. 1.16*A*). This character could not be scored in *Yavnella* TH02.

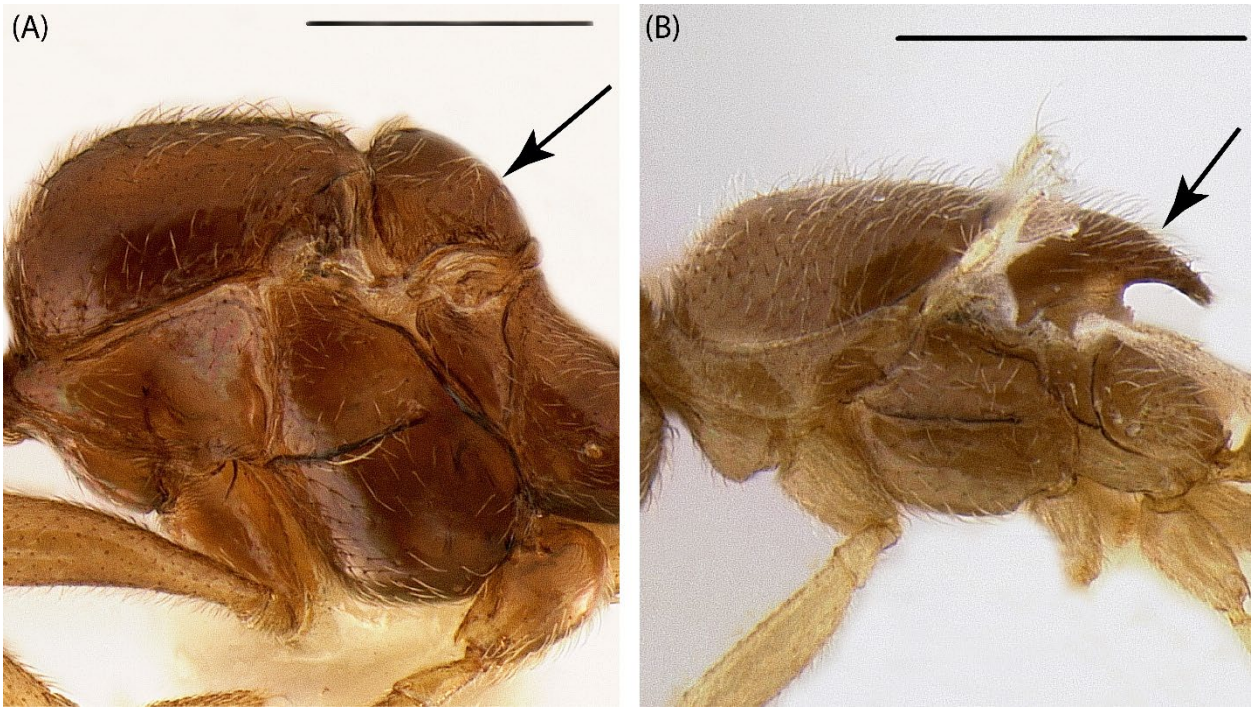

Figure 1.16. Presence (B: *Leptanilla* zhg-th01; CASENT0842619) versus absence (A: *Yavnella* zhg-th01; CASENT0842620) of the posterior prolongation of the mesoscutellum in male Leptanillini. Scale bar: 0.3 mm

17. Propodeum concave in profile view. This character state (1) (Fig. 1.17*A*) is an autapomorphy of *Yavnella s. l.* Under the alternative character state (0) the propodeum is convex in profile view (Fig. 1.17*C*) or produced into a right angle, with largely planar dorsal and posterior faces (the Bornean morphospecies-group: Fig. 1.17*B*).

Figure 1.17. Conditions of the propodeum in the Leptanilllinae. (A) Concave (*Yavnella* zhg-bt01; CASENT0106384); (B) convex with distinct dorsal face (*Leptanilla* zhg-my02; CASENT0106456); (C) convex without distinct dorsal face (*Protanilla lini* [OKENT0011097]; male described by Griebenow 2020) (not sequenced in this study).

18. Abdominal tergite II produced into distinct node. There is a shallow to pronounced dorsal node (Fig. 1.18*B*) present on the petiole (1) in *O. hungvuong*, *Protanilla* zhg-vn01 and TH01-2, *Yavnella* TH08, *Leptanilla* zhg-th01, the Bornean morphospecies-group, and *Leptanilla s. str*. except for *Leptanilla* zhg-au02. Under the alternative character state (0) the dorsal surface of the petiole is slightly convex (Fig. 1.18*A*), or planar without any supra-axial projection (as in *Leptanilla* zhg-au02).

Figure 1.18. Profile view of petiole in (A) *Yavnella* zhg-bt01 (CASENT0106384) and (B) *Protanilla lini* (OKENT0011097; male described by Griebenow 2020) (not sequenced in this study). Scale bars: A, 0.3 mm; B, 0.5 mm.

19. Abdominal sternite II with ventral process. A ventral rounded to angular process (1), shallow or well produced, is present on abdominal sternite II in *Protanilla* zhg-vn01 and

TH02, *Leptanilla* zhg-my02 (Fig. 1.19*C*) and -5, *Leptanilla s. str*. except for *Leptanilla* zhg-au02, and P. *javana*. Under the alternative character state (0) there is no ventrally projecting process on abdominal sternite II (Fig. 1.19*A*). A moderate ventral bulge without a distinct anterior face, posterior face or both, may be present under this character state (Fig. 1.19*B*). This character could not be scored in *Protanilla* TH01.

Figure 1.19. Profile view of petiole in (A) *Leptanilla* zhg-my04 (CASENT0842553), (B) *Yavnella* TH08 (CASENT0227555; Shannon Hartman) and (C) *Leptanilla* zhg-my02 (CASENT0106417). Scale bars: A, C, 0.5 mm; B, 0.2 mm.

20. Petiole higher than long including peduncle. This character state (Fig. 1.20*B*) is observed in profile view (1) in *Protanilla* zhg-vn01 and TH01-2, *Yavnella* cf. *indica*, MM01, TH05, and zhg-th01, *Leptanilla* TH01, the Bornean morphospecies-group, and *Noonilla*. This includes cases in which there is no distinct dorsal node. Under the alternative character state (0) the distance between two lines drawn tangential to the dorsal- and ventral-most points of the petiole in profile view is no greater than petiole length in profile view (Fig. 1.20*A*). This character could not be scored in *Yavnella* TH02.

Figure 1.20. Profile view of petiole in (A) *Yavnella* zhg-bt01 (CASENT0106384) and (B) *Protanilla lini* (OKENT0011097; male described by Griebenow 2020) (not sequenced in this study). Scale bars: A, 0.3 mm; B, 0.4 mm.

21. Cinctus present on abdominal segment III. The corollary of this character state (1) is the existence of a petiole (Fig. 1.21*B*), which has been secondarily lost (0) in *Yavnella* zhg-th01 (Fig. 1.21*A*), *Yavnella* TH02 (as noted by Boudinot 2015, p. 14), and *Noonilla* zhg-my02. There is a tendency towards petiolar reduction in *Yavnella s. l.* and *Noonilla*, but in many cases a cinctus on abdominal segment III is still discernible.

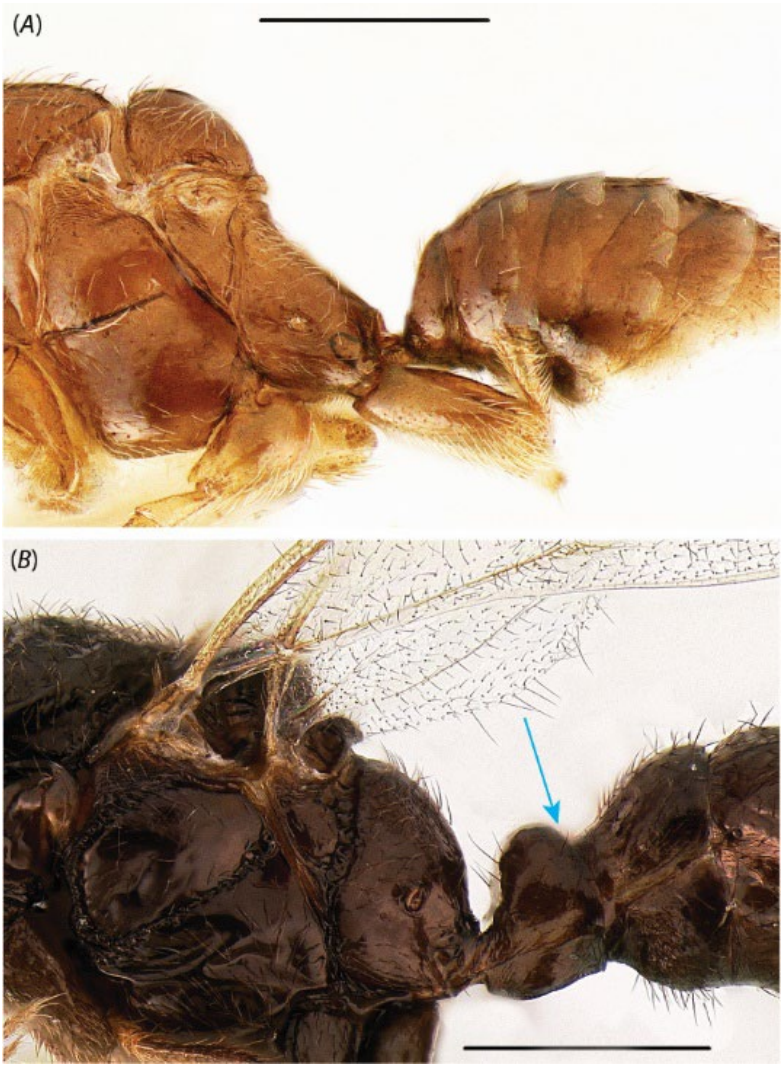

Figure 1.21. Profile view of petiole in (A) *Yavnella* zhg-th01 (CASENT0842620) and (B) *Protanilla lini* (OKENT0011097; male described by Griebenow 2020) (not sequenced in this study). Scale bars: A, 0.3 mm; B, 0.4 mm.

22. Cinctus present on abdominal segment IV. The corollary of this character state (1) is the presence of a postpetiole. This character state is unique to *Protanilla* TH03 (Fig. 1.22*B*),

although the anterior margin of abdominal segment IV may be slightly constricted relative to more posterior abdominal segments (0); otherwise, there is no constriction whatsoever (Fig. 1.22*A*).

Figure 1.21. Profile view of petiole in (A) *Yavnella* zhg-th01 (CASENT0842620) and (B) *Protanilla lini* (OKENT0011097; male described by Griebenow 2020) (not sequenced in this study). Scale bars: A, 0.3 mm; B, 0.4 mm.

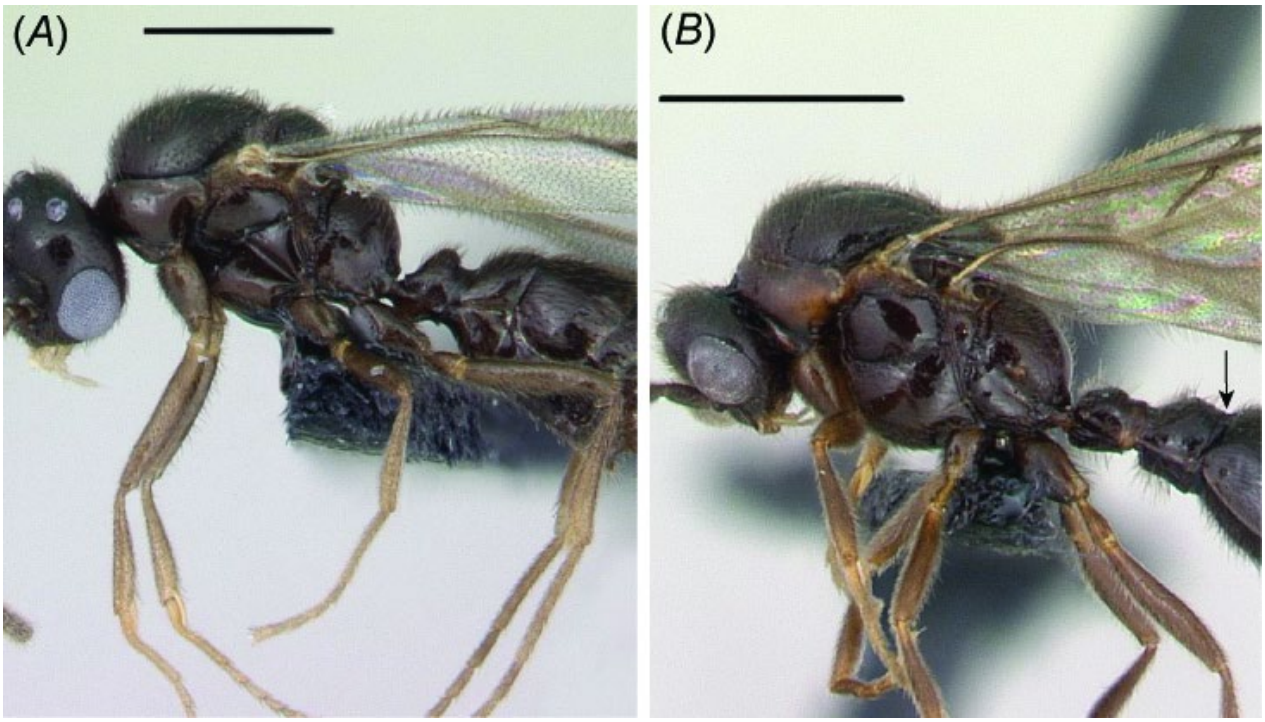

Figure 1.22. Profile view of (A) *Protanilla* TH02 (CASENT0128922; Erin Prado) and (B) *Protanilla* TH03 (CASENT0119791; Erin Prado). Scale bars: A, 0.5 mm; B, 1 mm.

23. Abdominal sternite IX with posteromedian filiform process. Illustration of this character state is unavailable on account of COVID-19. Although a posteromedian process of abdominal sternite IX is present in all male Anomalomyrmini and *O. hungvuong* (0), its filiform condition (1) is unique to *Yavnella* TH03. Abdominal sternite IX is not thus produced medially in all other male leptanillines sampled herein (0).

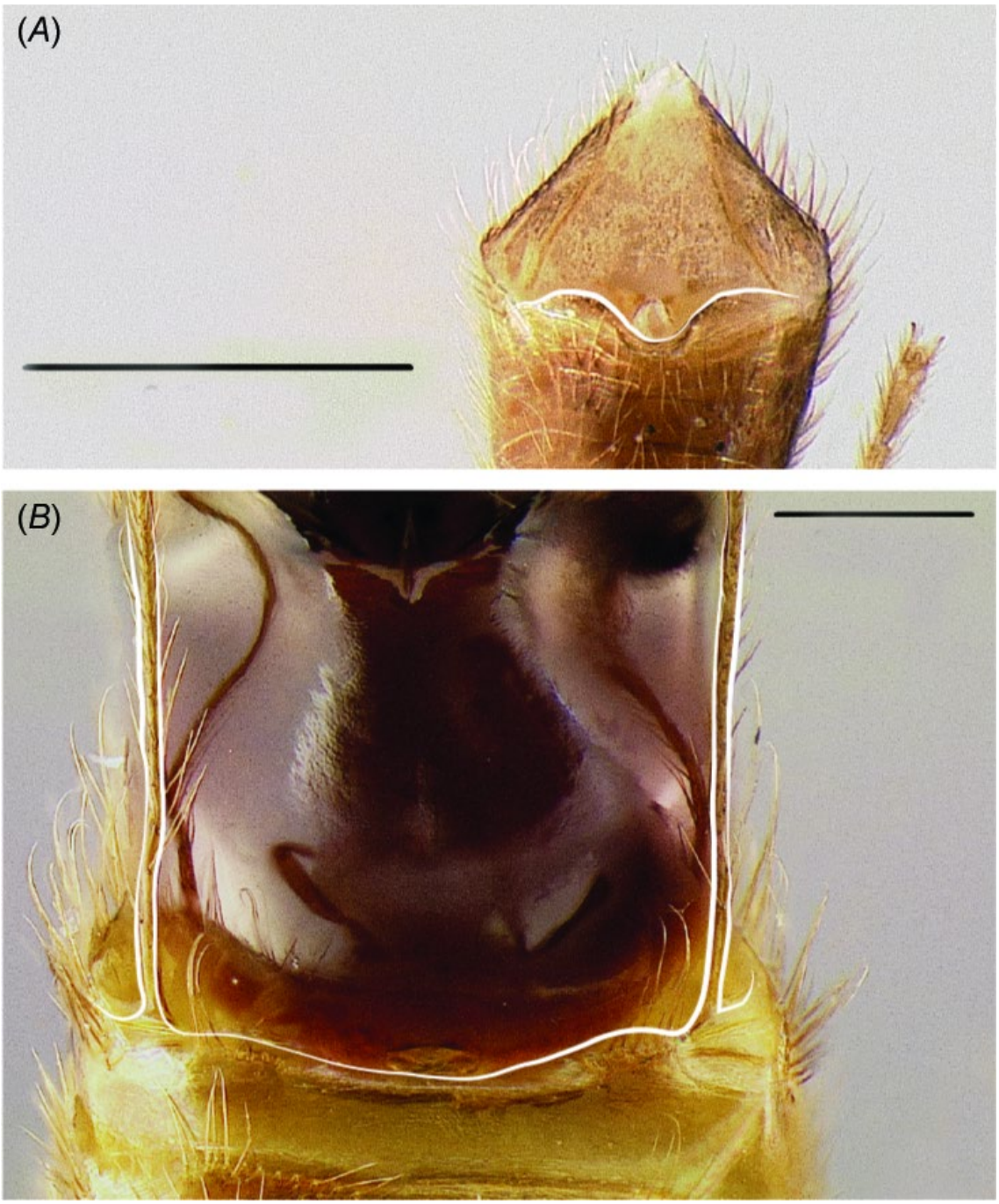

Figure 2.23. Ventral view ofabdominal sternite IX in (A) *Leptanilla* zhg-th01 (CASENT0842619) and (B) *Leptanilla* zhg-my04 (CASENT0842553). Scale bars: A, 0.3 mm; B, 0.2 mm.

24. Abdominal sternite IX with posterolateral filiform processes. These ‘bizarre, elongate, filamentous extensions’ of the metasoma were noted by Boudinot (2015, fig. 10D) as being extensions of the gonocoxae *sensu* Boudinot (2018). Detailed examination

demonstrates that these processes are in fact extensions of abdominal sternite IX (Fig. 1.23*B*). This character state is unique to the Bornean morphospecies-group. Under the alternative character state (0) the posterior margin of abdominal sternite IX may be medially indented (Fig. 1.23*A*), entire, or with a posteromedian process, as noted above. This character could not be scored in *Leptanilla* zhg-au02.

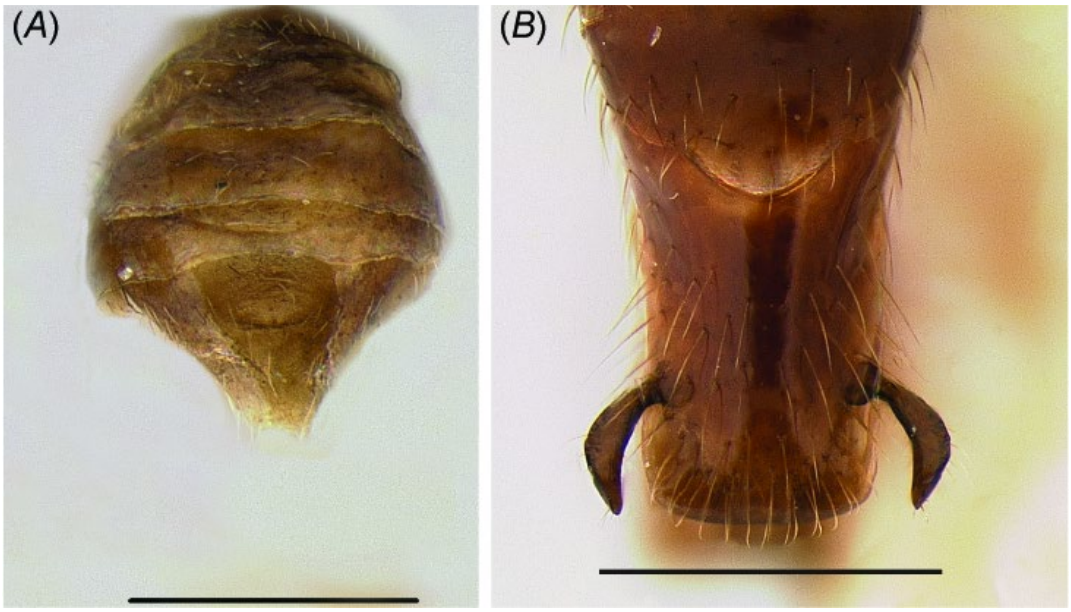

Figure 1.24. Posterior view of abdominal tergite VIII in male Leptanillini. (A) *Yavnella* zhg-th01 (CASENT0842620) and (B) *Noonilla* zhg-my02 (CASENT0842592). Scale bar: 0.3 mm.

25. Abdominal tergite XIII [sic!] broader than long. This character state is observed (1) in all male Leptanillinae scored (Fig. 1.24*A*) except for *Noonilla*, to which elongation of abdominal tergite XIII [sic!] (0) is unique (Fig. 1.24*B*). This character could not be scored in *Yavnella* MM01 and *P. javana*.

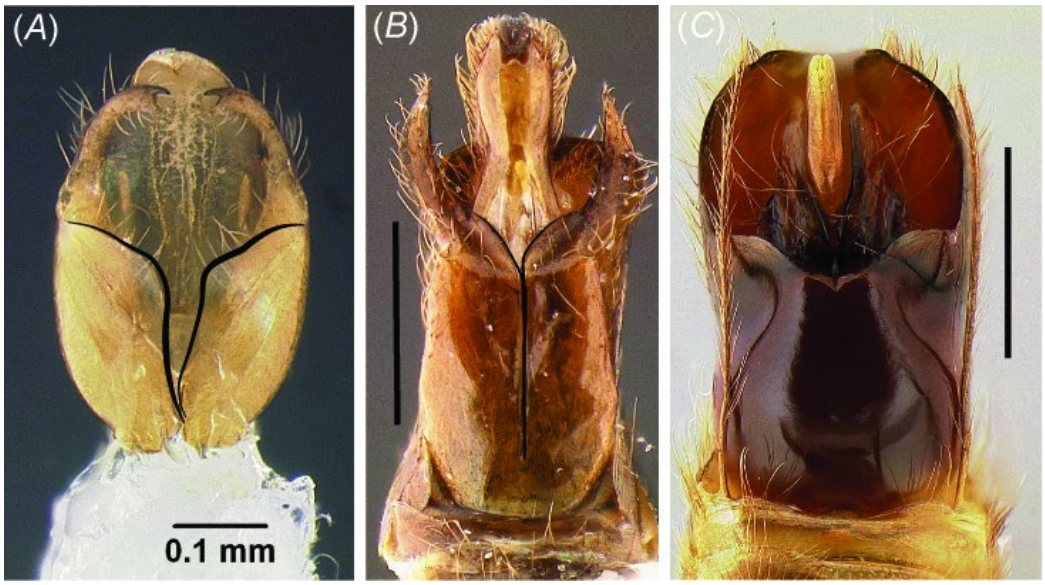

Figure 1.25. Ventral view of male genitalia across the Leptanillini. (A) *Leptanilla* ZA01 (CASENT0106354), (B) *Noonilla* zhg-my02 (CASENT0842595); (C) *Leptanilla* zhg-my04 (CASENT0842553). Scale bars: A, 0.1 mm; B, 0.3 mm; C, 0.5 mm.

26. Gonocoxae ventromedially fused along entire length. This character state (Fig. 1.25*C*) is observed in *O. hungvuong*, *Yavnella* TH03, and in all terminals within the Bornean morphospecies-group that could be scored (1). The alternative character state (0) encompasses partial (Fig. 1.25*B*) to complete (Fig. 1.25*A*) ventromedian separation of the gonocoxae. This character could not be scored in *Protanilla* TH01, *Yavnella* MM01, *Leptanilla* TH01, *Leptanilla* (Bornean morphospecies-group) zhg-my05, and *P. javana*.

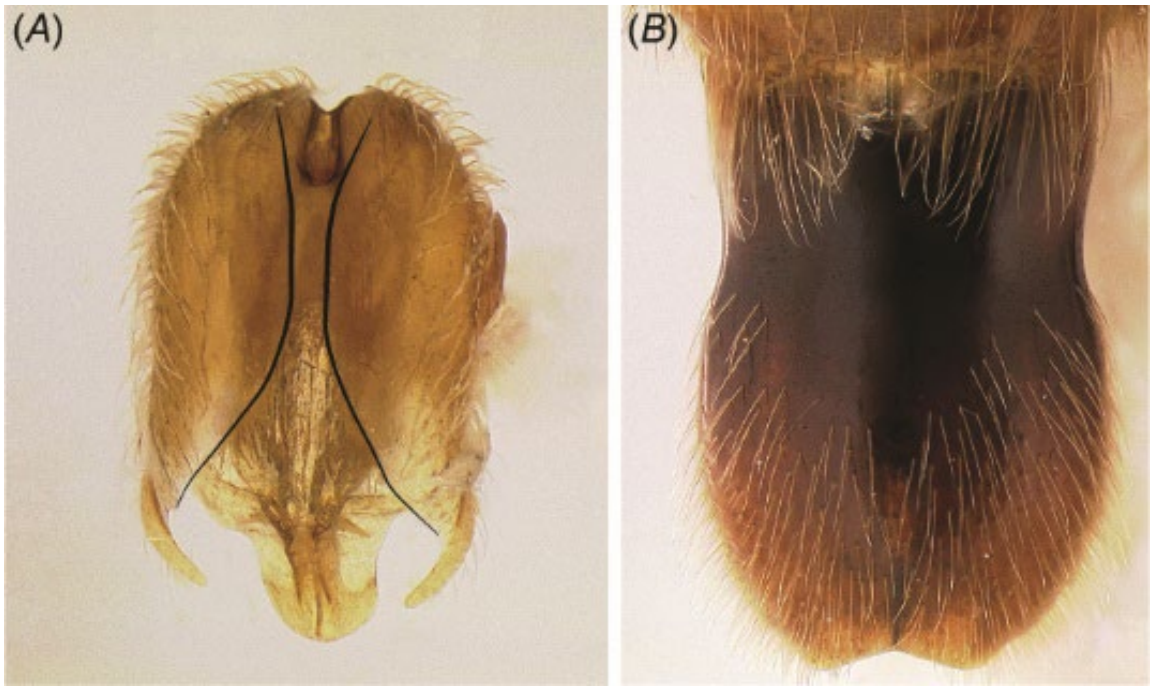

Figure 1.26. Dorsal view of genitalia in (A) *Yavnella* zhg-th01 (CASENT0842620) and (B) *Leptanilla* zhg-my04 (CASENT0842565). Scale bars: A, 0.3 mm; B, 0.4 mm.

27. Gonocoxae dorsomedially fused along entire length. This character state is observed (1) in *O. hungvuong*, *Yavnella* TH03 and the Bornean morphospecies-group (Fig. 1.26*B*). Under the alternative character state (0) the gonocoxae are fully (Fig. 1.26*A*) to partly separate medially. This character could not be scored without dissection in *Noonilla* (in which abdominal tergite XIII [sic!] conceals the gonocoxal dorsum) or in *Leptanilla* zhg-au02, -bt01, and ZA01; and *P. javana*.

Figure 1.27. Ventral view of genitalia (A) *Protanilla lini* (OKENT0018456; male described by Griebenow 2020) (not sequenced in this study) and (B) *Leptanilla* ZA01 (CASENT0106354). Scale bars: A, 0.3 mm; B, 0.1 mm.

28. Gonocoxa with ventromesal lamina. A ventromesal laminate margin, variably produced and shaped, is present (1) on the gonocoxa (Fig. 1.27*B*), or on the basal part of the gonopodite in those cases in which the gonocoxa and stylus are insensibly fused, in *Yavnella* cf. *indica*; *Leptanilla* zhg-th01; *Leptanilla* (Bornean morphospecies-group) zhg-

my02 and -5; and *Leptanilla* TH09, GR01-2, ZA01 (Fig. 1.27*B*), and zhg-au02. Under the alternative character state (0) no lamina is discernible whatsoever on the gonocoxa (Fig. 1.27*A*). Primary homology *sensu* de Pinna (1991) of the gonopodital lamina in *Leptanilla* zhg-my02 and -5 with the stylus is not stipulated, since this does not meet the criterion of conjunction (Patterson 1982; de Pinna 1991) in CASENT0178838 (Griebenow 2020, fig. 3), a heterospecific member of the Bornean morphospecies-group (misattributed to *Protanilla* by Boudinot 2015). This character could not be scored in *Protanilla* TH01, *Leptanilla* zhg-bt01, or P. *javana*.

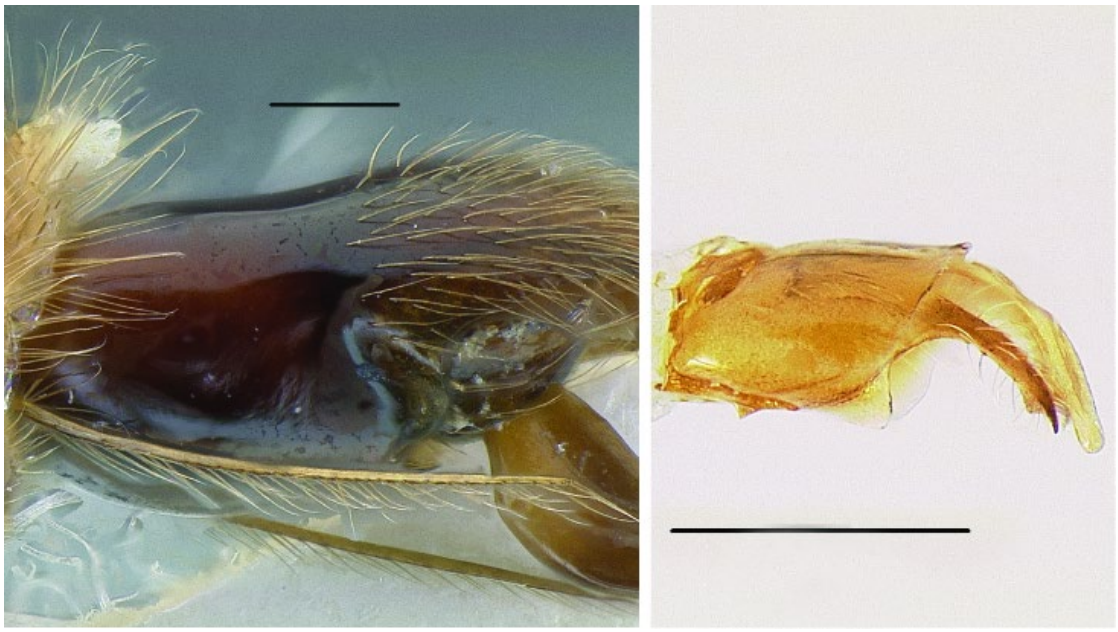

Figure 1.28. Profile view of genitalia in (A) *Leptanilla* zhg-my04 (CASENT0842558) and (B) *Leptanilla* ZA01 (CASENT0106354). Scale bars: A, 0.2 mm; B, 0.3 mm.

29. Stylus articulated to gonocoxa. This character state (1) includes cases in which the stylus is sharply deflexed relative to the gonocoxa (Fig. 1.28*B*) or a conjunctiva is visible between the gonopodital sclerites. Under the alternative character state (0) a suture might be visible (as in many *Yavnella s. l.*) or the gonocoxa and stylus insensibly fused (as in the Bornean morphospecies-group: Fig. 1.28*A*). Gonopodital articulation is fully present

in *O. hungvuong*, *Protanilla* zhg-vn01, *Yavnella* zhg-bt01, *Leptanilla* zhg-th01, all *Leptanilla s. str*. for which this character can be scored and both *Noonilla* included in this study. This character could not be scored in *Leptanilla* zhg-bt01.

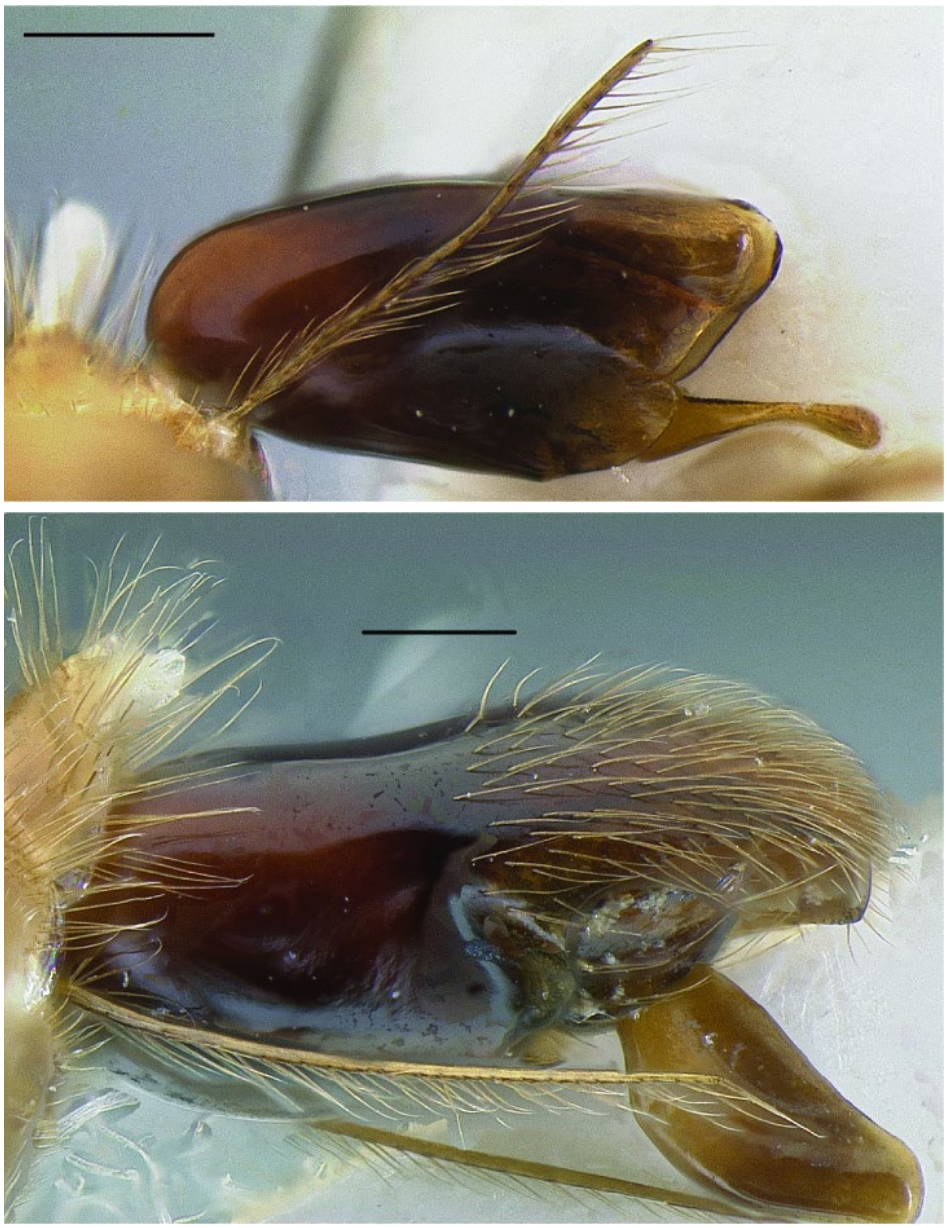

Figure 1.29. Profile view of genitalia in (A) *Leptanilla* zhg-my03 (CASENT0842545) and (B) *Leptanilla* zhg-my04 (CASENT0842558). Scale bar: 0.2 mm.

30. Gonopodital apex with vestiture. This character and the next are so termed in order to encompass cases in which the stylus is insensibly fused to the gonocoxa (Fig. 1.28*A*,

1.29*A*, *B*). The only terminals sampled here in which no vestiture is present on the gonopodital apex (0) are the Bornean morphospecies-group (Fig. 1.29*A*) except for *Leptanilla* zhg-my04. Otherwise (1) there are at least some setae present on the gonopodital apex (Fig. 1.29*B*). This character could not be scored in *Leptanilla* zhg-bt01.

31. Gonopodital apex bifurcated. This character state is observed (1) only in *Yavnella* TH08 (Fig. 1.30*B*), *Leptanilla* ZA01 and GR02. Under the alternative character state (0) the stylus may be entire (Fig. 1.30*A*) or may have a subapical tooth. This character could not be scored in *Leptanilla* zhg-bt01.

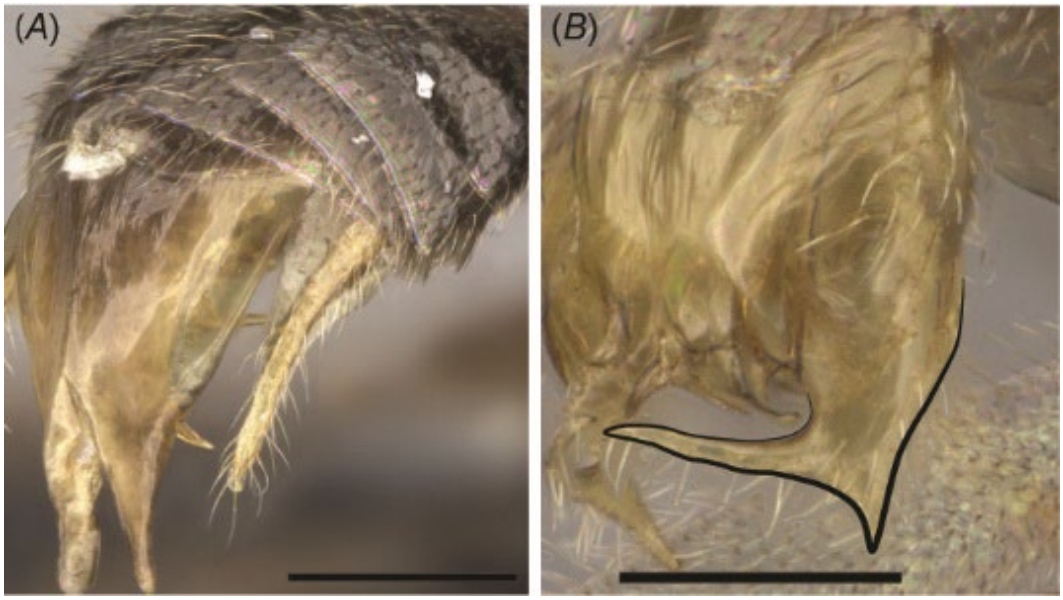

Figure 1.30. Profile view of genitalia in (A) *Leptanilla* zhg-my03 (CASENT0842545) and (B) *Leptanilla* zhg-my04 (CASENT0842558). Scale bar: 0.2 mm.

32. Penial sclerites enclosed dorsally by gonopodites at base. In this character state (1) the gonopodites may completely enclose (Fig. 1.31*C*) or partially overlap with (Fig. 1.31*B*) the penial sclerites. This character state is observed in *M. heureka*, *Yavnella* TH03, zhg-th01 and zhg-bt01, the Bornean morphospecies-group, and *Leptanilla* zhg-au02. Under the alternative character state (Fig. 1.31*A*) (0), the penial sclerites are never dorsally

surmounted by any portion of the gonopodites. This character could not be scored in *Noonilla* zhg-my06 and *P. javana*.

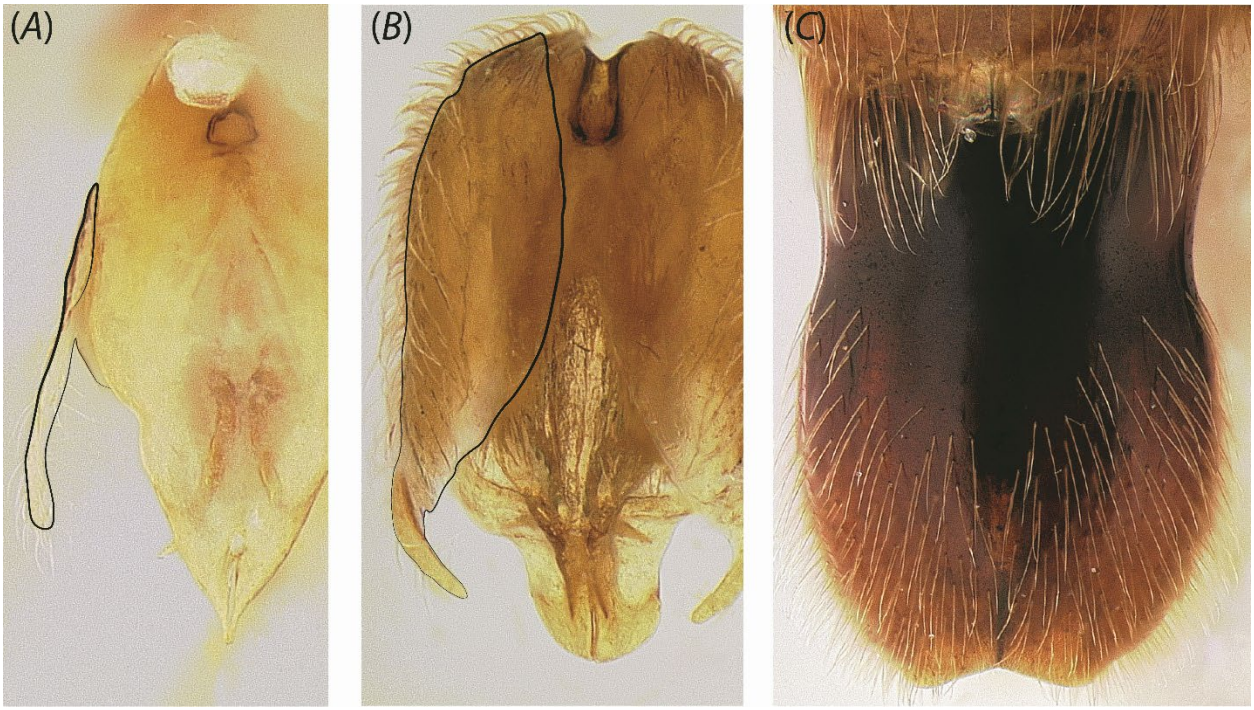

Figure 1.31. Posterior view of genitalia in (A) *Yavnella* cf. *indica* (CASENT0106378), (B) *Yavnella* zhg-th01 (CASENT0842620) and (C) *Leptanilla* zhg-my04 (CASENT0842565). Scale bar: 0.3 mm.

33. Penial sclerites dorsally recurved at base in profile view. Among the terminals sampled here, this bizarre character state (1) is present only in *Leptanilla* (Bornean morphospecies-group) zhg-my02 and -5 (Fig. 1.32*B*). In these morphospecies the penial sclerites are curved at the base so that in preserved specimens the apex is situated dorsally of the gonocoxae. Otherwise (0) in profile view the penial sclerites are slightly curved at the base towards the venter of the genital anteroposterior axis (Fig. 1.32*A*) or are parallel to that axis.

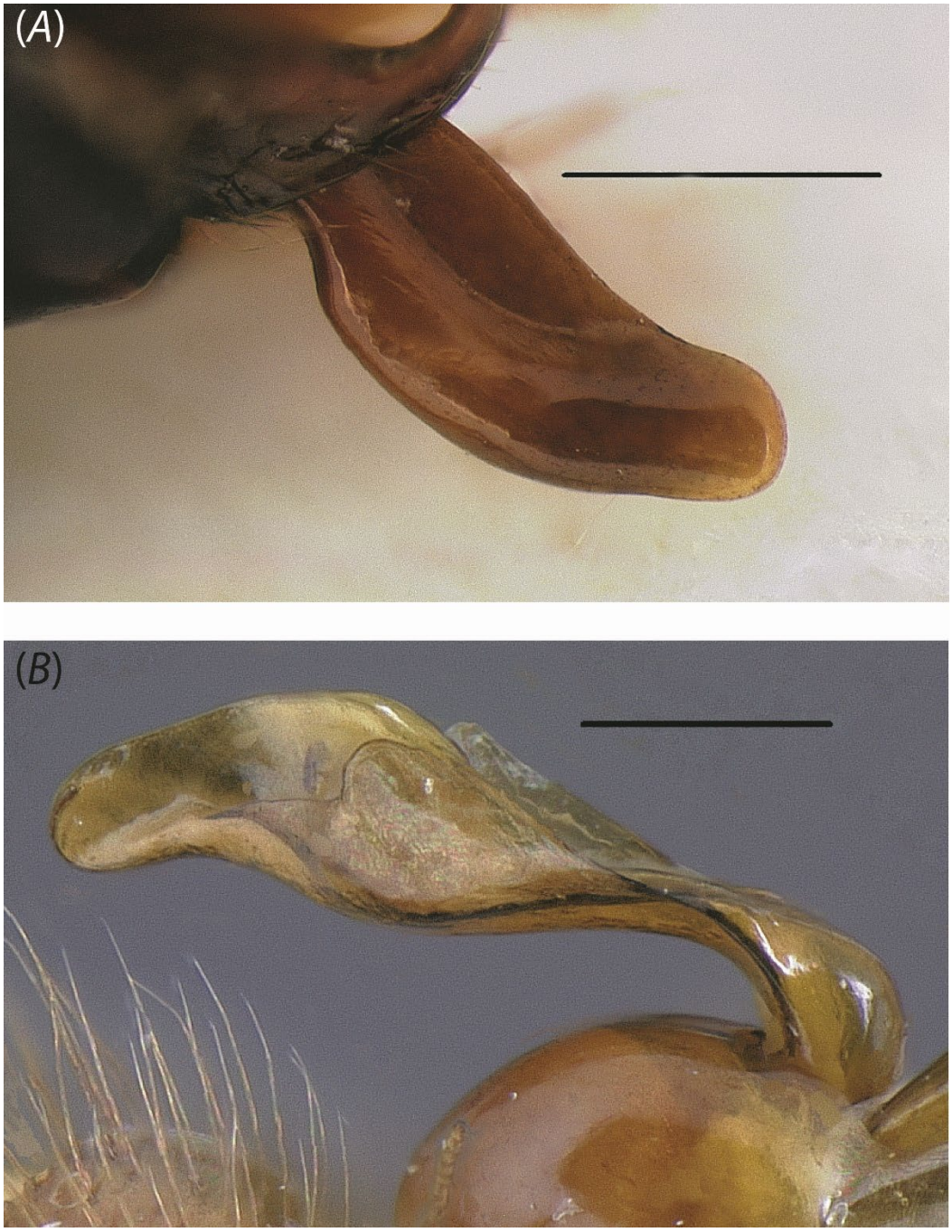

Figure 1.32. Profile view of penial sclerites in (A) *Leptanilla* zhg-my04 (CASENT0842550) and (B) *Leptanilla* zhg-my05 (CASENT0842571). Scale bars: A, 0.3 mm; B, 0.2 mm.

34. Penial sclerites dorsoventrally compressed at base. This character state is observed (1) in *M. heureka*, and all *Yavnella s. l.* (Fig. 1.33*B*) and *Leptanilla s. str*. for which this character can be scored. Under the alternative character state (0) the penial sclerites are basally wider along the dorsoventral axis, exclusive of any ventromedian processes, than

along the lateromedial axis (Fig. 1.33*A*). This character could not be scored in *O. hungvuong*, *Protanilla* TH02-3, *Yavnella* TH03-4 and zhg-bt01, *Leptanilla* TH01, *Noonilla* zhg-my06, and *P. javana*.

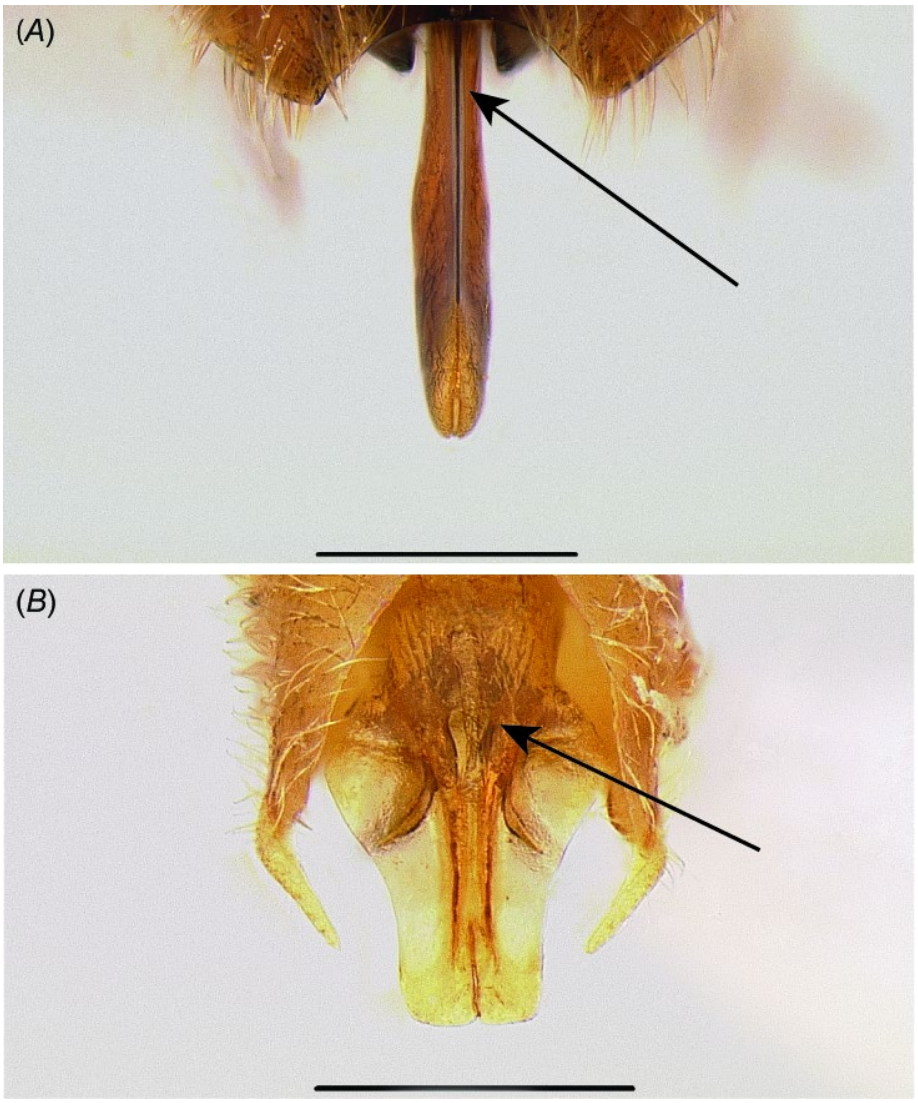

Figure 1.33. Posterior view of penial sclerites in (A) *Leptanilla* zhg-my04 (CASENT0842553) and (B) *Yavnella* zhg-th01 (CASENT0842620). Scale bar: 0.3 mm.

35. Penial sclerites dorsoventrally compressed at apex. This character state is observed (1) in *M. heureka*, *Yavnella s. l.* except for *Yavnella* TH03, *Leptanilla s. str.*, and *Leptanilla* zhg-my03 (Fig. 1.34*B*). Under the alternative character state (0) the penial sclerites are apically wider along the dorsoventral axis, exclusive of any ventromedian processes, than

along the lateromedial axis (Fig. 1.34*A*). The alternative character state (0) encompasses cases in which the penial sclerites are lateromedially compressed to varying extents (e.g. Anomalomyrmini) or are subcircular in cross-section (e.g. *Noonilla*). This character could not be scored in *O. hungvuong* or *Protanilla* TH02.

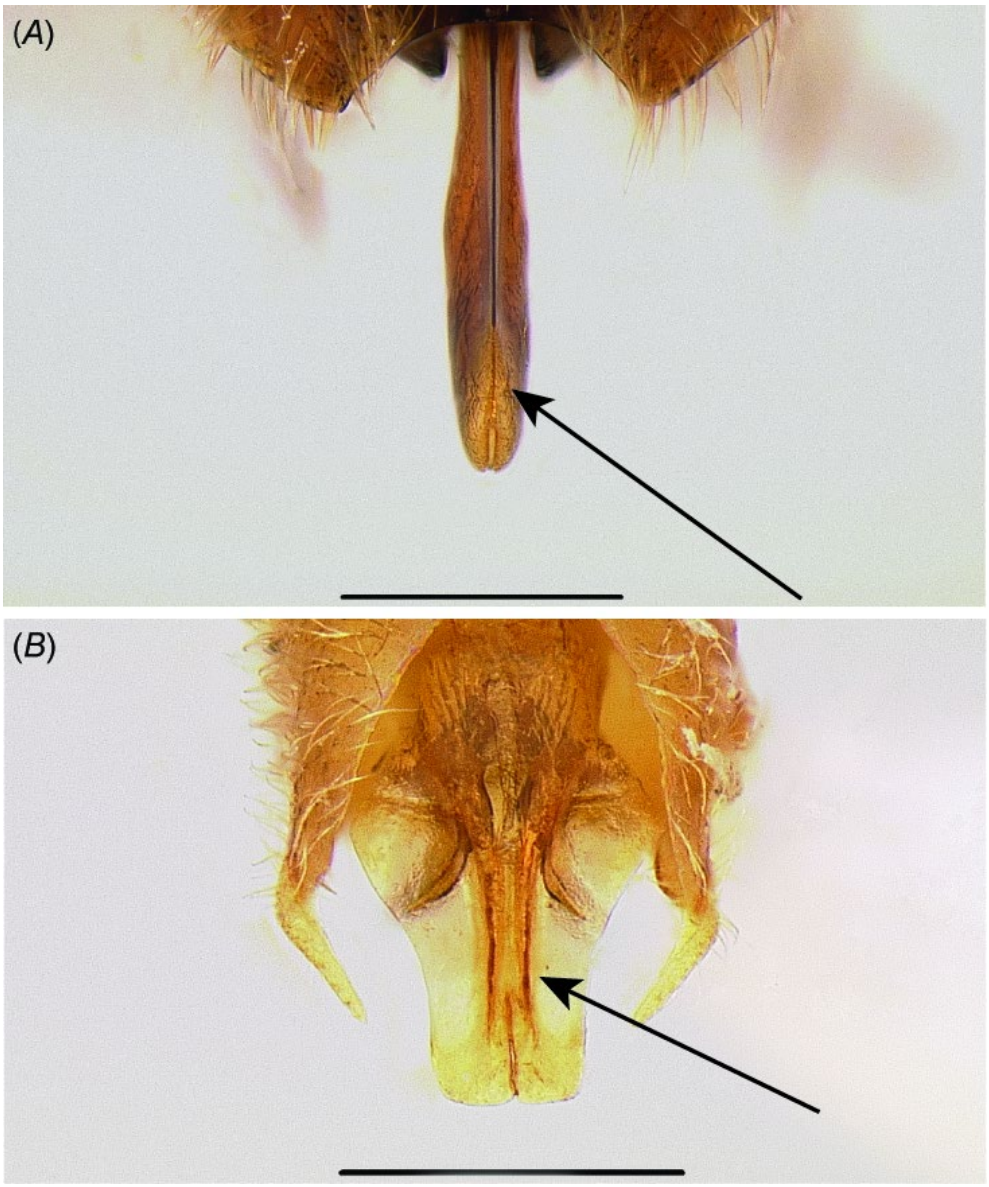

Figure 1.34. Posterior view of penial sclerites in (A) *Leptanilla* zhg-my04 (CASENT0842553) and (B) *Yavnella* zhg-th01 (CASENT0842620). Scale bar: 0.3 mm.

36. Lateral margins of penial sclerites laminate. This character state is observed (1) in *Yavnella* cf. *indica*, *Yavnella argamani*, TH02-5, MM01, and zhg-th01; *Leptanilla*

(Bornean morphospecies-group) zhg-my02 and -5; and all *Leptanilla s. str*. (Fig. 1.35*B*) for which this character can be scored, except for *Leptanilla* zhg-bt01. In the Bornean morphospecies-group the lateral laminae, when present, are strongly produced ventrally relative to the remainder of the penial sclerites. Under the alternative character state (0) (Fig. 1.35*A*) lateral flanges may be present or absent, but when present are not laminate. This character could not be scored in *M. heureka* and *Leptanilla* zhg-au02.

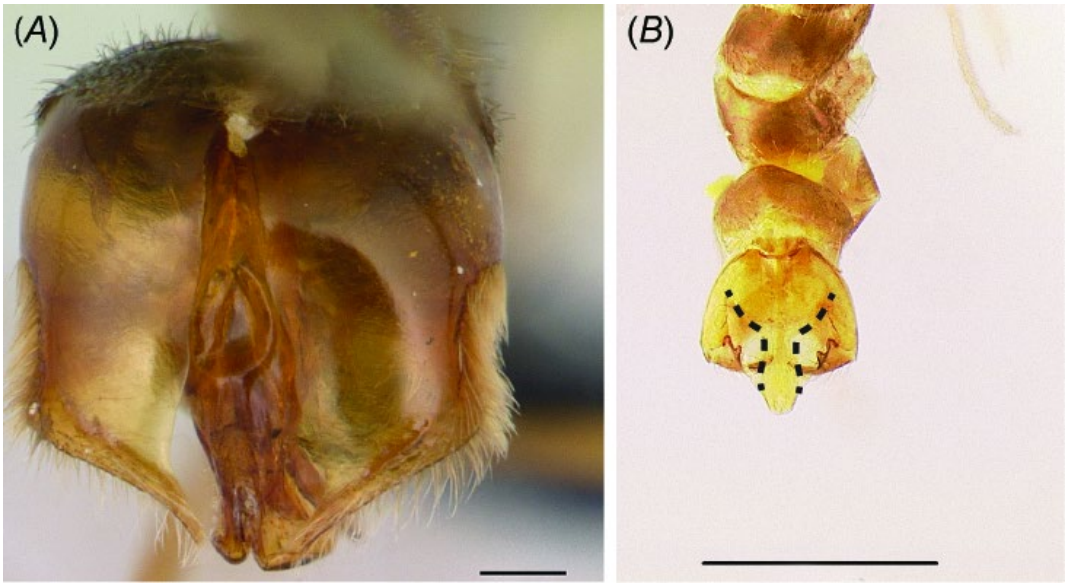

Figure 1.35. Posterior view of penial sclerites in (A) *Yavnella* TH06 (CASENT0129609; Erin Prado) and (B) *Leptanilla* GR02 (CASENT0106068). Scale bars: A, 0.1 mm; B, 0.3 mm.

37. Penial sclerites with dorsomedian carina. This character state is observed (1) only in *Leptanilla* TH01 and *Leptanilla* (Bornean morphospecies-group) zhg-my04 (Fig. 1.36*B*). In both cases the penial sclerites are strongly lateromedially compressed. Under the alternative character state (0) there is no dorsomedian penial carina, such that the dorsum of the penial sclerite(s) is or are rounded in cross-section (Fig. 1.36*A*). This character could not be scored in *Protanilla* TH03.

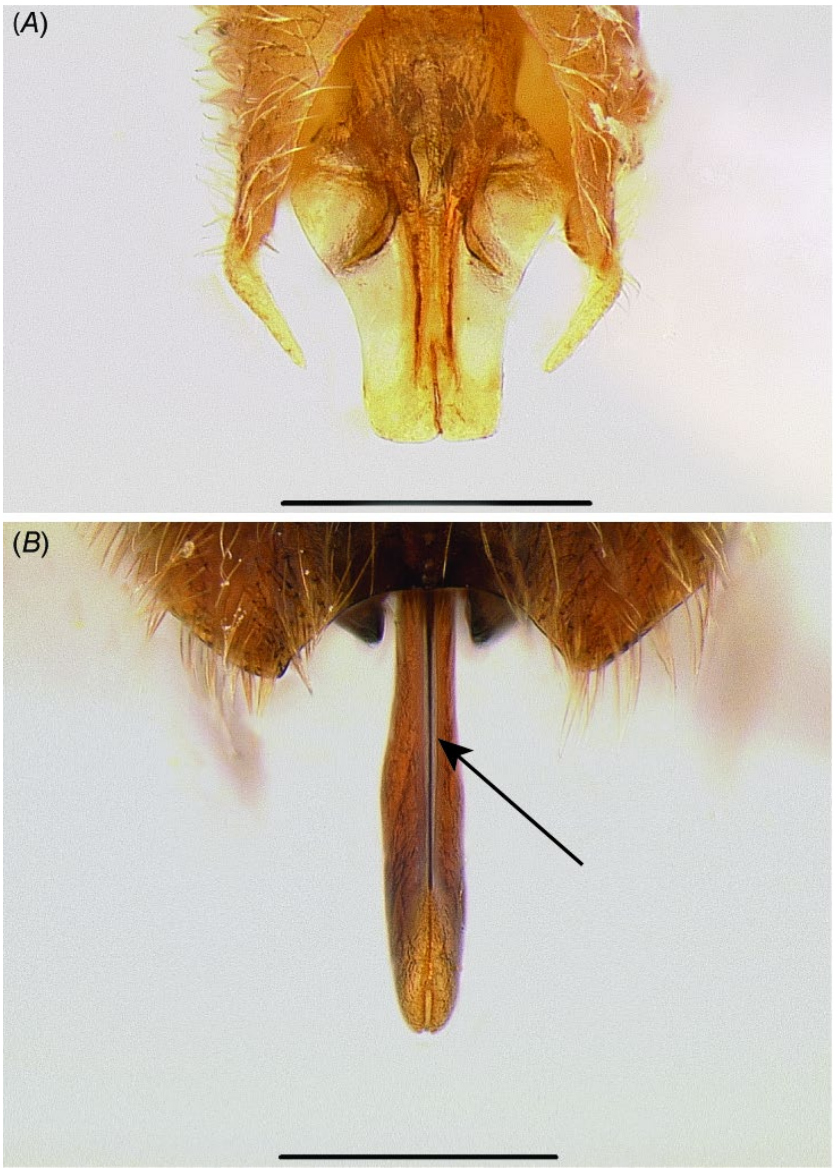

Figure 1.36. Dorsoventral (A) (*Yavnella* zhg-th01; CASENT0842620) versus lateromedial (B) (*Leptanilla* zhg-my04; CASENT0842553) compression of the penial sclerites in posterodorsal view. Dorsomedian carina marked with arrow. Scale bar: 0.3 mm.

38. Penial sclerites with ventromedian projection. This character state is observed (1) in *Leptanilla* zhg-my02 and zhg-my05; *Leptanilla* zhg-th01; and *Leptanilla* zhg-bt01, GR01-2, and zhg-au02. When present and discernible, the volsellae flank this projection, which can be rounded (as in *Leptanilla* zhg-my05: Fig. 1.37*B*) or carinate. Under the alternative character state (0) the penial sclerites are entirely separated, or if fused then lacking any ventromedian process (Fig. 1.37*A*). This character could not be scored in *M.*

heureka, the Anomalomyrmini, *Leptanilla* TH01 and *Yavnella* TH03-8 and *Yavnella* MM01.

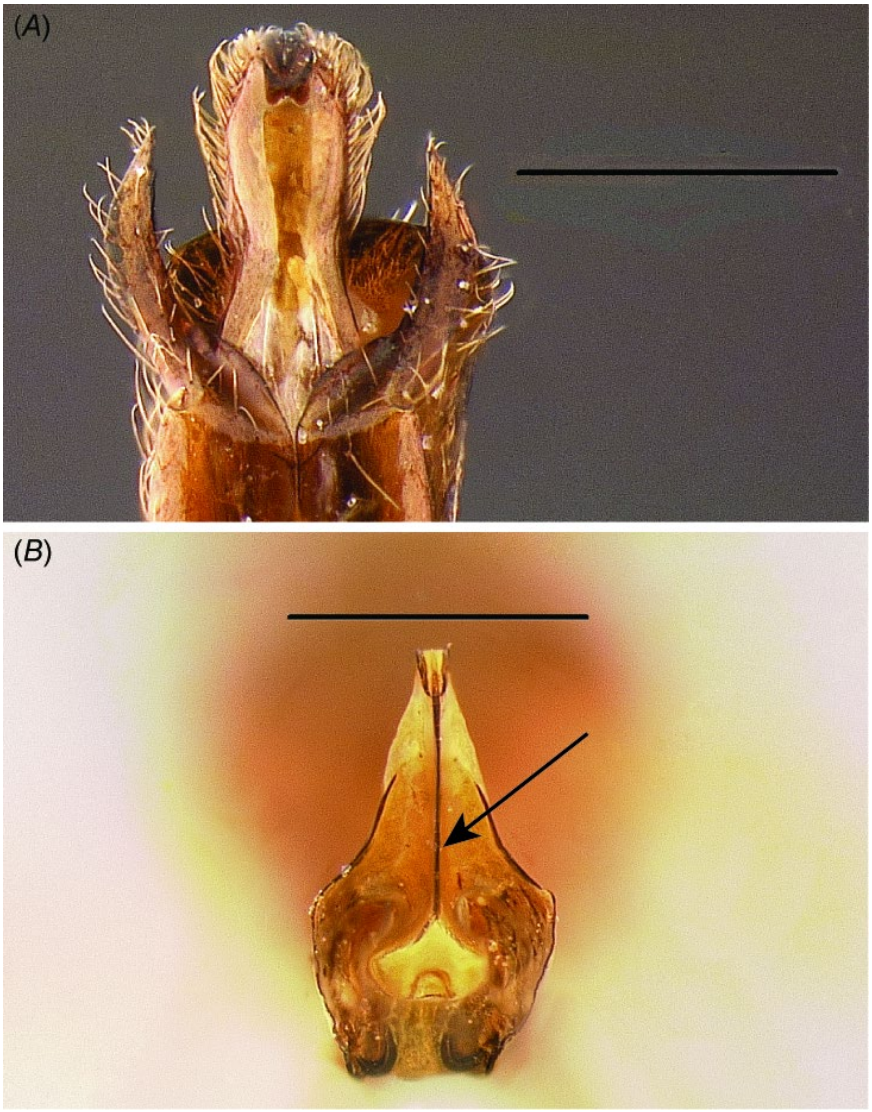

Figure 1.37. Posteroventral view of penial sclerites in (A) *Noonilla* zhg-my02 (CASENT0842595) and (B) *Leptanilla* zhg-my02 (CASENT0106432). Scale bar: 0.3 mm.

39. Phallotreme flanked with vestiture. This character state (1) occurs only in *Noonilla* (Fig. 1.38*B*). Under the alternative character state (0) the phallotremal rim is visibly bare of any setae (Fig. 1.38*A*). This character could not be scored in *P. javana* or *Yavnella* MM01.

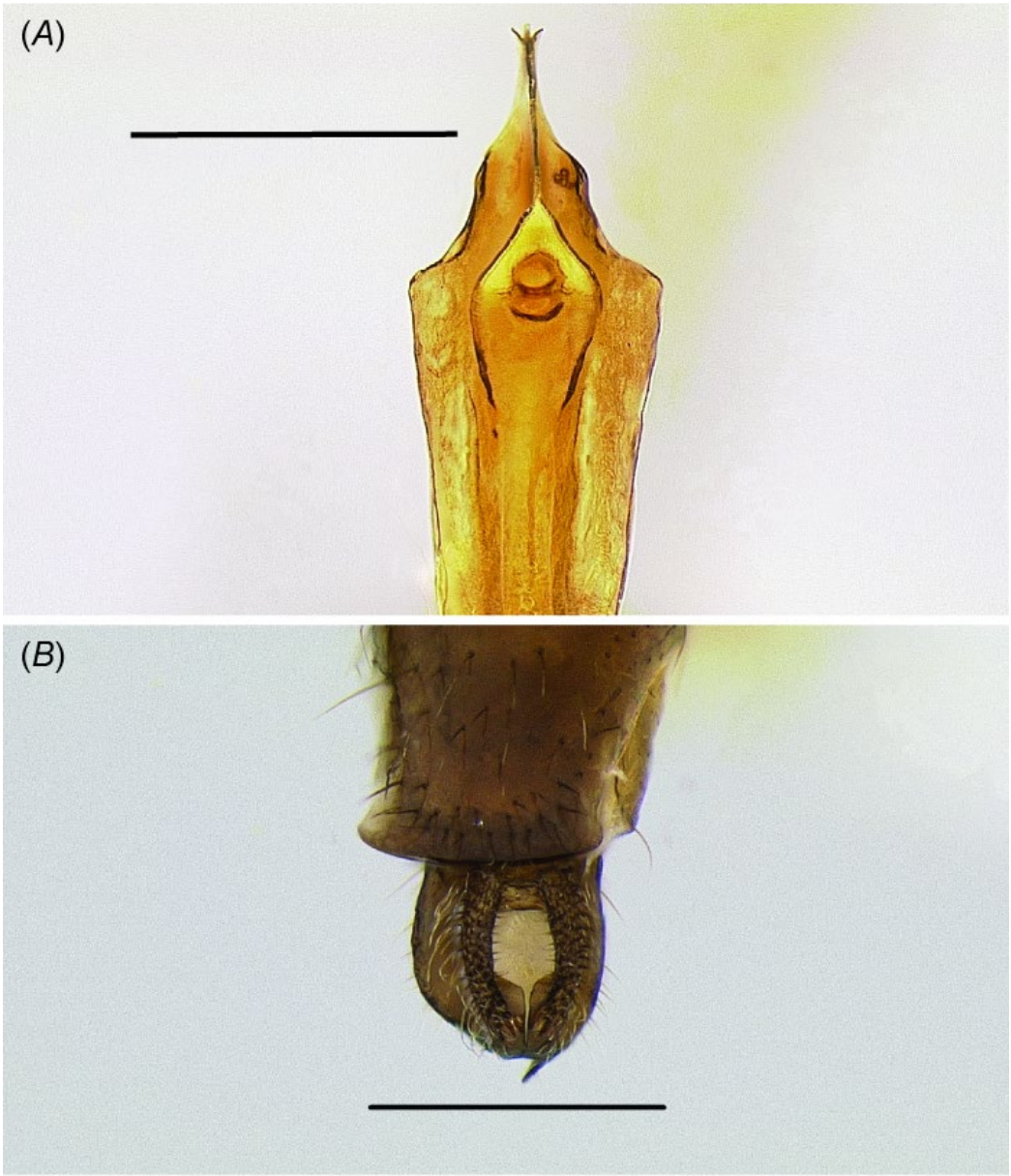

Figure 1.38. Posterior view of phallotreme in (A) *Leptanilla* zhg-my02 (CASENT0106432) and (B) *Noonilla* zhg-my02 (CASENT0842599). Scale bars: A, 0.4 mm; B, 0.3 mm.

40. Phallotreme preapical. Under the alternative character state (0) the phallotreme is situated adjoining the posterior penial margin or, if the penial sclerites are lateromedially compressed, at the penial apex (Fig. 1.39*A*). This includes cases in which the phallotreme is situated well basal to the penial apex but has a distal margin that extends to the penial apex. The phallotreme is therefore preapical (1) in *Leptanilla* (Bornean morphospecies-group) zhg-my02-3 and -5 (Fig. 1.39*B*), and in *Noonilla* zhg-my06. This character could

not be scored in *Protanilla* TH02-3; *Yavnella* TH04, -8, zhg-bt01, and MM01; *Leptanilla* zhg-bt01; and *P. javana*.

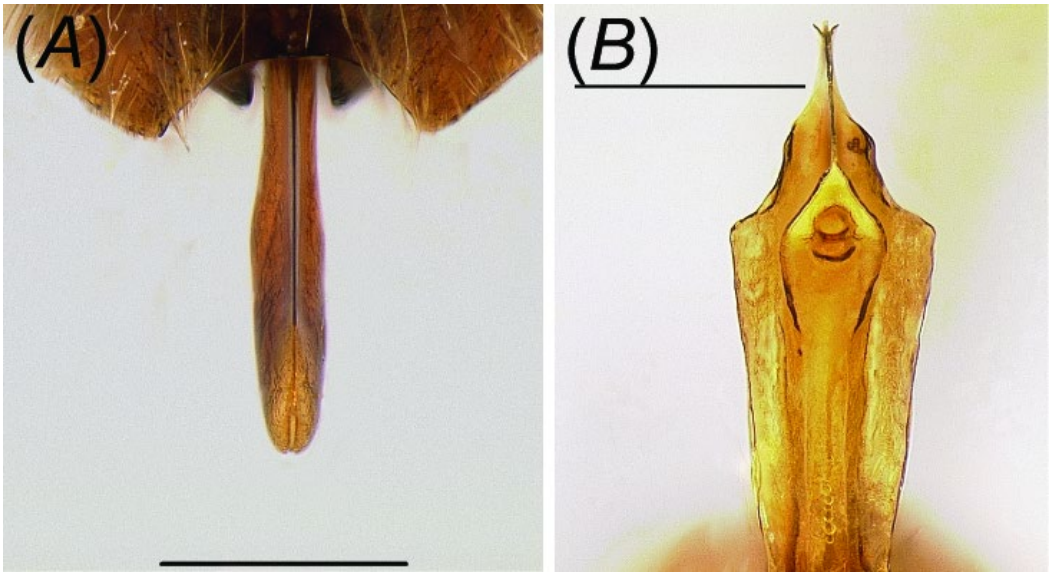

Figure 1.39. Dorsoposterior view of phallotreme in (A) *Leptanilla* zhg-my04 (CASENT0842553); ventroposterior view of phallotreme in (B) *Leptanilla* zhg-my02 (CASENT0106432). Scale bars: A, 0.3 mm; B, 0.4 mm.

41. Penial apex entire. The alternative (0) to this character state encompasses cases in which the penial sclerites are medially separated at the apex (as in *Protanilla* TH01-2), or strongly bifurcated (Fig. 1.40*A*). Under this character state (1) none of these observations apply (Fig. 1.40*B*), encompassing cases in which the distal phallotremal margin forms a narrow slit-like indentation in the penial sclerites (e.g. *Yavnella* cf. *indica*: Fig. 1.32*A*). The penial apex is entire in *M. heureka*; *Protanilla* TH03 and zhg-vn01; *Yavnella* cf. *indica*, TH02, -5-8, zhg-bt01, and zhg-th01; *Leptanilla* TH01; *Leptanilla* zhg-th01; the Bornean morphospecies-group; and *Leptanilla s. str*. except for *Leptanilla* ZA01.

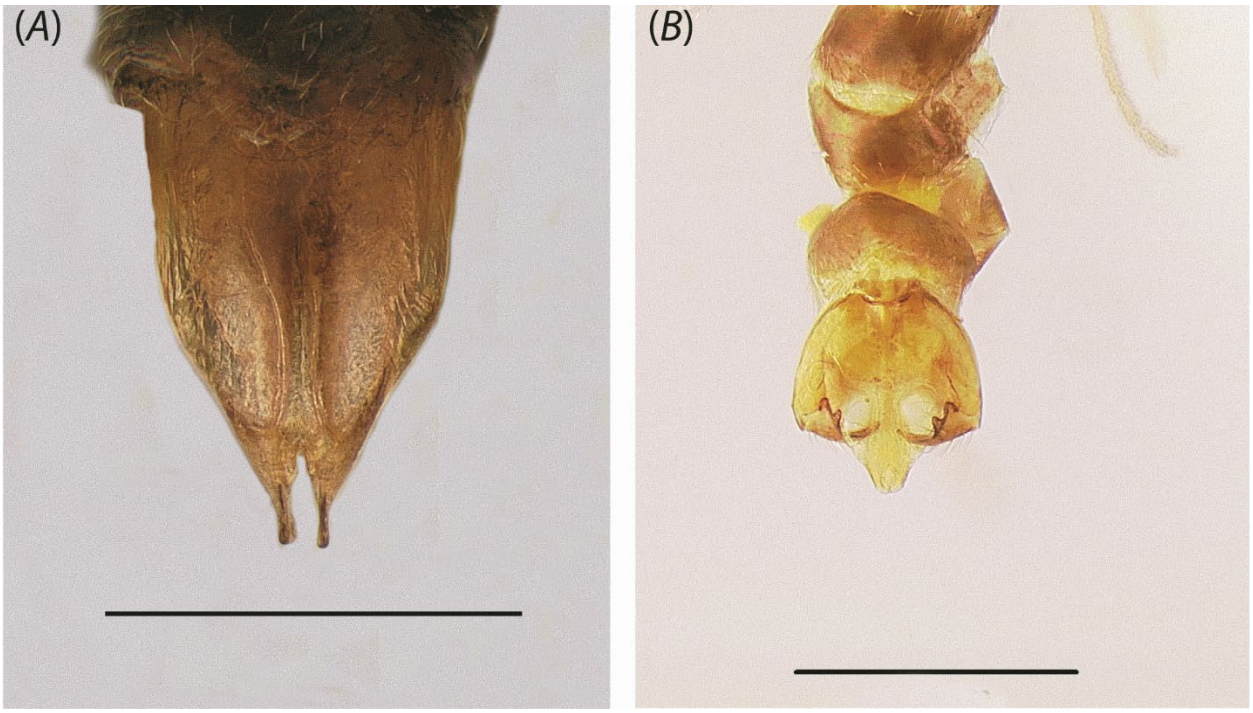

Figure 1.40. Posterodorsal view of the penial sclerites in (A) *Yavnella argamani* (CASENT0235253) and (B) *Leptanilla* GR02 (CASENT0106068). Scale bar: 0.3 mm.

Phylogenetic analyses

For the two legacy-locus molecular datasets, the partitioning scheme was inferred with PartitionFinder2 ver. 2.1.1 (Guindon *et al*. 2010; Lanfear *et al*. 2012, 2017) on the CIPRES Science Gateway, with subsets being asserted *a priori* according to locus and codon position. Introns were included. Models with I+G extensions were excluded from consideration due to undesirable behaviour in a model-based framework (Yang 1996). As an alternative *ad hoc* partitioning scheme for the 9351-bp alignment, all exonic loci were respectively partitioned so that 1st–2nd codon positions were placed in their own partition separate from the 3rd, and modelled nucleotide substitution in all partitions under GTR+G. Using AMAS (Borowiec 2016), the full 9351- and 9062-bp molecular alignments were respectively split according to partition scheme(s) for partitioned Bayesian total-evidence inference.

In total-evidence and morphology-only Bayesian phylogenetic analyses, the Mkv model (Lewis 2001) was used to model substitution of morphological character states, albeit with stationary frequencies of character states treated as free parameters (Felsenstein 1981) in order to accommodate asymmetry in character state frequencies. Variation in evolutionary rate among characters was accommodated by drawing rates from a gamma-distributed prior probability distribution (+G), approximated with eight discrete categories *k*.

All phylogenetic analyses were performed in a Bayesian statistical framework using RevBayes (ver. 1.0.11, see https://revbayes.github.io/download; Höhna *et al*. 2017) compiled on Ubuntu Linux (ver. 13.04, see http://old-releases.ubuntu.com/releases/13.04/). The following phylogenetic analyses were implemented: one using the 41-character male morphological dataset alone; one using the 9351-bp molecular dataset alone; two total-evidence analyses using the 9351-bp molecular alignment respectively with algorithmic or *ad hoc* partitioning schemes as described above; and a total-evidence analysis using the 9062-bp molecular alignment, partitioned algorithmically as described above with PartitionFinder2. Each analysis consisted of four independent Markov chain Monte Carlo (MCMC) chains, each run for 50 000 generations. Trees were sampled every 10 generations, with the first 25% of the run being discarded as burn-in. MCMCs with respect to all continuous parameters were considered converged if the effective sample sizes as given in Tracer (ver. 1.7.1, see http://tree.bio.ed.ac.uk/software/tracer/; Rambaut *et al*. 2018) were ≥200, with sufficiency of MCMC mixing across posterior probability landscapes being qualitatively assessed using traces of the respective log-likelihoods of each parameter across the course of the analysis. Maximum *a posteriori* trees were compiled from this sample of each run, with node support expressed as Bayesian posterior probability (BPP).

Data availability and nomenclature

All nucleotide and morphological data along with PartitionFinder2 configuration files, RevBayes scripts, and output of all phylogenetic analyses, are available at the Dryad Digital Repository (doi:10.25338/B8GP7C). Sequence Read Archives (SRAs) of raw UCE reads, and UCE assemblies, are publicly available on NCBI (Table 1.2).

Results

Phylogeny of the Leptanillinae

Bayesian total-evidence inference of leptanilline phylogeny using the 9351-bp legacy-locus dataset under the two partitioning schemes resulted in similar topologies, with none of the differences affecting the composition or interrelationship of major clades. All Bayesian total-evidence phylogenies inferred under the *ad hoc* partitioning schemes are provided on Dryad.

Most nodes in these phylogenies were supported with BPP ≥0.95. Those nodes supported with BPP ≤0.95 were scattered and shallow (Fig. 1.41), meaning that the interrelationships among all major leptanilline clades are well resolved. Although the sampling of the Leptanillinae differed from that of Borowiec *et al*. (2019) and Griebenow (2020), these inferences were largely congruent. Bayesian total-evidence inference from the 9062-bp alignment also drew a consilient conclusion (Fig. 1.42), indicating that the taxonomically biased distribution of missing data in the 9351-bp legacy-locus dataset does not have an appreciable effect on the backbone of inferred leptanilline phylogeny. Phylogenetic inference from the 9351-bp alignment alone, and therefore excluding *P. javana*, fully corroborates the conclusions of total-evidence Bayesian phylogenetic inference with high Bayesian posterior probabilities overall, while inference from the

morphological dataset alone was insufficient to resolve the phylogeny of the Leptanillinae (see Dryad). All discussion from here on refers to the phylogeny inferred under the partitioning scheme derived with PartitionFinder2 (Fig. 1.41) for the 9351-bp molecular alignment, unless otherwise noted.

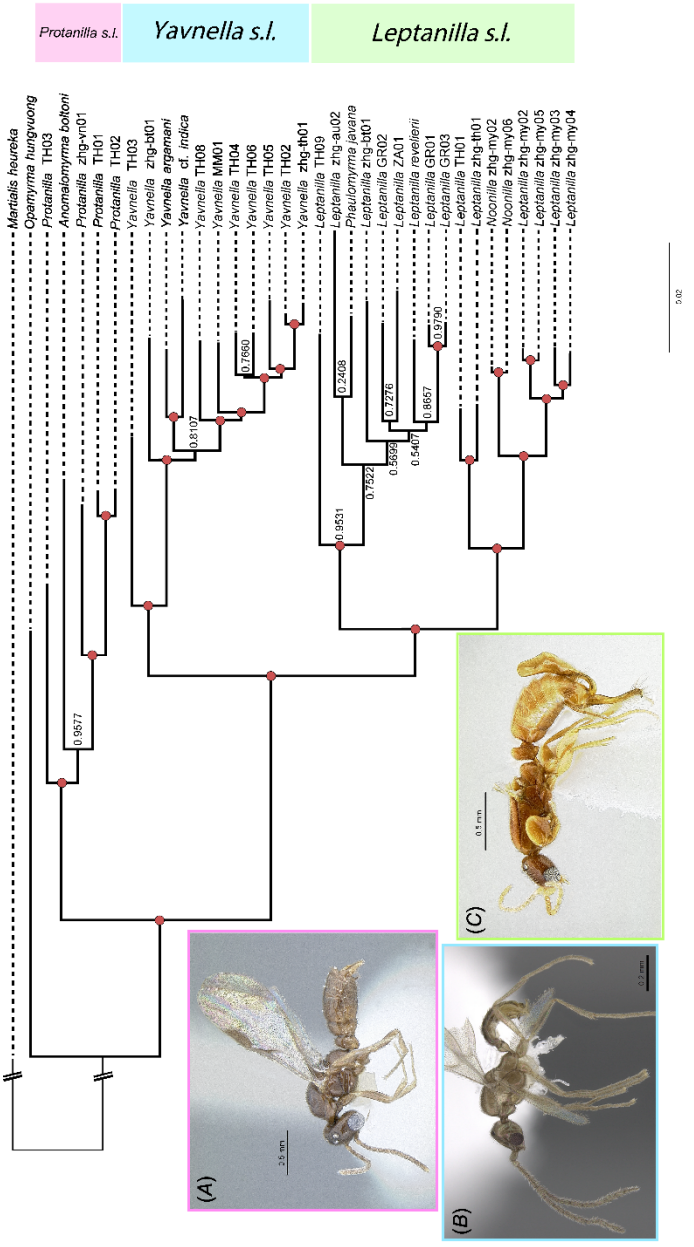

Figure 1.41. Bayesian total-evidence phylogeny of the Leptanillinae under partitioning scheme inferred with PartitionFinder2 for 9351-bp legacy-locus alignment. Phylogeny was rooted *a posteriori* on *Martialis heureka*. Nodes with BPP≥0.95 are marked in red. (A) *Protanilla* zhg-

vn01 (CASENT0842613); (B) *Yavnella* TH08 (CASENT0227555; Shannon Hartman); (C) *Leptanilla* zhg-my02 (CASENT0106416).

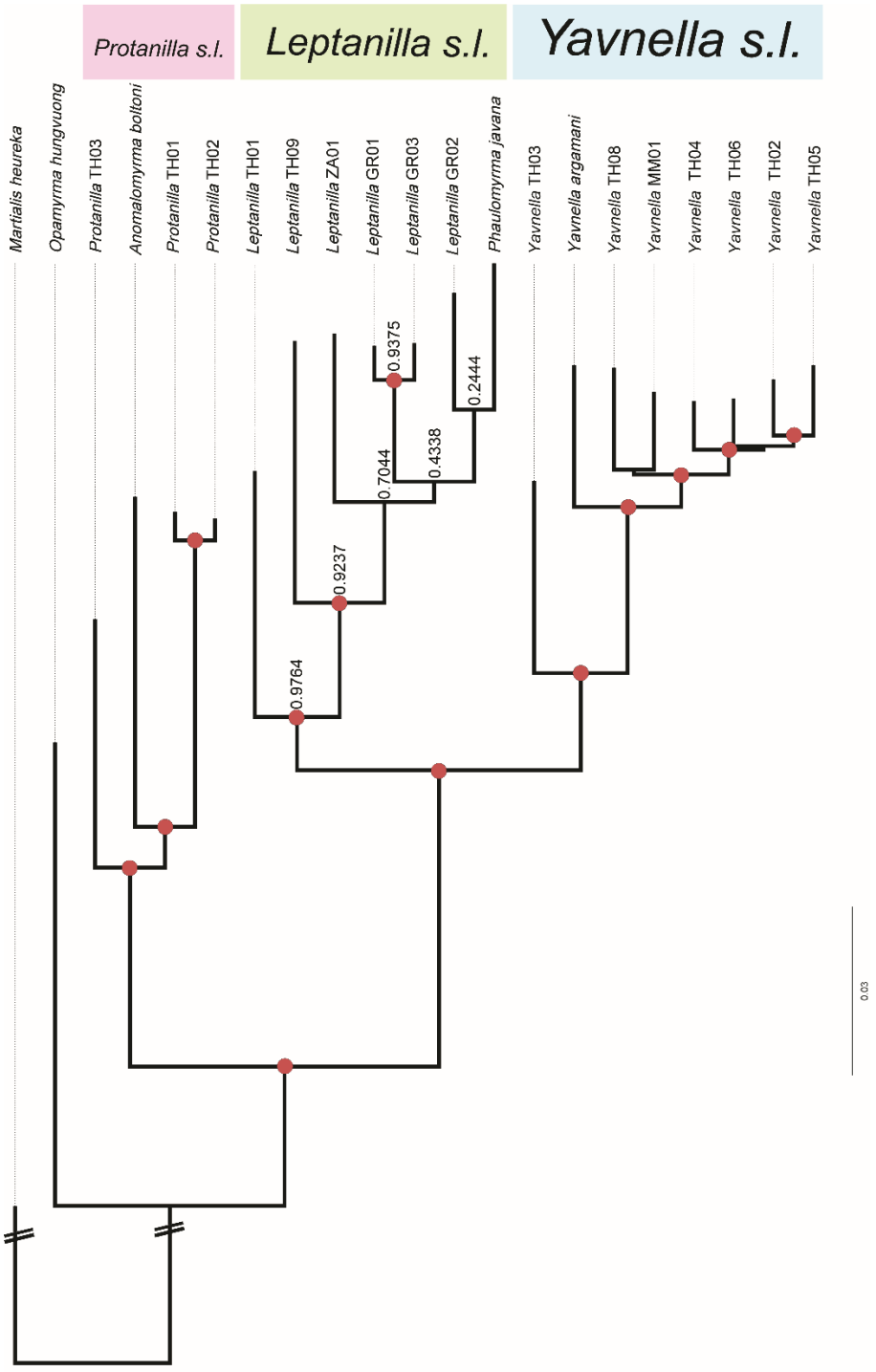

Figure 1.42. Bayesian total-evidence phylogeny of the Leptanillinae under partitioning scheme inferred with PartitionFinder2 for 9062-bp legacy-locus alignment. Phylogeny was rooted a posteriori on *Martialis heureka*. Nodes with BPP≥0.95 [sic!] are marked in red.

The clade corresponding to the tribe Anomalomyrmini (labelled as *Protanilla sensu lato* in Fig. 1.41 and 1.42) is recovered with maximal support (BPP = 1), with *A. boltoni* sister to all sampled *Protanilla* save *Protanilla* TH03 – thus rendering *Protanilla* paraphyletic – well supported (BPP = 0.9577). This same topology was recovered by Bayesian total-evidence analysis from the 9062-bp alignment, with higher support (BPP = 0.9947), and is supported by phylogenomic inference (Griebenow 2020) (Fig. 1.41). Borowiec *et al*. (2019) recovered *A. boltoni* as sister to *Protanilla* TH03 with weak support irrespective of statistical framework, albeit with more extensive sampling within the Anomalomyrmini, as did total-evidence inference from the 9351-bp dataset under the *ad hoc* partitioning scheme (BPP = 0.6535). However, the internal topology of the Anomalomyrmini does not have any bearing upon the status of *Phaulomyrma* relative to other leptanilline genera.

Noonilla, *Yavnella argamani* and *Yavnella* cf. *indica*, *Leptanilla revelierii*, and *Phaulomyrma javana* were firmly recovered within a clade corresponding to the Leptanillini (BPP = 1). As in Borowiec *et al*. (2019) and Griebenow (2020), the Leptanillini bifurcate robustly, with *Y. argamani* (and *Yavnella* cf. *indica*, which was not included in Borowiec *et al*. 2019) recovered in a clade otherwise without described representatives, which is hereinafter designated *Yavnella sensu lato* (BPP = 1). Although morphologically diverse (Fig. 1.43), the male morphospecies that comprise the sister-group to *Yavnella s. l.* are distinguished from that clade by (1) clypeus with a medial axis no longer than the diameter of the torulus, where the epistomal sulcus is distinct; and (2) pronotum and mesoscutum that are not extended posteriorly in profile view. Since *L. revelierii* is recovered within this clade, it is hereinafter referred to as *Leptanilla sensu lato* (BPP = 0.9964).

Figure 1.43. Selected diversity of male *Leptanilla s. l.* (A) *Leptanilla* TH01 (CASENT0119792; April Nobile); (B) *Leptanilla* zhg-bt02 (CASENT0842612; not sequenced in this study); (C) *Noonilla* zhg-my04 (CASENT0842610; not sequenced in this study); (D) *Leptanilla* (Bornean morphospecies-group) zhg-my05 (CASENT0842571). Scale bars: A, 0.2 mm; B, 1 mm; C, D, 0.5 mm.

Phylogenetic position of Phaulomyrma javana

Leptanilla s. l. bifurcates into two well supported clades: one is broadly Eurasian and Australian in its representation (with a single Afrotropical representative), including *L. revelierii* and *P. javana* (BPP = 0.9531); the other is Indo-Malayan, and includes *Noonilla* (BPP = 0.9839) (Fig. 1.41, 1.44). Since *L. revelierii* is included within the Afrotropical–Eurasian–Australian clade, that clade is hereinafter referred to as *Leptanilla sensu stricto*. The two circumscriptions of the name *Leptanilla* presented here are supported by male morphology (see Discussion).

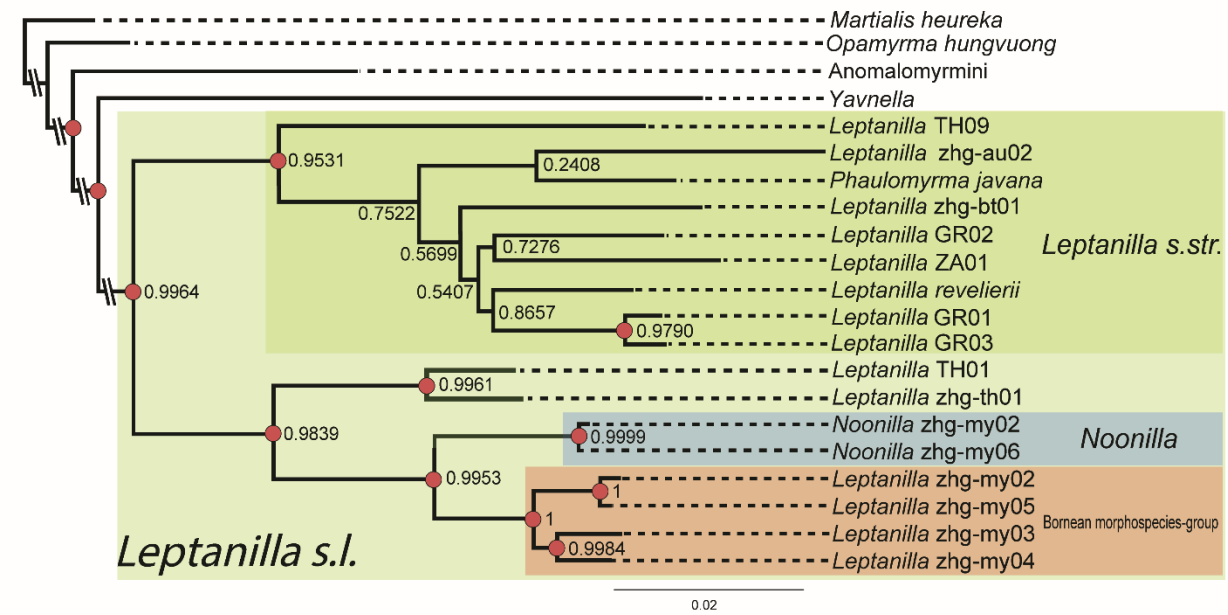

Figure 1.44. Bayesian total-evidence phylogeny of *Leptanilla s. l.* under partitioning scheme inferred with PartitionFinder2 for 9351-bp legacy-locus alignment. Phylogeny was rooted *a posteriori* on *Martialis heureka*. Nodes with BPP≥0.95 are marked in red.

Noonilla (BPP = 0.9999) is sister to a clade represented by highly distinctive male morphospecies, recovered with maximal support (BPP = 1) (Fig. 1.41, 1.44) and corroborated by Griebenow (2020, p. 238), that are immediately recognisable by bizarre metasomal processes (Griebenow 2020, fig. 3), heretofore hypothesised to be extensions of the gonocoxae *sensu* Boudinot (2018) (Boudinot 2015, p. 45); and a comb-like row of robust bristles on the protibia

(Fig. 1.45), in combination with a putatively grasping profemur. These morphospecies remain undescribed. Boudinot (2015, p. 33) adduced the grasping profemur of *Noonilla* as an autapomorphy of that genus, which could justify terming the undescribed clade as *Noonilla*_cf; but this profemoral condition is more widespread across male Leptanillini than Boudinot (2015) was aware, and better sampling is required to infer whether the grasping profemur is a synapomorphy of *Noonilla* and this undescribed clade. Said clade is therefore provisionally designated as the 'Bornean morphospecies-group': while present sampling is too sparse to judge whether this clade is precinctive to Borneo, available material exclusively originates on that island. Of the nine terminals recovered in the Indo-Malayan subclade, only *Leptanilla* TH01 was included in Borowiec *et al*. (2019) or in the 9062-bp legacy-locus alignment. The rather disparate morphospecies *Leptanilla* TH01 and *Leptanilla* zhg-th01 are recovered as a clade with high support (BPP = 0.9961), and this clade is in turn sister to *Noonilla* + Bornean morphospecies-group (Fig. 1.41, 1.44). *Leptanilla* zhg-th01 is unique among the Leptanillinae in possessing a recurved mesoscutellar horn (Fig. 1.16*B*).

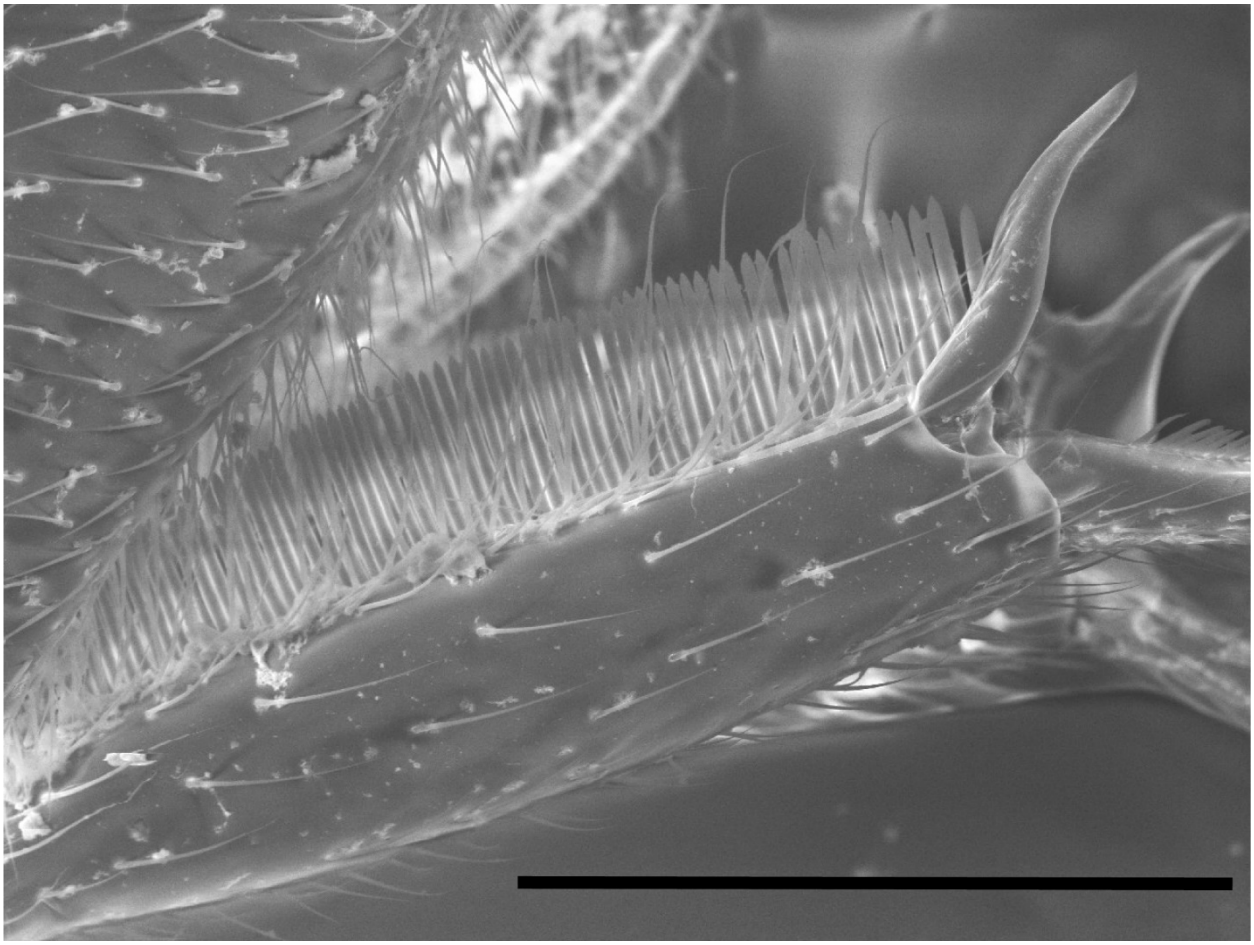

Figure 1.45. Protibia of *Leptanilla* zhg-my04 (CASENT0842555). Scale bar: 0.2 mm.

The support values of internal nodes within *Leptanilla s. str*. are generally poor under Bayesian total-evidence inference from the 9351-bp legacy-locus alignment, with the placement of *Leptanilla* ZA01 and *Leptanilla* zhg-bt01 differing according to partitioning scheme. The position of *P. javana* cannot be confidently resolved within this clade, but the basalmost node of *Leptanilla s. str*. is well supported, whether inferred under an algorithmic (BPP = 0.9531) or *ad hoc* (BPP = 0.9585) partitioning scheme. Although the internal phylogeny of *Leptanilla s. str*. cannot be resolved with Bayesian total-evidence inference, the monophyly of this clade is probable under the model and partitioning schemes used. The topology of *Leptanilla s. str*. is likely subject to strong stochastic error due to the inclusion of *P. javana*, for which molecular data are entirely absent. This is supported by Bayesian phylogenetic inference from molecular

data alone, which with only one exception recovers the internal phylogeny of *Leptanilla s. str*. with BPP ≥ 0.95 (see Dryad).

Bayesian total-evidence inference from the 9062-bp alignment (which does not include *Leptanilla revelierii*, zhg-au02 or zhg-bt01) gives mediocre support to *Leptanilla s. str*. (BPP = 0.9237) inclusive of *P. javana*, but also provides a phylogeny consilient with the results of other phylogenetic analyses (Fig. 1.42). The recovery of *P. javana* within *Leptanilla s. str*. is therefore supported by Bayesian total-evidence inference. Qualitatively, male morphological characters support *Leptanilla s. str*. (see Discussion).

Phaulomyrma javana and the taxon dubbed *Phaulomyrma* MM01 by Boudinot (2015) and Borowiec *et al*. (2019) were recovered distant from one another in the leptanilline phylogeny (Fig. 1.41, 1.42, 1.44). Total-evidence phylogenetic inference recovered the latter terminal within *Yavnella s. l*., indicating that it was incorrectly assigned to *Phaulomyrma* by these authorities, corroborating morphological evidence (see Discussion). An undescribed male morphospecies referred to as *Phaulomyrma* by Boudinot (2015, fig. 4F) was not sequenced in this study but also conforms morphologically to *Yavnella s. l*., and so likewise was incorrectly identified as *Phaulomyrma*. Conversely, *P. javana* is here recovered within *Leptanilla s. l*., and moreover within *Leptanilla s. str*. (BPP = 0.9531).

Discussion

Delimitation of subclades in Leptanillinae using male morphology

Male morphological characters corroborate inferred phylogeny at nodes of variable depth. *Opamyrma hungvuong* and the four male representatives of the Anomalomyrmini included in the

present study can easily be distinguished from male Leptanillini by the presence of a pterostigma (although wing venation may be inaccessible due to deciduous wings in some male Leptanillini) and the absence of an ocellar tubercle. Griebenow (2020) provides a formal description of female-associated male *Protanilla* and a male-based definition of the leptanilline tribes, as well as *O. hungvuong*. *Yavnella s. l.* is likewise well supported (Fig. 1.41, 1.42), as is *Leptanilla s. l.*, with the former clade diagnosed almost entirely by morphological symplesiomorphies: the only putative autapomorphy of *Yavnella s. l.* is concavity of the propodeum in profile view (Fig. 1.17*A*), which was previously noted by Kugler (1987) as being distinctive to *Yavnella*.

Leptanilla s. str. is identifiable relative to other subclades of *Leptanilla s. l.* based upon the following combination of male morphological characters: absence of posterior mesoscutellar prolongation (observed in *Leptanilla* zhg-th01 and *Leptanilla* TH01); propodeum convex and without distinct dorsal face (Fig. 1.17*C*); gonopodites articulated (otherwise among the Leptanillini articulated only in *Leptanilla* zhg-th01, *Yavnella* zhg-bt01 and some *Noonilla*); gonocoxae fully separated ventrally (this character state (Fig. 1.25*A*) elsewhere observed among sampled Leptanillini in all *Yavnella s. l.* except for Yavnella TH03, and *Leptanilla* zhg-th01); and penial sclerites dorsoventrally compressed along their entire length, entire, and lacking sculpture (Fig. 1.33*B*, 1.34*B*), this character state elsewhere observed in Leptanillini only among *Yavnella s. l.* (excluding *Yavnella* TH03) and *Leptanilla* zhg-th01.

Leptanilla TH09 is weakly recovered as sister to remaining *Leptanilla s. str.*, including *P. javana*, under all Bayesian total-evidence analyses (Fig. 1.41, 1.42, 1.44). Therefore, the phylogeny of *P. javana* relative to other *Leptanilla s. str.* would not be resolved if that clade were delimited to exclude *Leptanilla* TH09. However, *Leptanilla* TH09 conforms fully to the

diagnosis of *Leptanilla s. str*. given above, and aside from apomorphies of the foreleg (a perhaps opposable calcar and apical probasitarsal seta: Fig. 1.46*A*) is not a phenotypic outlier among the terminals representing *Leptanilla s. str*. Nor, given the weak BPP of *Leptanilla* TH09 as sister to the remainder of *Leptanilla s. str*., is there probabilistic support for qualitatively defining that clade to exclude *Leptanilla* TH09. Therefore, *P. javana* can be confidently placed within *Leptanilla s. str*., despite the inability of Bayesian total-evidence inference from these data and under these models to resolve its position within that clade.

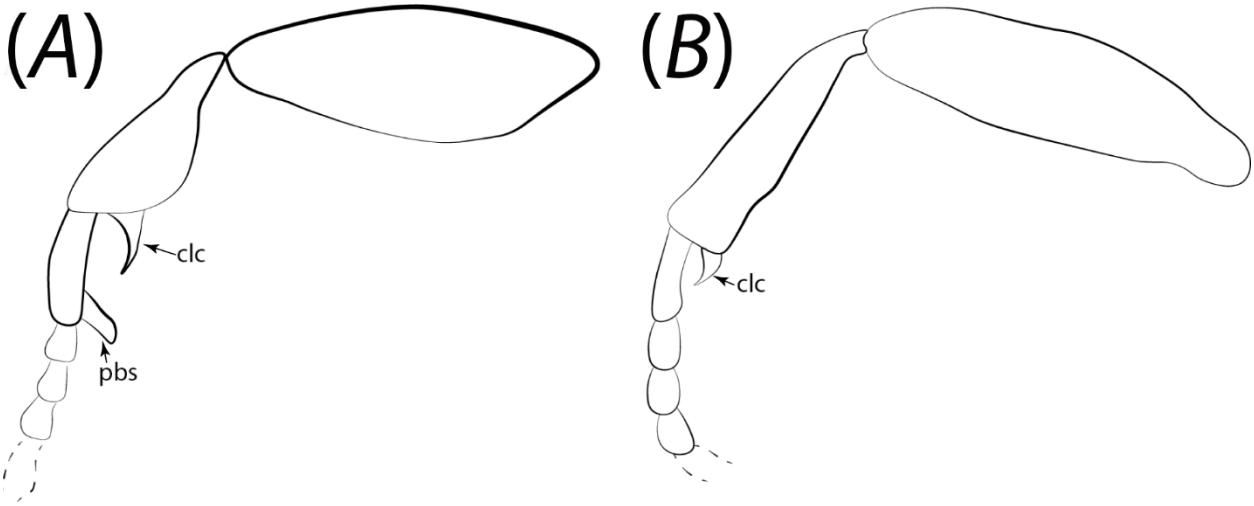

Figure 1.46. Profemur, protibia, and basal protarsomeres of (A) *Leptanilla* TH09 (CASENT0842664) and (B) *Leptanilla* zhg-bt01 (CASENT0842617). Abbreviations: clc, calcar; pbs, probasitarsal seta. Not to scale.

Unlike *Scyphodon*, *Noonilla*, and even the male-based species *Leptanilla palauensis* Smith, 1953 (Petersen 1968, p. 593), the status of *Phaulomyrma* as a leptanilline – and as an ant – has never been debated. Wheeler and Wheeler (1930) established the genus based upon the presence of wing veins and 'unusually large genitalia' (Wheeler and Wheeler 1930, p. 193), transferring also *Leptanilla tanit* Santschi, 1907 to *Phaulomyrma*. Their argument regarding wing venation has no merit, given that the forewing venation of *P. javana* falls within the range of variation observed in putative *Leptanilla* morphospecies (Petersen 1968, pp. 594–595), with all leptanilline males examined by Boudinot (2015) exhibiting at least one compound abscissa on the forewing.

Petersen (1968, p. 597) even referred to *Leptanilla* and *Phaulomyrma* as 'nearly identical' (when comparing these taxa to *L. palauensis*), and returned *L. tanit* to *Leptanilla*, but refrained from synonymising *Leptanilla* and *Phaulomyrma* on account of the apparent uniqueness of the genitalia of *P. javana* as illustrated by Wheeler and Wheeler (1930, fig. 2A, C). In passing, Taylor (1965, p. 365) also mentioned *Phaulomyrma* as being 'possibly synonymous' with *Leptanilla*.

Examination of a syntype of *P. javana* (lectotypified below) demonstrates that its genitalia are consistent with other sampled male *Leptanilla s. str*. to the exclusion of males within the Indo-Malayan sister-group of *Leptanilla s. str*. (Fig. 1.47). Although the preservation of this specimen (MCZ:Ent:31142) on a slide prevents direct confirmation of stylar articulation, the sharply recurved styli are consistent with the syndrome seen in dried male leptanillines with articulated gonopodites (Kugler 1987; Ward and Sumnicht 2012), indicating that the gonopodites are articulated in *P. javana*. *Contra* fig. 2C of Wheeler and Wheeler (1930), the volsellae of *P. javana* are not discernible *in situ* (Fig. 1.47*D*). If their condition is truly 'plate-like', as described by Wheeler and Wheeler (1930, p. 196), the volsellae of *P. javana* resemble those observed in undescribed Sicilian male morphospecies attributed to *Leptanilla* (Scupola and Ballarin 2009). Dissection of Anatolian *Leptanilla* GR03, and Spanish material that closely resembles sequenced males of *Leptanilla s. str*., demonstrates that the volsellae are likewise lamellate in these morphospecies, having much the same condition as in *Leptanilla africana* Baroni Urbani, 1977 (Baroni Urbani 1977, fig. 37) (not included in this study). Therefore, given the phylogeny of *P. javana* and its morphological conformity to *Leptanilla s. str*. there is no justification for maintaining the genus *Phaulomyrma*.

A complete male-based diagnosis of *Leptanilla* relative to other Leptanillinae under both broad and strict circumscriptions of *Leptanilla* is provided below, with putative synapomorphies for the two circumscriptions represented in italic. Only genital characters could be scored for *Leptanilla* ZA01.

Leptanilla javana Wheeler & Wheeler, **comb. nov.** (Fig. 47*A–D*)

Phaulomyrma javana – Wheeler and Wheeler (1930), p. 193, fig. 1, 2C.

Phaulomyrma javana – Petersen 1968, p. 293, fig. 16A–C.

ZooBank LSID (www.zoobank.com): 5f3becf6-3715-47b3-8d0f-de7d66e1da0a

Material examined

Lectotype (hereby designated). **Indonesia**: *Jawa Barat*: ♂ (fragments), Buitenzorg [Bogor], 6.59444°S, 106.78917°E ± 3 km [estimated with GeoLocate], iii.1907, F. A. G. Muir (MCZ:Ent:31142).

Paralectotype (hereby designated). Same data as for lectotype. No accession code.

Genus *Leptanilla* Emery, 1870

Type species: *Leptanilla revelierii* Emery, 1870: 196, by monotypy. Syntypes deposited at ZMHB (Museum für Naturkunde der Humboldt-Universität Berlin), Berlin, Germany.

=*Leptomesites* Kutter – Kutter (1948, p. 286, fig. 1–7). Synonymised by Baroni Urbani (1977, p. 433). Holotype deposited at MHNG (Muséum d'Histoire Naturelle, Geneva, Switzerland).

=*Phaulomyrma* Wheeler & Wheeler – Wheeler and Wheeler (1930, p. 193, fig. 1–2C); **syn. nov.** Lectotype and paralectotype (hereby designated) deposited at MCZC (Museum of Comparative Zoology, Cambridge, Massachusetts).

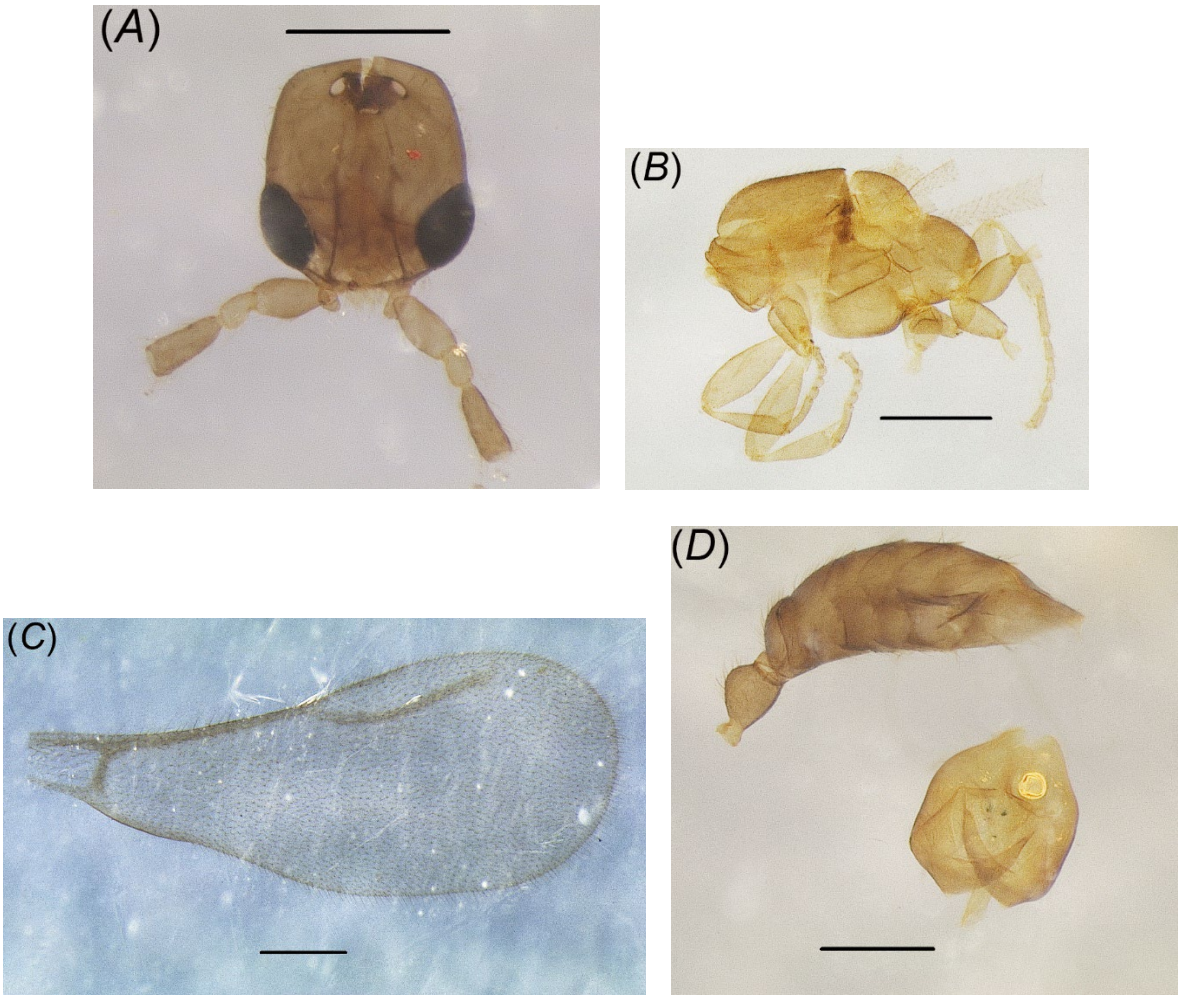

Figure 1.47. Lectotype of *Phaulomyrma javana* as designated by this study (MCZ:Ent:31142). (A) Full-face view; (B) profile view of mesosoma; (C) forewing; (D) metasoma and genitalia. Scale bar: 0.2 mm.

Male diagnosis of *Leptanilla s. l.* relative to other Leptanillinae

1. Mandibles articulated to gena (Fig. 1.8*B*).

2. *Medial axis of clypeus no longer than diameter of torulus, when epistomal sulcus is distinct.*

3. Antennomere 3 shorter than, or equal in length to, scape (Fig. 1.7*A*).

4. Ocelli present and *set on tubercle* (Fig. 1.48) (with exception of *Leptanilla* [Bornean morphospecies-group] zhg-my05).

5. *Pronotum and mesoscutum posteriorly extended* (Fig. 1.49*B*, *C*).

6. *Notauli absent.*

7. *Pterostigma absent.*

8. Propodeum not concave in profile view.

Figure 1.48. Full-face view of *Yavnella* TH02 (CASENT0119531; Michele Esposito), with ocellar tubercle marked. Scale bar: 0.1 mm.

Male diagnosis of *Leptanilla s. str.* relative to other *Leptanilla s. l.*

9. *Anteromedian ocellus and compound eye not intersecting line parallel to dorsoventral axis of cranium.*

10. Profemoral ventral cuticular hooks absent.

11. Ventromedian protibial comb-like row of setae absent.

12. Infuscation at juncture of Rf and 2s-rs+Rs+4-6 absent.

13. *Antero-admedian line absent* (HAO: 0000128).

14. Mesoscutellum not posteriorly prolonged.

15. Propodeum convex in profile view, without distinct dorsal face.

16. Abdominal sternite IX without posterolateral filiform processes.

17. Abdominal tergite VIII broader than long.

18. Gonocoxae medially separated*.

19. Gonopodites articulated.

20. *Volsella lamellate, entire distally, without denticles*.*

21. Penial sclerites dorsoventrally compressed, dorsomedian carina absent, ventromedian carina sometimes present.

22. Phallotreme situated at penial apex, without vestiture.

*These character states observed so far as is possible with available specimens.

Remarks

1. The mandibles are fused to the gena (Fig. 1.8*A*) in sampled *Yavnella s. l.* except for *Yavnella* TH04.

2. The epistomal sulcus is often difficult to distinguish in *Leptanilla s. l.*, but the anteroposterior reduction of the clypeus can be inferred by the situation of the toruli at the most anterior margin of the head (cf. Boudinot 2015, p. 30).

3. Antennomere 3 is longer than the scape in all sampled *Yavnella s. l.* except for *Yavnella* TH05.

4. Ocelli are entirely absent in *Yavnella* TH03 and *Yavnella* zhg-bt01. The ocellar tubercle is absent in the Anomalomyrmini and *O. hungvuong*; within *Leptanilla s. l.* it is absent in *Leptanilla* zhg-my05, which is here inferred to be a secondary loss.

5. As noted by Petersen (1968, p. 87), *N. copiosa* contrasts with other described male Leptanillinae by the lack of an 'elongated, laterally compressed' mesosoma. *Yavnella* was described by Kugler (1987) as sharing this condition, which Petersen (1968) adduced as plesiomorphic for the Leptanillinae. Although the relative modification of the mesosoma – here approximated by the proportions of the pronotum and mesoscutum – forms a morphocline across the male Leptanillinae, this morphocline is discontinuous, with a gap between the morphospace occupied by *Leptanilla s. l.* (Fig. 1.49*B*, *C*) and that occupied by *O. hungvuong*, the Anomalomyrmini, and *Yavnella s. l.* (Fig. 1.49*A*). Future sampling of male Leptanillinae may close this gap in morphospace, which would limit the diagnostic utility of pronotal and mesonotal length.

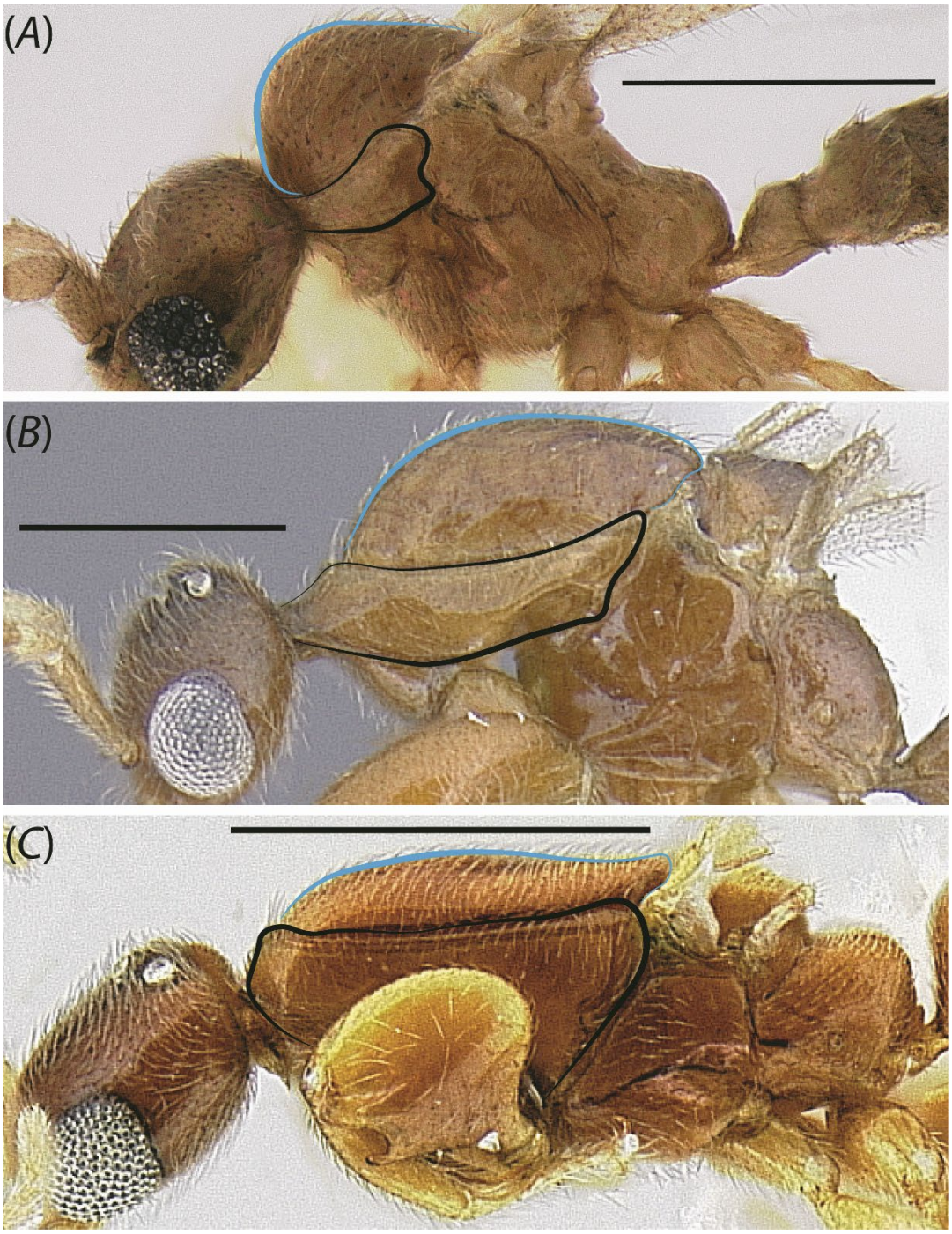

Figure 1.49. Profile of pronotum (black) and mesoscutum (blue) in male Leptanillini. (A) *Yavnella* zhg-bt01 (CASENT0106384); (B) *Noonilla* zhg-my04 (CASENT0842610; not sequenced in this study); (C) *Leptanilla* zhg-my02 (CASENT0106416).

6. The absence of notauli is a synapomorphy of the tribe Leptanillini. The notauli in *Protanilla* TH01 and *Protanilla* zhg-vn01, in the tribe Anomalomyrmini, are homoplastically absent.

7. The absence of the pterostigma (Fig. 1.50*A*, *C*) is a synapomorphy of the Leptanillini.

8. The convexity of the propodeum in profile view is plesiomorphic for the Leptanillinae. Its concave condition in *Yavnella* (Kugler 1987) is apomorphic for that genus.

9. The anteromedian ocellus is not situated orthogonally to the compound eye in profile view in *Leptanilla s. str.*, *Leptanilla* TH01 and zhg-th01, the Bornean morphospecies-group, and all examined *Noonilla*. The concomitant prognathy of the male cranium is unique among male Leptanillinae to *Leptanilla s. l.*, and, as adduced by Petersen (1968), this condition appears to be apomorphic among the Leptanillinae.

10. A profemoral ventral cuticular hook (Fig. 1.2*B*) is unique among the morphospecies sampled herein to *Leptanilla* ('Bornean morphospecies-group') zhg-my02 and -5.

11. The ventromedian comb-like row of setae on the protibia is an autapomorphy of the Bornean morphospecies-group.

12. The infuscation observed in the Bornean morphospecies-group at the juncture of Rf and 2s-rs+Rs+4-6 (Fig. 1.50*C*) is not enclosed anteriorly by an abscissa and appears to be homoplasious with the pterostigma observed in male Anomalomyrmini. Infuscation of the forewing is otherwise absent in the Leptanillini.

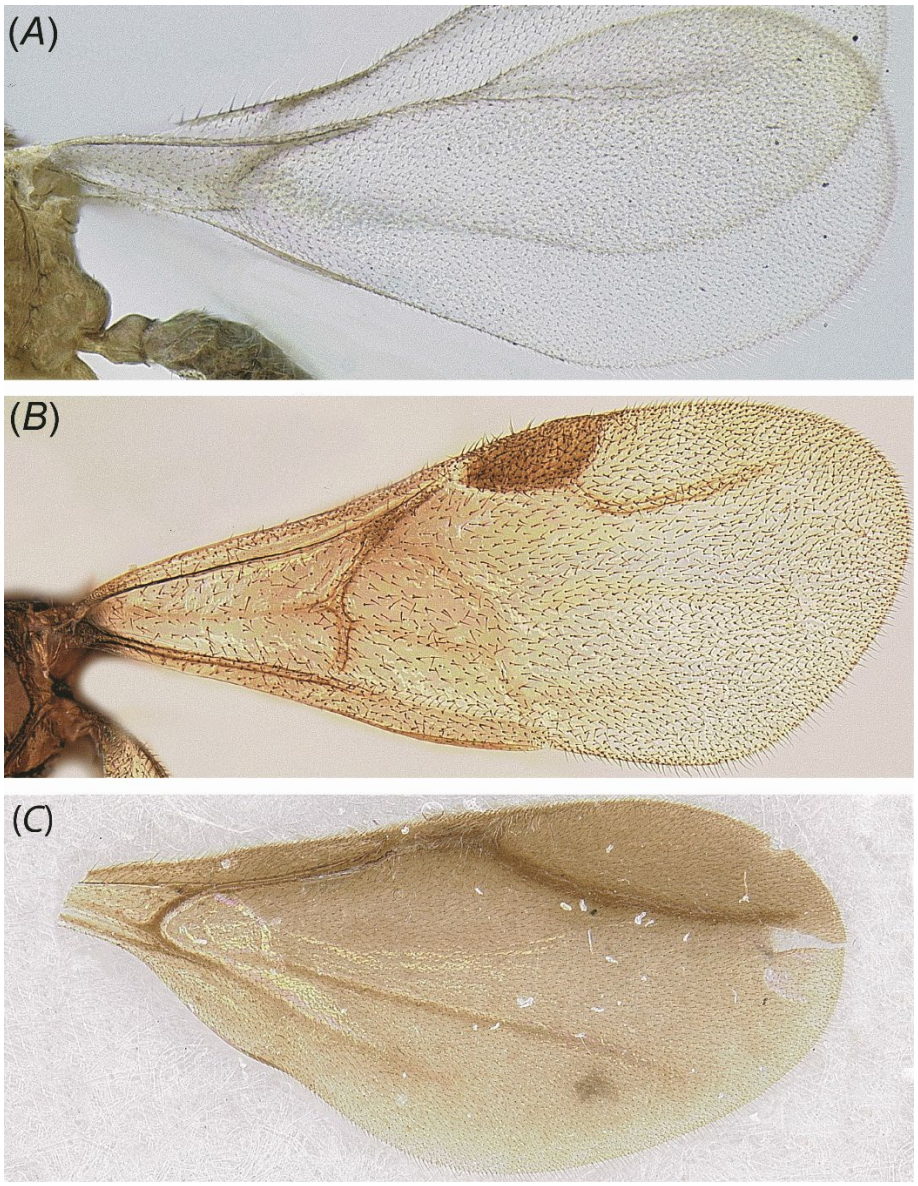

Figure 1.50. Examples of male forewing venation across the Leptanillinae. (A) *Yavnella* zhg-bt01 (CASENT0106384); (B) *Protanilla* zhg-vn01 (CASENT0842613); (C) *Leptanilla* zhg-my05 (CASENT0842571).

13. The antero-admedian line is present among sampled Leptanillini only among some *Yavnella* *s. l.*

14. The mesoscutellum is posteriorly prolonged in *Leptanilla* TH01 and *Leptanilla* zhg-th01 (Fig. 1.16*B*). The differences in mesoscutellar shape between these morphospecies (see Appendix) are such that the homology of posterior mesoscutellar prolongation is uncertain.

15.The propodeum has a distinct planar to depressed dorsal face in the Bornean morphospecies-group (Fig. 1.17*B*). This condition is an autapomorphy of that clade.

16. The posterior margin of abdominal sternite IX is variously emarginate to entire in male Leptanillinae or with a posteromedian process (e.g. *Protanilla* zhg-vn01, *Yavnella* TH03), but posterolateral filiform processes of abdominal sternite IX are an autapomorphy of the Bornean morphospecies-group.

17. Abdominal tergite VIII is longer than broad only in *Noonilla* (Fig. 1.24*B*), *Scyphodon* and a bizarre male morphospecies from Côte d'Ivoire (CASENT0102373) for which molecular data are unavailable.

18. The gonocoxae exhibit partial (Fig. 1.25*B*) to full (Fig. 1.25*C*) medial fusion at least in ventral view in *Yavnella* TH03, *Noonilla*, and all sampled members of the Bornean morphospecies-group. Within *Leptanilla s. l.*, complete lack of medial gonocoxal fusion (Fig. 1.25*A*) is a symplesiomorphy of *Leptanilla s. str.*, *Leptanilla* TH01, and *Leptanilla* zhg-th01.

19. Articulation of the gonopodites encompasses both cases in which conjunctival membrane is visible between the gonocoxa and stylus, and those in which the stylus is recurved relative to the gonocoxa without apparent conjunctival membrane. This character state is a symplesiomorphy of *Leptanilla s. str.*, and among *Leptanilla s. l.* included in this study is also observed in *Noonilla* zhg-my02 and -6, and *Leptanilla* zhg-th01.

20. The volsellae cannot be observed without dissection in many male Leptanillinae (e.g. *Noonilla*), limiting assessment of their condition. However, *Leptanilla s. str.* contrast with the Anomalomyrmini, *Yavnella s. l.*, and the Bornean morphospecies-group in that the volsellae

(where visible) are dorsoventrally flattened, entire, and lacking sculpture (Fig. 1.51). This is one of only two synapomorphies of *Leptanilla s. str*. relative to other *Leptanilla s. l.*

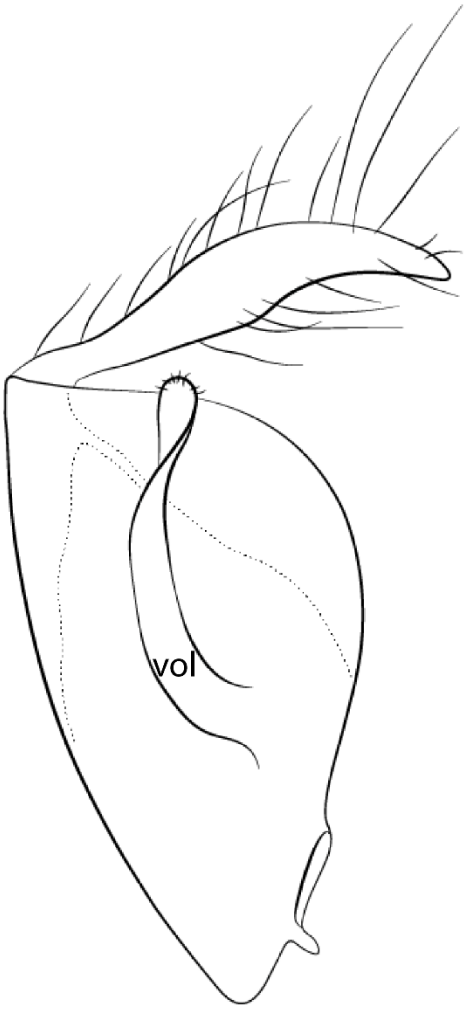

Figure 1.51. Gonopodite and volsella (vol) of *Leptanilla africana*, sketched after Baroni Urbani (1977, fig. 37) by M. K. Lippey. Top of image is distal to body.

21.Dorsoventral compression at the penial apex is also observed in *Yavnella s. l.* (except for *Yavnella* TH03). In the Indo-Malayan sister clade of *Leptanilla s. str*. the penial sclerites are lateromedially compressed to subcircular, at least basally. *Leptanilla* zhg-th01 exhibits an intermediate condition, with the penial apex being lateromedially compressed and this condition less pronounced towards the base.

22.Position of the phallotreme with distal margin adjoining the penial apex appears to be ancestral for the Leptanillini. The phallotreme is shifted basally in *Leptanilla* zhg-my02 and -5 (Fig. 1.38*A*), *Noonilla*, and *Scyphodon*. The outline of the phallotreme is subcircular in these morphotaxa. Setae surrounding the phallotreme are observed in *Noonilla* and *Scyphodon*; this character state is likely a synapomorphy of these genera.

Goals of future research

Two described male-based species of *Leptanilla* are worth noting here as requiring further study and acquisition of fresh material: *L. palauensis*, which was transferred with some reservation to *Leptanilla* from *Probolomyrmex* (Formicidae: Proceratiinae) by Taylor (1965), and *Leptanilla astylina* Petersen, 1968. Examination of the holotype of *L. palauensis* demonstrates that, according to the morphological hypotheses made herein, this species can be confidently referred to *Leptanilla s. l*., but beyond that its affinities are unclear. Based upon available illustrations (Petersen 1968, fig. 1) *L. astylina* likewise can be placed in *Leptanilla s. l*., and closely resembles *Leptanilla s. str*., excluding its genitalia, which to judge from Petersen (1968) are unlike those of any specimen that was examined in this study, and exclude it from the definition of *Leptanilla s. str*. given herein.

The case of *Scyphodon* must also be briefly addressed here. Examination of a specimen attributable to this monotypic male-based genus shows that it can be placed in *Leptanilla s. l*. As reported by Petersen (1968), the genitalia of *Scyphodon* conspicuously resemble those of *Noonilla*: there is no reason to conclude that *Scyphodon* belongs within *Leptanilla s. str*., and it is here predicted that *Scyphodon* is either sister to, or nested within, *Noonilla*. Future total-evidence Bayesian phylogenetic inference will resolve the relation of *Scyphodon* to other *Leptanilla s. l*.

Future acquisition and examination of novel material may necessitate revision of the male diagnosis of *Leptanilla* provided here, but this diagnosis is robust to all morphological observations made with sequenced material. As *Yavnella s. l.*, *Noonilla* and the Bornean morphospecies-group are known only from males, and *L. revelierii* is known only from female castes, no argument can yet be made regarding the ranking of the former clades relative to *Leptanilla*. *Yavnella* is here ranked as a genus, but the description of *Yavnella* workers may reveal a morphological basis for subjective arguments for the subsumption of *Yavnella* within *Leptanilla*. The delimitation of genera within the Leptanillini – including the status of *Noonilla* and undescribed male morphospecies more closely related to that genus than to *L. revelierii* – therefore depends not only upon phylogenetic resolution of the many lineages known only from male material, but upon the morphology of corresponding workers. Future molecular sequencing will be needed to associate workers and gynes to leptanilline lineages that are known only from males: such an effort has successfully linked *Protanilla lini* (Anomalomyrmini) with previously unassociated males (Griebenow 2020).

Conclusions

I have here demonstrated the utility of discrete morphological data within a total-evidence framework that includes molecular data in inferring the phylogeny of an ant taxon known only from male morphology. Using probabilistic models, the phylogenetic position of *Leptanilla javana* is robustly inferred in conjunction with taxa for which only molecular data, or both these and male morphological data, are available. In that phylogeny, *L. javana* and *L. revelierii* are confidently recovered within a subclade easily diagnosed by male morphological characters; disregarding future retrieval of worker material and novel male specimens, *Phaulomyrma* can be

synonymised with *Leptanilla* despite continued uncertainty in the bounds of the latter genus. Future work will employ this Bayesian total-evidence approach to infer the affinity of other, more peculiar leptanilline taxa for which molecular data are unavailable. With a robust phylogeny inferred for the Leptanillinae that is congruent with male morphology, the parallel taxonomy that bedevils this little-understood group of ants can begin to be resolved.

Conflicts of interest

The author declares that he has no conflicts of interest.

Declaration of funding

This research was supported by the University of California, Davis and by NSF grant DEB-1932405 to P. S. Ward.

Supplementary Tables, Chapter 1

Table 1.S1. Summary statistics for ultra-conserved element (UCE) assemblies, computed with BBMap (ver. 38.87, see https://sourceforge.net/projects/bbmap/files/, accessed 13 November 2020).

Table 1.S2. Summary statistics for each of the 11 loci in the 9351-bp alignment, computed with IQ-Tree (ver. 1.6.10, see http://www.iqtree.org/; Nguyen et al. 2015) on the CIPRES Science Gateway (ver. 3.3; Miller et al. 2010).

Table 1.S3. Discrete character matrix including the 33 terminals for which male morphology is known.

References

Bankevich, A., Nurk, S., Antipov, D., Gurevich, A. A., Dvorkin, M., Kulikov, A. S., Lesin, V. M., Nikolenko, S. I., Pham, S., Prjibelski, A. D., Pyshkin, A. V., Sirotkin, A. V., Vyahhi, N., Tesler, G., Alekseyev, M. A., and Pevzner, P. A. (2012). SPAdes: a new genome assembly algorithm and its applications to single-cell sequencing. *Journal of Computational Biology* **19**, 455–477.

Bapst, D. W., Wright, A. M., Matzke, N. J., and Lloyd, G. T. (2016). Topology, divergence dates, and macroevolutionary inferences vary between different tip-dating approaches applied to fossil theropods (Dinosauria). *Biology Letters* **12**, 20160237.

Barden, P., Boudinot, B. E., and Lucky, A. (2017). Where fossils dare and males matter: combined morphological and molecular analysis untangles the evolutionary history of the spider ant genus *Leptomyrmex* Mayr (Hymenoptera: Dolichoderinae). *Invertebrate Systematics* **31**, 765–780.

Baroni Urbani, C. (1977). Materiali per una revision della sottofamiglia Leptanillinae Emery (Hymenoptera: Formicidae). *Entomologica Basiliensia* **2**, 427–488.

Baroni Urbani, C., and de Andrade, M. L. (2006). A new *Protanilla* Taylor, 1990 (Hymenoptera: Formicidae: Leptanillinae) from Sri Lanka. *Myrmecologische Nachrichten* **8**, 45–47.

Belshaw, R., and Bolton, B. (1994). A survey of the leaf litter ant fauna in Ghana, West Africa (Hymenoptera: Formicidae). *Journal of Hymenoptera Research* **3**, 5–16.

Billen, J., Bauweleers, E., Hashim, R., and Ito, F. (2013). Survey of the exocrine system in *Protanilla wallacei* (Hymenoptera, Formicidae). *Arthropod Structure & Development* **42**, 173–183.

Bolton, B. (1990). The higher classification of the ant subfamily Leptanillinae (Hymenoptera: Formicidae). *Systematic Entomology* **15**, 267–282.

Bolton, B. (2003). Synopsis and classification of Formicidae. *Memoirs of the American Entomological Institute* **71**, 1–370.

Borowiec, M. L. (2016). AMAS: a fast tool for alignment manipulation and computing of summary statistics. *PeerJ* **4**, e1660.

Borowiec, M. L., Schulz, A., Alpert, G. D., and Baňar, P. (2011). Discovery of the worker caste and description of two new species of *Anomalomyrma* (Hymenoptera: Formicidae: Leptanillinae) with unique abdominal morphology. *Zootaxa* **2810**, 1–14.

Borowiec, M. L., Rabeling, C., Brady, S. G., Fisher, B. L., Schultz, T. R., and Ward, P. S. (2019). Compositional heterogeneity and outgroup choice influence the internal phylogeny of the ants. *Molecular Phylogenetics and Evolution* **134**, 111–121.

Boudinot, B. E. (2015). Contributions to the knowledge of Formicidae (Hymenoptera, Aculeata): a new diagnosis of the family, the first global male-based key to subfamilies, and a treatment of early-branching lineages. *European Journal of Taxonomy* **120**, 1–62.

Boudinot, B. E. (2018). A general theory of genital homologies for the Hexapoda (Pancrustacea) derived from skeletomuscular correspondences, with emphasis on the Endopterygota. *Arthropod Structure & Development* **47**, 563–613.

Brady, S. G., Schultz, T. R., Fisher, B. L., and Ward, P. S. (2006). Evaluating alternative hypotheses for the early evolution and diversification of ants. *Proceedings of the National Academy of Sciences of the United States of America* **103**, 18172–18177.

Branstetter, M. G., Longino, J. T., Ward, P. S., and Faircloth, B. C. (2017). Enriching the ant tree of life: enhanced UCE bait set for genome-scale phylogenetics of ants and other Hymenoptera. *Methods in Ecology and Evolution* **8**, 768–776.

Brazeau, M. D. (2011). Problematic character coding methods in morphology and their effects. *Biological Journal of the Linnaean Society* **104**, 489–498.

Brues, C. T. (1925). *Scyphodon*, an anomalous genus of Hymenoptera of doubtful affinities. *Treubia* **6**, 93–96.

Castresana, J. (2000). Selection of conserved blocks from multiple alignments for their use in phylogenetic analysis. *Molecular Biology and Evolution* **17**, 540–552.

Chen, Z.-L., Shi, F.-M., and Zhou, S.-Y. (2017). First record of the monotypic genus *Opamyrma* (Hymenoptera: Formicidae) from China. *Far Eastern Entomologist* **335**, 7–11.

de Pinna, M. C. C. (1991). Concepts and tests of homology in the cladistic paradigm. *Cladistics* **7**, 367–394.

Emery, C. (1870). Studi mirmecologici. *Bollettino della Società Entomologica Italiana* **2**, 193–201.

Faircloth, B. C. (2016). PHYLUCE is a software package for the analysis of conserved genomic loci. *Bioinformatics* **32**, 786–788.

Felsenstein, J. (1981). Evolutionary trees from DNA sequences: a maximum likelihood approach. *Journal of Molecular Evolution* **17**, 368–376.

Grabherr, M. G., Haas, B. J., Yassour, M., Levin, J. Z., Thompson, D. A., Amit, I., Adiconis, X., Fan, L., Raychowdhury, R., Zeng, Q., Chen, Z., Mauceli, E., Hacohen, N., Gnirke, A., Rhind, N., di Palma, F., Birren, B. W., Nusbaum, C., Lindblad-Toh, K., Friedman, N., and Regev, A. (2011). Full-length transcriptome assembly from RNA-Seq data without a reference genome. *Nature Biotechnology* **29**, 644–652.

Griebenow, Z. H. (2020). Delimitation of tribes in the subfamily Leptanillinae (Hymenoptera: Formicidae), with a description of the male of *Protanilla lini* Terayama, 2009. *Myrmecological News* **30**, 229–250.

Guindon, S., Dufayard, J. F., Lefort, V., Anisimova, M., Hordijk, W., and Gascuel, O. (2010). New algorithms and methods to estimate maximum-likelihood phylogenies: assessing the performance of PhyML 3.0. *Systematic Biology* **59**, 307–321.

Hoang, D. P., Chernomor, O., von Haeseler, A., Minh, B. Q., and Vinh, L. S. (2018). UFBoot2: improving the ultrafast bootstrap approximation. *Molecular Biology and Evolution* **35**, 518–522.

Höhna, S., Landis, M. J., and Heath, T. A. (2017). Phylogenetic inference using RevBayes. *Current Protocols in Bioinformatics* **57**, 6.16.1–6.16.34.

Hsu, P.-W., Hsu, F.-C., Hsiao, Y., and Lin, C.-C. (2017). Taxonomic notes on the genus *Protanilla* (Hymenoptera: Formicidae: Leptanillinae) from Taiwan. *Zootaxa* **4268**, 117–130.

Katoh, K., Asimenos, G., and Toh, H. (2009). Multiple alignment of DNA sequences with MAFFT. In 'Bioinformatics for DNA Sequence Analysis'. (Ed. D. Posada.) pp. 39–64. (Springer: New York, NY, USA.)

Katoh, K., Rozewicki, J., and Yamada, K. D. (2019). MAFFT online service: multiple sequence alignment, interactive sequence choice and visualization. *Briefings in Bioinformatics* **20**, 1160–1166.

Kjer, K., Borowiec, M. L., Frandsen, P. B., Ware, J., and Wiegmann, B. (2016). Advances using molecular data in insect systematics. *Current Opinion in Insect Science* **18**, 40–47.

Kück, P., Hita Garcia, F., Misof, B., and Meusemann, K. (2011). Improved phylogenetic analyses corroborate a plausible position of *Martialis heureka* in the ant tree of life. *PLoS One* **6**, e21031.

Kugler, J. (1987). The Leptanillinae (Hymenoptera: Formicidae) of Israel and a description of a new species from India. *Israel Journal of Entomology* **20**, 45–57.

Kutter, H. (1948). Beitrag zur Kenntnis der Leptanillinae (Hym. Formicidae): eine neue Ameisengattung aus Süd-Indien. *Mitteilungen der Schweizerische Entomologische Gesellschaft* **11**, 286–295.

Lanfear, R., Calcott, B., Ho, S. Y., and Guindon, S. (2012). PartitionFinder: combined selection of partitioning schemes and substitution models for phylogenetic analyses. *Molecular Biology and Evolution* **29**, 1695–1701.

Lanfear, R., Frandsen, P. B., Wright, A. M., Senfeld, T., and Calcott, B. (2017). PartitionFinder 2: new methods for selecting partitioned models of evolution for molecular and morphological phylogenetic analyses. *Molecular Biology and Evolution* **34**, 772–773.

Leong, C.-M., Yamane, S., and Guénard, B. (2018). Lost in the city: discovery of the rare ant genus *Leptanilla* (Hymenoptera: Formicidae) in Macau with description of *Leptanilla macauensis* sp. nov. *Asian Myrmecology* **10**, e010001.

Lewis, P. O. (2001). A likelihood approach to estimating phylogeny from discrete morphological character data. *Systematic Biology* **50**, 913–925.

López, F., Martinez, M. D., and Barandica, J. M. (1994). Four new species of the genus *Leptanilla* (Hymenoptera: Formicidae) from Spain – relationships to other species and ecological issues. *Sociobiology* **24**, 179–212.

Man, P., Ran, H., Chen, Z., and Xu, Z. (2017). The northernmost record of Leptanillinae in China with description of *Protanilla beijingensis* sp. nov. (Hymenoptera: Formicidae). *Asian Myrmecology* **9**, e009008.

Masuko, K. (1990). Behavior and ecology of the enigmatic ant *Leptanilla japonica* Baroni Urbani (Hymenoptera: Formicidae: Leptanillinae). *Insectes Sociaux* **37**, 31–57.

Matzke, N. J., and Wright, A. (2016). Inferring node dates from tip dates in fossil Canidae: the importance of tree priors. *Biology Letters* **12**, 20160328.

Miller, M. A., Pfeiffer, W., and Schwartz, T. (2010). Creating the CIPRES Science Gateway. In 'Proceedings, the Gateway Computing Environments Workshop (GCE)', 14 November 2010, New Orleans, LA, USA. INSPEC Accession Number 11705685. (Institute of Electrical and Electronics Engineers: Piscataway, NJ, USA.) 10.1109/GCE.2010.5676129

Moreau, C. S., Bell, C. D., Vila, R., Archibald, S. B., and Pierce, N. E. (2006). Phylogeny of the ants: diversification in the age of angiosperms. *Science* **312**, 101–104.

Nguyen, L.-T., Schmidt, H. A., von Haeseler, A., and Minh, B. Q. (2015). IQ-TREE: a fast and effective stochastic algorithm for estimating maximum-likelihood phylogenies. *Molecular Biology and Evolution* **32**, 268–274.

Niehuis, O., Hartig, G., Grath, S., Pohl, H., Lehmann, J., Tafer, H., Donath, A., Krauss, V., Eisenhardt, C., Hertel, J., Petersen, M., Mayer, C., Meusemann, K., Peters, R. S., Stadler, P. F., Beutel, R. G., Bornberg-Bauer, E., McKenna, D. D., and Misof, B. (2012). Genomic and morphological evidence converge to resolve the enigma of Strepsiptera. *Current Biology* **22**, 1309–1313.

O'Reilly, J. E., dos Reis, M., and Donoghue, P. C. J. (2015). Dating tips for divergence-time estimation. *Trends in Genetics* **31**, 637–650.

Ogata, K., Terayama, M., and Masuko, K. (1995). The ant genus *Leptanilla*: discovery of the worker-associated male of *Leptanilla japonica*, and a description of a new species from Taiwan (Hymenoptera: Formicidae: Leptanillinae). *Systematic Entomology* **20**, 27–34.

Patterson, C. (1982). Morphological characters and homology. In ‘Problems of Phylogenetic Reconstruction’. (Eds K. A. Joysey, and A. E. Friday.) pp. 21–74. (Academic Press: London, UK.)

Petersen, B. (1968). Some novelties in presumed males of Leptanillinae (Hym., Formicidae). *Entomologiske Meddelelser* **36**, 577–598.

Pleijel, P. (1995). On character coding for phylogeny reconstruction. *Cladistics* **11**, 309–315.

Rabeling, C., Brown, J., and Verhaagh, M. (2008). Newly discovered sister lineage sheds light on early ant evolution. *Proceedings of the National Academy of Sciences of the United States of America* **105**, 14913–14917.

Rambaut, A., Drummond, A. J., Xie, D., Baele, D., and Suchard, M. A. (2018). Posterior summarization in Bayesian phylogenetics using Tracer 1.7. *Systematic Biology* **67**, 901–904.

Robertson, H. G. (2000). Formicidae (Hymenoptera: Vespoidea). In ‘Dâures Biodiversity of the Brandberg Massif, Namibia’. (Eds A. H. Kirk-Spriggs, and E. Marais.) Cimbabesia Memoir 9, pp. 371–382. (National Museum of Namibia: Windhoek, Namibia.)

Robertson, J. A., and Moore, W. (2017). Phylogeny of *Paussus* L. (Carabidae: Paussinae): unravelling morphological convergence associated with myrmecophilous life histories. *Systematic Entomology* **42**, 134–170.

Ronquist, F., Klopfstein, S., Vilhelmsen, L., Schulmeister, S., Murray, D. L., and Rasnitsyn, A. P. (2012). A total-evidence approach to dating with fossils, applied to the early radiation of the Hymenoptera. *Systematic Biology* **61**, 973–999.

Sánchez, N., Yamasaki, H., Pardos, F., Sørensen, M. V., and Martínez, A. (2016). Morphology disentangles the systematics of a ubiquitous but elusive meiofaunal group (Kinorhyncha: Pycnophyidae). *Cladistics* **32**, 479–505.

Scupola, A., and Ballarin, R. (2009). The genus *Leptanilla* Emery, 1870 in Sicily (Hymenoptera: Formicidae). *Myrmecological News* **12**, 129–132.

Strong, E. E., and Lipscomb, D. (1999). Character coding and inapplicable data. *Cladistics* **15**, 363–371.

Taylor, R. W. (1965). A monographic revision of the rare tropicopolitan ant genus *Probolomyrmex* Mayr (Hymenoptera: Formicidae). *Transactions of the Royal Entomological Society of London* **117**, 345–365.

Ward, P. S., and Fisher, B. L. (2016). Tales of dracula ants: the evolutionary history of the ant subfamily Amblyoponinae (Hymenoptera: Formicidae). *Systematic Entomology* **41**, 683–693.

Ward, P. S., and Sumnicht, T. P. (2012). Molecular and morphological evidence for three sympatric species of *Leptanilla* (Hymenoptera: Formicidae). *Myrmecological News* **17**, 5–11.

Ward, P. S., Brady, S. G., Fisher, B. L., and Schultz, T. R. (2010). Phylogeny and biogeography of dolichoderine ants: effects of data partitioning and relict taxa on historical inference. *Systematic Biology* **59**, 342–362.

Wheeler, G. C., and Wheeler, E. W. (1930). Two new ants from Java. *Psyche* **37**, 193–201.

Wipfler, B., Letsch, H., Frandsen, P. B., Kapli, P., Mayer, C., Buckley, T. R., Donath, A., Edgerly-Rooks, A. S., Fujita, M., Liu, S., Machida, R., Mashimo, Y., Misof, B., Niehuis, O.,

Peters, R. S., Petersen, M., Podsiadlowski, L., Schütte, K., Shimizu, S., Uchifune, T., Wilbrandt, J., Yan, E., Zhou, X., and Simon, S. (2019). Evolutionary history of Polyneoptera and its implications for our understanding of early winged insects. *Proceedings of the National Academy of Sciences of the United States of America* **116**, 3024–3029.

Wong, M. K. L., and Guénard, B. (2016). *Leptanilla hypodracos* sp. n., a new species of the cryptic ant genus *Leptanilla* (Hymenoptera, Formicidae) from Singapore, with new distribution data and an updated key to oriental *Leptanilla* species. *ZooKeys* **551**, 129–144.

Yamada, A., Nguyen, D. D., and Eguchi, K. (2020). Unveiling the morphology of the Oriental rare monotypic ant genus *Opamyrma* Yamane, Bui & Eguchi, 2008 (Hymenoptera: Formicidae: Leptanillinae) and its evolutionary implications, with first descriptions of the male, larva, tentorium, and sting apparatus. *Myrmecological News* **30**, 27–52.

Yang, Z. (1996). Among-site rate variation and its impact on phylogenetic analyses. *Trends in Ecology & Evolution* **11**, 367–372.

Yoder, M. J., Miko, I., Seltmann, K. C., Bertone, M. A., and Deans, A. R. (2010). A gross anatomy ontology for Hymenoptera. *PLoS One* **5**, e15991.

Chapter 2. A remarkable troglomorphic ant, *Yavnella laventa* sp. nov. (Hymenoptera: Formicidae: Leptanillinae), identified as the first known worker of *Yavnella* Kugler by phylogenomic inference[2]

Zachary Hayes Griebenow[3], *Marco Isaia and Majid Moradmand*

Abstract. The ant subfamily Leptanillinae (Hymenoptera: Formicidae) consists of minute soil-dwelling species, with several genera within this clade being based solely upon males, including *Yavnella* Kugler. The dissociation of males and workers has resulted in taxonomic confusion for the Leptanillinae. We here describe the worker caste of *Yavnella*, facilitated by maximum-likelihood and Bayesian inference from 473 partitioned ultra-conserved element loci, this dataset including 49 other leptanilline species, both described and undescribed. *Yavnella laventa* sp. nov. is described from seven worker specimens collected in south-western Iran from the *Milieu Souterrain Superficiel*, a subterranean microhabitat consisting of air-filled cavities among rock and soil fragments, which is subject to similar environmental conditions as caves. This species has bizarrely elongated appendages, which suggests that it is confined to cavities, in contrast with the soil-dwelling behaviour observed in other leptanilline ants. Based on its gracile phenotype relative to other Leptanillinae, *Y. laventa* shows remarkable adaptations for subterranean life, making it one of a very few examples of this syndrome among the ants. Moreover, the discovery of the worker caste of *Yavnella* expands our morphological knowledge of the leptanilline ants. We provide worker- and male-based diagnoses of *Yavnella*, along with a key to the genera of the Leptanillinae for which workers are known. The worker caste of

[2]This chapter was originally published in *Invertebrate Systematics*, 2022, 36(12), 1118–1138, https://doi.org/10.1071/IS22035. Note that some of the information presented herein is superseded by Chapters 4-5.
[3]Lead author. Chapter 2 is included in thesis by approval of committee and permission of Graduate Program Chair of Dept. of Entomology & Nematology, Dr. Joanna Chiu.

Yavnella as known from this species is immediately recognisable, but the possibility must be noted that described workers of Leptanilla may in fact belong to *Yavnella*. Further molecular sampling is required to test this hypothesis.

Introduction

The Leptanillinae (Hymenoptera: Formicidae) are a group of miniscule, cryptic ants, found in many tropical and warm temperate areas of the Old World. Workers are completely blind and exclusively soil-dwelling. The biology of only a few leptanillines has been studied–these are specialized predators of geophilomorph centipedes (Masuko 1990; Hsu *et al.* 2017) or of forcepstails (Diplura: Japygidae) (Ito *et al.* 2021). The subfamily is divided into two monophyletic tribes, Leptanillini and Anomalomyrmini (Bolton 1990; Borowiec *et al.* 2019), with the monotypic genus *Opamyrma* unplaced to tribe (Ward and Fisher 2016). Of the tribe Leptanillini, in only *Leptanilla* Emery, 1870 are the worker and queen known, with the remaining three genera—*Scyphodon* Brues, 1925; *Noonilla* Petersen, 1968; and *Yavnella* Kugler, 1986—known only from male specimens. So far as is known, queens of *Leptanilla* are wingless and blind, resembling miniature versions of the dichthadiigynes observed in army ants of the subfamily Dorylinae (Hölldobler and Wilson 1990; Ito and Yamane 2020), while queens in the Anomalomyrmini are alate (Bolton 1990; Baroni Urbani and de Andrade 2006) or ergatoid (Billen *et al.* 2013).

Conversely, males of Leptanillinae are always fully winged. Due to collecting bias towards males, three genera in the tribe Leptanillini have been described solely from male specimens, as have some species of *Leptanilla*. Further, there is a large diversity of undescribed male morphospecies in the subfamily (Griebenow 2021). The Leptanillinae are therefore afflicted by parallel taxonomy. Out of more than sixty described species, the sexes have been associated only

in *Leptanilla japonica* Baroni Urbani, 1977 (Ogata *et al.* 1995), *Opamyrma hungvuong* Yamane, Bui & Eguchi, 2008 (Yamada *et al.* 2020), and *Protanilla lini* Terayama, 2009 (Griebenow 2020). Males were collected from the same nests as corresponding workers only in *L. japonica* and *O. hungvuong*, with the male of *P. lini* being indirectly identified using phylogenomic inference.

Yavnella is the most recently described of the male-based leptanilline genera, established by Kugler (1987) for two species from Israel and Kerala (India), by original designation. The phylogenetic analyses of Griebenow (2020, 2021) included a variety of undescribed male *Yavnella* morphospecies along with *Yavnella argamani* Kugler, 1987 and recovered the genus as monophyletic with high support, irrespective of data or inferential framework. The genus is most diverse in mainland Southeast Asia (this diversity remaining entirely undescribed), with additional representatives in the Indian subcontinent and the Arabian subcontinent as far south as Yemen (Collingwood and Agosti 1996). Borowiec *et al.* (2019) also robustly recovered this clade, under a sampling regime overlapping with Griebenow (2020, 2021), although Borowiec *et al.* (2019) did not explicitly identify this clade as *Yavnella*.

Here, we describe *Yavnella laventa* **sp. nov.** from Fārs Province, Iran, based on seven worker specimens, collected in the *Milieu Souterrain Superficiel* (MSS) at depths of 0.6-1 meters within a debris flow adjacent to a salt cave entrance. According to Uéno (1980) and Culver and Pipan (2014), the MSS is a subterranean network of empty air-filled cracks and voids. *Yavnella laventa* is here identified as belonging to *Yavnella* based upon phylogenomic inference from ultra-conserved elements (UCEs) and constitutes the first known representatives of the worker caste in that genus. The phenotype of *Y. laventa* is strikingly different from that of all other known leptanilline workers, with the mandibles, antennae and legs being elongated in what are

apparently examples of strong adaptation to subterranean habitats, i.e., troglomorphism. With the discovery of the worker caste of *Yavnella* we provide a revised worker-based key to the genera of the Leptanillinae, with figures.

A natural classification of the Leptanillinae is made difficult by dissociation of the dissimilar worker and male forms of leptanilline ants, which results in parallel taxonomy. Therefore, the identification of the worker caste of *Yavnella*, a major leptanilline clade heretofore known only from male specimens, begins to correct this parallel taxonomy. The phylogenomic approach by which *Y. laventa* was identified as *Yavnella*, despite the lack of known conspecific male specimens with which to determine the generic identity of this species, affirms the utility of molecular data in connecting unassociated and drastically divergent forms in polymorphic organisms.

From an ecological perspective, the troglomorphism exhibited by *Y. laventa* is remarkable in the context of the Formicidae as a whole. After *Leptogenys khammouanensis* Roncin & Deharveng, 2003 (Ponerinae: Ponerini) and *Aphaenogaster gamagumayaa* Naka & Maruyama, 2018 (Myrmicinae: Stenammini) *Y. laventa* is only the third arguably troglomorphic ant species described (Roncin and Deharveng 2003; Naka and Maruyama 2018), out of >15,000 described species. By contrast to *L. khammouanensis* and *A. gamagumayaa*, *Y. laventa* was not collected in an underground space between rocks accessible to humans (i.e., a “cave”), but in the network of subterranean fissures and voids that constitutes the MSS, which is known to harbor species with troglomorphic traits (see Mammola *et al.* [2016] for a comprehensive review on the topic).

Materials and Methods

Materials

In total, 63 specimens belonging to the Leptanillinae were included in this study, in addition to *Martialis heureka* Rabeling & Verhaagh, 2008 (Martialinae) as an outgroup. Ultra-conserved element (UCE) data are included in this study for 51 taxa of those 63, including *M. heureka*, a representative of *Y. laventa* (CASENT0842745), along with representatives of all major subclades of that subfamily. Fourteen of these specimens are newly sequenced in this study. Twelve specimens of *Protanilla* Taylor in Bolton, 1990 and *Leptanilla* along with one *Anomalomyrma* Taylor in Bolton, 1990 were morphologically examined, but not sequenced (Table 2.S1). Generic assignment of sequenced material follows Griebenow (2020) rather than Borowiec *et al.* (2019) where sampling overlaps with those studies. Additional collection data for these specimens are provided in a supplemental table (Table 2.S2).

Specimens are deposited at the following institutions (abbreviations follow Evenhuis 2021, where applicable): the California Academy of Sciences, San Francisco, USA (CAS); the California State Collection of Arthropods, Sacramento, USA (CSCA); the Biodiversity Museum, University of Hong Kong, Hong Kong, China (HKUBM); the Jalal Afshar Zoological Museum, Department of Plant Protection, College of Agriculture and Natural Resources, University of Tehran, Karaj, Iran (JAZM); Lund University, Lund, Sweden (MZLU); National Changhua University of Education, Changhua, Taiwan (NCUE); the Okinawa Institute of Science & Technology, Onna-son, Japan (OIST); the Royal Ontario Museum, Toronto, Ontario, Canada (ROME); the R. M. Bohart Museum of Entomology, University of California, Davis, USA (UCDC); the Museum für Naturkunde der Humboldt-Universität, Berlin, Germany (ZMHB); and Zoological Museum, University of Isfahan, Isfahan, Iran (ZMUI).

Collection and Specimen Preparation

Specimens of *Yavnella laventa* **sp. nov.** were collected using subterranean sampling devices, i.e., two buried pitfall traps, placed in the MSS. The buried pitfall traps (hereinafter "MSS traps") consisted of a rigid plastic cup, with holes bored in them midway from top to bottom to prevent flooding, and a horizontal stone placed on top. These were set in a clast on the bank of a wadi, opposite to a salt diapir (Fig. 2.1) (the Khoorab Salt Dome; Abbassi *et al.* 2015). These MSS traps were placed via slope boring at depths of 60-100 cm., baited with sardines and dates jointly contained in small vials, and half-filled with brine. We attempted to measure relative humidity (RH) within the MSS using a Lascar EL-USB-2 data logger buried adjacent to the MSS traps. Brine is not an ideal preservative for purposes of acquiring DNA but was used in a broad survey of salt karst fauna in the vicinity of Khoorab, due to low evaporative rate. Although extraction of a genome-scale molecular dataset was successful when attempted with a single specimen (see "Sequencing & Data Processing"), we recommend that future targeted efforts to collect leptanilline ants in the MSS or in salt caves use ethanol as a preservative, with traps being set for much briefer periods.

Traps were left for 15 months, from February 14, 2019 to June 26, 2020, at the end of which specimens were transferred to 80% or 95% ethanol, the latter if intended for non-destructive DNA extraction. A few specimens remained in brine and were used for dissection and imaging. In addition, four pitfall traps baited in the same way and containing the same liquid were placed at ground level inside an adjacent salt cave ("Last Cave") within the Khoorab Salt Dome, for the same duration as the MSS traps, but no *Y. laventa* were collected in these traps. We measured RH within Last Cave using the same data loggers as listed above.

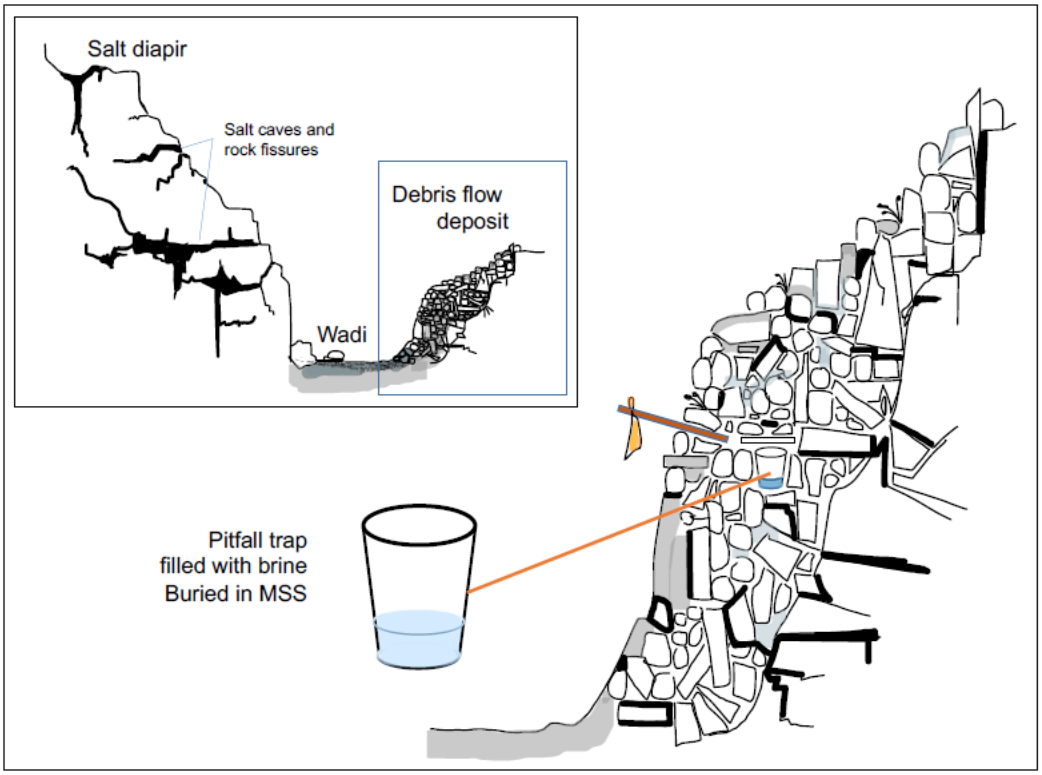

Figure 2.1. Layout of MSS traps, and position relative to the adjacent salt diapir (the Khoorab Salt Dome) in which Last Cave is located.

Sequencing & Data Processing

For the specimens newly sequenced for this study, DNA was extracted non-destructively using a Dneasy Blood & Tissue Kit (Qiagen Inc., Valencia, CA) with H_2O at room temperature to elute DNA, or, in the case of CASENT0842745 and several other samples, 56°C buffer AE (Cruaud *et al.* 2019) in order to increase DNA yield. Genomic concentrations were quantified for each sample with a Qubit 2.0 fluorometer (Life Technologies Inc., Carlsbad, CA). Input DNA was sheared using a Diagenode Bioruptor (Diagenode, Denville, NJ) or Qsonica Q800R3-110 (Qsonica Inc., Newtown, CT). Sheared product was used as input for the modified library preparation protocol of Branstetter *et al.* (2017), with the ant-specific version of the UCE probe set *hym-v2* (Branstetter *et al.* 2017). Enrichment success and size-adjusted DNA concentrations of pooled libraries were assessed using the SYBR FAST qPCR kit (Kapa Biosystems,

Wilmington, MA), and all pools were combined into an equimolar final pool. Final pools were sequenced on an Illumina HiSeq X at Novogene (Sacramento, CA) or prepared, enriched and sequenced using similar protocols at RAPiD Genomics (Gainesville, FL). Refer to Ward and Blaimer (2022) for further details on library preparation and enrichment. For sequencing protocols implemented for the phylogenomic data used in this study that have been previously published, refer to Griebenow (2020).

The FASTQ output was demultiplexed and cleansed of adapter contamination and low-quality reads using *illumiprocessor* (B. C. Faircloth, see https://github.com/faircloth-lab/illumiprocessor) in the PHYLUCE bioinformatic software package, v. 1.7.1 (Faircloth, 2016). Raw reads were assembled with SPAdes v. 3.12.0 (Bankevich *et al.* 2012). Species-specific contig assemblies were obtained with the ant-specific *hym-v2* probe set (Branstetter *et al.* 2017), aligned with MAFFT L-INS-I (Katoh and Toh 2010), and trimmed with Gblocks (Castresana 2000) within a PHYLUCE workflow modified from Faircloth (2016) with min_identity = 80 within *phyluce_assembly_match_contigs_to_probes.py*, resulting in an alignment 313,498 bp in length. This alignment was 76.79% complete, comprised of 39.1% parsimony-informative sites; AT content was 57.4%. Summary statistics for this alignment were computed with the *summary* command in AMAS (Borowiec, 2016) (Table 2.S1).

Phylogenomic Inference

Partitioning to generate subsets of each UCE locus was performed using PartitionUCE (Tagliacollo and Lanfear 2018). Using IQ-Tree v. 2.1.2 (Minh *et al.* 2020) on the CIPRES Science Gateway (v. 3.3) (Miller *et al.* 2010), partition schemes were inferred with ModelFinder (Kalyaanamorthy *et al.* 2017) using subsets generated by PartitionUCE for the complete alignment, with the Bayesian Information Criterion (BIC) deciding among available partitioning

schemes, followed by maximum-likelihood (ML) phylogenetic inference under these partition schemes (Chernomor *et al.* 2016) for 1,000 ultrafast bootstraps (UFBoot) (Hoang *et al.* 2018) and SH-like approximate likelihood ratio test (SH-aLRT) (Guindon *et al.* 2010) replicates. The relaxed hierarchical clustering algorithm was implemented in these analyses (Lanfear *et al.* 2014), with ModelFinder considering only the most likely 20% of partition schemes. Substitution models with I+G extensions to accommodate among-site rate heterogeneity were permitted, as IQ-Tree v. 2.1.2 implements an optimization heuristic that effectively compensates for the non-identifiability of these models (Nguyen *et al.* 2018). Bayesian inference was performed in ExaBayes v. 1.5.1 (Aberer *et al.* 2014) on the CIPRES Science Gateway under the partitioning scheme produced by ModelFinder in IQ-Tree (as described above) with GTR+G imposed across all partitions, all parameters unlinked, with the single Markov Chain Monte Carlo (MCMC) running until the average standard deviation of split frequencies (ASDSF) of topologies <0.05, for 100,000 generations, branch lengths treated as unlinked. Convergence of the MCMC with respect to continuous parameters was visually assessed in Tracer v. 1.7 (Rambaut *et al.* 2018).

Nomenclature

Nomenclature for sculpturation follows Harris (1979); setation, Wilson (1955) and Boudinot *et al.* (2020). Notation of palp and tibial spur formulae follows Bolton (2003). Cephalic nomenclature follows Richter *et al.* (2021) and Boudinot *et al.* (2021). Mesosomal nomenclature follows Liu *et al.* (2019); metasomal, Lieberman *et al.* (2022). Male genital nomenclature follows Boudinot (2018).

Measurements

Sorting and initial examination of the material was done using an Echo-Lab SM203H stereomicroscope (DEVCO, Milan, IT). Morphometric data for four specimens of *Y. laventa* are included in Table 2.1. Detailed morphological study of these specimens was performed with a Leica MZ75 compound microscope (Leica Microsystems, Oak Grove, IL) at magnifications of up to 50x. Photographs were obtained as image stacks via a Leica DMC2900 camera attached to a Leica MZ16A stereomicroscope or using the Visionary Digital Imaging System (Visionary Digital™, Richmond, VA), with *z*-stepping via the Leica Application Suite (LAS) software (v. 4.13.0) and montaged with Helicon Focus Pro (Helicon Software Ltd., Kharkiv, UP). Scanning electron microscopy was performed with a Hitachi TM4000 (Hitachi Global, Tokyo, JP). Measurement and index definitions are provided below.

HW = maximum width of cranium in full-face view

HL = Head Length, maximum length of head in full-face view from anterior margin of head to cranial vertex

SL = Scape Length, maximum length of scape in medial view, excluding bulbus

MaL = Mandible Length, maximum length of mandible from view orthogonal to lateral mandibular margin, measured from ventral mandibular articulation to mandibular apex

WL = Weber's Length, maximum diagonal length of mesosoma in profile view, measured from most anterior extent of pronotum excluding cervical shield to most posterior extent of propodeal lobes, when present

PrW = Pronotal width, maximum width of pronotum, measured in dorsal view

MW = Mesonotal width, maximum width of mesonotum in dorsal view, measured immediately anterior to mesocoxal foramina

PTL = Petiolar length, maximum length of petiole in dorsal view, not including presclerites

PTH = Petiolar height, maximum height of petiole in profile view, including sternal process and dorsal node, if distinct

PTW = Petiolar width, maximum width of petiole in dorsal view

PPL = Postpetiolar length, maximum length of postpetiole in dorsal view, not including presclerites

PPW = Postpetiolar width, maximum width of postpetiole in dorsal view

PPH = Postpetiolar height, maximum height of postpetiole in profile view, including sternal process and dorsal node, if distinct

Indices

CI = (HW / HL) × 100

SI = (SL / HW) × 100

MI = (MaL / HW) × 100

PI = (PTW / PTL) × 100

PPI = (PPW / PPL) × 100

PPHI = (PPH / PPL) × 100

	CASENT0842746	CASENT0842745	CASENT0842747	CASENT0842748
Measurements				
HW	0.353	N/A	0.358	0.332
HL	0.491	0.512	0.497	0.490
SL	0.564	0.588	0.585	0.554
MaL	0.264	0.256	0.275	0.265
WL	0.844	0.820	0.848	0.736
PrW	0.199	0.228	0.214	0.211
MW	0.159	0.163	0.165	0.143
PTL	0.232	0.230	0.238	0.222
PTH	0.097	0.096	0.100	0.089
PTW	0.071	0.067	0.069	0.071
PPL	0.133	0.139	0.133	0.122
PPW	0.086	0.085	0.083	0.072
PPH	0.119	0.118	0.121	0.119
Indices				
CI	71.894	N/A	72.032	68
SI	159.773	N/A	163.408	167
MI	53.768	50.000	55.332	80
PI	30.603	29.130	28.992	32
PPI	64.662	61.151	62.406	59
PPHI	72.269	72.034	68.595	98

Table 2.1. Measurements and indices for the type series of *Yavnella laventa*. Measurements are provided in millimeters.

Results

Phylogeny

Maximum-likelihood phylogenomic inference from a 313,498-bp alignment consisting of 473 UCEs, partitioned within-locus, corroborates the phylogeny of Leptanillinae as recovered by Griebenow (2020). All nodes along the backbone of the tree are recovered with high support under ML, with sub-maximal UFBoot/SH-aLRT values being restricted to the sister-group relationships of two terminals within *Yavnella*. Phylogenomic inference under a Bayesian framework, partitioned using a scheme derived according to an information-theoretic criterion (BIC) using ModelFinder in IQ-Tree v. 2.1.2, recovers all internal nodes of the phylogeny with maximal Bayesian posterior probability (BPP), with nearly all estimated parameters having an effective sample size (ESS) of >200 (the exceptions with ESS=190-191). *Yavnella laventa* is likewise robustly recovered within *Yavnella* with maximal support under ML and Bayesian frameworks (UFBoot, SH-aLRT=100; BPP=1) and sister to *Yavnella argamani* (UFBoot, SH-aLRT=100; BPP=1) (Fig. 2.2).

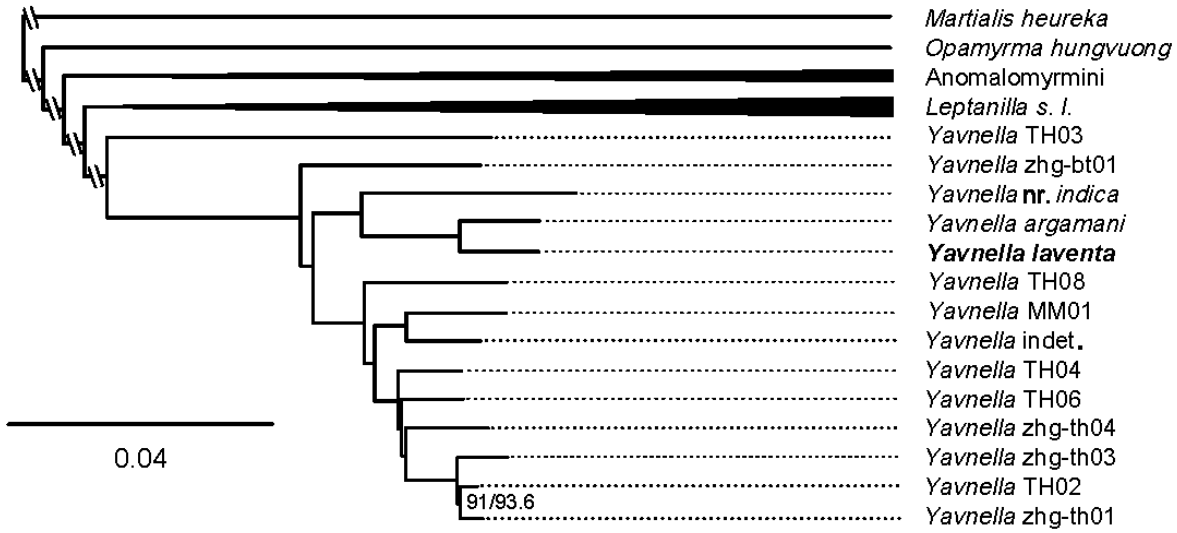

Figure 2.2. Maximum-likelihood phylogeny of the Leptanillinae, inferred from an alignment of 473 ultra-conserved elements (UCEs) partitioned within-locus (Tagliacollo & Lanfear 2018;

Kalyaanamorthy *et al.* 2017) and rooted *a posteriori* on *Martialis heureka* as an outgroup. The Anomalomyrmini (9 terminals) and *Leptanilla s. l.* (26 terminals) are collapsed. Node support values are UFBoot and SH-aLRT, respectively, and are only noted when <100. The phylogeny of the Leptanillinae inferred from the same data using a Bayesian approach was identical to the ML phylogeny shown here and is provided on Zenodo (10.5281/zenodo.5595290). Branch length is expressed in number of expected substitutions per site.

Class Insecta Linnaeus, 1758

Order Hymenoptera Linnaeus, 1758

Family Formicidae Latreille, 1809

Subfamily Leptanillinae Emery, 1910

Tribe Leptanillini Emery, 1910

Diagnosis (worker-based). Palp formula 2,1 or 1,1. Mandible without differentiated basal and masticatory margins. Medial mandibular margin without regularly spaced serration (Fig. 2.3C-D). Peg-like chaetae absent from mandible and labrum. Clypeus without median demarcation from frons by posterior carina, anteroposteriorly compressed anterior to antennal toruli, with antennal torulus adjacent to *or* abutting anterior margin of cranium (Fig. 2.3C-D); antennal socket fully exposed. Compound eye absent. Frontal carina absent. Antenna 12-merous. Promesonotal articulation highly flexible. Mesotibia with 0-2 apical spurs. Propodeal lobe absent; propodeal spiracle situated low on propodeum. Abdominal segments II-III with tergosternal fusion. Spiracle of abdominal segment III very large and placed far forward. Abdominal segment III posteriorly constricted, forming postpetiole (Fig. 2.4). Spiracles of abdominal segments IV-VII concealed by posterior margins of preceding tergites. Abdominal segment IV without tergosternal fusion; stridulitrum absent from abdominal presclerite IV. Abdominal tergite VII large, with simple posterior margin. Sting present. Pretarsal claw without apical tooth on inner margin.

Genus ***Yavnella*** Kugler, 1987

Yavnella Kugler, 1987 [“1986”]: 52. Type species: *Yavnella argamani*, original designation.

Diagnosis (worker-based)

Three mandibular teeth present (Fig. 2.5A). Palp formula 2,1 (Fig. 2.5C). Mesotibia with 2 apical spurs. Petiole much longer than wide in dorsal view (PI≤31) (Fig. 2.4), without distinct anterior peduncle. Abdominal segment IV constricted anteriorly in dorsal view; total length of abdominal segment IV greater than that of abdominal segments V-VII combined.

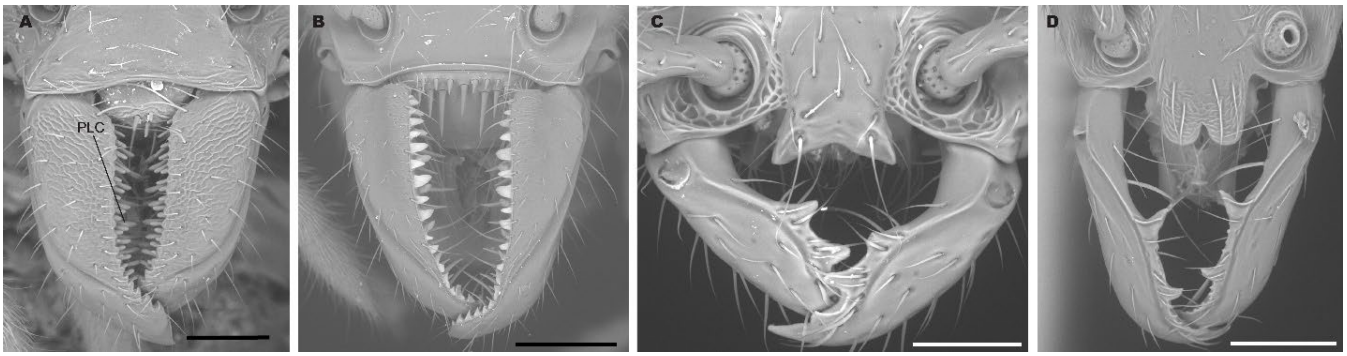

Figure 2.3. Full-face view of mandibular armature across the Leptanillinae. **A.** *Protanilla beijingensis* (CASENT0842639). Regular serration at mandibular apex outlined in red. **B.** *Anomalomyrma* indet. (CASENT0178553). **C.** *Leptanilla thai* (CASENT0842784). **D.** *Yavnella laventa* (CASENT0842745). PLC=peg-like chaetae. Scale bar A, B = 0.2 mm.; C = 0.04 mm.; D = 0.1 mm.

Diagnosis (male-based)

Palp formula 1,1. Ocelli present and set on a distinct tubercle (Griebenow 2020: fig. 5A), rarely absent (Griebenow 2020: fig. 6A); if present, anteromedian ocellus orthogonally dorsal to compound eye in profile view (Griebenow 2020: fig. 12Bi). Procoxa without distal transverse carina (cf. Petersen 1968: p. 583; fig. 8). Protrochanter not elongated relative to meso- and metatrochanter. Profemur without sinuate medial carina or ventral hook. Medioventral carina (Griebenow 2021: fig. 1) and comb (Griebenow 2021: fig. 3) absent from protibia. Notauli absent. Pronotum and mesoscutum not anteroposteriorly elongated. Pterostigma absent

(Griebenow 2020: fig. 4B). Recurved posteroventral process absent from mesoscutellum (Griebenow 2021: fig. 16A). Lower metapleuron indistinct. Propodeal declivity concave in profile view (Griebenow 2021: fig. 19B); propodeum without dorsolateral carina. Petiole reduced, without distinct dorsal node. Abdominal tergite VIII broader than long. Volsellae present, not dorsoventrally compressed and lamellate; fully articulated medially; parossiculus and lateropenite not distinguishable. Phallotreme apical, not surrounded with dense vestiture of setae.

Yavnella laventa Griebenow, Moradmand & Isaia, sp. nov.

(Figs. 2.4-11)

urn:lsid:zoobank.org:act:1BCBAA0B-753E-4DD4-8CFA-43CC25BCE68E

Material Examined

Holotype. Iran, Fārs: **1.3km E Khoorab** [in *Milieu Souterrain Superficiel*], 60 cm. [below surface], 28.59843°N 52.32863°E [±10m], alt. 620m, MSS2, 14.II.2019-26.VI.2020, M. Isaia & M. Moradmand leg. (ZMHB CASENT0842746), ☿.

Paratypes. Iran, Fārs: **1.3km E Khoorab** [in *Milieu Souterrain Superficiel*], 60 cm. [below surface], 28.59843°N 52.32863°E [±10m], alt. 620m, MSS2, 14.II.2019-26.VI.2020, M. Isaia & M. Moradmand leg., 1 ☿ (ZMUI CASENT0842745); **ibid.**, 3 ☿ (ZMUI CASENT0842747, ZMUI CASENT0842795, ZMUI CASENT0842796); **ibid.**, 1 ☿ (JAZM CASENT0842797); **1.3km E Khoorab** [in *Milieu Souterrain Superficiel*], 100 cm. [below surface], 28.59841°N 52.32856°E [±10m], alt. 618m, MSS4, 14.II.2019-26.VI.2020, M. Isaia & M. Moradmand leg., 1 ☿ (ZMHB CASENT0842748).

Other material examined. Iran, Fārs: **1.3km E Khoorab** [in *Milieu Souterrain Superficiel*], 60 cm. [below surface], 28.59843°N 52.32863°E ±10m, alt. 620m, MSS2, 14.II.2019-26.VI.2020, M. Isaia & M. Moradmand leg., 1 ☿ (head and hind leg) (ZMHB CASENT0842789); **ibid.**, 1 ☿ (mesothorax and metapectal-propodeal complex with hind leg) (ZMHB CASENT0842790).

Diagnosis (worker-based)

As for genus (see above).

Diagnosis (male-based)

Male unknown.

Etymology

Named after *La Venta Esplorazioni Geografiche*, the organization that facilitated the 2019 faunal survey of southwestern Iranian salt caves and their vicinity, during which the type series of this species was collected. The specific epithet is a noun in apposition and is therefore invariant.

Figure 2.4. Propodeum and abdominal segments II-IV of *Yavnella laventa* (CASENT0842746), dorsal view. Scale bar = 0.1 mm.

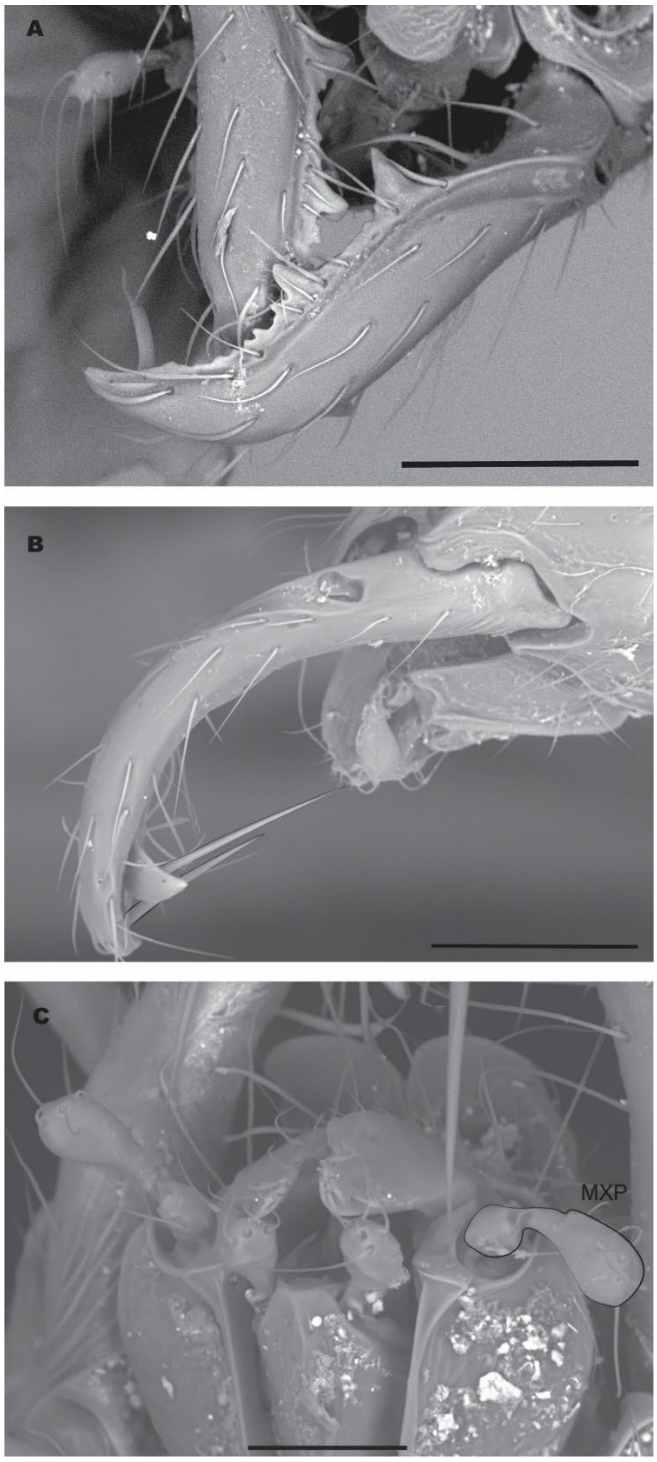

Figure 2.5. Mouthparts of *Yavnella laventa*. **A.** Mandibles, dorsal oblique view (CASENT0842789). **B.** Mandibles, profile view. Putative "trigger hairs" outlined in black. **C.** Mouthparts of *Yavnella laventa*, ventral view (CASENT0842789). MXP = maxillary palp. Scale bar A, B = 0.1 mm.; C = 0.05 mm.

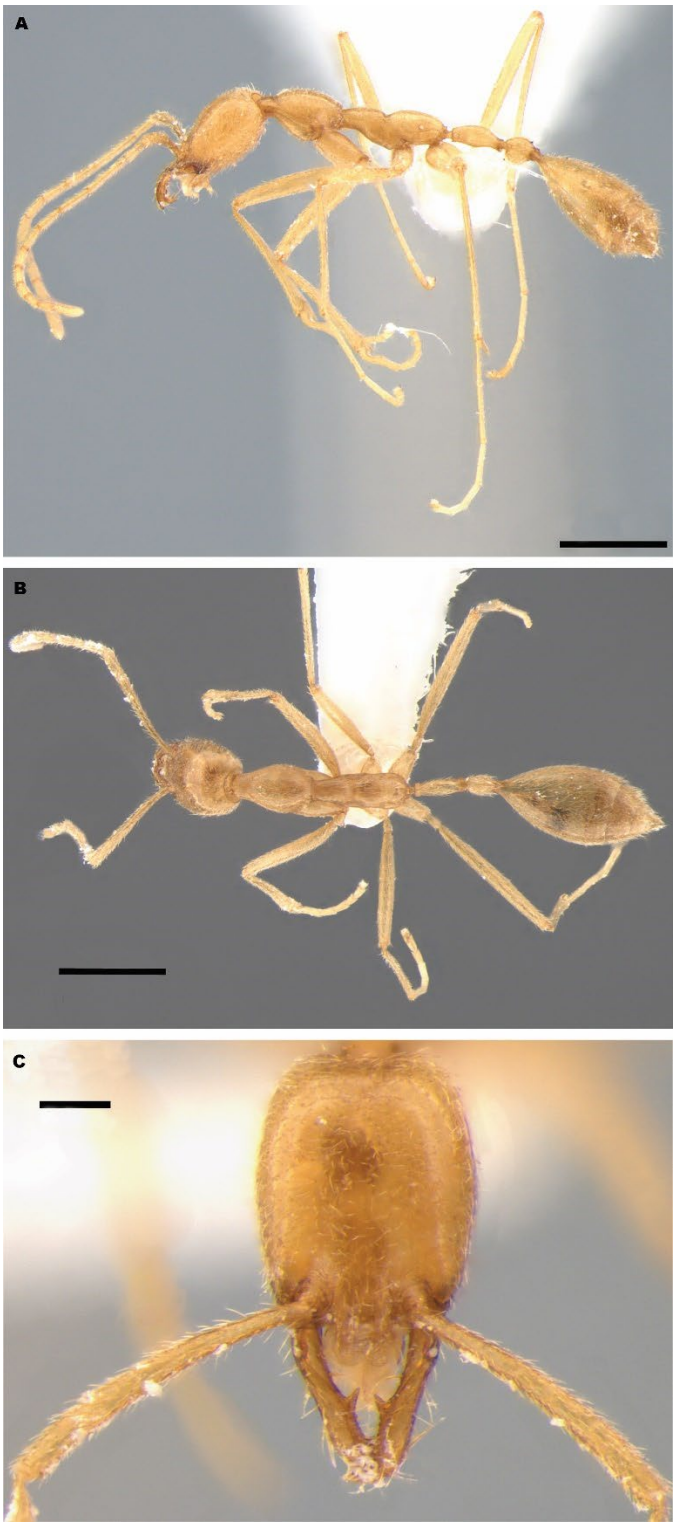

Figure 2.6. *Yavnella laventa*, holotype (CASENT0842746). **A.** Profile view. **B.** Dorsal view. **C.** Full-face view. Scale bar A, B = 0.5 mm.; C = 0.1 mm.

Description

Head. Cranium longer than wide in full-face view (CI=68-72). In full-face view, vertex of cranium emarginate; occiput anteroposteriorly narrow, occipital carina completely encircling occipital foramen (Fig. 2.7). Lateral margins of cranium slightly convex. Frontal carina absent. Antennal insertion exposed. Frontoclypeal process present, delimited from cranium by lateral carinae (Fig. 2.8), without posteromedian delimitation from cranium, projecting well anterior of labrum in full-face view; frontoclypeal process laminate, broad in outline, with apex emarginate, and anterolateral corners lobate (Fig. 2.8). Clypeus anteroposteriorly compressed anterior to antennal toruli; epistomal sulcus absent.

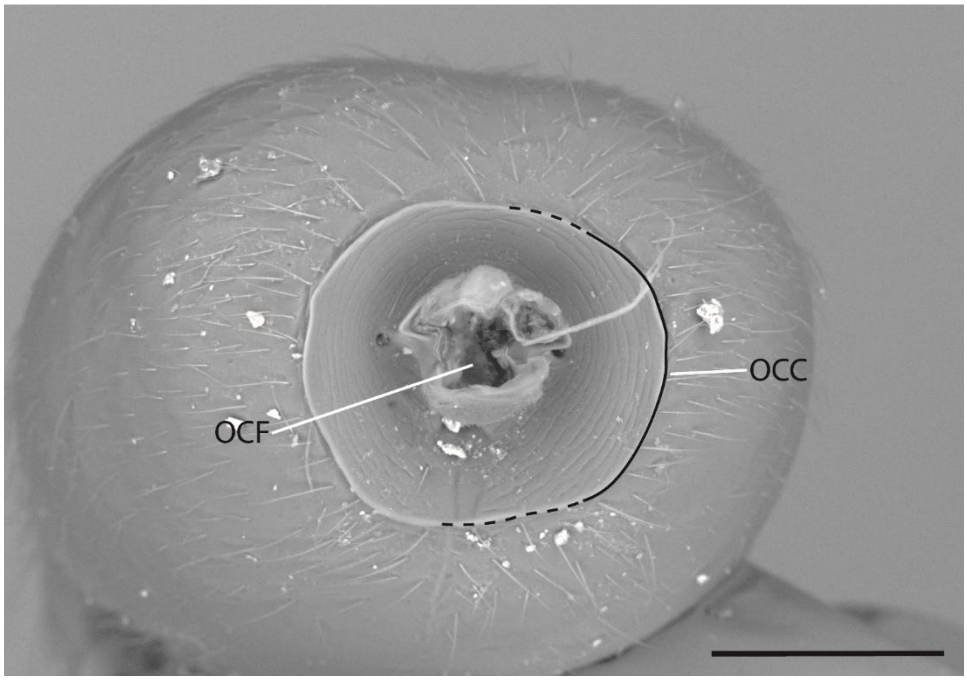

Figure 2.8. Cranium of *Yavnella laventa* (CASENT0842789), posterior view. OCC=occipital carina; OCF=occipital foramen. Scale bar = 0.1 mm.

Anterior tentorial pit not visible. Antennal torulus circular. Hypostomal carina present. Postgenal ridge extending from hypostoma to occipital carina. Mandible projecting anteriorly at rest (Fig. 2.3D). Mandalus small and bean-shaped in outline. Lateral mandibular groove extending along 1/3 of mandible surface, with a smaller groove laterad the longitudinal line, beginning at the basal tooth; both grooves merging proximad subapical tooth. Medial mandibular margin not

divided into basal and masticatory portions. Three teeth present on mandible, apical tooth acute; basal tooth larger than subapical tooth, tip recurved; margin distal to subapical tooth irregularly serrate (Fig. 2.5A). Large, tapering basal and subapical setae present on mandible (Fig. 2.5B). Peg-like chaetae absent from mandible. Labrum concealed by frontoclypeal process in full-face view; peg-like chaetae absent from labrum. Palp formula 2,1 (Fig. 2.5C). Ventral premental face elliptical. Antennae 12-merous. Scape elongated, extending well beyond cranial vertex at rest (SI=160-163); margins subparallel, slightly expanded towards apex. Pedicel longer than broad; constriction separating pedicel from flagellum not pronounced. Flagellum filiform; all flagellomeres longer than broad, with antennomere 3 longer than length of any of the distal antennomeres (Fig. 2.6A-B); apex of antennomere 12 slightly tapered.

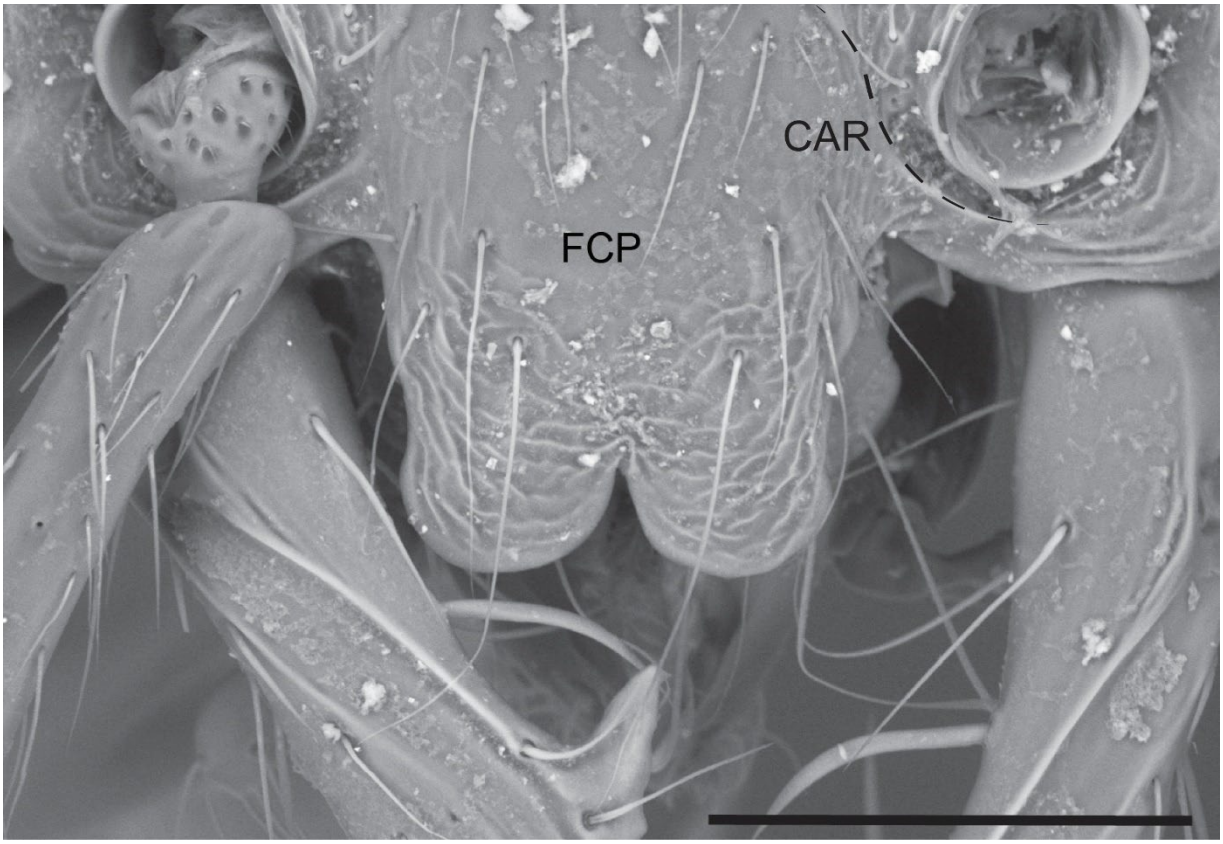

Figure 2.8. Frontoclypeal process of *Yavnella laventa* (CASENT0842789), full-face view. CAR=lateral carina; FCP=frontoclypeal process. Scale bar = 0.1 mm.

Mesosoma. In dorsal view, pronotal outline anteroposteriorly oblate, maximum width (PrW=0.199-0.228) greater than that of mesonotum, or of the propodeum (Fig. 2.6B). Pronotal dorsum convex, elevated above dorsal mesonotal vertex. Promesonotal suture present, highly flexible. Mesonotum constricted anteriorly in dorsal view, with maximum width <PrW (Fig. 2.6B); indistinct from mesopleural region. Mesothorax dorsoventrally constricted and anteroposteriorly elongated posterad the promesonotal suture in profile view (Fig. 2.6A). Meso-metapleural suture absent; in profile view, fusion of mesonotum with propodeum marked by excavation. Propodeum not constricted anteriorly in dorsal view, with outline subrectangular. Metapleural gland bulla large, anterior margin extending slightly anterior to anterior margin of propodeal spiracle. Metapleural gland orifice longitudinally elongated, curving posteriorly towards dorsum, overhung by longitudinal flange (Fig. 2.9).

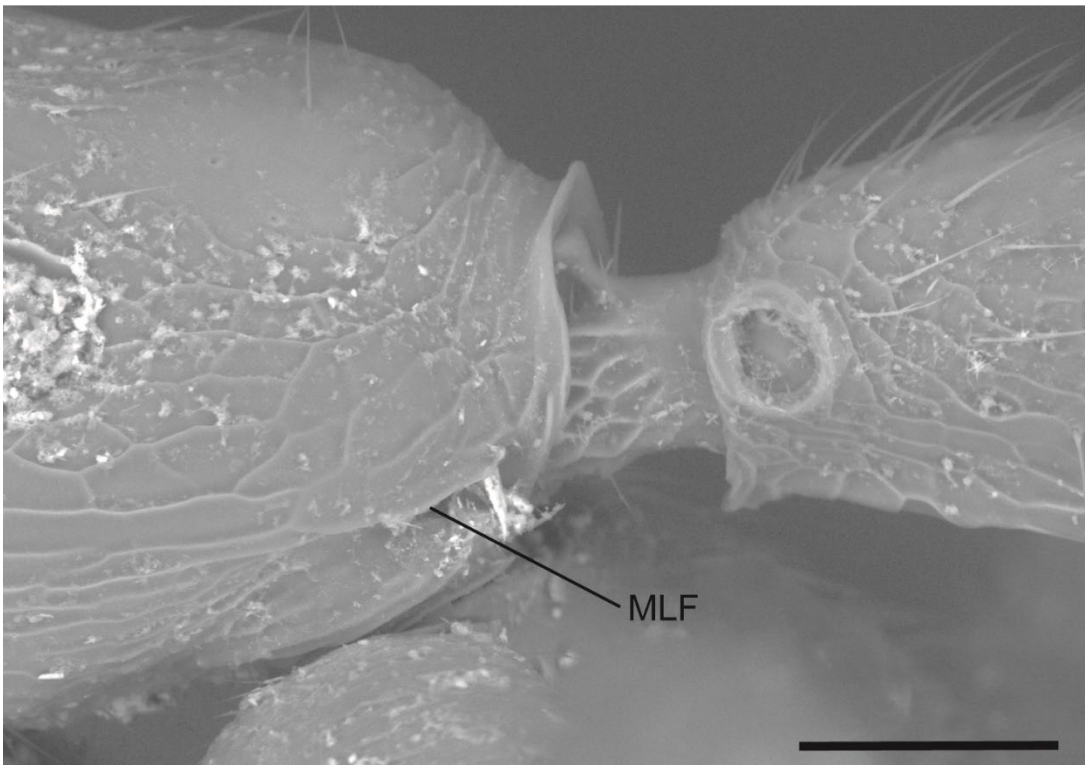

Figure 2.9. Propodeum and anterior petiole of *Yavnella laventa* (CASENT0842745), profile view. MLF = metapleural longitudinal flange. Scale bar = 0.05 mm.

Propodeal declivity convex in profile view. Coxae robust, pro- and mesocoxae well-separated; distal leg articles elongated (Fig. 2.10B). Metacoxal dorsum unarmed. Tibial spur formula 2b,1p. Calcar large, anterior margin densely pectinated (Fig. 2.10A), posterior surface bare, velum large; apex of posterior margin with two subapical spines (Fig. 2.10B); posterior stout seta absent from protibia. Anterior mesotibial spur reduced, barbulate with slight splintering; posterior mesotibial spur with pronounced barbulation. Metatibial spur pectinate (Fig. 2.10D). Meso- and metabasitarsus less than one half the length of meso- and metatibia, respectively. Anterior surface of probasitarsus with single row of acute scale-like cuticular processes (Fig. 2.10A); posterior surface bare of such processes. Tarsomeres with traction chaetae small and restricted to distal margins. Pretarsal claws unarmed, length less than that of tarsomere 5. Arolium present.

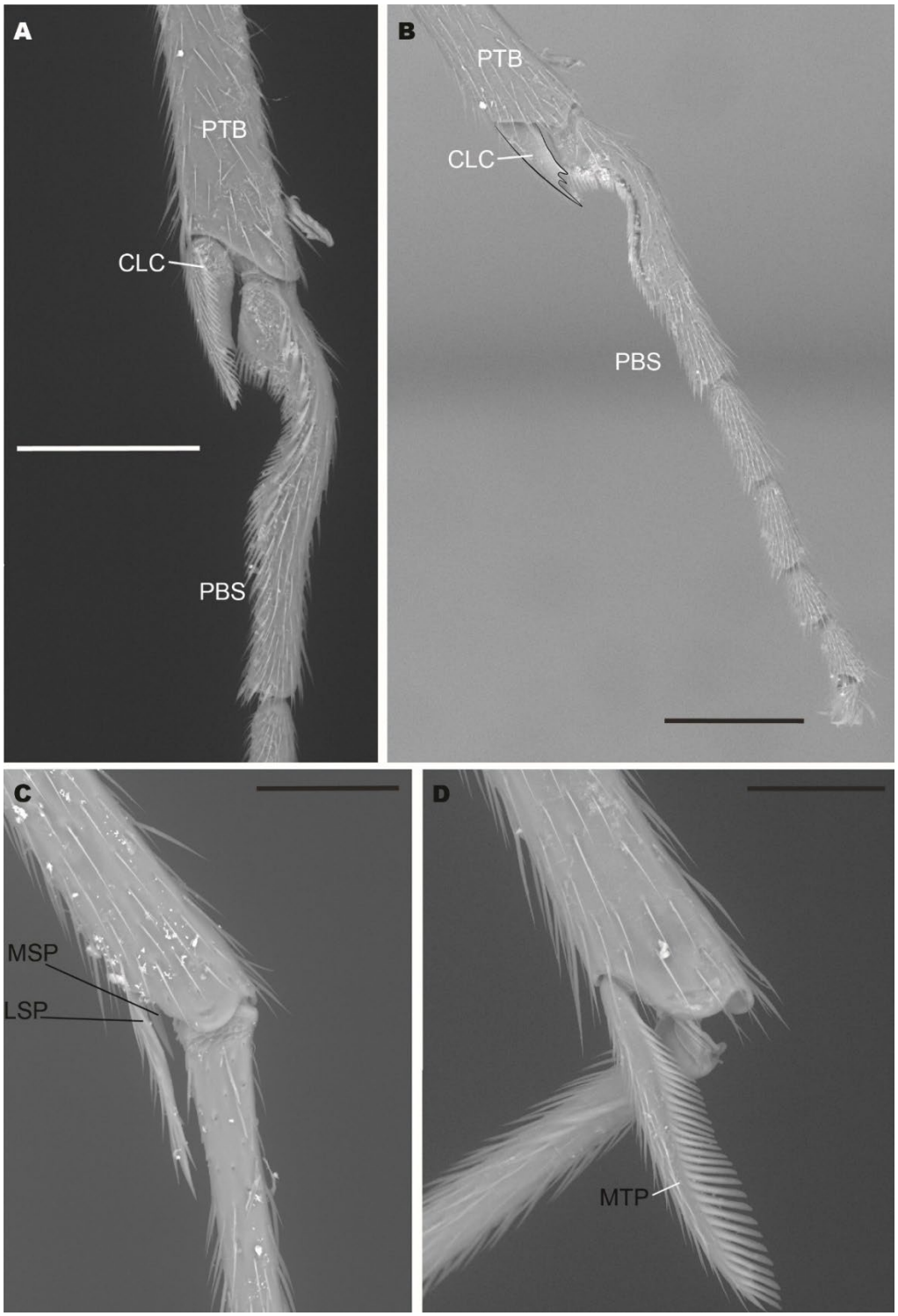

Figure 2.10. Tibial spurs of *Yavnella laventa*. **A.** Antennal strigil, anterior view (CASENT0842745). **B.** Protarsus, posterior view; calcar outlined (CASENT0842745). **C.** Mesotibia and mesobasitarsus, posterior view (CASENT0842746). **D.** Metatibial spur (CASENT0842789), posterior view. CLC=calcar; PTB=protibia; PBS=probasitarsus; MSP=anterior mesotibial spur; LSP=posterior mesotibial spur; MTP=metatibial spur. Scale bar A = 0.1 mm.; B = 0.2 mm.; C= 0.05 mm.; D = 0.1 mm.

Metasoma. Anterior margin of petiole linear in dorsal view. Abdominal spiracle II very large, situated well forward on petiole. Petiole much longer than wide (PI=29-32) (Fig. 2.4), without distinct dorsal node or ventral process; sessile; tergosternal fusion complete, with anterior ½ of abdominal sternite II delimited by longitudinal carinae, converging anteriorly in ventral view (Fig. 2.11); lateral margins subparallel in dorsal view. Dorsal and ventral surfaces of petiole shallowly convex in profile view. Abdominal spiracle III very large, situated well forward on postpetiole. Abdominal segment III posteriorly constricted, forming postpetiole; somewhat longer than wide (PPI=59-65); tergosternal fusion complete, with longitudinal sutures not converging anteriorly in ventral view; lateral margins convex in dorsal view (Fig. 2.4). Prora distinct. Abdominal segment IV longer than length of posterior abdominal segments combined, constricted into "neck" immediately posterior to abdominal segment III. Abdominal segments IV-VIII without tergosternal fusion. Abdominal sternite VII entire and unarmed. Sting well-developed.

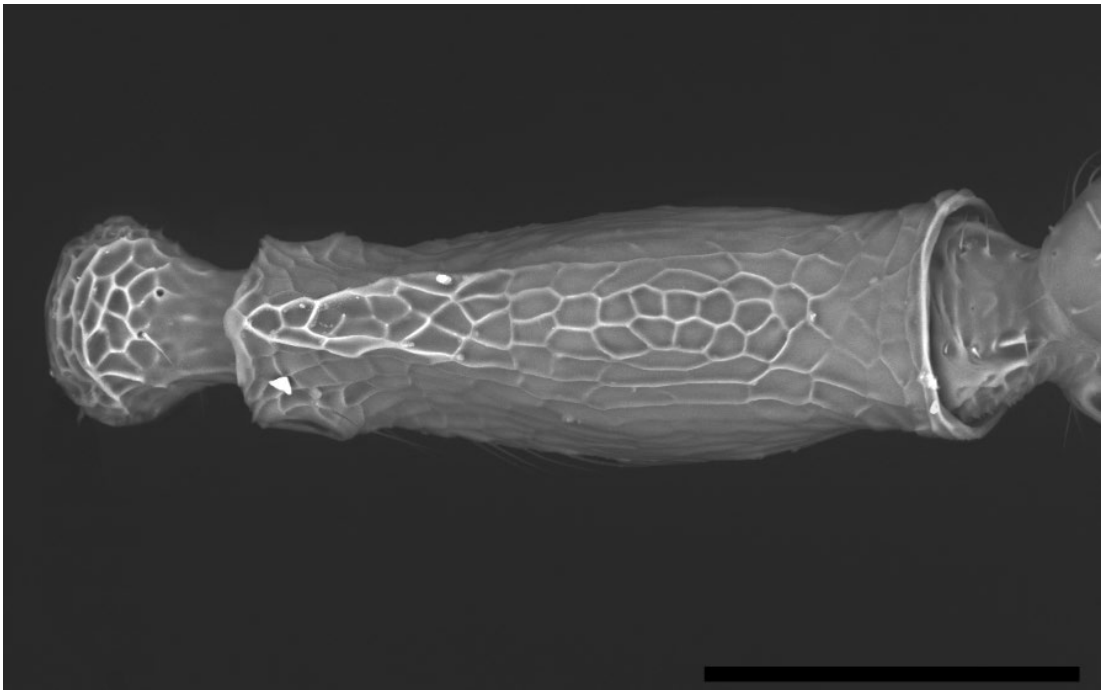

Figure 2.11. Ventral view of abdominal sternite II of *Yavnella laventa* (CASENT0842745). Scale bar = 0.1 mm.

Integument. Somal surface smooth to scabrous; mostly scabriculous. Anterior margins of pronotum, meso- and metapleuron, and abdominal sternite II areolate (Fig. 2.11) to rugose. Occiput substrigulose (Fig. 2.7). Appendages mostly unsculptured. Coloration orangish-yellow, extremities paler. Cuticle covered with short setae, subdecumbent to appressed; sparse on cranium, mesosoma, and abdominal sternite II. Setae longest on abdominal segments III and V-VII.

Distribution

Yavnella laventa is known only from the type locality, inhabiting the MSS within a debris flow on the bank of an ephemeral stream adjacent to a salt diapir (Fig. 2.12). The Khoorab Salt Dome is one of ~130 salt diapirs occurring in southern Iran (Talbot and Alavi 1996). It is therefore possible that *Y. laventa* occurs across this area, at least in microhabitats resembling those present at the type locality.

Habitat

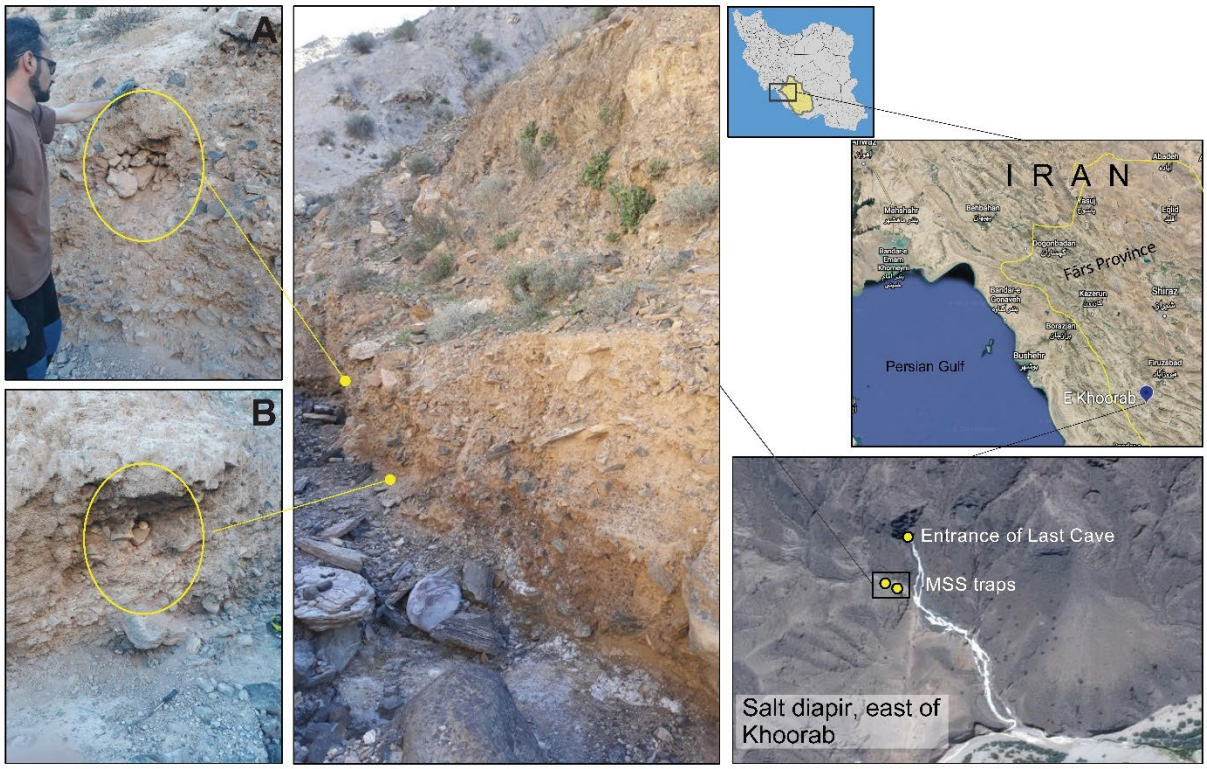

Figure 2.12. Map of the type locality within Iran, and the spatial relationship of the MSS traps in which *Yavnella laventa* was collected relative to each other and to Last Cave. Yellow marks indicate approximate positions of MSS traps, which were located below the surface of the ground. **A:** Location of MSS2. **B:** Location of MSS4.

Mean annual precipitation around the type locality is ~400 mm (Zarei 2010), meaning that moisture is a limiting abiotic factor. Microclimatic conditions in the MSS at the type locality were not directly measured due to data logger malfunctioning. Indeed, RH in the MSS is rarely measured for this reason (Mammola *et al.* 2016). Contrarily to cave habitats, in which relative humidity is generally constant, studies of this parameter in the MSS show seasonal variation, with a drop in spring through summer (Barranco *et al.* 2013). Via a data logger and RH in the nearby salt cave (the "Last Cave"), we found that RH varied seasonally from 50-80%, contrasting with the humidity and climatic constancy commonly associated with subterranean habitats (Badino 2010; Cigna 2002). We hypothesize that the hygroscopic property of salt causes a strong drop in humidity inside Last Cave, which may account for the absence of *Y. laventa*.

Key to genera of the Leptanillinae based on the worker caste

1. Abdominal segment III not constricted posteriorly (Fig. 2.13A); occiput visible in full-face view (Yamada *et al.* 2020: fig. 1A)……..*Opamyrma* Yamane, Bui and Eguchi, 2008
- Abdominal segment III constricted posteriorly, forming postpetiole (Fig. 2.13B-C); occiput not visible in full-face view…….2
2. Posterior face of petiolar node not distinct (Fig. 2.13C); abdominal segments II-III with tergotergal and sternosternal fusion partial to complete…..……...*Anomalomyrma* Taylor in Bolton, 1990
- Posterior face of petiolar node distinct (Fig. 2.13B); abdominal segments II-III without tergotergal or sternosternal fusion……...……..……..……..……..3
3. Mandible with peg-like chaetae on medial face (Fig. 2.3A); mandible with regularly spaced dorsomedial serration; mandible lacking subapical teeth (Fig. 2.3A-B)……..…….....…….*Protanilla* Taylor in Bolton, 1990
- Mandible without peg-like chaetae on medial face; serration present *or* absent from dorsomedial margin (Fig. 2.3C-D), *if* present *then* irregularly spaced; mandible with ≥1 subapical tooth..…….……..…..…..……4
4. Frontoclypeal process present *or* absent (Fig. 2.14A), *if* present apex entire (Fig. 2.14B) *or* emarginate, *if* emarginate *then* apicolateral margins angular (Fig. 2.14C); SI<100; PI>31…….……...…...*Leptanilla* Emery, 1870
- Frontoclypeal process present, apex emarginate, apicolateral margins lobate (Fig. 2.14D); SI≥100; PI≤31…….……..…*Yavnella* Kugler, 1987

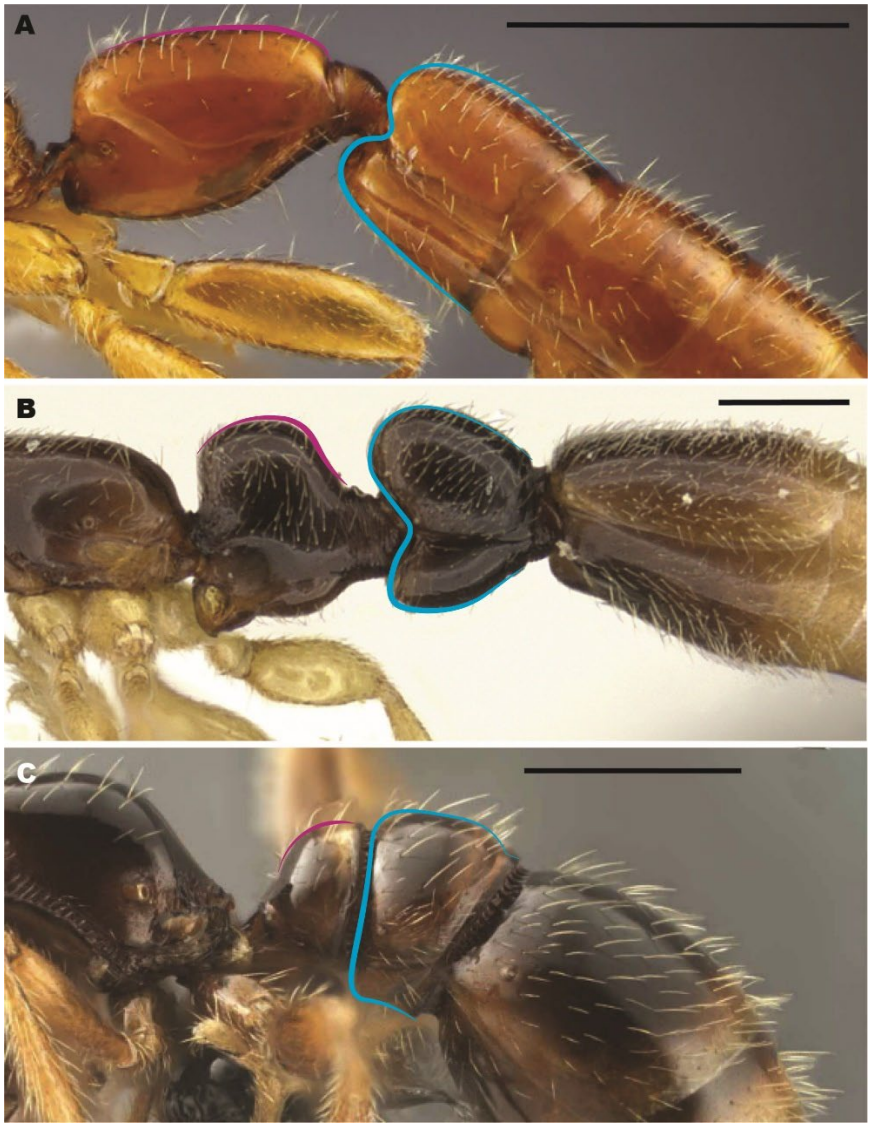

Figure 2.13. Profile view of abdominal segments II-III across the Leptanillinae. Profile of abdominal tergite II outlined in magenta; profile of abdominal segment III outlined in blue. **A.** *Opamyrma hungvuong* (AKY05vii17-06) (Yamada *et al.* 2020: fig. 1C). **B.** *Protanilla bicolor* (CASENT0235341), Estella Ortega (AntWeb 2022). **C.** *Anomalomyrma helenae* (CASENT0220220) (Borowiec *et al.* 2011: fig. 6). Scale bar A = 0.5 mm.; B = 0.2 mm.; C = 0.5 mm.

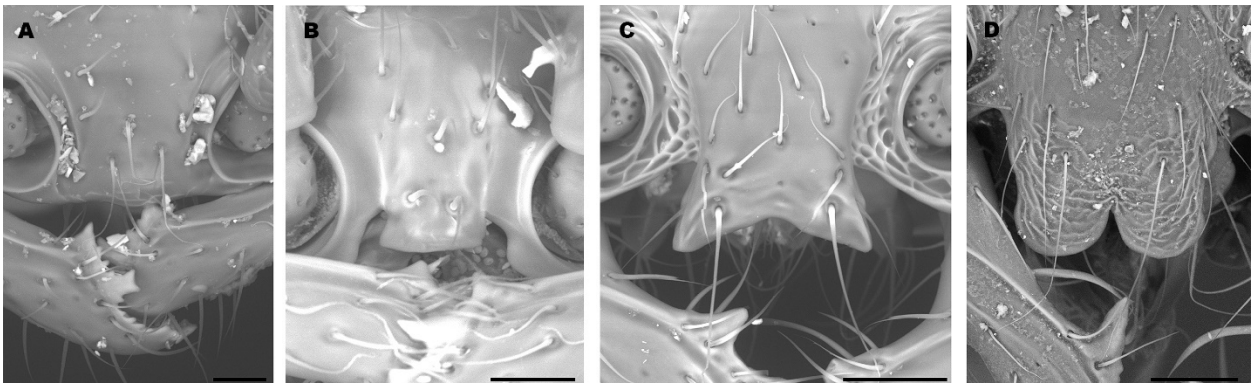

Figure 2.14. Full-face view of the frontoclypeal margin across the tribe Leptanillini. **A.** *Leptanilla* KE01 (CASENT0842721). **B.** *Leptanilla boltoni* (CASENT0260440). **C.** *Leptanilla thai* (CASENT0842784). **D.** *Yavnella laventa* (CASENT0842789). Scale bar A, B = 0.02 mm.; C = 0.035 mm.; D = 0.05 mm.

Discussion

Morphology

The habitus of *Y. laventa* is exceptional among worker Leptanillinae in the elongation of the appendages, including the scape (Table 2.2), flagellomeres, and tarsomeres (Figs. 2.6C, 15B). The anterior constriction of abdominal segment IV is also unique among the Leptanillinae, exceeding the constriction observed in *Leptanilla tanakai* Baroni Urbani, 1977 (Baroni Urbani 1977: fig. 33). *Protanilla* spp. have long scapes (SI>100) by comparison to *Leptanilla* (Richter *et al.* 2021), but these are less elongated than in *Y. laventa* (Table 2.2). Elongation of the scapes in *Protanilla* was hypothesized to be a secondary reversal from the ancestral condition in the Leptanillini (Richter *et al.* 2021). This implies that the elongation of the scape in *Y. laventa* is also a secondary reversal.

Species	**SI**	**PI**	**Reference**
Yavnella laventa (*n*=4)	160- 163†	29-31	This study
Martialis heureka (*n*=1)	72	70	Rabeling *et al.* (2008)

Species	**SI**	**PI**	**Reference**
Protanilla flamma (*n*=2)	86-90	110-112	Baidya & Bagchi (2020)
Leptanilla plutonia (*n*=20)	64-72	66-77	Pérez-González *et al.* (2020)
Leptanilla hypodracos (*n*=2)	69	60‡	Wong & Guénard (2016)
Leptanilla macauensis (*n*=4)	49-56	84-88	Leong *et al.* (2018)

†*n*=3
‡*n*=1

Table 2.2. Comparison of scape index (SI) and petiole index (PI) in *Yavnella laventa* to that observed in a selection of other leptanillomorph species.

The elongation of appendicular articles in *Y. laventa* is unparalleled in the "leptanillomorph clade", i.e., *Martialis* + Leptanillinae (Borowiec *et al.* 2019; Richter *et al.* 2021), as is the elongation of the petiole (PI=29-32) (Tables 2.2-3). Leptanillomorph workers generally have robust, short limbs, with a submoniliform antennal funiculus; this tendency is most pronounced in the Leptanillini. Along with positioning of the antennal toruli anterior to their ancestral position for the Formicidae, shortening of extremities is associated with motion in confined subterranean conditions (Eisenbeis and Wichard 1987; Richter *et al.* 2021). By contrast, the extremities of *Y. laventa* are attenuated and fragile, with the antennal funiculus filiform. This convincingly restricts this species to subterranean voids, as predicted for *M. heureka* (Rabeling *et al.* 2008: fig. 2). The sparseness of traction chaetae on the ventral tarsal surface (Figs. 2.10B, 2.15B) also implies limited digging capability in *Y. laventa* compared to examined *Leptanilla* spp. (Fig. 2.15).

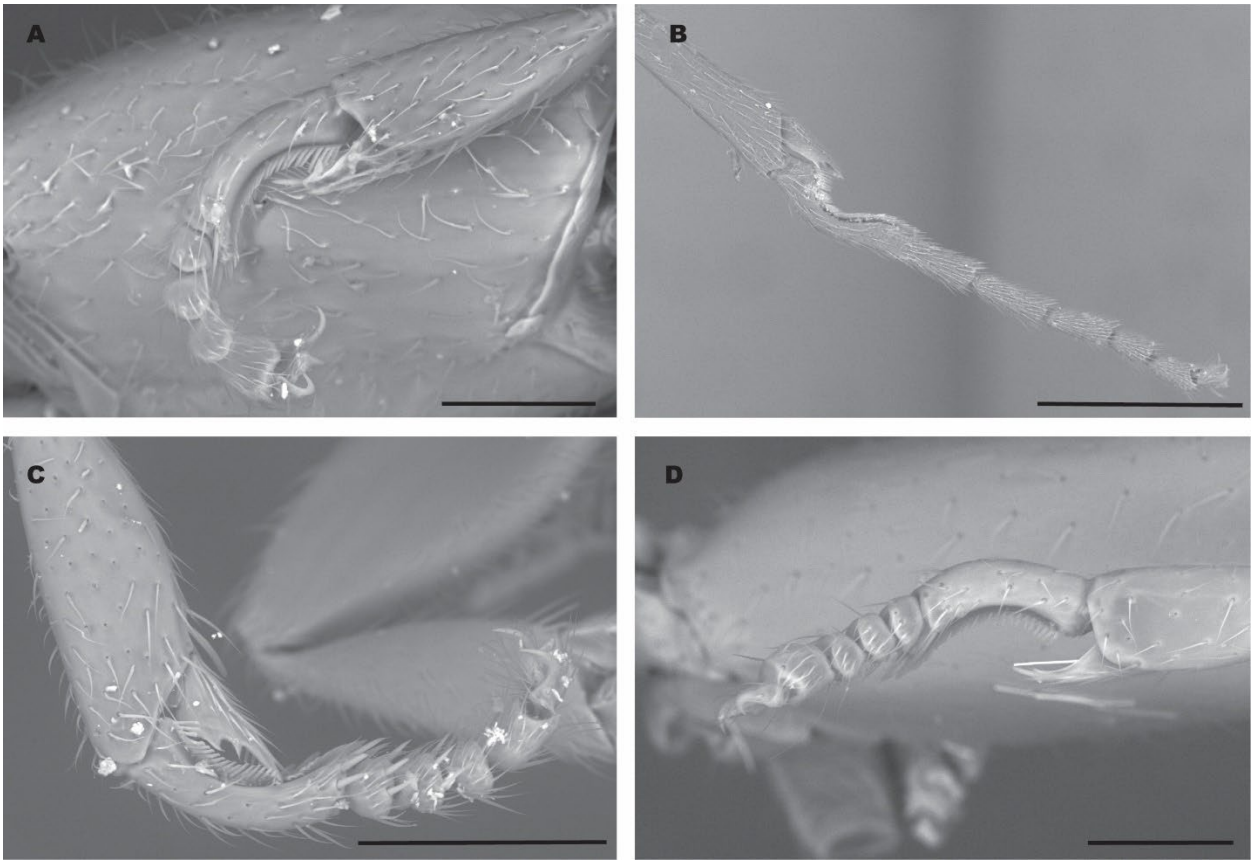

Figure 2.15. Protarsi of selected *Leptanilla* spp., lateral view. **A.** *Leptanilla boltoni* (CASENT0842753). **B.** *Yavnella laventa* (CASENT0842745). **C.** *Leptanilla thai* (CASENT0842752). **D.** *Leptanilla theryi* (CASENT0842751). TRC=traction chaetae. Scale bar A = 0.05 mm.; B = 0.2 mm.; C = 0.1 mm.; 0.05 mm.

The emarginate frontoclypeal process of *Y. laventa* resembles that observed in many *Leptanilla* spp., mostly distributed in the Indo-Malayan ecoregion. While regarded as clypeal in origin by previous authors (e.g., Leong *et al.* 2018), the homology of the frontoclypeal process is unclear, since it is difficult to delimit the clypeus in the absence of the epistomal sulcus.

The mandibular surface of *Y. laventa* bears sparse, tapering suberect setae of mostly uniform length and diameter. Two pairs of more robust, longer suberect setae are present on the medial mandibular surface, with the distal pair positionally homologous with the putative “trigger hairs” present in *Protanilla lini* and *Protanilla rafflesi* Taylor in Bolton, 1990 (Richter *et al.* 2021). This is the first purported example of trigger hairs in the Leptanillini. The definition of trigger

hairs has always been functional rather than anatomical, relying upon confirmation of "trap-jaw" behavior, or assertion by analogy to other ants for which behavioral observations exist (e.g., Creighton 1930; Barden & Grimaldi 2012; Richter *et al.* 2021). Observations of living *Y. laventa*, or three-dimensional modeling of mandibular movement in this species based upon micro-CT data, would test the hypothesized function of these mandibular setae (cf. Richter *et al.* 2021). Consultation of the primary literature (e.g., Man *et al.* 2017: fig. 5; Baidya and Bagchi 2020: fig. 1C; Aswaj *et al.* 2020: fig. 2C), photographs on AntWeb (2022), and available specimens showed that the subapical mandibular seta is present and robust in all described species of Anomalomyrmini for which this information is available. The presence of a robust subapical mandibular seta was also confirmed in all available undescribed specimens of that tribe (Table 2.3). There were few available worker specimens belonging to the Leptanillini in which mandibular setation could be assessed. A subapical mandibular seta is present in those that were examined and in *O. hungvuong* (Yamada *et al.* 2020: fig. 2E) (Table 2.3) but is less produced than in the Anomalomyrmini or *Y. laventa*, leaving its function as a trigger hair doubtful.

Specimen Identifier	**Species Identification**	**Subapical Mandibular Seta**	**Reference**
CASENT0178553	*Anomalomyrma* indet.	Present	This study
CASENT0217032	*Anomalomyrma boltoni*	Present	Borowiec *et al.* (2011: fig. 2)
CASENT0220221	*Anomalomyrma helenae*	Present	Borowiec *et al.* (2011: p. 6)

Specimen Identifier	Species Identification	Subapical Mandibular Seta	Reference
CASENT0101976	*Anomalomyrma taylori*	Present	Borowiec *et al.* (2011: fig. 12)
CASENT0842753	*Leptanilla boltoni*	Present	This study
CASENT0010809	*Leptanilla havilandi*	Present	This study
CASENT0842784	*Leptanilla thai*	Present	This study
AKY05vii17-06	*Opamyrma hungvuong*	Present	Yamada *et al.* (2020: fig. 2E)
CASENT0106383	*Protanilla* indet.	Present	This study
CASENT0898001	*Protanilla* indet.	Present	AntWeb (2022)
CASENT0842639	*Protanilla beijingensis*	Present	This study
CASENT0235341	*Protanilla bicolor*	Present	AntWeb (2022)
–	*Protanilla concolor*	?	Not examined
CESM-198516	*Protanilla flamma*	Present	Baidya & Bagchi (2020: fig. 1C)
–	*Protanilla furcomandibula*	Present	Xu (2011: p. 481)
–	*Protanilla gengma*	Present	Aswaj *et al.* (2020: fig. 2C)
CASENT0842850	*Protanilla izanagi*	Present	This study
CASENT0824693	*Protanilla jongi*	Present	This study
CASENT0172005	*Protanilla* jp02	Present	AntWeb (2022)

Specimen Identifier	Species Identification	Subapical Mandibular Seta	Reference
CASENT0709417	*Protanilla lini*	Present	Richter *et al.* (2021: Figs. 6D, 7A)
CASENT0746018	*Protanilla* MY01	Present	AntWeb (2022)
CASENT0842640	*Protanilla* psw-my01	Present	This study
CASENT0842972	*Protanilla rafflesi*	Present	Richter *et al.* (2021)
CASENT0902783	*Protanilla* rwt-tera	Present	AntWeb (2022)
CASENT0911228	*Protanilla schoedli*	Present	Baroni Urbani & de Andrade (2006: p. 45)
–	*Protanilla tibeta*	Present	Xu (2011: p. 488)
CASENT0179564	*Protanilla* VN01	Present	This study
CASENT0179565	*Protanilla* VN03	Present	This study
CASENT0842699	*Protanilla wallacei*†	Present	This study
CASENT0221924	*Protanilla wardi*	Present	This study
CASENT0842745	*Yavnella laventa*	Present	This study

†*Nomen nudum*

Table 2.3. Presence/absence of a subapical mandibular seta in all described species belonging to the tribe Anomalomyrmini, and in 10 specimens belonging to undescribed morphospecies of this tribe. Also included are *Opamyrma hungvuong* and the only three species of Leptanillini for which mandibular setation could be examined.

In *Y. laventa* the mandibles are elongated such that, when closed, these rest in a position subparallel to the anteroposterior axis of the cranium (Figs. 2.3D, 2.5B, 2.6C), resembling the Anomalomyrmini. This is not a condition previously observed in the Leptanillini. Save for the

posture of the mandibles at rest, *Y. laventa* has little morphological commonality with the Anomalomyrmini to the exclusion of other Leptanillini. Anomalomyrmine workers are uniformly distinguished from the Leptanillini, including *Yavnella*, by the presence of four maxillary palpomeres; the presence of regular serration on the medial mandibular margin, and absence of large teeth from that margin; the presence of at least one peg-like chaeta on the labrum; and the median demarcation of the clypeus from the frons by a carina.

Ecology

Yavnella laventa was collected ≥60 cm. below the surface, setting the workers of this species apart from other Leptanillinae for which soil depth of origin is recorded: these approach that of *Y. laventa* only in *Leptanilla taiwanensis* Ogata, Terayama & Masuko, 1995 and *Protanilla beijingensis* Man, Ran, Chen & Zhu, 2017 which have been collected with unbaited pitfall traps at depths of up to 55 cm. (Man *et al.* 2017).

That the biotope of *Y. laventa* appears to be the MSS, rather than soil as is the case in other leptanilline ants, is consistent with the strikingly gracile phenotype of this species. The elongated, delicate limbs preclude the endogean (i.e., soil-dwelling) biology otherwise observed in this subfamily, instead indicating hypogean habits. This elongation of extremities is consistent with troglomorphism. Worker Leptanillinae lack compound eyes, and so that condition in *Y. laventa* does not constitute troglomorphism *per se*, although it corroborates our supposition that this species is exclusively subterranean, as are all other leptanilline ants. Rather, the argument for troglomorphism in *Y. laventa* rests upon overall elongation of the extremities in conjunction with subterranean biology. This is analogous to troglomorphic Japygidae and Campodeidae (Hexapoda: Diplura), which likewise belong to an ancestrally eyeless, endogean clade, and differ from endogean relatives by larger size and elongation or multiplication of appendicular articles

(Sendra *et al.* 2021). A similar pattern is also recovered in subterranean spiders (Araneae), e.g. *Troglohyphantes* spp. (Linyphiidae), in which leg length appears to correlate with habitat (pore) size (Mammola and Isaia 2017).

We here follow the definition of Bichuette *et al.* (2015) for troglomorphism, regarding it as phenotypic traits selectively favored by subterranean biology and apomorphic relative to non-subterranean relatives of the putatively troglomorphic lineage. By this definition, troglomorphism does not necessarily coincide with habitation in subterranean voids that are considered caves by dint of being "commensurable to the human scale" (Mammola *et al.* 2016: p. 3). Therefore, that *Y. laventa* was collected in the MSS does not exclude its being troglomorphic. Indeed, this condition is unsurprising, since troglomorphic organisms are frequently encountered in the MSS (Christiansen 2005; Juberthie and Decu 2006; see Mammola *et al.* 2016 for further evidence from the literature).

Few ants are known to reside permanently in caves (Pape 2016) or exhibit troglomorphism (Christiansen 2005). While *Nylanderia pearsei* Wheeler, 1938 (Formicinae: Lasiini) from the Yucatán Peninsula and an undescribed *Leptogenys* sp. (Ponerinae: Ponerini) from central Texas are subterranean so far as is known (Wheeler 1938; Reddell 1977; Cokendolpher *et al.* 2009), neither is unambiguously troglomorphic in phenotype. Compelling arguments for troglomorphism among described ants have heretofore only been made for *Leptogenys khammouanensis* and *Aphaenogaster gamagumayaa*. When compared to their respective closest relatives, both display a gracile habitus, pale coloration, and reduced compound eyes (Roncin and Deharveng 2003; Naka and Maruyama 2018). Additionally, *L. khammouanensis* was collected in two large calcareous caves in Laos, ranging from 0.5 to several kilometers from the cave entrance (Roncin and Deharveng 2003); while *A. gamagumayaa* was collected

approximately 20 meters within a calcareous cave on Okinawa, apparently nesting in the floor of an aphotic guano hall (Naka and Maruyama 2018: pp. 138-139).

Generic Classification

Since *Y. laventa* is the sole species of *Yavnella* for which the worker has been identified, the range of morphological variation in the worker caste of *Yavnella* is unknown, as is the prevalence of troglomorphism in *Yavnella*. If all that is required for the evolution of troglomorphism in the Leptanillinae is the presence of the MSS, troglomorphism could be prevalent across the worker caste in *Yavnella*, since the geographical extent of the MSS is unknown (Juberthie and Decu 2006; Mammola *et al.* 2016).

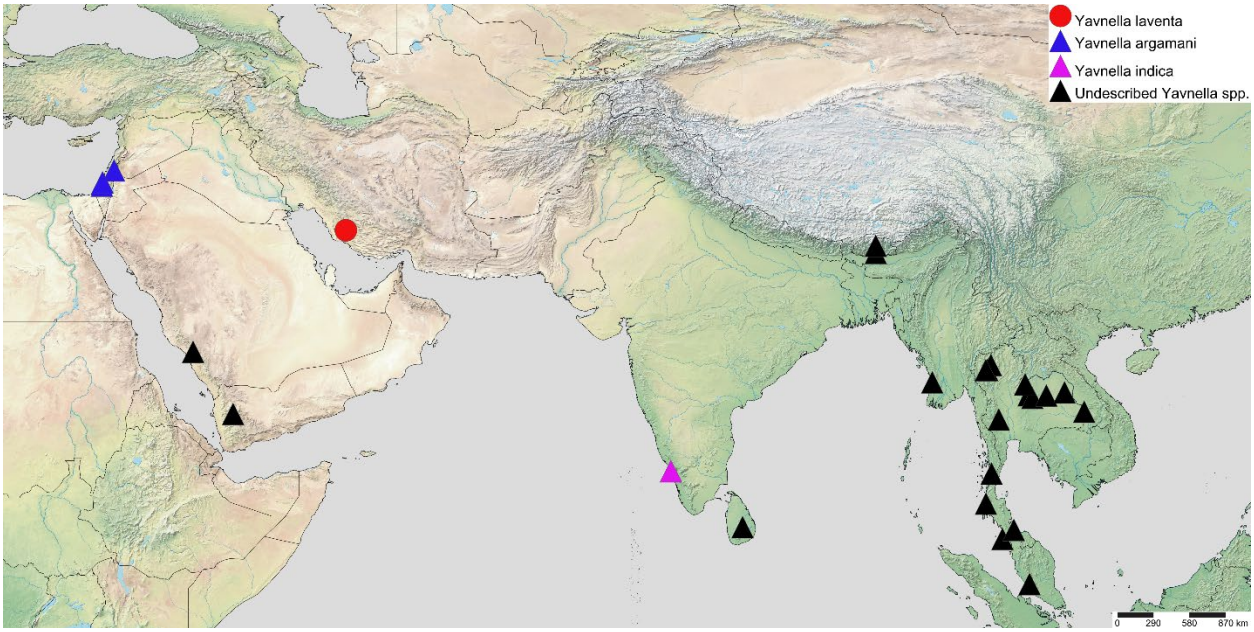

Figure 2.16. Distribution of known specimens attributed to *Yavnella*, according to Collingwood & Agosti (1994) and AntWeb (2022), with generic attribution of undescribed morphospecies following Griebenow (2021). Generated using SimpleMappr (https://www.simplemappr.net).

It must be cautioned that without troglomorphic elongation of the soma and extremities, and putative trigger hairs, workers of *Y. laventa* cannot be discriminated from those of *Leptanilla*. Disregarding these apomorphies, the phenotype of *Y. laventa* shows close affinity to *Leptanilla escheri* (Kutter, 1948) and *Leptanilla judaica* Kugler, 1987. The 2,1 palp formula of *Y. laventa*

(Fig. 2.5C) resembles that in *Leptanilla havilandi* Forel, 1901, *L. escheri*, *L. judaica*, and *Leptanilla ujjalai* Saroj *et al.*, 2022 (this study; Kugler 1987; Saroj *et al.* 2022), while the anteromedian frontoclypeal process of *Y. laventa* resembles that observed in these and other *Leptanilla* spp. (Kugler 1987; Wong and Guénard 2016: Figs. 1A-B; Leong *et al.* 2018: Figs. 14B-C, 15A; Saroj *et al.* 2022: Fig. 3B).

It is possible that *L. escheri* and *L. judaica* are non-troglomorphic representatives of *Yavnella*. In the absence of molecular data for *L. escheri*, *L. judaica*, or their close relatives, *Leptanilla lamellata* Bharti & Kumar, 2012 and *L. ujjalai*, we refrain from transferring any *Leptanilla* spp. to *Yavnella.* The hypothesis that these *Leptanilla* spp. represent *Yavnella* has biogeographical plausibility, since these species are known from the Indian subcontinent and Israel, with Iran intervening between these regions (Fig. 2.16). Under this hypothesis, it is plausible that *Yavnella indica* Kugler, 1987 and *Y. argamani* respectively represent the males of *L. escheri* and *L. judaica*, a prediction that could be tested with molecular data, as in this study and others (e.g., Ward and Brady 2009; Griebenow 2020).

Identification of *L. escheri* or any of its relatives as representatives of *Yavnella* would erase the distinction between that genus and *Leptanilla* in the worker caste. The subapical mandibular setae have not been comprehensively surveyed across the known diversity of the Leptanillini and therefore are not of monothetic use. *Yavnella* and *Leptanilla s. l.* are uniformly discriminated based upon male morphology (Griebenow 2021) and robustly recovered as reciprocally monophyletic by ML and Bayesian phylogenomic inference (Griebenow 2020, 2021; this study). Resolving the taxonomic status of the major subclades of the Leptanillini, including *Yavnella*, will require sequencing of further worker material across this tribe, including the as-yet-

unknown worker caste of *Scyphodon*, *Noonilla*, and the undescribed Bornean morphospecies-group (Griebenow 2020, 2021).

Acknowledgements

First, we would like to thank La Venta Esplorazioni Geografiche for the organization and funding of the Iran Salt Cave 2019 expedition that led to the discovery of *Y. laventa*. Without La Venta, this species would have remained unknown and the three of us would have never joined this publication. The expedition was led by Luca Imperio and Giuseppe Giovine, with the support of Younes Samaridati, our invaluable local guide and interpreter. We would like to thank the Iranian Cave and Speleology Association and the Iran Mountaineering and Sport Climbing Federation (Firuz Abad office) for local support in organizing the expedition. Special thanks go to Alessandro Uggeri for providing the geological description of the MSS sites.

The second expedition (2020) to collect the traps was assisted by colleagues of MM at the University of Isfahan and Yasouj University: Ali Mansouri, Alireza Ghahremani, Behzad Fathinia and Hamid Shahzeidi, for which we are thankful. We thank Jason Bond, Josh Gibson, and Charles Stephens for conceptual advice on this project; Michael Branstetter for assembling raw UCE reads; Phil Ward and Ziv Lieberman for writing advice; and Jadranka Rota (MZLU), Debbie Jennings (ANIC), Masashi Yoshimura (OIST), Kevin Williams (CSCA), Brian Fisher (CASC), Chris Darling (ROME), Benoit Guénard (HKUBM), Po-Wei Hsu (NCUE), Alberto Tinaut, Yu Hisasue, and José María Gómez-Durán for loaning material used in this study. We also thank Bui Tuan Viet, Katsuyuki Eguchi, Michael Ohl, Christian Rabeling, and Michael Sharkey for material sequenced by Borowiec *et al.* (2019) that was also included in this study.

Conflicts of Interest

The authors declare no conflicts of interest.

Declaration of Funding

This research was supported by the UC Davis Dept. of Entomology, UC Davis Jastro-Shields, and by NSF grant DEB-1932405 to P. S. Ward.

Data Availability

Configuration files, DNA alignment and output for all phylogenetic analyses employed in this study are available on Zenodo (10.5281/zenodo.5595290). Accession numbers for raw UCE reads, uploaded to the Sequence Read Archive (SRA) (https://www.ncbi.nlm.nih.gov/sra), are provided in Table 2.S1.

Supplementary Tables, Chapter 2

Table 2.S1. Specimens used in this study, with summary statistics pertaining to the 313,498-bp alignment in the cases of those specimens for which ultra-conserved elements (UCEs) were enriched using the *hym-v2* probe set of Branstetter *et al.* (2017).

Table 2.S2. Collection data for specimens included in this study.

References

Abbassi HR, Aleni MR, Feiznia S, Darvish M, Ahmadian M, Shahbazi A (2015) Effects of geological formation on desertification in the Mond watershed [in Farsi]. *Iranian Journal of Range & Desert Research* **22**(3), 583–593.

Aberer AJ, Kassian K, Stamatakis A (2014) ExaBayes: massively parallel Bayesian tree inference for the whole-genome era. *Molecular Biology & Evolution* **31**(10), 2553–2556. doi:10.1093/molbev/msu236

AntWeb. Version 8.68.7. California Academy of Sciences, online at https://www.antweb.org. Accessed 7 February 2022.

Aswaj P, Anoop K, Priyadarsanan DR (2020) First record of the rarely collected ant *Protanilla gengma* Xu, 2012 (Hymenoptera, Formicidae, Leptanillinae) from the Indian subcontinent. *Check List* **16**(6), 1621–1625. https://doi.org/10.15560/16.6.1621

Badino G (2010) Underground meteorology–"What's the weather underground?" *Acta Carsologica* **39**: 427–448.

Baidya P, Bagchi S (2020) A new species of *Protanilla* Taylor 1990 (Hymenoptera: Formicidae: Leptanillinae) from India. *Halteres* **11**, 19–24.

Bankevich A, Nurk S, Antipov D, Gurevich AA, Dvorkin M, Kulikov AS, Lesin VM, Nikolenko SI, Pham S, Prjibelski AD, Pyshkin AV, Sirotkin AV, Vyahhi N, Tesler G, Alekseyev MA, Pevzner PA (2012) SPAdes: a new genome assembly algorithm and its applications to single–cell sequencing. *Journal of Computational Biology* **19**(5), 455–477. doi:10.1089/cmb.2012.0021

Barden P, Grimaldi D (2012) Rediscovery of the bizarre Cretaceous ant *Haidomyrmex* Dlussky (Hymenoptera: Formicidae), with two new species. *American Museum Novitates* **3755**, 1–16.

Baroni Urbani C (1977) Materiali per una revisione della sottofamiglia Leptanillinae Emery (Hymenoptera: Formicidae) [in Italian]. *Entomologica Basiliensia* **2**, 427–488.

Baroni Urbani C, de Andrade ML (2006) A new *Protanilla* Taylor, 1990 (Hymenoptera: Formicidae: Leptanillinae) from Sri Lanka. *Myrmecologische Nachrichten* **8**, 45–47.

Barranco P, Gilgado JD, Ortuño VM (2013) A new mute species of the genus *Nemobius* Serville (Orthoptera, Gryllidae, Nemobiinae) discovered in colluvial, stony debris in the Iberian Peninsula: a biological, phenological and biometric study. *Zootaxa* **3691**(2), 201–219. doi:10.11646/zootaxa.3691.2.1

Bichuette ME, Rantin B, Hingst-Zaher E, Trajano E (2015) Geometric morphometrics throws light on evolution of the subterranean catfish *Rhamdiopsis krugi* (Teleostei: Siluriformes: Heptapteridae) in eastern Brazil. *Biological Journal of the Linnean Society* **114**, 136–151. https://doi.org/10.1111/bij.12405

Billen J, Bauweleers E, Hashim R, Ito F (2013) Survey of the exocrine system in *Protanilla wallacei* (Hymenoptera, Formicidae). *Arthropod Structure & Development* **42**(3), 173–183. doi:10.1016/j.asd.2013.01.001

Bolton B (1990) The higher classification of the ant subfamily Leptanillinae (Hymenoptera: Formicidae). *Systematic Entomology* **15**, 267–282.

Bolton B (2003) Synopsis and classification of Formicidae. *Memoirs of the American Entomological Institute* **71**, 1–370.

Borowiec ML (2016) AMAS: a fast tool for alignment manipulation and computing of summary statistics. *PeerJ* **4**, e1660.

Borowiec ML, Schulz A, Alpert GD, Baňař P (2011) Discovery of the worker caste and descriptions of two new species of *Anomalomyrma* (Hymenoptera: Formicidae: Leptanillinae) with unique abdominal morphology. *Zootaxa* **2810**, 1–14. doi:10.7717/ peerj.1660

Borowiec ML, Rabeling C, Brady SG, Fisher BL, Schultz TR, Ward PS (2019) Compositional heterogeneity and outgroup choice influence the internal phylogeny of the ants. *Molecular Phylogenetics & Evolution* **134**, 111–121. doi:10.1016/j.ympev.2019.01.024

Boudinot BE (2018) A general theory of genital homologies for the Hexapoda (Pancrustacea) derived from skeletomuscular correspondences, with emphasis on the Endopterygota. *Arthropod Structure & Development* **47**(6), 563–613.

Boudinot BE, Perrichot V, Chaul JCM (2020) †*Camelosphecia* gen. nov., lost ant-wasp intermediates from the mid-Cretaceous (Hymenoptera, Formicoidea). *ZooKeys* **1005**, 21–55.

Boudinot BE, Moosdorf, OTD, Beutel RG, Richter A (2021) Anatomy and evolution of the head of *Dorylus helvolus* (Formicidae: Dorylinae): patterns of sex- and caste-limited traits in the sausagefly and the driver ant. *Journal of Morphology* **282**, 1616–1658. doi:10.1111/1755-0998.13006

Branstetter MG, Longino JT, Ward PS, Faircloth BC (2017) Enriching the ant tree of life: enhanced UCE bait set for genome–scale phylogenetics of ants and other Hymenoptera. *Methods in Ecology & Evolution* **8**(6), 768–776. doi:10.1111/2041–210X.12742

Castresana J (2000) Selection of conserved blocks from multiple alignments for their use in phylogenetic analysis. *Molecular Biology & Evolution* **17**(4), 540–552. doi:10.1093/oxfordjournals.molbev.a026334

Chernomor O, von Haeseler A, Minh BQ (2016) Terrace aware data structure for phylogenomic inference from supermatrices. *Systematic Biology* **65**(6), 997–1008. doi:10.1093/sysbio/syw037

Christiansen KA (2005) Morphological adaptations. In 'Encyclopedia of Caves'. (Eds D Culver, WB White) pp. 517–527. (Elsevier: Amsterdam.)

Cigna AA (2002) Modern trend [sic!] in cave monitoring. *Acta Carsologica* **31**, 35–54.

Cokendolpher JC, Reddell JR, Taylor SJ, Krejca JK, Suarez AV, Pekins CE (2009) Further ants (Hymenoptera: Formicidae) from caves of Texas. *Texas Memorial Museum Speleological Monographs*, 7. *Studies on the Cave & Endogean Fauna of North America* **V**, 151–168.

Collingwood CA, Agosti D (1996) Formicidae (Insecta: Hymenoptera) of Saudi Arabia (part 2). *Fauna of Saudi Arabia* **15**, 300–385.

Creighton WS. (1930) A review of the genus *Myrmoteras* (Hymenoptera: Formicidae). *Journal of the New York Entomological Society* **38**, 177–192.

Cruaud A, Sabine N, Arnal P, Weber A, Fusu L, Gumovsky A, Huber J, Polaszek A, Rasplus J-Y (2019) Optimized DNA extraction and library preparation for minute arthropods: application to target enrichment in chalcid wasps used for biocontrol. *Molecular Ecology Resources* **19**(3), 702–710. doi:10.1111/1755–0998.13006

Culver DC, Pipan T. (2014) 'Shallow Subterranean Habitats: Ecology, Evolution, & Conservation.' (Oxford University Press: New York City, NY, United States of America)

Eisenbeis G, Wichard W (1987) *Atlas on the Biology of Soil Arthropods.* (Springer Berlin Heidelberg: Berlin, Germany)

Emery C (1870) Studi mirmecologici. *Bollettino della Società Entomologica Italiana* **2**, 193–201.

Emery C (1910) Hymenoptera. Fam. Formicidae. Subfam. Dorylinae. *Genera Insectorum* **102**, 1–34.

Evenhuis, N. L. (2021). The insect and spider collections of the world website. Available at http://hbs.bishopmuseum.org/codens/

Faircloth BC (2016). PHYLUCE is a software package for the analysis of conserved genomic loci. *Bioinformatics* **32**(5), 786–788. https://doi.org/10.1093/bioinformatics/btv646

Grabherr MG, Haas BJ, Yassour M, Levin JZ, Thompson DA, Amit I, Adiconis X, Fan L, Raychowdhury R, Zeng Q, Chen Z, Mauceli E, Hacohen N, Gnirke A, Rhind A, di Palma F, Birren BW, Nusbaum C, Lindblad-Toh K, Friedman N, Regev A (2011) Trinity: reconstructing a full-length transcriptome without a genome from RNA-Seq data. *Nature Biotechnology* **29**(7), 644–652. doi:10.1038/nbt.1883

Griebenow, ZH (2020) Delimitation of tribes in the subfamily Leptanillinae (Hymenoptera: Formicidae), with a description of the male of *Protanilla lini* Terayama, 2009. *Myrmecological News* **30**, 229–250. doi:10.25849/myrmecol.news_030:229

Griebenow ZH (2021) Synonymisation of the male–based ant genus *Phaulomyrma* (Hymenoptera: Formicidae) with *Leptanilla* based upon Bayesian total–evidence phylogenetic inference. *Invertebrate Systematics* **35**, 603–636. https://doi.org/10.1071/IS20059

Guindon S, Dufayard JF, Lefort V, Anisimova M, Hordjik W, Gascuel O (2010) New algorithms and methods to estimate maximum-likelihood phylogenies: assessing the performance of PhyML 3.0. *Systematic Biology* **59**(3), 307–321. doi:10.1093/sysbio/syq010

Harris RA (1979) A glossary of surface sculpturing. *Occasional Papers in Entomology* **28**, 1–31.

Hoang DT, Chernomor O, von Haeseler A, Minh BQ, Vinh LS (2018) UFBoot2: improving the ultrafast bootstrap approximation. *Molecular Biology & Evolution* **35**(2), 518–522. doi:10.1093/molbev/msx281

Hölldobler B, Wilson EO (1990) *The Ants.* (Harvard University Press: Cambridge, MS, United States of America)

Hsu P-W, Hsu F-C, Hsiao Y, Lin CC (2017) Taxonomic notes on the genus *Protanilla* (Hymenoptera: Formicidae: Leptanillinae) from Taiwan. *Zootaxa* **4268**(1), 117–130. doi:10.11646/zootaxa.4268.1.7

Ito F, Yamane S (2020) Behavior of the queen of *Leptanilla clypeata* Yamane *et* Ito collected in the Bogor Botanical Gardens, West Java, Indonesia (Hymenoptera; Formicidae), with a note on colony composition and a description of the ergatoid queen. *Asian Myrmecology* **12**, e012004. doi:10.20362/AM.012004

Ito F, Hashim R, Mizuno R, Billen J (2021) Notes on the biology of *Protanilla* sp. (Hymenoptera, Formicidae) collected in Ulu Gombak, Peninsular Malaysia. *Insectes Sociaux* _, 1–6 [online early]. https://doi.org/10.1007/s00040-021-00839-z

Juberthie C, Decu V. 2006. Interstitial habitat (terrestrial). In 'Encyclopedia of Caves & Karst Science'. (Ed Gunn J) pp. 984–987. Taylor and Francis Group: New York City, NY, United States of America.

Kalyaanamorthy S, Minh BQ, Wong TKF, von Haeseler A, Jermiin LS (2017) ModelFinder: fast model selection for accurate phylogenetic estimates. *Nature Methods* **14**(6), 587–589. doi:10.1038/nmeth.4285.

Katoh K, Toh H (2010) Parallelization of the MAFFT multiple sequence alignment program. *Bioinformatics* **26**(15), 1899–1900. doi:10.1093/bioinformatics/btq224

Kugler J (1987 ["1986"]) The Leptanillinae (Hymenoptera: Formicidae) of Israel and a description of a new species from India. *Israel Journal of Entomology* **20**, 45–47.

Leong C-M, Yamane S, Guénard B (2018) Lost in the city: discovery of the rare ant genus *Leptanilla* (Hymenoptera: Formicidae) in Macau with description of *Leptanilla macauensis* sp. nov. *Asian Myrmecology* 10: e010001.

Lanfear R, Calcott B, Kainer D, Mayer C, Stamatakis A (2018) Selecting optimal partitioning schemes for phylogenomic datasets. *BMC Evolutionary Biology* **14**, 82(2014). https://doi.org/10.1186/1471-2148-14-82

Lieberman ZE, Billen J, van de Kamp T, Boudinot BE (2022) The ant abdomen: the skeletomusculature of *Amblyopone australis* workers (Hymenoptera: Formicidae). *Journal of Morphology* **2022**, 1–78. doi:10.1002/jmor.21471

Liu SP, Richter A, Stoessel A, Beutel RG (2019) The mesosomal anatomy of *Myrmecia nigrocincta* workers and evolutionary transformations in Formicidae (Hymenoptera). *Arthropod Systematics & Phylogeny* **77**(1), 1–19.

Mammola S, Isaia M (2016) The ecological niche of a specialized subterranean spider. *Invertebrate Biology* **135**(1), 20–30.

Mammola S, Giachino PM, Piano E, Jones A, Barberis M, Badino G, Isaia M (2016) Ecology and sampling techniques of an understudied subterranean habitat: the *Milieu Souterrain Superficiel* (MSS). *The Science of Nature* **103**(88). doi:10.1007/s00114–016–1413–9

Mammola S, Arnedo MA, Fišer C, Cardoso P, Dejanaz AJ, Isaia M (2020) Environmental filtering and convergent evolution determine the ecological specialization of subterranean spiders. *Functional Ecology* **00**, 1–14. doi:10.1111/1365-2435.13527

Man P, Ran H, Chen Z, Xu Z (2017) The northernmost record of Leptanillinae in China with description of *Protanilla beijingensis* sp. nov. (Hymenoptera: Formicidae). *Asian Myrmecology* **9**:e009008. doi:10.20362/am.009008.

Minh BQ, Schmidt HA, Chernomor O, Schrempf D, Woodhams MD, von Haeseler A, Lanfear R (2020) IQ-TREE 2: new models and efficient methods for phylogenetic inference in the genomic era. *Molecular Biology & Evolution* **37**(5), 1530–1534. doi:10.1093/molbev/msaa015

Miller MA, Pfeiffer W, Schwartz T (2010) "Creating the CIPRES Science Gateway for inference of large phylogenetic trees", in *Proceedings of the Gateway Computing Environments Workshop (GCE)*, 14 Nov. 2010, New Orleans, LA (pp. 1–8).

Naka T, Maruyama M (2018) *Aphaenogaster gamagumayaa* sp. nov.: the first troglobiotic ant from Japan (Hymenoptera: Formicidae: Myrmicinae). *Zootaxa* **4450**(1), 135–141. doi:10.11646/zootaxa.4450.1.10

Nguyen L-T, von Haeseler A, Minh BQ, Susko E (2018) Complex models of sequence evolution require accurate estimators as exemplified with the invariable site plus gamma model. *Systematic Biology* **67**(3), 552–558. doi:10.1093/sysbio/syx092

Ogata K, Terayama M, Masuko K (1995) The ant genus *Leptanilla*: discovery of the worker–associated male of *L. japonica*, and a description of a new species from Taiwan (Hymenoptera: Formicidae: Leptanillinae). *Systematic Entomology* **20**(1), 27–34. doi:10.1111/j.1365–3113.1995.tb00081.x

Pape R (2016) The importance of ants in cave ecology, with new records and behavioral observations of ants in Arizona caves. *International Journal of Speleology* **45**(3), 185–205.

Pérez-González S, Gómez-Durán JM, Martínez-Ibáñez MD (2020) Highlighting the elusive: new findings and a redescription of the rare ant *Leptanilla plutonia* López, Martínez *et* Barandica, 1994, presenting morphological novelties for the genus. *Annales Zoologici (Warszawa)* **70**(2), 289–304. doi:10.3161/00034541ANZ2020.70.2.009

Petersen, B (1968) Some novelties in presumed males of Leptanillinae (Hym., Formicidae). *Entomologiske Meddelelser* **36**, 577–598.

Rabeling C, Brown JM, Verhaagh M (2008) Newly discovered sister lineage sheds light on early ant evolution. *Proceedings of the National Academy of Sciences* **105**(39), 14913–14917. https://doi.org/10.1073/pnas.0806187105

Rambaut A, Drummond AJ, Xie D, Baele G, Suchard MA (2018) Posterior summarization in Bayesian phylogenetics using Tracer 1.7. *Systematic Biology* **67**(5), 901–904. doi:10.1093/sysbio/syy032

Reddell JR (1977) A preliminary survey of the caves of the Yucatan peninsula. In 'Studies of the Caves & Cave Fauna of the Yucatan Peninsula'. (Ed Reddell JR) pp. 215–296. *Association for Mexican Cave Studies Bulletin* **6**. Speleo Press: Austin, TX, United States of America.

Richter A, Garcia FH, Keller RA, Billen J, Katzke J, Boudinot BE, Economo EP, Beutel RG (2021) The head anatomy of *Protanilla lini* (Hymenoptera: Formicidae: Leptanillinae), with a hypothesis of their mandibular movement. *Myrmecological News* **31**, 81–114. doi:10.25849/myrmecol.news_031:085

Roncin E, Deharveng L 2003. *Leptogenys khammouanensis* sp. nov. (Hymenoptera: Formicidae). A possible troglobitic species of Laos, with a discussion on cave ants. *Zoological Science* **20**(7), 919–924.

Saroj S, Mandi A, Dubey A (2022) A new species of the rare ant genus, *Leptanilla* Emery (Hymenoptera: Formicidae) from Eastern Himalaya, India. *Asian Myrmecology* **15**, e015005. doi:10.20362/am.015005

Sendra A, Komerički A, Lips J, Luan Y, Selfa J, Jiménez–Valverde A (2021) Asian cave–adapted diplurans, with the description of two new genera and four new species (Arthropoda, Hexapoda, Entognatha). *European Journal of Taxonomy* **731**, 1–46.

Tagliacollo VA, Lanfear R (2018) Estimating improved partitioning schemes for ultraconserved elements. *Molecular Biology & Evolution* **35**(7), 1798–1811. doi:10.1093/molbev/msy069

Talbot CJ, Alavi M (1996) The past of a future syntaxis across the Zagros. *Geological Society of London Special Publications* **100**, 89–109.

Tinaut A, López F (2001) Ants and caves: sociability and ecological constraints (Hymenoptera, Formicidae). *Sociobiology* **37**(3), 651–659.

Uéno SI (1980) The anophthalmic trechine beetles of the group of *Trechiama oshimai*. *Bulletin of the National Science Museum of Tokyo, Series A* **6**(4), 195–274.

Ward PS, & Brady SG (2009) Rediscovery of the ant genus *Amyrmex* Kusnezov (Hymenoptera: Formicidae) and its transfer from Dolichoderinae to Leptanilloidinae. *Zootaxa* **2063**, 46–54. doi:10.11646/zootaxa.2063.1.2

Ward PS, & Fisher BL (2016) Tales of dracula ants: the evolutionary history of the ant subfamily Amblyoponinae (Hymenoptera: Formicidae). *Systematic Entomology* **41**, 683–693.

Ward PS, Blaimer BB (2022) Taxonomy in the phylogenomic era: species boundaries and phylogenetic relationships among North American ants of the *Crematogaster scutellaris* group. *Zoological Journal of the Linnean Society* **194**(3), 893–937.

Wheeler, WM (1938) Ants from the caves of Yucatan. In Pearse, A. S. (ed.), *Fauna of the Caves of Yucatan* (pp. 251–255). Carnegie Institution of Washington Publication: Washington, D.C., United States of America.

Wilson EO (1955) A monographic revision of the ant genus *Lasius*. *Bulletin of the Museum of Comparative Zoology*, 113, 1–201.

Wong MKL, Guénard B (2016) *Leptanilla hypodracos* sp. n., a new species of the cryptic ant genus *Leptanilla* (Hymenoptera, Formicidae) from Singapore, with new distribution data and an

updated key to Oriental *Leptanilla* species. *ZooKeys* **551**, 129–144. doi:10.3897/zookeys.551.6686

Xu, Z-H (2011) *Furcotanilla*, a new genus of the ant subfamily Leptanillinae from China with descriptions of two new species of *Protanilla* and *P. rafflesi* Taylor (Hymenoptera: Formicidae). *Sociobiology* **59**, 477-491.

Yamada A, Nguyen DD, Eguchi K (2020) Unveiling the morphology of the Oriental rare monotypic ant genus *Opamyrma* Yamane, Bui & Eguchi, 2008 (Hymenoptera: Formicidae: Leptanillinae) and its evolutionary implications, with first descriptions of the male, larva, tentorium, and sting apparatus. *Myrmecological News* **30**, 27–52. doi:10.25849/myrmecol.news_030:027

Yamane S, Bui TV, Eguchi K (2008) *Opamyrma hungvuong*, a new genus and species of ant related to *Apomyrma* (Hymenoptera: Formicidae: Amblyoponinae). *Zootaxa* **1767**, 55–63.

Zarei M (2010) Hydrogeology of salt diapirs in the south of Iran. PhD dissertation, Shiraz University, Iran.

Chapter 3. Derivation and disparity in the male genitalia of the Leptanillinae (Hymenoptera: Formicidae): a comparative study of genital skeletomusculature[4]

Zachary H. Griebenow[5], Adrian Richter, Georg Fischer, Thomas van de Kamp, Evan Economo, Ziv E. Lieberman

Abstract. The male genitalia of the Insecta are famed for structural and functional diversity. Variation in this anatomical region shows ample phylogenetic signal, and this variation has proven indispensable for classification across the insects at multiple taxonomic ranks. However, in the ants (Hymenoptera: Formicidae) the male genital phenotype ancillary to the morphology of the worker caste for systematic purposes. Ants of the enigmatic subfamily Leptanillinae are an exception, as males are easier to collect than workers. Ongoing systematic revision of the Leptanillinae must therefore rely upon the male phenotype—particularly the male genitalia, which are spectacularly profuse. To thoroughly illuminate this anatomical region and aid comparative morphology of ant male genitalia, we present a comparative morphological study of the male genitalia in nine exemplar lineages spanning the Leptanillinae, plus three outgroups representing other major clades of the Formicidae. We use micro-computed tomography (micro-CT) to generate 3D volumetric reconstructions of male genital skeletomusculature in these specimens. Our descriptions use new muscular nomenclature compatible with topographic main-group systems for the rest of the pterygote soma, and applicable to all Hymenoptera. We find that male genitalia in the Leptanillinae show an overall trend towards skeletomuscular

[4]In review for publication in *Arthropod Systematics & Phylogeny*. Note that the taxonomy of the Leptanillinae used herein is superseded by that presented in Chapter 4.

[5]Lead author. Chapter 3 is included in thesis by approval of committee and permission of Graduate Program Chair of Dept. of Entomology & Nematology, Dr. Joanna Chiu.

simplification, with muscular reduction in some cases being unprecedented in ants, or even hymenopterans in general. In several lineages of the Leptanillinae we describe derivations of the male genitalia that are bizarre and unparalleled among the Hymenoptera. We conclude by discussing the functional implications of the often-extreme morphologies here observed.

1. Introduction

" *... Auteurs ne s'accordaient ni entre eux, ni avec eux-mêmes: autant de formes diverses, autant de noms différens."*

" ... Authors agreed neither among themselves, nor with themselves: so many varied forms, so many different names." – Pierre A. Latreille, in Audouin (1821: 287)

The structural diversity of the male genitalia in insects (Hexapoda: Ectognatha) is famously profuse. Snodgrass (1957: 11) referred to this diversity as being a dialectical "delight of taxonomists, [and] despair of morphologists". Empirical studies indicate that the genital variety observed in metazoans with internal fertilization, including insects, is attributable to sexual selection—this is not to the exclusion of other selective pressures, including reproductive antagonism (Hosken and Stockley 2004). Being intimately involved in pre-zygotic reproductive isolation, this anatomical region is regarded as a rich source of discrete characters for taxon delimitation (Tuxen 1970), useful at a broad span of taxonomic ranks, and is consequently used for classification and phylogenetic inference in myriad insect taxa (Dirsh 1956; Yoshizawa and Johnson 2006; Clarke 2011; Tarasov and Solodovnikov 2011; Buenaventura and Pape 2018; Chiquetto-Machado and Cancello 2021; Girón et al. 2022). Allaying concerns that the putative rapidity of male genital evolution in insects erases phylogenetic signal in this character set, a review of morphological cladistic analyses across the Insecta by Song & Bucheli (2010)

indicated that male genitalia display phylogenetic signal comparable to other anatomical regions (although without correction by these authors for systematic biases in the reviewed cladistic analyses; cf. Sanderson and Donoghue 1989). Even in the theoretical absence of character states that can be discretized, male insect genitalia are of morphometric utility as a source of continuous measurements that show negative allometry (Dreyer and Shingleton 2011; Mikó et al. 2013). Male insect genitalia are therefore unavoidably "an everlasting temptation" (Aspöck 2002: 161) to entomologists interested in classifying insects.

Compared to the general utility of male genitalia in insect taxonomy, ant classification has traditionally incorporated few male genitalic characters. Systematic myrmecology has overwhelmingly focused upon the female worker caste: workers are numerically more abundant than their reproductive counterparts, and males are short-lived, with rare exceptions (Boomsma et al. 2005; Fuessl et al. 2015). There has nonetheless been a recent increase in the study and description of male ant genitalia for taxonomic purposes at the species level (Schmidt and Heinze 2017) and higher (Wang et al. 2019; Ward and Boudinot 2021). In a number of lineages, male morphology, including that of the genitalia, provides phylogenetic signal absent from the phenotype of corresponding workers (Kempf 1954; Ward and Downie 2005; Eguchi et al. 2006; Lapolla et al. 2012; Barden et al. 2017; Boudinot et al. 2021).

The Old World ant subfamily Leptanillinae Emery is unusual among the Formicidae in that male morphology is integral to its taxonomy, rather than being supplemental to worker morphology. Leptanilline ants are minute, with the worker caste appearing to be strictly subterranean in biology (Masuko 1990; Yamada et al. 2020; Ito et al. 2021), although colonies have been also reported from dead wood (Hsu et al. 2017) and lone workers of *Protanilla lini* Terayama were collected in SLAM (Sea, Land & Air Malaise) traps (Griebenow 2020: 244). Male specimens are

more abundant in collections than females, with a variety of species and even several genera having been described based solely upon males unassociated with workers (Brues 1925; Petersen 1968; Kugler 1986). The classification of the Leptanillinae must therefore rely upon a firm understanding of male morphology. Comprehensive description of male genitalia in the Leptanillinae is indispensable to systematic revision of the clade, with the aim of devising a classification that integrates both sexes and acknowledges evolutionary relationships.

The largely undescribed morphological derivation of male genital skeletomusculature seen within the Leptanillinae relative to the remaining Formicidae is of broader scientific interest, as is the conspicuous morphological disparity of the male phenotype in the Leptanillinae (Fig. 3.1), particularly with respect to the genitalia. This disparity has not been scrutinized, beyond the use of discrete external skeletal characters of the male leptanilline genitalia in phylogenetic inference (Griebenow 2021), but has been superlatively alluded to in the literature: Boudinot (2015: 29) noted that "some [leptanilline] males are so derived as to be difficult to intuitively ascribe to the Formicidae", with reference to the whole of leptanilline male morphology; while Bolton (1990b: 271) remarked that male genitalia in the Leptanillinae are "often bizarre", without further elaboration.

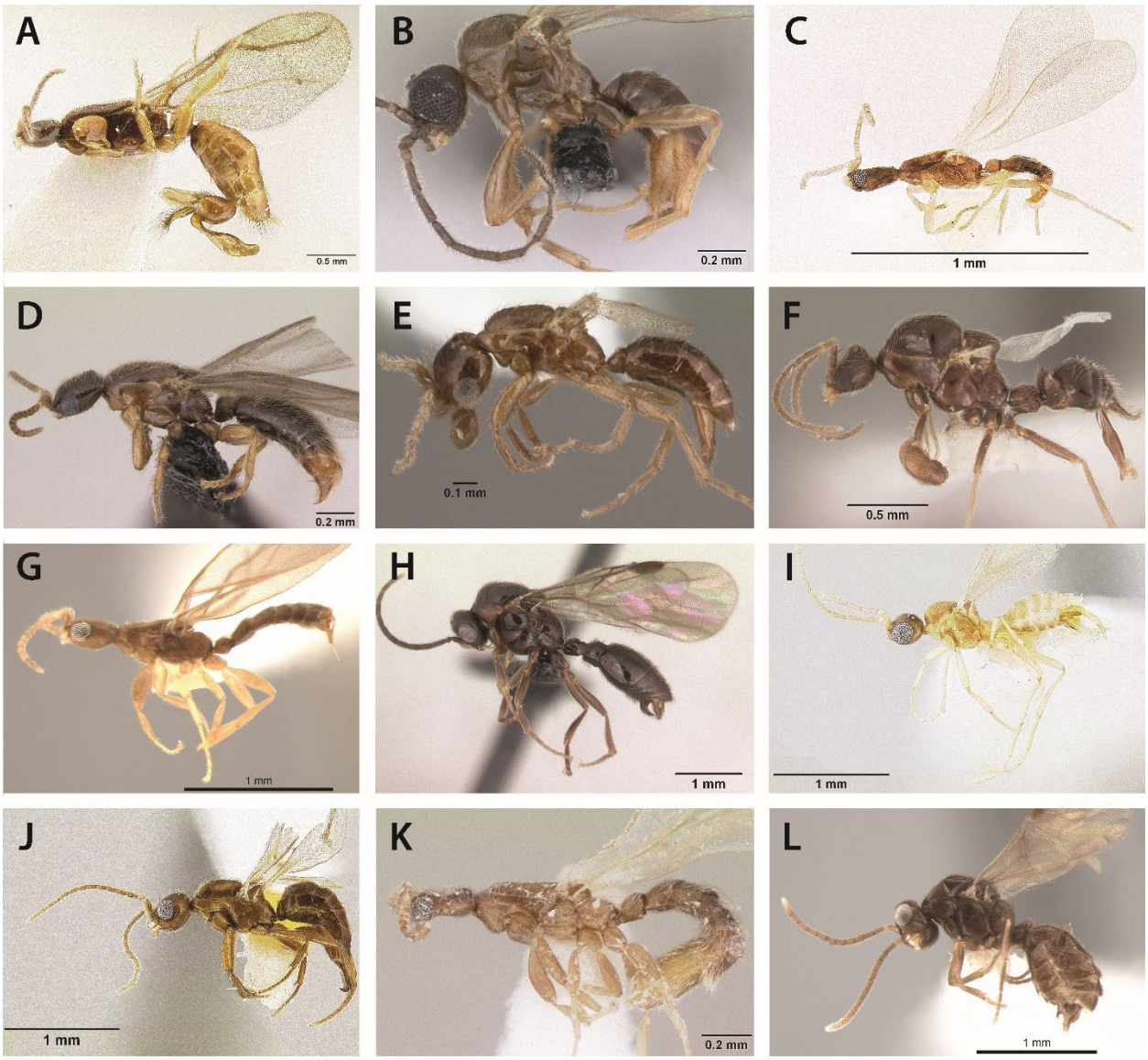

Figure 3.1. Variety of male habitus across the Leptanillinae, profile view; images from AntWeb.org. **A** *Leptanilla* zhg-my05 (CASENT042571; Zachary Griebenow) **B** *Yavnella* TH02 (CASENT0119531; April Nobile) **C** *Leptanilla* zhg-bt02 (CASENT0842612; Zachary Griebenow) **D** *Leptanilla* TH01 (CASENT0119792; April Nobile) **E** *Scyphodon* cf. *anomalum* (CASENT0106168; April Nobile) **F** *Leptanilla* ci01 (CASENT0102373; April Nobile) **G** *Leptanilla* zhg-mm01 (CASENT0842788; Zachary Griebenow) **H** *Protanilla* TH03 (CASENT0119791; Erin Prado) **I** *Yavnella* nr. *indica* (CASENT0106380; Zachary Griebenow) **J** *Noonilla* zhg-my06 (CASENT0106372; Zachary Griebenow) **K** *Leptanilla* indet. (CASENT0104306; April Nobile) **L** *Protanilla* zhg-my01 (CASENT0842734; Zachary Griebenow).

In the present study, we elucidate this “bizarre” quality by describing male genital skeletomusculature across all major subclades of the Leptanillinae for which males are known.

Male genital skeletomusculature is studied here according to the comparative method set out by evolutionary morphology *sensu* Richter and Wirkner (2014). To facilitate comprehensive comparison of tiny, often rare or unique specimens, we nondestructively generate high-resolution, three-dimensional (3D) anatomical data in a relatively large sample of taxa via micro-computed tomography (micro-CT). Where necessary and feasible, we supplement these 3D reconstructions, or "virtual dissections", with 2D imaging, including photomicrography and scanning electron microscopy (SEM). Scans of 21 specimens are published in the Supplementary Material for future comparative morphology.

We report spectacular modifications to the male genitalia in certain lineages of the Leptanillinae relative to homologous skeletomusculature observed in other Formicidae, some apparently unique not just among ants but among the Hymenoptera as a whole. We observe numerous striking autapomorphies of the posterior pregenital segments and the genital apparatus, in clades at the tribal, generic, and lower ranks. We discuss the degree of consilience of male genital morphology with the phylogeny of the Leptanillinae, as inferred by Borowiec et al. (2019) and Griebenow (2020, 2021), and compare this morphology with that documented in other ants, contrasting macroevolutionary tendencies across the entire genitalia and details thereof. In order to contextualize the Leptanillinae, facilitate comparison, and link male genitalic nomenclature to that of other body regions, we provide a new muscular nomenclature synthesizing interordinal holometabolan homologies (Boudinot, 2018) and the nomenclature for the neopteran thorax (Friedrich and Beutel 2008) and worker ant abdomen (Lieberman, Billen, van de Kamp, & Boudinot, 2022). Finally, though our approach is motivated by phenomenology rather than mechanism (Rodrigue and Philippe 2010), we speculate on the functional and evolutionary implications of the highly derived male genital modifications here described, and summarize

overall trends observed in the evolution of male genitalia in Leptanillinae, ants, and Hymenoptera. Our study is the first to address the male genitalia of any ant clade in such descriptive detail, explicitly grounded in phylogeny, and with a mind towards an evolutionary-morphological research program (Richter and Wirkner 2014).

2. Methods

2.1. Material Examined

2.1.1. Institutional Deposition

Specimens are deposited at the following institutions, with abbreviations following Evenhuis (2022) unless enclosed in brackets:

CAS = California Academy of Sciences, San Francisco, USA

CSCA = California State Collection of Arthropods, Sacramento, USA

[JMGDC] = personal collection of José María Gómez-Durán

MZLU = Lund University, Lund, Sweden

PMJ = Phyletisches Museum, Friedrich-Schiller-Universität, Jena, Germany

UCDC = R. M. Bohart Museum of Entomology, University of California, Davis, USA

ZMUC = Zoological Museum, University of Copenhagen, Copenhagen, Denmark

2.1.2. Scanned Specimens

Specimens with full descriptions of genital skeletomusculature in Section 3 are underlined. Other specimens below were scanned and examined but were not fully described in the Results. All image data are publicly available on Zenodo (10.5281/zenodo.7647890). All specimens are deposited as vouchers in their respective collections. Putative morphospecies are designated with numerical codes relating to their country of origin, following the generic assignments of Griebenow (2020) where relevant.

Odontomachus **indet.** 1 male; SRI LANKA, Central: Kandy District, University of Peradeniya, Mt. Hantana, 7°15′N 80°37′E, 10–14.viii.1999, Malaise trap, M. & J. Wasbauer, CASENT0842842. UCDC.

Lioponera **indet.** 1 male; MADAGASCAR, Antsiranana: Rés. Ankarana, 7 km SE Matsaborimanga, 12°54′S 49°7′E, 150 m, 1990.xi.28, blacklight, P. S. Ward, PSW11020–5, CASENT0844684. UCDC.

Aenictogiton **indet.** 1 male; GHANA, Western Region: Nini Suhien National Park, Ankasa Game Reserve, 5.248° -2.648°, 80 m, 2014.iv.24, M. Hauser & S. D. Gaimari. CASENT0866513. UCDC.

Myrmica ruginodis**.** 1 male; GERMANY, Thuringia: Jena, Lobeda West, meadow E Lobdeburgtunnel, 50.8793° 11.6148°, 24.vii.2021, A. Richter, PMJ:Hex:2205. PMJ.

Protanilla **zhg-vn01.** 1 male; VIETNAM, Vinh Phuc: Tam Dao National Park, 21°27′52″N 105°38′46″E, 1200 m, 19–22.vi.2014, Malaise trap, M. Hauser & N. von Ellenreider, CASENT0106408. CSCA.

***Protanilla lini*.** 1 male; JAPAN, Okinawa: Okinawa Institute of Science & Technology, Onna, 26.48059° 127.8419°, 107 m, 17.vi.–1.vii.2017, SLAM trap, OKEON, OKENT0011097. OIST.

***Yavnella* zhg-bt01**. 1 male; BHUTAN, Wangdue Phodrang: 3.5 km E Bajo, 27.486° 90.559°, 1480 m, 17–21.viii.2017, Malaise trap, C. J. Borkent & M. Hauser, FFP17BT050, CASENT0842743. CSCA.

***Yavnella* zhg-th03**. 1 male; THAILAND, Chaiyaphum: 2 km S Ruan Kluaymai Resort, road #2018, 16.529° 101.855°, 335 m, 20–28.iii.2019, Malaise trap, K.A. Williams, A.R. Chaves & Thaochan lab, CASENT0842741. CSCA.

***Leptanilla* zhg-id01.** 1 male; INDONESIA, Kalimantan Barat: Gunung Palung National Park, Cabang Panti Reserve Station, -1.25° 110.083°, 97 m, 15.vi.–15.vii.1991, Malaise trap, D.C. Darling *et al*., CASENT0842626. UCDC.

***Leptanilla* zhg-my02.** 1 male; MALAYSIA, Sabah: Sipitang District, Mendolong, 4.91667° 115.76667° [coordinates estimated to nearest minute], 16.iv.1988, S. Adebratt, CASENT0106416. MZLU.

***Leptanilla* zhg-my03.** 1 male; MALAYSIA, Sarawak: SW Gunung Buda, 64 km S Limbang, 4.2167° 114.9333°, 16–21.xi.1996, Malaise trap, S.L. Heydon & S. Fung, CASENT0106365. UCDC.

***Leptanilla* zhg-my04.** 1 male; MALAYSIA, Sabah: Sipitang District, Mendolong, 4.91667° 115.76667° [coordinates estimated to nearest minute], 3.v.1988, S. Adebratt, CASENT0842565. MZLU.

***Leptanilla* zhg-my06.** 1 male; MALAYSIA, Sarawak: SW Gunung Buda, 64 km S Limbang, 4.2167° 114.9333°, 8–15.xi.1996, Malaise trap, S.L. Heydon & S. Fung, CASENT0106370. UCDC.

***Noonilla* cf. *copiosa*.** 1 male; MALAYSIA, Sabah: Sipitang District, Mendolong, 4.91667° 115.76667° [coordinates estimated to nearest minute], 10.iii.1989, S. Adebratt, CASENT0842844. MZLU.

***Noonilla* zhg-my01.** 1 male; MALAYSIA, Sabah: Sipitang District, Mendolong, 4.91667° 115.76667° [coordinates estimated to nearest minute], 4.v.1988, S. Adebratt, CASENT0842577. MZLU.

***Noonilla* zhg-my02.** 1 male; MALAYSIA, Sabah: Sipitang District, Mendolong, 4.91667° 115.76667° [coordinates estimated to nearest minute], 6.v.1988, S. Adebratt, CASENT0842600.

***Noonilla* zhg-my03.** 1 male; MALAYSIA, Sabah: Sipitang District, Mendolong, 4.91667° 115.76667° [coordinates estimated to nearest minute], 3.v.1988, S. Adebratt, CASENT0842609. MZLU.

***Noonilla* zhg-my06.** 1 male; MALAYSIA, Sarawak; south of Gunung Buda, 64 km. south of Limbang, 4.21667° 114.93333°, 16–21.xi.1996, S. L. Heydon & S. Fung, CASENT0106371. UCDC.

***Leptanilla* cf. *zaballosi*.** 1 male; SPAIN, Madrid: Madrid, Instituto Nacional Investigación y Tecnología Agraria y Alimentaria, 40.45705° -3.74838°, 0.vii–ix.2013, experimental pool, J. M. G. Duran, CASENT0842782. JMGDC.

***Leptanilla* zhg-id04.** 1 male; INDONESIA, Sulawesi Tenggara: Kabupaten Kolaka, Mangolo Taman Wista, Alam Mangolo River Watershed, -3.98° 121.56833°, 85 m, 16–23. xi.2011, Malaise trap, ICGB Joint LIPI-U.C. Davis Entomology Survey Team, CASENT0106357. UCDC.

2.1.3. Other Specimens

***Diacamma* indet.** 1 male; MALAYSIA, Sabah: Penampang, Kipandi Butterfly Farm, 5.87222° 116.24806°, 720 m, 2013.iii.05–12, Malaise trap, M. Hauser, S. Gaimari, & J. Gokusing, SDG13-02, CASENT0842838. UCDC.

***Leptanilla astylina*.** 1 male; PHILIPPINES, Palawan: Pinigisan, Mantalingahan Range, 1969.ix.24, ZMUC00240037. ZMUC.

***Protanilla* zhg-th02.** 1 male; THAILAND, Chaiyaphum: 2km S Ruan Kluaymai Resort, road #2018, 16.529 101.855, 335 m, 2019.iii.20–28, Malaise trap, K. A. Williams, A. R. Chaves, Thaochan Laboratory, CASENT0842645. CSCA.

***Yavnella* TH03.** 1 male; THAILAND, Chiang Mai: Doi Inthanon National Park, checkpoint 2, 18.525984° 98.499016°, 1700 m, 2006.ix.27–x.5, Malaise trap, Y. Areeluck, T0349, CASENT0129721. CAS.

***Yavnella* zhg-th01.** 1 male; THAILAND, Phetchabun: Nam Nao National Park, helicopter landing ground, 16.71855° 101.58556°, 889 m, 2006.vii.10–17, Malaise trap, N. Hongyothi, CASENT0842620. CAS.

***Yavnella* zhg-my02.** 1 male; MALAYSIA, Selangor: Universiti Malaya, Botanical Garden, Kuala Lumpur, 3.11667° 101.65000°, 1996.vi.10–12, S. L. Heydon, CASENT0106369. UCDC.

***Noonilla* cf. *copiosa*.** 1 male; MALAYSIA, Sabah: Sipitang District, Mendolong, 4.9167° 115.7667°, 1989.iii.10, S. Adebratt, CASENT0842610. MZLU.

2.2. Methods

2.2.1. X-Ray microtomography

X-ray microtomography was performed using the following equipment and facilities: (1) Beamline 8.3.2 with a LuAD:CE scintillator and PCO.edge CMOS detector at the Lawrence Berkeley National Laboratory Advanced Light Source (ALS), University of California, Berkeley; (2) KIT Light Source of Karlsruhe Institute for Technology (KIT) using a 12-µm LSO:Tb scintillator and a 12-bit PCO.dimax detector. Laboratory X-ray microscopes used for this study were as follows: (1) a ZEISS Xradia 510 Versa 3D X-ray microscope, with the ZEISS Scout & Scan Control System (ZEISS, Oberkochen, Germany), at the Okinawa Institute of Science & Technology; (2) an XRadia 620 Versa at ZEISS X-ray Microscopy Inc., Dublin, CA; and (3) a Skyscan 2211 (Bruker, Belgium) at the Max Planck Institut for the Science of Human History Jena, equipped with a high resolution (4000 × 2600 pixel) X-ray sensitive CCD camera. Metadata for all scans published herein and relevant information on scan settings for all facilities are included in Table 3.S1.

Segmentation of micro-CT data was performed manually with Dragonfly v.2021.1–2, with the microtomography sequence being imported as a stack of .tif or DICOM images, with the latter being reconstructed using XMReconstructor (v. 10.7.2936). If unwieldy for system RAM, scan

data were cropped upon import into Dragonfly to include only structures that were relevant to the study. See Lieberman et al. (2022) for detailed explanation of tissue segmentation using Dragonfly. Segmentation labels were exported as image series for volume rendering using a custom code (K. Jandausch, pers. comm.). These series were cropped to the label extent, then imported to VG Studio Max 3.4.5 (Volume Graphics GmBH, Heidelberg, Germany) for volume rendering, with Phong interpolation shading. Scale for perspective renders was obtained from equivalent orthographic projections using *Rendering* > *Parallel*.

The minute size of most specimens belonging to the Leptanillinae largely prevented their suspension in fluid for imaging, therefore prohibiting iodine staining, except for *Yavnella* zhg-bt01. Therefore, leptanilline specimens were scanned dry on the end of cardstock points; if originally obtained in ethanol, these were treated with hexamethyldisilane (HMDS), preceded by two washes in absolute ethanol, to diminish distortion of muscles by desiccation. Outgroups were stained with iodine (PMJ:Hex:2205, CASENT0844684) or left unstained in conjunction with phase contrast (CASENT0842842), and scanned in ethanol.

2.2.2. Photomicrography and Scanning Electron Microscopy

Photomicrographs were acquired as focus stacks, either (1) using a JVC KY-F75 digital camera (JVC, Yokohama, Japan), with manual *z*-stepping; or (2) 3.1-megapixel Leica DMC2900 camera (Leica Microsystems, Wetzlar, Germany) mounted on a Leica MZ16A stereomicroscope, with automated *z*-stepping via the Leica Application Suite software (v. 4.13.0). Image stacks were combined into full-focus montages and manually retouched using the Syncroscopy AutoMontage Program (v. 5.02.0096) (Synoptics Ltd., Cambridge, UK) or Helicon Focus (Helicon Soft. Ltd., Kharkiv, Ukraine). Additional photomicrographs were obtained from AntWeb (Version 8.68.7,

California Academy of Sciences) and are attributed in figure captions. Scanning electron microscopy (SEM) was performed on uncoated specimens using a Hitachi TM4000.

2.3. Nomenclature

2.3.1. Scope

The male pregenital metasomal segments of Formicidae are abdominal segments II–VIII. Parts of abdominal segments IX–X comprise the genitalia, specifically abdominal sternite IX and its appendages and derivative structures, and the fused appendages of abdominal segment X (primary gonopods, i.e., the penis). Following prior convention, we do not consider abdominal tergites IX–XI to be part of the genital apparatus. In Formicidae, tergites X–XI cannot be clearly distinguished from one another. To describe the extreme derivations of the genitalia in certain lineages of Leptanillinae, we include the skeletomusculature of (pregenital) abdominal segment VIII if (1) the eighth tergite and sternite are fused to one another, or (2) when musculature of segment VIII is extrinsic and connects to genital sclerites. Visceral muscles, which have at least one non-skeletal attachment, were excluded from consideration in this study.

We caution that the muscular nomenclature introduced here is solely applicable to the male genitalia of Hymenoptera. For comparison of male genital skeletomusculature across the Hexapoda, we suggest retaining the system of Boudinot (2018), with which our nomenclature is congruent. We also caution that nomenclatural correspondence with terms used in topographic main-group nomenclature of female hymenopteran genitalia in the Hymenoptera does not imply homology between the sexes.

2.3.2. Genital Terminology

The terminology used for sclerites of male genitalia in the Formicidae is highly variable (Table 3.S2), recapitulating the longstanding profusion of genital terms across the Insecta as a whole (>5,400 listed by Kaestner and Wetzel 1972) and resulting in redundancy and confusion. Most publications make no theoretical justification for nomenclature, but may implicitly follow either the coxopodal (Michener 1944) or phallic-periphallic (Snodgrass 1935b, 1957) hypotheses of male genital evolution in the insects. Conversely, this study follows the skeletomuscular homology hypotheses of Boudinot (2018). This model is preferred to the coxopodal and phallic-periphallic models in that it homologizes male genital skeletomusculature across the entire Hexapoda with reference to the Remipedia, the sister taxon of the Hexapoda (von Reumont et al. 2012; Misof et al. 2014). By contrast, the coxopodal and phallic-periphallic hypotheses of male genital skeletomuscular homology assumed the falsified "orthodox views" (Brusca 2001: 1084) of arthropod phylogeny promulgated by Snodgrass and others, which posited that the Myriapoda are sister to the Hexapoda. Terminological correspondences with selected previous descriptions of male ant genitalia are summarized in Tables 3.1–2.

The genital appendages of males in the Ectognatha (Insecta *s. str.*) are derived from abdominal limbs, or coxopods, of abdominal segments IX–X, which constitute secondary and primary gonopods respectively; the protopods of gonopods X (i.e., gonocoxae) are medially fused to form the penis (Boudinot 2018). In the Endopterygota, the penis is developmentally integrated with gonopods IX, such that extrinsic penial musculature originates within gonocoxae IX, rather than on sternite IX. Additionally, in the endopterygote ancestor, bilateral portions of the penis split off, forming the paired *lateropenites*. The Hymenoptera are further derived relative to the endopterygote groundplan by 1) the fusion of fragments of abdominal tergite IX and the (ninth) gonocoxae to form the cupula; and 2) the fusion of the lateropenite with the *parossiculus*, a

ventromedial fragment of the gonocoxite (gonocoxal sclerite IX), the parossiculus and lateropenite together forming a paired appendage called the *volsella*.

2.3.3. General definitions

We consider homology of anatomical structures to refer to the phenomenon of morphological character states that are shared between individual organisms due to inheritance from a common ancestor. We recognize homological structures according to the criteria presented by Remane (1952), chiefly the first three: (1) parts correspond in location relative to other parts; (2) components of given parts correspond in location relative to other components of those given parts; and (3) parts that are disparate in appearance are related by intermediate forms.

The integument is here regarded as a continuous exoskeletal surface enclosing the fluid-filled haemocoel. Features situated on the exterior of this surface are called *ectal*; those within, *mesal*. For internalized sclerites which do not enclose a lumen, ectal indicates the outer surface (towards the body wall), and mesal indicates the inner surface (towards the anteroposterior axis). Along the transverse axis, features are referred to in mediolateral order.

Anatomically, sclerites are regions of the cuticle that are reinforced with exocuticle and separated by flexible conjunctivae, which consist only of endocuticle. A much more general definition is provided by the Anatomy of the Insect Skeleto-Muscular System (AISM; Girón et al. 2022), which considers a sclerite (AISM:0000003) to be a region of cuticle (AISM:0000174) that is less flexible than the neighboring, conjunctival cuticle (AISM:0000004). Because we neither examined the integument histologically or by manual manipulation, we recognize

sclerites by a combination of their higher contrast and thickness in micro-CT images, as well as visually by degree of melanization and opacity, relative to adjacent membrane.

For orientation of parts within the male genitalia, we divide this region into *axial* and *appendicular* anatomical categories. These categories are informed both by genital homologies across the Hymenoptera and the phenotype of genital components in the Leptanillinae. Abdominal sternite IX and the cupula are considered axial (unpaired and derived in whole or in part from segmental sclerites); the gonopodites, volsellae and penial sclerites are considered appendicular (paired and derived in whole from appendages). Axial structures are oriented along the craniocaudal axis, even when fused completely to components of the appendicular genitalia. Appendicular structures are oriented along a proximodistal axis relative to the abdomen, with abdominal sternite IX and cupula (when present) being the collective proximal point of reference. When skeletomuscular features could not be resolved due to limitations of the dataset, these features are referred to as *not discernible*.

2.3.4. Skeletal Nomenclature (Fig. 3.2)

Abdominal segments are abbreviated **A** and numbered in an anteroposterior direction using Roman numerals, with AII being the petiole, and AIII–XI comprising the gaster (in some outgroup subfamilies, AIII comprises the postpetiole and AIV–XI the gaster). Abdominal tergites and sternites are abbreviated **T** and **S**, respectively. Abdominal tergite IX may be a continuous, unpaired sclerite, as in the unmodified pregenital segments, or it may be fully divided into disjunct lateral fragments, or *hemitergites*. In species with undivided ATIX, the distinction between ATIX and ATX is usually unclear, due to weak sclerotization and continuity of the membranous surfaces between the tergites confusing the intersegmental boundary;

Richards (1934) contended that ATIX–ATX are indistinct in all male Aculeata. However, as pointed out by Peck (1937), the insertions of the longitudinal intertergal muscles IX–X, and the extrinsic proctiger muscles (cf. Lieberman et al. 2022) may serve as landmarks. Since the anatomy of ATX is beyond the scope of the present study, we did not investigate these traits in detail.

The skeletal nomenclature of Boudinot (2018) is followed here for the genitalia, with the following extensions. The sclerotized portion of the endophallus called the wedge sclerite (e.g., Forbes and Do-Van-Quy 1965) or *sperrkeil* (Clausen 1938) in the Formicidae, or endophallite more generally (Génier 2019), is here termed the *endophallic sclerite* (Fig. 3.2A, D) as in other taxa described by Boudinot (2018). The term *mulceator* is hereby coined to describe posterolateral filiform processes of the male abdominal sternite IX, a character state that is an autapomorphy of the Bornean morphospecies-group within *Leptanilla s. l.* Mulceators are observed nowhere else in the order Hymenoptera. The name derives from the Latin *mulceō*, meaning “I caress”.

External cuticular processes which do not enclose apparent haemocoelic lumina and are compressed enough to result in transparency to visible light are termed *laminae*. The gonopodites are considered *inarticulate* if there is no trace of a conjunctiva separating the gonocoxite and gonostylus, and the gonostylus is not reflexed relative to the gonocoxite, which in deceased specimens implies articulation of the gonopodite (Ward and Sumnicht 2012).

Table 3.S2 provides an abbreviated list of synonyms in skeletal nomenclature from a selection of the literature on male genitalia in the Formicidae, along with respective Uniform Resource Identifiers (URIs) from the Hymenoptera Anatomy Ontology (HAO; Yoder et al. 2010, Seltmann

et al. 2012) when available. For more extensive comparisons of terms across Hymenoptera, see Boulangé (1924) and especially Schulmeister (2001, fig. 3).

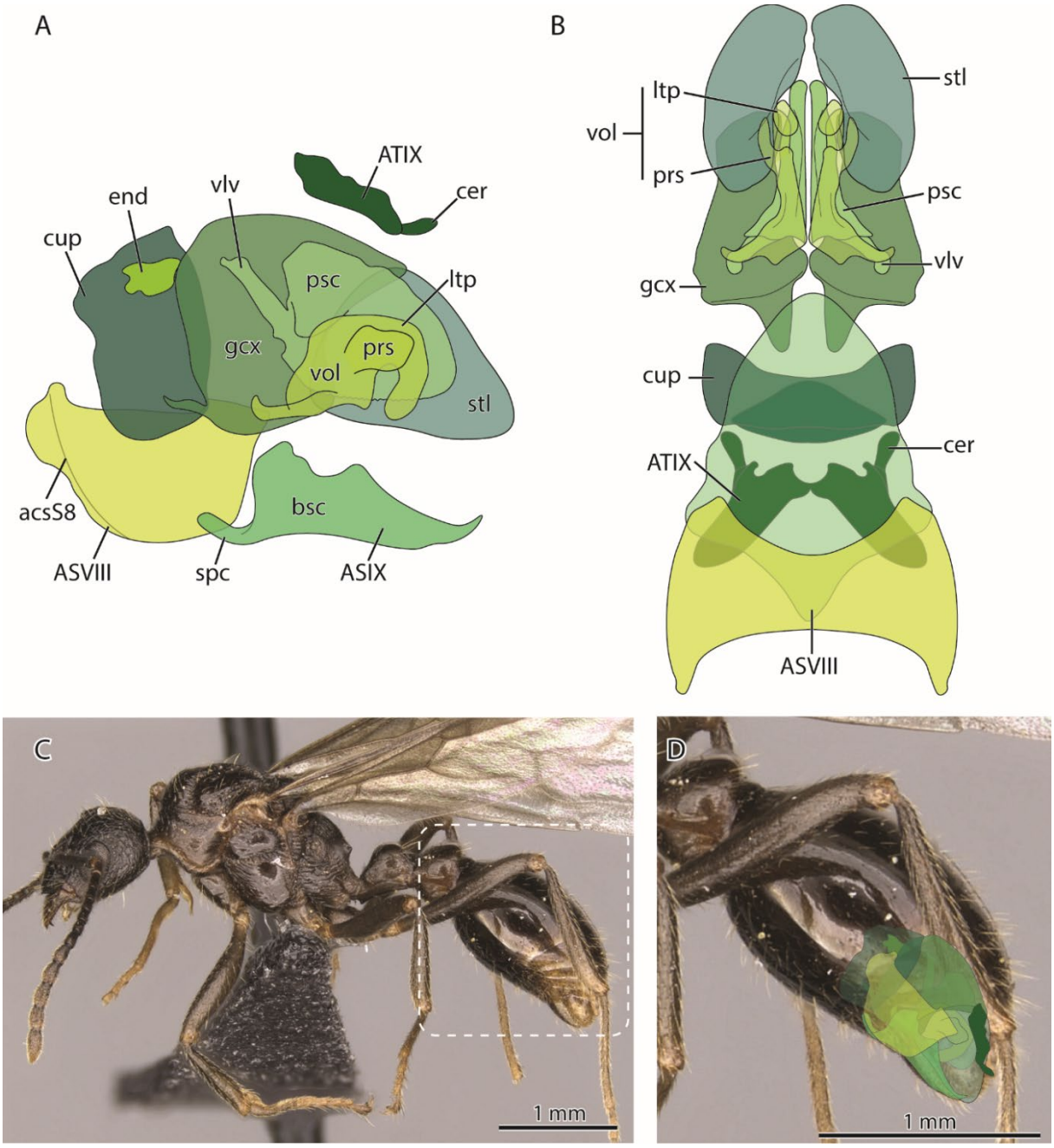

Figure 3.2. Diagrammatic summary of ♂ genital and pregenital sclerites in the Formicidae considered in the scope of this study, using *Myrmica ruginodis* Nylander as template. Order of overlapping sclerites in Figure 2A is not true to life, for clarity. Caps in muscle diagrams signify origin; lack of caps, insertion. **A** profile view of considered male genital and pregenital sclerites, exploded **B** ventral view of male genital and pregenital sclerites, exploded **C** Habitus of male *Myrmica ruginodis*, profile view (CASENT0902305; from AntWeb.org, Ziv Lieberman) **D** inset of same profile view, with included genital and pregenital sclerites diagrammed *in situ.* Abbreviations: acsS8=antecosta of abdominal sternite VIII; ASVIII=abdominal sternite VIII; ASIX=abdominal sternite IX; spc=spiculum; bsc=basal disc; ATIX=abdominal tergite IX; cer=cercus; cup=cupula; gcx=gonocoxite; stl=gonostylus; vol=volsella; prs=parossiculus; ltp=lateropenite; psc=penial sclerites; vlv=valvura; end=endophallic sclerite

2.3.5 Muscular Nomenclature

2.3.5.1. General terminology

A muscle is *extrinsic* if it attaches two different body segments, two true segments of an appendage, or connects an appendage to the body; it is *intrinsic* if both attachments are within the same body segment or segment of an appendage. The *origin* (**O**) of an extrinsic muscle is the attachment on the cephalad segment of the body, the proximad segment of an appendage, or the body segment if it attaches an appendage to the body; its *insertion* (**I**) is the attachment on the caudad body segment, distad appendage segment, or the appendage if the muscle attaches an appendage to the body. For intrinsic muscles, the origin is point of putatively fixed attachment, while the insertion is the point of mobile attachment (von Kéler 1955). Certain muscles that attach to two putatively mobile elements, present in outgroups to the Leptanillinae, are assigned origin and insertion based on their form and most likely function. We also designate muscles originating and inserting within the volsella as intrinsic, indicated in the Latin name by the descriptor *interior*, while those that originate on the gonopod and insert in the volsella are considered extrinsic (*exterior*). We choose not to use the term *tendon* in reference to insertions, as we did not examine myotendinous junctions histologically (Chapman et al. 2013).

In our expansion of Boudinot (2018) to include all known male Hymenopteran genital muscles (see following section), we in part apply the topographic main-group approach of Friedrich & Beutel (2008) for the thorax in the Neoptera and Lieberman et al. (2022) for the worker ant abdomen. Topographic main groups refer to the general spatial position and orientation of muscle origins and insertions, providing a framework for recognizing subdivisions. Where possible, we align our main groups with interordinal homologies and use topography to

distinguish within such homology classes. A “homology class” in this context is a set of structures which can be reasonably inferred to derive from the same ancestral structure, and are variably expressed among the considered exemplars.

Terminology and enumeration for pregenital musculature follows Lieberman et al. (2022). Although these authors described a worker ant (Amblyoponinae: *Amblyopone australis* Erichson), in which the genital segments are AVIII and AIX and lack sternites, homonymy is clear between the muscles of the male eighth segment and the serial homologues in the female pregenital abdomen, as additionally supported by descriptions of the posterior pregenital musculature by Boulangé (1924), (Peck 1937), Snodgrass (1942), and Youssef (1969).

2.3.5.2. Genital musculature

We introduce an expansion of the homology inferences of Boudinot (2018), providing designations both for subdivisions of the neopteran groundplan muscles occurring in male Hymenoptera, and for main groups which cannot be decisively homologized with those of outgroup neopterans. We note that the recognition of subdivisions as separate muscles is somewhat subjective; see Sections 4.3.1.1–2 for discussion of our approach to identifying homologies and recognizing subdivisions.

While the system applied here generally refers to muscle groups plesiomorphic for the Hexapoda, the numeration and descriptors of muscles apply strictly to male Hymenoptera. That is, the system used here is not intended to apply across insect orders and does not imply intersexual homology with female Hymenoptera. We are aware of potential drawbacks in introducing new nomenclature, especially of limited scope and in systems rife with historical

synonymy and terminological homonymy. Nevertheless, we consider the application of the system justifiable. The most common schema for genital nomenclature in male Hymenoptera is the homology-neutral alphabetic system of Boulangé (1924) with occasional modification (e.g., (Schulmeister 2001, 2003). We avoid this system for practical and epistemological reasons. Operationally, the Boulangé names only provide very coarse and approximate spatial information (with lettering broadly proceeding cephalad to caudad) and are inconsistently constructed. For instance, the compound name *qr* implies the close association of subgroups *q* and *r*, while *si* refers to an intermediate position between *s* and *i* on the transverse axis (Boulangé 1924). Our epistemology holds that homology-oriented terms are preferable to purely anatomical (descriptive) terms, when the homology adduced is robust and consistent across the focal taxa, although we do appreciate the value of neutral morpheme-based nomenclature in some systems (Richter and Wirkner 2014). We choose not to use the terms employed by HAO (Yoder et al. 2010) for similar reasons; while the HAO names do provide information on origin and insertion, they are homology-neutral and unwieldy for our purposes (referring, e.g., to the "gonostyle/volsella complex" rather than to the gonocoxite, gonostylus, parossiculus, or lateropenite specifically). Additionally, other schemata are incomplete relative to our system: of the 28 muscles recognized here, Schulmeister (2003) named 26, and Boulangé (1924) 23.

The alternate system available for muscle names is Boudinot (2018), who established homology of genital muscles across hexapod orders with respect to the Remipedia, the sister-group of the Hexapoda (von Reumont et al. 2012; Misof et al. 2014). Because most muscles of the male genitalia can be confidently identified as subsets of these homology classes, we adopt these groups where applicable. However, we make certain modifications to both convey evolutionary-anatomical information and provide an intuitive and usable shorthand for communicating spatial

information. To these ends, we combine the homologies of Boudinot (2018) with the topographical main-group approach. Where relevant, we prioritize the homological class of muscles with plastic or secondarily modified topography with respect to origin or insertion. In general, attachments tend to be plastic with respect to fused or closely associated sclerites, especially those that derive from the same ancestral structure. Specifically, origins may drift to a limited degree between the gonocoxites and gonostyli, and insertions between the parossiculus and lateropenite. For clarity, we list here the cases where observed topography may be apparently incongruent with the homological class designation. (1) The anterior coxo-stylar muscle (9csm1) is secondarily intrinsic to the gonocoxite, and the intrinsic coxo-stylar muscle (9csm4, *v*) in outgroups is secondarily intrinsic to the gonostylus; (2) the coxo-lateropenital muscles are frequently labile in insertion, and in ants generally insert on the parossiculus, or at the proximal junction of parossiculus and lateropenite; and (3) the dorsal coxo-penial remotors may originate at or somewhat distad the coxo-stylar articulation.

We enact the following additions or modifications to Boudinot (2018): (1) we designate the remotors and promotors of the penial sclerites as "coxo-penial" to explicitly reference the origin; (2) we recognize subsets of the coxo-penial muscles (9cppv1–2) and the coxo-lateropenital muscles (9clm1, –4, *s*, *o*) not addressed in Boudinot (2018); (3) we interpret the muscle *si* to be derived from the ventral coxo-penial remotors, rather than promotors (9cprv1); (4) we recognize the pene-lateropenital muscles (10plm1–2, *m, n*); (5) we designate the muscles attaching the gonocoxite to the gonostylus as coxo-stylar muscles (9csm1–3, *t, w, u, v*) rather than adductors and abductors of the exopod; and (6) we recognize the intrinsic penial and coxal muscles (10ppm1–2, *x, z*; 9ccim, *y*), and the ninth intrinsic sterno-sternal muscle (9vvim), which are autapomorphies of particular families or genera (Schulmeister, 2001; 2003). We also provide

new abbreviations and modified Latinized names for readability and consilience with analogous systems.

Relative transverse position is stabler at deeper nodes than anteroposterior or dorsoventral position, as in the worker abdomen (Lieberman et al. 2022). Therefore, for sequential numbering of muscles in the same group, we order origins from medial to lateral, anterior to posterior (proximal to distal), and dorsal to ventral, in that sequence.

We recognize thirteen homological-topographic groups in male Hymenoptera, of which eight are known in ants. Table 3.S3 lists the full complement of muscles with terminological equivalencies; for ease of comparison, the Boulangé (1924) labels are provided throughout. Not all groups designated here have equivalent alphabetic labels. Groups known in ants and outgroups are: (1) **sterno-coxal muscles** (**9vcm1–3**, *a, b, c*) which originate on ASIX and insert on the cupula; (2) **tergo-coxal muscles** (**9dcm1–4**, *g, f, e, d*), which originate on the cupula and insert on the gonocoxite; (3) **dorsal coxo-penial promotors** (**9cppd**, *j*) which originate dorsally on the gonocoxite and insert apically on the valvura; (4) **dorsal coxo-penial remotors (9cprd1–2**, *k, l*) which originate dorsally on the gonocoxite and insert basally on the penial sclerite; (5) **ventral coxo-penial promotors** (**9cppv1–2**, *h*) which originate ventrally on the gonocoxite and insert apically on the valvura; (6) **ventral coxo-penial remotors (9cprv1–2**, *si, i*) which originate ventrally on the gonocoxite and insert basally on the penial sclerite, usually on a lateral apodeme; (7) **coxo-stylar muscles (9csm1–4**, *t, u, v*), which originate on the gonocoxite and insert on the gonostylus (or are secondarily intrinsic to the gonocoxite in 9csm1, or the stylus in 9csm4, *v*); and **(8) coxo-lateropenital muscles** (**9clm1–4**, *s, qr, p, o*), which originate on the gonocoxite or parossiculus (both of which are gonocoxal fragments; Boudinot 2018) and insert

on the lateropenite or secondarily on the parossiculus. Groups present in outgroup Hymenoptera are: **(9) pene-lateropenital muscles (10plm1–2**, *m, n*) which originate on the valvura and insert on the lateropenite, sometimes associated with the membranes of the endophallus; (10**) pene-penial muscles (10ppm1–2,** *x, z*) which are intrinsic to the penial sclerites; (11) **coxo-coxal muscles (9ccim**, *y*) which connect the left and right parossiculi; and finally (12) **sterno-sternal intrinsic muscles** (**9vvim**) which are intrinsic to ASIX.

For the coxo-penial muscles, the names "promotor" and "remotor" are used to indicate homology with other Neoptera, although in the Hymenoptera these muscles may not protrude or retract the genitalia. The heuristic definition of these terms is that promotors insert apically on the valvurae while remotors insert at the base of the valvurae on the mesal surface or a lateral apodeme on the ectal surface. In some cases, the insertions are secondarily expanded, as in 9cprd1 (*k*) which may insert broadly on the mesal surfaces of the penial sclerites, both distally, and on parts of the valvurae. Functionally, the dorsal and ventral promotors are usually antagonists of one another.

We use Latinized names to take advantage of differences in grammatical word order between Latin and English, allowing the presentation of information hierarchically while also providing cogent English names. Latin names give homological, spatial, and orientational information in order from general to specific (origin-insertion, main descriptor, detailed descriptors) and parallel the construction of abbreviations (segment of origin, origin-insertion, numeration of subsets). An English term can be derived by reading the Latin name in reverse. For example, 9clm2, *Musculus coxo-lateropenitalis interior lateralis* is the "lateral intrinsic coxo-lateropenital muscle [of AIX]", while 9cprd1, *M. coxo-penialis remotor dorsalis mesalis* is the mesal dorsal coxo-penial remotor [of AIX]".

2.4. Taxonomy and Phylogeny

2.4.1. Taxonomy

The tribal, generic, and species-group phylogeny of the exemplars used here is provided in Fig. 3.3. This paper follows the treatment of leptanilline taxonomy in Boudinot et al. (2022), which erected the monobasic tribe Opamyrmini and synonymized the Anomalomyrmini under Leptanillini. The generic limits of *Leptanilla* follow Chapter 1, with *Leptanilla sensu lato* encompassing both *Scyphodon* Brues and *Noonilla* Petersen. The phylogenetic position of the monotypic *Scyphodon* relative to the multiple sequenced exemplars of *Noonilla* remains unclear, but *Scyphodon* + *Noonilla* exhibit many synapomorphies; therefore, this clade is here conservatively referred to as *Scyphodon s. l.* according to the principle of priority. A depauperate clade (not examined), that we here term the Indochinese morphospecies-group, is sister to *Scyphodon s.l.* + the Bornean morphospecies-group (Chapter 1); these three groups comprise the "Indomalayan clade". Males of *Anomalomyrma* remain unknown, and so the taxonomic problem presented by the paraphyly of *Protanilla* with respect to *Anomalomyrma* (Borowiec et al. 2019; Griebenow 2020; Chapters 2, 5) is moot for the purposes of this study.

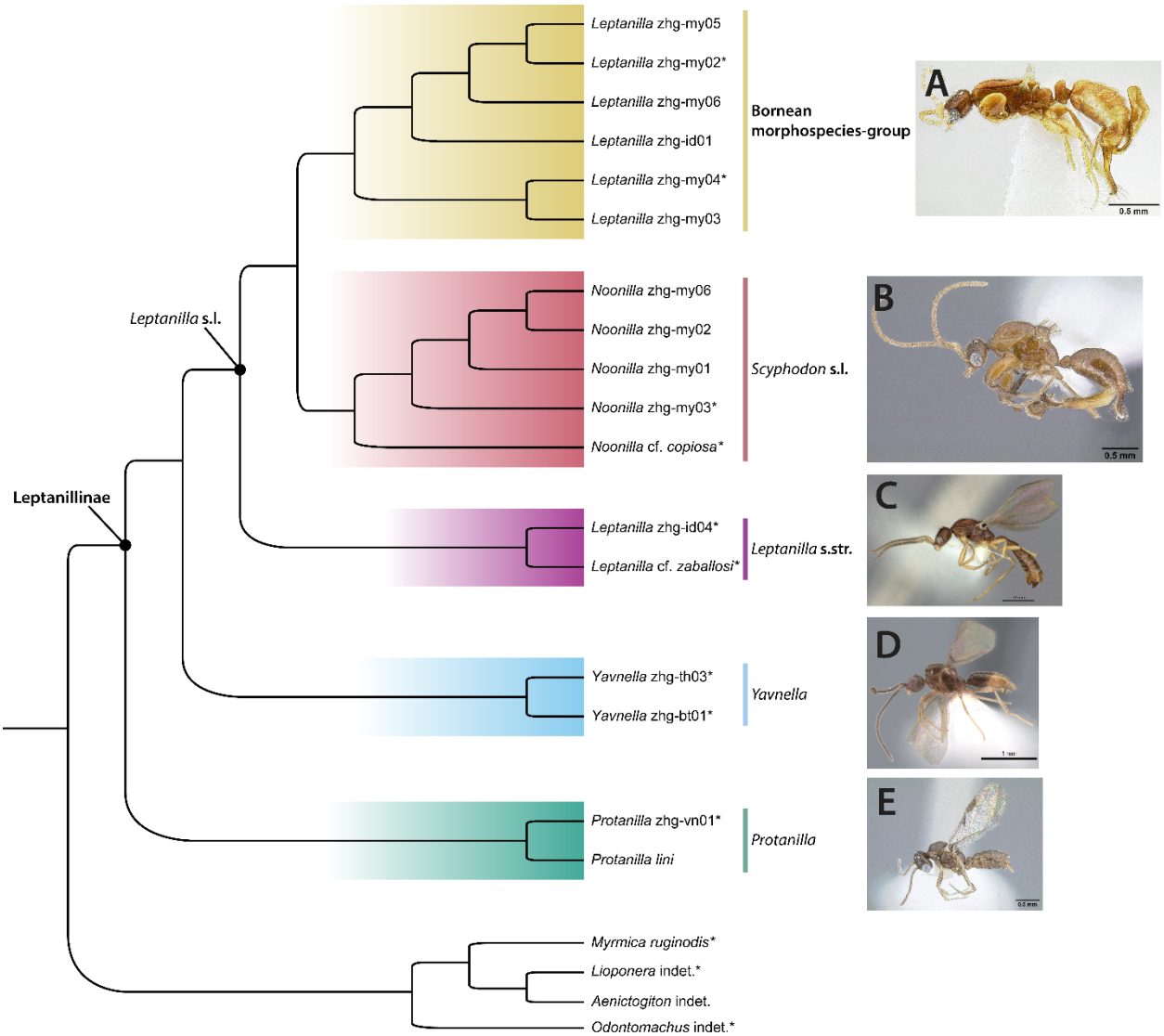

Figure 3.3. Cladogram of exemplars for which scan data are published in this study. Terminals that received a full male genital skeletomuscular description in this study are marked with an asterisk.

2.4.2. Taxon sampling

Except for *Noonilla* zhg-my03, *Leptanilla* zhg-my06, and *Leptanilla* zhg-id04, all leptanilline morphospecies for which micro-CT data were obtained in this study have been sequenced using ultraconserved elements (UCEs; Griebenow 2020, Chapter 2). Morphospecies for which UCEs are not yet available can be confidently situated in one of the major leptanilline subclades based

upon morphology alone, since this morphology is contextualized by robust molecular or total-evidence phylogenies (Griebenow 2020; Chapters 1–2).

Scans are hereby published for all major subclades of the Leptanillini, with at least two morphospecies being scanned per subclade. Males of three outgroups to the Leptanillinae were scanned and described in full (Sections 3.1.2, 3.2.2), representing both major ant clades: the "poneroids" (Ponerinae: Ponerini: *Odontomachus* indet.) and the "core formicoids" (Myrmicinae: Myrmicini: *Myrmica ruginodis* Nylander), and the latter's comparatively minor sister lineage, the Dorylinae (*Lioponera* indet.; Branstetter et al. 2017).

Descriptive sampling within the Leptanillinae in this study focuses largely on the tribe Leptanillini *s. str.*, with a single exemplar (*Protanilla* zhg-vn01) of their sister clade, the former Anomalomyrmini. The only conspicuous gap in our sampling of the Leptanillini *s. str.* is the Indochinese morphospecies-group, which is known only from undescribed male morphospecies and was represented in previous studies by *Leptanilla* TH01, –7, and *Leptanilla* zhg-th01 (Borowiec et al. 2019; Griebenow 2020; Chapters 1–2).

The former Anomalomyrmini are less speciose than the Leptanillini *s. str.*, and variation in the external morphology of all available male specimens is so limited as to obviate any apparent need for description of multiple morphospecies, with the following exceptions. *Protanilla* TH03 (CASENT0119791) differs from all other known males of the former Anomalomyrmini in several conspicuous morphological characters (Griebenow 2020: 240), as does *Protanilla* zhg-th02 (CASENT0842645), but neither of these morphospecies nor any related ones were available for micro-CT scanning or dissection. Phylogenetic inference confidently recovers both these

morphospecies distantly from one another and outside the subclade of the former Anomalomyrmini which contains both *Protanilla* sampled in this study (Chapter 4).

Males of the monotypic genus *Opamyrma*, which is sister to the remaining Leptanillinae (Ward and Fisher 2016), were unavailable for micro-CT scanning; however, the skeletal morphology of the male genitalia in *Opamyrma* was thoroughly described by Yamada et al. (2020) using manual dissection. The male genital musculature of this lineage remains unknown and will require the collection of fresh specimens. Likewise, description of the male genital musculature of *Martialis heureka* Rabeling & Verhaagh (Martialinae), the sister taxon of the Leptanillinae, will require collection of fresh material. The genital skeleton of the putative male of *M. heureka* was described by Boudinot (2015).

3. Results

3.1. Integument

3.1.1. Summary

The following is a summary of the totality of variation observed in the male genital sclerites of the Formicidae, compiling previous literature and the findings described in the present paper. This summary cannot be construed as representative of the ancestral condition of the male genital sclerites for the Formicidae.

The terminal pregenital segment is *abdominal segment VIII* (**AVIII**), which comprises the dorsal *tergite VIII* (**ATVIII**), and ventral *sternite VIII* (**ASVIII**), which lacks limbs. Both these sclerites bear an anterior marginal invaginated ridge, the *antecosta* (**acs**) which represents the apparent segmental boundary (i.e., secondary segmentation; Snodgrass 1935a) and serves as a point for

muscle attachment. The anterior margin of abdominal sternite VIII is entire but may be produced into diverging *anterolateral apodemes* homologous with those in the female metasoma (Lieberman et al. 2022). The remnant of *abdominal tergite IX* (**ATIX**) is situated dorsal to the genitalia and is fused to the fused remnants of abdominal tergites X and XI, which bear the median proctiger, here defined as the area of cuticle surrounding the anus, and lateral *cerci* (also known as pygostyles; Table 3.S2) (**cer**); abdominal tergite IX may be divided into hemitergites, i.e., incontiguous lateral sclerites.

The genital skeleton comprises *abdominal sternite IX* (**ASIX**, Fig. 3.2A–B) and its appendages, and the fused remnants of the appendages of abdominal sternite X. ASIX is variably integrated with the copulatory appendages; its main body is the *basal disc* (**bsc**; Fig. 3.2A) which variably bears an antecosta (**acsS9**) and diverging *anterolateral processes* (**atpS9**) which may be serially homologous the anterolateral apodemes of the pregenital segments. ASIX is often produced anteriorly into a median *spiculum* (**spc**, Fig. 3.2A–B), a "spiniform apodeme" (MacGown et al. 2014); rarely, two to three spicula are present, or the spiculum is absent (Barden et al. 2017). The *cupula* (**cup**, Fig. 3.2A–B) is usually annular in shape, comprising a complete ring that outlines the *foramen genitale* (**fog**; Fig. 3.3.24A–C), through which the paired *ducti ejaculatorii* or unpaired *endophallus* run; or the cupula is reduced to a slat ventrad the gonopodites (Boudinot et al. 2022). The anteroventral margin of the cupula may be produced into a median process called the *gonocondyle* (**gcy**). The paired *gonopodites* (**gpd**) are distal to the cupula and each comprise a proximal *gonocoxite* (**gcx**, Fig. 3.2A–B) (equivalent to the *gonocoxa* of Griebenow [2021]) and distal *gonostylus* (**stl**, Fig. 3.2A–B), with the gonostylus being sometimes articulated with a mesal condyle, or rarely absent; the paired *volsellae* (**vol**, Fig. 3.2A–B) originate medially on the gonocoxites, and each consist of a lateral *parossiculus* (**prs**, Fig. 3.2A–B) and distomedial

lateropenite (**ltp**, Fig. 3.2A–B). The proximoventral surface of the volsella may bear a basivolsellar process (Boudinot, 2015; Barden et al., 2017). The parossiculus may bear *recurved medial processes* (**prp**). Medial to the volsellae are the paired *penial sclerites* (**psc**, Fig. 3.2A–B), which are proximally produced into paired apodemes called *valvurae* (**vlv**, Fig. 3.2A–B), serving as the origin or insertion of much of the penial musculature; in some cases, the penial sclerites bear proximal apodemes that are not homologous with valvurae, and so these are here agnostically designated as *posterior penial processes* (**ppp**; Fig. 3.11D, Fig. 3.12D, Fig. 3.18D). Posterior penial processes are not to be confused with the "penisvalva lateral apodeme[s]" (Boudinot 2013: 39) or lower oblique carinae (Ward 2001), both of which are variably present on the proximolateral surfaces of the penial sclerites in the Formicidae. The portion of the penial sclerites distal to the penial sclerite base may be produced into lateral *penial condyles*. The penial sclerites are medially separated by dorsal thickened conjunctiva, or medially conjoined by a proximodorsal "sclerotic bridge" of cuticle (Boudinot et al. 2016) or are medially fused along the entire length of the penial sclerites. If medially fused, the penial sclerites may be perforated proximally by a *proximomedian foramen*, which admits the endophallus to the penial sclerites. A small, unpaired *endophallic sclerite* (**end**, Fig. 3.2A–B**)** may be situated at the proximal end of the endophallus. The distal opening of the endophallus is the *phallotreme* (**pht**; Fig. 3.13B, Fig. 3.14A, Fig. 3.15A), which is surrounded by the penial sclerites when the latter are medially fused.

3.1.2. Outgroups

3.1.2.1. Odontomachus indet. (Figs 4–5)

Abdominal sternite VIII (**ASVIII**; Fig. 3.4A–D, Fig. 3.5) elongate, with lateral portions longer than medial region, anterior margin linear; antecosta of abdominal sternite VIII present;

anterolateral apodemes of abdominal sternite VIII absent; laterally separate from abdominal tergite VIII; posteriorly separate from abdominal sternite IX, posterior margin widely excavated medially. Abdominal sternite IX (**ASIX**; Fig. 3.4A–D, Fig. 3.5) elongate, shallowly hull-shaped, narrowing laterally along anteroposterior axis; basal disc present, anterior margin not produced into diverging anterolateral processes; anterolateral processes absent; spiculum present, anterior apex bluntly acuminate, lateromedial breadth decreasing anteriorly; abdominal sternite IX produced posteriorly into broad, elongated process with entire apex, process not anteriorly delimited from basal disc by transverse carina; posteriorly separate from gonopodites. Mulceators absent. Antecosta of abdominal sternite IX present, weakly developed. Abdominal tergite IX (**ATIX**; Fig. 3.4A, C–D, Fig. 3.5) not divided into hemitergites, elongate, posterior margin gently produced medially. Cerci (**cer**; Fig. 3.4A, C–D) present. Cupula (**cup**; Fig. 3.4A, C–D) present; annular, dorsum and lateral surfaces anteroposteriorly prolonged, anteroposteriorly narrow along the ventromedian axis, posterior margin not mesally recurved; mesal anterolateral surfaces with dorsally curved carinae, carinae not adjoining anterior or posterior margins; mesal ventral surfaces with sinuate carinae, converging medially, adjoining both anterior and posterior margins. Gonocondyle absent. Gonopodites proximally distinct from abdominal sternite IX, articulate, with complete medial separation. Dorsum of gonocoxites (**gcx**; Fig. 3.4A, Fig. 3.5) enclosing and separated from penial sclerites; apicolateral laminae absent from gonocoxites; gonocoxites with mesal articulatory condyles associated with and proximomediad the bases of the volsellae, ventrally articulated with the gonostyli. Gonostyli (**stl**; Figs 4A–D, Fig. 3.5) unfused to gonocoxites and separated from gonocoxites by ventral conjunctiva, but not distinguishable from gonocoxites dorsal to conjunctiva; outline of gonostyli bluntly cuneiform in dorsolateral view, anteroposterior length greater than that of gonocoxites.

Volsellae (**vol**; Fig. 3.4D) present, fully articulated with gonopodites; not medially fused; parossiculus and lateropenites dorsally articulated, ventrally indistinct; recurved medial processes absent. Penial sclerites (**psc**; Fig. 3.4A, C–D, Fig. 3.5) medially conjoined by conjunctiva along basal ½ of dorsum and venter, medially separated at apex; entirely unsculptured; valvurae (**vlv**; Fig. 3.5) present, proximolateral processes that are sub-elliptical in cross-section, proximal apices directed dorsally; endophallic sclerite apparently absent (see Section 4.1.1); phallotreme enlarged, situated at penial apex, not surrounded by sclerotized portions of the penial sclerites, not recessed; apices of penial sclerites not ventrally recurved, dorsolateral margins slightly divergent.

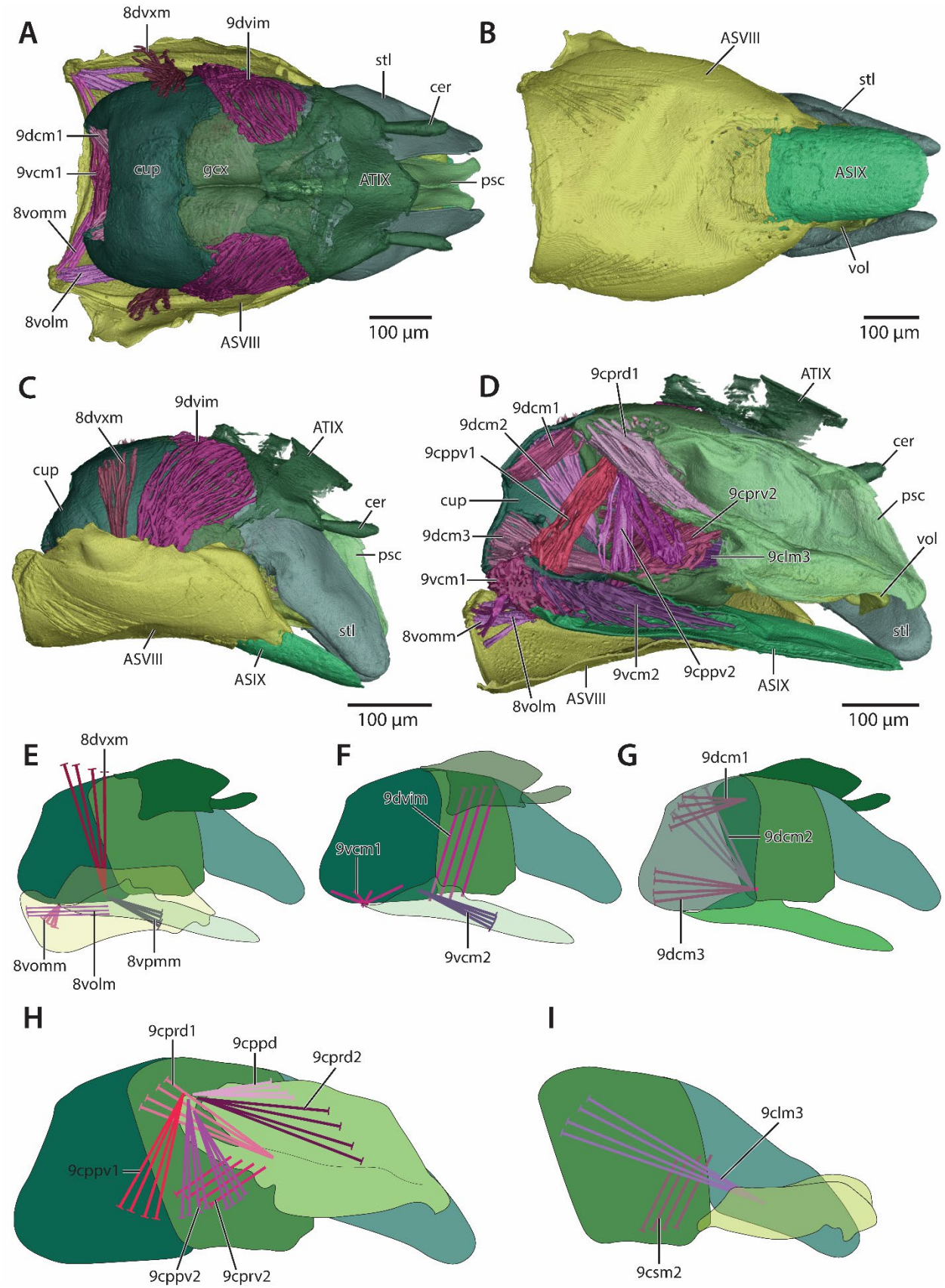
A
8dvxm
9dvim
stl
cer
9dcm1
9vcm1
cup
gcx
ATIX
psc
8vomm
8volm
ASVIII
100 µm
B
ASVIII
stl
ASIX
vol
100 µm
C
9dvim
8dvxm
ATIX
cup
cer
psc
stl
ASVIII
ASIX
100 µm
D
9cprd1
ATIX
9dcm1
9dcm2
cer
9cppv1
cup
9cprv2
psc
9dcm3
9clm3
vol
9vcm1
8vomm
stl
9vcm2
9cppv2
ASIX
8volm
ASVIII
100 µm
E
8dvxm
8vomm
8vpmm
8volm
F
9dvim
9vcm1
9vcm2
G
9dcm1
9dcm2
9dcm3
H
9cprd1
9cppd
9cprd2
9cppv1
9cppv2
9cprv2
I
9clm3
9csm2

Figure 3.4. ♂ genitalia of *Odontomachus* indet. (CASENT0842842), 3D reconstructions (A–D) and summary diagrams (E–H). Caps in muscle diagrams signify origin; lack of caps, insertion. **A** dorsal view **B** ventral view **C** profile view **D** sagittal cross-section **E** ventral longitudinal muscles VIII-IX and dorsoventral extrinsic muscles VIII-IX, profile view **F** intrinsic dorsoventral muscles IX and sterno-coxal muscles IX, profile view **G** tergo-coxal muscles IX, profile view **H** coxo-penial muscles sagittal cross-section **I** coxo-stylar and coxo-lateropenital muscles, profile view. Abbreviations: ASVIII=abdominal sternite VIII; ASIX=abdominal sternite IX; ATIX=abdominal tergite IX; cer=cercus; cup=cupula; gcx=gonocoxite; stl=gonostylus; vol=volsella; psc=penial sclerites; 8vomm=ventral orthomedial muscles VIII-IX; 8vpmm=ventral paramedial muscles VIII-IX; 8volm=ventral ortholateral muscles VIII-IX; 8dvxm=dorsoventral extrinsic muscles VIII-IX; 9dvim=dorsoventral intrinsic muscles IX; 9vcm1=anteromedial sterno-coxal muscles; 9vcm2=posteromedial sterno-coxal muscles; 9dcm1=dorsal tergo-coxal muscles; 9dcm2=dorsolateral tergo-coxal muscles; 9dcm3=ventrolateral tergo-coxal muscles; 9csm2=intermediate coxo-stylar muscles; 9clm3=medial extrinsic coxo-lateropenital muscles; 9cppd=dorsal coxo-penial promotors; 9cprd1=dorsal coxo-penial remotors; 9cppv1=anterior ventral coxo-penial promotors; 9cppv2=posterior ventral coxo-penial promotors; 9cprv2=lateral ventral coxo-penial remotors

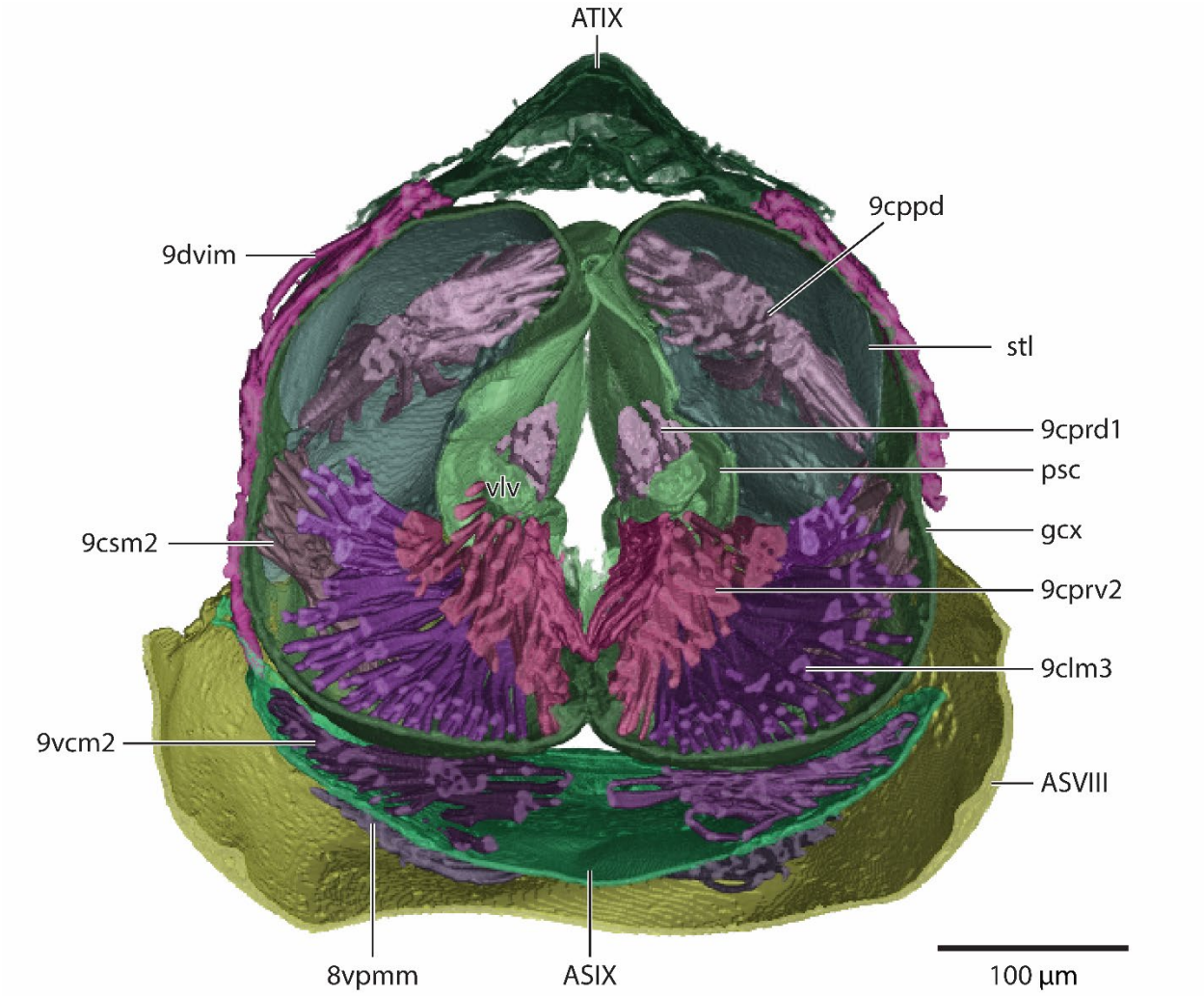

Figure 3.5. ♂ genitalia of *Odontomachus* indet. (CASENT0842842), 3D reconstruction in transverse cross-section. Abbreviations: ASVIII=abdominal sternite VIII; ASIX=abdominal sternite IX; ATIX= gcx=gonocoxite; stl=gonostylus; vol=volsella; psc=penial sclerites; vlv=valvura; 8vpmm=ventral paramedial muscles VIII-IX; 9dvim=dorsoventral intrinsic muscles IX; 9vcm2=posteromedial sterno-coxal muscles; 9csm2=intermediate coxo-stylar muscles; 9cppd=dorsal coxo-penial promotors; 9clm3=medial extrinsic coxo-lateropenital muscles; 9cprd1=dorsal coxo-penial remotors; 9cprv2=lateral ventral coxo-penial remotors

3.1.2.2. Myrmica ruginodis (Figs 6–7)

Abdominal sternite VIII (**ASVIII**; Figs 6A–D, Fig. 3.7) anteroposteriorly reduced medially, anterior margin shallowly concave in ventral view; antecosta of abdominal sternite AVIII present, narrow; anterolateral apodemes of abdominal sternite AVIII present, broadly lobate; laterally separate from ATVIII; posteriorly separate from abdominal sternite IX, with a large, well-developed carina on the dorsal surface. Abdominal sternite IX (**ASIX**; Fig. 3.6A–D, Fig. 3.7) elongate, shallowly hull-shaped, narrowing laterally posteriorly; basal disc present, anterior margin produced into lobate anterolateral processes; spiculum (**spc**; Fig. 3.6B) present, robustly triangular, with a strong but short dorsal median longitudinal carina; abdominal sternite IX moderately narrowed posteriorly along transverse axis, posterior not anteriorly delimited from basal disc by transverse carina; posteriorly separate from gonopodites. Mulceators absent. Antecosta of abdominal sternite IX present, well-developed. Abdominal tergite IX (**ATIX**; Figs 6A, C–D) not divided into hemitergites, not elongate, medially emarginate, medial connection entirely membranous. Cerci (**cer**; Fig. 3.6A–D) present. Cupula (**cup**; Fig. 3.6A–D) present; annular, anteroposteriorly compressed along ventromedian axis; margin of foramen genitale continuously carinate, carina prolonged dorsomedially into a small, anteriorly directed triangle. Gonocondyle absent. Gonopodites proximally distinct from abdominal sternite IX, articulate, with complete medial separation. Dorsum of gonocoxites (**gcx**; Fig. 3.6A, C–D, Fig. 3.7) enclosing and separated from penial sclerites, medial proximoventral margins produced into

anteriorly projecting lobes; apicolateral laminae absent from gonocoxites; mesal surfaces with longitudinal carinae, not converging medially, extending from proximoventral lobes to distal margins. Gonostyli (**stl**; Fig. 3.6A–D) unfused to gonocoxites and separated by ventral conjunctiva, but not distinguishable from gonocoxites dorsal to conjunctiva; outline of gonostylus bluntly lobate in dorsolateral view, anteroposterior length subequal to that of gonocoxite. Volsellae (**vol**; Fig. 3.6D, Fig. 3.7) present, fully articulated with gonopodites; not medially fused; parossiculus and lateropenite dorsally articulated, ventrally distinct; lateropenite ventrally recurved, apex rounded; recurved medial processes absent. Penial sclerites (**psc**; Fig. 3.6A, C–D, Fig.7) medially joined by dorsal conjunctiva along proximal 3/4 of length, medially separated at apex; not dorsoventrally or lateromedially compressed; unsculptured, except for fine, regular dentition on ventromedial margins, save for base and apices; ventromesal septa present, apparently arising by conjunctival connection with the ventral penial margins and sclerotic connection by a distal bridge, forming roughly round distomesal spaces at penial apex; valvurae (**vlv**; Fig. 3.7) present, proximolateral processes that are roughly sub-elliptical in cross-section, with ectal flanges at anterior base, proximal apices directed dorsolaterally; endophallic sclerite (**end**; Fig. 3.6D) present, sagittate in dorsal view and deeply hull-like, margins carinate; phallotreme surrounded by sclerotized portions of the penial sclerites, not recessed; apices of penial sclerites not ventrally recurved, dorsolateral margins convergent.

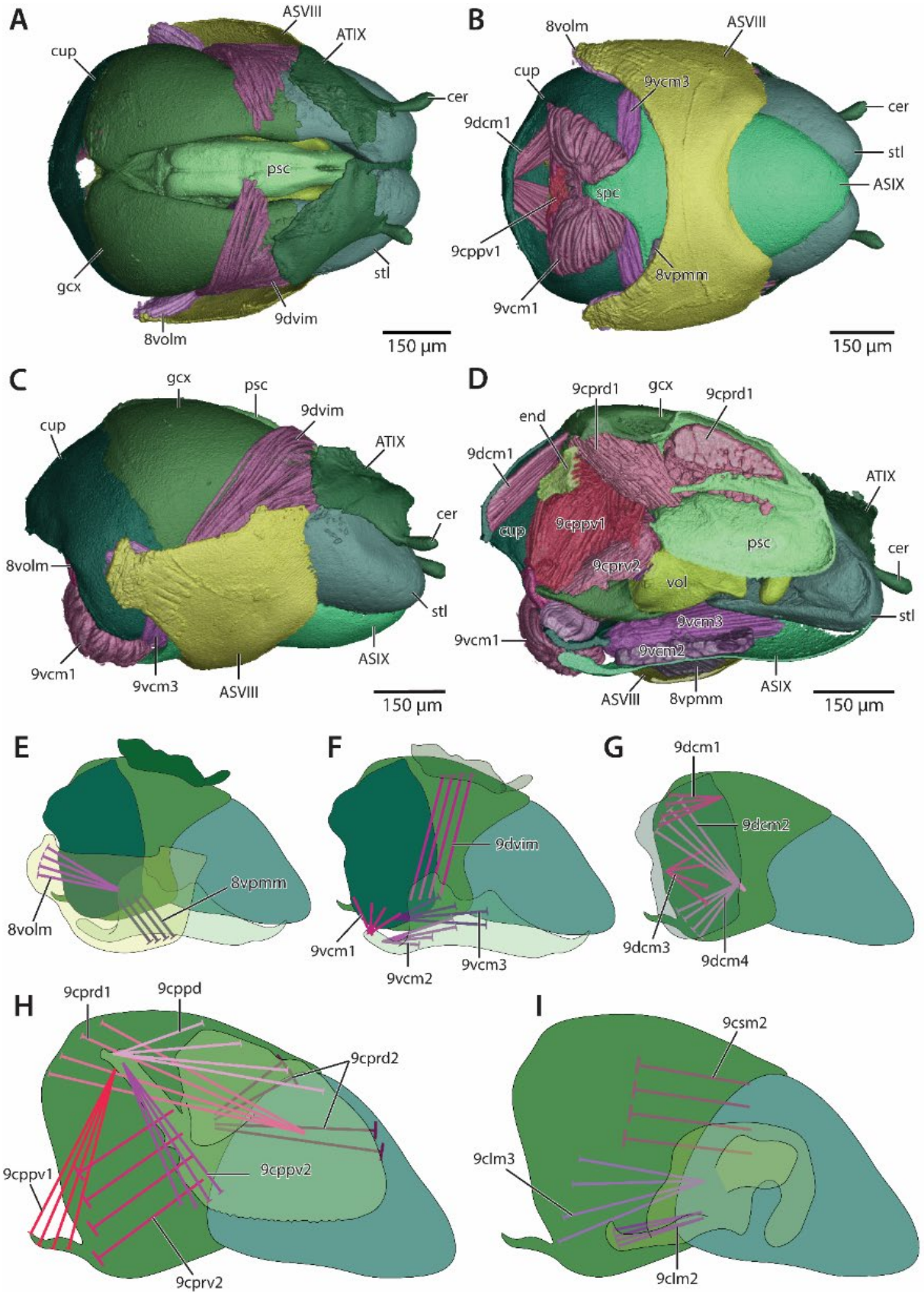
A
ASVIII
ATIX
cup
cer
psc
gcx
stl
9dvim
8volm
150 µm
B
8volm
ASVIII
cup
9vcm3
cer
9dcm1
stl
ASIX
spc
9cppv1
8vpmm
9vcm1
150 µm
C
gcx
psc
cup
9dvim
ATIX
cer
8volm
stl
ASIX
9vcm1
9vcm3
ASVIII
150 µm
D
9cprd1
gcx
9cprd1
end
9dcm1
ATIX
cup
9cppv1
psc
cer
9cprv2
vol
stl
9vcm3
9vcm1
9vcm2
ASVIII
8vpmm
ASIX
150 µm
E
8vpmm
8volm
F
9dvim
9vcm1
9vcm2
9vcm3
G
9dcm1
9dcm2
9dcm3
9dcm4
H
9cprd1
9cppd
9cprd2
9cppv1
9cppv2
9cprv2
I
9csm2
9clm3
9clm2

Figure 3.6. ♂ genitalia of *Myrmica ruginodis* (PMJ:Hex:2205), 3D reconstructions (A–D) and summary diagrams (E–H). Caps in muscle diagrams signify origin; lack of caps, insertion. **A** dorsal view **B** ventral view **C** profile view **D** sagittal cross-section **E** ventral longitudinal muscles, profile view IX **F** intrinsic dorsoventral muscles IX and sterno-coxal muscles IX, profile view **G** tergo-coxal muscles IX, profile view **H** coxo-penial muscles, sagittal cross-section **I** coxo-stylar and coxo-lateropenital muscles, profile view. Abbreviations: ASVIII=abdominal sternite VIII; ASIX=abdominal sternite IX; ATIX=abdominal tergite IX; cer=cercus; cup=cupula; gcx=gonocoxite; stl=gonostylus; vol=volsella; psc=penial sclerites; end=endophallic sclerite; 8vpmm=ventral paramedial muscles VIII-IX; 8volm=ventral ortholateral muscles VIII-IX; 9dvim=dorsoventral intrinsic muscles IX; 9vcm1=anteromedial sterno-coxal muscles; 9vcm2=posteromedial sterno-coxal muscles; 9vcm3=lateral sterno-coxal muscles; 9dcm1=dorsal tergo-coxal muscles; 9dcm2=dorsolateral tergo-coxal muscles; 9dcm3=ventrolateral tergo-coxal muscles; 9dcm4=ventral tergo-coxal muscles; 9csm2=intermediate coxo-stylar muscles; 9clm2=lateral intrinsic coxo-lateropenital muscles; 9clm3=medial extrinsic coxo-lateropenital muscles; 9cppd=dorsal coxo-penial promotors; 9cprd1=dorsal coxo-penial remotors; 9cprd2=ectal dorsal coxo-penial remotors; 9cppv1=anterior ventral coxo-penial promotors; 9cppv2=posterior ventral coxo-penial promotors; 9cprv2=lateral ventral coxo-penial remotors

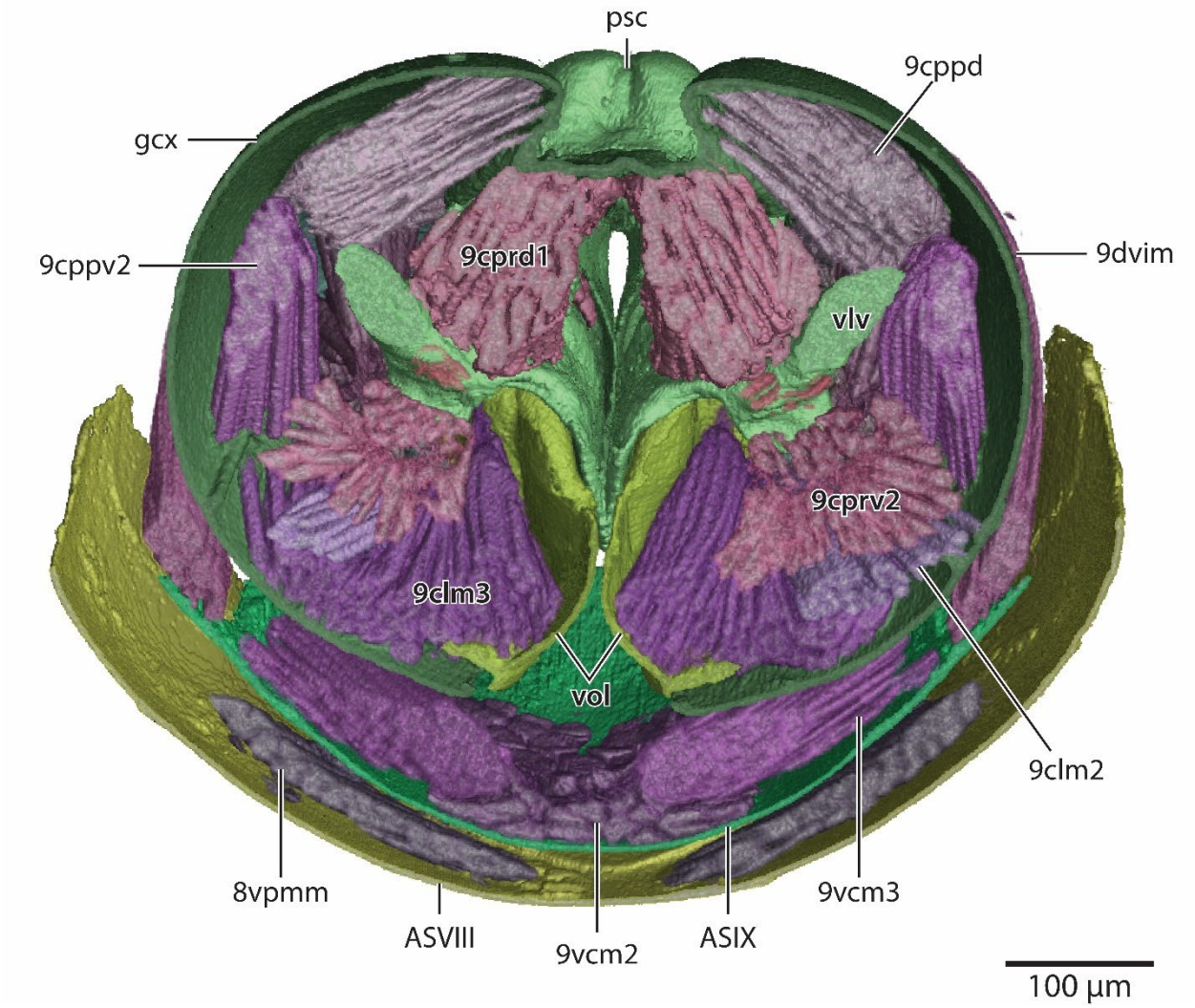

Figure 3.7. ♂ genitalia of *Myrmica ruginodis* (PMJ:Hex:2205), 3D reconstruction in transverse cross-section. Abbreviations: ASVIII=abdominal sternite VIII; ASIX=abdominal sternite IX; gcx=gonocoxite; vol=volsella; psc=penial sclerites; vlv=valvura; 8vpmm=ventral paramedial muscles VIII-IX; 9dvim=dorsoventral intrinsic muscles IX; 9vcm2=posteromedial sterno-coxal muscles; 9vcm3=lateral sterno-coxal muscles; 9clm2=lateral intrinsic coxo-lateropenital muscles; 9clm3=medial extrinsic coxo-lateropenital muscles; 9cppd=dorsal coxo-penial promotors; 9cprd1=dorsal coxo-penial remotors; 9cppv2=posterior ventral coxo-penial promotors; 9cprv2=lateral ventral coxo-penial remotors

3.1.2.3. Lioponera indet. (Figs 8–9)

Abdominal sternite VIII (**ASVIII**; Fig. 3.8A–D, Fig. 3.9) elongate, with length equivalent along most of median span, much greater laterally, with anterolateral corners produced into diverging processes; antecosta of abdominal sternite VIII absent; diverging anterolateral apodemes of

abdominal sternite VIII present, lobate in profile view; laterally separate from abdominal tergite VIII; posteriorly separate from abdominal sternite IX. Abdominal sternite IX (**ASIX**; Fig 8A–D) elongate, shallowly hull-shaped, not narrowing laterally along anteroposterior axis; basal disc present, anterior margin produced into diverging anterolateral processes; divergent anterolateral processes of abdominal sternite IX present, lobate in profile view; spiculum (**spc**; Fig. 3.8B–D) present, anterior apex narrowly truncate, lateromedial breadth constant along most of anteroposterior length; abdominal sternite IX produced posteriorly into bifid process, posterolateral points of process with lateral subapical teeth, process not delimited from basal disc by transverse carina; separate posteriorly from gonopodites; mulceators absent. Antecosta of abdominal sternite IX present. Abdominal tergite IX (**ATIX**; Figs 8A, C; Fig. 3.9) separated into hemitergites; hemitergital outline Z-shaped in dorsolateral view, angular, broadly truncate anteriorly, tapering posteriorly. Cerci absent. Cupula (**cup**; Fig. 3.8A, C–D) present; annular, dorsum and lateral surfaces anteroposteriorly prolonged, anteroposteriorly narrow along ventromedian axis, posterior margin mesally recurved to form antecosta-like "lip". Gonocondyle vestigial. Gonopodites (**gpd**; Fig 8A–D, Fig. 3.9) proximally separated from abdominal sternite IX, inarticulate; with complete medial separation; dorsum enclosing penial sclerites; apicolateral laminae absent; mesal articulatory condyles absent; apices of gonopodites lobate in profile view. Gonocoxites (**gpd (gcx)**; Fig 8C–D; Fig. 3.9) present, indistinct from gonostyli. Gonostyli (**gpd (stl)**, Fig. 3.8B, C) present, indistinct from gonocoxites. Volsellae (**vol**; Figs 8C–D; Fig. 3.9) present, fully articulated with gonopodites; not medially fused; lateropenite proximally indistinct from and not articulated to parossiculus; volsellae with robust proximolateral condyles and basomedial articulatory condyles, distally divergent, apices lobate in profile view; recurved medial processes absent. Penial sclerites (**psc**; Fig. 3.8A–D, Fig. 3.9) medially conjoined by

conjunctiva along most of proximodistal length, including apex; unsculptured except for coarse dentition on ventral margins; valvurae (**vlv**; Fig. 3.9) present, proximolateral processes that are subcircular in cross-section, proximal apices directed dorsally; endophallic sclerite **(end**; Fig. 3.8D) present, large and dorsally concave, bifurcating anteriorly, anterior apices truncate**;** phallotreme distal, situated at penial apex, surrounded by sclerotized portions of the penial sclerites, not recessed; penial sclerites distad phallotreme lobate in outline, not produced ventrally, dorsolateral margins subparallel.

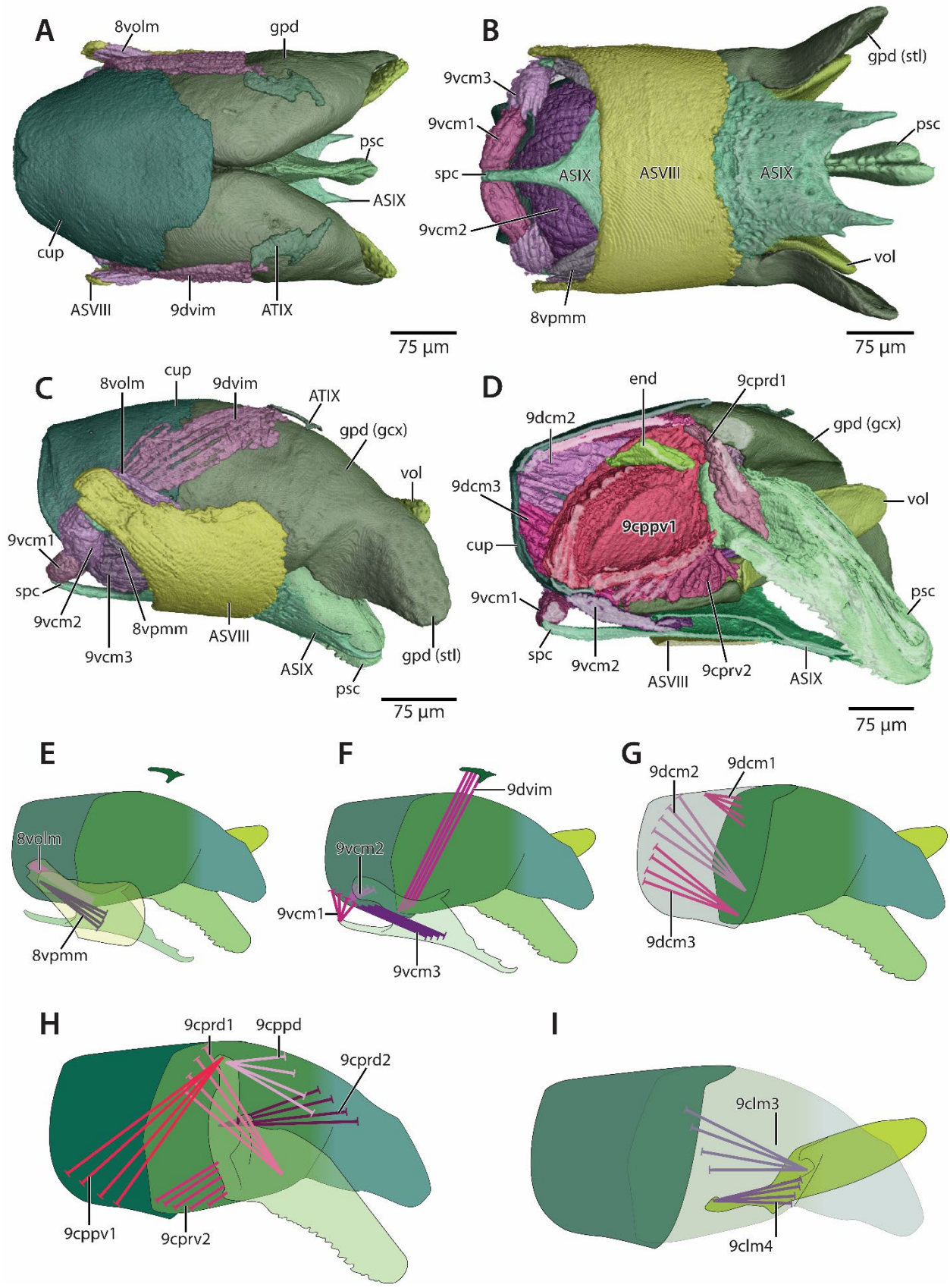
A
8volm
gpd
psc
ASIX
cup
ASVIII
9dvim
ATIX
75 µm
B
gpd (stl)
9vcm3
9vcm1
psc
spc
ASIX
ASVIII
ASIX
9vcm2
vol
8vpmm
75 µm
C
8volm
cup
9dvim
ATIX
gpd (gcx)
vol
9vcm1
spc
9vcm2
8vpmm
9vcm3
ASVIII
ASIX
gpd (stl)
psc
75 µm
D
end
9cprd1
9dcm2
gpd (gcx)
9dcm3
vol
9cppv1
cup
psc
9vcm1
spc
9vcm2
ASVIII
9cprv2
ASIX
75 µm
E
8volm
8vpmm
F
9dvim
9vcm2
9vcm1
9vcm3
G
9dcm2
9dcm1
9dcm3
H
9cprd1
9cppd
9cprd2
9cppv1
9cprv2
I
9clm3
9clm4

Figure 3.8. ♂ genitalia of *Lioponera* indet. (CASENT0844684), 3D reconstructions (A–D) and summary diagrams (E–H). Caps in muscle diagrams signify origin; lack of caps, insertion. **A** dorsal view **B** ventral view **C** profile view **D** sagittal cross-section **E** ventral longitudinal muscles IX, profile view **F** intrinsic dorsoventral muscles IX and sterno-coxal muscles, profile view IX **G** tergo-coxal muscles IX, profile view **H** coxo-penial muscles, sagittal cross-section **I** coxo-lateropenital muscles, profile view. Abbreviations: ASVIII=abdominal sternite VIII; ASIX=abdominal sternite IX; spc=spiculum; ATIX=abdominal tergite IX; cup=cupula; gpd=gonopodite; gcx=gonocoxite; stl=gonostylus; vol=volsella; psc=penial sclerites; 8vpmm=ventral paramedial muscles VIII-IX; 8volm=ventral ortholateral muscles VIII-IX; 9dvim=dorsoventral intrinsic muscles IX; 9vcm1=anteromedial sterno-coxal muscles; 9vcm2=posteromedial sterno-coxal muscles; 9dcm1=dorsal tergo-coxal muscles; 9dcm2=dorsolateral tergo-coxal muscles; 9dcm3=ventrolateral tergo-coxal muscles; 9clm3=medial extrinsic coxo-lateropenital muscles; 9clm4=lateral extrinsic coxo-lateropenital muscles; 9cppd=dorsal coxo-penial promotors; 9cprd1=dorsal coxo-penial remotors; 9cprd2= ectal dorsal coxo-penial remotors; 9cppv1=anterior ventral coxo-penial promotors; 9cprv2=lateral ventral coxo-penial remotors

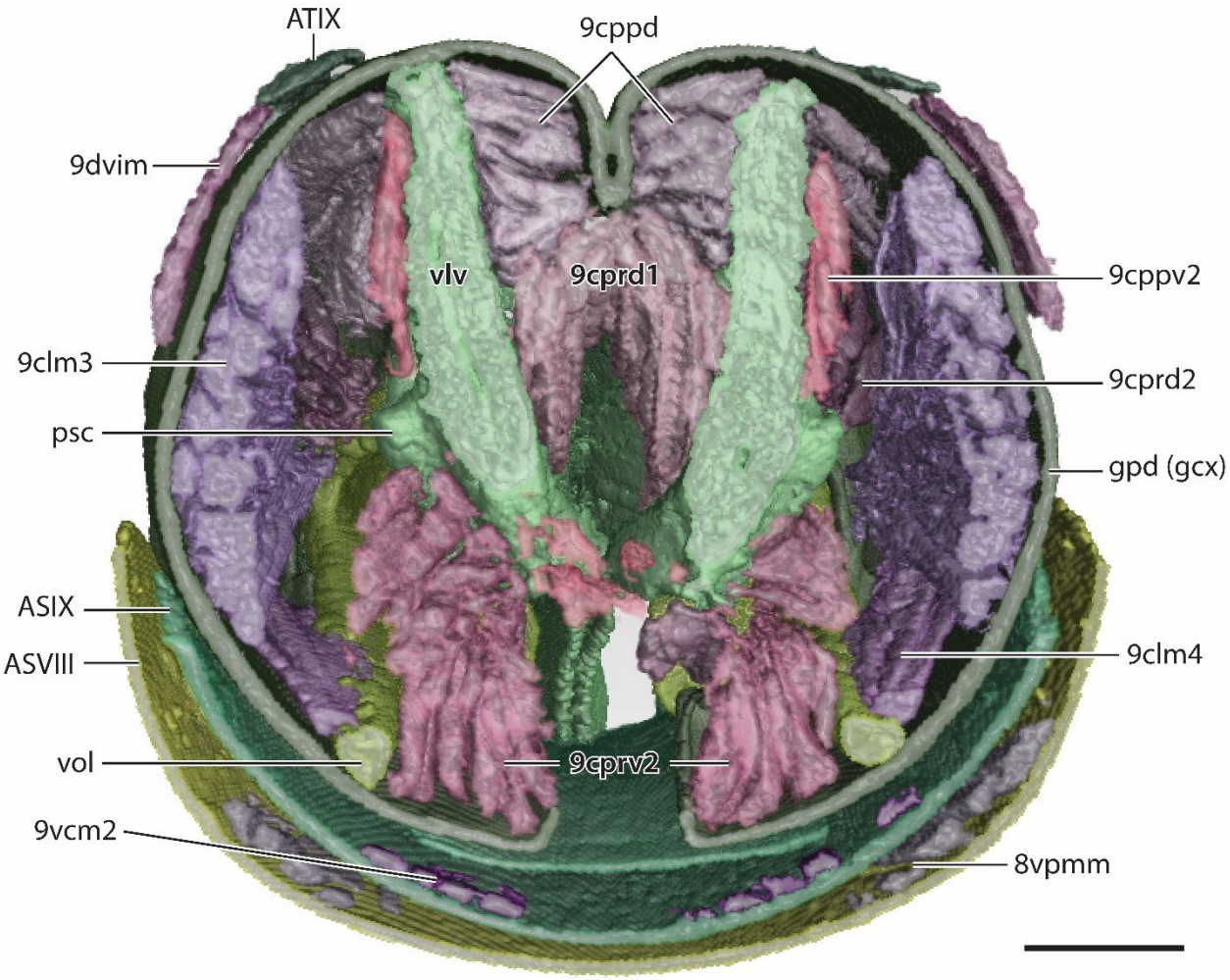

Figure 3.9. ♂ genitalia of *Lioponera* indet. (CASENT0844684), 3D reconstruction in transverse cross-section. Abbreviations: ASVIII=abdominal sternite VIII; ASIX=abdominal sternite IX; ATIX=abdominal tergite IX; gpd=gonopodite; gcx=gonocoxite; vol=volsella; psc=penial sclerites; vlv=valvura; 9dvim=dorsoventral intrinsic muscles IX; 9vcm2=posteromedial sterno-coxal muscles; 9clm3=medial extrinsic coxo-lateropenital muscles; 9clm4=lateral extrinsic coxo-lateropenital muscles; 9cprd2= ectal dorsal coxo-penial remotors; 9cppv2=posterior ventral coxo-penial promotors

3.1.3. Protanilla

3.1.3.1. Protanilla zhg-vn01 (Fig. 3.10)

Abdominal sternite VIII (**ASVIII**; Fig. 3.10A–E) elongate, with length equivalent across lateromedial span; antecosta of abdominal sternite VIII not discernible; diverging anterolateral apodemes of abdominal sternite VIII absent; laterally separate from abdominal tergite VIII;

posteriorly separate from abdominal sternite IX. Abdominal sternite IX (**ASIX**; Fig. 3.10B–D) elongate, hull-shaped, not narrowing laterally along anteroposterior axis; basal disc present, with anterolateral corners angular, not produced into diverging anterolateral processes; diverging anterolateral processes absent; spiculum (**spc**; Fig. 3.10B–D) present, anterior apex narrowly truncate, lateromedial breadth constant along most of anteroposterior length; abdominal sternite IX produced posteriorly into triangular, truncate posteromedian process, delimited from basal disc by transverse carina; separate posteriorly from gonopodites; mulceators absent. Antecosta of abdominal sternite IX present. Abdominal tergite IX (**ATIX**; Fig. 3.10A, C–E) divided into hemitergites; outline sigmoidal in dorsolateral profile view, tapering medially and laterally. Cerci absent. Cupula (**cup**; Fig. 3.10A–D) present; non-annular and crescentiform, situated ventral to proximodistal axis of genitalia, narrowing laterally along anteroposterior axis; lateral extremities with posterodorsal processes. Gonocondyle absent. Gonopodites proximally separated from abdominal sternite IX, articulate. Gonocoxites (**gcx**; Fig. 3.10A, C, E) with complete medial separation along dorsum; along venter, medially fused along apical 1/3 of length; dorsum proximally enclosed by, and separated from, penial sclerites; apicolateral laminae absent; gonocoxites with mesal articulatory condyles associated with gonostyli, ventrally articulated with gonostyli. Gonostyli (**stl**; Fig. 3.10A–D) present, unfused to gonocoxites and separated from gonocoxites by ventral conjunctiva, but not distinguishable from gonocoxites dorsal to conjunctiva; outline of gonostyli bluntly cuneiform in dorsolateral view, anteroposterior length subequal to that of the gonocoxites. Volsellae (**vol**; Fig. 3.10A–E) present, proximally indistinct from gonopodites; not medially fused; lateropenite (**ltp**; Fig. 3.10B, D) and parossiculus (**prs**; Fig. 3.10B, D) present, proximally indistinct; two recurved, dorsoventrally compressed medial processes present, placed successively along medioventral margin. Penial sclerites (**psc**; Fig.

3.10A–E) medially joined by dorsal conjunctiva along proximal 4/7 of length, medially separated at apex; not dorsoventrally or lateromedially compressed, unsculptured; valvurae present, lamellate proximolateral processes, proximal apices of valvurae not directed dorsally; posterior penial processes absent; endophallic sclerite absent; phallotreme distodorsal, situated at apex of penial conjunctiva, not surrounded by sclerotized portions of the penial sclerites, not recessed; penial sclerites distad phallotreme produced ventrally, dorsolateral margins bowed outwards.

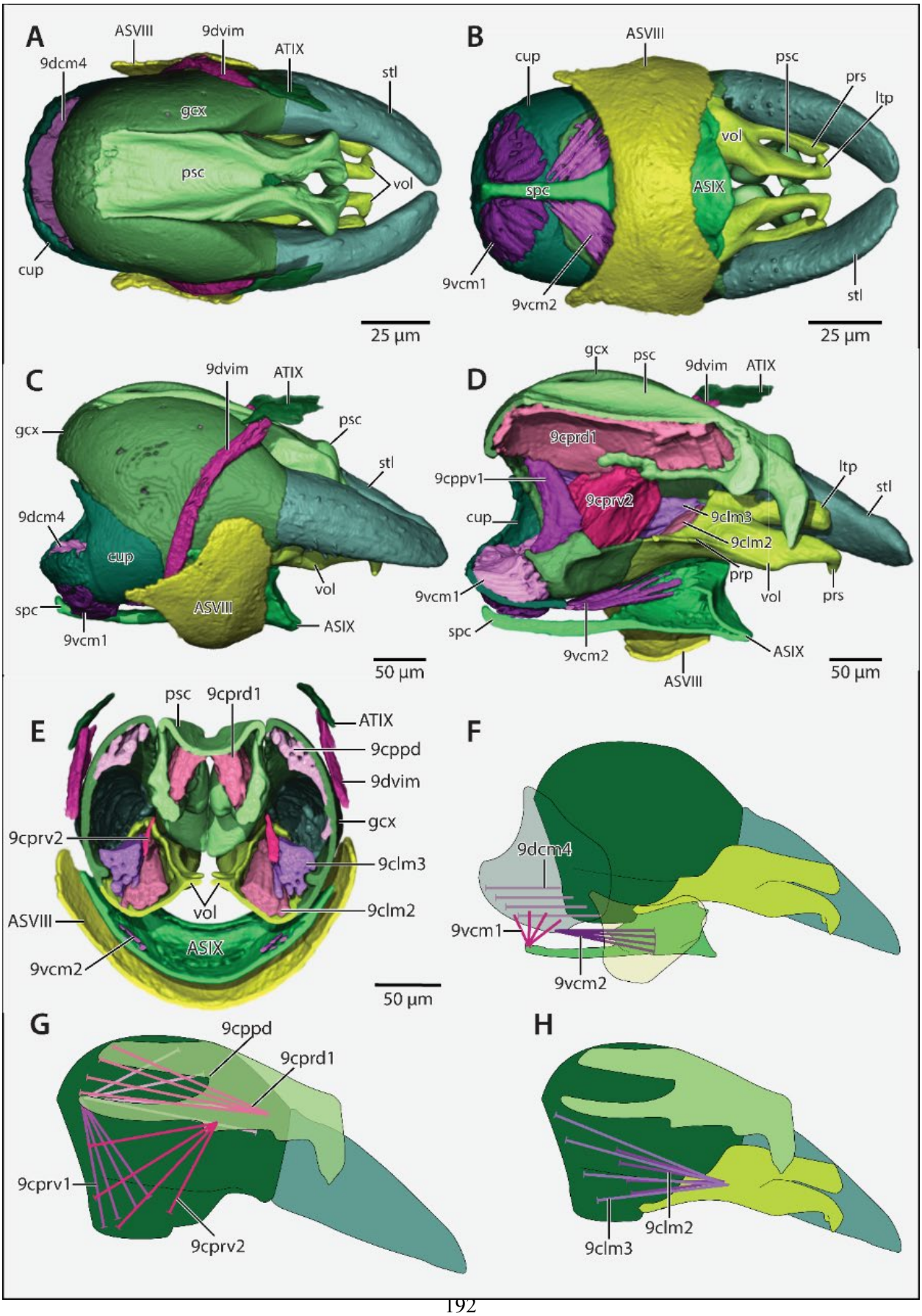
A
ASVIII
9dvim
ATIX
9dcm4
stl
gcx
psc
vol
cup
25 µm
B
ASVIII
cup
psc
prs
ltp
vol
spc
ASIX
9vcm1
9vcm2
stl
25 µm
C
9dvim
ATIX
gcx
psc
stl
9dcm4
cup
vol
spc
ASVIII
ASIX
9vcm1
50 µm
D
gcx
psc
9dvim
ATIX
9cprd1
ltp
9cppv1
stl
9cprv2
cup
9clm3
9clm2
prp
vol
prs
9vcm1
spc
9vcm2
ASIX
ASVIII
50 µm
E
psc
9cprd1
ATIX
9cppd
9dvim
gcx
9cprv2
9clm3
vol
9clm2
ASVIII
ASIX
9vcm2
50 µm
F
9dcm4
9vcm1
9vcm2
G
9cppd
9cprd1
9cprv1
9cprv2
H
9clm2
9clm3

Figure 3.10. ♂ genitalia in *Protanilla* zhg-vn01 (CASENT0106408), 3D reconstructions (A–E) and summary diagrams (F-H). Figure 10G is a sagittal cross-section. Caps in muscle diagrams signify origin; lack of caps, insertion. **A** dorsal view **B** ventral view **C** profile view **D** sagittal cross-section **E** transverse cross-section **F** sterno-coxal and tergo-coxal muscles, profile view **G** coxo-penial muscles, sagittal cross-section **H** coxo-lateropenital muscles, profile view Abbreviations: ASVIII=abdominal sternite VIII; ASIX=abdominal sternite IX; spc=spiculum; ATIX=abdominal tergite IX; cup=cupula; gcx=gonocoxite; stl=gonostylus; vol=volsella; prs=parossiculus; lateropenite=ltp; prp=lateropenital recurved processes; psc=penial sclerites; 9dvim=dorsoventral intrinsic muscles IX; 9vcm1=anteromedial sterno-coxal muscles; 9vcm2=posteromedial sterno-coxal muscles; 9dcm4=ventral tergo-coxal muscles; 9clm2=lateral intrinsic coxo-lateropenital muscles; 9clm3=medial extrinsic coxo-lateropenital muscles; 9cppd=dorsal coxo-penial promotors; 9cprd1=dorsal coxo-penial remotors; 9cppv1=anterior ventral coxo-penial promotors; 9cprv2=lateral ventral coxo-penial remotors

3.1.4. Yavnella

3.1.4.1. Yavnella zhg-bt01 (Fig. 3.11)

Abdominal sternite VIII (**ASVIII**; Fig. 3.11B–D) anteroposteriorly compressed laterally, anteroposteriorly expanded medially, posteromedian margin produced into paired obtuse processes; antecosta of abdominal sternite VIII absent; laterally separate from abdominal tergite VIII; posteriorly separate from abdominal sternite IX. Abdominal sternite IX narrowly fused to abdominal tergite IX, anteroposteriorly compressed, anterior margin simple; antecosta absent; basal disc absent; diverging anterolateral processes absent; spiculum absent; posteromedian process absent, posteriorly separate from gonopodites; mulceators absent. Abdominal segment IX (**AIX**; Fig. 3.11A) forming a narrow ring surrounding a broad, circular abdominal foramen IX. Abdominal tergite IX insensibly fused to abdominal sternite IX, not divided into hemitergites. Cerci absent. Cupula absent. Gonopodites (**gpd**; Fig. 3.11A–E) proximally separate from abdominal sternite IX, inarticulate. Gonocoxites (**gcx**; Fig. 3.11A–D) present, not externally distinct from gonostyli, with complete medial separation along dorsum; along venter, medially fused along proximal 1/4 of length; dorsum proximally enclosed by penial sclerites, fused with penial sclerites along proximodorsal margin; apicolateral laminae absent. Mesal

articulatory condyles absent. Gonostyli (**stl**; 11A–E) present, not articulated to gonocoxites, internally delimited from gonocoxites by mesal articulatory condyles; outline rounded in profile view, length less than that of the gonocoxites. Volsellae (**vol**; Fig. 3.11A–E) present, proximally distinct from gonopodites; medially separate; parossiculus and lateropenite not distinct; recurved medial processes absent; volsella bifid. Penial sclerites (**psc**; Fig. 3.11A, C–E) completely medially fused, proximally separate from gonopodites; dorsoventrally compressed, unsculptured; valvurae absent; posterior penial processes absent; endophallic sclerite absent; phallotreme distal, situated at penial apex; penial apex dorsoventrally compressed, not laminate, margins convergent.

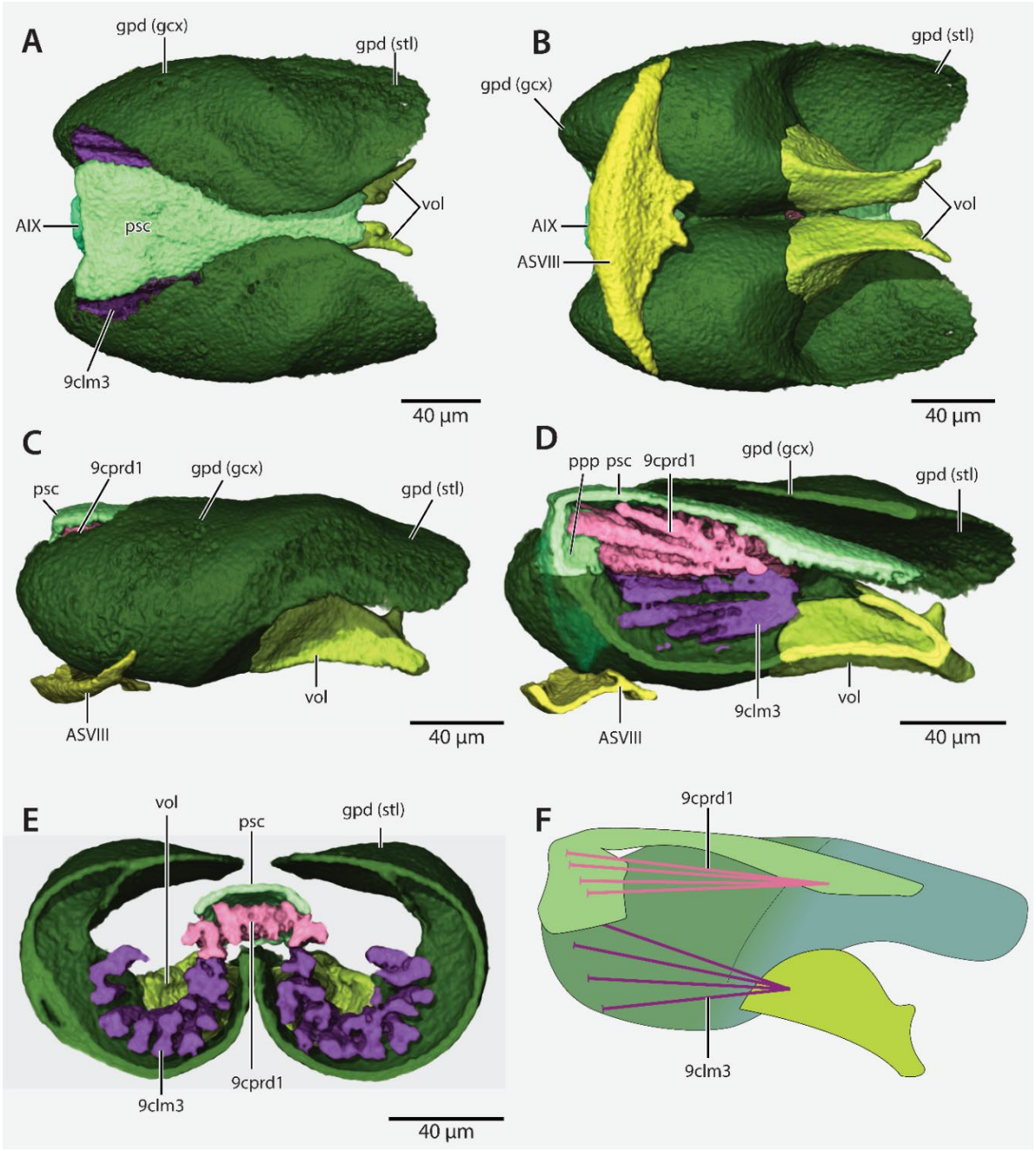

Figure 3.11. ♂ genitalia of *Yavnella* zhg-bt01 (CASENT0842743), 3D reconstructions (A-E) and summary diagram (F). Caps in muscle diagrams signify origin; lack of caps, insertion. **A** rendering, dorsal view **B** rendering, ventral view **C** rendering, profile view **D** rendering, sagittal cross-section **E** rendering, transverse cross-section **F** genital musculature, sagittal cross-section. Abbreviations: ASVIII=abdominal sternite VIII; AIX=abdominal segment IX; gpd=gonopodites; gcx=gonocoxite; stl=gonostylus; vol=volsella; pen=penial sclerites; 9clm3=medial extrinsic coxo-lateropenital muscles; 9cprd1=dorsal coxo-penial remotors

3.1.4.2. Yavnella zhg-th03 (Fig. 3.12)

Abdominal sternite VIII (**ASVIII**; Fig. 3.12A–D) expansive, enclosing dorsal base of genitalia; antecosta of abdominal sternite VIII present laterally, absent medially, where present rotated and projecting ventrad anteroposterior; diverging anterolateral apodemes absent; laterally separate from abdominal tergite VIII; posteromedially fused to abdominal segment IX, delimited posteriorly from abdominal sternite IX by dorsoventral apodemes, on each side of median fusion of abdominal sternites VIII–IX. Abdominal sternite IX (**AIX** [**ASIX**]; Fig. 3.12D) lateromedially compressed, posteriorly prolonged; antecosta of abdominal sternite IX absent; basal disc absent; diverging anterolateral processes absent; spiculum absent; posteromedian process absent, posteriorly separate from gonopodites; mulceators absent. Abdominal segment IX (**AIX**; Fig. 3.12A–B, D) with complete tergosternal fusion, lateromedially compressed, anteroposteriorly prolonged, with abdominal foramen IX as a dorsoposterior opening. Abdominal tergite IX (**AIX** [**ATIX**]; Fig. 3.12A–B, D) insensibly fused to abdominal sternite IX, not divided into hemitergites. Cerci absent. Cupula absent. Gonopodites (**gpd**; Fig. 3.12A–E) proximally separate from abdominal sternite IX, inarticulate. Gonocoxites (**gpd** (gcx); Fig. 3.12A–D) present, not externally distinct from gonostyli, with complete medial separation along dorsum; along venter, medially fused along proximal 1/3 of length; dorsum proximally enclosed by penial sclerites; fused with penial sclerites along ventromedial face; apicolateral laminae absent. Mesal articulatory condyles absent. Gonostyli (**gpd** (stl); Fig. 3.12A–D) present, not separated from gonocoxites by mesal articulatory condyles; tapering, apices medially recurved. Volsellae (**vol**; Fig. 3.12B–E) present, not medially fused; fully articulated to gonopodites; basal ½ of volsella subcylindrical in cross-section, with ectal longitudinal costae on medial face; apical ½ of volsella produced into dorsal linear process and ventral hook-like process, with latter process proximally recurved, surface of processes unsculptured. Penial sclerites (**psc**; Fig. 3.12A–E) completely

medially fused, fused to gonocoxites along proximal 1/3 of length, subtriangular proximomedian notch present; proximal longitudinal carinae present on penial dorsum, absent medially and laterally; valvurae absent; ventral longitudinal posterior penial processes (**ppp**; Fig. 3.12D) present at base, insensibly fused with gonocoxites; endophallic sclerite absent; phallotreme posterodorsal, not recessed, outline teardrop-like, narrowing distally; narrow linear apicomedian slit present, distal to phallotreme; penial apex dorsoventrally compressed, laminate, with linear lateral margins.

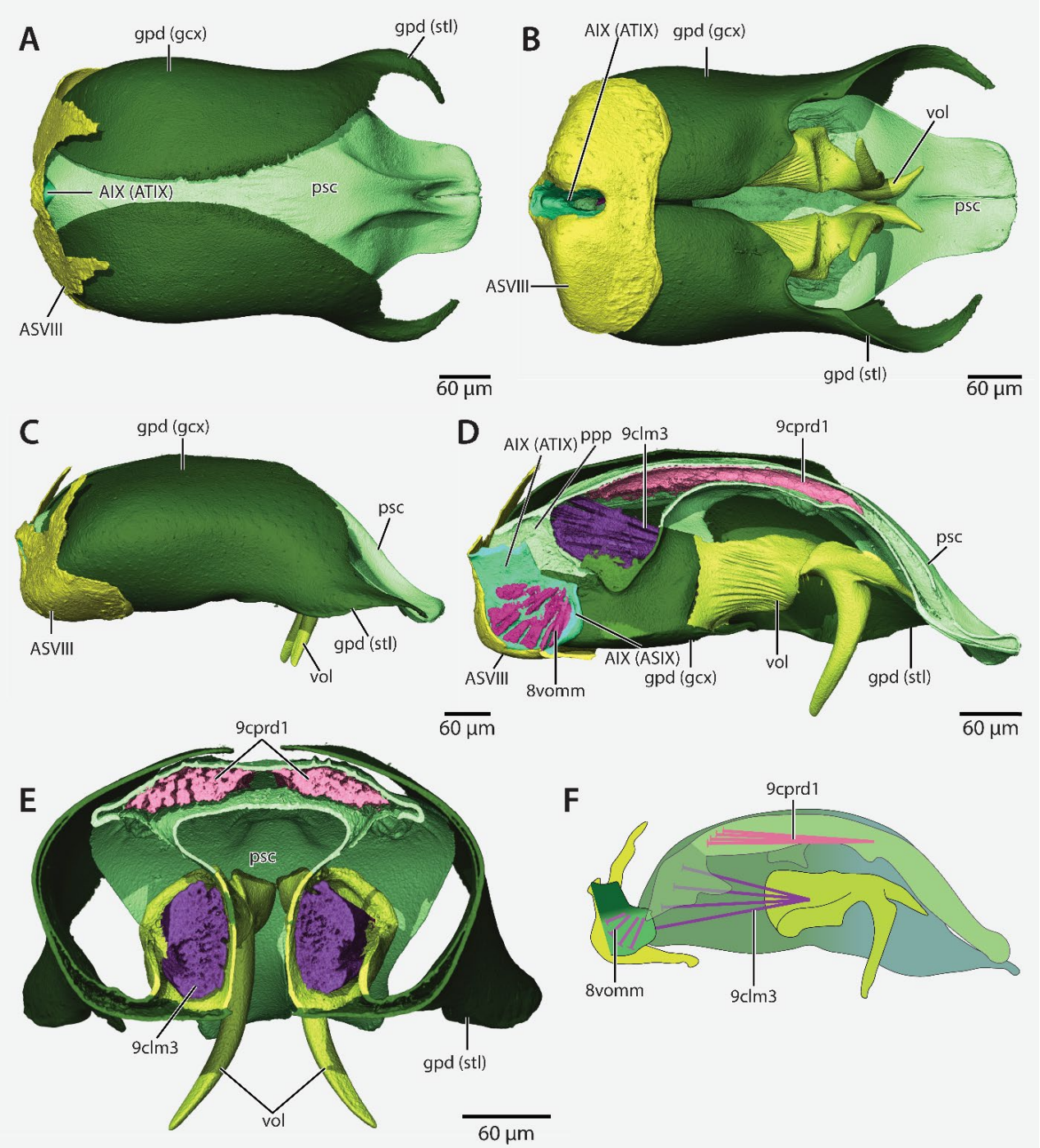

Figure 3.12. ♂ genitalia of *Yavnella* zhg-th03 (CASENT0842741), 3D reconstructions (A-E) and summary diagram (F). Caps in muscle diagrams signify origin; lack of caps, insertion. **A** dorsal view **B** ventral view **C** profile view **D** sagittal cross-section **E** transverse cross-section **F** genital musculature, sagittal cross-section. Abbreviations: ASVIII=abdominal sternite VIII; AIX=abdominal segment IX; ASIX=abdominal sternite IX; spc=spiculum; ATIX=abdominal tergite IX; gpd=gonopodites; gcx=gonocoxite; stl=gonostylus; vol=volsella; pen=penial sclerites; 8vomm=ventral orthomedial muscles VIII-IX; 9clm3=medial extrinsic coxo-lateropenital muscles; 9cprd1=dorsal coxo-penial remotors

3.1.5. Scyphodon s. l.

3.1.5.1. Noonilla zhg-my03 (Fig. 3.13)

Abdominal sternite VIII (**ASVIII**; Fig. 3.13A–D) anteroposteriorly compressed, bar-like, with anteroposterior breadth equivalent across lateromedial span; antecosta present, weakly developed; diverging anterolateral apodemes absent; abdominal sternite VIII laterally separate from abdominal tergite VIII; posteriorly separate from abdominal sternite IX. Abdominal sternite IX (**ASIX**; Fig. 3.13A–B, C) anteroposteriorly compressed medially; antecosta present, not hypertrophied, abdominal sternite IX not reduced to antecosta; basal disc absent; spiculum absent; diverging anterolateral processes absent; posteromedian process absent, abdominal sternite IX fused to gonocoxites posteriorly, intersecting with gonocoxites at obtuse angle in profile view, delimited from gonocoxites by mesal transverse carina; mulceators absent. Abdominal tergite IX (**ATIX**; Fig. 3.13A, C–D) with posteromedian fusion, insensibly blending posteriorly into proctiger, expanded into apodemes anterolaterad median fusion; abdominal tergite IX anteroposteriorly narrowing laterad apodemes. Cerci absent. Cupula absent. Gonopodites proximally fused to abdominal sternite IX, articulate. Gonocoxites (**gcx**; Fig. 3.13A–E) present, proximally fused to abdominal sternite IX, distinct from gonostyli; with complete medial fusion along dorsum and venter, delimited by ventromedian carina; dorsum not proximally enclosed by, and insensibly fused to, penial sclerites; apicolateral laminae absent. Gonostyli (**stl**; Fig. 3.13A–E) present, separated dorsally from gonocoxites by invaginated conjunctiva, ventrally fused to gonocoxites along proximal ½ of length; medially fused at base, delimited by shallow median sulcus, unfused distally; each gonostylus distally produced into lobate, medially recurved processes, subequal in length. Volsellae absent. Penial sclerites (**psc**; Fig. 3.13A–E) with complete median fusion, insensibly fused to gonocoxites at base, proximal

margin entire, dorsum intersecting that of the gonocoxites at a 90° angle; unsculptured; valvurae absent; posterior penial processes absent; endophallic sclerite absent; phallotreme (**pht**; Fig. 3.13B) posterodorsal, outline elliptical, slightly narrowing proximally, not recessed; penial apex not dorsoventrally compressed, dorsal surface concave, not laminate, distal margin entire, lateral margins converging.

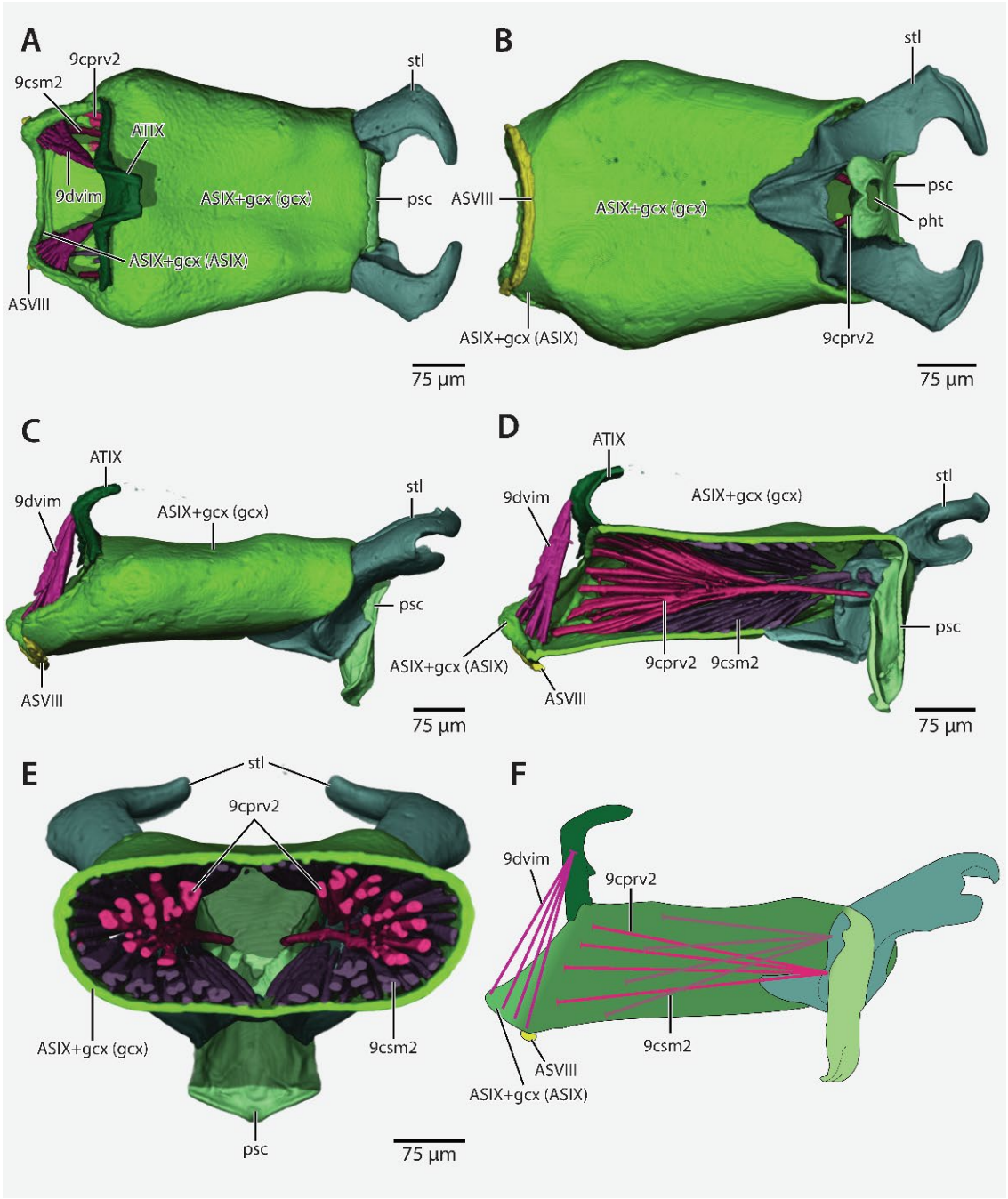

Figure 3.13. ♂ genitalia of *Noonilla* zhg-my03 (CASENT0842609), 3D reconstructions (A-E) and summary diagram (F). Caps in muscle diagrams signify origin; lack of caps, insertion. **A** dorsal view **B** ventral view **C** profile view **D** sagittal cross-section **E** transverse cross-section **F** genital musculature, sagittal cross-section. Abbreviations: ASVIII=abdominal sternite VIII; ASIX=abdominal sternite IX; ATIX=abdominal tergite IX; gcx=gonocoxite; stl=gonostylus; psc=penial sclerites; pht=phallotreme; 9dvim=dorsoventral intrinsic muscles IX; 9csm2=intermediate coxo-stylar muscles; 9cprv2=lateral ventral coxo-penial remotors

3.1.5.2. Noonilla cf. *copiosa* (Fig. 3.14)

Abdominal sternite VIII (**ASVIII**; Fig. 3.14A–D) anteroposteriorly compressed, bar-like, with anteroposterior length equivalent across lateromedial span; antecosta (**acsS8**; Fig. 3.14B, D) present, well-developed; diverging anterolateral apodemes absent; laterally fused to abdominal tergite VIII; not posteriorly fused to abdominal sternite IX. Abdominal sternite IX (**ASIX**; Fig. 3.14B–C) anteroposteriorly extended, posteriorly constricted along lateromedial axis; antecosta (**acsS9**; Fig. 3.14B) hypertrophied, extending along median faces of diverging anterolateral processes, medially prolonged into recurved triangular process, abdominal sternite IX not reduced to antecosta; diverging anterolateral processes (**atpS9**; Fig. 3.14D) present, outline of abdominal sternite IX being yoke-shaped dorsally; basal disc absent; posteromedian process absent, abdominal sternite IX insensibly fused to gonocoxites posteriorly, intersecting with gonocoxites at 45° angle in profile view; mulceators absent. Abdominal tergite IX (**ATIX**; Fig. 3.14) divided into hemitergites; hemitergites anteroposteriorly compressed, tapering laterally. Cerci absent. Cupula absent. Gonopodites proximally fused to abdominal sternite IX, articulate. Gonocoxites (**gcx**; Fig. 3.14A–E) with narrow proximal fusion to abdominal sternite IX, distinct from gonostyli; with complete medial fusion along dorsum and venter, delimited by shallow ectal ventromedian sulcus and dorsomedian mesal carina; dorsum not proximally enclosed by, and insensibly fused to, penial sclerites; apicolateral laminae absent. Gonostyli (**stl**; Fig. 3.14A–E) present, articulated dorsally with gonocoxites, insensibly fused to gonocoxites ventrally; without medial fusion; apex of each gonostylus entire, medially recurved. Volsellae absent. Penial sclerites (**psc**; Fig. 3.14A–E) completely medially fused; insensibly fused to gonocoxites at base, proximal margin absent, dorsum at same dorsoventral level as that of the gonocoxites; ventromedian margin irregularly serrated, sculpturation otherwise absent; lateromedially compressed, valvurae absent; posterior penial processes absent; endophallic sclerite absent;

phallotreme (**pht**; Fig. 3.14A) posterodorsal, recessed, outline teardrop-shaped; penial apex lateromedially compressed, rounded, outline entire, subapically produced into ventromedian "trigger", consisting of a proximal, proximally recurved process and apical proximally recurved process with length ~130% that of proximal process.

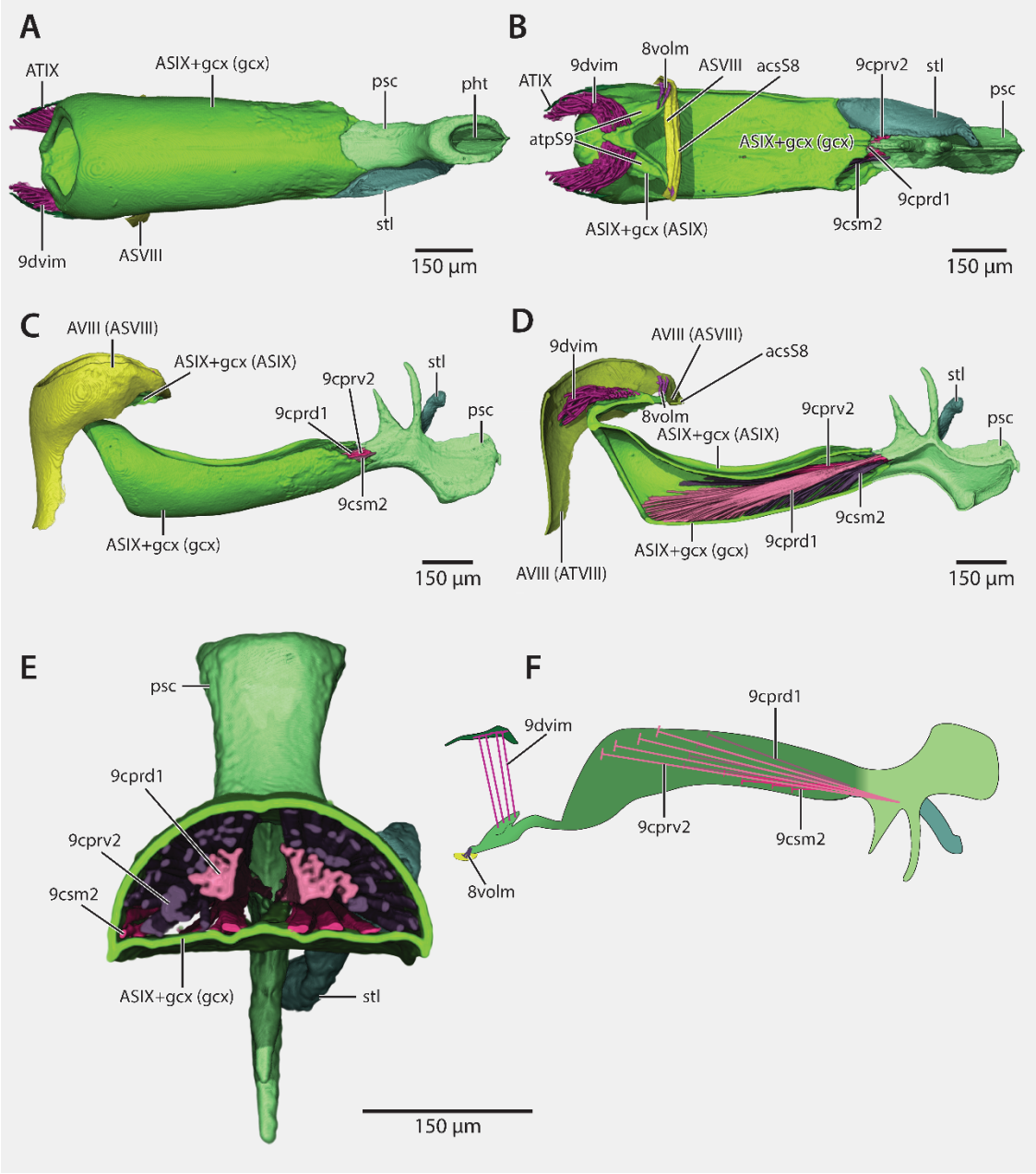

Figure 3.14. ♂ genitalia of *Noonilla* cf. *copiosa* (CASENT0842844), 3D reconstructions (A–E) and summary diagram (F). Caps in muscle diagrams signify origin; lack of caps, insertion. **A** dorsal view **B** ventral view **C** profile view **D** sagittal cross-section **E** transverse cross-section **F** genital musculature, sagittal cross-section; abdominal sternite IX is shown rotated 180° relative to its position *in situ*. Abdominal sternite VIII is shown without sagittal cross-section. Abbreviations: AVIII=abdominal segment VIII; ASVIII=abdominal sternite VIII; ATVIII=abdominal tergite VIII; ASIX=abdominal sternite IX; atpS9=anterolateral processes of abdominal sternite IX; ATIX=abdominal tergite IX; gcx=gonocoxite; stl=gonostylus; psc=penial sclerites; 8volm=ventral ortholateral muscles VIII-IX; 9dvim=dorsoventral intrinsic muscles IX; 9csm2=intermediate coxo-stylar muscles; 9cprd1=dorsal coxo-penial remotors; 9cprv2=lateral ventral coxo-penial remotors

3.1.6. The Bornean morphospecies-group

3.1.6.1. Leptanilla zhg-my02 (Fig. 3.15)

Abdominal sternite VIII (**ASVIII**; Fig. 3.15A–D) anteroposteriorly compressed; antecosta present, not well-developed, abdominal sternite VIII medially reduced to antecosta; diverging anterolateral apodemes absent; laterally separate from abdominal tergite VIII; posteriorly separate from abdominal sternite IX. Abdominal sternite IX (**ASIX**; Fig. 3.15A–D) anteroposteriorly compressed, strap-like with posterolateral corners expanded and rounded, narrowing medially along anteroposterior axis; antecosta absent medially, not produced into recurved lateral apodemes; diverging anterolateral processes absent; basal disc absent; spiculum absent; posteromedian process absent, abdominal sternite IX with posteromedian fusion to gonocoxites, ventral to gonocoxital foramen; mulceator (**mul**; Fig. 3.15A–E) present, subcircular in cross-section towards apex. Abdominal tergite IX (**ATIX**; Fig. 3.15A–D) divided into hemitergites; hemitergites anteroposteriorly compressed, lozenge-shaped in outline. Cerci absent. Cupula absent. Gonopodites with narrow proximomedian fusion to abdominal sternite IX. Gonocoxites (**gcx**; Fig. 3.15A–E) present, with medial fusion complete, not medially delimited by sulcus, carina, or both; circular gonocoxital foramen present; dorsum enclosing, and separate from, penial sclerites; apicolateral laminae (**all**; Fig. 3.15A–C, E) present, outline subulate. Gonostyli absent. Volsellae (**vol**; Fig. 3.15A–E) present, fully articulated to gonocoxites at base, medially fused by narrow bridge of cuticle at base; lateropenite insensibly fused to parossiculus; parossiculus insensibly fused to lateropenite; recurved medial processes absent; lateral faces of volsellar apices produced into dorsally recurved hook. Penial sclerites (**psc**; Fig. 3.15A–E) completely medially fused, fully articulated to gonocoxites along proximodorsal margin, subcircular in proximal cross-section, dorsally recurved, unsculptured; penial condyles present;

valvurae absent; posterior penial processes absent; endophallic sclerite absent; phallotreme (**pht**; Fig. 3.15A) distoventral, subapical, recessed, on platform-like ventromedian process, outline elliptical; penial apex produced into median ventral carina distad phallotreme, with lateral margins produced into ventral carinae that converge apically.

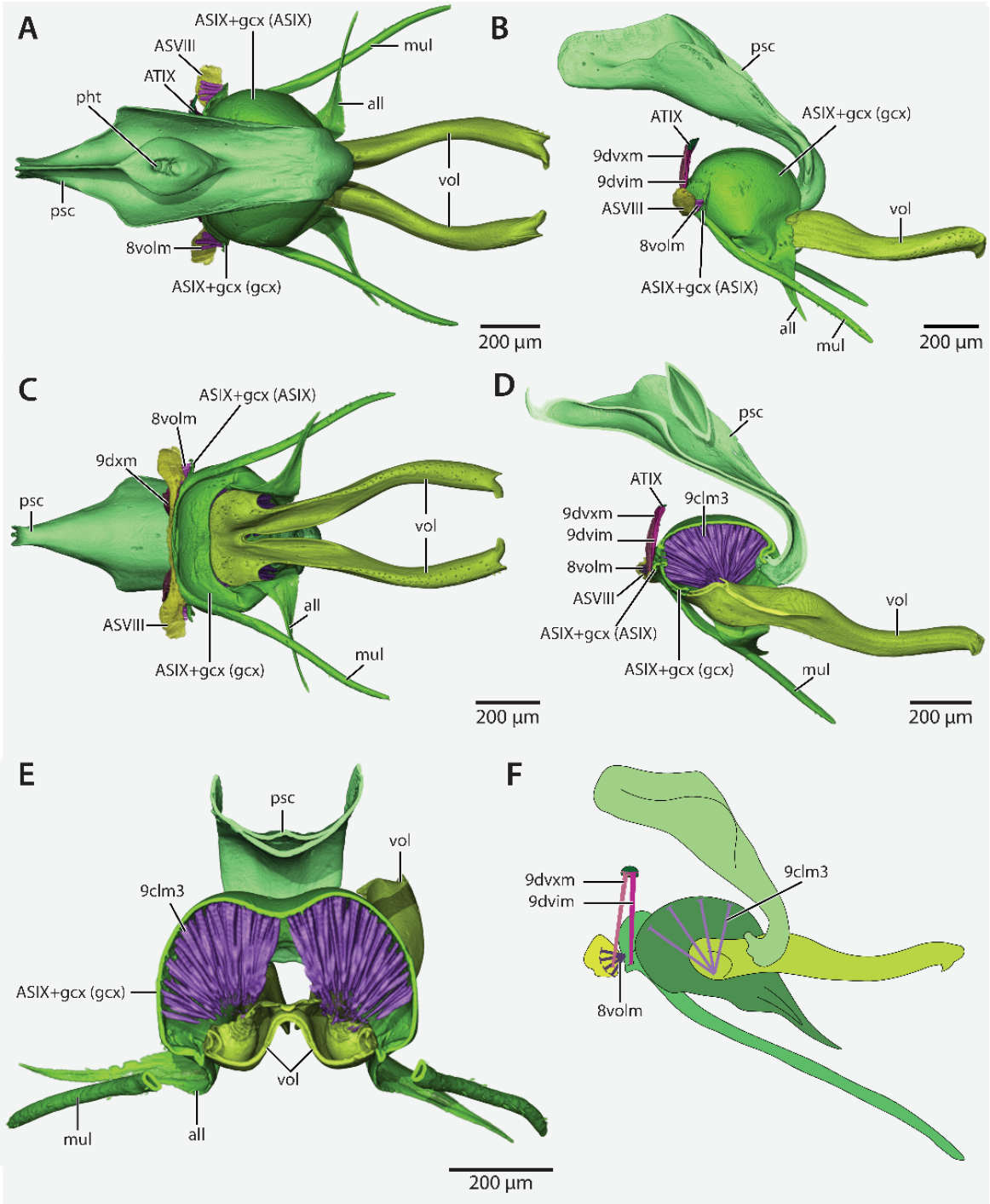

Figure 3.16. ♂ genitalia of *Leptanilla* zhg-my02 (CASENT0106416), 3D reconstructions (A–E) and summary diagram (F). Caps in muscle diagrams signify origin; lack of caps, insertion. **A** dorsal view **B** ventral view **C** profile view **D** sagittal cross-section **E** transverse cross-section **F** genital musculature, sagittal cross-section. Abbreviations: ASVIII=abdominal sternite VIII; ASIX=abdominal sternite IX; mul=mulceator; ATIX=abdominal tergite IX; gcx=gonocoxite; all=apicolateral lamina; vol=volsella; psc=penial sclerites; pht=phallotreme; 8volm=ventral ortholateral muscles VIII-IX; 9dvxm=dorsoventral extrinsic muscles IX-VIII; 9dvim=dorsoventral intrinsic muscles IX; 9clm3=medial extrinsic coxo-lateropenital muscles

3.1.6.2. Leptanilla zhg-my04 (Fig. 3.16)

Abdominal sternite VIII (**ASVIII**; Fig. 3.16A–D) anteroposteriorly compressed medially; antecosta present, not well-developed, abdominal sternite VIII not reduced to antecosta; diverging anterolateral apodemes absent; laterally separate from abdominal tergite VIII; broadly fused to abdominal sternite IX posteriorly, delimited from abdominal sternite IX by mesal transverse apodeme. Abdominal sternite IX (**ASIX**; Fig. 3.16A–D) anteroposteriorly compressed, strap-like with posterolateral corners expanded and rounded, narrowing medially along anteroposterior axis; antecosta present medially; antecosta of abdominal sternite IX produced into recurved lateral apodemes; basal disc absent; spiculum absent; anterolateral processes absent; posteromedian process absent, abdominal sternite IX with insensible posteromedian fusion to gonocoxites, fusion forming ring surrounding gonocoxital foramen; mulceators (**mul**; Fig. 3.16A–E) present, originating medially to lateral apodeme, lateromedially compressed towards apex. Abdominal tergite IX (**ATIX**; Fig. 3.16A, C) divided into hemitergites; hemitergites anteroposteriorly compressed. Cerci absent. Cupula absent. Gonopodites with narrow proximomedian fusion to abdominal sternite IX. Gonocoxites (**gcx**; Fig. 3.16A–E) present, with medial fusion complete, not medially delimited by sulcus, carina, or both; circular gonocoxital foramen present; dorsum enclosing penial sclerites, which are fused to the gonocoxites surrounding the gonocoxital foramen; apicolateral laminae absent. Gonostyli absent. Volsellae present, fully articulated to gonocoxites, medially fused by narrow bridge of cuticle 1/3 of length from base; parossiculus and lateropenite insensibly fused to lateropenite; recurved medial processes absent; volsellar apex produced into large, dorsally recurved hook, penial sclerites supported by proximomedial volsellar condyles. Penial sclerites (**psc**; Fig. 3.16A–E) completely medially fused, with insensible proximal fusion to gonocoxites, fusion

surrounding gonocoxital foramen, proximal margin entire, unsculptured, lateromedially compressed along entire length; penial condyles absent; posterior penial processes absent; valvurae absent; endophallic sclerite absent; phallotreme situated apically, not recessed, outline slit-like; penial apex lateromedially compressed, lacking distinct lateral margins, dorsomedian carina present; apical margin entire.

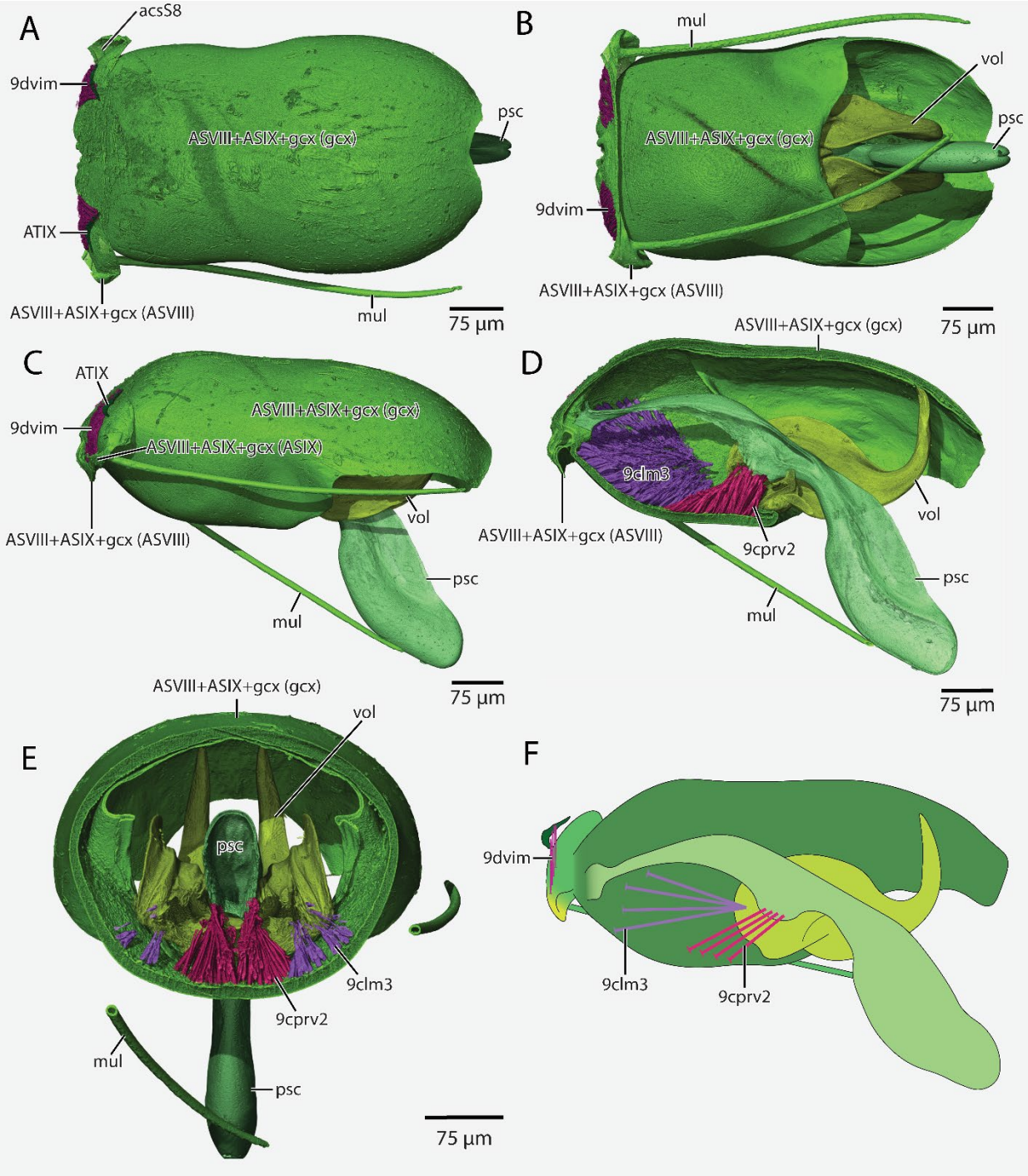

Figure 3.16. ♂ genitalia of *Leptanilla* zhg-my04 (CASENT0842565), 3D reconstructions (A–E) and summary profile diagram (F). Caps in muscle diagrams signify origin; lack of caps, insertion. **A** dorsal view **B** ventral view **C** profile view **D** sagittal cross-section **E** transverse cross-section **F** genital musculature, sagittal cross-section. Abbreviations: ASVIII=abdominal sternite VIII; ASIX=abdominal sternite IX; mul=mulceator; ATIX=abdominal tergite IX; gcx=gonocoxite; vol=volsella; psc=penial sclerites; 9dvim=intrinsic dorsoventral muscles IX; 9clm=medial extrinsic coxo-lateropenital muscles; 9cprv2=lateral ventral coxo-penial remotors

3.1.7. Leptanilla s. str.

3.1.7.1. Leptanilla zhg-id04 (Fig. 3.17)

Abdominal sternite VIII (**ASVIII**; Fig. 3.17A–D) anteroposteriorly compressed, with anteroposterior breadth equivalent across lateromedial span; antecosta not discernible; diverging anterolateral apodemes absent; laterally separate from abdominal tergite VIII; posteriorly separate from abdominal sternite IX. Abdominal sternite IX (**ASIX**; Fig. 3.17A–D) elongate, moderately narrowing laterally along anteroposterior axis; antecosta not discernible; basal disc indistinct; spiculum absent; diverging anterolateral processes absent; small, obtuse posteromedian process present, not delimited from anterior mesal surface of abdominal sternite IX by transverse carina, separate posteriorly from gonocoxites; mulceators absent. Abdominal tergite IX not discernible. Cerci absent. Cupula absent. Gonopodites proximally separate from abdominal sternite IX, articulate. Gonocoxites (**gcx**; Fig. 3.17A–E) present, with narrow proximal ventromedian fusion, otherwise with complete medial articulation; dorsum proximally enclosed by penial sclerites; narrowly fused with penial sclerites along proximal ventromedian face; apicolateral laminae absent. Gonostyli (**stl**; Fig. 3.17A–E) present, fully articulated to dorsomedial apex of the gonocoxites; not medially fused; apex of each gonostylus bifid, not medially recurved, apical teeth truncate. Volsellae (**vol**; Fig. 3.17E) present, proximally articulated to gonocoxites; completely medially separate; parossiculus and lateropenite insensibly fused; lamellate, unsculptured, not medially recurved; recurved medial processes absent. Penial sclerites (**psc**; Fig. 3.17A–E) medially fused, without ventromedian carina; narrowly fused to gonocoxites at proximal margin, proximal margin entire, with a proximomedian foramen; dorsoventrally compressed at base, unsculptured; penial condyles absent; posterior penial processes present distolaterad proximal margin, obtusely rounded;

valvurae absent; endophallic sclerite absent; phallotreme distodorsal, not recessed, outline subcircular; penial apex dorsoventrally compressed, laminate, unsculptured, margin entire, lateral margins converging.

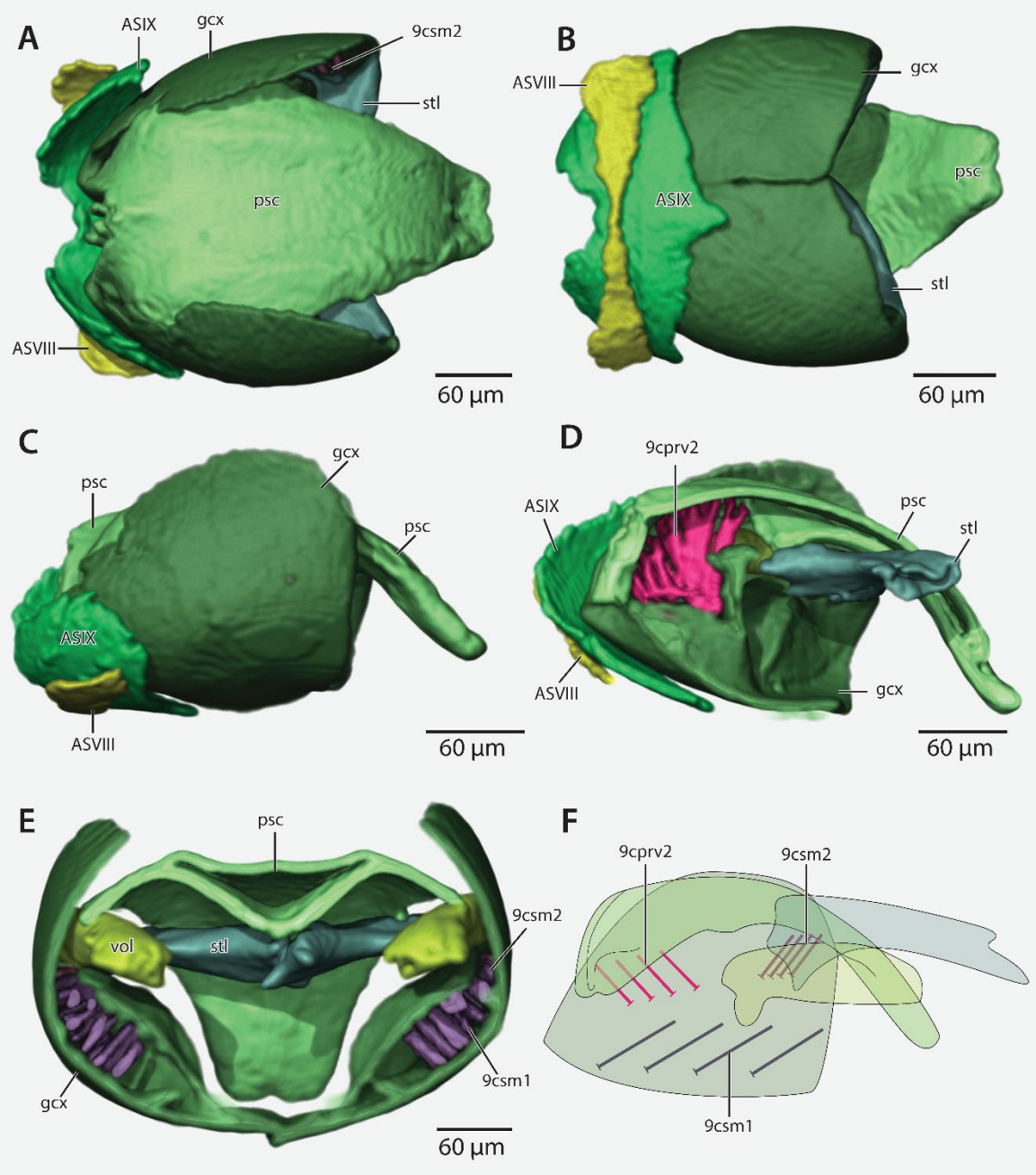

Figure 3.17. ♂ genitalia of *Leptanilla* zhg-id04 (CASENT0106357), 3D reconstructions (A–E) and summary diagram (F). Caps in muscle diagrams signify origin; lack of caps, insertion. **A** dorsal view **B** ventral view **C** profile view **D** sagittal cross-section **E** transverse cross-section **F** genital musculature, external profile view. Abbreviations: ASVIII=abdominal sternite VIII; ASIX=abdominal sternite IX; gcx=gonocoxite; stl=gonostylus; vol=volsella; psc=penial

sclerites; 9csm1=anterior coxo-stylar muscle; 9csm2=intermediate coxo-stylar muscle; 9cprv2=lateral ventral coxo-penial remotors

3.1.7.2. Leptanilla cf. *zaballosi* (Fig. 3.18)

Abdominal sternite VIII present, posteriorly separate from abdominal sternite IX, but not discernible *in toto*. Abdominal sternite IX (**ASIX**; Fig. 3.18A–D) elongate, moderately narrowing laterally along anteroposterior axis; antecosta absent; basal disc indistinct; spiculum absent; diverging anterolateral processes absent; small, obtuse posteromedian process present, not delimited from anterior mesal surface of abdominal sternite IX by transverse carina, posteriorly distinct from gonocoxites; mulceators absent. Abdominal tergite IX not discernible. Cerci absent. Cupula absent. Gonopodites proximally separate from abdominal sternite IX, articulate. Gonocoxites (**gcx**; Fig. 3.18A–E) present, with complete medial separation; dorsum proximally enclosing penial sclerites; fully articulated to penial sclerites (**psc**; Fig. 3.18A–E); apicolateral laminae absent from gonocoxites. Gonostyli (**stl**; Fig. 3.18B–E) present, fully articulating with dorsomedial apices of the gonocoxites; not medially fused; apex of each gonostylus entire, tapering, somewhat medially recurved. Volsellae (**vol**; Fig. 3.18D–E) present, proximally articulated to gonocoxites; completely medially separate; parossiculus and lateropenite insensibly fused; falcate, not dorsoventrally compressed, proximal 1/6 of length recurved ventrolaterad relative to proximodistal axis of genitalia; recurved medial processes absent. Penial sclerites (**psc**; Fig. 3.18A–D) medially fused, with ventromedian carina; posterior penial processes (**ppp**; Fig. 3.18D) present, broad, and dicondylic, articulating narrowly with gonocoxites; proximal condyle obtuse; distal condyle (**ppp2**; Fig. 3.18D) tapering; proximal margin entire, without proximomedian foramen; dorsoventrally compressed at base, unsculptured; valvurae absent; endophallic sclerite absent; phallotreme distodorsal, not recessed,

outline elliptical; penial apex dorsoventrally compressed, laminate, margin entire, lateral margins converging.

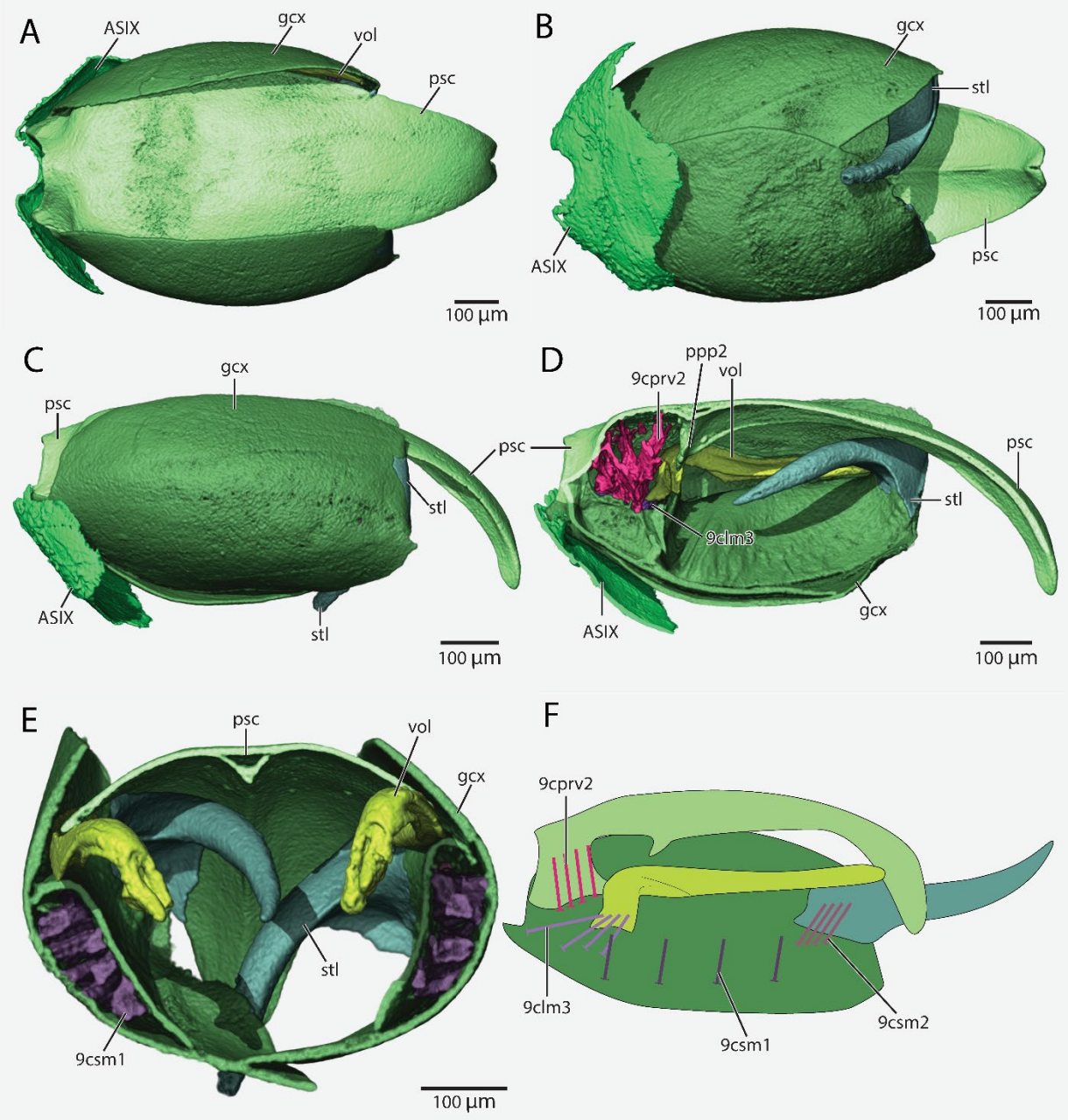

Figure 3.18. ♂ genitalia of *Leptanilla* cf. *zaballosi* (CASENT0842782), 3D reconstructions (A–E) and summary diagram (F). Caps in muscle diagrams signify origin; lack of caps, insertion. **A** dorsal view **B** ventral view **C** profile view **D** sagittal cross-section **E** transverse cross-section **F** genital musculature, sagittal cross-section. Abbreviations: ASVIII=abdominal sternite VIII; ASIX=abdominal sternite IX; gcx=gonocoxite; stl=gonostylus; vol=volsella; psc=penial sclerites; ppp=posterior penial process; 9csm1=anterior coxo-stylar muscles; 9csm2=intermediate coxo-stylar muscles; 9clm3=medial extrinsic lateropenital muscles; 9cprv2=lateral ventral coxo-penial remotors

3.2. Musculature

3.2.1. Summary

As in Section 3.1.1, the following summarizes the totality of muscular variation in the male genitalia of the Formicidae, based upon previous literature (Boudinot, 2013) and the findings described in the present study. This summary of genital musculature includes the intrinsic dorsoventral muscles IX, extrinsic dorsoventral muscles VIII–IX and ventral longitudinal muscles VIII–IX but excludes dorsal longitudinal muscles VIII–IX and intrinsic dorsoventral muscles VIII.

Ventral longitudinal muscles VIII–IX (8vlm) originate on abdominal sternite VIII and insert on abdominal sternite IX. These include the ventral longitudinal orthomedial (**8vomm)**, paramedial (**8vpmm**) and ortholateral (**8volm**) muscles. The ventral paramedial muscles VIII–IX (**8vpmm**) originate on abdominal sternite VIII posterior to their insertion on abdominal sternite IX and are therefore reversed in position relative to the orthomedial and -lateral ventral longitudinal muscles**.** In many cases sampled in this study, these subsets of 8vlm cannot be distinguished. Intrinsic dorsoventral muscles IX (**9dvim**) originate on abdominal tergite IX (**ATIX**) and insert on abdominal sternite IX; extrinsic dorsoventral muscles IX–VIII (**9dvxm**) originate on abdominal tergite IX and insert on abdominal sternite VIII (these muscles are documented for the first time in this study and are only known in *Leptanilla* zhg-my02 and -my05). Median sterno-coxal muscles (**9vcm1–2**; *a, b; M. sterno-coxalis antero-*, *posteromedialis*) and lateral sterno-coxal muscles (**9vcm3**; *c; M. sterno-coxalis lateralis*) originate on abdominal sternite IX and insert on the cupula (**cup**); 9vcm1 (*a*) are paired, originating on the anterior end of the spiculum (**spc**) and inserting on the anteroventral margin of the cupula (**cup**); 9vcm2 (*b*) are unpaired, originating posteriorly or around the longitudinal midpoint of abdominal sternite IX, sometimes

on a transverse carina ("cranial apodeme", Boudinot, 2013, p. 38), and inserting on the ventromedian margin of the cupula (**cup**); 9vcm3 (*c*) are paired, originating on anterolateral projections of abdominal sternite IX, inserting on the anteroventral margin of the cupula (cup), anterad the insertions of 9vcm1. Tergo-coxal muscles (**9dcm1**–**4**; *g, f, e, d*; *M. tergo-coxalis dorsalis*, *dorsolateralis*, *ventrolateralis*, and *ventralis*) originate on the cupula (**cup**) and insert on the gonocoxites (**gcx**), of which 9dcm1–3 (*g, e, f*) are paired; 9dcm4 may be paired or unpaired. The coxo-stylar muscles (**9csm**, *M. coxo-stylalis*) originate within the gonocoxite (**gcx**) and insert within the gonostylus (**stl**); these are rarely divided into a proximal, intrinsic (**9csm1**, *M. coxo-stylalis anterior*) and intermediate, extrinsic (**9csm2**; *t*; *M. coxo-stylalis intermedialis*) subsets, with the anterior subset inserting on the mesomedial surfaces of the gonocoxites; note that 9csm2 (*t*) is termed *intermediate* due to the presence of a third, distal coxo-stylar muscle in outgroup taxa (9csm3, *u*). Lateral intrinsic coxo-lateropenital muscles (**9clm2**, *M. coxo-lateropenitalis interior lateralis; qr*) and medial extrinsic coxo-lateropenitals (**9clm3**, *M. coxo-lateropenitalis exterior medialis; p*) originate on the medial surfaces of the parossiculus (**prs**) and gonocoxites, respectively. 9clm2 always insert on the mesal surfaces of the volsellae, while 9clm3 may insert mesally or ectally on the parossiculus; very rarely the origin of 9clm3 shifts in part to the penial sclerites (**psc**). Lateral extrinsic coxo-lateropenital muscles (**9clm4**, *M. coxo-lateropenitalis exterior lateralis*) originate distally on the gonocoxite and insert anterad their origin on the proximal part of the volsella; these muscles are only rarely present. Dorsal coxo-penial promotors (**9cppd**, *j*; *M. coxo-penialis promotor dorsalis*) originate on the mesal distodorsal surfaces of the gonocoxites, inserting on anterodorsal surfaces of the valvurae, anterad their origin. Mesal dorsal coxo-penial remotors (**9cprd1**, *k*; *M. coxo-penialis remotor dorsalis mesalis*) originate on the gonocoxites (**gcx**) medial to origin of 9cppd, and insert distally

on mesal surfaces of the penial sclerites (**psc**); ectal dorsal coxo-penial remotors (**9cprd2** *l*; *M. coxo-penialis remotor dorsalis ectalis*) originate distomesally on the gonocoxite near the gonostylar articulation, or on the dorsomedial mesal surfaces of the gonostyli at the proximal margin, inserting distad the insertions of 9cprv2 (*i*), sometimes on a penial apodeme resembling the ergot of symphytan Hymenoptera (e.g., Schulmeister, 2001). Ventral coxo-penial promotors (**9cppv1**, *h*, **–2**; *M. coxo-penialis promotor ventralis anterior, posterior*) insert on the proximoventral surfaces of the valvurae; **9cppv1** originate on the ventromesal surface of the cupula (cup), while **9cppv2** originate on the ventromesal surfaces of the gonocoxites (**gcx**). Ventral coxo-penial remotors (**9cprv2**, *i*; *M. coxo-penialis remotor ventralis lateralis*) originate on the proximoventral mesal surfaces of the gonocoxites (**gcx**), and insert on the proximolateral surfaces of the penial sclerites.

3.2.2. Outgroups

3.2.2.1 Odontomachus indet. (Figs 4–5)

Ventral longitudinal muscles AVIII–IX: **8vomm**, ventral orthomedial muscles. **O**: narrowly on ASVIII, anteromediad O: 8vpmm. **I**: narrowly on ASIX at the anterior apex of the spiculum. **8vpmm**, ventral paramedial muscles. **O**: broadly on median mesal surface of ASVIII. **I**: narrowly, ventrally on anterolateral corners of ASIX. **8volm**, ventral ortholateral muscles. **O**: narrowly on mesal surfaces of anterolateral margins of ASVIIII. **I**: broadly on anterolateral margins of ASIX.

Dorsoventral muscles AVIII: **8dvxm**, dorsoventral extrinsic muscles VIII–IX. **O**: broadly on dorsolateral margins of ATVIII. **I**: narrowly on anterolateral corners of the basal disc of ASIX.

Dorsoventral muscles AIX: **9dvim**, dorsoventral intrinsic muscles IX. **O**: narrowly on anterolateral margins of ATIX. **I**: broadly on mesal anterolateral surfaces of the basal disc of ASIX.

Sterno-coxal muscles: **9vcm1** (*a*), anteromedial sterno-coxal muscles. **O**: narrowly at the anterior apex of the spiculum. **I**: broadly on the ventro-ectal surface of the cupula. **9vcm2** (*b*) posteromedial sterno-coxal muscles. **O**: broadly on mesal surface of ASIX, posterolaterad I:9dvim. **I**: narrowly on the ectal posteromedian surface of the cupula.

Tergo-coxal muscles: **9dcm1** (*g*), dorsal tergo-coxal muscles. **O**: broadly on posterodorsal margin of the cupula **I**: broadly on posterodorsal margins of the gonocoxites. **9dcm2** (*f*), dorsolateral tergo-coxal muscles. **O**: broadly on dorsomesal surface of the cupula. **I**: narrowly on ventral proximolateral margins of the gonocoxites. **9dcm3** (*e*), ventrolateral tergo-coxal muscles. **O**: broadly on anteromesal surface of the cupula. **I**: broadly on proximal ventro-ectal margins of the gonocoxites.

Coxo-stylar muscles: **9csm2** (*t*), intermediate coxo-stylar muscles. **O**: broadly on distodorsal margins of the gonocoxites. **I**: narrowly on lateral extremity of the mesal articulatory condyles of the gonocoxites; intrinsic to the gonocoxites.

Coxo-lateropenital muscles: **9clm3** (*p*), medial extrinsic coxo-lateropenital muscles. Partially differentiated into two bundles, origins adjacent: **O**: one bundle, broadly on mesal ventral surfaces of the gonopodites; the other bundle just proximodorsad the first. **I**: narrowly on proximomedial apodemes of the parossiculi; and narrowly on the mesal proximolateral margin of the parossiculi.

Dorsal coxo-penial promotors: **9cppd** (*j*). Partially differentiable into an anterior and posterior bundle. Anterior partition **O**: broadly on the dorsomesal surfaces of the gonopodites, **I**: on medial surface of the posterior apices of the valvurae. Posterior partition **O**: broadly on the dorsomesal surfaces of the gonostyli. **I**: narrowly on the apices of the valvurae, distad insertion of the anterior partition.

Dorsal coxo-penial remotors: **9cprd1** (*k*), mesal dorsal coxo-penial remotors. **O**: broadly on dorsomesal proximomedian surfaces of gonocoxites. **I**: broadly on mesal surfaces of the valvurae.

Ventral coxo-penial promotors: **9cppv1** (*h*), anterior ventral coxo-penial promotors. **O**: broadly on mesal ventromedian surface of the cupula. **I**: narrowly at proximal apices of the valvurae. **9cppv2**, posterior ventral coxo-penial promotors. **O**: broadly along proximoventral margins of the gonocoxites, and on ventromedian apodemes of gonocoxites. **I**: narrowly distad I: 9cppv1.

Ventral coxo-penial remotors: **9cprv2** (*i*), lateral ventral coxo-penial remotors. **O**: broadly on proximolateral margins of the gonocoxites. **I**: broadly on the distoventral surface of the base of the valvurae.

3.2.2.2 Myrmica ruginodis (Figs 6–7)

Ventral longitudinal muscles AVIII–IX: 8vpmm, ventral paramedial muscles. **O**: broadly on the posterolateral surface of ASVIII, anterad the posterior marginal carina**, I**: broadly on ventral surfaces of anterolateral processes of ASIX. **8volm**, ventral ortholateral muscles. **O**: broadly on mesal surfaces of anterolateral apodemes of ASVIII**, I**: broadly on anterior edges of antecosta and anterolateral processes of ASIX.

Dorsoventral muscles AIX: 9dvim, dorsoventral intrinsic muscles. **O**: broadly on the anterolateral margin of ATIX; **I**: narrowly on the mesal surfaces of the anterolateral processes of ASIX.

Sterno-coxal muscles: 9vcm1 (*a*), anteromedial sterno-coxal muscles. **O**: on entire lateral edges of the spiculum, **I**: extensively on anterior rim and anteroventral surfaces of cupula. **9vcm2** (*b*), posteromedial sterno-coxal muscles. **O:** dorsomedial surface of ASIX, at around the anteroposterior midlength, immediately adjacent to midline, paired but partially coalesced, **I**: posterior margin of spiculum and antecosta of ASIX just laterad spiculum. **9vcm3** (*c*), lateral sterno-coxal muscles. **O**: very extensively on lateromesal surfaces of ASIX, from slightly posterad O:9vcm2 to and including anterolateral processes of ASIX, dorsad 9vcm2, **I**: broadly on anteroventral rim of cupula, laterad and ventrad 9vcm1.

Tergo-coxal muscles: 9dcm1 (*g*), dorsal tergo-coxal muscles. **O**: on the dorsomedian mesal surface of the cupula, coalesced at origin but diverging to paired insertions, **I**: on the anterodorsal edge of the anterior gonocoxital margin. **9dcm2** (*f*), dorsolateral tergo-coxal muscles. **O**: broadly on the dorsolateral mesal surface of the cupula, mostly laterad O:9dcm1 but partially overlapping. **I**: on the ventrolateral edge of the anterior gonocoxital margins, ventrolaterad I:9dcm1. **9dcm3** (*e*), ventrolateral tergo-coxal muscles. **O**: ventrolateral mesal surfaces of the cupula, ventrolaterad O:9dcm2, **I**: more narrowly on the anterodorsal edges of the proximal processes of the gonocoxites, thus muscles triangular and transverse in orientation. **9dcm4** (*d*), ventral tergo-coxal muscles. **O**: ventromedially on the cupula, ventromediad O:9dcm3, **I**: on the anterior surfaces of the proximal processes of the gonocoxites, ventromediad 9dcm3.

Coxo-stylar muscles: 9csm2 (*t*), intermediate coxo-stylar muscles. **O:** at or slightly beyond the distoventral margins of the gonocoxites, **I**: distodorsally on the mesomedial surfaces of the gonostyli, muscles strongly curved along gonostylar profile.

Coxo-lateropenital muscles: 9clm2 (*qr*), lateral intrinsic coxo-lateropenital muscles. **O**: at the junctions of the distoventral gonocoxites and the proximoventral parossiculi, **I**: on the mesal surfaces of the parossiculi, slightly distad (and mesad) I:9clm3. **9clm3** (*p*), medial extrinsic coxo-lateropenital muscles. **O**: broadly on ventromesal surfaces of the gonocoxites, ventrad longitudinal gonocoxital carinae, **I**: broadly on ectal dorsolateral surfaces of parossiculi.

Dorsal coxo-penial promotors: 9cppd (*j*). **O**: very extensively on entire dorsomesal surfaces of the gonocoxites and slightly beyond the coxo-stylar articulation, **I**: apicodorsally, and the dorsal subapical surfaces of the valvurae, dorsad I:9cppv2.

Dorsal coxo-penial remotors: **9cprd1** (*k*), mesal dorsal coxo-penial remotors. **O**: dorsomedially on proximal surfaces of the gonocoxites, **I**; extensively on the mesal surfaces of the penial sclerites, including somewhat differentiated bundles that are located entirely within the penial sclerites, extending nearly to the phallotreme; these posterior partitions divided by a medial sclerotic septum. **9cprd2** (*l*), ectal dorsal coxo-penial remotors. **O**: subdivided at origins; anterior origins distodorsally on the gonocoxites, posterior origins distodorsally on the gonostyli, **I**: both partitions coalescing at long narrow insertions on the ventral and distal ectal surfaces of the lateral apodemes at the base of the valvurae, ventrad 9cppv2, distad I:9cprv2.

Ventral coxo-penial promotors: **9cppv1** (*h*), anterior ventral coxo-penial promotors. **O**: broadly on proximoventral processes of gonocoxites and apparently on medial gonocoxital conjunctiva, **I:** broadly on proximoventral surfaces of the valvurae; some fibers reaching transversely across

the endophallic membrane at the location of the endophallic sclerite. **9cppv2**, posterior ventral coxo-penial remotors. **O**: broadly on distomesal ventral surfaces of gonocoxites, posterad O:9cprv2, **I**: apically on the ectal surfaces of the valvurae, laterad apical parts of I:9cppv1.

Ventral coxo-penial remotors: **9cprv2** (*i*), lateral ventral coxo-penial promotors. **O:** very extensively on the mesal surfaces of the gonocoxites, both dorsad and ventrad the longitudinal gonocoxital carinae, ventrolaterad 9cppv1, **I**: extensively on anterior surfaces of lateral apodemes at bases of valvurae.

3.2.2.3 Lioponera indet. (Figs 8–9)

Ventral longitudinal muscles AVIII–IX: **8vpmm**, ventral paramedial muscles. **O:** broadly on the ventrolateral surface of ASVIII, **I:** broadly on the ectal surfaces of the diverging anterolateral processes of ASIX. **8volm**, ventral ortholateral muscles. **O:** broadly on the mesodorsal surfaces of the diverging anterolateral apodemes of ASVIII, **I:** broadly on the ectal dorsal margin of ASIX posterad the base of the posterolateral lobate apodemes of ASIX.

Dorsoventral muscles AIX: 9dvim, dorsoventral intrinsic muscles. **O:** narrowly on anterior margins of abdominal hemitergites IX, **I:** narrowly on dorsal margins of diverging anterolateral processes of ASIX.

Sterno-coxal muscles: **9vcm1** (*a*), anteromedial sterno-coxal muscles. **O:** narrowly on anterior apex of spiculum, **I:** narrowly on anteroventral rim of cupula. **9vcm2** (*b*), posteromedial sterno-coxal muscles. **O:** broadly on the posteromesal surface of abdominal sternite IX, **I:** broadly on the ventral surface of the cupula, posterad the I: 9vcm1. **9vcm3** (*c*), lateral sterno-coxal muscles. **O:** broadly on anterior margins of diverging anterolateral processes of abdominal sternite IX, **I:** broadly on anteroventral rim of cupula, immediately laterad I: 9vcm1.

Tergo-coxal muscles: **9dcm1** (*g*), dorsal tergo-coxal muscles. Unpaired; **O:** broadly on dorsomedian mesal surface of the cupula. **I:** broadly on proximodorsal margins of the gonocoxites dorsad I: 9dcm2. **9dcm2** (*f*), dorsolateral tergo-coxal muscles. **O:** broadly on anteromesal surface of the cupula dorsad the O: 9dcm3. **I:** broadly on proximo-ectal margins of the gonocoxites dorsad I: 9dcm3. **9dcm3** (*e*), ventrolateral sterno-coxal muscles. **O:** broadly on anteromesal surface of the cupula. **I:** broadly on proximal ventro-ectal margins of the gonocoxites.

Coxo-lateropenital muscles: 9clm3 (*p*), medial extrinsic coxo-lateropenital muscles. **O:** broadly on mesal dorsal surfaces of the gonopodites. **I:** narrowly on ectal surface of volsellae, distal to base of proximal volsellar apices: **9clm4** (*o*), lateral extrinsic coxo-lateropenital muscles. **O:** broadly on ventral dorsal surfaces of the gonopodites. **I:** narrowly on ectal surfaces of the proximal volsellar apices.

Dorsal coxo-penial promotors: 9cppd (*j*). **O:** broadly on the dorsomesal surfaces of the gonopodites, **I:** narrowly on anterior surfaces of the apices of the valvurae.

Dorsal coxo-penial remotors: **9cprd1** (*k*), mesal dorsal coxo-penial remotor. **O:** narrowly on median proximodorsal margin of the gonopodites. **I:** broadly on median ventromesal surfaces of the penial sclerites, distad the bases of the valvurae. **9cprd2** (*l*), ectal dorsal coxo-penial remotor. **O:** broadly on the dorsomesal surfaces of the gonopodites distad O: 9cppd. **I:** narrowly on ventro-ectal surfaces of the lateral posterior penial processes.

Ventral coxo-penial promotors: 9cppv1 (*h*), anterior ventral coxo-penial promotors. **O:** broadly on mesal ventromedian surface of the cupula. **I:** extensively on the proximal and lateral surfaces of the apices of the valvurae.

Ventral coxo-penial remotors: 9cprv2 (*i*), lateral ventral coxo-penial remotor. **O:** extensively on mesal surfaces of the gonocoxites. **I:** broadly along margin of the lateral posterior penial processes, proximad and ventrad I: 9cprd2.

3.2.3 Protanilla

3.2.3.1 Protanilla zhg-vn01 (Fig. 3.10)

Dorsoventral muscles AIX: **9dvim**, dorsoventral intrinsic muscles. **O**: narrowly on anterior margin of abdominal hemitergites IX. **I**: narrowly on anterolateral corners of basal disc of ASIX.

Sterno-coxal muscles: **9vcm1** (*a*), anteromedial sterno-coxal muscles. **O**: on anterior half of spiculum. **I**: posterolaterally on cupula. **9vcm2** (*b*), posteromedial sterno-coxal muscles. **O**: on posterior margin of cupula. **I**: posterolaterally on disc of ASIX.

Tergo-coxal muscles: **9dcm4** (*d*), ventral tergo-coxal muscles. Unpaired; **O**: widely on cupula, **I**: on the ectal anteroventral surfaces of the gonocoxites.

Coxo-lateropenital muscles: **9clm2** (*qr*), lateral intrinsic coxo-lateropenital muscles. **O**: at base of parossiculi. **I**: narrowly basad the base of the lateropenite. **9clm3** (*p*), medial extrinsic coxo-lateropenital muscles. **O**: broadly on posterolateral mesal surfaces of the gonocoxites. **I**: narrowly basad the base of the lateropenites, adjacent to I: 9clm2.

Dorsal coxo-penial promotors: **9cppd** (*j*). **O**: on the mesal anterodorsal surfaces of the gonocoxites. **I**: broadly on anterodorsal surfaces of valvurae.

Dorsal coxo-penial remotors: **9cprd1** (*k*), mesal dorsal coxo-penial remotors. **O**: on gonocoxites, mediad O: 9cppd. **I**: broadly on mesal surfaces of the penial sclerites.

Ventral coxo-penial promotors: **9cppv1** (*h*), anterior ventral coxo-penial promotors. **O**: on mesal proximoventral surfaces of the gonocoxites, proximomediad O:9cprv2. **I**: narrowly on ventral surfaces of the proximal apices of the valvurae.

Ventral coxo-penial remotors: **9cprv2** (*i*), lateral ventral coxo-penial remotors. **O**: on the mesal proximoventral surfaces of the gonocoxites, **I**: broadly on ectal ventral surfaces of the penial sclerites, at and distal to the base of valvurae.

3.2.4. Yavnella

3.2.4.1 Yavnella zhg-bt01 (Fig. 3.11)

Coxo-lateropenital muscles: **9clm3** (*p*), medial extrinsic coxo-lateropenital muscles. **O:** broadly on posterior and medial mesal surfaces of the gonocoxites. **I**: narrowly at proximoventral margins of the volsellae.

Dorsal coxo-penial remotors: 9cprd1 (*k*), mesal dorsal coxo-penial remotors. **O:** narrowly on the proximodorsal mesal margin of the penial sclerites. **I**: narrowly on proximodorsal margins and distodorsal mesal surfaces of the penial sclerites.

3.2.4.2 Yavnella zhg-th03 (Fig. 3.12)

Ventral longitudinal muscles AVIII–AIX: One pair of 8vlm present, identity uncertain (see Section 4.1.2), here identified as **8vomm**, ventral orthomedial muscles. **O**: on apodeme of ASVIII. **I**: along mesal surface of ventral end of ninth tergosternal complex (ATIX+ASIX).

Coxo-lateropenital muscles: **9clm3** (*p*), medial extrinsic coxo-lateropenital muscles: **O**: broadly on posterior and medial mesal surfaces of the gonocoxites, along with proximoventral surfaces of the penial sclerites. **I**: narrowly within the volsellae.

Dorsal coxo-penial remotors: **9cprd1** (*k*), mesal dorsal coxo-penial remotors: **O**: on proximodorsal mesal surfaces of the penial sclerites, apical to ventral posterior penial processes. **I**: broadly on distodorsal mesal surfaces of the penial sclerites.

3.2.5. Scyphodon s. l.

3.2.5.1 Noonilla zhg-my03 (Fig. 3.13)

Dorsoventral muscles AIX: **9dvim**, dorsoventral intrinsic muscles. **O**: narrowly on ATIX. **I**: broadly on most anterior ventral surface of the sterno-gonocoxital complex (ASIX+gcx+psc), anterior to antecosta of ASIX.

Coxo-stylar muscles: **9csm2** (*t*), intermediate coxo-stylar muscles. **O**: broadly on mesal gonocoxital surface, both dorsally and ventrally. **I**: along median edge of gonostyli.

Ventral coxo-penial remotors: 9cprv2 (*i*), lateral ventral coxo-penial remotors. **O**: broadly on mesal proximal surfaces of the gonocoxites, origin forming dorsoventral parabola proximad O: 9csm2. **I**: narrowly on anatomical venter of posterior penial processes.

3.2.5.2 Noonilla cf. *copiosa* (Fig. 3.14)

Ventral longitudinal muscles AVIII–AIX: One pair of 8vlm present and extremely reduced, identity uncertain (see Section 4.1.2), here identified as **8volm**, ventral ortholateral muscles. **O**: on medial apodemes of ASVIII. **I**: on apodeme of ASIX near most proximolateral extent of anterolateral processes.

Dorsoventral muscles AIX: **9dvim**, dorsoventral intrinsic muscles. **O**: narrowly on abdominal hemitergites IX. **I**: narrowly on anteromedian region of antecosta ASIX.

Coxo-stylar muscles: 9csm2 (*t*), intermediate coxo-stylar muscles. **O**: broadly on mesal dorsal surface of sterno-gonocoxital complex, along entire length of sterno-gonocoxital complex. **I**: along median edge of gonostyli.

Dorsal coxo-penial remotors: 9cprd1 (*k*), mesal dorsal coxo-penial remotors. **O**: broadly on mesal dorsal surface of the sterno-gonocoxital complex, proximomediad O: 9csm2. **I**: narrowly along mesal ventral surfaces of the penial sclerites, at base of ventromedian "trigger."

Ventral coxo-penial remotors: 9cprv2 (*i*), lateral ventral coxo-penial remotors. **O**: broadly along distal third of the mesal ventral surfaces of the gonocoxites. **I**: on the penial sclerites. medial to bases of gonostyli.

3.2.6. Bornean morphospecies-group

3.2.6.1 Leptanilla zhg-my02 (Fig. 3.15)

Ventral longitudinal muscles AVIII–AIX: **8volm**, ventral ortholateral muscles. **O**: on ASVIII and **I:** on ASIX dorsal to bases of mulceators.

Dorsoventral muscles AIX: **9dvim**, dorsoventral intrinsic muscles. **O**: on abdominal hemitergites IX. **I**: mediad I: 8volm. **9dvxm**, dorsoventral extrinsic reversed muscles: **O**: on abdominal hemitergites IX. **I**: on dorsal surfaces of ASVIII.

Coxo-lateropenital muscles: **9clm3** (*p*), medial extrinsic coxo-lateropenital muscles. **O**: broadly on dorsomesal surfaces of the gonocoxites. **I**: broadly on apical margin of proximal volsellar aperture.

3.2.6.2 Leptanilla zhg-my04 (Fig. 3.16)

Dorsoventral muscles AIX: **9dvim**, dorsoventral intrinsic muscles. **O**: along entire lateromedial lengths of abdominal hemitergites IX. **I**: narrowly posterior to antecosta of ASIX, medial to bases of mulceators.

Coxo-lateropenital muscles: **9clm3** (*p*), medial extrinsic coxo-lateropenital muscles. **O**: broadly on mesal ventral surfaces of the gonocoxites. **I**: narrowly on proximomedian processes of the volsellae.

Ventral coxo-penial remotors: **9cprv2** (*i*), lateral ventral coxo-penial remotors. **O**: broadly on distomedian mesal surfaces of the gonocoxites. **I**: narrowly on the ventrolateral margins of the penial sclerites, proximad the proximomedial volsellar condyles.

3.2.7. Leptanilla s. str.

3.2.7.1 Leptanilla zhg-id04 (Fig. 3.17)

Ventral longitudinal muscles AVIII–IX and **dorsoventral intrinsic muscles AIX** not discernible.

Coxo-stylar muscles: **9csm1**, intrinsic coxo-stylar muscles. **O**: broadly on mesolateral surfaces of the gonocoxites. **I**: broadly on mesomedial surfaces of the gonocoxites. **9csm2** (*t*), intermediate coxo-stylar muscles. **O**: on the distal mesolateral surfaces of the gonocoxites. **I**: narrowly at proximoventral margins of gonostyli.

Ventral coxo-penial remotors: **9cprv2** (*i*), lateral ventral coxo-penial remotors. **O**: narrowly on mesal proximomedian apodemes of the gonocoxites. **I**: broadly on mesal proximal surfaces of the penial sclerites.

3.2.7.2 Leptanilla cf. *zaballosi* (Fig. 3.18)

Ventral longitudinal muscles AVIII–IX: One pair of 8vlm present, identity indeterminate between 8vomm, 8vpmm, 8volm, but likely not 8vpmm.

Dorsoventral intrinsic muscles AIX not discernible.

Coxo-stylar muscles: **9csm1**, intrinsic coxo-stylar muscles. **O**: broadly on mesolateral surfaces of the gonocoxites. **I**: broadly on mesomedial surfaces of the gonocoxites. **9csm2** (*t*), intermediate coxo-stylar muscles. **O**: on the distal mesolateral surfaces of the gonocoxite. **I**: narrowly at proximomedial margins of gonostyli.

Coxo-lateropenital muscles: **9clm3** (*p*), medial extrinsic coxo-lateropenital muscles. **O**; broadly on ventral proximomesal surfaces of the gonocoxites and on proximoventral surfaces of the penial sclerites. **I**: narrowly on medial surfaces of proximomedial condyles of the volsellae.

Ventral coxo-penial remotors: **9cprv2** (*i*), lateral ventral coxo-penial remotors. **O**; narrowly on ventromedian apodemes of the gonocoxites. **I**: broadly on mesal proximoventral surfaces of the penial sclerites.

4. Discussion

4.1. Ambiguities

The extremely small size of many of the structures described herein, and the inability to confirm some observations based on micro-CT using manual dissection or SEM, means that the interpretation of these primary observations is sometimes uncertain. Moreover, extreme derivation of male genital skeletomusculature in certain lineages of the Leptanillinae means that assertion of primary homology (de Pinna 1991) can be debatable. While Section 3 described the male genital skeletomusculature of 11 exemplar ants according to what appeared to be the most

likely interpretation of these ambiguous aspects, with the awareness that these conclusions are provisional, the following is a list of observations that must be regarded as particularly unclear.

4.1.1. Skeletal ambiguity

The transverse posterior mesal carina of abdominal sternite IX in *Scyphodon s. l.* may not correspond to the antecosta of abdominal sternite IX, rather being an invagination of abdominal sternite IX derived in *Scyphodon s. l.* independently from the antecosta of abdominal sternite IX that is plesiomorphic for the Formicidae, which appears to have been ancestrally lost in male Leptanillinae. This reasoning assumes that the antecosta of abdominal sternite IX is sufficiently complex to not be regained once lost (Simpson 1953). Nonetheless, the transverse posterior mesal carina of abdominal sternite IX in *Scyphodon s. l.* appears to be positionally and functionally equivalent to the antecosta of abdominal sternite IX.

Petersen (1968) interpreted the paired, articulated distal appendages in *Noonilla copiosa* Petersen as volsellae, an interpretation that we contest based upon micro-CT scans from across a broad sampling of *Scyphodon s. l.* The ambiguity arises from the fact that gonostyli and volsellae do not co-occur in any *Scyphodon s. l.* scanned in this study or observed by Petersen. The origins of the coxo-lateropenital and coxo-stylar muscles also have very little utility in identifying these appendages, as a single muscle attaches the gonocoxite to the mesal surface of the appendage, running laterad to the coxo-penial remotors, which, absent other landmarks, could reasonably be either 9clm3 (*p*) or 9csm2 (*t*). The mesal insertion on the appendage is also of little use as both 9clm3 (p) and 9csm2 (t) can insert ectally or mesally on the volsella or gonostylus respectively. One suggestive analogy to other leptanillines is that the muscle originates extensively on the mesal surfaces of the gonocoxite, including the ventral, lateral, and dorsal surfaces, a condition observed for 9csm2 (*t*) in *Leptanilla s. str.* but never for 9clm3 (*p*). Nevertheless, we observe that

these appendages articulate at the distolateral margins of the gonocoxites, a positioning contrary to that observed for the volsellae, which in this study and available literature always articulate medially with the gonocoxites and proximad the distal gonocoxital margins.

Relative contrast between sclerite and conjunctiva in micro-CT data is sometimes insufficient to discriminate these forms of the integument from each other. This results in the following points of interpretive ambiguity:

1. The tergosternal fusion of abdominal segment VIII in *Noonilla* cf. *copiosa* (Fig. 3.14C–D) can only be assessed with certainty by manual dissection or histology, and since Petersen (1968) did not mention the tergosternal condition of this segment in the description of *N. copiosa*, it is possible that the tergosternal fusion here inferred from micro-CT scans of *Noonilla* cf. *copiosa* is erroneous. Alternatively, this fusion may simply be more pronounced than in the type series of *N. copiosa*.

2. Abdominal sternites VIII–IX may be (sternosternally) fused in *Leptanilla* zhg-my02 and -5. The extreme median anteroposterior compression of abdominal sternites VIII-IX, and their adjacency (Fig. 3.15D), makes it difficult to be certain that the intervening cuticle is conjunctival in form.

3. It is uncertain if the endophallic sclerite is indeed absent in *Odontomachus* indet., as opposed to present but weakly developed. The endophallic sclerite is widely reported in the Formicidae (Marcus 1953; Forbes 1954; Hagopian 1963; Trakimas 1967; Shyamalanath and Forbes 1983; Ball and Vinson 1984) and appears evolutionarily labile, but has not been included in any comprehensive anatomical or morphological survey of male ant genitalia. To our knowledge, the condition of the endophallic sclerite has never been examined in the Ponerinae or even the

"poneroids" *sensu* Moreau & Bell (2013). Therefore, the condition in *Odontomachus* cannot be predicted based upon other, more readily observable characters, nor extrapolated from observations of related poneroids. It is possible that this sclerite is present in *Odontomachus* but poorly developed, such that contrast of the micro-CT scans was insufficient to differentiate it from the adjacent membranous endophallus.

4.1.2. Muscular ambiguity

The homology of the penial muscles present in *Scyphodon s. l.* is open to debate since the reduction of the penial sclerites in this clade removes topological points of reference necessary for the assertion of primary homology. For similar reasons, the precise identity of the ventral longitudinal muscles VIII–IX observed in *Yavnella* zhg-th03 is debatable, although their origin on the antecosta of ASVIII excludes identification as ventral paramedial muscles (Fig. 3.12D). The sole muscles belonging to this topographic main-group in *Yavnella* zhg-th03 are here regarded as the ventral longitudinal orthomedial muscles VIII–IX (8volm).

4.2. Overview and phylogenetic context

A pronounced tendency towards skeletomuscular simplification is apparent in the Leptanillinae relative to the remainder of the Formicidae. This trend is most striking in the Leptanillini *s. str.* (Figs 19–23; Table 3.S4) but is also applicable to *Protanilla* zhg-vn01, in which the coxo-stylar adductors are absent—muscles that are retained in certain lineages of the Leptanillini *s. str.* (Table 3.S4).

Several of these skeletal or muscular simplifications are homoplasious. The intermediate coxo-stylar muscles (9csm2, *t*) are lost in *Protanilla* zhg-vn01, the Bornean morphospecies-group and *Yavnella*; concomitantly, the gonopodite is fully to partly inarticulate in all these lineages, while

in the remaining sampled lineages the presence of the intermediate coxo-stylar muscles is always associated with articulated gonopodites. It can be inferred that the intermediate coxo-stylar muscles are absent in all *Yavnella* and members of the Bornean morphospecies-group, and may be absent in many, if not all, male *Protanilla*. The extrinsic medial coxo-lateropenital muscles (9clm3, *p*) were lost at least twice within the Leptanillini *s. str.*, while the anterior dorsal coxo-penial remotors (9cprd1, *k*) are retained within the sampled Leptanillini *s. str.* in *Noonilla* cf. *copiosa*, implying independent losses of this muscle pair in *Leptanilla s. str.* and the Bornean morphospecies-group.

In terms of scleritic simplification, there is a tendency towards median fusion of paired structures. In addition to the synapomorphic fusion of the penial sclerites in Leptanillini *s. str.*, the gonocoxites are medially fused along their entire anteroposterior length in the Bornean morphospecies-group and *Scyphodon s. l.*, and partial gonocoxital fusion is observed in *Yavnella*; while the complete medial fusion of the volsellae is an autapomorphy of the Bornean morphospecies-group, observed nowhere else in male Formicidae. The medial fusion of the gonostyli in *Noonilla* zhg-my03 is apparently unique to that morphospecies throughout the entire Hymenoptera, providing a serial parallel to the medial fusion of the volsellae in the Bornean morphospecies-group.

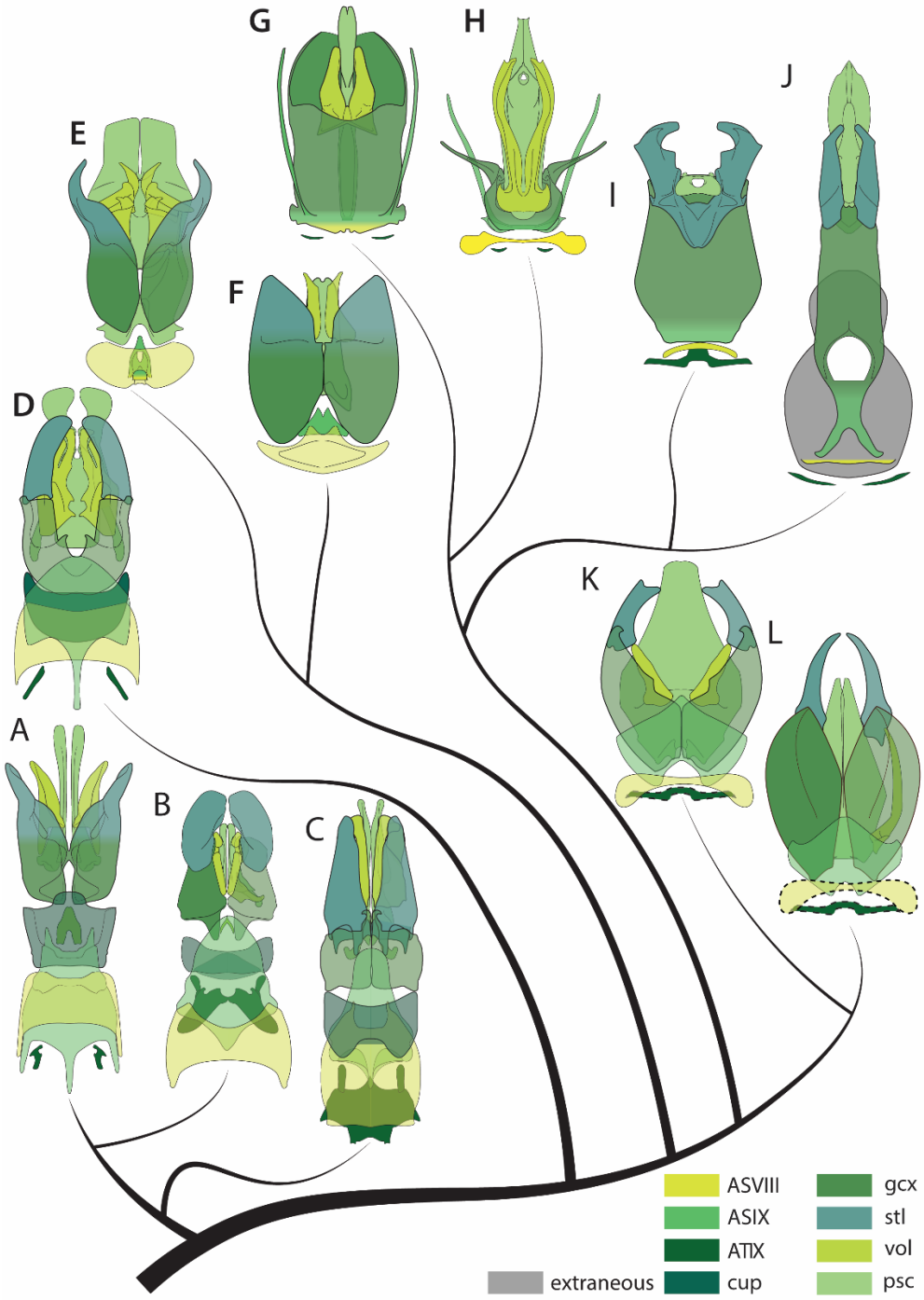

Figure 3.19. Diagrammatic cladogram of genital and pregenital sclerites, ventral view. Sclerites bounded by dashed lines were indiscernible; those bounded with dotted lines were discernible, but not fully segmented. **A** *Lioponera* indet. **B** *Myrmica ruginodis* **C** *Odontomachus* indet. **D** *Protanilla* zhg-vn01 **E** *Yavnella* zhg-th03 **F** *Yavnella* zhg-bt01 **G** *Leptanilla* zhg-my04 **H** *Leptanilla* zhg-my02 **I** *Noonilla* zhg-my03 **J** *Noonilla* cf. *copiosa* **K** *Leptanilla* zhg-id04 **L** *Leptanilla* cf. *zaballosi*. Abbreviations: ASVIII=abdominal sternite VIII; ASIX=abdominal sternite IX; ATIX=abdominal tergite IX; cup=cupula; gcx=gonocoxite; stl=gonostylus; vol=volsella; psc=penial sclerites.

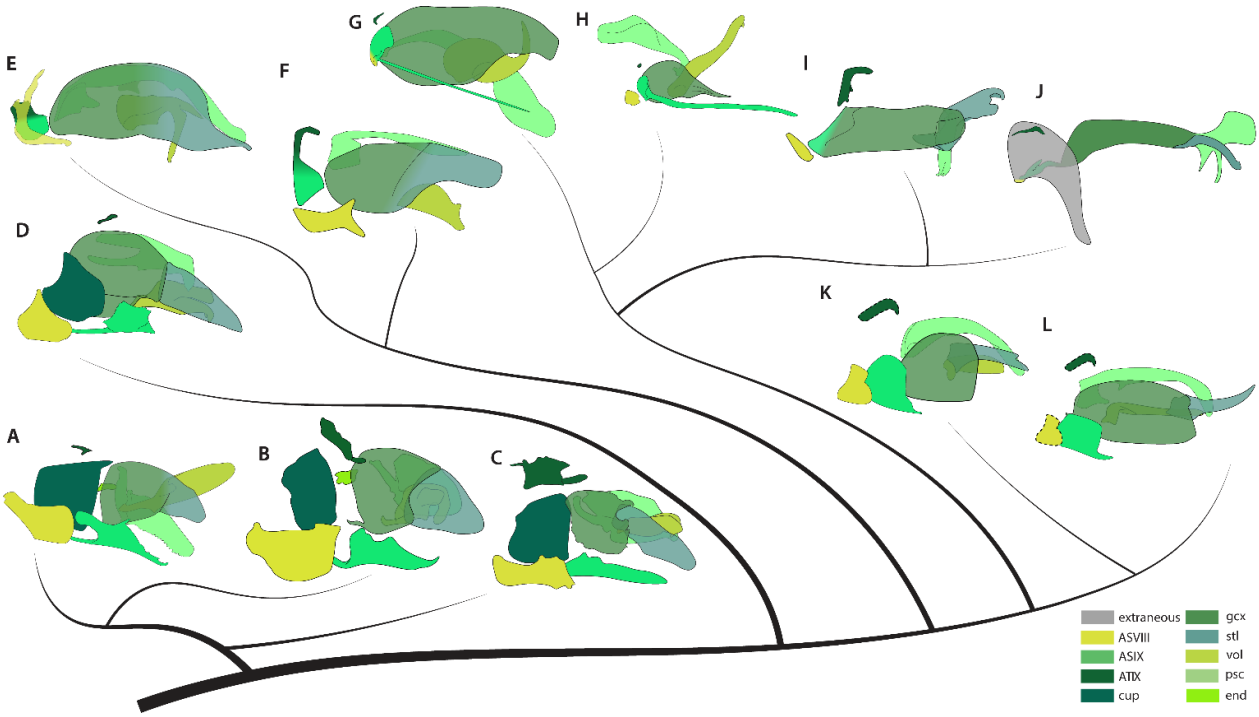

Figure 3.20. Diagrammatic cladogram of genital and pregenital sclerites of exemplars, profile view. Sclerites bounded by dashed lines were indiscernible; those bounded with dotted lines were discernible, but not fully segmented. Abdominal sternite IX of *Noonilla* cf. *copiosa* is rotated 180° relative to *in situ* position. **A** *Lioponera* indet. **B** *Myrmica ruginodis* **C** *Odontomachus* indet. **D** *Protanilla* zhg-vn01 **E** *Yavnella* zhg-th03 **F** *Yavnella* zhg-bt01 **G** *Leptanilla* zhg-my04 **H** *Leptanilla* zhg-my02 **I** *Noonilla* zhg-my03 **J** *Noonilla* cf. *copiosa* **K** *Leptanilla* zhg-id04 **L** *Leptanilla* cf. *zaballosi*. Abbreviations: ASVIII=abdominal sternite VIII; ASIX=abdominal sternite IX; ATIX=abdominal tergite IX; cup=cupula; gcx=gonocoxite; stl=gonostylus; vol=volsella; psc=penial sclerites; end=endophallic sclerite.

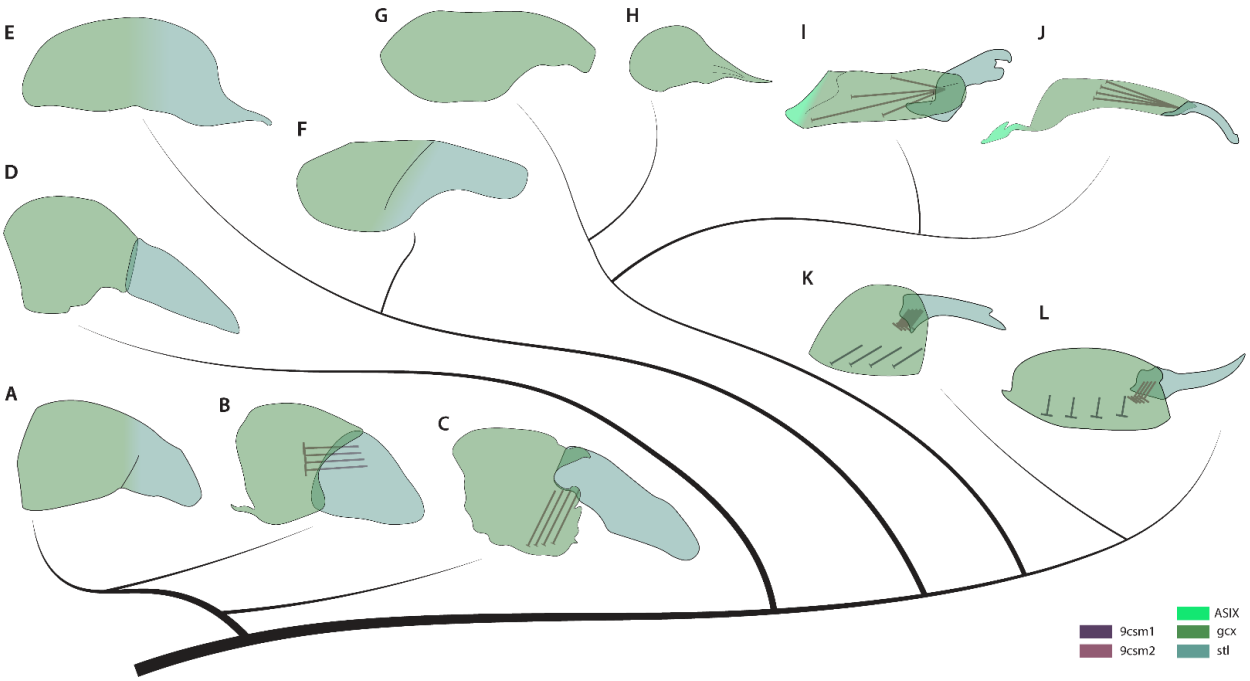

Figure 3.21. Diagrammatic cladogram of coxo-stylar skeletomusculature, profile view. Abdominal sternite IX of *Noonilla* cf. *copiosa* is rotated 180° relative to *in situ* position. Caps in muscle diagrams signify origin; lack of caps, insertion. **A** *Lioponera* indet. **B** *Myrmica ruginodis* **C** *Odontomachus* indet. **D** *Protanilla* zhg-vn01 **E** *Yavnella* zhg-th03 **F** *Yavnella* zhg-bt01 **G** *Leptanilla* zhg-my04 **H** *Leptanilla* zhg-my02 **I** *Noonilla* zhg-my03 **J** *Noonilla* cf. *copiosa* **K** *Leptanilla* zhg-id04 **L** *Leptanilla* cf. *zaballosi*. Abbreviations: ASIX=abdominal sternite IX; gcx=gonocoxite; stl=gonostyli; 9csm1=anterior coxo-stylar muscles; 9csm2=intermediate coxo-stylar muscles.

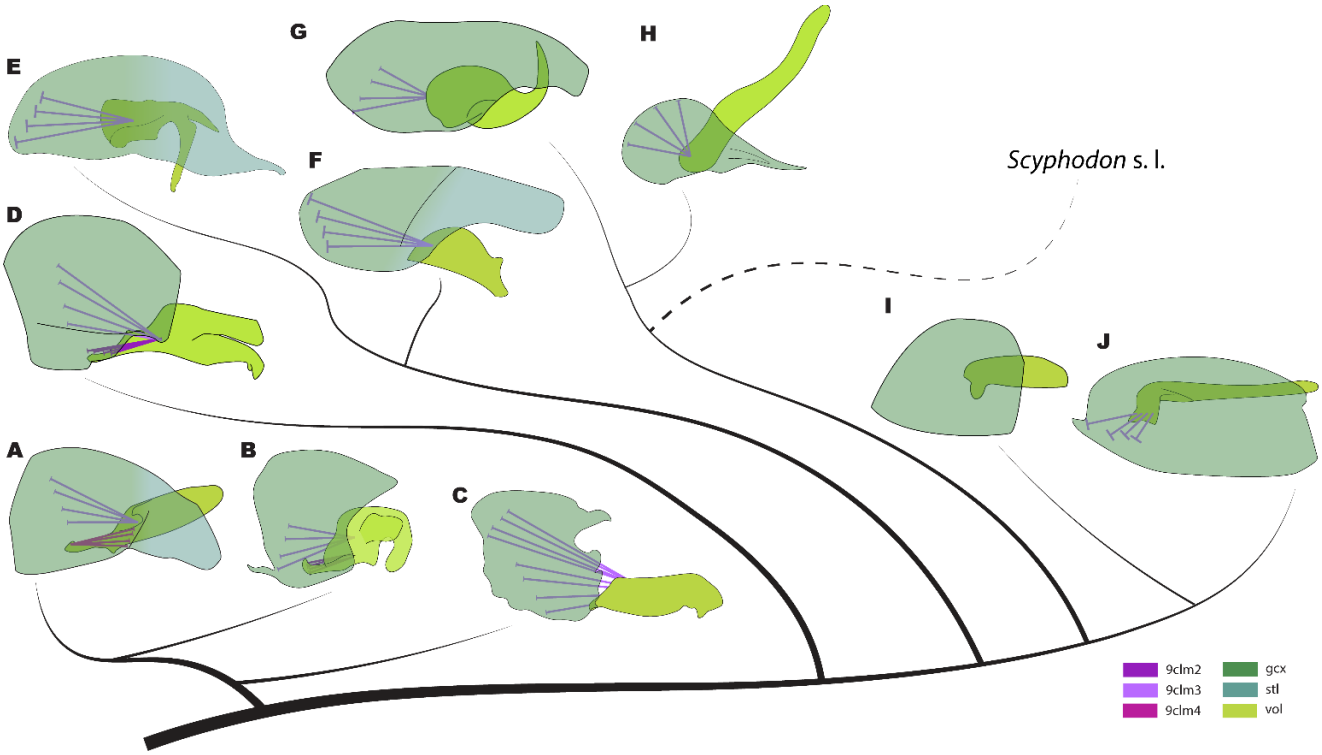

Figure 3.22. Diagrammatic cladogram of coxo-lateropenital skeletomusculature, profile view. The volsellae are absent in *Scyphodon s. l.*, so the exemplars belonging to this clade are not shown here. Caps in muscle diagrams signify origin; lack of caps, insertion. **A** *Lioponera* indet. **B** *Myrmica ruginodis* **C** *Odontomachus* indet. **D** *Protanilla* zhg-vn01 **E** *Yavnella* zhg-th03 **F** *Yavnella* zhg-bt01 **G** *Leptanilla* zhg-my04 **H** *Leptanilla* zhg-my02 **I** *Leptanilla* zhg-id04 **J** *Leptanilla* cf. *zaballosi*. Abbreviations: gcx=gonocoxite; stl=gonostylus; vol=volsella; 9clm2=lateral intrinsic coxo-lateropenital muscles; 9clm3=medial extrinsic coxo-lateropenital muscles; 9clm4=lateral extrinsic coxo-lateropenital muscles.

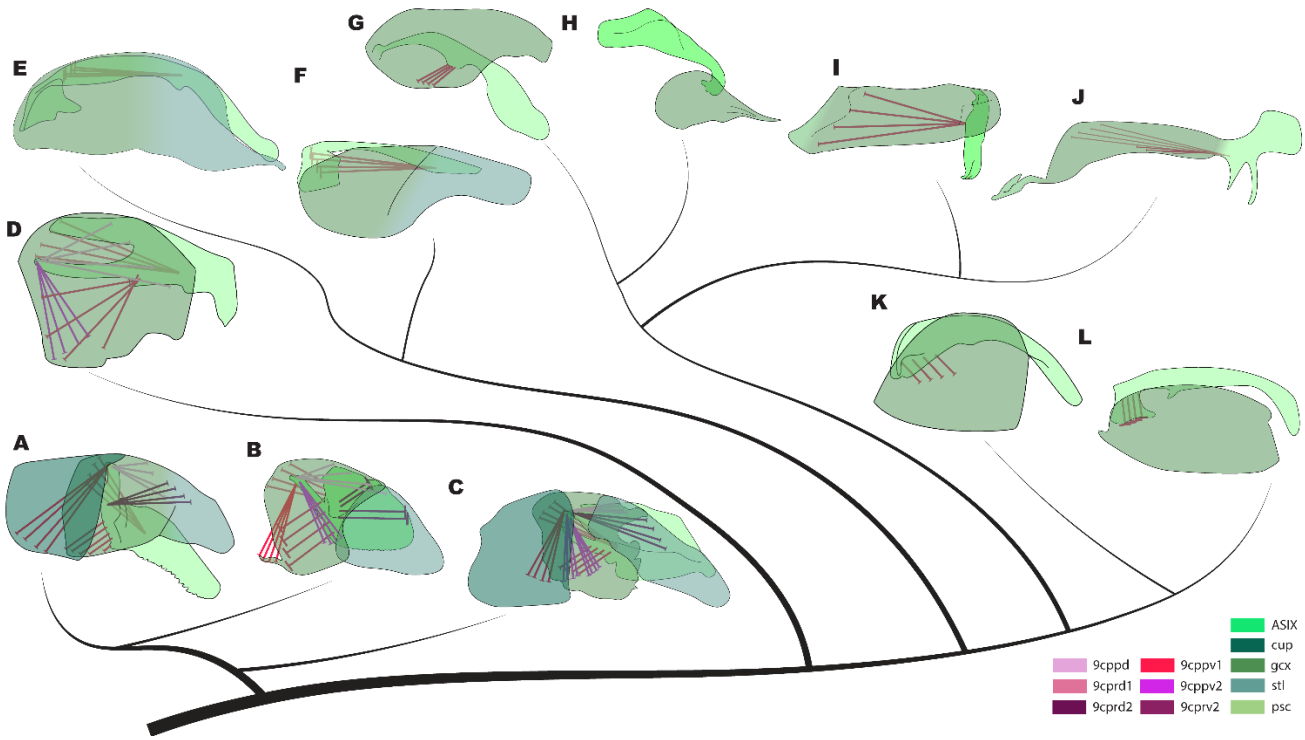

Figure 3.23. Diagrammatic cladogram of coxo-penial skeletomusculature, profile view. Abdominal sternite IX of *Noonilla* cf. *copiosa* is rotated 180° relative to *in situ* position. Caps in muscle diagrams signify origin; lack of caps, insertion. **A** *Lioponera* indet. **B** *Myrmica ruginodis* **C** *Odontomachus* indet. **D** *Protanilla* zhg-vn01 **E** *Yavnella* zhg-th03 **F** *Yavnella* zhg-bt01 **G** *Leptanilla* zhg-my04 **H** *Leptanilla* zhg-my02 **I** *Noonilla* zhg-my03 **J** *Noonilla* cf. *copiosa* **K** *Leptanilla* zhg-id04 **L** *Leptanilla* cf. *zaballosi*. Abbreviations: ASIX=abdominal sternite IX; cup=cupula; gcx=gonocoxite; stl=gonostylus; psc=penial sclerites; 9cppd=dorsal coxo-penial promotors; 9cprd1=mesal dorsal coxo-penial remotors; 9cprd2=ectal dorsal coxo-penial remotors; 9cppv1=anterior ventral coxo-penial promotors; 9cppv2=posterior ventral coxo-penial promotors; 9cprv2=lateral ventral coxo-penial remotors

The apparent tergosternal fusion of abdominal segment VIII in *Noonilla* cf. *copiosa* (see Section 4.4.1), and the tergosternal fusion of abdominal segment IX in both sampled *Yavnella* (see Section 4.4.2), are conditions unique among described male Formicidae and possibly throughout the Hymenoptera as a whole, with one exception: Petersen (1968: p. 580) reported tergosternal fusion of abdominal segment IX in *L. astylina*. Examination of the holotype could not confirm, but there is no reason to doubt this observation. This condition is homoplasious with *Yavnella*, although the phylogenetic position of *L. astylina* within the Leptanillini *s. str.* is enigmatic.

Anteroposterior fusion of sclerites is also a notable tendency. Abdominal sternite IX is at least partly fused to the gonocoxites in all sampled representatives of *Scyphodon s. l.* and the Bornean morphospecies-group, with this fusion being homoplasious between the two clades (see Section 4.4.2). Complete posterior fusion of abdominal sternite VIII to abdominal sternite IX has evolved at least three separate times in the Leptanillini *s. str.* (see Section 4.4.1). Another case of homoplasy is the partial fusion of the penial sclerites to the gonocoxites in *O. hungvuong* (Yamada et al. 2020), *Protanilla* zhg-vn01 (Fig. 3.10), and both sampled *Yavnella* (Figs 11–12), with complete fusion of the gonocoxites and penial sclerites being observed in *Leptanilla* zhg-my03, -4 and all sampled *Scyphodon s. l*. (see Section 4.4.4) (Figs 13–16).

Although these homoplasies appear straightforward at a coarse comparative scale, further examination may show noteworthy functional differences. An example is the parallel fusion of the penial sclerites to the gonocoxites in *Scyphodon s. l.* and the clade comprising *Leptanilla* zhg-my03 and -4. In both cases, the penial sclerites are musculated by a single muscle pair. In *Leptanilla* zhg-my03 and -my04, the penial sclerites are narrowly but firmly fused to the medially fused gonocoxites at the most proximal penial extremity (Fig. 3.15D, F), surrounding the gonocoxital foramen; contraction of the lateral ventral coxo-penial remotors (9cprv2, *i*) affords limited motion of the penial sclerites relative to the rigid gonocoxital capsule. Conversely, the anterior and venter of the penial sclerites in *Scyphodon s. l.* are broadly fused to the medially fused gonocoxites, forming an inarticulate gonocoxital complex (Figs 13D, F; 14D, F); in these cases, the anterior dorsal coxo-penial remotors (9cprd1, *k*) or lateral ventral coxo-penial remotors (9cprv2, *i*) move the entire gonocoxital complex relative to the gonostyli.

Based upon the micro-CT data for the 20 exemplars presented here, and physical examination of additional specimens, along with the published description of male *Opamyrma hungvuong*

(Yamada et al. 2020), the loss of the spiculum, cupula, and valvurae, and complete medial fusion of the penial sclerites, are synapomorphies of the Leptanillini *s. str.* The absence of the lateropenites was suggested to be a synapomorphy of the Leptanillinae excluding the former Anomalomyrmini by Boudinot (2015, p. 33), by which was meant the clade here referred to as the Leptanillini *s. str.* (*Opamyrma* was at the time still classified in the Amblyoponinae; Yamane, Bui, & Eguchi, 2008); if the distal volsella of the Leptanillini *s. str.* is indeed homologous with the apex of the parossiculus, this hypothesis is correct, although tests are not possible with present sampling. Loss of the anterior ventral and dorsal coxo-penial promotors (9cppv1, *h*; 9cppd, *j*) is also synapomorphic for the Leptanillini *s. str.*, while the loss of the medial coxo-lateropenital muscles is a synapomorphy of *Leptanilla s. l.* The loss of the spiculum is also observed in some *Leptomyrmex* spp. (Dolichoderinae: Leptomyrmecini) (Barden et al., 2017) and is widespread among symphytan hymenopterans (Schulmeister 2003: fig.14). As noted by Boudinot et al. (2022), the non-annularity of the cupula in the Leptanillinae, whether due to reduction to an anteroventral strip (as in *Opamyrma* and *Protanilla*; Fig. 3.24D) or complete loss (as in the Leptanillini *s. str.*), is an autapomorphy of the clade within the Formicidae. In most ants, the cupula forms a "basal ring" (Crampton, 1919) proximad the remainder of the genital capsule (Fig. 3.24A–C). Outside the ants, the loss of the cupular dorsum is paralleled by *Gasteruption* and *Pseudofoenus* indet. (Evanioidea: Gasteruptiidae) (Mikó et al. 2013), while the loss or fusion of the cupula to the gonopodites is observed in *Mymaromma anomalum* (Blood & Kryger) (Mymarommatidae) and universally among the Chalcidoidea (Gibson 1986). Beyond the Apocrita, the cupula is insensibly fused to the gonocoxites or entirely lost in the Argidae and Pergidae (Schulmeister 2003).

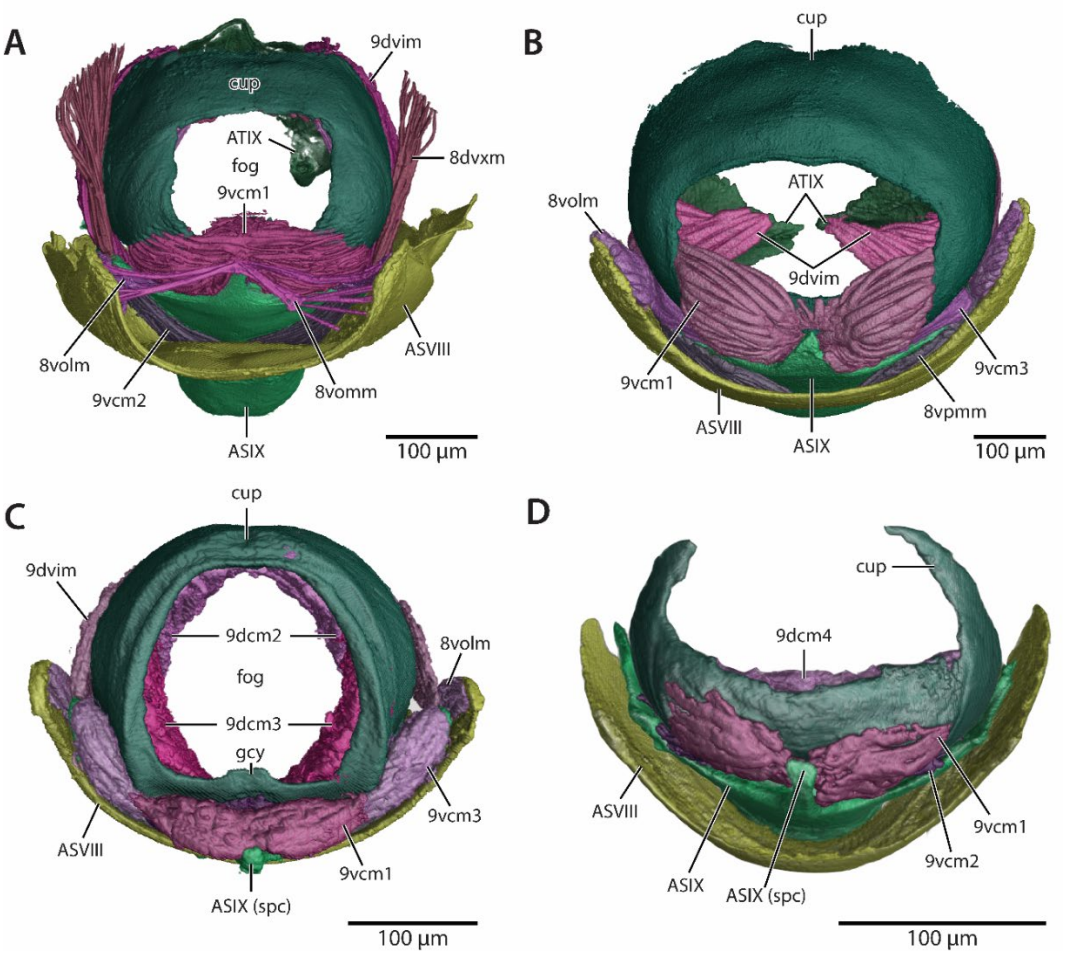

Figure 3.24. Morphology of the cupula, 3D reconstructions in anterior view. **A** *Odontomachus* indet. **B** *Myrmica ruginodis* **C** *Lioponera* indet. **D** *Protanilla* zhg-vn01. Abbreviations: ASVIII=abdominal sternite VIII; ASIX=abdominal sternite IX; spc=spiculum; ATIX=abdominal tergite IX; cup=cupula; gcy=gonocondyle; fog=foramen genitale; gcx=gonocoxite; stl=gonostylus; 8volm=ventral ortholateral muscles VIII-IX; 8vpmm=ventral paramedial muscles VIII-IX; 9dvim=dorsoventral intrinsic muscles IX; 9vcm1=anteromedial sterno-coxal muscles; 9vcm2=posteromedial sterno-coxal muscles; 9vcm3=lateral sterno-coxal muscles; 9dcm2=dorsolateral tergo-coxal muscles; 9dcm3=ventrolateral tergo-coxal muscles; 9dcm4=ventral tergo-coxal muscles

The total absence of the cupula in the Leptanillini *s. str.* is associated with the absence of tergo-coxal and sterno-coxal muscles IX, along with the spiculum. In most Leptanillini *s. str.*, therefore, the genitalia are not musculated from abdominal segment IX. Although the cupula is extremely reduced in other ant lineages, e.g. the Old World army ants (Dorylinae: *Aenictogiton*, *Aenictus*, and *Dorylus*) the absence of extrinsic male genital musculation from the metasoma is unique to the Leptanillini *s. str.* among the Formicidae. Musculation has been functionally

regained secondarily in *Scyphodon s. l.* and the Bornean morphospecies-group by fusion of abdominal sternite IX to the gonocoxites, with the movement of the genitalia thus being mediated by ventral longitudinal muscles VIII–IX, intrinsic dorsoventral muscles IX, both, or in the case of *Leptanilla* zhg-my02 and -5, the autapomorphic extrinsic dorsoventral muscles IX–VIII in addition (Fig. 3.15B, D, F).

Although the phylogeny of the Leptanillini *s. str.* is well-resolved, with subclades readily diagnosed by multiple non-genitalic male morphological characters (Griebenow 2020, 2021), this internal phylogeny is not reflected by male genital skeletomusculature with plain fidelity. For example, we may speculate that the posterior fusion of abdominal sternite IX to the gonocoxites in *Scyphodon s. l.* and the Bornean morphospecies-group is homoplasious due to differences in Remanean "special qualities," despite these being sister clades, with this hypothesis being untestable with available taxon sampling. In addition, we can propose no definitive male genital synapomorphies of *Leptanilla s. l.* or for the "Indomalayan clade" within *Leptanilla s. l.* Members of the latter clade that do not belong to *Scyphodon s. l.* or the Bornean morphospecies-group, i.e., the Indochinese morphospecies-group, have medially separated gonocoxites, based upon external examination, unlike *Scyphodon s. l.* and the Bornean morphospecies-group.

4.3. Male genital musculature in the Leptanillinae compared to other Hymenoptera

4.3.1.1. Framework of muscle evolution

Our understanding of muscle evolution is generally based in a modification of the *a priori* assumptions of Boudinot (2018: 565): (1) evolutionary sequences of muscle movement occur in steps of local movement, without spontaneous "leaps" from sclerite to sclerite; (2) shifts of

attachment across conjunctiva, and transverse translation across other muscles, are rare; (3) topographic reorganization is usually due to local plasticity within a sclerite or to "vicariant" drift of attachments concomitant with scleritic modification; and (4) new muscles are derived from fission (gain) or fusion (loss) of existing muscles rather than *de novo* innovation. Relative probability of transformation series is guided by the principle of parsimony.

4.3.1.2. Muscle subdivisions and nomenclature

While insect muscles are frequently arranged in discrete groups, they lack an epimysial sheath like that of vertebrates, such that recognition of specific bundles of fibers as separate sets is somewhat subjective. Here, we consider both the degree of separation at both origin and insertion, and implied transformations, as evidence to discern subsets of the homological-topographic main groups, but acknowledge that there is no solid, global criterion for recognizing individual subgroups. In terms of subdivisions within a main group, we consider that distinct lack of overlap of attachments of bundles within a main group indicates a mechanical reorganization, implying a semi-independent ontogenetic and therefore evolutionary program, which should be addressed through nomenclature. Part of our aim in designing the numeration is that future authors may further expand our schema by addition of numbers, if necessary, based on additional splits in particular taxa. Nevertheless, we performed an exhaustive review of the literature (Kluge 1895; Beck 1933; Peck 1937; Snodgrass 1941, 1942; Alam 1952; Kempf 1956; Smith 1969, 1970, 1972; Youssef 1969; Chiappini and Mazzoni 2000; Schulmeister 2001, 2003; Boudinot 2013; Mikó et al. 2013) to identify stable designations for all major muscles observed in male Hymenoptera.

In two cases, we observe partial differentiation of 9cprd2 (*l*) into anterior and posterior partitions, which we do not designate separately. These partitions in *Odontomachus* indet. are somewhat differentiable visually but overlap extensively in both origin and insertion (Fig. 3.4H); in *M. ruginodis¸* the origins of the partitions are widely separated, with the anterior partition originating in the gonocoxite and the posterior part in the gonostylus; however, the partitions coalesce into unified insertions (Fig. 3.6H). Potential subdivisions of 10plm2 (*n*) and 9clm4 (*o*) discussed by Schulmeister (2001, 2003) are not designated individually due to uncertainty on the part of Schulmeister (2001, 2003), and because we did not primarily observe 10plm2, while our observations of 9clm4 are limited. We do note that if parts of 10plm2, 9clm4, and 9prd2 are formally recognized in the future, such a modification could append names to our schema without altering the existing nomenclature.

4.3.1.3. Potentially apomorphic states of genital musculature in ants

Most muscles named here are clearly homologous across Hymenoptera. Specifically, the sterno-coxal, tergo-coxal, and most coxo-lateropenital and coxo-penial muscles are most certainly homologous. However, a few likely exceptions can be postulated in which topography corresponds among taxa but may represent independent derivations. The most probable exception is the exact correspondences of the coxo-stylar muscles 9csm1 and 9csm2 (*t*). Three main states of these muscles are observed in various hymenopteran lineages: (1) in the plesiomorphic condition, there is a single 9csm2 (which may be bifid distally) which connects the gonocoxite to the gonostylus; (2) in a few taxa, there is a single muscle intrinsic to the gonocoxite; and (3) there may be both an intrinsic (anterior) gonocoxital muscle and extrinsic coxo-stylar muscle. Schulmeister (2003) observed state (2) in Vespidae and termed the single

muscle *w*. On the other hand, following the principle of parsimony, we hypothesize that in state (2) the muscle is truly 9csm2 (*t*), having shifted its insertion proximally. In state (3), we designate the intrinsic muscle 9csm1 as different from the extrinsic 9csm2. The orientation of muscle *w* in *Dolichovespula* spp. and *Odontomachus* indet., as described here (Fig. 3.25B), is dorsoventral; while the intrinsic coxo-stylar muscle (9scm1) here observed only in *Leptanilla s. str.* is transverse in orientation, spanning the medial and lateral surfaces of the gonocoxite (Figs 17E, 18E, 25D–E). Therefore, we do not equate 9csm1 with *w*. We do caution that many possible transformation series could lead to the observed topographies of the coxo-stylar muscles and emphasize that the present hypothesis is based on limited information, given the infrequent presence of an intrinsic coxo-stylar muscle in Hymenoptera.

For two other muscles (9cppv2, 9clm4, *o*), our primary observations were too limited to confidently assert homology at the ordinal scale. The posterior subdivision of the ventral coxo-penial promotors, 9cppv2, occurs in a few ant taxa and in at least *Stenobracon deesae* (Braconidae; Alam, 1952), most probably having derived independently from 9cppv1 (*h*) in Formicidae and Braconidae, and perhaps multiply within ants. It is also probable that the lateral extrinsic coxo-lateropenital muscle 9clm4 (*o*), which we observe in *Lioponera* (Figs 8I, 9) and was previously reported in *Cephalotes pusillus* (Klug) by Kempf (1956), derive independently from a subdivision of 9clm3 (*p*), rather than corresponding to the putatively homoplasious 9clm4 in non-ant taxa.

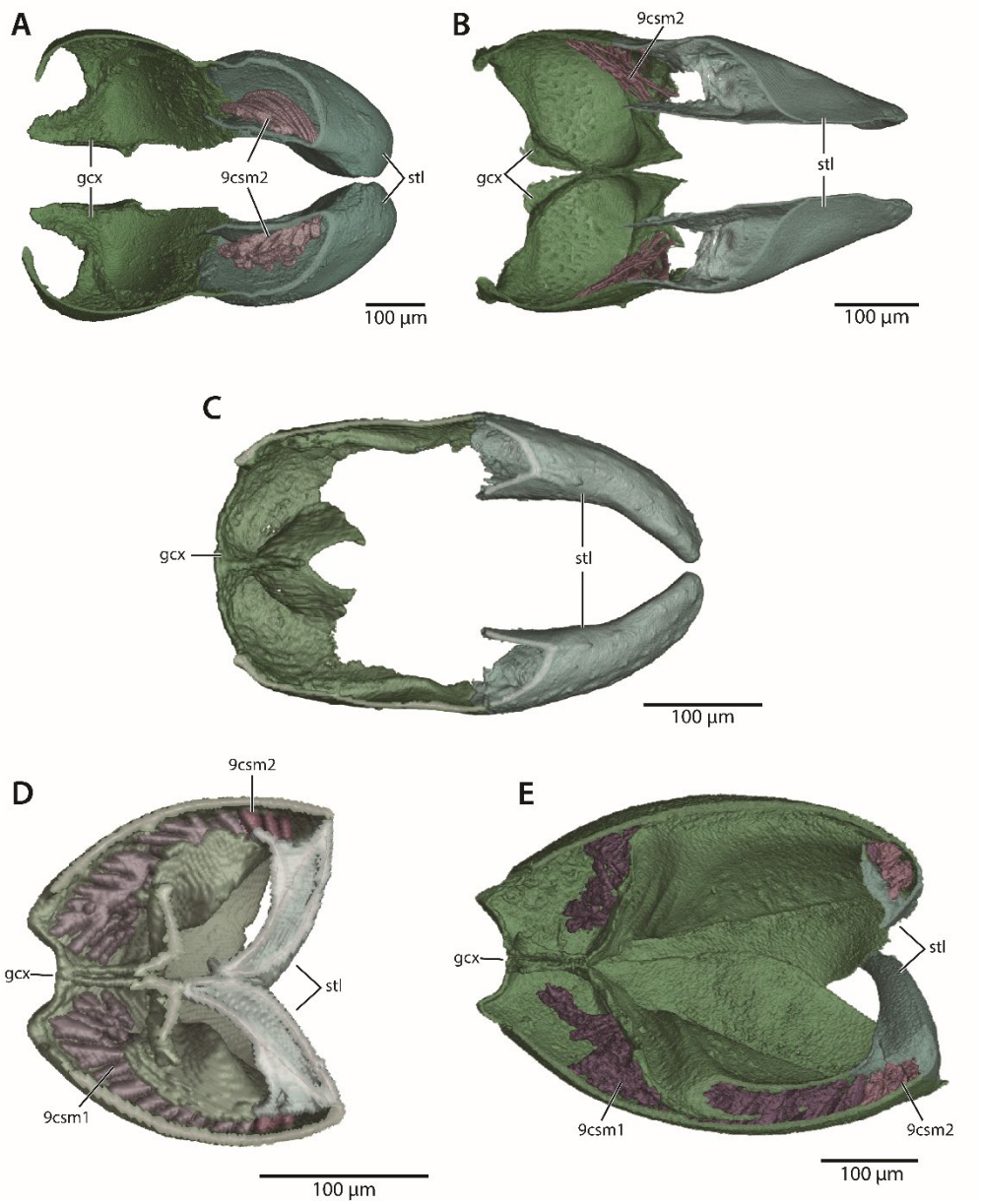

Figure 3.25. Coxo-stylar skeletomusculature, 3D reconstructions in coronal cross-section. **A** *Myrmica ruginodis* **B** *Odontomachus* indet. **C** *Protanilla* zhg-vn01 **D** *Leptanilla* zhg-id04 **E** *Leptanilla* cf. *zaballosi*. Abbreviations: gcx=gonocoxite; stl=gonostylus; 9csm1=anterior coxo-stylar muscles; 9csm2=intermediate coxo-stylar muscles

4.3.2. Muscle evolution and variation in Hymenoptera

Based on the evolutionary sequence inferred by Boudinot (2018), informed by the phylogenetic analysis of Schulmeister (2003) and our recoding of muscle presence and absence across Hymenoptera, some hypotheses may be made regarding the evolution of the male genital

musculature in this clade. The main difference between our interpretation and that of Schulmeister (2003) regards the evolution of muscle 9clm1 (*s*) with respect to muscles 9cprv1 (*si*) and 9clm2 (*qr*). We consider 9cprv1 (*si*) to be a coxo-penial muscle since it originates on the parossiculus (gonocoxal fragment) or on the gonocoxite itself and inserts on the penial sclerite. This is also the suggestion of Boudinot (2018), although we infer 9cprv1 (*si*) is a remotor, rather than a promotor. In this interpretation, 9cprv1 (*si*) derives from a split of 9cprv2 (*i*) into a lateral and medial group, followed by limited movement of origin and insertion on the anteroposterior axis. We hypothesize that muscle 9clm1 (*s*) similarly derived from a simple subdivision of the plesiomorphic intrinsic coxo-lateropenital muscle 9clm2 (*qr*) into a medial and lateral group, with 9clm1 shifting its insertion to the base of the lateropenite. By contrast, Schulmeister (2003) infers that *s* derives from *si* by splitting followed by a transition in insertion of *s* to the lateropenite and the origin to a more definitively parossicular location. We consider the latter interpretation less parsimonious because it involves migration of insertions across disparate, unfused sclerites. The partial differentiability of 9clm2 into portions labeled *q* and *r* in some taxa may additionally support our hypothesis, though we here consider 9clm2 to constitute a single muscle group, as in Snodgrass (1941) and Schulmeister (2001, 2003).

The mesal dorsal coxo-penial remotors (9cprd1; *k*) is labile in origin across Hymenoptera, potentially leading to confusion regarding its designation here as associated with 9cprd2 (*l*). In ants, the gonocoxites usually have a well-developed, sclerotized, continuous surface area that extends anterad the valvural apices. In these cases, 9cprd1 (*k*) has a definitively anteroposterior orientation, inserting distad the origin and often being mostly or entirely located anterad 9cprd2 (*l*) and 9cppd (*j*). This positioning leaves 9cprd1(*k*) rather proximad 9cprd2 (*l*) and mesad 9cppd (*j*). The latter muscles have closely approximated origins and similar orientations, suggesting that

if 9cprd1 and 9cprd2 (*k, l*) are derived from the same ancestral muscle, there must have been a shift both along the anteroposterior axis and the transverse axis, "hopping" over 9cppd (*j*). The latter translation is *a priori* unlikely, given the usual high conservation of mediolateral relationships among muscles. However, the insertion of both dorsal coxo-penial remotors is on the base of the penial apodeme, while that of 9cppd (*j*) is on the valvural apex, as predicted for the Neoptera. Further, in many symphytan Hymenoptera, the sclerotized gonocoxital surface area is strongly reduced to proximal "gonostipital arms" and distodorsal "parapenes." The parapenes are generally shorter than valvurae, such that their apices are posterad the main body of the penial apodeme. 9cprd1 (*k*) in these taxa originates proximally on the apex of the parapenis and has a reversed position, inserting anterad its origin on the mesal base of the valvura (see Schulmeister, 2001, fig. 9A); alternately, it may be unreversed but still not so proximal as in ants (see Schulmeister, 2001, fig. 7E–F). 9cprd2 (*l*) originates in a similar location, but laterad of 9cppd (*j*) and somewhat more ventrally on the parapenis. In these cases, the dorsal penial remotors "straddle" the promotor. This indicates that the two groups of remotors were already present and located both mediad and laterad the promotors in the common ancestor of Hymenoptera, implying a simple anterior "vicariance" of 9cprd1 (*k*) in ants as the gonocoxital surface area expanded. Functionally, it seems more probable that the dorsal remotors would subdivide, as 9cppd is a definitive depressor of the penial sclerites, and is physically more robust than either subset of 9cprd; this suggests that the weak retractor/pronator is more liable to splitting than the strong, conserved depressor.

The pene-lateropenital (10plm1–1; *m, n*) and pene-penial muscles (10ppm1–2; *x*, *z*) are considered muscles of AX, since they originate on the penial sclerites, which derive from the tenth gonocoxae. Both groups can be considered intrinsic to the penis, since the lateropenite is a

penial fragment. However, the homology of these muscles cannot be definitely asserted based on our review of the literature or our primary observations (these muscles are absent in ants), so it is possible, though unparsimonious, that they truly derive from ninth segmental muscles, having moved their origin during the evolution of ontogenetic integration of gonopods X with gonopods IX in the endopterygote ancestor (Boudinot 2018). In general, the homologies of intrinsic penial muscles are obscure in the Endopterygota, given their apparent lability and distribution of occurrence among holometabolan orders. The Phalloneoptera groundplan includes two intrinsic penial muscles, which are inferred to have been retained in the Endopterygota groundplan and which frequently have their distal attachment on membranes of the penis or the primary gonopore specifically (XAp, Boudinot 2018). One or more intrinsic penial muscles are variably present in Neuropteroidea and Antliophora, where they may participate in the semen pumping apparatus; they are known in Trichoptera, but not Lepidoptera (Boudinot 2018). That these muscles are homologous across orders, having been variously lost or modified in taxa that lack them, seems probable, but primary homology cannot be definitively asserted presently. The evolutionary origin of 10plm (*m, n*) and 10ppm (*x, z*) in Hymenoptera may therefore be of broader significance, given the sister-group relationship of Hymenoptera with the remaining Endopterygota.

Within Hymenoptera, the pene-lateropenital muscles occur much more frequently than the pene-penials, the latter being mostly restricted to Siricidae and Cephidae (Schulmeister, 2003). The most commonly retained muscle, 10plm2 (*n*), often inserts partially or entirely on the membranes of the primary gonopore (*nb, nd*, Schulmeister 2003), suggesting that if 10plm are not homologous with XAp in outgroup orders, they have both functionally and topographically converged. The major difference between 10plm and XAp as described by Boudinot (2018) is

that 10plm may also insert on the lateropenite, a penial derivative which became discrete in the endopterygote ancestor. This suggests that if XAp and 10plm are homologous, then 10plm moved their insertion to the lateropenite in the stem Hymenoptera, prior to the integration of the lateropenite with the parossiculus in the crown Hymenoptera (Boudinot 2018). Our preferred, though largely speculative, inference is that 10plm correspond to XAp, with 10ppm deriving from 10plm to connect the valvurae of Ichneumonidae (10ppm1, *x*) or the "median sclerotized style" (Ross 1937), a ventromedian interpenial sclerite which may be a fragment of the penial sclerites, or a secondary sclerotization of the ventromedian penial membrane (10ppm2, *z*). The muscle connecting the proximal aedeagal apodemes and another set of longitudinally-oriented penial apodemes in *Anagrus* (Mymaridae) is likely an independent derivation, possibly of 10plm1, but cannot be decisively identified based on the description or figures of Chiappini and Mazzoni (2000). Multiple losses would account for the scattered presence of the pene-lateropenital muscles across Hymenoptera. Under this interpretation, the coxo-coxal intrinsic muscle, here conservatively termed 9ccim (*y*), could also reasonably derive from 10ppm1, shifting anteriorly in origin from the valvurae to the parossiculi.

4.3.3. Trends of skeletomuscular simplification of male genitalia in the Formicidae

Of the 28 species of Formicidae for which the genital muscles have been completely described or coded (Kempf 1956; Birket-Smith 1981; Ogata 1991; Boudinot 2013), in only *Leptanilloides* sp. (Dorylinae) is muscular reduction comparable to that observed in the Leptanillinae. To wit, the anterior ventral, anterior dorsal, and posterolateral ventral coxo-penial muscles are absent in *Leptanilloides* sp. (Boudinot, 2013, table 3), with some or all these penial muscles being absent in sampled exemplars of Leptanillini *s. str.*, whereas these muscles are present in all other male ants examined by Boudinot (2013). Reduction of male genital musculature is quantitatively more

extreme in the Leptanillini *s. str.* than in *Leptanilloides* sp., since the posteromedial sterno-coxal muscles, ventrolateral tergo-coxal muscles, and posteromedial dorsal coxo-penial muscles are present in the latter taxon but are absent in the former; further, the lateral coxo-lateropenital muscles and intermediate coxo-stylar muscles remain in the unidentified *Leptanilloides* species sampled by Boudinot (2013), but have been lost in multiple lineages within the Leptanillini *s. str.* and in *Lioponera* indet.

Leptanilloides males are unusual among the Formicidae in equaling the smallness of certain leptanilline males. Skeletomuscular simplification of the male genitalia in the Leptanillinae and across the Formicidae as a whole may therefore correlate with miniaturization, although the trends of skeletomuscular simplification paralleled in multiple anatomical regions across the phylogeny of the Endopterygota coincide with various evolutionary factors beyond miniaturization *per se* (Beutel et al. 2022), meaning that this hypothesis concerning the evolutionary impetus behind male genital skeletomuscular simplification in the Leptanillinae must be tested further. Male genital skeletomuscular simplification as correlate of miniaturization in the Leptanillinae could be corroborated by the extreme scleritic simplification observed in male genitalia throughout the Chalcidoidea (Snodgrass 1941; Hansson 1996), which are for the most part miniaturized relative to other Hymenoptera, with a distinct cupula being universally lost in that superfamily (Domenichini 1953; Viggiani 1973), and also absent in the similarly minute Mymarommatoidea (Gibson et al. 2007). All members of the Leptanillini *s. str.* sampled herein equal or surpass the degree of muscular reduction observed in *Anagrus* spp. (Chalcidoidea: Mymaridae), as four muscles or less are associated with the appendicular sclerites, although the identity of these muscles differs somewhat between *Anagrus* and the Leptanillini *s. str.* (Chiappini & Mazzoni, 2000).

4.4. Comparative discussion of sclerites of interest across the Leptanillinae

4.4.1. Abdominal sternite VIII

The pregenital abdominal sternite VIII is peculiarly modified in some lineages of the Leptanillinae, associated with derivation of abdominal sternite IX (see Section 4.4.2). Yamada et al. (2020) did not describe or figure abdominal sternite VIII for *O. hungvuong*. In *Protanilla* zhg-vn01 and sampled *Leptanilla s. str.*, abdominal sternite VIII is unmodified relative to the ancestral condition of homonomy with immediately preceding abdominal sternites. There is a tendency towards anteroposterior reduction of abdominal sternite VIII observed in sampled *Scyphodon s. l.* and the Bornean morphospecies-group, with median loss of post-antecostal sternite VIII in *Leptanilla* zhg-my02 and complete loss of post-antecostal sternite VIII in *Noonilla* zhg-my03. In *Leptanilla* zhg-my03, -4 and *Noonilla* zhg-my02 and -6, abdominal sternite VIII is completely fused to abdominal sternite IX to form an inarticulate S8+ASIX+gcx+psc (Fig. 3.15).

Abdominal sternite VIII is completely fused to abdominal segment IX in *Yavnella* zhg-th01 and -3. This expanded fusion of abdominal sternite VIII to abdominal segment IX corresponds to the hypertrophied condition of the former sclerite in *Yavnella* zhg-th01, -3 and -my02, forming a dorsally recurved “dish” surrounding the base of the appendicular genitalia, seemingly a sclerotized analog to the genital pouch referred to by Boulangé (1924), which is absent in *Yavnella*. Conversely, abdominal sternite VIII is only moderately expanded medially in *Yavnella* zhg-bt01, in which case it is posteriorly separate from abdominal segment IX. Therefore, posterior fusion of abdominal sternite VIII to abdominal sternite IX has evolved separately at least once in *Yavnella*, *Scyphodon s. l.*, and the Bornean morphospecies-group, respectively (see Section 4.4.2). This is comparable to the condition observed in *Dolichovespula maculata* (Linn.)

and *Dolichovespula adulterina* (Buysson) (Vespidae: Vespinae), in which ASVIII–ASIX are fused, but remain distinguishable by the retention of antecostae (Peck, 1937, Figs 36, 37; Schulmeister, 2003, fig. 14W) (Fig. 3.26).

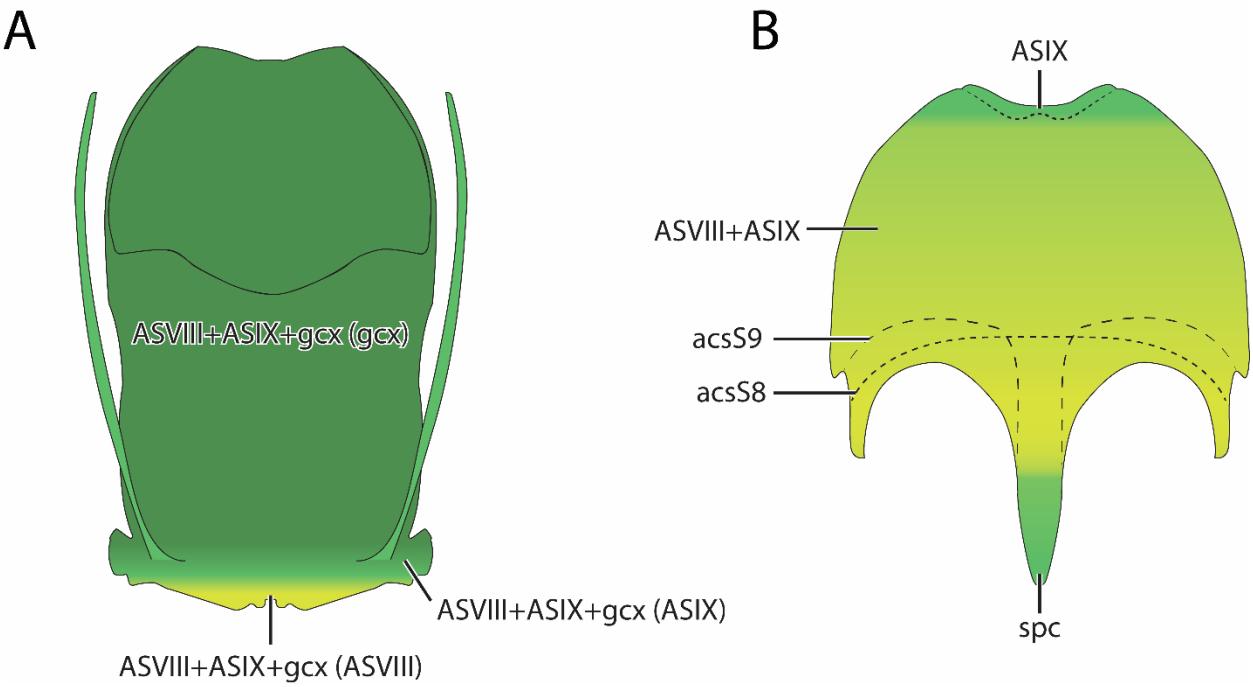

Figure 3.26. Diagrammatic comparison of fusion of male abdominal sternites VIII-IX in the Hymenoptera, ventral view. Figure 26B redrawn from Peck (1937: fig. 37). **A** *Leptanilla* zhg-my04 **B** *Dolichovespula maculata* (Linn.). Abbreviations: ASVIII=abdominal sternite VIII; acsS8=antecosta of abdominal sternite VIII; ASIX=abdominal sternite IX; acsS9=antecosta of abdominal sternite IX; spc=spiculum; gcx=gonocoxite.

In *Yavnella* zhg-bt01, abdominal sternite VIII is medially bifurcated (Fig. 3.11B), recalling derivation of the male abdominal sternite IX elsewhere among the Formicidae (Section 4.4.2) and the median emargination of the male abdominal sternite VII in *Ooceraea* (Dorylinae) (Borowiec 2016). This serial analogy between abdominal sternites VIII and IX may apply to *Yavnella* TH03, meaning that it is conceivable that this posteromedian sternal process observed in *Yavnella* TH03 is in fact anatomically derived from abdominal sternite VIII. Further specimens of *Yavnella* TH03 would be required to assess this possibility.

We speculate that the structural reinforcement afforded by tergosternal fusion of abdominal segment VIII in *Noonilla* cf. *copiosa* aids the maneuverability of the genital capsule. This maneuverability is presumably greater in *Noonilla* cf. *copiosa* relative to other *Scyphodon s. l.* included in this study, which have lost all ventral longitudinal muscles VIII–IX, and thus the capacity for movement of the genital capsule along the craniocaudal or transverse axes.

4.4.2. Abdominal sternite IX

The modification of abdominal sternite IX is diverse across the Leptanillinae sampled herein, and anatomical and structural integration of this sclerite with the appendicular genitalia is variable (Fig. 3.27). In *Protanilla* zhg-vn01 and *O. hungvuong*, abdominal sternite IX is separate from all adjacent pregenital and genital sclerites and ventrally vaulted, with an anteromedian spiculum and posteromedian triangular process. This posteromedian process is visible without dissection in *O. hungvuong* (Yamada et al., 2020, fig. 13C) and all available *Protanilla*, implying that this condition of abdominal sternite IX is plesiomorphic for the Leptanillinae. The spiculum and associated sterno-coxal muscles are lost in the Leptanillini *s. str.*, and in that tribe the posteromedian process of abdominal sternite IX, if present, is broadly triangular or filiform, as in *Yavnella* TH03 (Griebenow 2021: 616).

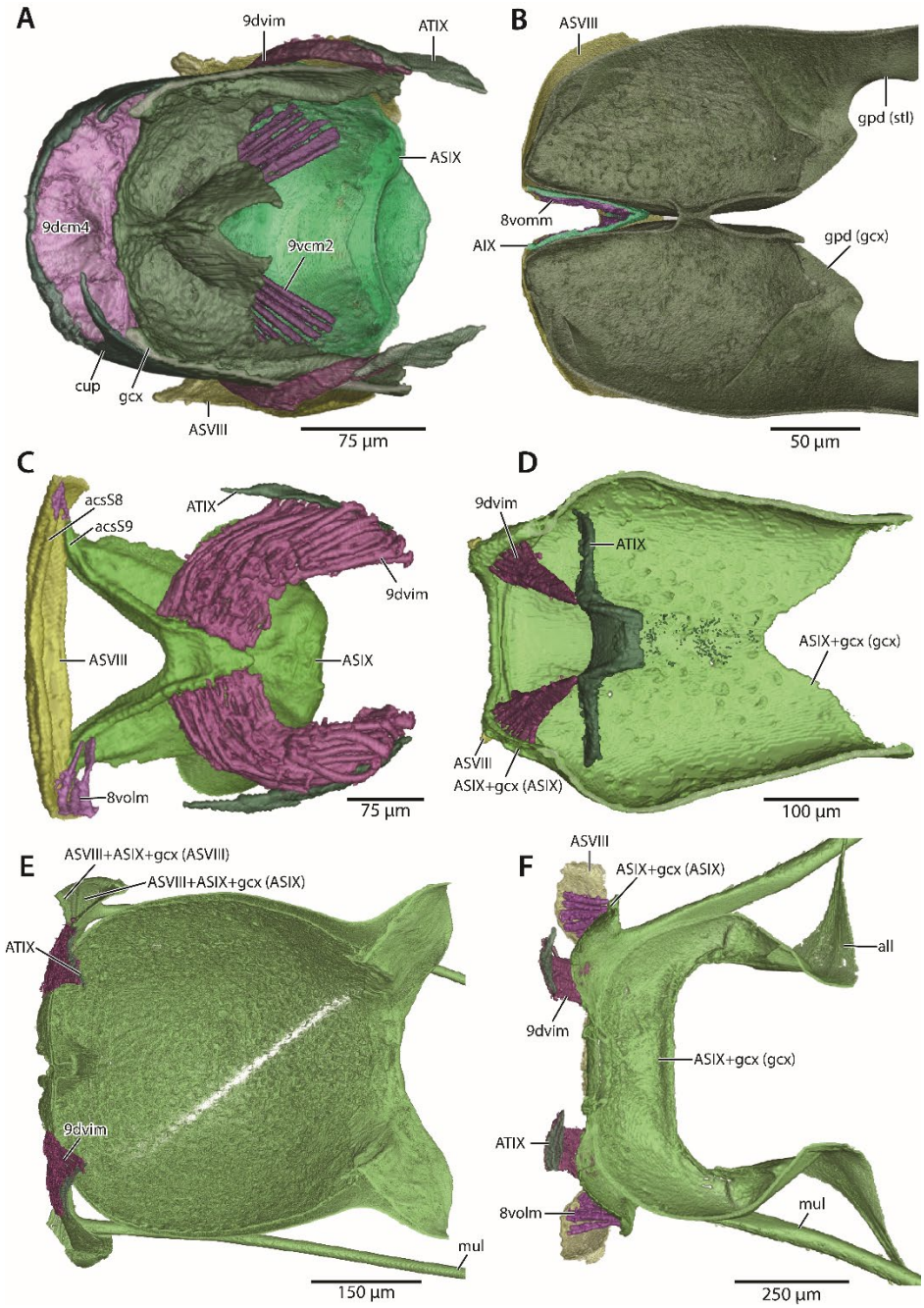

Figure 3.27. Morphology of the axial sclerites, gonopodites, and associated musculature, 3D reconstructions in coronal cross-section. **A** *Protanilla* zhg-vn01 **B** *Yavnella* zhg-th03 **C** *Noonilla* cf. *copiosa* **D** *Noonilla* zhg-my03 **E** *Leptanilla* zhg-my04 **F** *Leptanilla* zhg-my02. Abbreviations: ASVIII=abdominal sternite VIII; acsS8=antecosta of abdominal sternite VIII; AIX=abdominal segment IX; ASIX=abdominal sternite IX; acsS9=antecosta of abdominal sternite IX; mul=mulceator; ATIX=abdominal tergite IX; cup=cupula; gpd=gonopodite; gcx=gonocoxite; all=apicolateral lamina; stl=gonostylus; 8vomm=ventral orthomedial muscles VIII-IX; 8volm=ventral ortholateral muscles VIII-IX; 9dvim=dorsoventral intrinsic muscles IX; 9vcm2=posteromedial sterno-coxal muscles; 9dcm4=ventral tergo-coxal muscles.

According to Petersen (1968) tergosternal fusion of abdominal segment IX occurs in *L. astylina.* Abdominal tergite IX in *L. astylina* is expanded laterally, with the rhomboid abdominal sternite IX (Petersen 1968: fig. 2) completing the ring, which differs from abdominal segment IX as observed in *Yavnella* in that the tergite and sternite remain distinguishable. Abdominal segment IX in *L. astylina* is "a cup-shaped holder which fits the anterior end of the genitalia and is hidden inside the abdomen" (Petersen 1968: 581), in a striking functional parallel with the hypertrophied abdominal sternite VIII of *Yavnella* zhg-th03 and related morphospecies. A comprehensive survey of metasomal skeletomusculature across the Apocrita would be required to determine the singularity of tergosternal fusion in abdominal segments VIII–IX.

In *Leptanilla s. str.*, abdominal sternite IX is unmodified relative to the ancestral condition for Leptanillini *s. str.* or is reduced to an anteroposteriorly narrow strip. The posterior margin may be entire; bear a truncate posteromedian process; medially incised (Petersen 1968: fig. 13); or be shallowly emarginate (Griebenow 2021: fig. 23A). Further derivation of abdominal sternite IX is observed in other subclades of *Leptanilla s. l.*, as follows.

In *Yavnella* zhg-th01, zhg-th03, and zhg-my02, abdominal sternite IX is insensibly fused with abdominal tergite IX (Figs 11–12). Abdominal segment IX forms a ring in *Yavnella* zhg-bt01, but in the other morphospecies of *Yavnella* cited above is lateromedially compressed and dorsoventrally prolonged to form a median keel, confirmed in *Yavnella* zhg-th01 and -3 to be fully fused anteriorly with the hypertrophied abdominal sternite VIII. The functional implications of this modification are unknown.

In the Bornean morphospecies-group, abdominal sternite IX is reduced to an anteroposteriorly narrow strip and posterolaterally produced into mulceators (Figs 15–16), which are an unequivocal autapomorphy of this clade. The neologism *mulceator* aids concision. Since the

term describes a structure that is unique among the Hymenoptera, this nomenclatural addition does not overturn preexisting conventions. Among ants excluding the Leptanillinae, paired posterior processes of the male abdominal sternite IX occur in *Paraponera clavata* (Fab.) (Paraponerinae) (Boudinot, 2015), *Nothomyrmecia macrops* Clark (Myrmeciinae: Prionomyrmecini) (Taylor 1978), and are a synapomorphy of the Dorylinae (secondarily lost in *Leptanilloides*: Ward, 2007; Borowiec, 2016), but these processes are not elongate and filiform. Furthermore, in contrast with the Bornean morphospecies-group, abdominal sternite IX in male *P. clavata*, *N. macrops* and the Dorylinae is anteroposteriorly prolonged and robust, rather than exhibiting median compression along the anteroposterior axis to form a ductile strap, as in the Bornean morphospecies-group. Abdominal sternite IX in the Bornean morphospecies-group also shows partial to complete median fusion to the gonocoxites. The posteromedian fusion of abdominal sternite IX in *Leptanilla* zhg-my02, -5, -6, and -id01 to the gonocoxites anchors this sternite medially, allowing differential motion of the lateral portions of abdominal sternite IX and thus of the mulceators, mediated by the ventral ortholateral muscles VIII–IX (Fig. 3.27C, F).

In sampled *Scyphodon s. l.*, abdominal sternite IX is insensibly fused to the medially fused gonocoxites along the ventral gonocoxital margin. The "reversed *v*-shaped, strongly sclerotized structure in firm connection with the genitalia" described by Petersen (1968, p. 584) for *N. copiosa* is here identified as abdominal sternite IX (Fig. 3.27C), as suggested by Petersen (1968). The posteromedian fusion of abdominal sternite IX to the gonocoxites in the Bornean morphospecies-group is much less pronounced than that in *Scyphodon s. l.* and is functionally different in the absence of mulceators. We therefore regard the posterior fusion of ASIX to the appendicular genitalia as homoplasious between *Scyphodon s. l.* and the Bornean morphospecies-group.

4.4.3. Volsellae

The variation observed in volsellar anatomy across the Leptanillinae is dramatic, ranging from presence and complete articulation of the parossiculus and lateropenite in *O. hungvuong* to complete absence of the volsella in *Scyphodon s. l.* (Fig. 3.22). The loss of distinction between the parossiculus and lateropenite is a synapomorphy of the Leptanillini *s. str.* As noted above, due to a lack of intermediates in volsellar form between the former Anomalomyrmini and Leptanillini *s. str.*, it is not externally evident if the volsellar sclerite observed in the latter clade is homologous with the parossiculus or with the lateropenite. The proximal insertion of the extrinsic medial coxo-lateropenital muscles on the volsellae would identify at least the proximal portion of that sclerite as parossicular, implying that the whole of the sclerite perhaps corresponds to the parossiculus rather than to the lateropenite in part.

The volsella in the Leptanillini *s. str.* therefore consists of a single article, which in many *Yavnella*, including *Yavnella* zhg-th03, is divided into proximal and distal sections (cf. Kugler, 1986, Figs 18, 22) by an ectal transverse sulcus on the medial face. This division is not observed in *Yavnella* zhg-bt01 or *Yavnella* TH03, and so may be synapomorphic for the Southeast Asian clade comprising most of the species-level diversity in this genus, but to which *Yavnella* zhg-bt01 and *Yavnella* TH03 do not belong (Griebenow et al. 2022). These proximodistal volsellar sections are not respectively homologous with the basi- and distivolsella observed in symphytan Hymenoptera, since the distinction between proximodistal articles was apparently lost in the most recent common ancestor of the Leptanillini *s. str.*; the proximodistal division described here for some *Yavnella* spp. is a secondary derivation.

In the remainder of the Leptanillini *s. str.* the volsella (if present) exhibits no trace of a transverse sulcus. As mentioned above, the medial fusion of the volsellae, synapomorphic for the Bornean

morphospecies-group, is unique among the Formicidae but paralleled in *Sceliphron caementarium* (Drury) (Sphecidae: Sceliphrini) in the form of a "basivolsellar bridge" (Schulmeister 2003, fig. 11C). The shape and proportions of the volsellae in the Bornean morphospecies-group differ markedly on the morphospecies level, particularly when considering the clade comprising *Leptanilla* zhg-my03 and -4 contrasted with their sister-group (which constitutes the remainder of the Bornean morphospecies-group), but are always large and prominent. The shape of the volsellae appears to be less variable in *Leptanilla s. str.*, in which these sclerites are reduced proportionally to the gonopodites and largely concealed by the latter appendages *in situ*. *Leptanilla* zhg-id04 shows an odd juxtaposition of character states in that the volsellae are present and seemingly articulated to the gonocoxites yet are unmusculated (Fig. 3.17). It seems clear that this interpretation is not artifactual. The loss of volsellar musculature has never been previously observed in the ants (Schulmeister, 2003; Boudinot, 2013, table 2), nor has the concomitant loss of the volsellae autapomorphic for *Scyphodon s. l.* No trace of volsellae could be discerned in any *Scyphodon s. l.* examined with micro-CT: it appears that what Petersen (1968) identified as volsellae are in fact gonostyli (see Section 4.2).

4.4.4. Penial sclerites

The complete medial fusion of the penial sclerites is a synapomorphy of the Leptanillini *s. str.* (Fig. 3.19), here inferred to be homoplasious with the condition observed in *M. heureka* (Boudinot 2015). In *Protanilla* zhg-vn01, and all known *Protanilla* by extension, the penial sclerites are not medially fused, as is reported for *O. hungvuong* (Yamada et al. 2020), instead being separated by a medial conjunctiva. Within the Leptanillinae, the medial fusion of the penial sclerites is associated with the loss of the posteromedial dorsal coxo-penial muscles and valvura—conditions that are synapomorphic for the Leptanillini *s. str.* as well. The penial

sclerites in *Yavnella* TH03 and *Leptanilla astylina* Petersen appear to be medially separated, at least in part, but dissection would be required to determine the penial condition of these lineages.

Despite the tendency towards fusion of the penial sclerites with the gonocoxites in scanned exemplars of the Leptanillini *s. str.*, at least one pair of coxo-penial muscles is retained in those scanned specimens in which partial (*Yavnella* zhg-th03) to complete fusion (*Scyphodon s. l.*, *Leptanilla* zhg-my03, -4) is observed. Complete loss of penial musculature is observed among scanned male Leptanillinae in certain members of the Bornean morphospecies-group (*Leptanilla* zhg-my02, -5, -6, and *Leptanilla* zhg-id01), which display remarkable modification of the penial sclerites: these are proximally recurved (less so in *Leptanilla* zhg-id01 than the others), with paired penial condyles articulating to the gonocoxites, and the recessed phallotreme situated on the anatomical venter proximal to the penial apex.

Certain outgroup taxa exhibit sclerotized structures mediad the penial sclerites, which are almost certainly non-homologous with the fused penial sclerites in Leptanillini *s. str.* but may provide informative comparative data. Birket-Smith (1981: 385) notes that a proximodorsal, interpenial sclerite, which he terms the "*patella intermediare*," occurs "in several species" of Dorylinae, but unfortunately does not list these species by name. Among the Apoidea, and in *Sceliphron caementarium* (Drury), the dorsal membranes are variably sclerotized (Snodgrass 1941); the sclerites in these cases are unmusculated. In Cephidae and Siricidae, the median sclerotized style is a ventral strip of sclerite, proximally fused to the gonocoxite in cephids (Schulmeister 2003). Smith (1970), who posited intersexual genital homology, interpreted the median sclerotized style to be the detached ninth gonapophyseal rhachies; this could be broadly brought into alignment with our understanding of sclerite homologies as a fragment of the penial sclerites. Alternately, the style could be a secondary sclerotization of the penial conjunctiva. In cephids and siricids this

sclerite may bear the insertion of 10ppm2 (*z*, Schulmeister, 2001). We note that the term "median rod" has been variably used to refer to either the dorsal (e.g., Snodgrass, 1941) or ventral interpenial sclerite (Schulmeister 2001), while "spatha" has been applied to both sclerotizations of the dorsal and ventral interpenial membranes, as well as to parts of the gonocoxites (Audouin 1821).

4.5. Comparative discussion of muscles of interest across the Leptanillinae

Musculation of abdominal sternites VIII–IX is diverse among those lineages in which these sclerites have derived morphologies. Ventral longitudinal muscles VIII–IX are absent in *Noonilla* zhg-my03, *Leptanilla* zhg-my03, and -4, concomitant with the anteroposterior fusion of abdominal sternites VIII–IX. This is unlike *D. maculata*, *D. adulterina*, and *Yavnella* zhg-th03 in which abdominal sternites VIII–IX are anteroposteriorly fused and sternosternal musculature is retained (Peck 1937). Ventral longitudinal muscles VIII–IX in *Yavnella* zhg-th03 originate on a posteromedian apodeme of abdominal sternite VIII and insert along the ventral mesal length of abdominal segment IX. Intrinsic dorsoventral muscles IX are uniquely lost in *Yavnella*. Ventral longitudinal muscles VIII–IX are retained in *Noonilla* cf. *copiosa* and *Leptanilla* zhg-my02, -5 as ventral ortholateral muscles VIII–IX.

Based on outgroup sampling, the ancestral insertion of the dorsoventral intrinsic muscles IX in Formicidae is at the anterolateral corners of abdominal sternite IX, and this condition is retained in *Protanilla* zhg-vn01. Dorsoventral intrinsic muscles IX are indiscernible in both sampled *Leptanilla s. str.* and *Yavnella* zhg-bt01, but where discernible in the Leptanillini show varying degrees of derivation, in conjunction with often extreme modifications to abdominal sternite IX. In *Yavnella* zhg-th03, these muscles are absent, and indeed are spatially excluded by the ventral longitudinal orthomedial muscles VIII–IX due to pronounced lateromedial compression of

abdominal sternite IX (Figs 11D, 27B); if this is a corollary of the tergosternal fusion of abdominal segment IX, we can predict that the dorsoventral intrinsic muscles IX are absent in *Yavnella* zhg-bt01 and zhg-th01 as well. In *Noonilla* zhg-my01, -2, -3, and -6 the insertions of the dorsoventral intrinsic muscles IX retain their ancestral position (Fig. 3.13A), whereas in all examined members of the Bornean morphospecies-group these insertions are well mediad the lateral extremities of abdominal sternite IX (Fig. 3.27E–F). In *Noonilla* cf. *copiosa* this tendency is developed still further, with the insertions of the dorsoventral intrinsic muscles IX being closely approximated medially (Fig. 3.27C). These insertions are restricted to the anterior margins of the antecosta of abdominal sternite IX, which forms an anteriorly directed triangle in dorsal view.

Leptanilla zhg-my02 and -5 exhibit unique extrinsic dorsoventral muscles IX that insert on abdominal sternite VIII from origins on abdominal hemitergites IX (9dvxm) (Fig. 3.15D, F). Extrinsic muscles are expected to insert on the segment caudad the segment of origin, as observed across the insects. Both intrinsic and extrinsic dorsoventral muscles in the Hymenoptera almost always originate on the tergite and insert on the sternite. Therefore, the orientation of the dorsoventral muscles that are here termed 9dvxm is confounding, and the lack of descriptions of pregenital musculature in male Hymenoptera further obscures evolutionary derivation. We therefore emphasize the importance of descriptions of at least some of the muscles of AVIII–AIX in treatments of the male genitalia. These are largely absent from the literature, with a few notable exceptions (Birket-Smith, 1981; Boulangé, 1924; Kempf, 1956; Youssef, 1969) and occasional mention of 9dvim. We propose two alternate interpretations for the identity of what is here designated 9dvxm but acknowledge that neither of these interpretations are parsimonious. The one notable exception to the orientation of origins and

insertions in extrinsic muscles cited above is the muscle 7vdxm (*M. sterno-tergalis exterior*) in female Aculeata, which is clearly homologous among the lineages in which it is present but cannot be serially homologized (Lieberman et al. 2022) and certainly does not correspond to the male 9dvxm. Therefore, the two possibilities for the correspondence of 9dvxm appear to be: (1) these muscles properly belong to AVIII, potentially being sterno-sternal longitudinal muscles which shifted their insertion to the tergite, possibly through a series of local translations beginning with movement from the sternite to the ventral tergite, which seems unlikely given the reduction of ATIX to hemitergites in those lineages in which 9dvxm is observed, and lack of correlates to 9dvxm in species with ATIX not so divided; and (2) 9dvxm corresponds to the external intrinsic dorsoventral muscles of AIX, having shifted their insertion to ASVIII during extreme reduction and modification of both ATIX and ASVIII. We here tentatively infer the latter with according nomenclatural designation, but the identity of this ludicrous muscle deserves further investigation.

4.6. Functional and evolutionary-biological speculation

4.6.1. Part-wise overview of putative mechanics

Leptanilline ants are rarely observed alive, and among the tribe Leptanillini, only the males of *Leptanilla japonica* Baroni Urbani (Ogata et al. 1995) and *O. hungvuong* (Yamada et al., 2020) have been collected in association with conspecific females. Therefore, we have no direct observations of male ethology in the Leptanillinae and can only speculate on the functional implications of the disproportionately diverse male genital morphology here described from that clade. The sheer novelty of some of the morphological character states observed herein, both among the ants and among the Hymenoptera, makes extrapolation of mechanical function difficult. Nonetheless, the mechanical functions of some conditions can be reasonably inferred.

Any case of recurved serration, or recurved processes, presumably serves an anchoring function, extrapolating from Kamimura (2008). This condition is observed in all three of the non-leptanilline outgroups included in this study, and in other formicids (Forbes and Hagopian 1965: fig. 5; Boudinot 2013: fig.13), despite the phylogenetic distance of these taxa from one another. When coincident with medial articulation of the penial sclerites, such serration can be inferred to gain purchase on the female genital tract "via a motion analogous to mastication" (Boudinot 2013: 41), mediated by the mesal dorsal coxo-penial remotors, 9cprd1, and perhaps aided by the lateral ventral coxo-penial remotors (Boudinot, 2013). Concomitant with the medial fusion of the penial sclerites in the Leptanillini *s. str.* is the loss of 9cprd1 in all exemplars except *Noonilla* cf. *copiosa*, precluding masticatory motion of the penial sclerites in this tribe. Nonetheless, the recurved process at the penial apex, ventrad the phallotreme, observed in some *Scyphodon s. l.* (Griebenow 2020: fig. 13A) would serve an anchoring function analogous to the penial serration observed in many other male ants, as would the ventromedian genital "trigger" unique to *N. copiosa*, with the longitudinal pairing of proximal and distal ventromedian penial processes here described in *Noonilla* cf. *copiosa* granting opposability (Fig. 3.14C–D). An obvious anchoring function is otherwise only observed for the penial sclerites among the Leptanillinae in sampled *Protanilla*, in which the penial sclerites exhibit plesiomorphic medial separation.

An anchoring function is inferred for the volsellae of examined *Protanilla* and *Yavnella* zhg-th03, in which ventral penial serration is not observed: this is indicated in both *Protanilla* sampled in this study by recurved medial processes of the parossiculus (Fig. 3.28E), which in *P. lini* would work in concert with shagreened cuticular denticles (Griebenow 2020: Figs:19A, C). An anchoring function of the volsellae in *Yavnella* zhg-th03 is indicated by dorsal volsellar serration, analogous to that observed in the penial sclerites across the Formicidae. Recurved

spines with a similar putative function are observed on the volsellae in *Anagrus* spp., although these are distal, and laterally rather than medially recurved (Chiappini & Mazzoni, 2000).

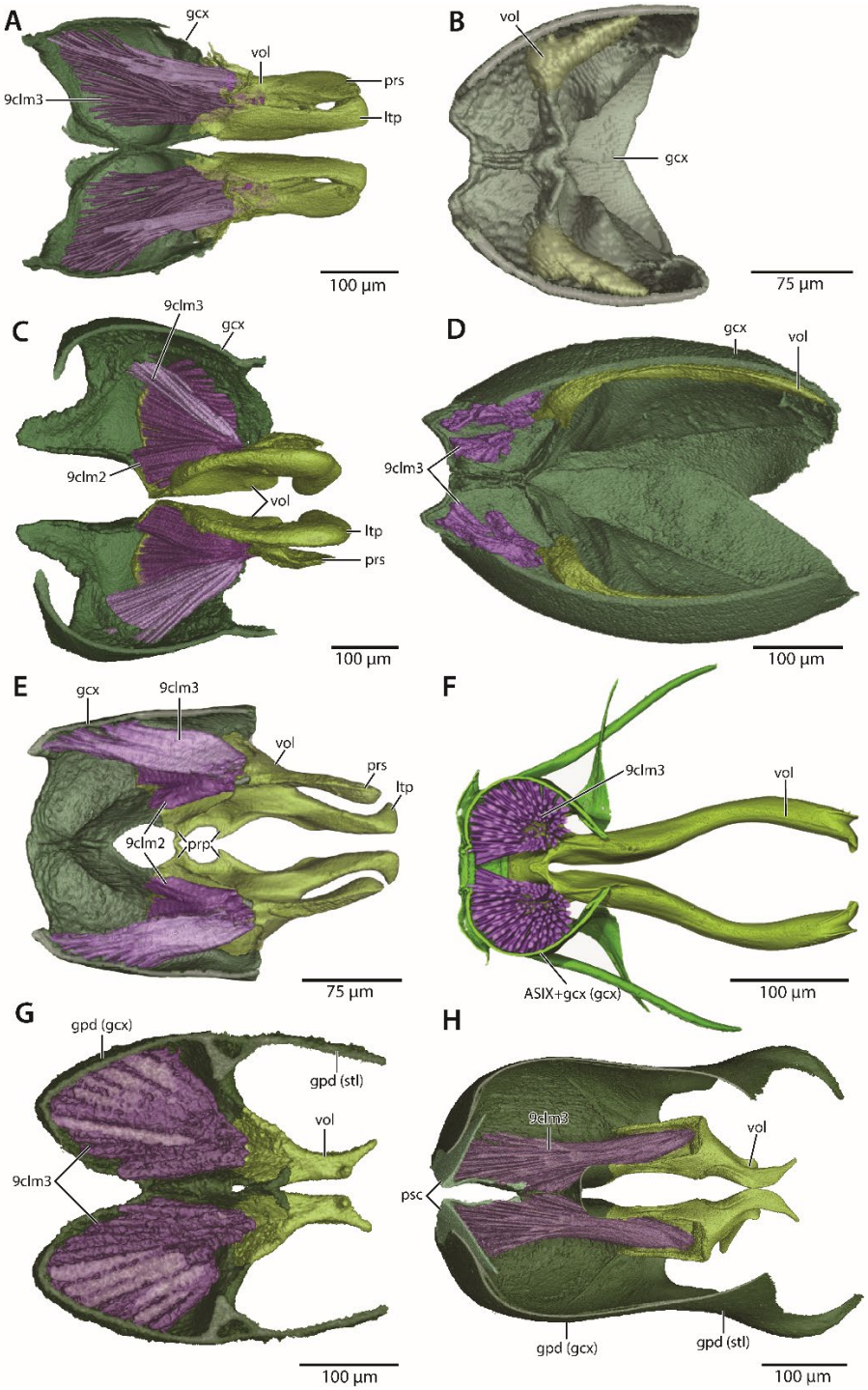

Figure 3.28. Morphology of the coxo-lateropenital musculature and associated sclerites, 3D reconstructions in sagittal cross-section. **A** *Lioponera* indet. **B** *Protanilla* zhg-vn01 **C** *Yavnella* zhg-bt01 **D** *Yavnella* zhg-th03 **E** *Leptanilla* zhg-id04 **F** *Leptanilla* cf. *zaballosi* **G** *Leptanilla* zhg-my04 **H** *Leptanilla* zhg-my02. Abbreviations: ASIX=abdominal sternite IX; gpd=gonopodite; gcx=gonocoxite; vol=volsella; prs=parossiculus; ltp=lateropenite; psc=penial sclerites; 9clm2=lateral intrinsic coxo-lateropenital muscles; 9clm3=medial extrinsic coxo-lateropenital muscles; 9clm4=lateral extrinsic coxo-lateropenital muscles.

It can be surmised that the ancestral function of the volsellae for the Hymenoptera was a pincing one (Snodgrass 1941; Smith 1970; Schulmeister 2001, 2003). Loss of the medial ventral coxo-penial remotors (9cprv1, *si*) and intrinsic medial coxo-lateropenital muscles (9clm1, *s*) in the Formicidae prevents opening of the parossiculus and lateropenite relative to the resting position of the volsella, a function probably ancestral in the Hymenoptera given the wide distribution of these muscles among symphytan Hymenoptera (Schulmeister, 2001). The synapomorphic loss of distinction between the parossiculus and lateropenite in the Leptanillini *s. str.* is therefore associated with loss of the plesiomorphic grasping function of the volsellae, parallel to the Ceraphronoidea and some Proctotrupomorpha (Mikó et al. 2013). Furcation of the volsellar apices is prevalent in the predominantly Southeast Asian clade constituting almost all known *Yavnella* and is somewhat correlated with the secondary proximodistal articulation of the volsella in that clade. It is tempting to infer that the volsella here anchors the genitalia, with contraction of the coxo-lateropenital muscles facilitating a grasping function not accomplished by the gonopodites, which in *Yavnella* are always firmly inarticulate.

The medial fusion of the volsellae in the Bornean morphospecies-group is intriguing from a functional standpoint. In *Leptanilla* zhg-my03 and -4, the volsellar apices are dorsally recurved (Fig. 3.29G), and therefore would function analogously to furcated or falcate volsellae observed in most *Yavnella*. In the remainder of the Bornean morphospecies-group sampled here (which constitute a monophyletic group), the volsellae are elongated, and fit into slots in the penial sclerites laterad the elevated, recessed phallotreme. Uniquely among hymenopterans, so far as is known, coxo-penial muscles are here found to be absent in *Leptanilla* zhg-id01, zhg-my02, -5, and -6. Movement of the penial sclerites along the dorsoventral axis in this clade is therefore mediated by retraction of the basomedially fused volsellae, musculated by lateral coxo-

lateropenital muscles, with the penial sclerites articulating with the gonocoxites via penial condyles. Recurved teeth at the volsellar apices in *Leptanilla* zhg-my02, -5, and -6 (Fig. 3.28F, Fig. 3.29H) imply that the volsellae serve an anchoring function in these morphospecies, concurrent with indirect movement of the penial sclerites by way of the volsellae; no such function is implied for *Leptanilla* zhg-id01, since in this morphospecies the volsellar apices are entire. Rather, such a function is obviously served in *Leptanilla* zhg-id01 by a small falcate hook, at the penial apex, dorsally recurved (Griebenow 2020: fig. 13C).

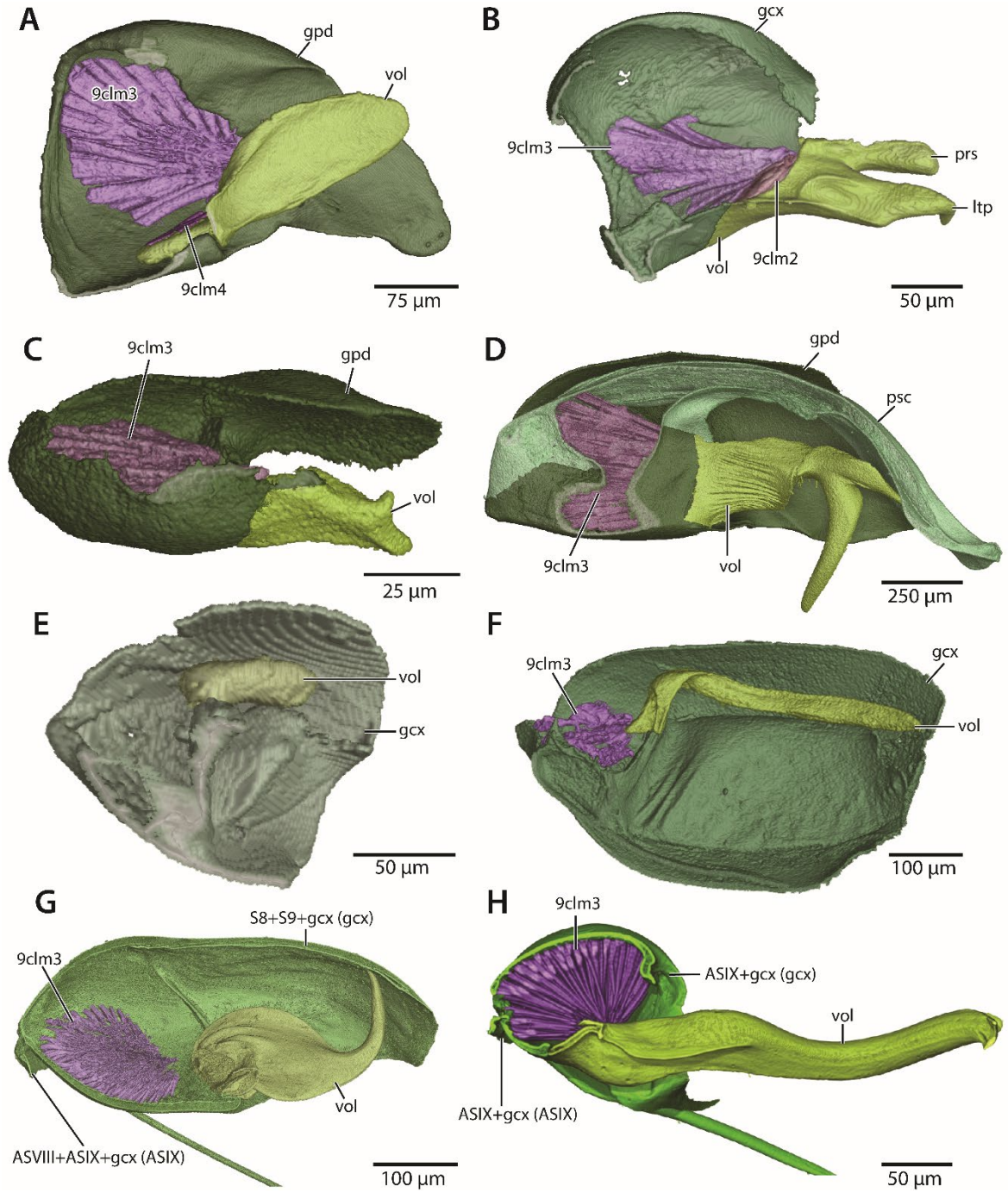

Figure 3.29. Morphology of the coxo-lateropenital musculature and associated sclerites, 3D reconstructions in coronal cross-section. **A** *Odontomachus* indet. **B** *Leptanilla* zhg-id04 **C** *Myrmica ruginodis* **D** *Leptanilla* cf. *zaballosi* **E** *Protanilla* zhg-vn01 **F** *Leptanilla* zhg-my02 **G** *Yavnella* zhg-bt01 **H** *Yavnella* zhg-th03. Abbreviations: gpd=gonopodite; gcx=gonocoxite; stl=gonostylus; vol=volsella; prs=parossiculus; ltp=lateropenite; prp=lateropenital recurved processes; psc=penial sclerites; 9clm2=lateral intrinsic coxo-lateropenital muscles; 9clm3=medial extrinsic coxo-lateropenital muscles.

The absence of the volsellae in *Scyphodon s. l.* is associated among the exemplars of that clade sampled in this study with irregular ventral serration or a recurved process proximoventrad the penial apex, as noted above. *Noonilla* zhg-my03 is an exception, with a penial venter that is unsculptured and lacks any recurved processes proximad the apex. Notably, the gonostylar apex in *Noonilla* zhg-my03 is unique among known *Scyphodon s. l.* in its bifurcation into recurved lobes; we infer that in the absence of penial serration, the gonostyli in this morphospecies act in an anchoring capacity, unlike the clasping or curbing observed in other ants. Moreover, the exceptional medial fusion of the gonostyli in *Noonilla* zhg-my03 constitutes serial parallelism with the volsellae of the Bornean morphospecies-group, suggesting a similar function.

Although we do not examine membranous structures in detail here, a few observations of apparently derived skeletomusculature likely relate to the function of the endophallus through direct or indirect muscular action. First is the presence and expression of the endophallic sclerite, which is located within the ejaculatory duct at or near the primary gonopore, i.e., the point at which the paired *ducti ejaculatorii* merge to form the endophallus. This sclerite may or may not be homologous in the various ants in which it occurs, or with the endophallic sclerite in other orders, including Coleoptera (see, e.g., Boudinot 2018, Génier 2019 and references therein), or the anterior sclerite in the endophallic *bulbalis* of Siphonaptera (Günther 1961). Possible homology has also been questioned between the formicid endophallic sclerite and the *fibula ducti* in symphytan Hymenoptera or even the musculated *Ostialsklerit* of some Mecoptera (Schulmeister 2001). The term *fibula ducti* has been applied to two dissimilar forms: a small, unpaired sclerite within the endophallus or *ductus ejaculatorius* of various sawflies; and, in Pergidae and Argidae, a larger pair of plates on the ectodorsal and ectoventral surfaces of the *ducti ejaculatorii*, connected to one another by a sclerotic bridge in “the median plane”

(Schulmeister 2001:339, 2003). It seems likely that the endophallic sclerite corresponds to the former, internal form, while homology with the external sclerites is more doubtful, although the two forms may indeed be homologous, as suggested by the presence of the median bridge. In Mecoptera, the Ostialsklerit is unpaired, and approximates the form of the formicid endophallic sclerite; however, the term has been applied both to an ectal sclerite, as in *Bittacus*, and to an internal sclerite at the distal end of the endophallus as in *Apteropanorpa* (Willmann 1981).

Inferring the evolutionary origin of the endophallic sclerite is complicated by the lack of intermediate forms indicating that it is, e.g., derived by fragmentation and internalization of an existing penial sclerite, or represents a novel sclerotization of the endophallus itself. The *ducti ejaculatorii* and endophallus are ectodermal organs with cuticular surfaces and thus may be expected to display ontogenetic plasticity between conjunctiva and sclerite as in exoskeletal surfaces, albeit within a different set of constraints, for example, of optimum flexibility and space-filling.

The endophallic sclerite is not directly musculated in any known ants, and therefore likely functions through indirect action of muscles associated ectally with the endophallus. Contraction of 9cppv1 (*h*) in *Myrmica ruginodis*, for example, close the endophallus and allow accumulation of potential energy through pressure on the endophallic sclerite, the release of which could increase the velocity of ejaculation. An alternate hypothesis is that the endophallic sclerite serves as simple reinforcing structure against pressure during ejaculation, or more specifically as a stent to keep the endophallus dilated during contractions of other powerful genital muscles, a situation which may be more probable in lineages that lack muscles near the primary gonopore.

In many sawflies, the lateral pene-lateropenital muscles 10plm2 (*n*) are frequently associated medially with the endophallic membrane, probably playing a role in closing or opening the genital tract (Schulmeister, 2001). A compelling preliminary observation is that in some ants, which lack pene-lateropenital muscles, other muscles appear to be partially or totally associated with the endophallus. In *M. ruginodis*, some partially differentiated fibers of 9cppv1 (*h*) wrap ventromedially around the endophallus in its proximal region, near the primary gonopore, and may serve to compress the duct dorsoventrally. Similarly, 9cppv2 (*h'*) in *Dorylus funereus* Emery "embrace the vesica ejaculatorius" and "cause a powerful contraction. . .presumably essential for the ejaculation of sperm" (Birket-Smith 1981: 385). In at least *Aenictogiton* (Dorylinae), there is a massive, approximately toroidal "knot" of muscles surrounding the endophallus, which appears to comprise at least 9cppv1 and likely includes other coxo-penial muscles. Contraction of this effectively circular muscle group might cause forceful ejaculation or extension of the membranous elements of the genitalia. A dedicated comparative study of the structure and function of the endophallic sclerite and muscles acting on the genital tract is merited, preferably histological.

4.6.2. "Detachable Penis": implications of putative suicidal mating in the Leptanillinae

As noted above, copulation in the Leptanillinae has never been observed. Given that the queens of *Opamyrma*, *Protanilla*, and *Anomalomyrma* are usually alate (Bolton 1990b; Baroni Urbani and de Andrade 2006; Chen et al. 2017; Ito et al. 2021) it is theoretically feasible for queens and males of these taxa to be observed *in copula*, but all known queens within the tribe Leptanillini *s. str.* are wingless, with reduced eyes (Kutter 1948; Ito and Yamane 2020): this dichthadiiform phenotype would suggest that copulation is subterranean in the Leptanillini *s. str.*, and so it is extremely improbable that mating behaviors will ever be observed in this clade. This limitation is

disappointing from a biomechanical perspective, since all leptanilline lineages in which the male genitalia are most extreme in derivation and interspecific variation belong to the Leptanillini *s. str.* Due to these limitations, the biological implications of the skeletomusculature and macroevolutionary trends described herein are for now only the subjects of well-informed speculation.

The loss of the cupula, and therefore of sterno-cupular and tergo-coxal muscles, which is here inferred to be a synapomorphy of the Leptanillini *s. str.*, is presumably associated with suicidal mating. This is by analogy to copulation in *Apis* (Apidae: Apinae: Apini), in which suicidal mating by detachment of the male genital capsule (Koeniger and Koeniger 1991) is enabled by the absence of the cupula and associated musculature, with there being extrinsic musculation by a single pair of muscles that proceed from abdominal sternite VIII to the gonocoxites (Snodgrass 1942). The corollary of this hypothesis is that suicidal mating does not occur in *Scyphodon s. l.* and the Bornean morphospecies-group, since in these clades sterno-sternal and dorsoventral tergosternal musculature connects the male genital capsule to the remainder of the metasoma. Such a conclusion cannot be assumed however, since suicidal mating is common in *Dinoponera* and *Diacamma* (Ponerinae: Ponerini) (Monnin and Peeters 1998; Allard et al. 2002) but is not associated in these clades with reduction or loss of the cupula and associated musculature (Tozetto and Lattke 2020, this study).

In metazoans that use internal fertilization, genital morphology is often conspicuously varied relative to other anatomical regions, with the male genitalia having received more descriptive study than the female counterparts (Sloan and Simmons 2019). Empirical studies continue to indicate that sexual selection is the primary evolutionary force behind this phenomenon (Hosken and Stockley 2004) rather than pleiotropic effects (Mayr 1963) or the lock-and-key hypothesis

(Dufour 1848), but the mechanisms that are at play in sexual selection, and their proportional significance in the evolution of a given lineage, often cannot be discriminated experimentally. Under the theoretical synthesis of Eberhard (1985), one would hypothesize that the diversity of male genitalia in the Leptanillinae results from Fisherian sexual selection (Fisher 1930) and is therefore driven by female choice. Other hypothesized selective mechanisms, such as sexual antagonism, that would give rise to observed morphological divergence which is disproportionate in genitalia relative to other anatomical regions, are not mutually exclusive with female choice (Simmons 2014). These may operate on male genitalia in the Leptanillinae as well.

Qualitatively, the male genitalia of *Scyphodon s. l.* and the Bornean morphospecies-group show increased morphological disparity relative to that observed in *Leptanilla s. str.* This could indicate that posterior fusion of abdominal sternite IX to the genital capsule is associated with an increased tempo of morphological evolution in the genitalia—an observation that invites macroevolutionary scrutiny. Quantitative tests of this hypothesis would require phylogenetic comparative analyses utilizing landmark-based geometric morphometrics, applied to scleritic structures. While such an enterprise is theoretically challenging, due to operational obstacles and analytical conundrums presented by phylogenetic variance in articulation of adjacent sclerites (Vidal-García et al. 2018), and the absence of definitively homologous landmarks in certain leptanilline lineages (cf. Borgard et al. 2020), it is conceivable given the scan data published here.

5. Conclusion

Male genitalia in the insects are profuse in morphology and corresponding function, with this profusion often covarying with phylogenetic structure. The male genitalia are therefore of

enduring functional, evolutionary, and taxonomic interest. Despite the ecological prevalence and diversity of the Formicidae, little descriptive work has focused on the male genitalia of this clade for classificatory purposes, when compared to congruent scientific attention that the male genitalia in other insect taxa have received. The peculiar ant subfamily Leptanillinae deserves further scrutiny in this regard, since the male genitalia in this clade show high morphological disparity and sometimes spectacular derivation, which have received only piecemeal description (e.g., Santschi 1907, 1908; Wheeler and Wheeler 1930; Petersen 1968).

In this study we provide the first descriptions of male genital skeletomusculature within the Leptanillinae, supplemented by description of several exemplars sampled from across the remainder of the Formicidae, from the perspective of comparative morphology. These descriptions are guided by phylogeny, as inferred from molecular and morphological data (Griebenow 2020; Chapters 1–2). Our observations are facilitated by virtual dissection of male genital skeletomuscular components, as reconstructed from scans acquired with micro-computed tomography, or directly derived from these scans without virtual dissection. To describe the range of muscular modifications relative to the putative ancestral condition for the Hymenoptera that are observed across sampled leptanilline lineages, we present a standardized nomenclature for male genital musculature, using the hypothesized interordinal genital homologies proposed by Boudinot (2018) for the Endopterygota, and designed to be practically extensible across the whole of the order Hymenoptera. While this nomenclature is applicable strictly to hymenopteran male genitalia, the notational conventions of this nomenclature combine homological inference with the topographic main-group approach, which is deliberately congruent with that used for other insect anatomical regions (e.g., Friedrich and Beutel 2008).

Taxonomy in the Leptanillinae relies on male morphological characters, especially those of the genitalia, due to the scarcity of female specimens and lack of phylogenetic signal from worker morphology; our observations clarify and expand our understanding of male genital morphology in the Leptanillinae, therefore aiding future systematic revision of this clade. We find that male genital skeletomusculature in the Leptanillinae is characterized by an overall trend of skeletomuscular reduction relative to the remainder of the Formicidae, in some lineages to an extreme otherwise not observed among ants. Many apomorphic scleritic fusions and muscular losses are homoplasious amongst different lineages of the Leptanillinae and are therefore examples of evolutionary parallelism *sensu* Futuyma (1998), but have no known morphological parallels in other ant lineages, and few known parallels across the Hymenoptera as a whole. Other modifications are autapomorphies of certain leptanilline subclades, relative to the remainder of the Formicidae: particularly striking among these is the complete tergosternal fusion of abdominal segment IX in *Yavnella*, and the total loss of the volsellae in *Scyphodon s. l.*

Despite our inability to observe copulation in most leptanilline ants, and the complete absence to date of such observations, we extrapolate the function of some derived skeletomuscular character states observed in this study. Most striking among these in its behavioral implications is the absence of sterno-coxal and tergo-coxal muscles, conjunct with the complete loss of the cupula, which are together a synapomorphy of Leptanillini *s. str.* and to our knowledge unique among the ants. The loss of extrinsic musculation of the genital capsule would mechanically oblige detachment of the genitalia during copulation. Certain subclades of the Leptanillini *s. str.* are here found to exhibit posterior fusion of abdominal sternite IX to the appendages of the genital capsule; by consequence, the genital capsule is extrinsically musculated in these clades by

ventral longitudinal and dorsoventral abdominal muscles, with this musculation therefore being a secondary derivation of these subclades.

While provincial in scope—focusing upon a species-poor clade of ants, sister to nearly all other members of the formicid crown-group (Borowiec et al. 2019; Romiguier et al. 2022)—this comparative study is the first of its kind for the Formicidae, explicitly contextualizing male genital skeletomuscular observations on a robust phylogeny inferred *a priori*. It is on account of its evolutionary-morphological perspective that, so far as is possible given the cryptic biology of our study system, we address the functional and evolutionary implications of our findings; further, we communicate our findings with nomenclature that incorporates hypothesized homology and accommodates male genital variation not just in the Leptanillinae but the Hymenoptera as a whole. This establishes a foundation for a synthetic view of male genital evolution in the Leptanillinae, and indeed to the whole of the ants.

6. Author Contributions

Zachary Griebenow: Conceptualization, Methodology, Data Curation, Writing – Original Draft, Writing – Review & Editing, Visualization **Adrian Richter:** Investigation, Resources, Data Curation, Writing – Review & Editing, Visualization **Georg Fischer:** Investigation, Data Curation **Thomas van de Kamp:** Investigation **Evan Economo:** Data Curation, Funding Acquisition **Ziv Lieberman:** Conceptualization, Writing – Original Draft, Writing – Review & Editing, Visualization

7. Acknowledgements

We thank Dilworth Parkinson and Douglas Rowland for their tireless help in obtaining additional scan data for ingroup exemplars, despite the perpetually challenging minuteness of these

specimens. We also thank Phil Ward for providing feedback on the contents of the manuscript, along with advice and enduring support throughout the course of this project. We are grateful to Elias Hamann and Mathias Hurst for their assistance during the tomographic measurements at KIT and thank Tomáš Faragó for tomographic raw data reconstruction. Lastly, we thank all who provided specimens included in this study: José María Gómez-Durán, Brian Fisher (CASC), Jadranka Rota (MZLU), Lars Vilhelmsen (ZMUC), Kevin Williams (CSCA), and Masashi Yoshimura. This research used resources of the Advanced Light Source, which is a DOE Office of Science User Facility under contract no. DE-AC02-05CH11231. We acknowledge the KIT Light Source for provision of instruments at their beamlines and we would like to thank the Institute for Beam Physics and Technology (IBPT) for the operation of the storage ring, the Karlsruhe Research Accelerator (KARA).

REFERENCES

Alam SM (1952) Studies on “skeleto-muscular mechanism” of the male genitalia in *Stenobracon deesae* Cam. (Hymenoptera: Braconidae). Beiträge zur Entomologie, Band 2 2(6): 620–634.

Allard D, Gobin B, Ito F, Billen J, Tsuji K (2002) Sperm transfer in the Japanese queenless ant *Diacamma* sp. (Hymenoptera: Formicidae). Netherlands Journal of Zoology 52(1): 77–86. https://doi.org/10.1163/156854202760405203

Aspöck U (2002) Male genital sclerites of Neuropterida: An attempt at homologisation (Insecta: Holometabola). Zoologischer Anzeiger 241(2): 161–171. https://doi.org/10.1078/S0044-5231(04)70071-6

Audouin JV (1821) Observations sur les organes copulateurs mâles des Bourdons. Rapport lit par Latreille en lundi 9 avril. Annales générales des sciences physiques 8: 285–289.

Ball DE, Vinson SB (1984) Anatomy and histology of the male reproductive system of the fire ant, *Solenopsis invicta* Buren (Hymenoptera: Formicidae). International Journal of Insect Morphology and Embryology 13: 283–294.

Barden P, Boudinot BE, Lucky A (2017) Where fossils dare and males matter: combined morphological and molecular analysis untangles the evolutionary history of the spider ant genus *Leptomyrmex* Mayr (Hymenoptera: Dolichoderinae). Invertebrate Systematics 31(6): 765–780. https://doi.org/10.1071/IS16067

Baroni Urbani C, de Andrade ML (2006) A new *Protanilla* Taylor, 1990 (Hymenoptera: Formicidae: Leptanillinae) from Sri Lanka. Myrmecologische Nachrichten 8: 45–47.

Beck DE (1933) A morphological study of the male genitalia of various genera of bees. Doctor of Philosophy, Iowa State University, Digital Repository, Ames, 77 pp.: 6882999pp. https://doi.org/10.31274/rtd-180813-14568

Beutel RG, Friedrich F, Economo EP (2022) Patterns of morphological simplification and innovation in the megadiverse Holometabola (Insecta). Cladistics 38: 227–245. https://doi.org/10.1111/cla.12483

Birket-Smith J (1981) Male genitalia of Hymenoptera - a review based on morphology in Dorylidae (Hymenoptera: Formicoidea). Entomologia Scandinavica Supplement 15: 377–397.

Bolton B (1990a) Abdominal characters and status of the cerapachyine ants (Hymenoptera, Formicidae). Journal of Natural History 24(1): 53–68. https://doi.org/10.1080/00222939000770051

Bolton B (1990b) The higher classification of the ant subfamily Leptanillinae (Hymenoptera: Formicidae). Systematic Entomology 15: 262–282.

Boomsma JJ, Baer B, Heinze J (2005) The evolution of male traits in social insects. Annual Review of Entomology 50(1): 395–420. https://doi.org/10.1146/annurev.ento.50.071803.130416

Borgard HL, Baab K, Pasch B, Riede T (2020) The shape of sound: A geometric morphometrics approach to laryngeal functional morphology. Journal of Mammalian Evolution 27(3): 577–590. https://doi.org/10.1007/s10914-019-09466-9

Borowiec ML (2016) Generic revision of the ant subfamily Dorylinae (Hymenoptera, Formicidae). ZooKeys 608: 1–280. https://doi.org/10.3897/zookeys.608.9427

Borowiec ML, Rabeling C, Brady SG, Fisher BL, Schultz TR, Ward PS (2019) Compositional heterogeneity and outgroup choice influence the internal phylogeny of the ants. Molecular Phylogenetics and Evolution 134: 111–121. https://doi.org/10.1016/j.ympev.2019.01.024

Boudinot BE (2013) The male genitalia of ants: Musculature, homology, and functional morphology (Hymenoptera, Aculeata, Formicidae). Journal of Hymenoptera Research 30: 29–49. https://doi.org/10.3897/jhr.30.3535

Boudinot BE (2015) Contributions to the knowledge of Formicidae (Hymenoptera, Aculeata): A new diagnosis of the family, the first global male-based key to subfamilies, and a treatment of early branching lineages. European Journal of Taxonomy (120). https://doi.org/10.5852/ejt.2015.120

Boudinot BE (2018) A general theory of genital homologies for the Hexapoda (Pancrustacea) derived from skeletomuscular correspondences, with emphasis on the Endopterygota. Arthropod Structure & Development 47(6): 563–613. https://doi.org/10.1016/j.asd.2018.11.001

Boudinot BE, Moosdorf OTD, Beutel RG, Richter A (2021) Anatomy and evolution of the head of *Dorylus helvolus* (Formicidae: Dorylinae): Patterns of sex- and caste-limited traits in the sausagefly and the driver ant. Journal of Morphology: jmor.21410. https://doi.org/10.1002/jmor.21410

Boudinot BE, Probst RS, Brandão CRF, Feitosa RM, Ward PS (2016) Out of the Neotropics: newly discovered relictual species sheds light on the biogeographical history of spider ants (Leptomyrmex, Dolichoderinae, Formicidae). Systematic Entomology 41(3): 658–671. https://doi.org/10.1111/syen.12181

Boudinot BE, Khouri Z, Richter A, Griebenow ZH, van de Kamp T, Perrichot V, Barden P (2022) Evolution and systematics of the Aculeata and kin (Hymenoptera), with emphasis on the ants (Formicoidea: †@@@idae fam. nov., Formicidae). https://doi.org/10.1101/2022.02.20.480183

Boulangé H (1924) Recherces sur l'áppareil copulateur des Hyménopterès et spécialement des Chalastogastres. Mémoires et Travaux de la Faculté Catholique de Lille 28: 1–444.

Branstetter MG, Longino JT, Ward PS, Faircloth BC (2017) Enriching the ant tree of life: Enhanced UCE bait set for genome-scale phylogenetics of ants and other Hymenoptera. Methods in Ecology and Evolution 8(6): 768–776. https://doi.org/10.1111/2041-210X.12742

Brues CT (1925) *Scyphodon*, an anomalous genus of Hymenoptera of doubtful affinities. Treubia 6: 93–96.

Brusca RC (2001) Origin of the Hexapoda. Journal of Crustacean Biology 21(4): 1084–1086. https://doi.org/10.1163/20021975-99990201

Buenaventura E, Pape T (2018) Phylogeny, evolution and male terminalia functionality of Sarcophaginae (Diptera: Sarcophagidae). Zoological Journal of the Linnean Society 183(4): 808–906. https://doi.org/10.1093/zoolinnean/zlx070

Chapman RF, Simpson SJ, Douglas AE (2013) The insects: Structure and function. Fifth edition. Cambridge University Press, New York, 929 pp.

Chen Z-L, Shi F-M, Zhou S-Y (2017) First record of the monotypic genus *Opamyrma* (Hymenoptera: Formicidae) from China. Far Eastern Entomologist 335: 7–11.

Chiappini E, Mazzoni E (2000) Differing morphology and ultrastructure of the male copulatory apparatus in species-groups of *Anagrus* Haliday (Hymenoptera: Mymaridae). Journal of Natural History 34(8): 1661–1676. https://doi.org/10.1080/00222930050117549

Chiquetto-Machado PI, Cancello EM (2021) Cladistic analysis of *Paraphasma* (Phasmatodea: Pseudophasmatidae) highlights the importance of the phallic organ for phasmid systematics. Zoological Journal of the Linnean Society 193(1): 158–198. https://doi.org/10.1093/zoolinnean/zlab004

Clarke DJ (2011) Testing the phylogenetic utility of morphological character systems, with a revision of *Creophilus* Leach (Coleoptera: Staphylinidae). Zoological Journal of the Linnean Society 163(3): 723–812. https://doi.org/10.1111/j.1096-3642.2011.00725.x

Clausen R (1938) Untersuchungen über den männlichen Copulationsapparat der Ameisen, speziell der Formicinae. Mitteilungen der Schweizerischen Entomologischen Gesellschaft 17: 233–346.

Crampton GG (1919) The genitalia and terminal abdominal structures of males, and the terminal structures of the larvae of "chalastogastrous" Hymenoptera. Proceedings of the Entomological Society of Washington 21: 129–151.

Dirsh VM (1956) The phallic complex in Acridoidea (Orthoptera) in relation to taxonomy. Transactions of the Royal Entomological Society of London 108(7): 223–270. https://doi.org/10.1111/j.1365-2311.1956.tb02270.x

Domenichini G (1953) Studio sulla morfologia dell'addome degli Hymenoptera Chalcidoidea. Bollettino di Zoologia Agraria e Bachicultura, Milano 19: 183–298.

Dreyer AP, Shingleton AW (2011) The effect of genetic and environmental variation on genital size in male *Drosophila*: canalized but developmentally unstable. PLOS ONE 6(12): e28278. https://doi.org/10.1371/journal.pone.0028278

Dufour L (1848) Anatomie générale des Dipteres. Annuare de Science Naturelle 1: 244–264.

Eberhard WG (1985) Sexual Selection and Animal Genitalia. Harvard University Press, Cambridge, Mass. Available from: http://www.degruyter.com/search?f_0=isbnissn&q_0=9780674330702&searchTitles=true (April 8, 2022).

Eguchi K, Yoshimura M, Yamane S (2006) The Oriental species of the ant genus *Probolomyrmex* (Insecta: Hymenoptera: Formicidae: Proceratiinae). Zootaxa 1376(1): 1. https://doi.org/10.11646/zootaxa.1376.1.1

Evenhuis NL (2022) The insect and spider collections of the world website. Available from: http://hbs.bishopmuseum.org/codens/.

Fisher RA (1930) The genetical theory of natural selection. Oxford Clarendon Press, 306 pp. Available from: http://archive.org/details/geneticaltheoryo00fishuoft (April 8, 2022).

Forbes J (1954) The anatomy and histology of the male reproductive system of *Camponotus pennsylvanicus* DeGeer (Formicidae, Hymenoptera). Journal of Morphology 95: 523–555.

Forbes J, Do-Van-Quy D (1965) The anatomy and histology of the male reproductive system of the legionary ant, *Neivamyrmex harrisi* (Haldeman) (Hymenoptera: Formicidae). Journal of the New York Entomological Society 73: 95–111. https://doi.org/10.25849/myrmecol.news_030:229

Forbes J, Hagopian M (1965) The male genitalia and terminal segments of the ponerine ant *Rhytidoponera metallica* F. Smith (Hymenoptera: Formicidae). Journal of the New York Entomological Society 73(4): 190–194.

Friedrich F, Beutel RG (2008) The thorax of *Zorotypus* (Hexapoda, Zoraptera) and a new nomenclature for the musculature of Neoptera. Arthropod Structure & Development 37(1): 29–54. https://doi.org/10.1016/j.asd.2007.04.003

Fuessl M, Heinze J, Schrempf A (2015) Queen and male longevity in the Southeast Asian ant *Cardiocondyla tjibodana* Karavaiev, 1935. Asian Myrmecology 7: 137–141.

Futuyma DJ (1998) Evolutionary Biology. 3rd ed. Sinauer Associates Inc., Massachusetts.

Génier F (2019) Endophallites: a proposed neologism for naming the sclerotized elements of the insect endophallus (Arthropoda: Insecta). Annales de la Société entomologique de France (N.S.) 55(6): 482–484. https://doi.org/10.1080/00379271.2019.1685907

Gibson GAP (1986) Evidence for monophyly and relationships of Chalcidoidea, Mymaridae, and Mymarommatidae (Hymenoptera: Terebrantes). The Canadian Entomologist 118(3): 205–240. https://doi.org/10.4039/Ent118205-3

Gibson GAP, Read J, Huber JT (2007) Diversity, classification and higher relationships of Mymarommatoidea (Hymenoptera). Journal of Hymenoptera Research 16(1): 51–146.

Girón JC, Tarasov S, González Montaña LA, Matentzoglu N, Smith AD, Koch M, Boudinot BE, Bouchard P, Burks R, Vogt L, Yoder M, Osumi-Sutherland D, Friedrich F, Beutel R, Mikó I (2022) Formalizing insect morphological data: A model-based, extensible insect anatomy

ontology and its potential applications in biodiversity research and informatics. https://doi.org/10.20944/preprints202201.0254.v1

Griebenow ZH (2020) Delimitation of tribes in the subfamily Leptanillinae (Hymenoptera: Formicidae), with a description of the male of *Protanilla lini* Terayama, 2009. Myrmecological News 30: 229–250. https://doi.org/10.25849/myrmecol.news_030:229

Griebenow ZH (2021) Synonymisation of the male-based ant genus *Phaulomyrma* (Hymenoptera: Formicidae) with *Leptanilla* based upon Bayesian total-evidence phylogenetic inference. Invertebrate Systematics 35: 603–636. https://doi.org/10.1071/IS20059

Griebenow ZH, Isaia M, Moradmand M (2022) A remarkable troglomorphic ant, *Yavnella laventa* sp. nov. (Hymenoptera: Formicidae: Leptanillinae), identified as the first known worker of *Yavnella* Kugler by phylogenomic inference. Invertebrate Systematics 36(12): 1118–1138. https://doi.org/10.1071/IS22035

Günther KK (1961) Funktionell-anatomische Untersuchung des männlichen Kopulationsapparates der Flöhe unter Berücksichtigung seiner postembryonalen Entwicklung (Siphonaptera). Deutsche Entomologische Zeitschrift 8: 258–349.

Hagopian M (1963) An anatomical and histological study of the male ponerine ant, *Rhytidoponera metallica* F. Smith (Formicidae, Hymenoptera). Doctor of Philosophy, Fordham University, New York, 110 pp.

Hansson CT (1996) A new genus of Eulophidae (Hymenoptera: Chalcidoidea) with remarkable male genitalia. Systematic Entomology 21(1): 39–62. https://doi.org/10.1111/j.1365-3113.1996.tb00598.x

Hosken DJ, Stockley P (2004) Sexual selection and genital evolution. Trends in Ecology & Evolution 19(2): 87–93. https://doi.org/10.1016/j.tree.2003.11.012

Hsu P-W, Hsu F-C, Hsiao Y, Lin C-C (2017) Taxonomic notes on the genus *Protanilla* (Hymenoptera: Formicidae: Leptanillinae) from Taiwan. Zootaxa 4268(1): 117–130. https://doi.org/10.11646/zootaxa.4268.1.7

Ito F, Yamane S (2020) Behavior of the queen of *Leptanilla clypeata* Yamane et Ito collected in the Bogor Botanical Gardens, West Java, Indonesia (Hymenoptera; Formicidae), with a note on colony composition and a description of the ergatoid queen. Asian Myrmecology 12: e012004. https://doi.org/10.20362/AM.012004

Ito F, Hashim R, Mizuno R, Billen J (2021) Notes on the biology of *Protanilla* sp. (Hymenoptera, Formicidae) collected in Ulu Gombak, Peninsular Malaysia. Insectes Sociaux 69(1): 13–18. https://doi.org/10.1007/s00040-021-00839-z

Kaestner A, Wetzel A (1972) Lehrbuch der Speziellen Zoologie: Band 1: Wirbellose: 3. Teil: Insecta: A. Algemeiner Teil. Fischer Verlag.

Kamimura Y (2008) Copulatory wounds in the monandrous ant species *Formica japonica* (Hymenoptera, Formicidae). Insectes Sociaux 55(1): 51–53. https://doi.org/10.1007/s00040-007-0968-z

von Kéler S (1955) Entomologisches Worterbuch. Akademie-Verlag, Berlin, 679 pp.

Kempf WW (1954) A descoberta do primeiro macho do gênero *Thaumatomyrmex* Mayr (Hymenoptera: Formicidae). Revista Brasileira de Entomologia 1: 47–52.

Kempf WW (1956) A morphological study on the male genitalia of *Paracryptocerus (P.) pusillus* (Hymenoptera: Formicidae). Revista Brasileira de Entomologia 5: 101–110.

Kluge MHE (1895) Das männliche Geschlechtsorgan von *Vespa germanica*. Archiv für Naturgeschichte (a) 61: 159–168.

Koeniger N, Koeniger G (1991) An evolutionary approach to mating behaviour and drone copulatory organs in *Apis*. Apidologie 22(6): 581–590. https://doi.org/10.1051/apido:19910602

Kugler J (1986) The Leptanillinae (Hymenoptera: Formicidae) of Israel and a description of a new species from India. Israel Journal of Entomology 20: 45–57.

Kutter H (1948) Beitrag zur Kenntnis der Leptanillinae (Hym. Formicidae). Eine neue Ameisengattung aus Süd-Indien. Mitteilungen der Schweizerischen Entomologischen Gesellschaft 21: 286–295.

Lapolla JS, Kallal RJ, Brady SG (2012) A new ant genus from the Greater Antilles and Central America, *Zatania* (Hymenoptera: Formicidae), exemplifies the utility of male and molecular character systems. Systematic Entomology 37(1): 200–214. https://doi.org/10.1111/j.1365-3113.2011.00605.x

Lieberman ZE, Billen J, van de Kamp T, Boudinot BE (2022) The ant abdomen: The skeletomuscular and soft tissue anatomy of *Amblyopone australis* workers (Hymenoptera: Formicidae). Journal of Morphology 283(6): 693–770. https://doi.org/10.1002/jmor.21471

MacGown JA, Boudinot BE, Deyrup M, Sorger DM (2014) A review of the Nearctic *Odontomachus* (Hymenoptera: Formicidae: Ponerinae) with a treatment of the males. Zootaxa 3802(4): 515. https://doi.org/10.11646/zootaxa.3802.4.6

Marcus H (1953) Estudios mirmecológicos. Folia Universitaria Cochabamba 6: 14–68.

Masuko K (1990) Behavior and ecology of the enigmatic ant *Leptanilla japonica* Baroni Urbani (Hymenoptera: Formicidae: Leptanillinae). Insectes Sociaux 37(1): 31–57.

Mayr E (1963) Animal Species and Evolution. Harvard University Press. Available from: https://doi.org/10.4159/harvard.9780674865327 (April 8, 2022).

Michener CD (1944) A comparative study of the appendages of the eighth and ninth abdominal segments of insects. Annals of the Entomological Society of America 37(3): 336–351. https://doi.org/10.1093/aesa/37.3.336

Mikó I, Masner L, Johannes E, Yoder MJ, Deans AR (2013) Male terminalia of Ceraphronoidea: morphological diversity in an otherwise monotonous taxon. Insect Systematics & Evolution 44(3–4): 261–347. https://doi.org/10.1163/1876312X-04402002

Misof B, Liu S, Meusemann K, Peters RS, Donath A, Mayer C, Frandsen PB, Ware J, Flouri T, Beutel RG, Niehuis O, Petersen M, Izquierdo-Carrasco F, Wappler T, Rust J, Aberer AJ, Aspöck U, Aspock H, Bartel D, Blanke A, Berger S, Bohm A, Buckley TR, Calcott B, Chen J, Friedrich F, Fukui M, Fujita M, Greve C, Grobe P, Gu S, Huang Y, Jermiin LS, Kawahara AY, Krogmann L, Kubiak M, Lanfear R, Letsch H, Li Y, Li Z, Li J, Lu H, Machida R, Mashimo Y, Kapli P, McKenna DD, Meng G, Nakagaki Y, Navarrete-Heredia JL, Ott M, Ou Y, Pass G, Podsiadlowski L, Pohl H, von Reumont BM, Schutte K, Sekiya K, Shimizu S, Slipinski A,

Stamatakis A, Song W, Su X, Szucsich NU, Tan M, Tan X, Tang M, Tang J, Timelthaler G, Tomizuka S, Trautwein M, Tong X, Uchifune T, Walzl MG, Wiegmann BM, Wilbrandt J, Wipfler B, Wong TKF, Wu Q, Wu G, Xie Y, Yang S, Yang Q, Yeates DK, Yoshizawa K, Zhang Q, Zhang R, Zhang W, Zhang Y, Zhao J, Zhou C, Zhou L, Ziesmann T, Zou S, Li Y, Xu X, Zhang Y, Yang H, Wang J, Wang J, Kjer KM, Zhou X (2014) Phylogenomics resolves the timing and pattern of insect evolution. Science 346(6210): 763–767. https://doi.org/10.1126/science.1257570

Monnin T, Peeters C (1998) Monogyny and regulation of worker mating in the queenless ant *Dinoponera quadriceps*. Animal Behaviour 55(2): 299–306. https://doi.org/10.1006/anbe.1997.0601

Moreau CS, Bell CD (2013) Testing the museum versus cradle tropical biological diversity hypothesis: Phylogeny, diversification, and ancestral biogeographic range evolution of the ants. Evolution 67(8): 2240–2257. https://doi.org/10.1111/evo.12105

Ogata K (1991) A generic synopsis of the poneroid complex of the family Formicidae (Hymenoptera). Part II. Subfamily Myrmicinae. Bulletin of the Institute of Tropical Agriculture Kyushu University 14: 61–149.

Ogata K, Terayama M, Masuko K (1995) The ant genus *Leptanilla*: Discovery of the worker-associated male of *L. japonica*, and a description of a new species from Taiwan (Hymenoptera: Formicidae: Leptanillinae). Systematic Entomology 20: 27–34.

Peck O (1937) The male genitalia in the Hymenoptera (Insecta), especially the family Ichneumonidae: I. Comparative morphology. Canadian Journal of Research 15d(11): 221–252. https://doi.org/10.1139/cjr37d-018

Petersen B (1968) Some novelties in presumed males of Leptanillinae (Hym., Formicidae). Entomologiske Meddelelser 36: 577–598.

de Pinna MCC (1991) Concepts and tests of homology in the cladistic paradigm. Cladistics 7(4): 367–394. https://doi.org/10.1111/j.1096-0031.1991.tb00045.x

Remane A (1952) Die Grundlagen des natürlichen Systems, der vergleichenden Anatomie und der Phylogenetik. Geest & Portig K.-G., Leipzig, 400 pp.

von Reumont BM, Jenner RA, Wills MA, Dell'Ampio E, Pass G, Ebersberger I, Meyer B, Koenemann S, Iliffe TM, Stamatakis A, Niehuis O, Meusemann K, Misof B (2012) Pancrustacean phylogeny in the light of new phylogenomic data: Support for Remipedia as the possible sister group of Hexapoda. Molecular Biology and Evolution 29(3): 1031–1045. https://doi.org/10.1093/molbev/msr270

Richter S, Wirkner CS (2014) A research program for evolutionary morphology. Journal of Zoological Systematics and Evolutionary Research 52(4): 338–350. https://doi.org/10.1111/jzs.12061

Rodrigue N, Philippe H (2010) Mechanistic revisions of phenomenological modeling strategies in molecular evolution. Trends in Genetics 26(6): 248–252. https://doi.org/10.1016/j.tig.2010.04.001

Romiguier J, Borowiec ML, Weyna A, Helleu Q, Loire E, La Mendola C, Rabeling C, Fisher BL, Ward PS, Keller L (2022) Ant phylogenomics reveals a natural selection hotspot preceding the origin of complex eusociality. Current Biology: S0960982222007606. https://doi.org/10.1016/j.cub.2022.05.001

Ross HH (1937) A generic classification of the Nearctic sawflies (Hymenoptera, Symphyta). Illinois Biological Monographs 15(2): 1–173.

Sanderson MJ, Donoghue MJ (1989) Patterns of variation in levels of homoplasy. Evolution 43(8): 1781–1795. https://doi.org/10.1111/j.1558-5646.1989.tb02626.x

Santschi F (1907) Fourmis de Tunisie capturées en 1906. Revue Suisse de Zoologie 15: 305–334.

Santschi F (1908) Nouvelles fourmis de l'Afrique du Nord (Égypte, Canaries, Tunisie). Annales de la Société Entomologique de France 77: 517–534.

Schmidt CV, Heinze J (2017) Genital morphology of winged and wingless males in the ant genus *Cardiocondyla* (Formicidae, Myrmicinae). Insect Systematics & Evolution 49(1): 59–80. https://doi.org/10.1163/1876312X-48022163

Schulmeister S (2001) Functional morphology of the male genitalia and copulation in lower Hymenoptera, with special emphasis on the Tenthredinoidea s. str. (Insecta, Hymenoptera, 'Symphyta'). Acta Zoologica 82(4): 331–349. https://doi.org/10.1046/j.1463-6395.2001.00094.x

Schulmeister S (2003) Genitalia and terminal abdominal segments of male basal Hymenoptera (Insecta): morphology and evolution. Organisms Diversity & Evolution 3(4): 253–279. https://doi.org/10.1078/1439-6092-00078

Seltmann K, Yoder M, Mikó I, Forshage M, Bertone M, Agosti D, Austin A, Balhoff J, Borowiec M, Brady SG, Broad G, Brothers D, Burks R, Buffington M, Campbell H, Dew K, Ernst A, Fernández-Triana J, Gates M, Gibson G, Jennings J, Johnson N, Karlsson D, Kawada R, Krogmann L, Kula R, Mullins P, Ohl M, Rasmussen C, Ronquist F, Schulmeister S, Sharkey M, Talamas E, Tucker E, Vilhelmsen L, Ward PS, Wharton R, Deans A (2012) A hymenopterists' guide to the Hymenoptera Anatomy Ontology: utility, clarification, and future directions. Journal of Hymenoptera Research 27: 67–88. https://doi.org/10.3897/jhr.27.2961

Shyamalanath S, Forbes J (1983) Anatomy and histology of the male reproductive system in the adult and pupa of the doryline ant, *Aenictus gracilis* Emery (Hymenoptera: Formicidae). Journal of the New York Entomological Society 91(4): 377–393.

Simmons LW (2014) Sexual selection and genital evolution. Austral Entomology 53(1): 1–17. https://doi.org/10.1111/aen.12053

Simpson GG (1953) The Major Features of Evolution. Columbia University Press, New York Chichester, West Sussex, 436 pp. Available from: doi.org/ 9780231895330.

Sloan NS, Simmons LW (2019) The evolution of female genitalia. Journal of Evolutionary Biology 32(9): 882–899. https://doi.org/10.1111/jeb.13503

Smith EL (1969) Evolutionary morphology of external insect genitalia. 1. Origin and relationships to other appendages. Annals of the Entomological Society of America 62(5): 1051–1079.

Smith EL (1970) Evolutionary morphology of the external insect genitalia. 2. Hymenoptera. Annals of the Entomological Society of America 63(1): 1–27. https://doi.org/10.1093/aesa/63.1.1

Smith EL (1972) Biosystematics and morphology of symphyta—III. External genitalia of *Euura* (Hymenoptera: Tenthredinidae): Sclerites, sensilla, musculature, development and oviposition behavior. International Journal of Insect Morphology and Embryology 1(4): 321–365. https://doi.org/10.1016/0020-7322(72)90016-5

Snodgrass RE (1935a) Principles of Insect Morphology. McGraw-Hill Book Company, Inc.

Snodgrass RE (1935b) The abdominal mechanisms of a grasshopper. Smithsonian Miscellaneous Collections 94(6).

Snodgrass RE (1941) The male genitalia of Hymenoptera. Smithsonian Miscellaneous Collections 99(14): 123.

Snodgrass RE (1942) The skeleto-muscular mechanisms of the honey bee. Smithsonian Miscellaneous Collections 103(2): 124.

Snodgrass RE (1957) A revised interpretation of the external reproductive organs of male insects. Smithsonian Miscellaneous Collections 135(6): 64.

Song H, Bucheli SR (2010) Comparison of phylogenetic signal between male genitalia and non-genital characters in insect systematics. Cladistics 26(1): 23–35. https://doi.org/10.1111/j.1096-0031.2009.00273.x

Tarasov SI, Solodovnikov AY (2011) Phylogenetic analyses reveal reliable morphological markers to classify mega-diversity in Onthophagini dung beetles (Coleoptera: Scarabaeidae: Scarabaeinae). Cladistics 27(5): 490–528. https://doi.org/10.1111/j.1096-0031.2011.00351.x

Taylor RW (1978) *Nothomyrmecia macrops*: A living-fossil ant rediscovered: The most primitive living ant, previously an enigma, rediscovered and the subject of international study. Science 201(4360): 979–985. https://doi.org/10.1126/science.201.4360.979

Tozetto L, Lattke JE (2020) Revealing male genital morphology in the giant ant genus *Dinoponera* with geometric morphometrics. Arthropod Structure & Development 57: 100943. https://doi.org/10.1016/j.asd.2020.100943

Trakimas WB (1967) An anatomical and histological study of the male myrmicine ant, *Myrmica rubra*, L. (Hymenoptera: Formicidae). Doctor of Philosophy, Fordham University, New York, 125 pp.

Tuxen SL (Ed.) (1970) Taxonomist's glossary of genitalia in insects. 2nd ed. Munksgaard, Copenhagen, 362 pp. Available from: http://antbase.org/ants/publications/21060/21060.pdf (April 8, 2022).

Vidal-García M, Bandara L, Keogh JS (2018) ShapeRotator: An R tool for standardized rigid rotations of articulated three-dimensional structures with application for geometric morphometrics. Ecology and Evolution 8(9): 4669–4675. https://doi.org/10.1002/ece3.4018

Viggiani G (1973) Osservazioni morfobiologiche sull'*Azotus pulcherrimus* Merc. (Hymenoptera: Aphelinidae). Bollettino del Laboratorio di Entomologia Agraria "Filippo Silvestri", Portici 30: 300–311.

Wang WY, Yamada A, Eguchi K (2019) Discovery of a new ant species of the elusive termitophilous genus *Metapone* in Singapore (Hymenoptera, Formicidae, Myrmicinae), with the first detailed description of male genitalia of the genus. ZooKeys 876: 125–141. https://doi.org/10.3897/zookeys.876.35739

Ward PS (2001) Taxonomy, phylogeny and biogeography of the ant genus *Tetraponera* (Hymenoptera: Formicidae) in the Oriental and Australian regions. Invertebrate Taxonomy 15: 589–665.

Ward PS (2007) The ant genus *Leptanilloides*: Discovery of the male and evaluation of phylogenetic relationships based on DNA sequence data. Memoirs of the American Entomological Institute 80: 637–649.

Ward PS, Downie DA (2005) The ant subfamily Pseudomyrmecinae (Hymenoptera: Formicidae): Phylogeny and evolution of big-eyed arboreal ants. Systematic Entomology 30(2): 310–335. https://doi.org/10.1111/j.1365-3113.2004.00281.x

Ward PS, Sumnicht TP (2012) Molecular and morphological evidence for three sympatric species of Leptanilla (Hymenoptera: Formicidae) on the Greek island of Rhodes. Myrmecological News 17: 5–11.

Ward PS, Fisher BL (2016) Tales of dracula ants: the evolutionary history of the ant subfamily Amblyoponinae (Hymenoptera: Formicidae). Systematic Entomology 41(3): 683–693. https://doi.org/10.1111/syen.12186

Ward PS, Boudinot BE (2021) Grappling with homoplasy: Taxonomic refinements and reassignments in the ant genera *Camponotus* and *Colobopsis* (Hymenoptera: Formicidae). Arthropod Systematics & Phylogeny 79: 37–56. https://doi.org/10.3897/asp.79.e66978

Wheeler GC, Wheeler EW (1930) Two new ants from Java. Psyche (Cambridge) 37: 193–201.

Willmann VR (1981) Das Exoskelett der männlichen Genitalien der Mecoptera (Insecta): I. Morphologie. Journal of Zoological Systematics and Evolutionary Research 19(2): 96–150. https://doi.org/10.1111/j.1439-0469.1981.tb00235.x

Yamada A, Nguyen D, Eguchi K (2020) Unveiling the morphology of the Oriental rare monotypic ant genus *Opamyrma* Yamane, Bui & Eguchi, 2008 (Hymenoptera: Formicidae: Leptanillinae) and its evolutionary implications, with first descriptions of the male, larva, tentorium, and sting apparatus. Myrmecological News 30: 27–52. https://doi.org/10.25849/myrmecol.news_030:027

Yamane S, Bui TV, Eguchi K (2008) *Opamyrma hungvuong*, a new genus and species of ant related to *Apomyrma* (Hymenoptera: Formicidae: Amblyoponinae). Zootaxa 1767(1): 55. https://doi.org/10.11646/zootaxa.1767.1.3

Yoder MJ, Mikó I, Seltmann KC, Bertone MA, Deans AR (2010) A gross anatomy ontology for Hymenoptera. PLOS ONE 5(12): e15991. https://doi.org/10.1371/journal.pone.0015991

Yoshizawa K, Johnson KP (2006) Morphology of male genitalia in lice and their relatives and phylogenetic implications. Systematic Entomology 31(2): 350–361. https://doi.org/10.1111/j.1365-3113.2005.00323.x

Youssef NN (1969) Musculature, nervous system and glands of metasomal abdominal segments of the male of *Nomia melanderi* Ckll. (Hymenoptera, Apoidea). Journal of Morphology 129(1): 59–79. https://doi.org/10.1002/jmor.1051290105

Supplementary Tables, Chapter 3

Table 3.S1. Scan settings for all 19 datasets here published. Fundamental differences in modality between X-ray microscopes and synchrotrons result in reciprocal inapplicability of some scan parameters here reported.

Table 3.S2. Nomenclatural equivalencies in hymenopteran male genital sclerites across a selection of morphological studies. HAO URIs are unique reference identifiers; the associated webpage can be accessed by appending the URI to the URL https://purl.obolibrary/org/obo/.

Table 3.S3. Muscular nomenclature used in this study and equivalencies with selected systems. The Boulangé (1924) names are supplemented by the additions of Schulmeister (2001; 2003) and Boudinot (2013). HAO URIs are unique reference identifiers; the associated webpage can be accessed by appending the URI to the URL https://purl.obolibrary/org/obo/.

Table 3.S4. Muscular observations across the 12 exemplars described in detail in this study. 1 = presence; 0 = absence; - = inapplicable (sclerite hosting muscle origin or insertion absent).

Chapter 4. Systematic revision of the ant subfamily Leptanillinae (Hymenoptera, Formicidae)

Abstract. The genus-level taxonomy of the ant subfamily Leptanillinae (Hymenoptera: Formicidae) is here revised, with the aim of delimiting genus-level taxa that are reciprocally monophyletic and readily diagnosable based upon all adult forms. This new classification reflects molecular phylogenetic results and is informed by joint consideration of both male and worker morphology. Three valid genera are recognized in the Leptanillinae: *Opamyrma*, *Leptanilla* (= *Scyphodon* **syn. nov.**, *Phaulomyrma*, *Noonilla* **syn. nov.**, *Yavnella* **syn. nov.**), and *Protanilla* (= *Anomalomyrma* **syn. nov.**, *Furcotanilla*). *Leptanilla* and *Protanilla* are respectively divided into five and four informal putatively monophyletic species-groups. Eight and one species are respectively left unplaced to species-group in *Leptanilla* and *Protanilla*. Synoptic diagnoses are provided for all genera and informal supraspecific groupings. In addition, the following keys are provided: a worker-based key to all described species within the Leptanillinae for which the worker caste is known; a male-based key to all species for which males are known, plus undescribed male morphospecies for which molecular data are published; and worker- and male-based keys to the genera as defined in this study. The following species are described as new: *Protanilla wallacei* **sp. nov.**, *Leptanilla acherontia* **sp. nov.**, *Leptanilla belantan* **sp. nov.**, *Leptanilla najaphalla* **sp. nov.**, and *Leptanilla bethyloides* **sp. nov.**

Introduction

The subfamily Leptanillinae (Hymenoptera: Formicidae), sometimes called *legionary vampire ants* (Ward and Boudinot, 2021), consists of cryptic, hypogaeic ants largely restricted to tropical and warm temperate regions of the Old World, although *Protanilla beijingensis* Man *et al.* and

Leptanilla taiwanensis Ogata *et al.* have been collected in a cold temperate climate . Most of their diversity is concentrated in the Indo-Malayan region. While the affinities of the Leptanillinae to other ants have historically been controversial, phylogenetic inference from molecular data that corrects for compositional heterogeneity in nucleotides supports the monotypic Neotropical genus *Martialis* Rabeling and Verhaagh as the sister-group of the Leptanillinae, with this clade collectively being sister to all other extant Formicidae (Borowiec et al., 2019; Romiguier et al., 2022; Chapter 5).

Colonies of *Protanilla jongi* Hsu *et al.* and *Leptanilla belantan* **sp. nov.** were collected in decaying wood (Hsu et al., 2017; this study), and foraging workers of *Protanilla lini* Terayama in Sea, Land and Air Malaise (SLAM) traps (Griebenow, 2020), but leptanilline workers are otherwise exclusively subterranean. Based on limited observations of live colonies, it appears that leptanilline ants are specialized predators of geophilomorph centipedes or forcepstails (Diplura: Japygidae) (Hsu et al., 2017; Ito et al., 2022; Masuko, 1990), with *P. lini* feeding on other prey (e.g., lithobiomorph centipedes, cockroaches) in captivity (Katayama and Tsuji, 2011; Yamamuro, 2018). *Leptanilla* display aspects of the "army ant syndrome" commonly associated with *Dorylus*, *Eciton*, and related lineages in the subfamily Dorylinae: *Leptanilla japonica* Baroni Urbani and *Leptanilla clypeata* Yamane and Ito engage in synchronized brood production (Ito and Yamane, 2020; Masuko, 1990) and regular colony migration, with the physogastry reported in *Leptanilla charonea* Barandica *et al.* and *Leptanilla zaballosi* Barandica *et al.* indicating synchronized brood production in at least those species as well (López et al., 1994). Gynes of *Leptanilla* are always wingless and blind. It is unclear whether *Protanilla* (the only other leptanilline genus for which any bionomic data are available) display legionary behavior, but the alate condition of *Protanilla* gynes (except for *Protanilla wallacei* **sp. nov.** [Billen et al.,

2013; Ito et al., 2022]) contraindicate this. Intracolonial conformity of larval instar in an undescribed *Protanilla* nr. *bicolor* Griebenow et al. (in prep.) indicates synchronized brood production in at least that species. Gynes of *L. japonica* and *L. clypeata*, and the worker of *L. clypeata*, engage in larval hemolymph feeding (LHF) via a specialized "larval hemolymph tap" (Masuko, 1989) that acts as an exudatorium (Wheeler, 1918), facilitating non-traumatic LHF (Ito and Yamane, 2020; Masuko, 1989); such an exudatorium is otherwise known in ants only in *Proceratium itoi* (Proceratiinae) (Masuko, 2019). Larvae of *Leptanilla* bear a prothoracic process (Barandica et al., 1994; Kugler, 1987; Wheeler and Wheeler, 1988; Wheeler, 1918) that is used as a grip by workers during colony migration (Masuko, 1990). The larvae of *Protanilla jongi* examined in this study lack this process.

The internal taxonomy of the Leptanillinae has been afflicted with probable parallelism, since males are collected more often than workers or gynes: both genus- and species-group names were established based solely upon male specimens. The sexes are only directly associated in *L. japonica* (Ogata et al., 1995) and *Opamyrma hungvuong* Yamane et al. (Yamada et al., 2020), while Griebenow (2020) associated the sexes of *P. lini* with phylogenomic inference. The genera *Scyphodon* Brues, *Noonilla* Petersen, and *Yavnella* Kugler were all described solely from male material, with the worker of *Yavnella* being identified *ex post facto* by phylogenomic inference (Chapter 2). Total-evidence Bayesian inference recovered the male-based genus *Phaulomyrma* Wheeler and Wheeler within *Leptanilla s. str.* (Chapter 1), resulting in its synonymy under *Leptanilla*, with Griebenow (2020; Chapter 1) delimiting *Leptanilla s. l.* to also include *Noonilla* and *Scyphodon*, along with two major clades known only from undescribed male morphospecies. The boundaries of *Leptanilla* relative to the three male-based genera must therefore be formally revised. Generic boundaries in the former Anomalomyrmini require revision as well, with

phylogenetic inference consistently recovering *Protanilla* as paraphyletic relative to *Anomalomyrma* irrespective of dataset or statistical framework (e.g., Borowiec et al., 2019; Chapter 5).

With the internal phylogeny of the tribe Leptanillini confidently resolved by a combination of total-evidence and phylogenomic approaches (Chapter 5), including the identification of workers of *Yavnella* and *Scyphodon s. l.*, worker and male morphology can be contextualized on this robust phylogeny. Therefore, the time is ripe for revision of the Leptanillinae at the genus level. What follows is a systematic revision of the subfamily to establish reciprocally monophyletic and consistently diagnosable genera and species-groups. In addition, *Protanilla wallacei* **sp. nov.**, *Leptanilla belantan* **sp. nov.** and *Leptanilla acherontia* **sp. nov.** are described based upon worker specimens. To provide a formal name for the Bornean morphospecies-group of *Leptanilla s. l.* (Griebenow, 2020) (Chapter 1), known only from bizarre males, *Leptanilla najaphalla* **sp. nov.** is described based solely upon male specimens. Likewise, to establish a formal name for the Indochinese morphospecies-group (Chapter 3), *Leptanilla bethyloides* **sp. nov.** is described based on male specimens. The first global worker-based key to all species of the Leptanillinae is also included, along with a male-based species-level key revised from Griebenow (2020: pp. 241-244).

Methods

Methods and material examined

Specimens were imaged using the same equipment as reported in Griebenow (2020) and Chapters 1-2, with the addition of a VHX-970F digital microscope (Keyence, Osaka, Japan). Specimens are deposited in the following institutions, with abbreviations following Evenhuis (2021): the Bernice P. Bishop Museum, Honolulu, USA (BPBM); the California Academy of

Sciences, San Francisco, USA (CAS); the California State Collection of Arthropods, Sacramento, USA (CSCA); the Biodiversity Museum, University of Hong Kong, China (HKUBM); the Jalal Afshar Zoological Museum, Department of Plant Protection, College of Agriculture and Natural Resources, University of Tehran, Karaj, Iran (JAZM); the Los Angeles County Museum of Natural History, Los Angeles, USA (LACM); the Museum of Comparative Zoology, Cambridge, USA (MCZC); Lund University, Lund, Sweden (MZLU); National Changhua University of Education, Changhua, Taiwan (NCUE); the Okinawa Institute of Science and Technology, Onna-son, Japan (OIST); the Royal Ontario Museum, Toronto, Canada (ROME); the R. M. Bohart Museum of Entomology, University of California, Davis, USA (UCDC); the Museum für Naturkunde der Humboldt-Universität, Berlin, Germany (ZMHB); and the Zoological Museum, University of Isfahan, Isfahan, Iran (ZMUI). I also consulted the personal collections of José María Gómez-Durán (JMGDC), John T. Longino (JTLC), and Philip Ward (PSWC). Discrepancy in provisional morphospecies identifiers with those used in previous studies is resolved by Table 5.1.

Measurements

HW = maximum width of cranium in full-face view

HL = Head Length, maximum length of head in full-face view from anterior margin of head capsule to cranial vertex

SL = Scape Length, maximum length of scape in medial view, excluding bulbus

LF2 = Third Antennomere Length, length of the basal flagellomere

MaL = Mandible Length, maximum length of mandible from view orthogonal to lateral mandibular margin, measured from ventral mandibular articulation to mandibular apex

WL = Weber's Length, maximum diagonal distance measured from most anterior extent of pronotum excluding cervical shield to most posteroventral extremity of the mesosoma, including propodeal lobes if present

PrW = Pronotal width, maximum width of pronotum, measured in dorsal view

MW = Mesonotal width, maximum width of mesonotum in dorsal view, measured immediately anterior to mesocoxal foramina

PTL = Petiolar length, maximum length of petiole in dorsal view, not including presclerites

PTH = Petiolar height, maximum height of petiole in profile view, including sternal process and dorsal node, if distinct

PTW = Petiolar width, maximum width of petiole in dorsal view

PPL = Postpetiolar length, maximum length of postpetiole in dorsal view, not including presclerites

PPW = Postpetiolar width, maximum width of postpetiole in dorsal view

PPH = Postpetiolar height, maximum height of postpetiole in profile view, including sternal process and dorsal node, if distinct

TW4 = Width of abdominal tergite IV, maximum width of abdominal tergite IV measured in dorsal view

Indices

CI = (HW / HL) × 100

SI = (SL / HW) × 100

MI = (MaL / HW) × 100

PI = (PTW / PTL) × 100

PPI = (PPW / PPL) × 100

TI1 = (PPW / TW4) × 100

Nomenclature

Nomenclature for sculpturation and setation combines Harris (1979), Wilson (1955), and Boudinot et al. (2020). Notational conventions for palp and tibial spur formulae follow Bolton (2003). Cephalic nomenclature follows Richter et al. (2021) and Boudinot et al. (2021). Mesosomal nomenclature follows Liu et al. (2019); metasomal, Lieberman et al. (2022). Male genital nomenclature follows Boudinot (2018). Descriptive terms for larval morphology follow Wheeler and Wheeler (1986, 1976). Wing venation is described using Brown and Nutting (1949) and Ogata (1991), with interpretation of homologies in male wing venation following Boudinot (2015) in some ambiguous cases observed in *Leptanilla*. Any morphological terms unaddressed in these publications follow the Hymenoptera Anatomy Ontology (Yoder et al., 2010). Glossaries of external morphological terms for worker and male Leptanillinae are summarized in Figs. 4.1-3.

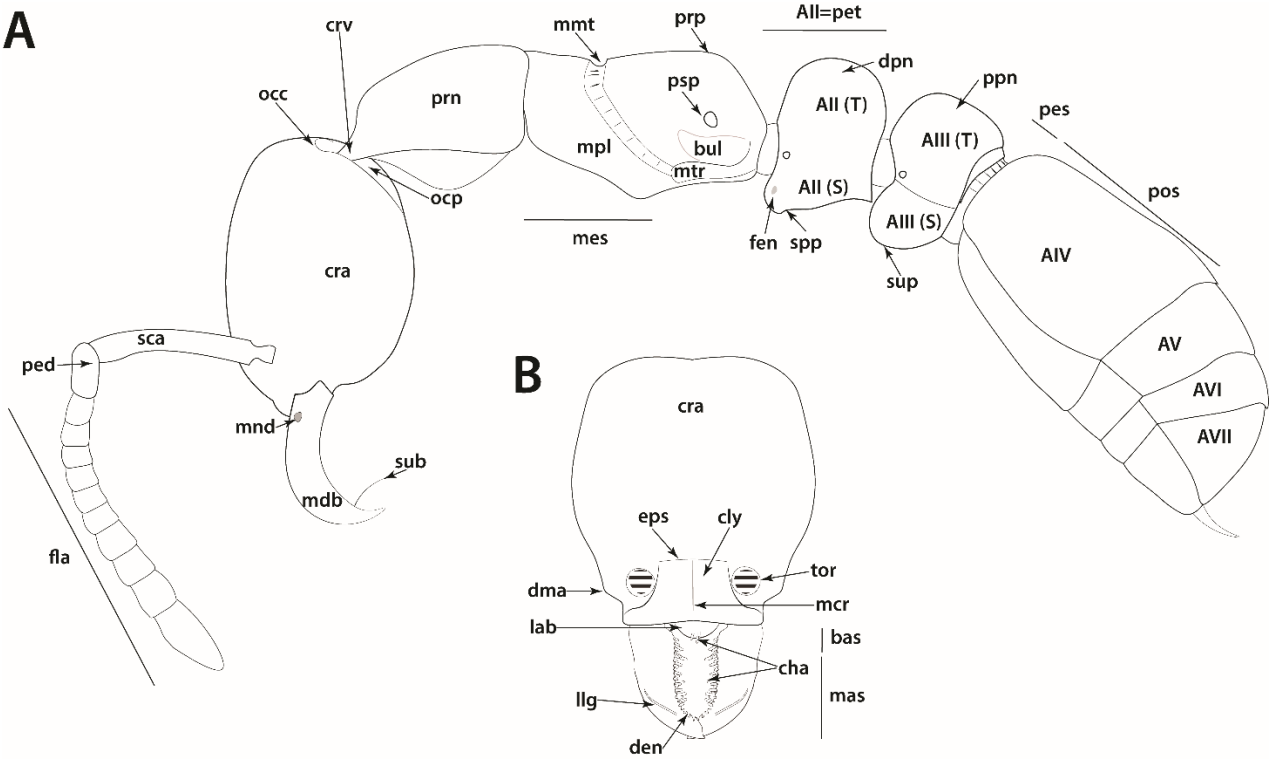

Figure 4.1. Glossary of morphological terms used to describe the worker soma in the Leptanillinae, with *Protanilla beijingensis* as template. **a.** Profile habitus **b.** Full-face view. Abbreviations: A = abdominal segment; bas = basal mandibular margin; bul = bulla; cha = chaetae; cly = clypeus; cra = cranium; crv = cervical shield; den = denticle; dma = dorsal mandibular articulation; dpn = petiolar node; eps = epistomal sulcus; fen = fenestra; fla = flagellum; lab = labrum; llg = laterodorsal longitudinal groove; mas = masticatory mandibular margin; mcr = median clypeal ridge; mdb = mandible; mes = mesothorax; mmt = meso-metapleural suture; mnd = mandalus; mpl = mesopleuron; mtr = metapleural trench; occ = occipital carina; ocp = occiput; ped = pedicel; pes = presternite; pos = poststernite; ppn = postpetiolar node; prn = pronotum; prp = propodeum; psp = propodeal spiracle; S = sternite; sca = scape; spp = subpetiolar process; sub = subapical mandibular seta; sup = subpetiolar process; T = tergite; tor = torulus

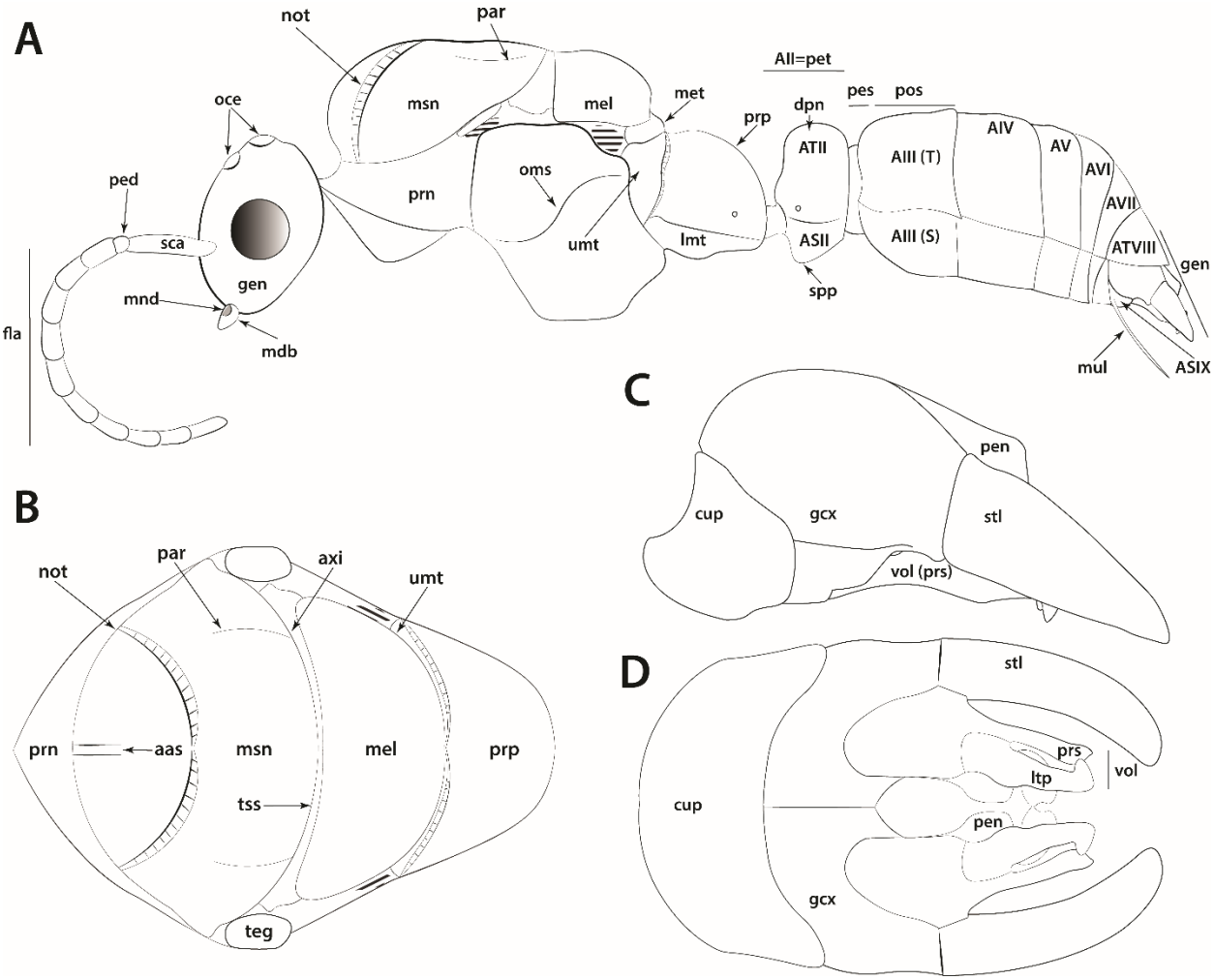

Figure 4.2. Glossary of morphological terms used to describe male morphology in the Leptanillinae. Representation of soma is chimeric, but *Protanilla* zhg-vn01 is the template for the genital diagrams. **a** Profile habitus **b** Mesosomal dorsum **c** Genitalia, profile view **d** Genitalia, ventral view. Abbreviations: A = abdominal segment; aas = antero-admedian signum; axi = axilla; cup = cupula; dpn = petiolar node; fla = flagellum; gcx = gonocoxites; gen = genital capsule; gen = gena; lmt = lateropenite; mdb = mandible; mel = mesoscutellum; met = metascutellum; mnd = mandalus; msn = mesonotum; mul = mulceators; not = notauli; oce = ocelli; oms = oblique mesopleural sulcus; par = parapsidal signa; ped = pedicel; pen = penial sclerites; pes = presternite; pet = petiole; prn = pronotum; prp = propodeum; prs = parossiculus; S = sternite; sca = scape; spp = subpetiolar process; stl = gonostylus; T = tergite; teg = tegula; tss = transscutal line; umt = upper metapleuron; vol = volsella.

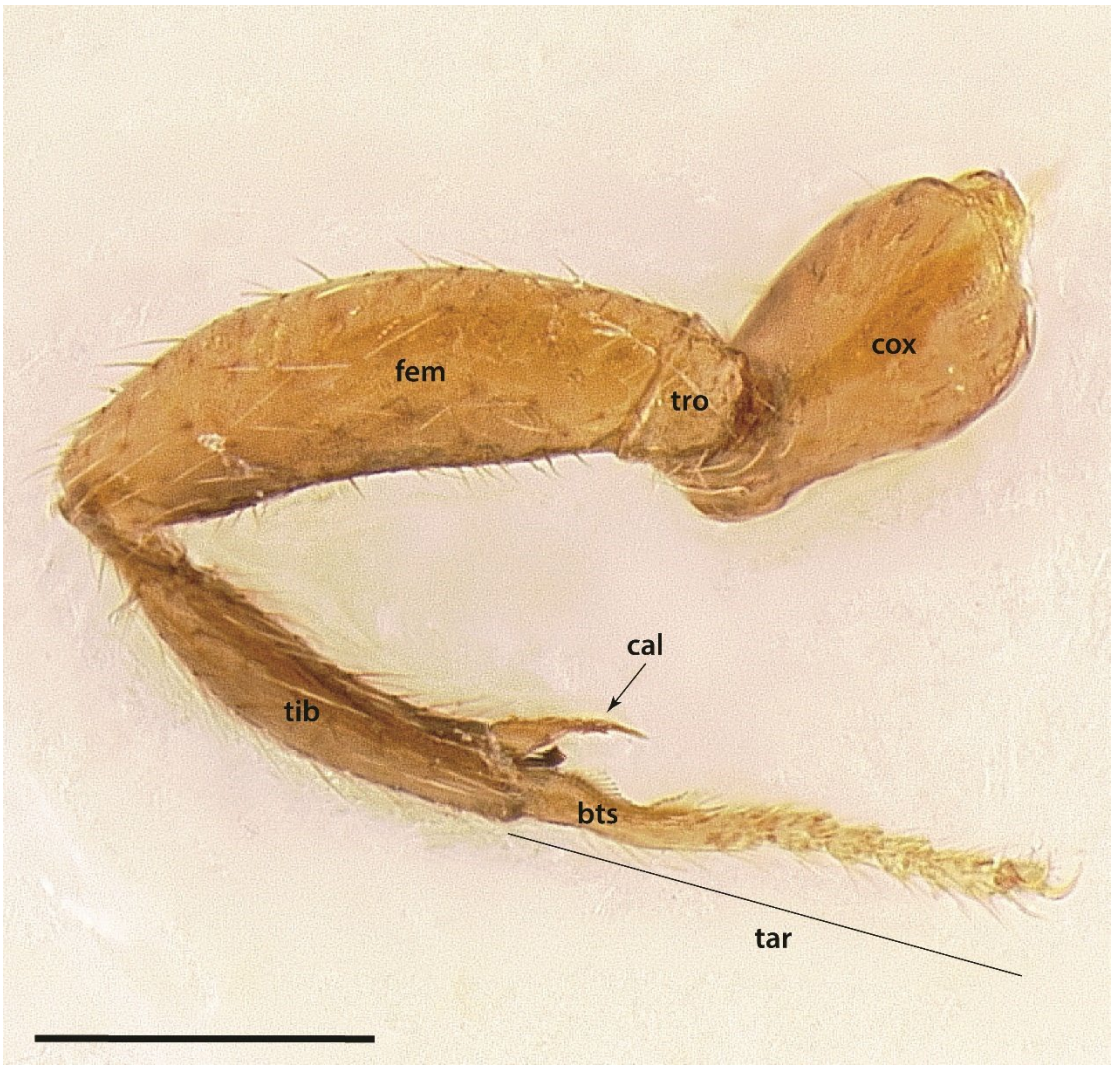

Figure 4.3. Glossary of leg nomenclature used for the Formicidae, with the foreleg of *Leptanilla* zhg-my11 (CASENT0842596) as template. Abbreviations: bts = basitarsus; cal = calcar; cox = coxa; fem = femur; tar = tarsus; tib = tibia; tro = trochanter. Scale bar = 0.2 mm.

Species concept

I here follow Barraclough (2019) in treating a species as an evolutionarily independent population of organisms that is genetically and phenotypically distinct from other such populations (Simpson, 1961). In sexually reproducing organisms, such as the Leptanillinae (so far as is known), reproductive isolation sufficient to maintain interspecific distinctiveness—in other words, the absence of genotypic and phenotypic intermediates—is an expected property of species. Mechanically incompatible genitalia are an expected corollary of reproductive isolation,

and thus would indicate interspecific differentiation, but may only be asserted to be so for sibling populations that occur in sympatry and exhibit consistent phenotypic differentiation. The degree of differentiation between such species serves as a "yardstick" by which to assess whether allopatric populations diverge sufficiently in phenotype to be considered heterospecific (Tobias et al., 2010; Ward and Branstetter, 2022). Scenarios that allow this calibration of phenotypic difference are fulfilled twice among the leptanilline morphospecies for which UCEs have been successfully enriched: one instance being *Leptanilla najaphalla* **sp. nov.** and *Leptanilla* zhg-my05 (Sabah, Malaysia), and the other *Leptanilla charonea* López *et al.* and *Leptanilla* cf. *zaballosi* (Madrid, Spain). In both cases the two putative sympatric species are recovered as closely related terminals by phylogenomic inference (Griebenow, 2020; Chapters 1-2, 5), and males of each species pair exhibit a phenotype uniformly distinguishable across all available specimens by the proportions of the genitalia. Variation among the syntopic specimen series assigned to these morphotypes is bimodal, giving no indication that any differentiation in genital shape among sympatric species is intraspecific.

Worker-based key to the genera of the Leptanillinae

1. Abdominal segment III not petiolate (Fig. 2.13A); abdominal segment II without complete tergosternal fusion; occiput visible in full-face view……...*Opamyrma* Yamane, Bui and Eguchi, 2008
- Abdominal segment III petiolate (Fig. 2.13B-C); abdominal segment II with complete tergosternal fusion; occiput not visible in full-face view……..……..……..……...2
2. Peg- to pencil-like chaetae present on labrum, present (Fig. 2.3A) *or* absent on medial mandibular surface; medial mandibular surface with regular, saw-like cuticular denticles (Fig. 2.3A); dorsomedial mandibular teeth absent……..*Protanilla* Taylor in Bolton, 1990

- Peg-like chaetae absent from labrum and medial mandibular surface; medial mandibular surface with (Fig. 2.5A) or without (Fig. 2.3C) irregular cuticular denticles; 2-4 dorsomedial mandibular teeth present (Fig. 2.3C-D)….....*Leptanilla* Emery, 1870

Male-based key to the genera of the Leptanillinae

1. Discal cell present; abdominal segment II without complete tergosternal fusion…….……..…….....*Opamyrma* Yamane, Bui and Eguchi, 2008
- Discal cell absent; abdominal segment II with complete tergosternal fusion….……2
2. Ocelli present, not set on distinct tubercle (Fig. 4.4A); pterostigma present; penial sclerites with medial articulation; cupula present……*Protanilla* Taylor in Bolton, 1990b
- Ocelli present *or* absent (Fig. 4.4B), *if* present *then* set on distinct tubercle (Fig. 4.4C); pterostigma absent; penial sclerites almost always without medial articulation; cupula absent……..…*Leptanilla* Emery, 1870

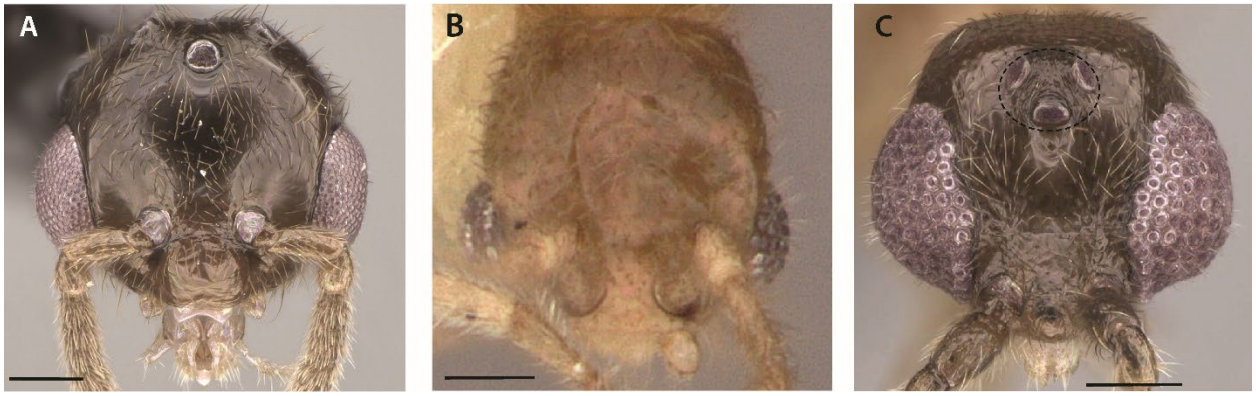

Figure 4.4. Condition of the male ocelli across the Leptanillini, full-face view. The ocellar tubercle is delimited in Fig. 4.4C by a dashed line. **a** *Protanilla* TH01 (CASENT0119776; Michele Esposito) **b** *Leptanilla* zhg-my03 (CASENT0106384) **c** *Leptanilla* TH02 (CASENT0119531; Shannon Hartman). Scale bars: A = 0.2 mm.; B-C = 0.1 mm.

Worker-based key to the species of the Leptanillinae

Dias et al. (2019) described the putative worker of *Protanilla schoedli*; however, given known morphological variation in the worker caste among described species of *Protanilla*, we here consider this as representing an undescribed species. Therefore, *P. schoedli* and *Protanilla taylori* (Taylor in Bolton) **comb. nov.** are excluded from this key, being known only from gynes.

Most subclades show strong morphological conservatism in the worker caste. It is consequently difficult to assess the scope of intraspecific phenotypic variation in workers, and the sparseness of collected specimens prevents algorithmic species delimitation using molecular data. Therefore, morphospecies known only from a single specimen are excluded from this key, and no new species are described in this study based upon worker singletons. Any such species hypothesis would be weak due to lack of comparative context, and be falsifiable simply by the discovery of additional specimens (Bond et al., 2022).

1. Abdominal segment III not petiolate; occiput visible in full-face view (Opamyrmini) …*Opamyrma hungvuong* Yamane *et al.*, 2008 / VIETNAM: Ha Tinh, Son La; CHINA: Hainan, Guangxi
- Abdominal segment III petiolate; occiput not visible in full-face view (Leptanillini).……..…….…2
2. Clypeus extending posteriorly between antennal toruli (Fig. 4.5A); epistomal sulcus present medially (*Protanilla*)…….....3
- Clypeus not extending posteriorly between antennal toruli (Fig. 4.5B); epistomal sulcus indistinct medially (*Leptanilla*)……..……..……...…...17
3. Abdominal tergite II without distinct posterior face (Fig. 2.13B); regular serration extending along entirety of medial mandibular face (*Protanilla taylori* species-group)…4

- Abdominal tergite II with distinct posterior face (Fig. 2.13A); regular serration not extending along entirety of medial mandibular face……..……..5

4. Cranium, pronotum and mesopleuron puncticulate to roughly sculptured; subpetiolar process lacking fenestra in profile view……...*Protanilla boltoni* (Borowiec *et al.*, 2011) **comb. nov. /** MALAYSIA: Perak
- Cranium, pronotum and mesopleuron glabrous; subpetiolar process with fenestra in profile view…*Protanilla helenae* (Borowiec *et al.*, 2011) **comb. nov.** / PHILIPPINES: Palawan

5. Clypeus oblate-trapezoidal in outline, elevated above frons posteriorly (Fig. 4.6A); mandible bowed along anteroposterior axis of cranium.....*Protanilla izanagi* Terayama, 2013 / JAPAN: Honshu
- Clypeus campaniform in outline (Fig. 4.1B), not elevated above frons posteriorly (Fig. 4.6B); mandible sublinear…….……..….6

6. Mesotibia with one spur; mandible without laterodorsal longitudinal groove (*Protanilla bicolor* species-group)……..……..…….……7
- Mesotibia without spurs; mandible with laterodorsal longitudinal groove (*Protanilla rafflesi* species-group)……...……..8

7. Cranium black-brown; anterior face of petiolar node sloping in profile view…….*Protanilla gengma* Xu, 2012 / CHINA: Yunnan; INDIA: Mizoram
- Cranium yellowish; anterior face of petiolar node subvertical in profile view……*Protanilla bicolor* Xu, 2002 / CHINA: Yunnan

8. Abdominal sternite III linear to slightly concave in profile view; abdominal segments III-IV broadly conjoined, with abdominal tergite III lacking a distinct posterior face……..9

- Abdominal sternite III convex in profile view; abdominal segments III-IV not broadly conjoined, with abdominal tergite III having a distinct posterior face……..10

9. Anterior margin of abdominal tergite IV emarginate in dorsal view; two ventrolateral teeth present on mandible…*Protanilla furcomandibula* Xu and Zhang, 2002 / CHINA: Yunnan

- Anterior margin of abdominal tergite IV entire in dorsal view; one ventrolateral tooth present on mandible…….…….…….*Protanilla jongi* Hsu *et al.*, 2017 / TAIWAN

10. Anterior face of petiolar node concave in profile view…….11

- Anterior face of petiolar node linear in profile view…….12

11. In profile view anterodorsal corner of petiolar node projecting anteriorly; larger species (WL 0.86-0.89 mm.)……*Protanilla rafflesi* Taylor in Bolton, 1990 / SINGAPORE; MALAYSIA: Sabah, Sarawak

- In profile view anterodorsal corner of petiolar node not projecting anteriorly; smaller species (WL 0.70-0.80 mm.)……*Protanilla wardi* Bharti and Akbar, 2015 / INDIA: Kerala

12. In dorsal view petiolar node breadth and length subequal; postpetiolar node not inclined anteriorly in profile view …..……...…..……...……...…….13

- In dorsal view petiolar node distinctly broader than long; postpetiolar node inclined anteriorly in profile view…...……...…….…….....16

13. Coloration castaneous; larger species (HL=0.628-0.700 mm.; WL=0.99 mm.)……..*Protanilla beijingensis* Man *et al.*, 2017 / CHINA: Beijing; PAKISTAN: Khyber Pakhtunkhwa

- Coloration coppery or yellowish; smaller species (HL=0.425-0.59 mm.; WL=0.640-0.936 mm.)…...……..…14

14. Scape not extending beyond occipital vertex of cranium in full-face view (SI≤90); coloration coppery……...*Protanilla flamma* Baidya and Bagchi, 2020 / INDIA: Goa

- Scape extending beyond occipital vertex of cranium in full-face view (SI>90); coloration yellowish……15

15. Larger species (WL≥0.75 mm.); postpetiolar node prominent in profile view, with anterior and posterior declivities equally rounded (Fig. 4.7A)……..*Protanilla lini* Terayama, 2009 / TAIWAN; JAPAN: Okinawa, Ryukyu Islands; Senkaku Islands

- Smaller species (WL<0.75 mm.); postpetiolar node shallow in profile view, with posterior declivity more gradual than anterior declivity (Fig. 4.7B)…...……..*Protanilla wallacei* **sp. nov.** / MALAYSIA: Sabah, Selangor

16. Lateral margin of head without dorsal mandibular articulation apparent in full-face view (Fig. 4.8A); anteroventral corner of sub-post-petiolar process rounded……....*Protanilla concolor* Xu, 2002 / CHINA: Yunnan

- Lateral margin of head with acute dorsal mandibular articulation in full-face view; anteroventral corner of sub-post-petiolar process obliquely truncated…*Protanilla tibeta* Xu, 2012 / CHINA: Xizang

17. Meso-metapleural suture present……...……..……..18

- Meso-metapleural suture vestigial to absent…..……...…….19

18. Frontoclypeal margin not protruding, anterior margin entire; postpetiolar node breadth and length subequal in dorsal view…*Leptanilla hunanensis* Tang *et al.*, 1992 / CHINA: Hunan

- Frontoclypeal margin protruding, anterior margin concave; postpetiolar node distinctly wider than long in dorsal view……....*Leptanilla kunmingensis* Xu and Zhang, 2002 / CHINA: Yunnan

19. Frontoclypeal margin entire (Fig. 2.14A) or not entire in full-face view, *if* not entire *then* never produced into emarginate median frontoclypeal process (Fig. 2.14B)……20

- Frontoclypeal margin not entire in full-face view, produced into emarginate median frontoclypeal process (Fig. 2.14C-D)……..……..……44

20. Frontoclypeal margin not entire, produced into median process (Fig. 2.14B)…….....21

- Frontoclypeal margin entire or not entire, never produced into median process……...23

21. Mandible with four teeth.....*Leptanilla boltoni* Baroni Urbani, 1977 / GHANA

- Mandible with three teeth……..22

22. Posteriorly recurved subpetiolar process present; PPI=122-138 mm…..……...*Leptanilla macauensis* Leong *et al.*, 2018 / CHINA: Macau

- Posteriorly recurved subpetiolar process absent; PPI=80-86 mm…….……...*Leptanilla buddhista* Baroni Urbani, 1977 / NEPAL

23. Frontoclypeal margin not entire…….24

- Frontoclypeal margin entire……...28

24. Frontoclypeal margin with pair of anterolateral processes; mandible with two teeth……..….*Leptanilla kebunraya* Yamane and Ito, 2001 / INDONESIA: Java

- Frontoclypeal margin without anterolateral processes; mandible with 3-4 teeth……..25

25. Four mandibular teeth; greatest width of petiolar node in dorsal view distinctly posterior to midlength……...……....*Leptanilla vaucheri* Emery, 1899 / MOROCCO

- Three mandibular teeth; greatest width of petiolar node in dorsal view not distinctly posterior to midlength……....26

26. Length of abdominal segment II subequal to that of abdominal segment III in dorsal view; abdominal tergite IV narrowed anteriorly in dorsal view (Fig. 4.9A)…...*Leptanilla taiwanensis* Ogata *et al.*, 1995 / TAIWAN; CHINA: Beijing

- Abdominal segment II longer than abdominal segment III in dorsal view; abdominal tergite IV not narrowed anteriorly in dorsal view (Fig. 4.9B)..…….……..……..27

27. Outline of abdominal segment III campaniform in dorsal view; frontoclypeal margin convex……..*Leptanilla oceanica* Baroni Urbani, 1977 / JAPAN: Ogasawara Islands

- Outline of abdominal segment III subrectangular in dorsal view; frontoclypeal margin sublinear……....*Leptanilla swani* Wheeler, 1932 / AUSTRALIA: Western Australia

28. Ventral vertex of abdominal sternite II distinctly lower on dorsoventral axis compared to ventral vertex of abdominal sternite III; mandible with two teeth……..……..*Leptanilla butteli* Forel, 1913 / MALAYSIA: Selangor

- Ventral vertex of abdominal sternite II not distinctly lower on dorsoventral axis compared to ventral vertex of abdominal sternite III; mandible with 3-4 teeth ….…..…….….29

29. Mandible with four teeth (subapical tooth sometimes difficult to distinguish)…….30

- Mandible with three teeth……..……...…….……37

30. Propodeum angular in profile view, with distinct posterior and dorsal faces…….……..…..*Leptanilla ortunoi* López *et al.*, 1994 / SPAIN: Ceuta

- Propodeum rounded in profile view, without distinct posterior and dorsal faces.....31

31. Abdominal sternite II emarginate in profile view.....*Leptanilla poggii* Mei, 1995 / ITALY: Pantellaria

- Abdominal sternite II sublinear in profile view.....32

32. Frontal margin of cranium convex in full-face view; scape strongly constricted at base…….…..*Leptanilla nana* Santschi, 1915 / TUNISIA

- Frontal margin of cranium linear in full-face view; scape moderately constricted at base……...….33

33. Abdominal sternite II with distinct linear face in profile view…….34

- Abdominal sternite II without distinct linear face in profile view……35

34. Most proximal mandibular tooth large and distinct; abdominal tergite IV distinctly narrowed anteriorly in dorsal view….*Leptanilla tanakai* Baroni Urbani, 1977 / JAPAN: Yakushima

- Most proximal mandibular tooth small and indistinct; abdominal tergite IV not distinctly narrowed anteriorly in dorsal view……..….*Leptanilla japonica* Baroni Urbani, 1977 / JAPAN: Honshu, CHINA: Hong Kong

35. Height of metafemur in anterior view 0.5× metafemoral length in anterior view; coloration pale…….....……..*Leptanilla charonea* Barandica *et al.*, 1994 / SPAIN

- Height of metafemur in anterior view <0.5× of metafemoral length in anterior view; coloration yellowish……..……36

36. Larger species (HL=0.32-0.36 mm.)……*Leptanilla theryi* Forel, 1903 / ALGERIA; TUNISIA; SPAIN

……. *Leptanilla plutonia* López *et al.*, 1994 / SPAIN

- Smaller species (HL=0.22-0.28 mm.)…*Leptanilla zaballosi* Barandica *et al.*, 1994 / SPAIN

37. Abdominal sternite II emarginate in profile view, with narrow trough-like indentation……...*Leptanilla doderoi* Emery, 1915 / ITALY: Sardinia

- Abdominal sternite II entire to shallowly emarginate in profile view……...38

38. Petiole distinctly wider than long…..*Leptanilla yunnanensis* Xu, 2002 / CHINA: Yunnan

- Petiole not distinctly wider than long...…….…39

39. Frontal margin convex in full-face view……...….40

- Frontal margin linear in full-face view……...…….…..……...…….41

40. Mesothorax anteriorly constricted in dorsal view…*Leptanillla besucheti* Baroni Urbani, 1977 / SRI LANKA

- Mesothorax not anteriorly constricted in dorsal view…….*Leptanilla morimotoi* Yasumatsu, 1960 / JAPAN: Kyushu

41. Length of abdominal tergite V>0.5× length of abdominal tergite IV……*Leptanilla revelierii* Emery, 1870 / FRANCE: Corsica; ITALY: Sardinia; SPAIN; PORTUGAL; MOROCCO

- Length of abdominal tergite V≤0.5× length of abdominal tergite IV……42

42. Pedicel distinctly longer than wide…*Leptanilla kubotai* Baroni Urbani, 1977 / JAPAN: Shikoku

- Pedicel length and width subequal…….43

43. Smaller species (WL<0.3 mm.)…….……*Leptanilla okinawensis* Terayama, 2013 / JAPAN: Okinawa

- Larger species (WL≥0.3 mm.)…….……*Leptanilla acherontia* **sp. nov.** / KENYA

44. SI>100; length of petiole >3× greater than maximum breadth (Fig. 2.6B)…….....*Leptanilla laventa* (Griebenow et al., 2022) **comb. nov.** / IRAN: Fārs

- SI≤100; length of petiole ≤3× greater than maximum breadth (Fig. 4.10B)…...…….....45

45. Anterior margin of petiolar node emarginate in dorsal view…….....…….…46

- Anterior margin of petiolar node entire in dorsal view…….…….…….……...47

46. In full-face view, mandible with most proximal tooth long and well-defined; petiolar node almost twice as long as wide in dorsal view; postpetiolar node longer than wide in dorsal view……*Leptanilla hypodracos* Wong and Guénard, 2016 / SINGAPORE

- In full-face view, mandible without most proximal tooth long and well-defined; length and width of petiolar node subequal in dorsal view; postpetiolar node distinctly wider than long in dorsal view…*Leptanilla clypeata* Yamane and Ito, 2001 / INDONESIA: Java

47. Length of metasomal setae bimodal……..48

− Length of metasomal setae unimodal……50

48. Mandible with four teeth, with most proximal tooth truncate (Saroj et al., 2022: fig. 1E); ventromedian lamella of abdominal sternite II denticulate……*Leptanilla ujjalai* Saroj et al., 2022 / INDIA: West Bengal

- Mandible with three teeth, with most proximal tooth not truncate; ventromedian lamella of abdominal sternite II not denticulate…….……49

49. Lateral pronotal margins weakly convex in dorsal view; PPTI=73.68-76.47……*Leptanilla lamellata* Bharti and Kumar, 2012 / INDIA: Himachal Pradesh

− Lateral pronotal margins strongly convex in dorsal view; PPTI=84.62-85.71.....*Leptanilla escheri* (Kutter, 1948) / INDIA: Tamil Nadu

50. Petiole twice as long as wide in dorsal view, or more……...……....51

- Petiole less than twice as long as wide…….……...……..52

51. Meso-metapleural furrow present; mandible with three teeth, most proximal tooth acute.....*Leptanilla judaica* Kugler, 1987 / WEST BANK

– Meso-metapleural furrow absent; mandible with four teeth, most proximal tooth distally recurved, apex expanded……..……*Leptanilla belantan* **sp. nov.** / MALAYSIA: Selangor

52. Subpetiolar process present, angular; torular rim without areolate sculpture (Fig. 4.11A)……*Leptanilla havilandi* Forel, 1901 / SINGAPORE; MALAYSIA: Sabah

- Subpetiolar process absent; torular rim with medial and anterior areolate sculpture (Fig. 4.11B)…….*Leptanilla thai* Baroni Urbani, 1977 / THAILAND: Khao Chong

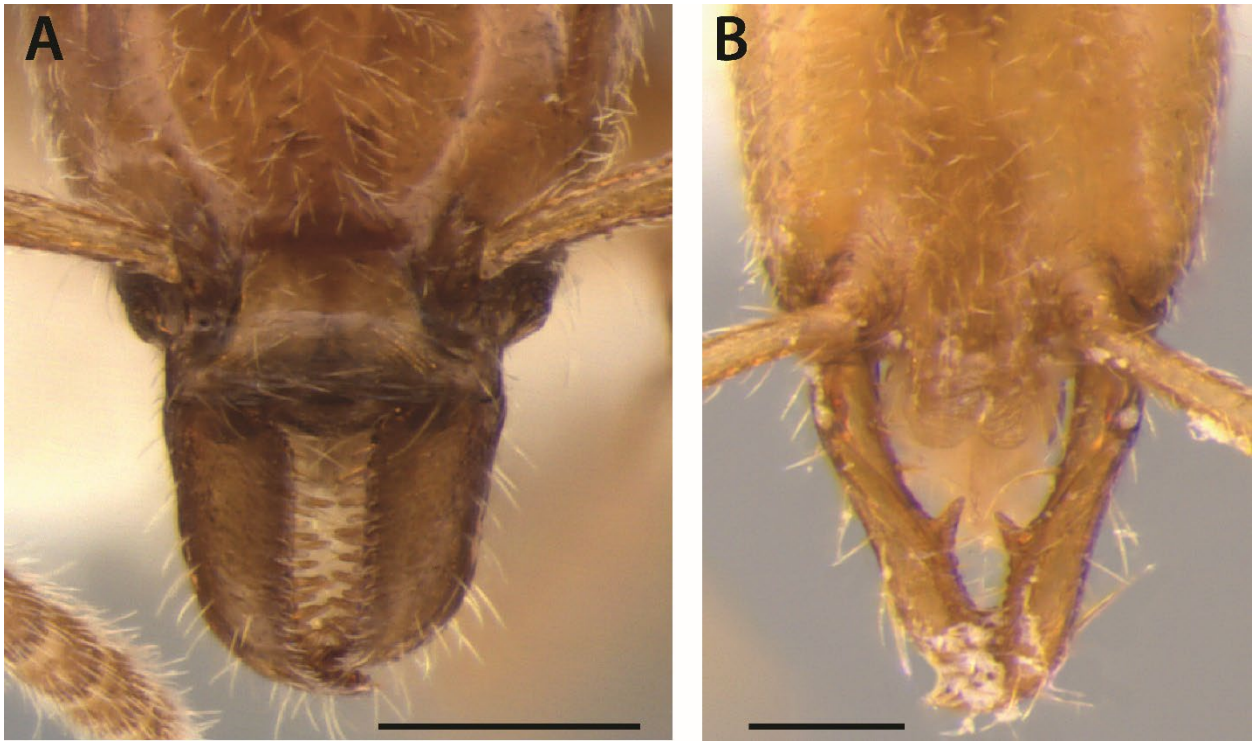

Figure 4.5. Condition of the frontoclypeal margin in *Protanilla* (**a**) and *Leptanilla* (**b**). **a** *Protanilla bejingensis* (CASENT0842639) **b** *Leptanilla laventa* (CASENT0842746). Scale bars: A = 0.5 mm.; B = 0.1 mm.

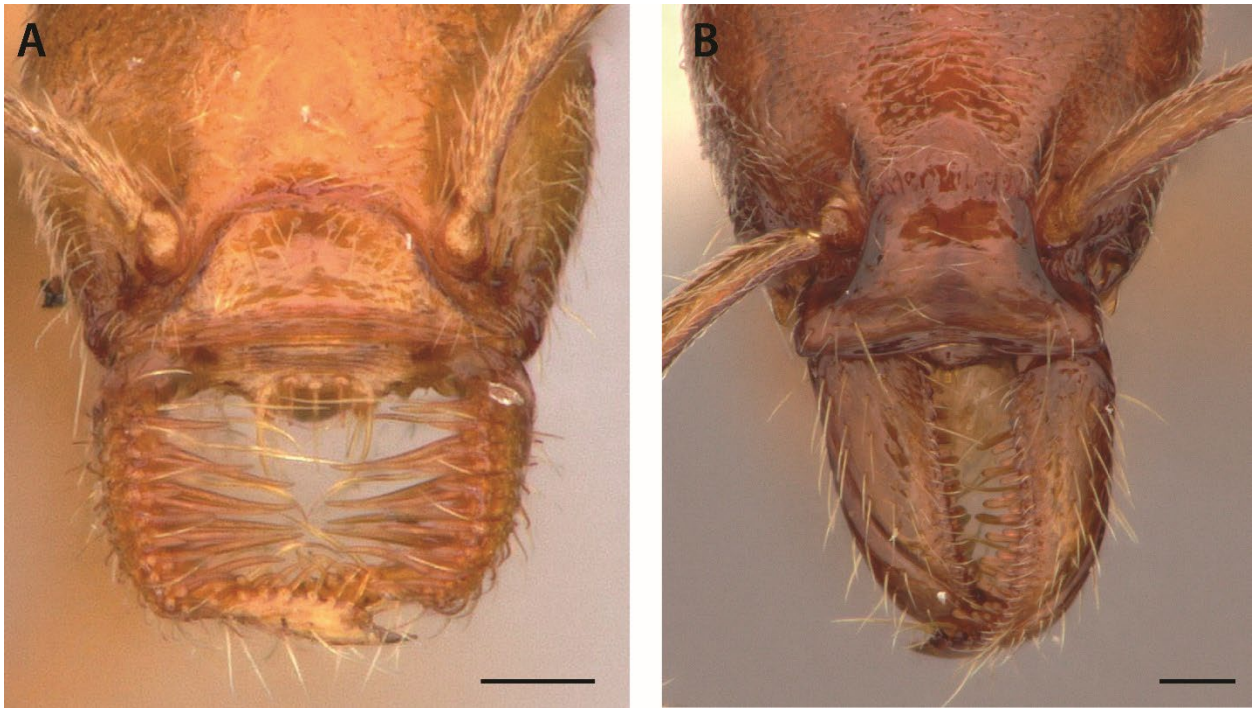

Figure 4.6. Anterior of the head in *Protanilla*, full-face view. **a** *Protanilla izanagi* (CASENT0842850) **b** *Protanilla jongi* (CASENT0842693). Scale bars: A-B = 0.1 mm.

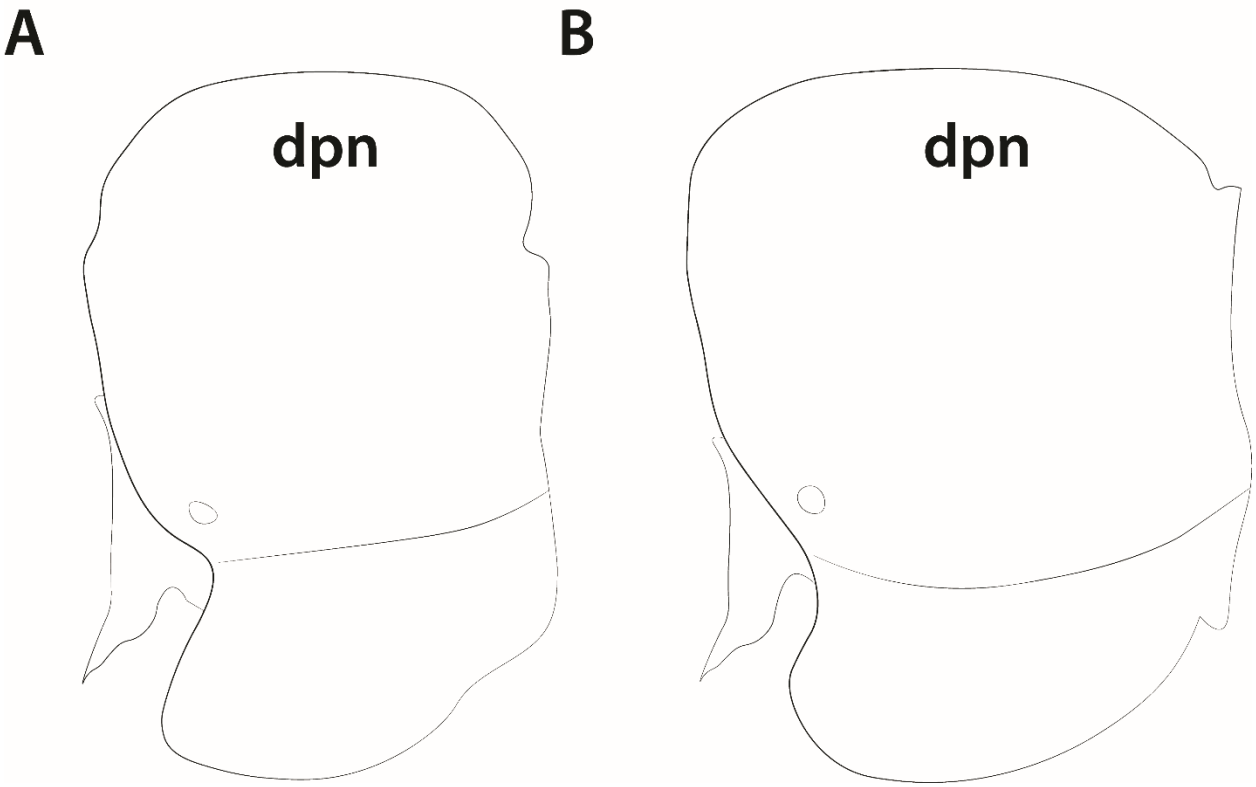

Figure 4.7. Petiole of *Protanilla lini* (**a**) and *Protanilla wallacei* **sp. nov.** (**b**), profile view. dpn = petiolar node.

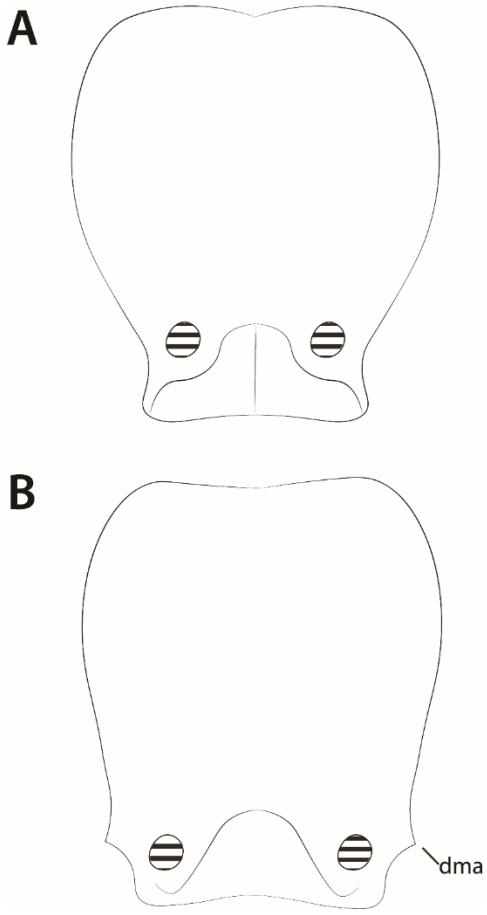

Figure 4.8. Cranium of *Protanilla concolor* (**a**) and *Protanilla bicolor* (**b**), diagrammatic full-face view, redrawn from Xu (2002: figs. 18, 21). dma = dorsal mandibular articulation.

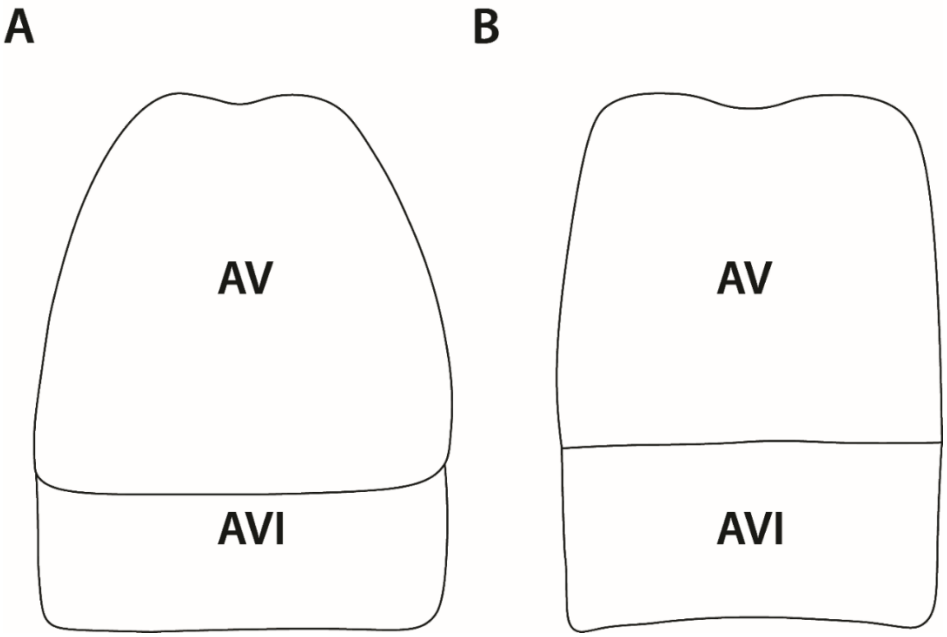

Figure 4.9. Abdominal segments V-VI (AV-AVI) in *Leptanilla taiwanensis* (**a**) and *Leptanilla oceanica* (**b**), diagrammatic. 4.8B redrawn from Baroni Urbani (1977: fig. 19).

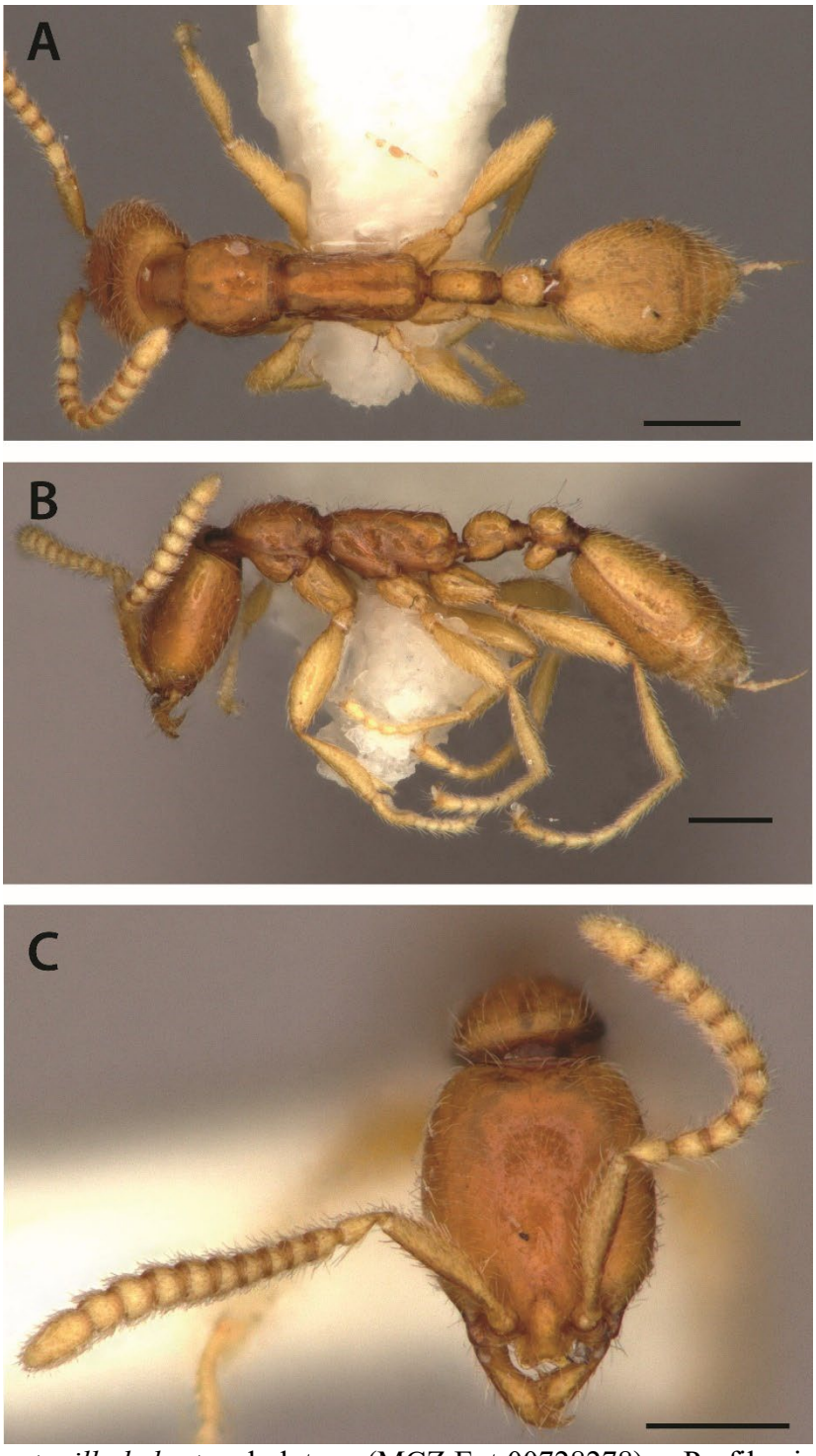

Figure 4.10. *Leptanilla belantan*, holotype (MCZ:Ent:00728278). **a** Profile view. **b** Dorsal view. **c** Full-face view. Scale bars = 0.2 mm.

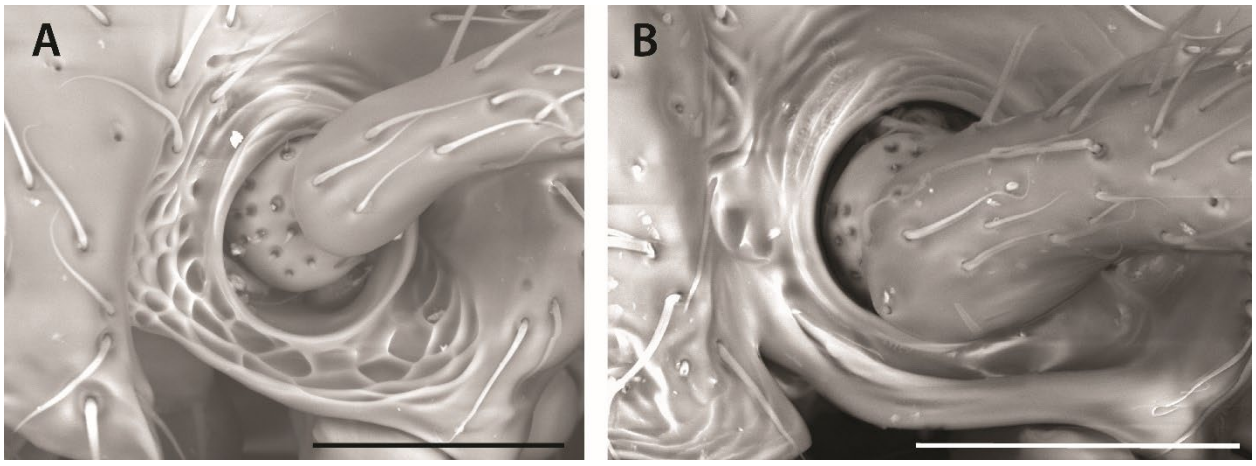

Figure 4.11. Antennal torulus in *Leptanilla thai* (**a**) and *Leptanilla havilandi* (**b**). Scale bars: A = 0.04 mm.; B = 0.05 mm.

Male-based species-level key to the Leptanillinae

Corrected and extended from Griebenow (2020), with updated generic assignments for undescribed morphospecies; concordances of these morphospecies identifiers with previous publications (Griebenow, 2020; Chapters 1-3) are provided in Table 4.1. Includes all described species for which males are known, and all undescribed male morphospecies for which molecular data are available, except for *Leptanilla* ZA01 (for which only genital morphology is known), *Leptanilla* TH07 and *Leptanilla* zhg-mm14 (for which genital morphology is unknown). Based on phylogenetic inference from both molecular and morphological data (Chapters 1, 5), these three morphospecies belong to the *Leptanilla revelierii* species-group, the *Leptanilla bethyloides* species-group, and the *Leptanilla thai* species-group, respectively.

1. Discal cell present (Fig. 4.12A); parossiculus and lateropenite distinct, articulated……....……..……...*Opamyrma hungvuong* Yamane *et al.*, 2008 / VIETNAM: Ha Tinh, Son La; CHINA: Hainan, Guangxi

- Discal cell absent (Fig. 4.12B-D); if volsella discernible, parossiculus and lateropenite distinct or indistinct, *if* distinct *then* inarticulate (Leptanillini)……..……2

2. Pterostigma present (Fig. 1.14A); ocelli present, with ocellar tubercle absent (Fig. 4.4A)…….……..……3

- Pterostigma absent (Fig. 1.14B); ocelli present *or* absent (Fig. 4.4B), *if* present *then* set on ocellar tubercle (Fig. 4.4C)……...…..…8

3. Notauli present (Fig. 4.13A)...……...…….……...……..……...4

- Notauli absent (Fig. 4.13B)...……...……..…….……..…...6

4. Notauli not scrobiculate, not intersecting transscutal line.…….....…….*Protanilla* TH02 / THAILAND: Chaiyaphum

- Notauli scrobiculate, intersecting transscutal line…….……..……5

5. Mandalus not extending to mandibular apex; abdominal segment III not petiolate (Fig. 1.22A)…….…...…..*Protanilla* zhg-th02 / THAILAND: Chaiyaphum

- Mandalus extending to mandibular apex; abdominal segment III petiolate (Fig. 1.22B)……..……...*Protanilla* TH03 / THAILAND: Chiang Mai

6. Gonostylar apex pointed (Griebenow, 2020: fig. 9Ci)…*Protanilla* TH01 / THAILAND: Khon Kaen

- Gonostylar apex rounded (Griebenow, 2020: fig. 9Cii)……..…...…7

7. Anterior face of subpetiolar process nearly perpendicular to craniocaudal axis in profile view; abdominal tergite III slightly narrower than IV in dorsal view (TI1 62-92) (Fig. 4.14A)……...*Protanilla* zhg-vn01 / VIETNAM: Vinh Phuc
……..*Protanilla* zhg-my01 / MALAYSIA: Sarawak

- Anterior face of subpetiolar process gently sloping relative to craniocaudal axis; abdominal tergite III much narrower than IV in dorsal view (TI1 50-55) (Fig.

4.14B)…*Protanilla lini* Terayama, 2009 / TAIWAN; JAPAN: Ryukyu Islands, Senkaku Islands

8. Propodeum concave in profile view (Fig. 1.17A); pronotum and mesoscutum not posteriorly prolonged (*Leptanilla thai* species-group)……..……...…...9
- Propodeum not concave in profile view (Fig. 1.17B-C); pronotum and mesoscutum posteriorly prolonged……..……..…..…….…….…….22
9. Gonocoxites entirely fused medially; posterior margin of abdominal sternite IX with median extension……..……..….*Leptanilla* TH03 / THAILAND: Chiang Mai
- Gonocoxites partly to fully separate medially; posterior margin of abdominal sternite IX entire……..……10
10. Ocelli absent (Fig. 4.4B); mandible articulated to gena (Fig. 4.15A)…..*Leptanilla* zhg-bt03 / BHUTAN
- Ocelli present; mandible fused to gena (Fig. 4.15B), rarely articulate (*Leptanilla* TH04)……..…11
11. Gonopodite distinctly longer than penial sclerites (Fig. 4.16A)……...…….....…...…..12
- Gonopodite shorter than (Fig. 4.16B), or subequal in length to, penial sclerites……..20
12. Profemur arcuate, constricted proximally (Griebenow, 2020: fig. 11Bi).....….....13
- Profemur sublinear, not constricted proximally (Griebenow, 2020: fig. 11Bii).…....…16
13. Volsella bifid, ventral process bifurcated (Griebenow, 2020: fig. 11Ci)……...……...*Leptanilla* zhg-th02 / THAILAND: Phetchabun
- Volsella bifid, ventral process entire (Griebenow, 2020: fig. 11Cii)…….14
14. Dorsal and ventral parossicular processes oriented in opposite directions; lengths of processes subequal…….……..……..*Leptanilla* TH02 / THAILAND: Khon Kaen

- Dorsal and ventral parossicular processes not oriented in opposite directions; ventral parossicular process 3× longer than length of dorsal process…….……...……15

15. Diameter of compound eye >4× span of ocellar tubercle; gonopodital apices not recurved towards medial axis...…….…… *Leptanilla* zhg-th04 / THAILAND: Chaiyaphum

- Diameter of compound eye only slightly greater than span of ocellar tubercle; gonopodital apices sharply recurved towards medial axis……..…...*Leptanilla* zhg-th05 / THAILAND: Chaiyaphum

16. Gonostylar apex subtriangular, entire……....*Leptanilla* MM01 / BURMA: Rakhine

- Gonostylar apex tapering, entire or bifid…….……...…..……17

17. Head not broader than long in full-face view (Fig. 1.4A), including compound eyes; gonostylar apex bifurcated…*Leptanilla* TH08 / THAILAND: Surat Thani

- Head broader than long in full-face view, including compound eyes; gonostylar apex entire……...…….……..18

18. Volsella bifid; mandible articulated to gena….*Leptanilla* TH04 / THAILAND: Chiang Mai

- Volsella entire; mandible fused to gena…….19

19. Gonostylar apex lobate in outline, covered with dense vestiture; coloration castaneous.……..*Leptanilla* TH06 / THAILAND: Chiang Mai

- Gonostylar apex acuminate, glabrous; coloration beige……...……..*Leptanilla* zhg-my16 / MALAYSIA: Selangor

20. Internal margins of apical penial cleft distinctly separated; posteroventral gonocoxital margin entire (Fig. 4.17B)..…*Leptanilla argamani* **comb. nov.** (Kugler, 1987) / ISRAEL, LEBANON

- Internal margins of apical cleft of penial sclerites subparallel; posteroventral gonocoxital margin sinuate (Fig. 4.17A)……...……...…….…….21

21. Color castaneous; posterior margin of compound eye linear in profile view ……..….*Leptanilla indica* **comb. nov.** (Kugler, 1987) / INDIA: Kerala

- Color yellowish to pallid; posterior margin of compound eye convex in profile view……..…….……*Leptanilla* nr. *indica* / SRI LANKA

22. Dorsolateral carina present on propodeum; penial sclerites lateromedially compressed……*Leptanilla palauensis* (M.R. Smith, 1953) / PALAU

- Dorsolateral carina absent from propodeum; penial sclerites sometimes lateromedially compressed, more often not…….…….…….……23

23. Gonostylus ellipsoid in outline (Griebenow, 2020: fig. 11E); penial sclerites medially articulated …….*Leptanilla astylina* Petersen, 1968 / PHILIPPINES: Palawan

- Gonostylus not ellipsoid in outline; penial sclerites not medially articulated……..24

24. Phallotreme surrounded with dense setae (Griebenow, 2020: fig. 12Ai); procoxa with distal transverse carina (*Leptanilla havilandi* species-group) (Fig. 4.18B)…….25

- Phallotreme bare (Griebenow, 2020: fig. 12Aii); procoxa without distal transverse carina (Fig. 4.18A)…….……..…...…...……...29

25. ML≥SL, with mandible flattened and paddle-like; lower metapleuron indistinct……*Leptanilla anomala* **comb. nov.** (Brues, 1923) / INDONESIA: Sumatra, Kalimantan Barat

- ML<SL, with mandible nub-like; lower metapleuron distinct…..…...……26

26. Mandalus not extending to mandibular apex; anteromedian ocellus orthogonally dorsal to compound eye in profile view (Griebenow, 2020: fig. 12Bi)…...…….*Leptanilla copiosa* **comb. nov.** (Petersen, 1968) / PHILIPPINES: Palawan; MALAYSIA: Sabah

- Mandalus extending to mandibular apex; anteromedian ocellus positioned posterodorsal to compound eye in profile view (Griebenow, 2020: fig. 12Bii)…….……..27

27. Gonostylus longer than gonocoxite (Griebenow, 2020: fig. 13Aii)……*Leptanilla* zhg-my10 / MALAYSIA: Sabah

- Gonostylus shorter than, or subequal in length to gonocoxite (Griebenow, 2020: fig. 13Ai)…….…….…...……28

28. Penial apex entire……....*Leptanilla* zhg-my14 / MALAYSIA: Sabah

- Penial apex cleft……...…….…..*Leptanilla* zhg-my11 / MALAYSIA: Sabah

29. Dorsal propodeal face long, parallel to craniocaudal axis (Fig. 1.17B); protibial comb present (Fig. 1.3B) (*Leptanilla najaphalla* species-group)……...…….30

- Dorsal propodeal face short, with propodeal outline in profile view convex, *if* long and parallel to craniocaudal axis *then* upper metapleuron distinct from metapectal-propodeal complex; protibial comb absent (Fig. 1.3A)….....…….....34

30. Phallotreme at penial apex.……..……..……31

- Phallotreme proximad penial apex, anatomically ventral.…….…....……...32

31. Penial sclerites dorsoventrally compressed at apex, without dorsomedian lamina……..…….……*Leptanilla* zhg-my03 / MALAYSIA: Sabah, Sarawak

- Penial sclerites lateromedially compressed at apex, with dorsomedian lamina……..……..…*Leptanilla* zhg-my04 / MALAYSIA: Sabah

32. Gonostylus present, penial sclerites with recurved apical hook (Griebenow, 2020: fig. 13Ci)……..…….*Leptanilla* zhg-id01 / INDONESIA: Kalimantan Barat

- Gonostylus absent, penial sclerites without recurved apical hook…….…..33

33. Apicolateral gonocoxital lamina subulate (Fig. 4.19A)..……..….…….*Leptanilla najaphalla* **sp. nov.** / MALAYSIA: Sabah

- Apicolateral gonocoxital lamina lanceolate (Griebenow, 2020: fig. 13Ciii).....*Leptanilla* zhg-my05 / MALAYSIA: Sabah

34. Metapleuron at least partly distinct; vestiture dense and pubescent (*Leptanilla bethyloides* species-group)……..……..35

- Metapleuron never distinct; vestiture rarely dense, never pubescent……...….38

35. Mesoscutellum produced into recurved posterior process (Fig. 1.16B); third antennomere longer than scape…….……..……*Leptanilla* zhg-th01 / THAILAND: Chiang Mai

- Mesoscutellum not produced into recurved posterior process; third antennomere equal in length to, or greater than, length of scape……...…….……..36

36. Penial sclerites lateromedially compressed, with dorsomedian carina……..……...…*Leptanilla* TH01 / THAILAND: Chiang Mai

- Penial sclerites dorsoventrally compressed, without dorsomedian carina; gonopodital apex bifid…….……..……37

37. Smaller species; abdominal postsclerites V-VII anteroposteriorly compressed relative to III-IV.....……..……...*Leptanilla* zhg-mm05, -6 / BURMA: Taninthayi

- Larger species; abdominal postsclerites V-VII with anteroposterior lengths subequal to those of III-IV……..*Leptanilla bethyloides* **sp. nov.** / CHINA: Hong Kong

38. Gonostylus absent; Sc+R+Rs and Rf1 nebulous, *2s-rs*+Rsf4-6 absent, M+Cu absent…….….*Leptanilla santschii* Wheeler and Wheeler, 1930 / INDONESIA: Java

- Gonostylus present; Sc+R+Rs and Rf1 present or rarely absent, *2s-rs*+Rsf4-6 present or absent, M+Cu absent or rarely present……...……...39

39. Protibial length 0.5× profemoral length……..…….....40

- Protibial length >0.5× profemoral length …….……41

40. Probasitarsal seta not hypertrophied, length subequal to that of calcar……..*Leptanilla africana* Baroni Urbani, 1977 / NIGERIA

- Probasitarsal seta hypertrophied, length subequal to that of calcar (Fig. 1.46B)..…….……..*Leptanilla* TH09 / THAILAND: Phetchabun

41. Gonostylus bifurcated…….…...…..……..42

- Gonostylus entire…...…….……...……..…….51

42. Abdominal segment II broadly joined to abdominal segment III (Santschi, 1907: fig. 3)…..…….…....*Leptanilla minuscula* Santschi, 1907 / TUNISIA

- Abdominal segment III narrowly joined to abdominal segment III…….....43

43. Ventromedial gonocoxital margin with sinuate process……...*Leptanilla tanit* Santschi, 1907 / TUNISIA

− Ventromedial gonocoxital margin entire……..….....44

44. Gonostylar apex with obtuse tooth subtending dorsal process……..*Leptanilla* GR02 / GREECE: Rhodes

- Gonostylar apex lacking obtuse tooth subtending dorsal process……..……..45

45. Ventromedian margin of gonostylus excavated proximad apical furca……..*Leptanilla* zhg-au02 / AUSTRALIA: New South Wales

- Ventromedian margin of gonostylus entire proximad apical furca…….…..….46

46. Dorsal process of gonostylar apex acuminate……...47

- Dorsal process of gonostylar apex rounded…….…..48

47. Processes of gonostylar apex large, with apex appearing deeply bifurcated; pedicel with strong proximal constriction…….*Leptanilla tenuis* Santschi, 1907 / TUNISIA

- Processes of gonostylar apex small, with apex appearing nearly truncate; pedicel with moderate proximal constriction…….*Leptanilla* zhg-mm02 / BURMA: Taninthayi

48. Penial apex entire..….....…….....49

- Penial apex emarginate.....50

49. PTL≈PTH……..…….*Leptanilla* GR01 / GREECE: Rhodes

- PTL>PTH…….…..……..*Leptanilla* zhg-id02 / INDONESIA: Sulawesi Tenggara

50. Internal margins of apical penial cleft distinctly separated, ventral gonostylar process narrower than dorsal process……...….*Leptanilla bifurcata* Kugler, 1987 / ISRAEL

− Internal margins of apical penial cleft adjacent, gonostylar processes subequal in breadth…….....…….*Leptanilla israelis* Kugler, 1987 / ISRAEL

51. Gonostylus not tapered.…….…..……...52

- Gonostylus tapered…….…….……..54

52. Gonostylus with expanded, rounded apex…*Leptanilla islamica* Baroni Urbani, 1977 / YEMEN; OMAN

- Gonostylus with apex not expanded……..……...…….…….53

53. Outline of penial sclerites attenuate in posterodorsal view……*Leptanilla alexandri* Dlussky, 1969 / UZBEKISTAN

- Outline of penial sclerites elliptical in posterodorsal view……*Leptanilla japonica* Baroni Urbani, 1977 / JAPAN: Honshu; CHINA: Hong Kong

54. Gonostylar apex acuminate……...……...…….…….55

- Gonostylar apex digitate……...……...…..……...…...61

55. Oblique mesopleural sulcus traversing posterior >0.5× of mesopleuron…….....56

- Oblique mesopleural sulcus traversing posterior ≤0.5× of mesopleuron…….....57

56. Penial sclerites broad in posterodorsal view, apex entire; Rsf1+Mf1 present……..*Leptanilla javana* (Wheeler and Wheeler , 1930) / INDONESIA: Java

- Penial sclerites narrow in posterodorsal view, apex emarginate; Rsf1+Mf1 absent……*Leptanilla* zhg-ke01 / KENYA: Laikipia

57. Abdominal sternite II without distinct subpetiolar process..……*Leptanilla* zhg-bt02 / BHUTAN

- Abdominal sternite II with distinct subpetiolar process.…….……..58

58. *2s-rs*+R+4-6 absent (Fig. 4.20A)……...…….……...59

- *2s-rs*+R+4-6 present (Fig. 4.20B)...……...…….……...60

59. Posterior face of petiolar node shallower than anterior face; genital capsule subequal in overall dimensions to abdominal segment II……..*Leptanilla* zhg-bt01 / BHUTAN

- Posterior face of petiolar node not shallower than anterior face; dimensions of genital capsule conspicuously greater than those of abdominal segment II……*Leptanilla* zhg-ke02 / KENYA: Kakamega

60. Apicolateral margins of penial sclerites emarginate; smaller species (WL=0.37-0.44 mm.) (*n*=6)……...……*Leptanilla charonea* Barandica *et al.*, 1994 / SPAIN

- Apicolateral margins of penial sclerites entire; larger species (WL=0.46-0.50 mm.) (*n*=3)……...……..*Leptanilla* cf. *zaballosi* López *et al.*, 1994 / SPAIN

61. Penial sclerites broader than long.…*Leptanilla* GR03 / GREECE: Rhodes; TURKEY: Muğla

    ……...*Leptanilla* zhg-tr01 / TURKEY: Muğla

- Penial sclerites longer than broad……...……..…….……62

62. Gonostylus not articulated to gonocoxite…..*Leptanilla exigua* Santschi, 1908 / TUNISIA

- Gonostylus articulated to gonocoxite…….……....63

63. Oblique mesopleural sulcus present; Sc+R+Rs tubular….*Leptanilla* zhg-au01 / AUSTRALIA: Queensland

- Oblique mesopleural sulcus absent; Sc+R+Rs absent…*Leptanilla australis* Baroni Urbani, 1977 / SOUTH AFRICA: Cape Province

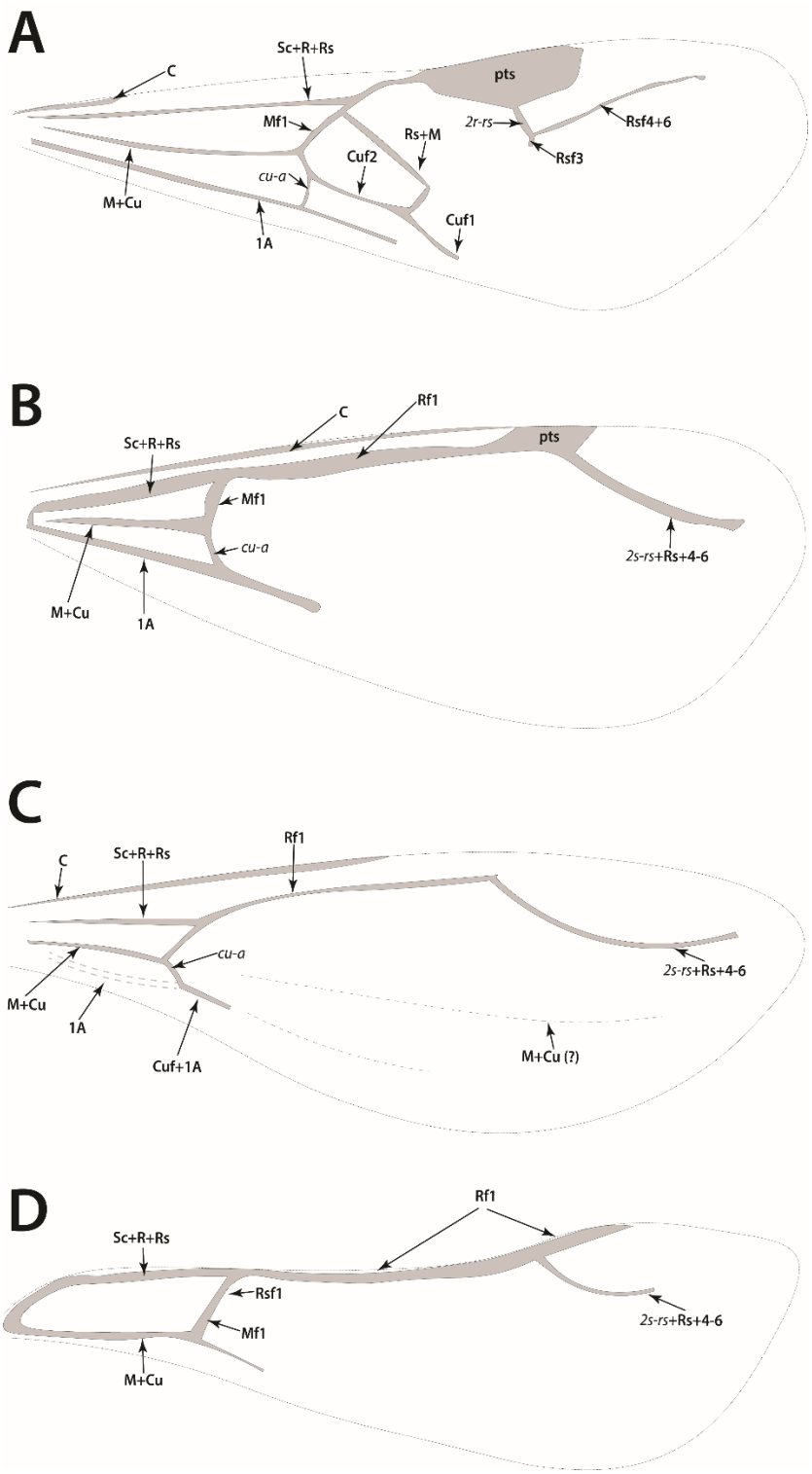

Figure 4.12. Exemplars of male wing venation across the Leptanillinae, diagrammatic. **b-c** are typological generalizations of male wing venation in the clades that they represent. **a** *Opamyrma hungvuong* **b** *Protanilla* **c** *Leptanilla najaphalla* species-group **d** *Leptanilla javana*. pts=pterostigma.

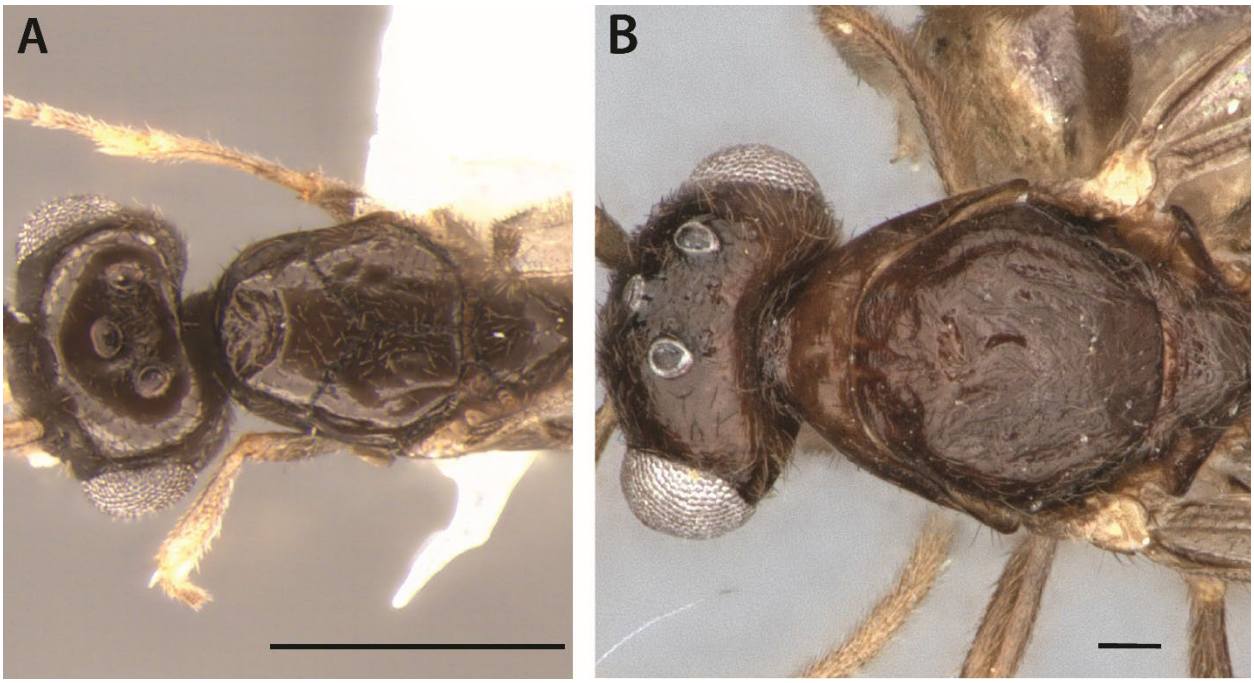

Figure 4.13. Mesoscutum in *Protanilla*. **a** *Protanilla* zhg-th02 (CASENT0842645) **b** *Protanilla lini* (OKENT0027514). Scale bars: A = 0.5 mm.; B = 0.2 mm.

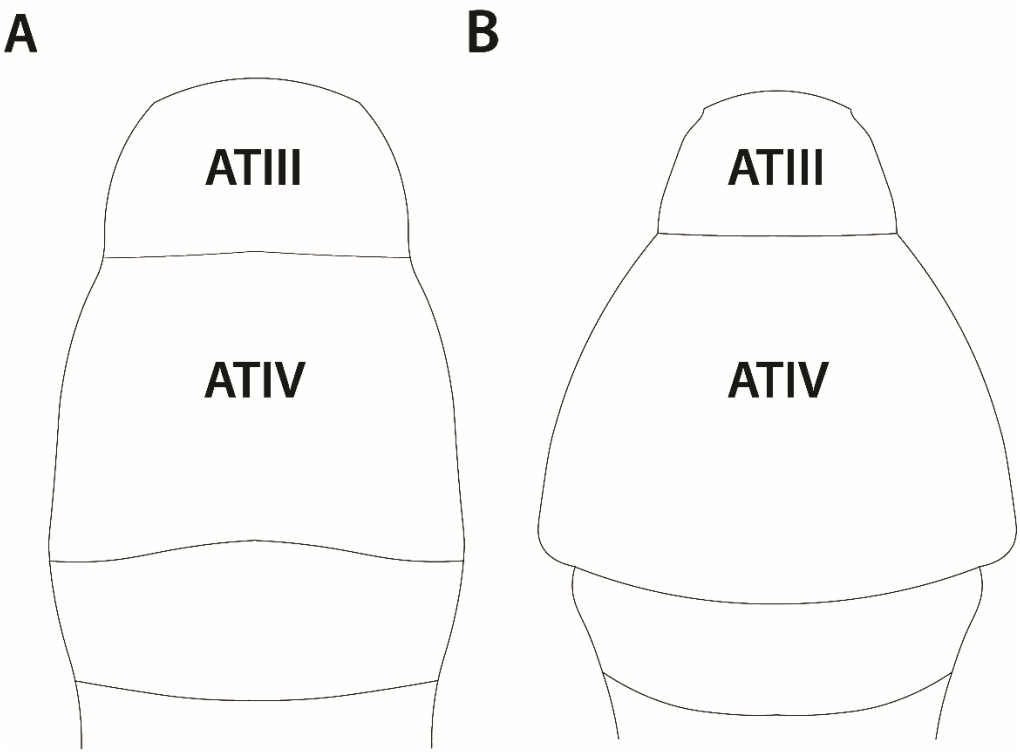

Figure 4.14. Proportions of abdominal tergites III-IV in *Protanilla* zhg-vn01 (**a**) versus *Protanilla lini* (**b**), diagrammatic.

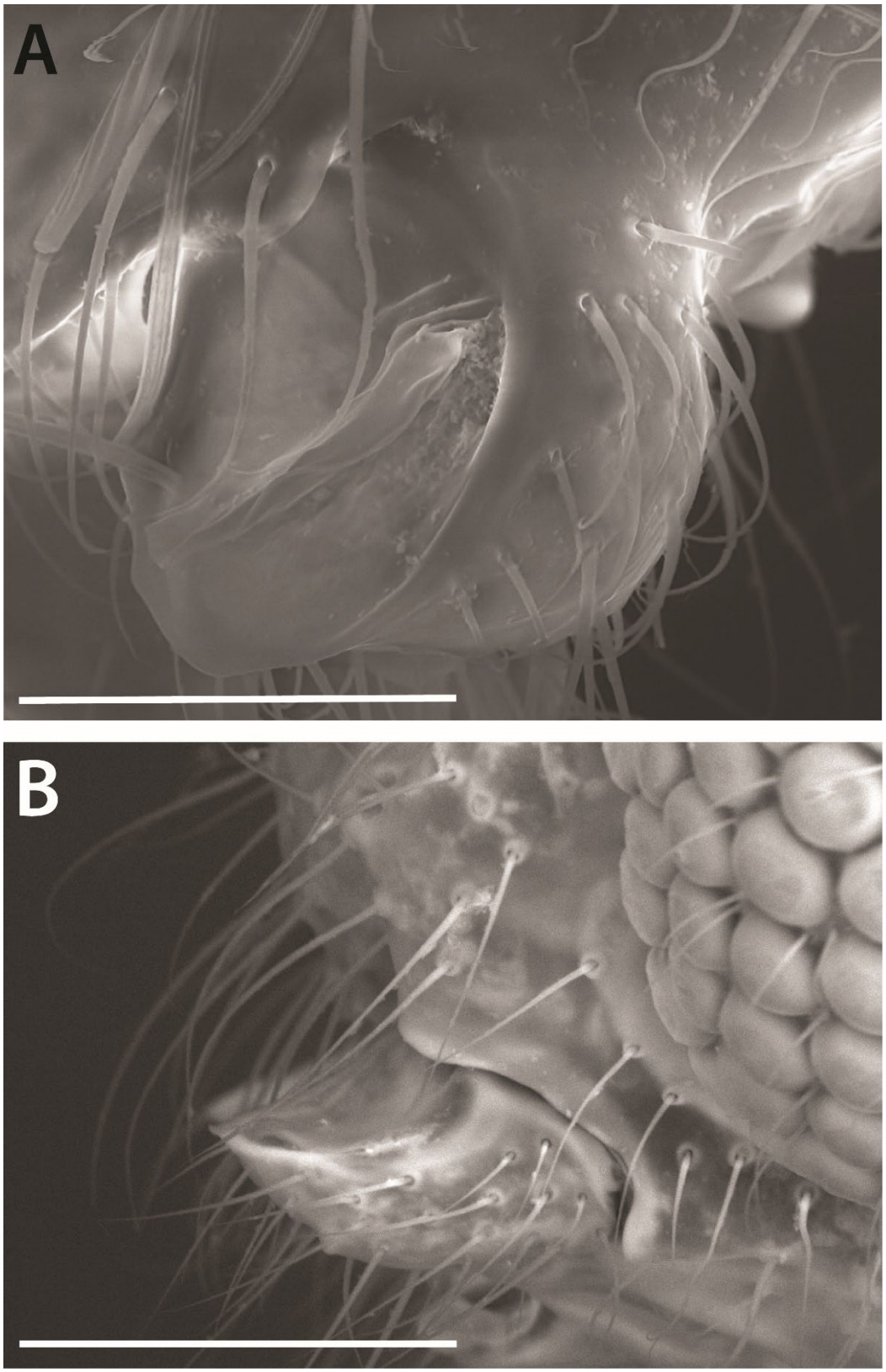

Figure 4.15. Articulation of the male mandible in the *Leptanilla thai* species-group. **a** *Leptanilla* nr. *indica* **b** *Leptanilla* zhg-bt03. Scale bars: A = 0.03 mm.; B = 0.04 mm.

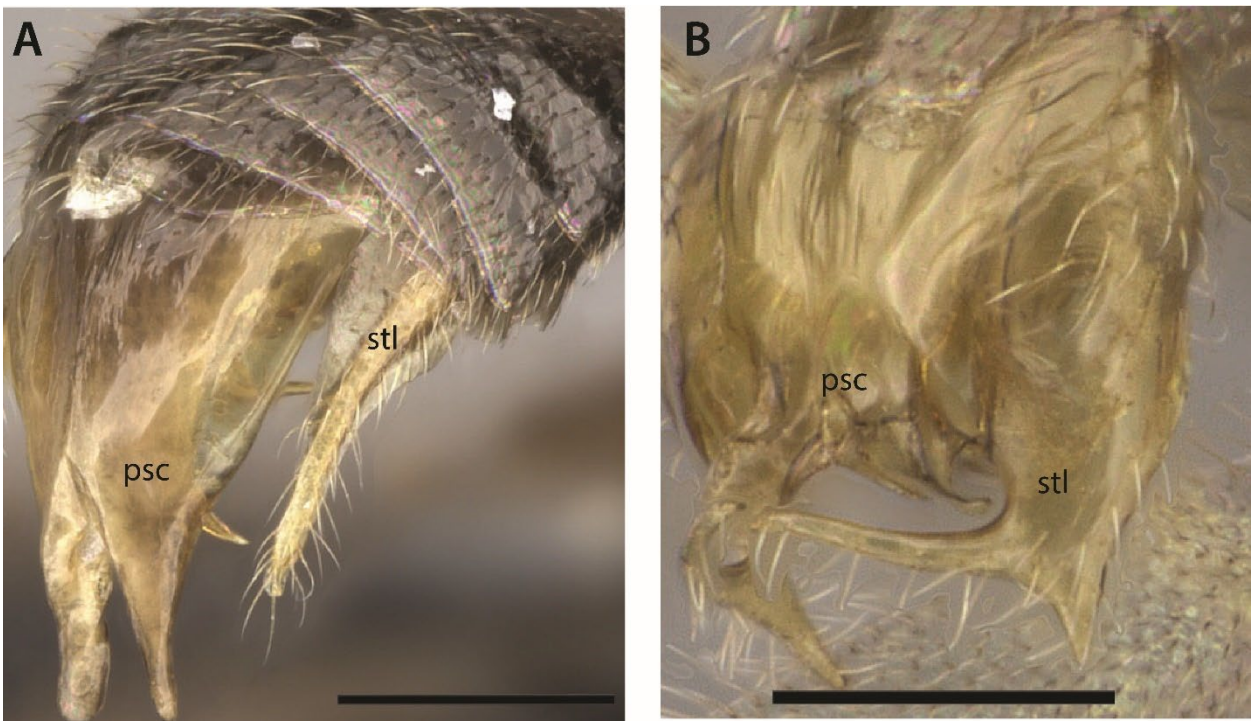

Figure 4.16. Proportions of the penial sclerites to the gonopodites in the *Leptanilla thai* species-group. **a** *Leptanilla argamani* **b** *Leptanilla* TH08. Abbreviations: stl = gonostyli; psc = penial sclerites. Scale bars: A = 0.2 mm.; B = 0.1 mm.

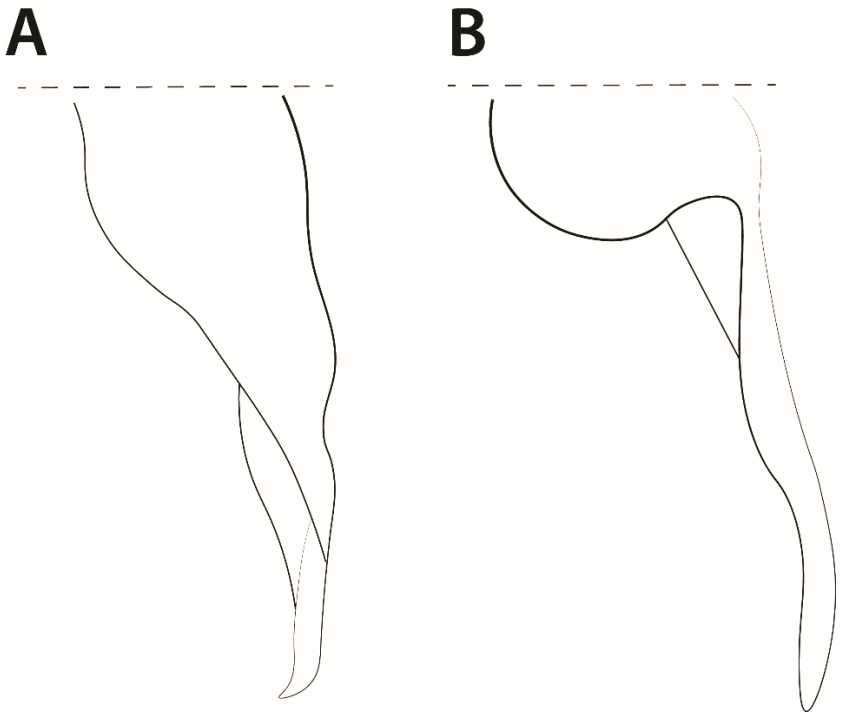

Figure 4.17. Outline of the gonopodites in *Leptanilla indica* (**a**) and *Leptanilla argamani* (**b**), ventral view, diagrammatic. Redrawn from Kugler (1987: figs. 18, 22).

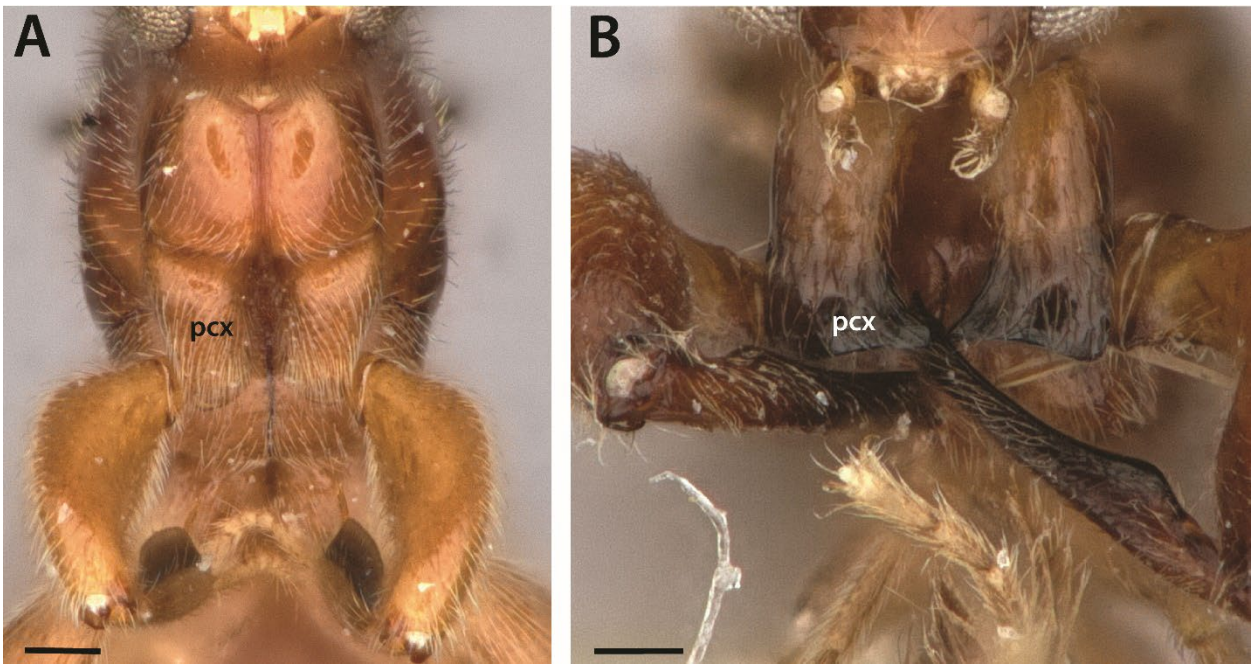

Figure 4.18. Condition of the male procoxa in *Leptanilla*, anterior view. **a** *Leptanilla* zhg-my04 (CASENT0842567) **b** *Leptanilla* cf. *copiosa* (CASENT0842844). Abbreviation: pcx = procoxa. Scale bars = 0.1 mm.

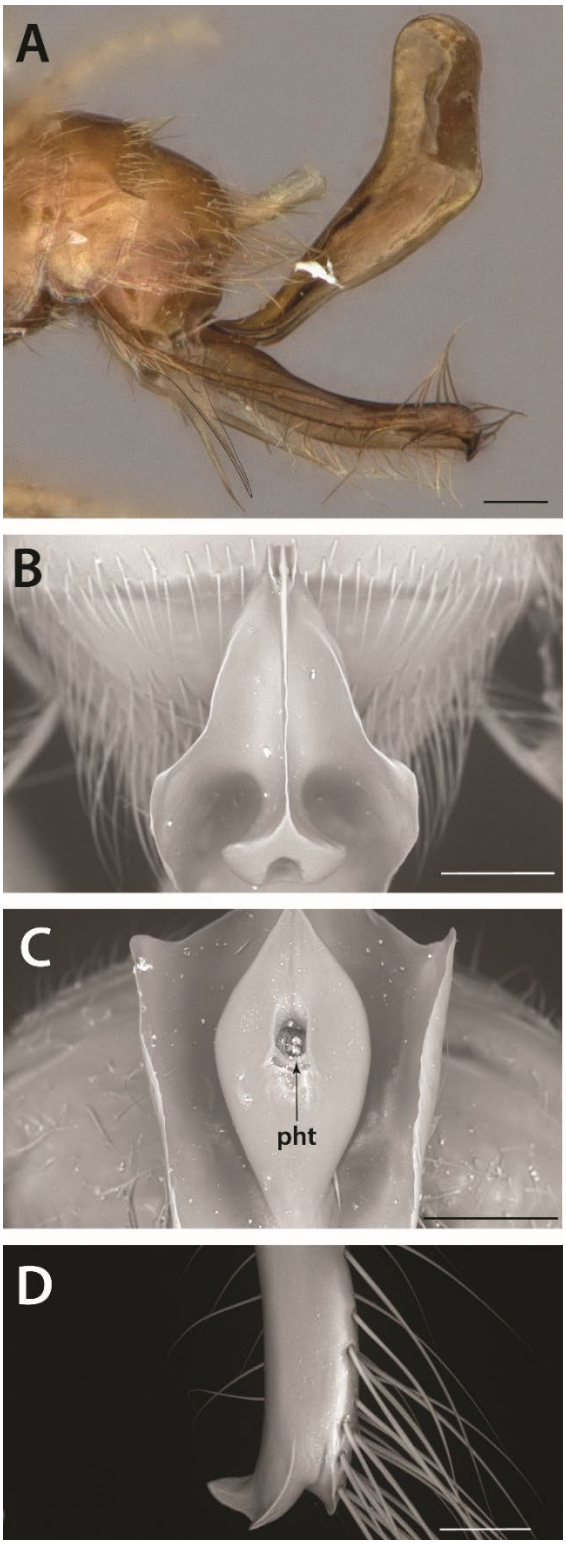

Figure 4.19. Genitalia of *Leptanilla najaphalla*. **a** Profile view, apicolateral gonocoxital lamina outlined (CASENT0106424) **b** Penial apex, posteroventral view (CASENT0106421) **c** Penial sclerites and phallotreme, ventral view (CASENT0106433) **d** Volsellar apex, dorsal view (CASENT0106421). Abbreviations: pht = phallotreme. Scale bars: A, C-D = 0.1 mm.; B = 0.2 mm.

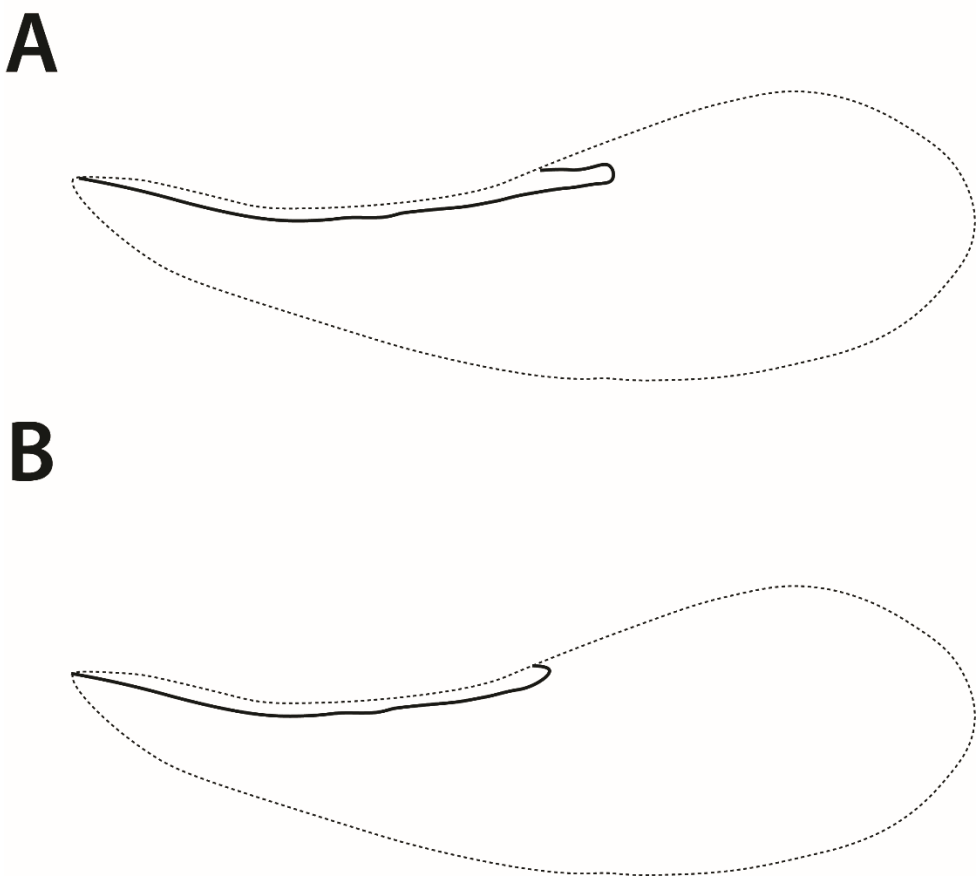

Figure 4.20. Presence (**a**) versus absence (**b**) of *2s-rs*+R+4-6 in males of the *Leptanilla revelierii* species-group, diagrammatic.

Current identifier	**Previous identifier**
Leptanilla MM01	*Yavnella* MM01
Leptanilla TH02	*Yavnella* TH02
Leptanilla TH03	*Yavnella* TH03
Leptanilla TH04	*Yavnella* TH04
Leptanilla TH06	*Yavnella* TH06
Leptanilla TH07	*Leptanilla* TH07
Leptanilla TH08	*Yavnella* TH08
Leptanilla zhg-bt03	*Yavnella* zhg-bt01
Leptanilla zhg-mm14	*Yavnella* indet.
Leptanilla zhg-my11	*Noonilla* zhg-my02
Leptanilla zhg-my14	*Noonilla* zhg-my06
Leptanilla zhg-my16	*Yavnella* zhg-my02
Leptanilla zhg-th02	*Yavnella* zhg-th01
Leptanilla zhg-th04	*Yavnella* zhg-th03
Leptanilla zhg-th05	*Yavnella* zhg-th04
Protanilla id01	*Anomalomyrma* indet.

Table 4.1. Concordance of morphospecies identifiers used in this study that conflict with previous publications.

Results

Protanilla wallacei sp. nov. (Fig. 4.21A-C)

Holotype. MALAYSIA – Sarawak • 1 ☿; Gunung Mulu National Park, 4th division; May-Aug. 1978, P. M. Hammond and J. E. Marshall leg.; CASENT0902782; BM1978-49, BMNH(E) 1015826. BMNH.

Paratypes. MALAYSIA – Sabah • 1 ☿; Gunung Silam, Lahad Datu; 4.96°N 118.17°E [estimated from Google Earth to nearest minute]); 630m a.s.l.; 1983; R. Leakey leg; CASENT0842699; UCDC.

MALAYSIA – Sabah • 1 ☿; 8km S Sapulut, 4.62844°N 116.47175°E; 325m a.s.l.; 31.vii.2014; P. S. Ward leg.; sifted litter (leaf mold, rotten wood), rainforest; CASENT0842640; PSW17199-01. UCDC.

Description. Lateral cranial margins converging anteriorly; cranium not bulging towards vertex. Genal angle laterad antennal toruli obtuse. Outline of clypeus campaniform in full-face view, laterally elevated above cranium, posteriorly not elevated above frons; clypeal surface planar; anterior clypeal margin slightly emarginate, posteromedian clypeal margin emarginate; median clypeal ridge present on mesal surface of clypeus, externally visible. Labrum visible in full-face view; anterodorsal apex of labrum armed with 3-4 dentiform, peg-like chaetae; venter with vestiture of suberect lamose setae. Mandibles elongate relative to head (CI=79-80), sublinear, apex curved downward distally; vertical dorsal lamella absent; laterodorsal longitudinal groove present; dorsomedial margin of mandible with single row of ~12 dentiform, peg-like chaetae;

lateral mandibular face glabrous. Labial palp 1-merous. Anterior tentorial pits faint, situated anterad the toruli, not visible in full-face view. Postgenal ridge complete. Scape long (SL 0.34-0.39 mm.), reaching slightly beyond occipital margin when antennae retracted. Flagellum submoniliform; apical flagellomere 3× longer than broad. Pronotum broader than mesonotum in dorsal view, with lateral margins convex. Mesonotum narrow, with lateral margins parallel in dorsal view. Meso-metapleural suture narrow laterally, broader along dorsal surface; scrobiculate, with transverse ridges larger and more widely spaced along dorsal surface of meso-metapleural suture; posteriorly distinct from metapleural trench. Maximum breadth of metapectal-propodeal complex greater than that of mesonotum in dorsal view, slightly narrowed anteriorly, posterior outline convex in profile view. Bulla large, extending anterior to propodeal spiracle. Propodeum rounded in profile view. Tarsomeres longer than broad. Meso- and metatibial spur formula 0,1p. Petiole sessile. Abdominal segments II-III without tergotergal and sternosternal fusion. Abdominal segment II slightly longer than wide in dorsal view (PI 94-99), with distinct dorsal node, in profile view anterior and posterior faces subequal in height; anterior face of petiolar node linear in profile view. Subpetiolar process present, abdominal sternite II with concavity posterior to subpetiolar process so that margin of abdominal sternite II is sinuate in profile view; fenestra present, elliptical, anteroposteriorly compressed. Lengths of abdominal segments II-III subequal. Abdominal sternite II projecting no further than abdominal sternite III towards venter. Abdominal segment III slightly broader than long in dorsal view (PPI=105-113), with distinct dorsal node; in profile view, anterior face of dorsal node abruptly vertical and bulging, posterior face gently sloping. Post-petiole with distinct tergosternal suture. Abdominal segments III-IV separated by pronounced constriction, with presclerites of abdominal segment IV distinct; pretergite IV planar in profile view, shorter than presternite IV; presternite IV

slightly convex in profile view; cinctus of abdominal segment IV scrobiculate. Anterior margin of abdominal post-tergite IV shallowly emarginate in dorsal view. Outline of postpetiolar node trapezoidal in dorsal view, corners rounded, slightly narrowed anteriorly. Soma concolorous, color castaneous. Vestiture of suberect to erect setae present; length of setae variable.

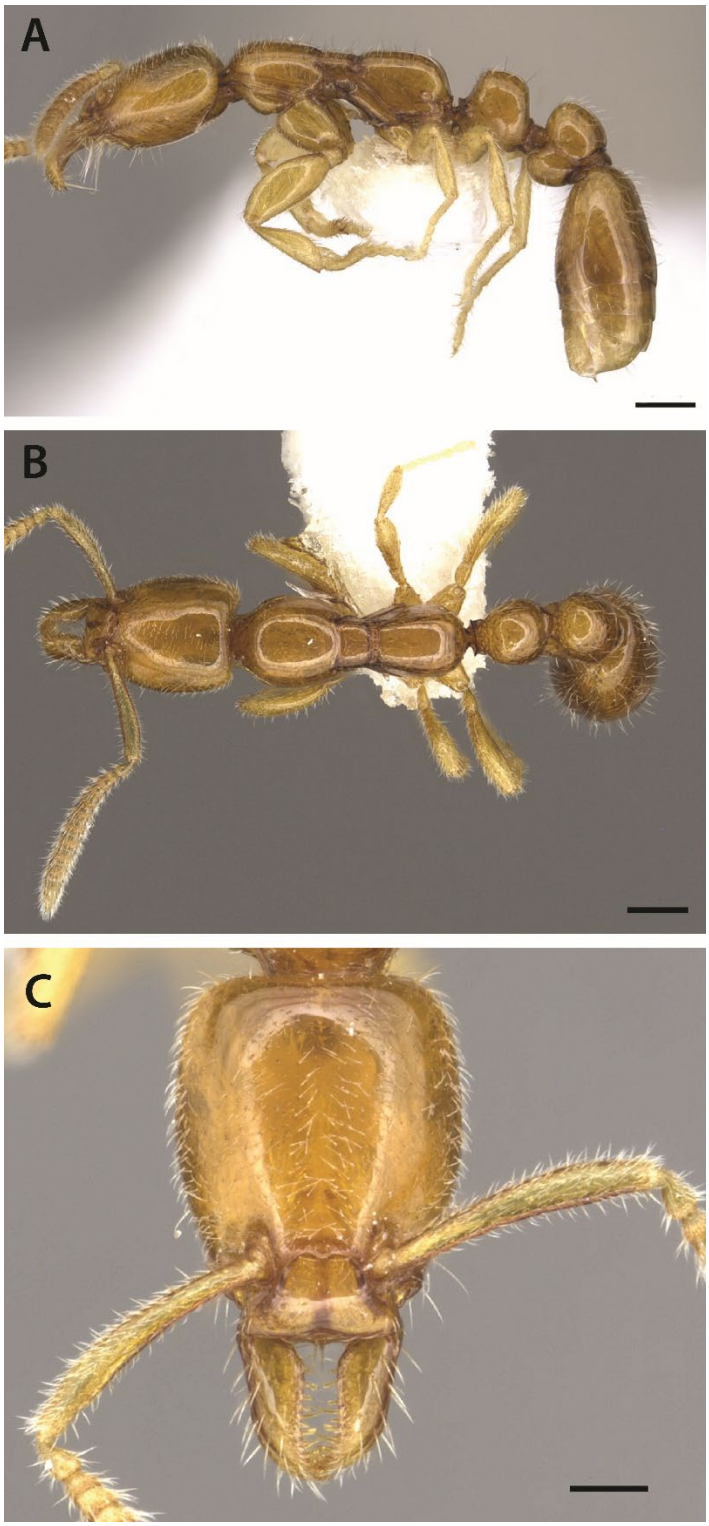

Figure 4.21. *Protanilla wallacei*, holotype (CASENT0902782; Ziv Lieberman). **a** Profile view. **b** Dorsal view. **c** Full-face view. Scale bars: A, B = 0.2 mm.; C = 0.1 mm.

Etymology. Named for Alfred Russel Wallace, commonly thought to be the progenitor of the discipline of biogeography and still well-regarded for his study of the biota of the Malay Archipelago, where this ant is native.

Diagnosis. The worker caste of *P. wallacei* is extremely close to that of *P. lini* but differs in overall smaller size (Table 4.2) and the shallowness of the postpetiolar node, with the posterior declivity being gradual (Fig. 4.7B) rather than abrupt (Fig. 4.7A). PPI tends to be greater in *P. wallacei* ($\underline{x} = 109$) than in *P. lini* ($\underline{x} = 100$) but cannot be consistently used to discriminate the two (Table 4.3). Interestingly, all known gynes of *P. wallacei* are ergatoid (Billen *et al.* 2013; Ito *et al.* 2021), whereas those of *P. lini* are alate (Hsu *et al.* 2017).

Remarks. Protanilla wallacei appeared as a *nomen nudum* in Hölldobler and Wilson (1990), with the name purportedly being under description by R. W. Taylor based upon material from Sabah. Such a description has not appeared. CASENT0842699 was identified as *P. wallacei* by Barry Bolton with reference to "type" material under description by Taylor, which, based on a paratype label assigned by Taylor, included CASENT0902782. Billen et al. (2013) described the glandular complement of specimens from peninsular Malaysia that was attributed to this *nomen nudum* by Taylor, while Ito et al. (2022) reported on the behavioral observations of specimens from that same series, referring to this species as *Protanilla* sp. *P. wallacei* is here made an available name, described based upon worker specimens from Sabah. Judging from Billen et al. (2013: fig. 5E), the series referred to in that study and in Ito et al. (2022) conforms to the diagnosis of *P. wallacei* here given. The unidentified *Protanilla* that was the sole representative of the Leptanillinae in the phylogenomic analyses of Branstetter et al. (2017) (CASENT0634862) is here identified as *P. wallacei*. Putatively intraspecific variation in labral chaeta count is here observed in sympatry for *P. wallacei*: this is also observed in putatively

conspecific allopatric specimens of *Protanilla gengma* (Aswaj et al., 2020) and *Protanilla beijingensis* (this study).

Protanilla wallacei and *P. lini* are recovered as sister taxa in phylogenomic inference sampling from across the geographical range of the latter species (Chapter 5). *P. lini* ranges across Taiwan and the Ryukyu Islands, while the *P. wallacei* specimens examined in this study originate in the Sundan region. This allows for the possibility that these putative species are populations from extreme ends of a contiguous swath of metapopulations extending throughout southeast Asia. Further sampling in mainland southeast Asia may reciprocally efface the morphometric distinction between these species, and with the other members of the *Protanilla lini* species-complex.

Protanilla wallacei	**HL**	**HW**	**SL**	**ML**	**PW**	**WL**	
CASENT0842699	0.425	0.334	0.342	0.218	0.265	0.677	
CASENT0842640	0.458	0.364	0.387	0.211	0.291	0.722	
CASENT0634862	0.429	0.345	0.334	0.24	0.264	0.64	
Protanilla lini							
OKENT0035688	0.509	0.413	0.428	0.225	0.321	0.779	
CASENT0842681	0.562	0.467	0.451	N/A	0.347	0.849	
CASENT0842755	0.555	0.456	0.497	0.298	0.349	0.888	
CASENT0842756	0.579	0.493	0.524	0.327	0.36	0.891	
CASENT0842757	0.59	0.466	0.525	0.319	0.36	0.936	
CASENT0842758	0.535	0.468	0.456	0.303	0.338	0.832	
CASENT0842759	0.552	0.457	0.458	N/A	0.335	0.837	
CASENT0842760	0.549	0.458	0.448	0.315	0.333	0.813	
CASENT0842761	0.553	0.45	0.463	0.314	0.331	0.853	
CASENT0842762	0.569	0.472	0.482	0.261	0.349	0.859	
CASENT0842763	0.565	0.464	0.484	0.322	0.353	0.859	
CASENT0842764	0.575	0.462	0.473	N/A	0.352	0.882	
CASENT0842765	0.554	0.469	0.469	0.281	0.349	0.86	
CASENT0842749	0.582	0.485	0.497	0.246	0.35	0.891	
CASENT0842700	0.578	0.483	0.478	0.275	0.365	0.895	
CASENT0842702	0.582	0.469	0.485	0.299	0.357	0.896	
Protanilla wallacei	**WL**	**PNL**	**PNH**	**PNW**	**PPNL**	**PPNW**	**PPNW**

CASENT0842699	0.677	0.198	0.121	0.186	0.187	0.068	0.203
CASENT0842640	0.722	0.206	0.143	0.203	0.206	0.059	0.233
CASENT0634862	0.64	0.194	0.125	0.196	0.193	0.06	0.204
Protanilla lini							
OKENT0035688	0.779	0.183	0.128	0.22	0.182	0.076	0.211
CASENT0842681	0.849	0.21	0.162	0.202	0.209	0.093	0.204
CASENT0842755	0.888	0.218	0.152	0.224	0.205	0.107	0.221
CASENT0842756	0.891	0.228	0.175	0.227	0.226	0.129	0.222
CASENT0842757	0.936	N/A	N/A	0.237	0.229	0.112	0.236
CASENT0842758	0.832	0.208	0.187	0.219	0.22	N/A	0.22
CASENT0842759	0.837	0.205	0.16	0.205	0.21	0.114	0.204
CASENT0842760	0.813	0.222	N/A	0.217	0.216	0.082	0.212
CASENT0842761	0.853	0.223	0.153	0.221	0.223	0.109	0.223
CASENT0842762	0.859	0.217	0.156	0.203	0.217	0.103	0.214
CASENT0842763	0.859	0.207	0.158	0.21	0.213	0.109	0.217
CASENT0842764	0.882	N/A	0.141	0.206	0.216	0.111	0.218
CASENT0842765	0.86	0.211	0.206	0.207	0.202	0.106	0.21
CASENT0842749	0.891	0.216	0.156	0.224	0.219	0.123	0.222
CASENT0842700	0.895	0.21	0.15	0.226	0.224	0.104	0.204
CASENT0842702	0.896	0.221	0.157	0.218	0.223	0.117	0.204

Table 4.2. Morphometric data for *Protanilla wallacei* **sp. nov.** and *Protanilla lini*.

Protanilla wallacei	**CI**	**SI**	**PI**	**PPI**
CASENT0842699	78.5882	102.395	93.9394	108.556
CASENT0842640	79.476	106.319	98.5437	113.107
CASENT0634862	80.4196	96.8116	101.031	105.699
Protanilla lini				
OKENT0035688	81.1395	103.632	120.219	115.934
CASENT0842681	83.0961	96.5739	96.1905	97.6077
CASENT0842755	82.1622	108.991	102.752	107.805
CASENT0842756	85.1468	106.288	99.5614	98.2301
CASENT0842757	78.9831	112.661	N/A	103.057
CASENT0842758	87.4766	97.4359	105.288	100
CASENT0842759	82.7899	100.219	100	97.1429
CASENT0842760	83.4244	97.8166	97.7477	98.1481
CASENT0842761	81.3743	102.889	99.1031	100
CASENT0842762	82.9525	102.119	93.5484	98.6175
CASENT0842763	82.1239	104.31	101.449	101.878
CASENT0842764	80.3478	102.381	N/A	100.926
CASENT0842765	84.657	100	98.1043	103.96
CASENT0842749	83.3333	102.474	103.704	101.37

Protanilla lini				
CASENT0842700	83.564	98.9648	107.619	91.0714
CASENT0842702	80.5842	103.412	98.6425	91.4798

Table 4.3. Selected morphometric indices for *Protanilla wallacei* **sp. nov.** and *Protanilla lini*.

Leptanilla belantan **sp. nov.** (Figs. 4.9A-C, 4.22, 4.23A-C)

Holotype. MALAYSIA – Selangor • 1 ☿; Genting Highlands, below Sri Layan; 1.iv.1981; W. L. Brown leg.; hill forest, red-rotten wood; MCZ:Ent:00728278. MCZC

Paratypes. MALAYSIA – Selangor • 1 ♀; same data as for holotype; MCZ:Ent:00728275; MCZC • 3 ☿, same data as for holotype; MCZ:Ent:00728276, MCZ:Ent:00728277, MCZ:Ent:00793731; MCZC • 2 ☿, same data as for holotype; MCZ:Ent:00793729, MCZ:Ent:00793730; UCDC

Worker. Lateral margins of cranium slightly convex. Occipital carina distinct. Frontoclypeal process present, delimited from cranium by lateral carinae, with posteromedian delimitation from cranium, projecting well anterior of labrum in full-face view; apex robust, broad in outline, emarginate, bordered by laminae. Mandible short relative to head. Four teeth present on mandible; two teeth proximad apical tooth acute, subequal in size, with two denticles interposed; most proximal tooth large, distally recurved, blunt, enlarged apically (Fig. 4.22). Large, tapering basal seta absent from mandible; subapical tapering seta present (Fig. 4.22). Maxillary palp 2-merous. Scape short, not reaching cranial vertex at rest, somewhat expanded towards apex. Pedicel length subequal to that of basal flagellomere. Flagellum submoniliform; antennomere 3 subequal in length to distal antennomeres; apical flagellomere 2× longer than subapical flagellomere. In dorsal view, pronotal margins strongly convex, pronotal width distinctly greater than mesonotal width. Pronotal dorsum moderately convex, slightly elevated above dorsal

mesonotal vertex. Lateral margins of mesonotum and metapectal-propodeal complex subparallel in dorsal view; mesonotum not constricted anteriorly. Meso-metapleural suture entirely absent; fusion of mesonotum with propodeum marked by shallow excavation. Propodeum angular in profile view; propodeal declivity slanted; posterolateral corners rounded. Tarsomeres longer than broad. Meso- and metatibial spur formula 2b,2(1s,1p). Anterior margin of petiole linear in dorsal view. Abdominal segment II longer than wide, with distinct dorsal node; margins parallel in dorsal view; margin of abdominal sternite II sublinear in profile view, angled ventrally anteriorly; subpetiolar process present, not lamellate, anterior face concave in profile view. Length of abdominal segment II distinctly greater than that of III. Abdominal segment III longer than wide in dorsal view. Breadth of abdominal segment III less than half the breadth of abdominal segment IV in dorsal view (TI1=30-33) (Tables 4.4-5). Anteroposterior length of abdominal tergite IV greater than that of V-VIII combined. Respective anteroposterior lengths of abdominal segments V-VII subequal. Coloration brown.

Gyne. As for genus. Mandible with distinct basal and masticatory margins, edentate, not demarcated by a distinct subapical incisor; masticatory margin longer than basal margin. In dorsal view, breadth of mesonotum less than that of pronotum or metanotal-propodeal complex. Petiole longer than broad in dorsal view (PI=0.719), constricted anteriorly along both transverse and dorsoventral axes; subpetiolar process absent. Dorsal node situated towards posterior of petiole. Abdominal segment III axial relative to posterad abdominal segments. Postsclerites of abdominal segments III-VII subequal in length. Vestiture consisting of short subdecumbent to suberect setae, longer and more abundant on gaster than on remainder of soma.

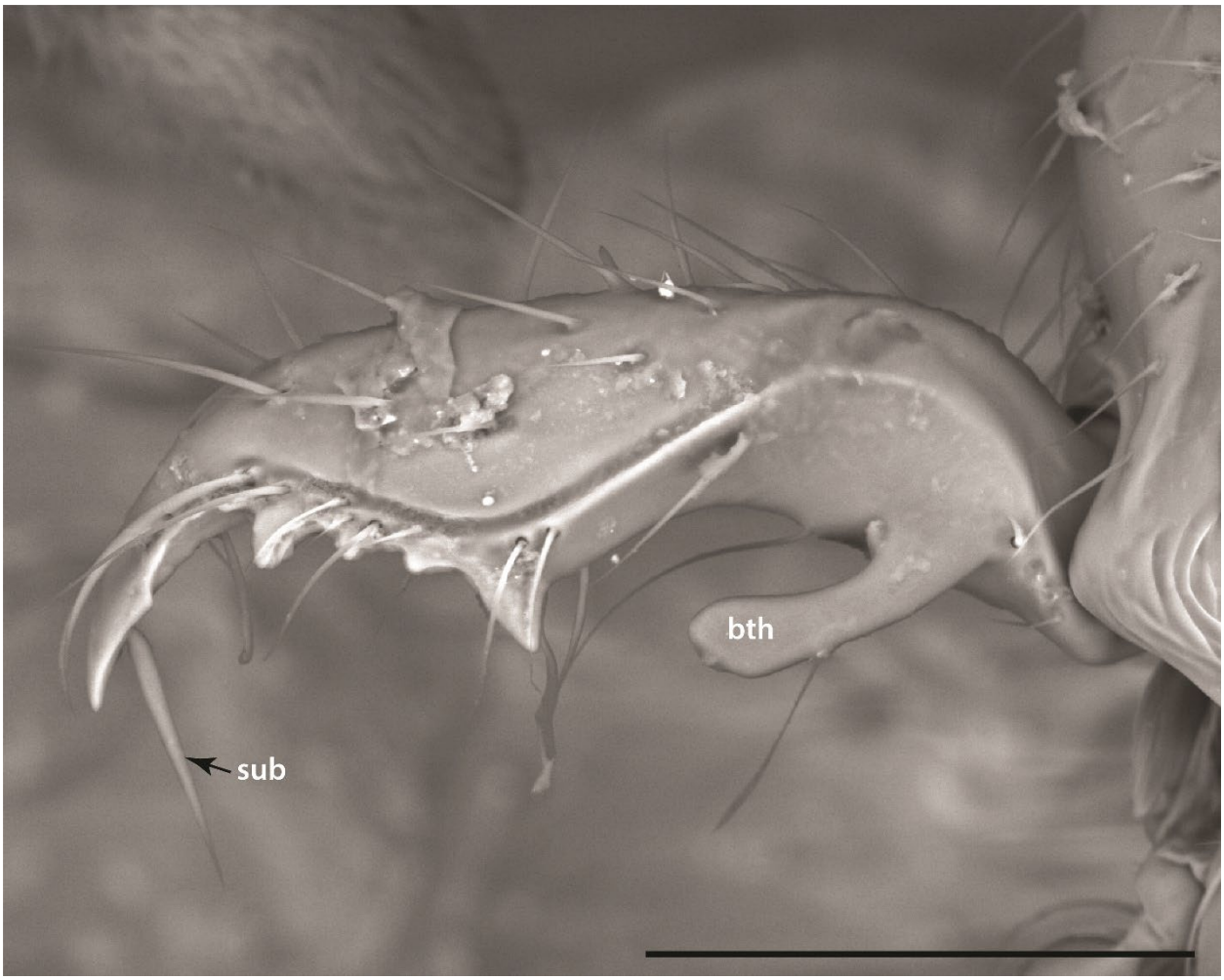

Figure 4.22. Mandible of *Leptanilla belantan* (MCZ:Ent:00728277), dorsal view. Abbreviations: sub = subapical mandibular seta; bth = most proximal tooth. Scale bar = 0.1 mm.

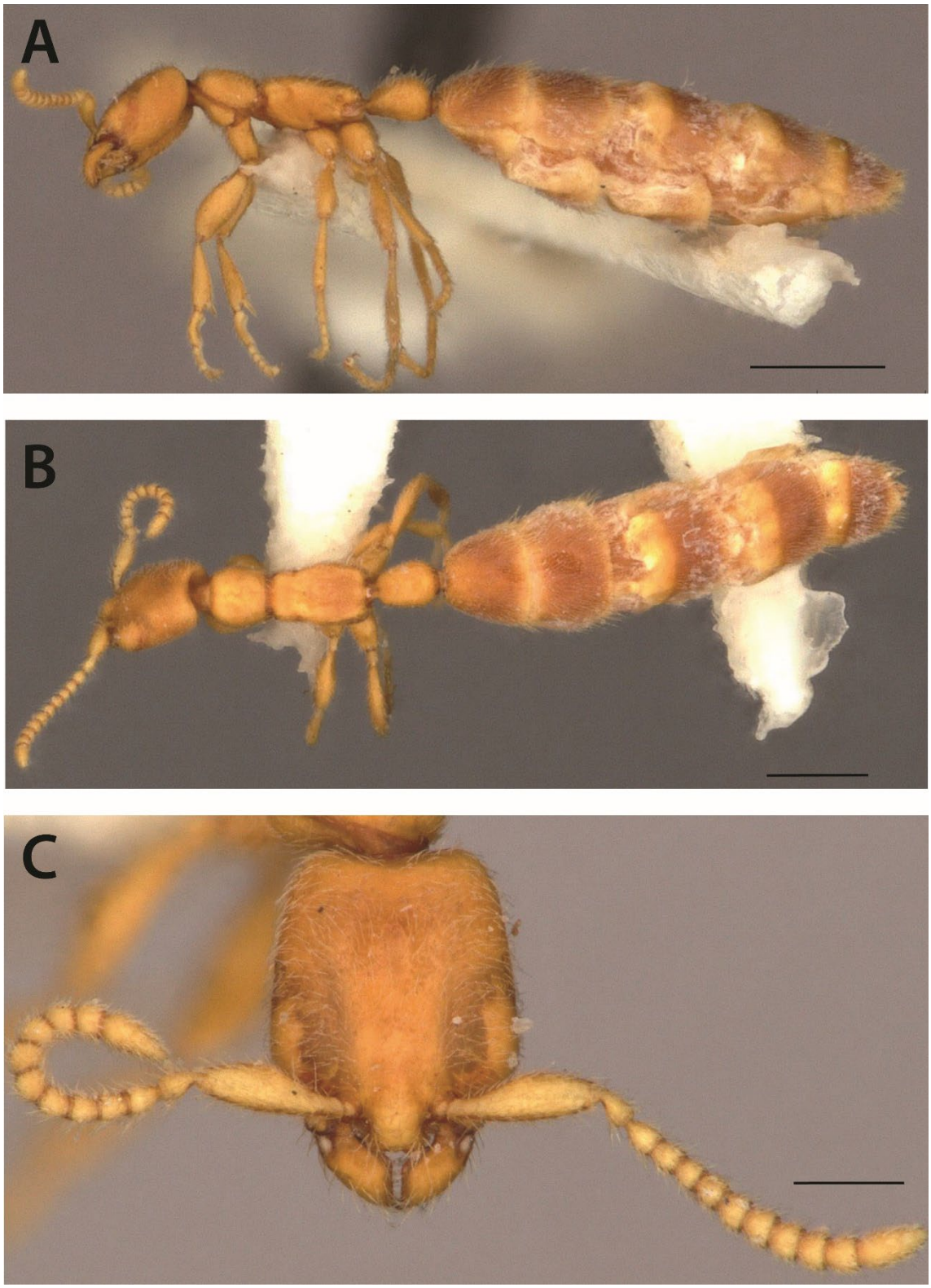

Figure 4.23. Gyne of *Leptanilla belantan* (MCZ:Ent:00728275). **a** Profile view **b** Dorsal view **c** Full-face view. Scale bars: A, B = 0.5 mm.; C = 0.2 mm.

Etymology. “Belantan” is Malay for a club-like weapon, in reference to the shape of the proximal tooth of the worker mandible, the apical expansion of which is unique in mandibular teeth observed in *Leptanilla*. The specific epithet is a noun in apposition and therefore invariant.

Diagnosis. The worker of *Leptanilla belantan* is closest to that of *Leptanilla judaica* and *Leptanilla ujjalai* in appearance. Like *L. ujjalai*, *L. belantan* possesses an enlarged, truncate proximal tooth on the mandible, which in the latter species is bent distally; *L. belantan* differs from *L. ujjalai* in not having a serrated subpetiolar process and in the apex of the frontoclypeal process being emarginate, rather than entire. Castaneous coloration and lack of a meso-metapleural furrow set *L. belantan* apart from *L. judaica*. The gyne habitus of *L. belantan* is nearest to *L. escheri* (Kutter, 1948), differing in the elongation of the masticatory margin and the complete absence of ommatidia.

Remarks. It is quite possible that the specimens identified as *L. escheri* and mentioned by Hölldobler et al. (1989) in fact belong to this species, since these also originated in peninsular Malaysia, although this speculation is unprovable because the repository of those specimens was not reported. It is also possible but unconfirmable that the undescribed *Leptanilla* species portrayed in Bolton (1990b: figs. 8-11) corresponds to *L. belantan*. As with these relatives, the placement of *L. belantan* in the *Leptanilla thai* species-group must be regarded with some caution until this hypothesis can be tested with phylogenomic inference. It is conceivable that *L. belantan* instead belongs to the *Leptanilla havilandi* species-group, since the worker caste of the two clades are at times distinguishable only by phenetic minutiae such as sculpturation. Unlike its putative close relatives within the *Leptanilla thai* species-group, *L. belantan* exists in parapatry with the *Leptanilla havilandi* species-group, allowing for the possibility that this species belongs to the latter clade.

The mandible of the gyne of *L. belantan* differs from the falcate facies observed in all other *Leptanilla* gynes, with the masticatory margin being longer than the basal margin. The gyne mandible in *L. belantan* therefore converges with the synapomorphic condition of the Poneroformicines (Richter et al., 2022).

Worker	**HW**	**HL**	**SL**	**LF2**	**MaL**	**WL**	**PrW**
MCZ:ENT:00793729	0.338	0.442	0.256	0.055	0.177	0.568	0.232
MCZ:ENT:00793730	0.327	0.422	0.241	0.045	N/A	0.54	0.227
MCZ:ENT:00793731	0.337	0.445	0.259	0.056	0.204	0.574	0.237
MCZ:ENT:00728276	0.345	0.45	0.275	0.045	0.206	0.565	0.229
MCZ:ENT:00728277	0.333	0.442	0.253	0.052	N/A	0.541	0.224
MCZ:ENT:00728278	0.335	0.435	0.276	0.048	0.195	0.558	0.225
Gyne							
MCZ:ENT:00728275	0.47	0.558	0.286	0.064	0.203	0.834	0.305
Worker	**MW**	**PTL**	**PTH**	**PTW**	**PPL**	**PPW**	**PPH**
MCZ:ENT:00793729	0.157	0.148	0.114	0.081	0.107	0.098	0.159
MCZ:ENT:00793730	0.154	0.137	0.118	0.079	0.11	0.1	0.154
MCZ:ENT:00793731	0.152	0.146	0.123	0.085	0.095	0.093	0.164
MCZ:ENT:00728276	0.156	0.155	0.125	0.085	0.102	0.103	0.175
MCZ:ENT:00728277	0.155	0.143	0.123	0.08	0.104	0.093	0.159
Gyne							
MCZ:ENT:00728275	0.308	0.302	0.209	0.217	N/A*	N/A*	N/A*
Worker	**TW4**						
MCZ:ENT:00793729	0.298						
MCZ:ENT:00793730	0.285						
MCZ:ENT:00793731	0.314						
MCZ:ENT:00728276	0.311						
MCZ:ENT:00728277	0.306						
MCZ:ENT:00728278	0.292						

Table 4.4. Morphometric data for *Leptanilla belantan* **sp. nov**. Asterisk indicates morphometrics inapplicable in the gyne.

Worker	**CI**	**SI**	**MI**	**PI**	**PPI**	**TI1**
MCZ:ENT:00793729	0.76471	0.7574	0.52367	0.5473	0.91589	32.8859
MCZ:ENT:00793730	0.77488	0.737	N/A	0.57664	0.90909	35.0877
MCZ:ENT:00793731	0.7573	0.76855	0.60534	0.58219	0.97895	31.8471
MCZ:ENT:00728276	0.76667	0.7971	0.5971	0.54839	1.0098	33.119
MCZ:ENT:00728277	0.75339	0.75976	N/A	0.55944	0.89423	30.3922
MCZ:ENT:00728278	0.77011	0.82388	0.58209	0.59441	0.91509	33.2192
Gyne						
MCZ:ENT:00728275	0.84229	0.60851	0.43191	0.71854	N/A*	N/A†

Table 4.5. Morphometric indices for *Leptanilla belantan* **sp. nov.** Asterisk signifies index inapplicable in the gyne; dagger signifies index not reported due to diagnostic irrelevance.

Leptanilla acherontia **sp. nov.** (Figs. 4.24A-C, 25)

Holotype. KENYA – Kakamega • 1 ☿; Kakamega Forest, Isecheno; 00.24°N 34.85°E; 6 Nov. 2002; 1550m a.s.l.; W. Okeka leg.; equatorial rainforest, sifted litter in soil under *Morus mesozygia*; CASENT0842720; UCDC

Paratype. KENYA – Kakamega • 1 ☿; same data as for holotype; CASENT0178284; LACM.

Description. Lateral margins of cranium subparallel. Occipital carina indistinct. Frontoclypeal process absent; frontoclypeal margin with median portion slightly raised, entire. Mandibles short relative to head. Three teeth present on mandible; apical and subapical teeth entire, intermediate tooth shallowly bifid (Fig. 4.25); irregular denticles interposed between all three teeth. Large, tapering basal seta absent from mandible; subapical tapering seta present. Scape short, not reaching cranial vertex at rest, somewhat expanded towards apex. Pedicel length distinctly greater than that of basal flagellomere. Flagellum submoniliform; length of basal flagellomere distinctly less than that of distal antennomeres; apical flagellomere 2× longer than subapical flagellomere. In dorsal view, pronotal margins moderately convex, pronotal width only slightly greater than mesonotal width. Pronotal dorsum planar, not elevated above dorsal mesonotal

vertex. Lateral margins of mesonotum and metapectal-propodeal complex subparallel in dorsal view; mesonotum not constricted anteriorly. Meso-metapleural suture absent dorsally; pleural portion visible as sinuate signum in oblique anterior view. Propodeum convex in profile view; propodeal declivity vertical and linear; posterolateral corners of propodeum rounded. Tarsomeres broader than long. Meso- and metatibial spur formula 1b,2(1b,1p). Anterior margin of petiole linear in dorsal view. Length and breadth of abdominal segment II subequal, distinct dorsal node present; margins parallel in dorsal view; subpetiolar process absent. Lengths of abdominal segments II-III subequal. Abdominal segment III slightly broader than long in dorsal view. Breadth of abdominal segment III approximately half that of abdominal segment IV in dorsal view (TI1=47-54) (Tables 4.6-7). Abdominal tergites IV-VII visible in posterodorsal view. Anteroposterior length of abdominal tergite IV twice anteroposterior length of abdominal tergite V in dorsal view. Anteroposterior lengths of abdominal tergites V-VI subequal; anteroposterior length of abdominal tergite VII much less than that of abdominal tergite VI. Sculpture largely absent. Vestiture consisting of short subdecument setae, longer and more abundant on gaster than on remainder of soma. Coloration yellowish.

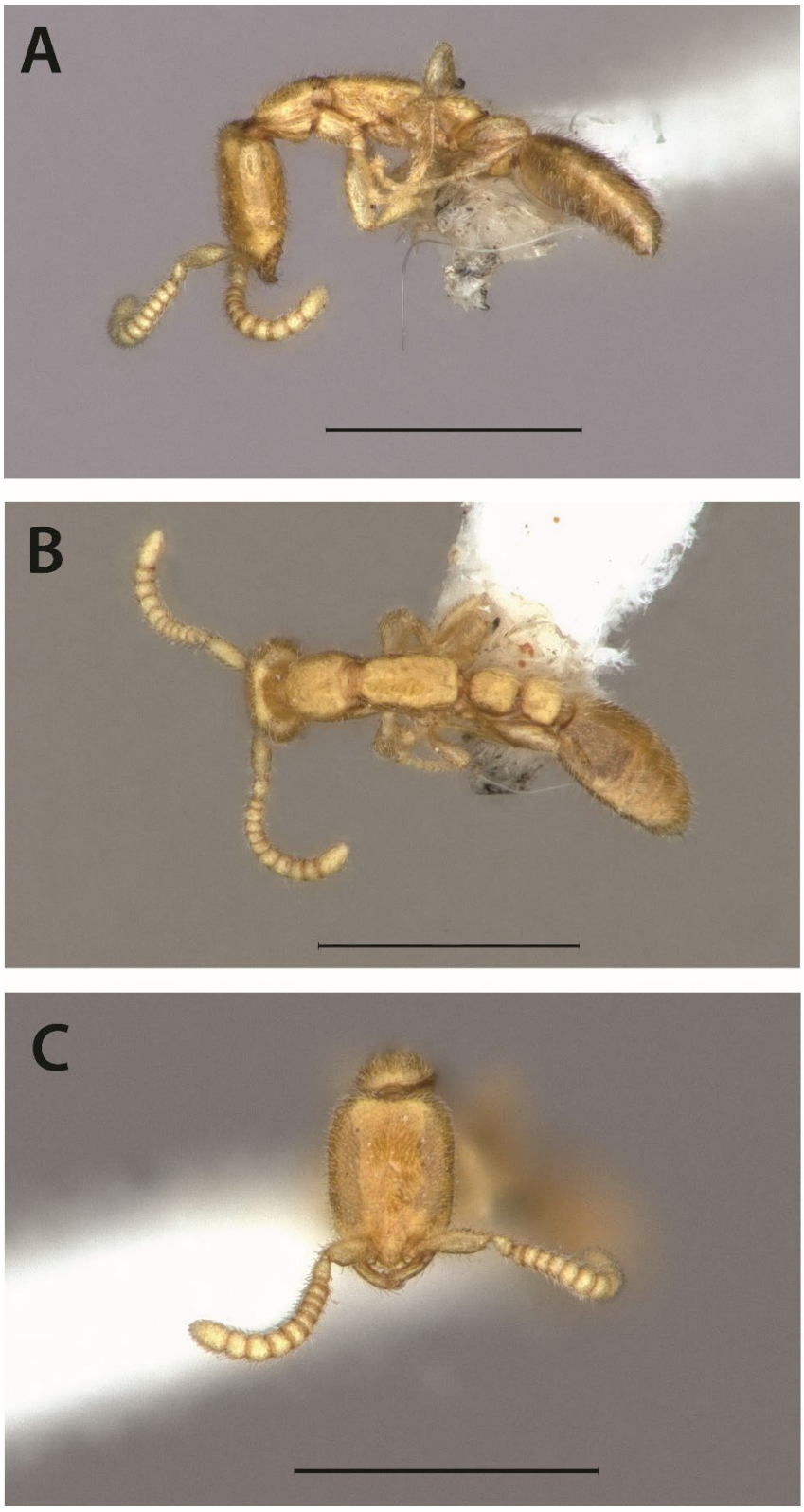

Figure 4.24. *Leptanilla acherontia* (CASENT0842720), holotype. **a** Profile view **b** Dorsal view **c** Full-face view. Scale bars: 0.5 mm.

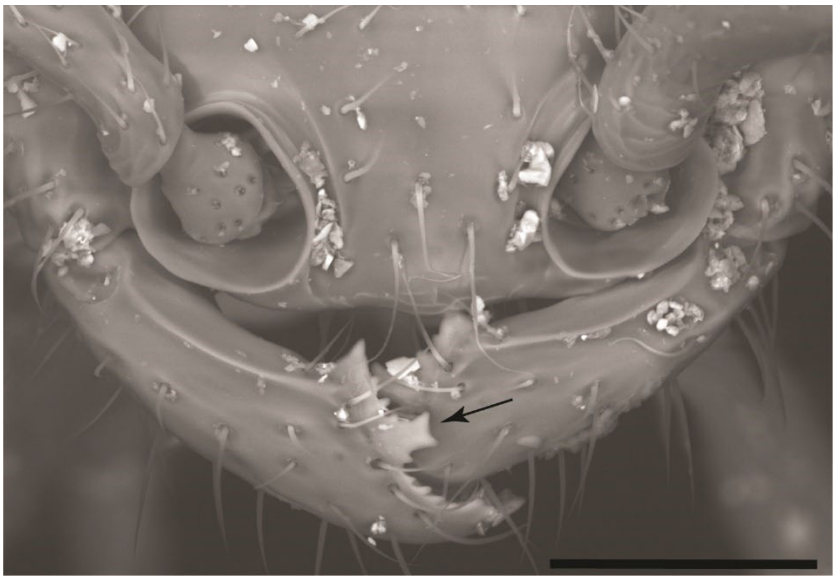

Figure 4.25. Mandibles of *Leptanilla acherontia* (CASENT0842721), dorsal view. Bifid tooth marked with arrow. Scale bar = 0.05 mm.

Etymology. The specific epithet refers to Acheron, a subterranean river in Greek mythology, continuing a theme established by the specific epithets of the related Iberian species *Leptanilla charonea* Barandica *et al.* and *Leptanilla plutonia* López *et al*. The gender is feminine.

Diagnosis. Leptanilla acherontia **sp. nov.** most closely resembles *Leptanilla revelierii* Emery, *Leptanilla kubotai* Baroni Urbani, and *Leptanilla okinawensis* Terayama, with 3 mandibular teeth and a linear clypeal margin. Abdominal tergite V is proportionally longer in dorsal view in *L. acherontia* than *L. revelierii*, while *L. acherontia* differs from *L. kubotai* and *L. okinawensis* in pedicel shape and larger body size, respectively. Based on consultation of AntWeb images, *Leptanilla* UG01, known only from equatorial rainforest in Kibale National Park, Uganda, is almost certainly conspecific with *L. acherontia*.

Remarks. Along with *Leptanilla boltoni* Baroni Urbani, *L. acherontia* is one of only two described Afrotropical *Leptanilla* species for which the worker caste is known. Phylogenomic inference indicates that *Leptanilla* zhg-ke02 may represent the male of *L. acherontia* (Chapter 5), but further sampling of sympatric *Leptanilla* would be required for this association to be

decisive. The type locality of *L. acherontia* is situated in perhumid equatorial rainforest, contrasting with the semi-arid provenance of *Leptanilla* zhg-ke01 and other Afrotropical and Western Palaearctic *Leptanilla*. It is unclear to what degree climatic conditions dictate the distributions of *Leptanilla* species.

	HW	**HL**	**MaL**	**SL**	**WL**	**PNW**	**PNL**
CASENT0842720	0.216	0.289	0.112	0.134	N/A	0.139	0.177
CASENT0842721	0.206	0.276	0.114	0.12	0.374	0.131	0.183
	MW	**PTL**	**PTH**	**PTW**	**PPL**	**PPW**	**TW4**
CASENT0842720	0.117	0.11	N/A	0.098	0.089	0.114	0.208
CASENT0842721	0.111	0.098	N/A	0.088	0.086	0.097	0.205

Table 4.6. Morphometric data for *Leptanilla acherontia* **sp. nov.**, worker.

CI	**SI**	**MI**	**PI**	**PPI**	**TI1**
74.7405	62.037	51.8519	N/A	128.09	54.8077
74.6377	58.2524	55.3398	N/A	112.791	47.3171

Table 4.7. Morphometric indices for *Leptanilla acherontia* **sp. nov.**, worker.

Leptanilla najaphalla **sp. nov.** (Figs. 4.19A-D, 4.26A-C, 4.27, 5.28)

Holotype. MALAYSIA – Sabah • 1 ♂; Sipitang Dist., Mendolong; 4.917°N, 115.767°E [estimated from Google Earth to nearest minute]; 27 Apr. 1988; S. Adebratt leg.; A1L; CASENT0106427 [MZLU00174197]; MZLU

Paratypes. MALAYSIA – Sabah • 2 ♂; same locality as for holotype; 7 Apr. 1988; S. Adebratt leg.; A1L; CASENT0106435, CASENT0106437; MZLU • 5 ♂; same locality as for preceding; 16 Apr. 1988; S. Adebratt leg.; A1L; CASENT0106416, CASENT0106417, CASENT0106438, CASENT0106444, CASENT0106457; MZLU · MALAYSIA, Sabah • 5 ♂; same locality as for preceding; 19 Apr. 1988; S. Adebratt leg.; W5L; CASENT0106421, CASENT0106432, CASENT0106433, CASENT0106449, CASENT0106450; MZLU • 2 ♂; same locality as for preceding; 25 Apr. 1988; S. Adebratt leg.; T1B/W4; CASENT0106443, CASENT0106454; MZLU • 1 ♂; same locality as for preceding; 27 Apr. 1988; S. Adebratt leg.; A1L;

CASENT0106413; MZLU • 6 ♂; same locality as for preceding; 1 May 1988; S. Adebratt leg.; A1L; CASENT0106422, CASENT0106423, CASENT0106424, CASENT0106426, CASENT0106428, CASENT0106430; MZLU • 2 ♂; same locality as for preceding; 3 May 1988; S. Adebratt leg.; T4/R; CASENT0106420, CASENT0106458; MZLU • 2 ♂; same locality as for preceding; 4 May 1988; S. Adebratt leg.; T4/R; CASENT0106412, CASENT0106456; MZLU • 2 ♂; same locality as for preceding; 5 May 1988; S. Adebratt leg.; A1L; CASENT0106418, CASENT0106453; MZLU • 3 ♂; MALAYSIA, Sabah: same locality as for preceding; 13 May 1988; T4/R; CASENT0106414, CASENT0106415, CASENT0106429; MZLU

Description. Cranial outline quadrate. Occiput emarginate in full-face view. Frons produced into anterior shelf. Mandible articulated to gena; distinctly longer than broad. Mandalus large, covering most of anterodorsal mandibular surface. Maxillary palp 1-merous. Clypeus anteroposteriorly reduced, concealed by frontal shelf in full-face view. Anterior tentorial pits not discernible. Compound eyes longer than wide in profile view, posterior margin slightly emarginate, all other margins convex. Anteromedian ocellus and compound eyes not intersecting line drawn perpendicular to anteroposterior axis of cranium. Scape anteroposteriorly compressed, longer than wide, shorter than anteroposterior length of compound eye; pedicel short, subcylindrical, lateral margins parallel, length 0.5 that of scape; antennomere 3 short, subcylindrical, length less than that of pedicel or scape; flagellum submoniliform, not extending posterior to mesoscutellum if folded flat over mesosoma. Pronotum and mesoscutum posteriorly prolonged. In profile view anterodorsal pronotal face slightly convex, diagonal to craniocaudal axis at ~45° angle. Mesoscutal dorsum planar; mesoscutum longer than broad. Antero-admedian signum absent. Notauli absent. Parapsidal signa present, not impressed. Mesoscutellum longer

than tall, dorsum not lower than that of mesoscutum, posterodorsal mesoscutellar face convex, not posteriorly produced. Oblique mesopleural sulcus present, not intersecting metapectal-propodeal complex. Metapleuron indistinct. Metapleural gland absent. Propodeum convex in profile view, with distinct dorsal and posterior faces; areas of these faces subequal. Procoxa longer than meso- and metacoxa; procoxa without distal transverse carina. Protrochanters sphenoid in outline, distally truncate. Profemur markedly constricted at base, anteroposteriorly compressed, incrassate; acute distal flange on posterior surface present; Arcuate medial carina absent. Protibia >0.5× length of profemur, not dorsoventrally compressed, without ventromedian carina; protibial comb present, length of processes decreasing distally; probasitarsal seta not hypertrophied. Meso- and metatibial spur formula 2b,2b. C, Sc+R+Rs, *2s-rs*+R+4-6, Rf, Mf1, *cu-a*, and Cuf+1A tubular; M+Cu and 1A nebulous; all other venation absent. Cuf+1A spectral apically, not reaching anal margin. Costal infuscation present proximal to *2s-rs*+R+4-6; C extending well beyond infuscation. Abdominal segment II anteroposteriorly compressed, not broader than long in dorsal view; dorsal node present, well-developed, without median excavation. Abdominal sternite II with process along posterior 0.5 of length, outline cuneiform in profile view, apex rounded. Presclerites of abdominal segments IV-VIII inconspicuous. Abdominal segments III-IX without tergosternal fusion (Chapter 3). Abdominal tergites IV-VII each broader than preceding tergite in dorsal view, lateral margins diverging posteriorly; breadth of abdominal tergite VIII less than that of abdominal tergite VII in posterodorsal view. Abdominal sternite VIII anteroposteriorly compressed, not visible without dissection, posterior margin entire (Chapter 3). Abdominal sternite IX with posteromedian fusion to gonocoxites; anteroposteriorly compressed along median axis, laterally expanded and lobate. Mulceators present, subcircular in cross-section, longer than anteroposterior length of gonocoxites.

Gonocoxites bulging, with complete dorsomedian and ventromedian fusion; apicoventral laminae present, subulate in outline. Gonostyli absent. Volsellae present, with complete proximomedian fusion, subcircular in cross-section; sclerotized medial carina present at volsellar apex, produced into pair of denticles, dorsal denticle shorter than ventral one. Penial sclerites not dorsoventrally compressed, basally recurved, proximal ¼ subcircular in cross-section, apical 1/3 with ventromedian carina; rounded platform proximad this median carina with outline elliptical; phallotreme subapical and ventral, recessed, not surrounded by vestiture of setae; lateral laminate flanges present. Most sclerites with vestiture of subdecumbent to appressed setae; elongated on posterior margins of abdominal tergites III-VIII, increasing in length posteriorly; anterior faces of mulceators with elongate suberect setae; ectal faces of volsellae with suberect to erect setae, genitalia otherwise bare. Cuticle bearing piligerous punctae; sculpture fatiscent distad and proximad phallotreme (Fig. 4.28).

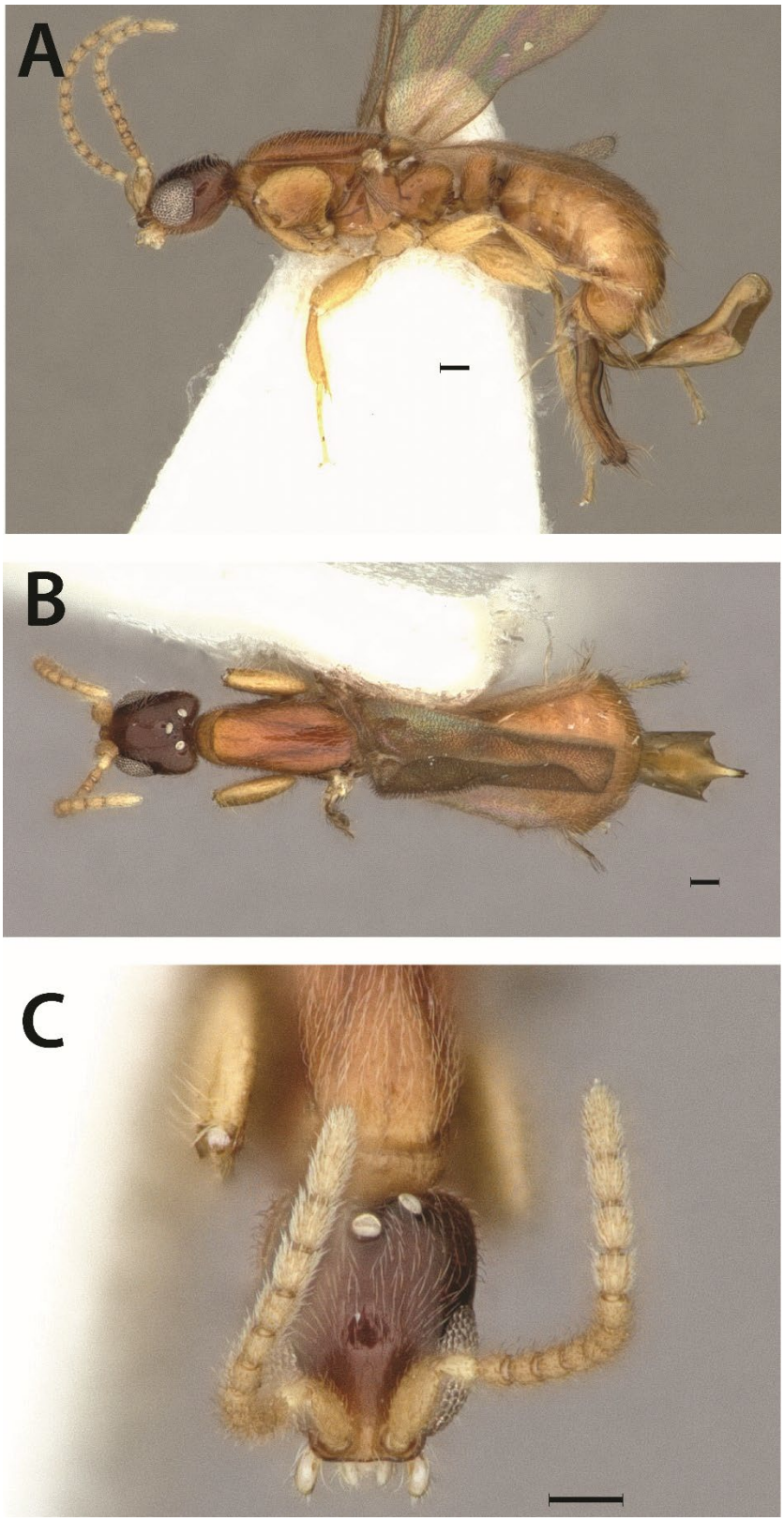

Figure 4.26. *Leptanilla najaphalla*, holotype (CASENT0106427). **a** Profile view **b** Dorsal view **c** Full-face view. Scale bar = 0.1 mm.

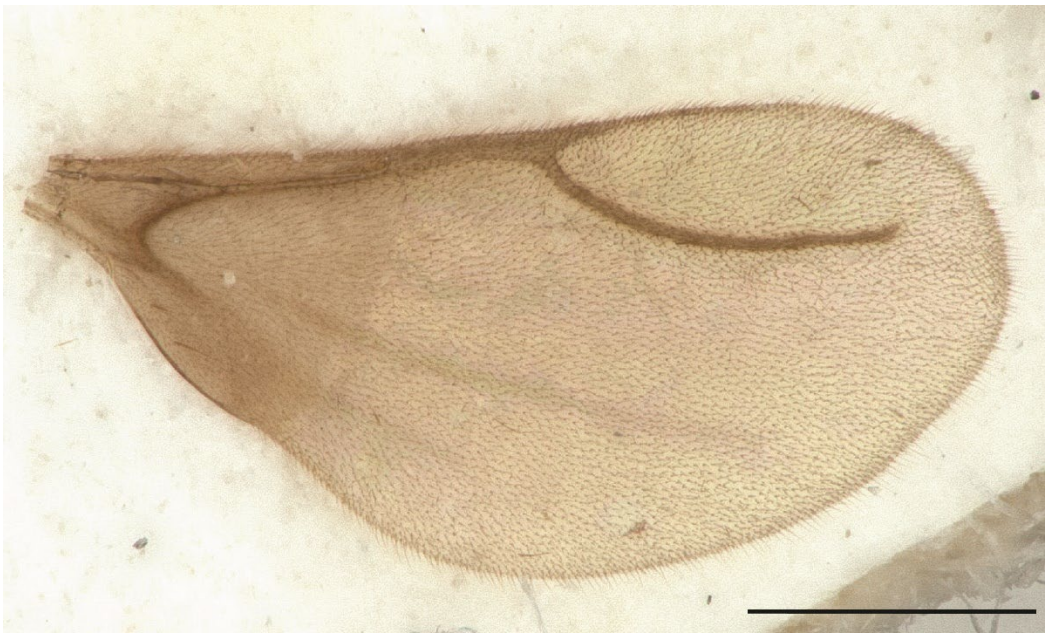

Figure 4.27. Forewing of *Leptanilla najaphalla* (CASENT0106419). Scale bar = 0.5 mm.

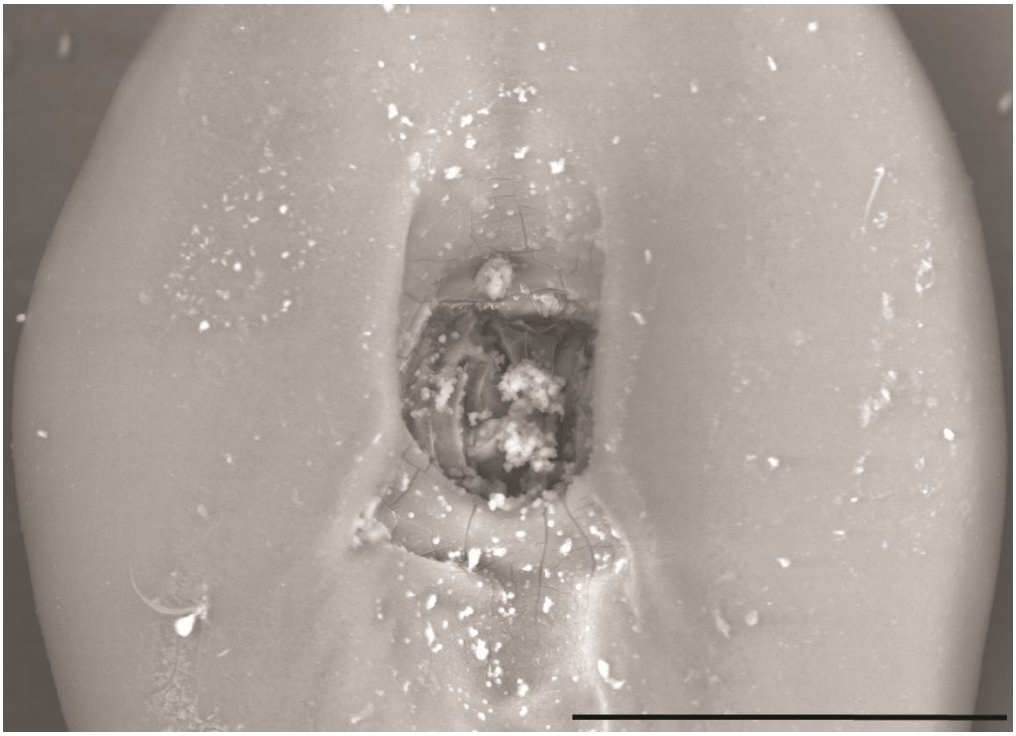

Figure 4.28. Phallotreme of *Leptanilla najaphalla* (CASENT0106433). Scale bar = 0.5 mm.

Etymology. The specific epithet derives from *Naja* (Squamata: Elapidae), the cobra, and *-phalla*, meaning penis. This refers to the florid facies of the penial sclerites, which recalls the threat display of these snakes: the dorsal curvature of the penial sclerites resembles the rearing posture,

while the lateral laminae resemble the extended “hood” of the cobra. The specific epithet is feminine.

Diagnosis. Leptanilla najaphalla is so far the only formally described species belonging to the *Leptanilla najaphalla* species-group. The males of *L. najaphalla* uniformly differ from the sympatric undescribed morphospecies *Leptanilla* zhg-my05 in the outline of the apicolateral gonocoxital lamina and the proportions of the penial sclerites and volsellae to the gonocoxites.

Remarks. Leptanilla najaphalla was included in the phylogenetic analyses of Griebenow (2020) and Chapters 2-3 under the provisional identifier *Leptanilla* zhg-my02, with the genitalia being the subject of detailed morphological study using micro-computed tomography presented in Chapter 3, under that same provisional identifier. Describing a new species of *Leptanilla* based solely upon male specimens, as here done for *L. najaphalla*, was eloquently argued against by Bolton (1990b), since it exacerbates the probable redundancy that plagues the taxonomy of *Leptanilla*. This description of *L. najaphalla* is justified only to give a formal species-group name to the Bornean morphospecies-group. This subclade of *Leptanilla* remains known only from males and is robustly supported by all phylogenetic analyses that have addressed its monophyly, in addition to being supported by several conspicuous morphological autapomorphies. Accordingly, the Bornean morphospecies-group is here termed the *Leptanilla najaphalla* species-group (see Discussion).

Leptanilla bethyloides **sp. nov.** (Figs. 4.29A-C, 30)

Holotype. CHINA – Hong Kong • 1 ♂; Tai Po Kau; 22.44°N 114.18°E [estimated from Google Earth to nearest minute], 15 Jun. 1964; W. J. Voss and W. M. Hui leg.; CASENT0842864. BPBM.

Paratype. CHINA – Hong Kong • 1 ♂; same locality as for preceding; 2-6 Jul. 1964; L. K. and H. W. Ming leg.; light trap; CASENT0842865. BPBM.

Description. Cranial outline quadrate. Occiput emarginate in full-face view. Frons not produced into anterior shelf. Mandible articulated to gena; broader than long. Mandalus large, covering entire anterodorsal mandibular surface. Maxillary palp 1-merous. Clypeus anteroposteriorly reduced, not discernible in full-face view. Anterior tentorial pits not discernible. Compound eyes longer than wide in profile view, posterior margin slightly emarginate, all other margins convex. Anteromedian ocellus and compound eyes not intersecting line drawn perpendicular to anteroposterior axis of cranium. Scape anteroposteriorly compressed, longer than wide, shorter than anteroposterior length of compound eye; pedicel short, subcylindrical, lateral margins parallel, length 0.5× that of scape; antennomere 3 short, subcylindrical, length subequal to that of pedicel; flagellum submoniliform, not extending to posterior to mesoscutum if folded flat over mesosoma. Pronotum and mesoscutum posteriorly prolonged. In profile view anterodorsal pronotal face diagonal to craniocaudal axis at ~45° angle, but profile of pronotum otherwise obscured by vestiture. Mesoscutal dorsum slightly convex; mesoscutum longer than broad. Antero-admedian signum absent. Notauli absent. Parapsidal signa present, impressed. Mesoscutellum longer than tall, dorsum not lower than that of mesoscutum, posterodorsal mesoscutellar face convex, posteriorly produced, not recurved. Oblique mesopleural sulcus present, not intersecting metapectal-propodeal complex. Metapleuron distinct, transected by transverse sulcus. Metapleural gland absent. Propodeum convex in profile view, without distinct dorsal and posterior faces. Pro- and metacoxa subequal in length, metacoxal somewhat more massive; mesocoxa shorter than pro- and metacoxa. Protrochanters sphenoid in outline, distally truncate. Profemur not markedly constricted at base, anteroposteriorly compressed, incrassate;

acute distal flange on posterior surface absent; Arcuate medial carina absent. Protibial and profemoral length subequal; protibia not dorsoventrally compressed, without ventromedian carina; protibial comb absent; probasitarsal seta not hypertrophied. Meso- and metatibial spur formula 2b,2(1b,1p). C and Sc+R+Rs fused, tubular; *2s-rs*+R+4-6 and M+Cu tubular; all other venation absent. Costal infuscation absent. Abdominal segment II anteroposteriorly compressed, broader than long in dorsal view; dorsal node present, well-developed; with median excavation. Abdominal sternite II without process, planar in profile view. Presclerites of abdominal segments IV-VIII inconspicuous. Abdominal segments III-VII without tergosternal fusion. Tergosternal fusion of abdominal segment VIII-IX unknown. Abdominal tergites III-VIII not anteroposteriorly compressed, lateral margins subparallel; breadth of abdominal tergite VIII subequal to that of abdominal tergite VII in posterodorsal view. Abdominal sternite VIII anteroposteriorly compressed, visible without dissection, posterior margin entire. Abdominal sternite IX not visible without dissection. Mulceators absent. Gonocoxites without complete dorsomedian and ventromedian fusion; ventromedial margin of gonocoxite with lamina; apicoventral laminae absent. Gonostylus present, outline lanceolate, apex entire. Volsellae absent. Penial sclerites dorsoventrally compressed, not basally recurved, ventromedian carina extending along most of length, without lateral laminate margins. Phallotreme dorsal, concealed by gonostyli in available specimens. Somal sclerites with thick vestiture of decumbent to suberect setae, sparsest on mesopectus and metapleuron; setae appressed to decumbent on antennae and legs; gonostyli with similar vestiture to abdominal postsclerites, genitalia otherwise glabrous. Base of forewing costa bearing row of exceptionally long, suberect setae. Cuticle bearing piligerous punctae; sculpture otherwise absent.

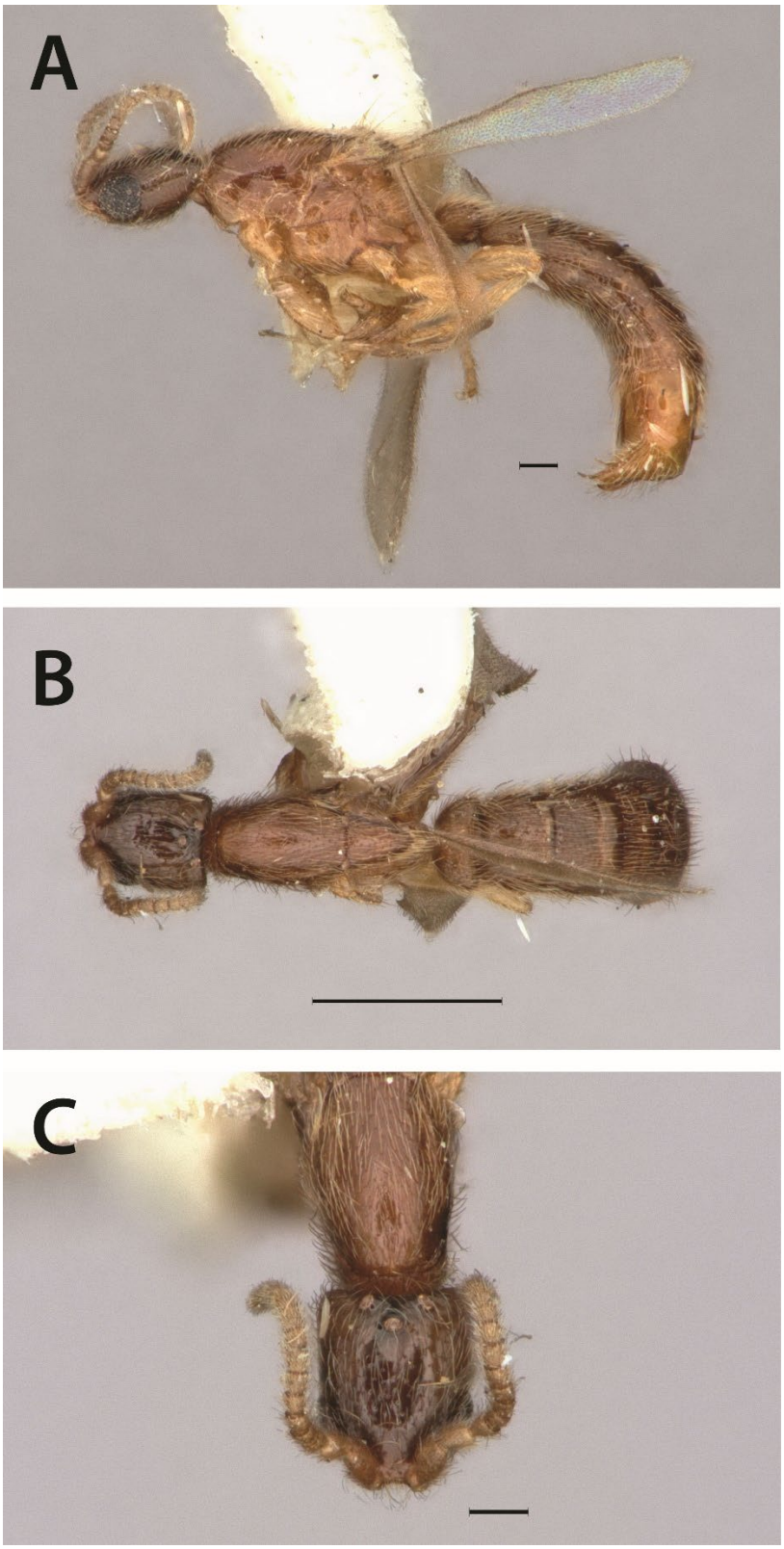

Figure 4.29. *Leptanilla bethyloides*, holotype (CASENT0842864). **a** Profile view **b** Dorsal view **c** Full-face view. Scale bars: A, C = 0.1 mm.; B = 0.5 mm.

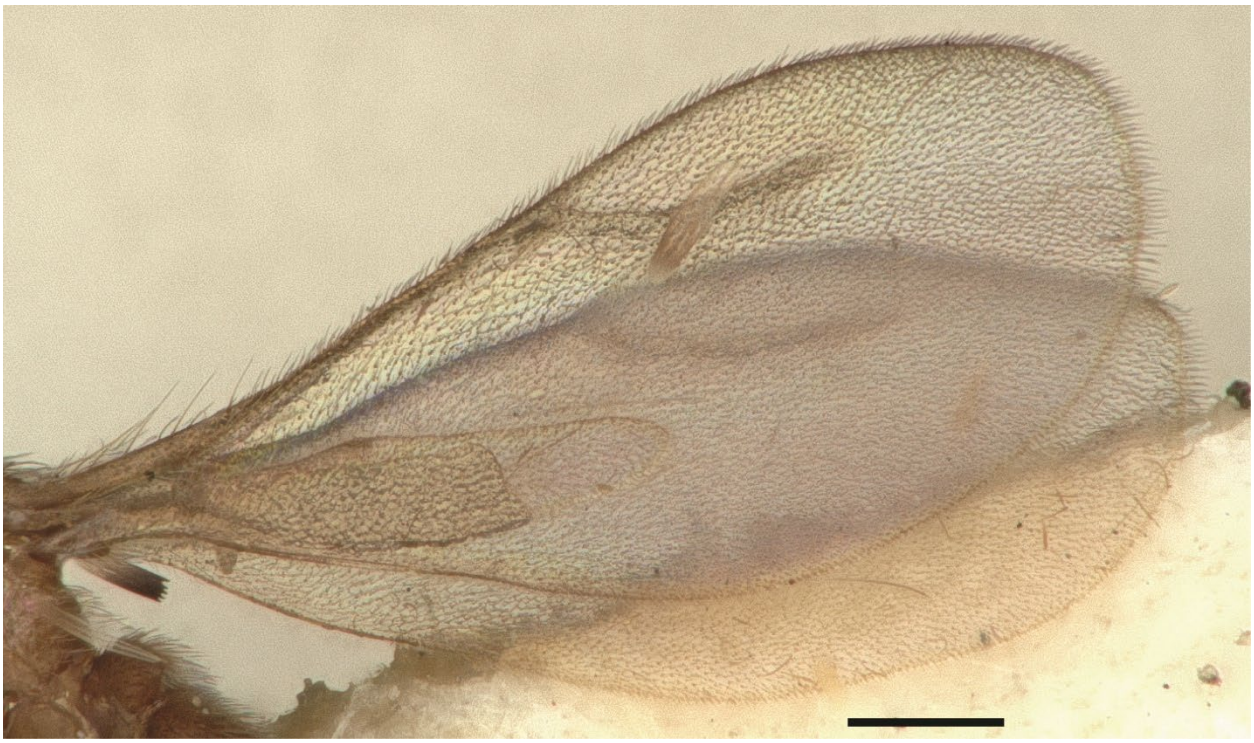

Figure 4.30. Wings of *Leptanilla bethyloides* (CASENT0842865). Scale bar = 0.2 mm.

Etymology. The specific epithet refers to the gestalt of this ant, which resembles that of the flat wasps (Chrysidoidea: Bethylidae). While superficial, this resemblance was pronounced enough that the holotype and paratype of *L. bethyloides* were initially mis-sorted to Bethylidae *incertae sedis* at the Bishop Museum. The specific epithet is neuter.

Diagnosis. Among the *Leptanilla bethyloides* species-group, of which this is the only described species, *L. bethyloides* most closely resembles multiple undescribed morphospecies from southern Burma, differing in larger size and the proportions of the metasomal segments.

Remarks. Leptanilla bethyloides is here described based only upon male specimens, for the same nomenclatural reasons as *Leptanilla najaphalla* (see above): the clade to which it belongs heretofore consisted solely of undescribed species, and is therefore here referred to as the *Leptanilla bethyloides* species-group. It is due to this close resemblance that I here infer the complete absence of the volsellae in *L. bethyloides*; these appendages are known to be wholly

lacking in *Leptanilla* zhg-mm03, which shows very close morphological affinity to *L. bethyloides*. This condition cannot yet be falsified in any other representatives of the *Leptanilla bethyloides* species-group besides *Leptanilla* zhg-mm03.

Given the relative lack of phylogenetic signal in the worker phenotype of *Leptanilla* and the scarcity of species in which the worker caste and phylogenetic position are both known, it is difficult to predict the morphology of the unknown worker of *L. bethyloides*, beyond a probable 1,1 palpal formula. It is conceivable that *Leptanilla macauensis* Leong *et al.* represents this worker, although unlikely, given the conformity of *L. macauensis* to the worker diagnosis for the *Leptanilla revelierii* species-group, where it is placed in this study.

Discussion

Taxonomic history

Writing of the subfamily Leptanillinae, Brown (1954: p. 28) opined that " … it is doubtful that we shall ever be certain of its true affinities." Concomitantly, the classification of the Leptanillinae relative to other Formicidae has a convoluted history. Extreme morphological derivation (in males, larvae, and both female castes), varying markedly across the few lineages of the clade, is responsible for this.

For most of its taxonomic history, the subfamily Leptanillinae was subsumed within (Emery 1910), or affiliated with, the army ants (Dorylinae *sensu* Ashmead) (Baroni Urbani, 1989; Hölldobler and Wilson, 1990), with *Leptanilla* having been described within the Dorylinae (Emery, 1870). Despite ill-interrogated placement in the Myrmicinae by many early authors (Ashmead, 1905; Dalla Torre, 1893; Emery, 1910; Emery and Forel, 1879), the description of dichthadiiform gynes in *Leptanilla* was interpreted as supporting its placement within the

Dorylinae (Emery, 1904), while Santschi (1907) asserted the similarity of putative male *Leptanilla* to male army ants. Wheeler (1923) was the first to elevate the then-monobasic Leptanillini to subfamily rank, an action also argued for by Wheeler (1928) and Wheeler and Wheeler (1965) due to the dissimilarity of the larval habitus between the Dorylinae and Leptanillinae. *Leptanilloides* (Dorylinae) was placed as Formicidae *incertae sedis* and likened to the Leptanillinae by Borgmeier (1955) due to that genus exhibiting "a mixture of characters of the Ecitonini [i.e., New World army ants] and Leptanillinae" (Borgmeier, 1955: p. 652), but Brown (1975: p. 34) classified *Leptanilloides* within the "doryline section" (Bolton, 1990a) due to its close resemblance to *Sphinctomyrmex sensu lato*, a classification followed by all subsequent authors and confirmed by phylogenetic inference from molecular data (e.g., Brady et al. 2014).

With the description of the tribe Anomalomyrmini within the Leptanillinae, Bolton (1990b: p. 267) "dispute[d] the indisputability" of leptanilline kinship with army ants, since *Protanilla* gynes are not dichthadiiform (Baroni Urbani and de Andrade, 2006; Billen et al., 2013; Hsu et al., 2017), and dichthadiigynes are unequivocally homoplasious in their other occurrences across the Formicidae (Bolton, 1990a). Bolton (1990b) transferred *Apomyrma* to the Leptanillinae from the Ponerinae *sensu* Bolton (1990c) and proposed that the resemblance of doryline to leptanilline gynes was homoplasious. Based on the theorized kinship of *Apomyrma* to the Leptanillinae (Apomyrminae and Leptanillinae constituting the "leptanillomorph subfamilies" *sensu* Bolton [2003]), these lineages were hypothesized to have affinity with the Amblyoponinae, or more generally the "poneroid" clade (Ward, 2007).

The advent of molecular sequencing supported none of the above hypotheses: instead, Leptanillinae was consistently supported as an early-diverging lineage of the Formicidae not akin

to *Apomyrma*, which was recovered as a poneroid, sister to the Amblyoponinae. In addition, Ward and Fisher (2016) robustly recovered the monotypic genus *Opamyrma*, which had been described within the Amblyoponinae on account of character states closely resembling those of *Apomyrma* (e.g., abdominal sternite II reduced), as sister to the remaining Leptanillinae (Ward and Fisher, 2016). This inference is corroborated by male morphology (see "Remarks" concerning *Opamyrma* below).

The Leptanillinae have been afflicted by a dual taxonomy since the description of the first putative males by Santschi (1907, 1908). The first males of *Leptanilla* were described without association with workers, justified by purported similarity in head morphology, and "only with some doubt [*n'est qu'avec doute*]" (Santschi, 1907: p. 312). The genus *Phaulomyrma* was erected for *Leptanilla javana* (Wheeler and Wheeler) and *Leptanilla tanit* Santschi, both known only from males (Wheeler and Wheeler, 1930), whereas the bizarre monotypic genus *Scyphodon*, described by Brues (1925) as Hymenoptera *incertae sedis*, was found to represent a male leptanilline (Boudinot, 2015; Petersen, 1968), although Ogata et al. (1995) argued against the placement of *Scyphodon* in the Formicidae. The genera *Noonilla* and *Yavnella* were also described in the Leptanillinae based solely upon male specimens (Kugler, 1987; Petersen, 1968). Ogata et al. (1995) was the first to associate male and worker leptanilline specimens, describing the male of *Leptanilla japonica*, which was previously known from workers (Baroni Urbani, 1977), and confirming the hypothesis of Santschi (1907). The two genera for which the tribe Anomalomyrmini was established were each initially known only from workers (*Protanilla*) or gynes (*Anomalomyrma*), therefore leaving a potential for taxonomic redundancy in this tribe until the description of all female castes of both these genera confirmed their reciprocal diagnosability —although consideration of morphology illuminated by phylogenetic inference

(Borowiec et al., 2019; Griebenow, 2020) (Chapters 1-2, 5) here demonstrates a lack of reciprocal monophyly, and the two are here synonymized. Males were only subsequently associated with *Protanilla* (namely the *Protanilla rafflesi* species-group) by means of phylogenomic inference (Griebenow, 2020). The Opamyrmini have avoided comparable taxonomic problems, with the collection of the male of *O. hungvuong* in association with females (Yamada et al., 2020).

Biogeography and ecology

The Leptanillinae are, as per the 95% credibility interval inferred for the crown age of this clade by Borowiec et al. (2019), no older than the beginning of the Cenozoic Era (66 mya). The crown age of the Leptanillinae is no older than the estimated origins of several ant clades that have a circumtropical or cosmopolitan distribution, including *Odontomachus* (Ponerinae: Ponerini) (Schmidt, 2013) and *Camponotus* (Formicinae: Camponotini) (Blaimer et al., 2015). Yet, curiously, the Leptanillinae are restricted to the Old World. The bulk of leptanilline diversity resides in the humid tropics, with the few temperate lineages (e.g., *L. taiwanensis*; Man et al., 2017) being close kin of tropical ones. This implies that the origin of the Leptanillinae occurred in tropical climates, conforming to the overall tendency observed in the Formicidae (Economo et al., 2018). In the absence of other data to explain the absence of this clade from the New World, I predict that leptanilline ants originated after the closure of the Thulean and Beringian land bridges to tropical biota, but this prediction remains to be tested.

The notable absence of the Leptanillinae from the Neotropics elicits inquiry into which ants occupy a similar ecological niche in this ecoregion. In terms of functional morphology and behavior, *Leptanilloides* differs from leptanilline ants in the presence of cincti on abdominal segments IV-VII and in being an obligate predator of ant brood, rather than hunting

geophilomorph centipedes; despite their name, these minute dorylines are not a Neotropical analog to the Leptanillinae. Rather, it is probable that centipede predators such as *Prionopelta* and *Fulakora* (Amblyoponinae), which often display LHF (Ito and Billen, 1998), are ecological counterparts to the Leptanillinae in the New World. This hypothesis is further supported by remarkable homoplasy between the Amblyoponinae and Leptanillinae, which resulted in the erroneous hypothesis that these clades were akin (Bolton, 2003, 1990b).

Typhlomyrmex (Ectatomminae: Ectatommini), which are minute hypogaeic ants precinctive to the Neotropics, are also worth noting here on account of the leptanilloid gestalt of the worker. Coarse but pronounced resemblance in habitus implies functional parallels in *Typhlomyrmex* with the Leptanillinae, with the articulated meso-metapleural suture that is unique to *Typhlomyrmex* among the Ectatomminae (Bolton, 2003) recalling that feature in *Protanilla* and certain *Leptanilla* species, while the tergosternal fusion of abdominal segment II constitutes convergence with the Leptanillini. Miniaturized and flexible relative to the robust, epigaeic members of their sister clade, *Gnamptogenys sensu stricto* (Camacho et al., 2022), *Typhlomyrmex* represent Ectatomminae that occupy a morphospace occupied outside the New World by the Leptanillinae.

Revised diagnosis and generic classification of Leptanillinae

Based upon total-evidence and phylogenomic inference (Chapter 5) corroborated by previous studies (Griebenow, 2020, Chapter 1), I here enact a revised classification of the Leptanillinae, reducing the number of genera to three. Summaries of character states that in combination differentiate major clades of the Leptanillinae from their relatives are provided below. These summary diagnoses are based upon all adult castes and larvae, when available. Apomorphies

relative to the parent taxon are italicized; characters of uncertain polarity are marked with an asterisk.

Leptanillinae Emery, 1910

Type genus. Leptanilla Emery, 1870: 196.

Worker diagnosis.

1. Mandibles without differentiated basal and masticatory margins.
2. At least one preapical tooth or lobe present on mandible.
3. Frontal lobes absent.
4. *Antennal sockets dorsal, fully exposed.*
5. *Compound eyes absent*, if present (*Protanilla izanagi*) then reduced to two ommatidia (Fig. 4.31A).
6. Ocelli absent.
7. Antenna 12-merous.
8. Promesonotal suture fully articulated.
9. *Propodeal lobes weakly present (Opamyrmini) or absent (Leptanillini).
10. Propodeal spiracle situated low on propodeum.
11. *Metacoxal foramen small, fully closed* (Fig. 4.32).
12. Suture absent from annulus surrounding metacoxal foramen.
13. Metapleural gland present.
14. *Orifice of metapleural gland covered by dorsal cuticular flange.
15. *Helcial sternite reduced and partly covered by corresponding tergite.*
16. Spiracle of abdominal segment III large and placed far forward.

17. Spiracles of abdominal segments IV-VII concealed by posterior margins of preceding tergites.
18. *Petiole sessile, rarely subsessile (*Protanilla taylori* species-group).
19. *Abdominal postsclerites II with (Leptanillini)* or without (Opamyrmini) complete tergosternal fusion.
20. *Abdominal postsclerites III with (Leptanillini)* or without (Opamyrmini) tergosternal fusion.
21. *Abdominal segment III petiolate (Leptanillini) or not (Opamyrmini).
22. Abdominal segment IV without tergosternal fusion.
23. Stridulitrum absent from abdominal segment IV.
24. *Abdominal tergite VII large*, with simple posterior margin.
25. Sting present.
26. Pretarsal claws edentate.

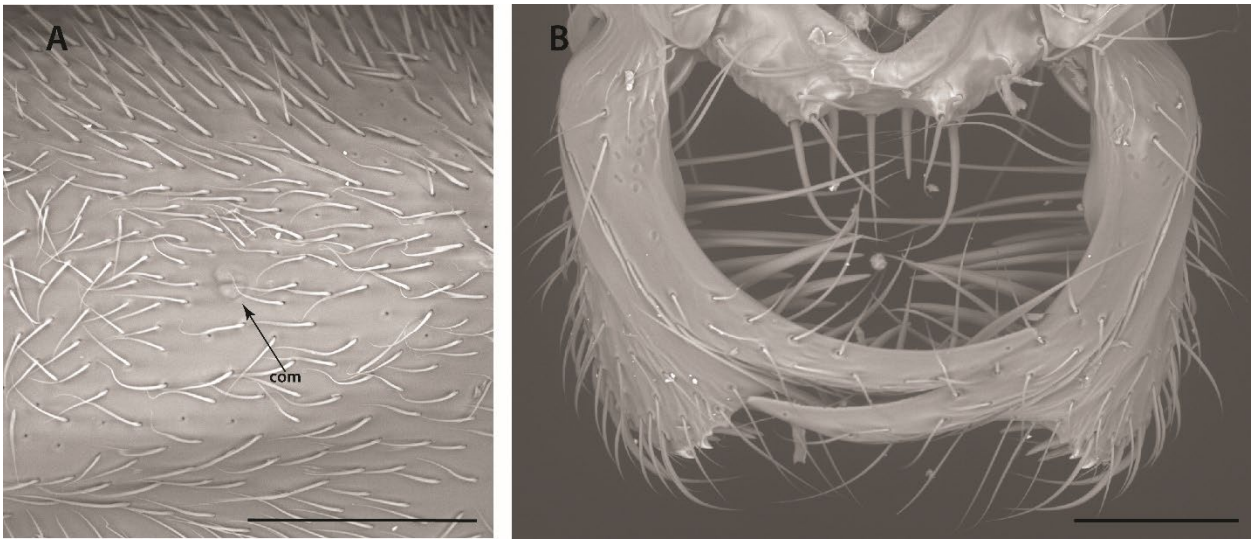

Figure 4.31. Aspects of *Protanilla izanagi*. **a** Profile view of posterior half of cranium **b** Ventral view of the mandibles. Abbreviations: com = compound eye. Scale bars: A = 0.1 mm.; B = 0.2 mm.

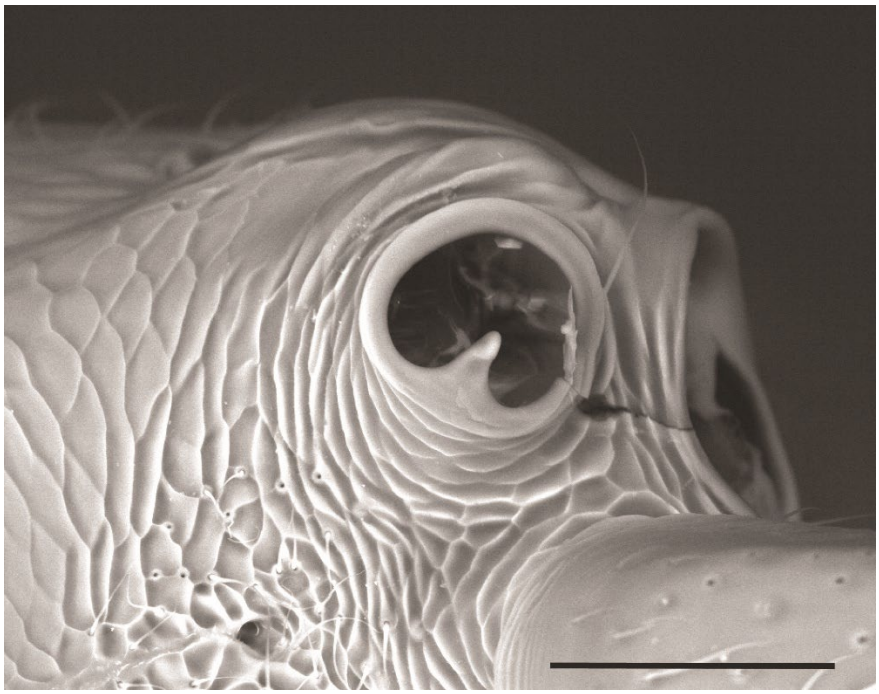

Figure 4.32. Metacoxal foramen of *Leptanilla havilandi* (CASENT0010809), ventral view. Scale bar = 0.05 mm.

Gyne diagnosis. As above, but alate or dichthadiiform (rarely ergatoid). *If* alate *then* with ocelli and pterostigma; hindwing with R + Rs and 1A tubular, not intersecting distal wing margin. If dichthadiiform *then* compound eyes reduced to 1-2 ommatidia, or absent; ocelli absent; mandibles sometimes edentate.

Male diagnosis.

1. *Mandible edentate, nub-like or spatulate* (*Leptanilla anomala* **comb. nov.**).
2. Frontal carinae absent.
3. Cuticular pegs absent from anterior clypeal margin.
4. Antenna 13-merous.
5. Funiculus filiform *to submoniliform*.
6. Oblique mesopleural sulcus present *or absent*.
7. *Metapleural spiracular plate absent.*

8. *Propodeal lobes inconspicuous or absent*.
9. Metacoxal cavities closed.
10. Mesotibia with 1-2 spurs *or none*.
11. Metatibia with 1-2 spurs.
12. Metatarsus lacking posterolateral line of dense differentiated setae.
13. Pretarsal claws edentate.
14. Pterostigma present *or absent*.
15. *Rs+M absent* (Leptanillini) or present, nebulous (Opamyrmini).
16. 1m-cu *absent* (Leptanillini) or present, nebulous (Opamyrmini).
17. *Jugal lobe absent*.
18. *Hindwing venation reduced, at most R+Rs and 1A tubular*.
19. *Metapleural gland absent* or rarely present (Fig. 4.33) (e.g., *Leptanilla* zhg-th02).
20. Petiole present *or reduced to absent* (*Leptanilla thai* species-group, *Leptanilla havilandi* species-group)
21. Helcium axial *or infra-axial*.
22. Abdominal segment III not petiolate, *or rarely petiolate* (*Protanilla bicolor* species-group).
23. *Abdominal segment IV not vaulted, as long as, or distinctly longer than posterad abdominal segments.
24. Abdominal spiracles IV-VIII obscured by preceding tergites.
25. Posterior margin of abdominal sternite IX with posteromedian process, *entire*, *emarginate*, *or with mulceators* (Chapter 3).
26. *Cerci absent*.

27. Cupula present *or absent*, if present, *non-annular* (Chapter 3).

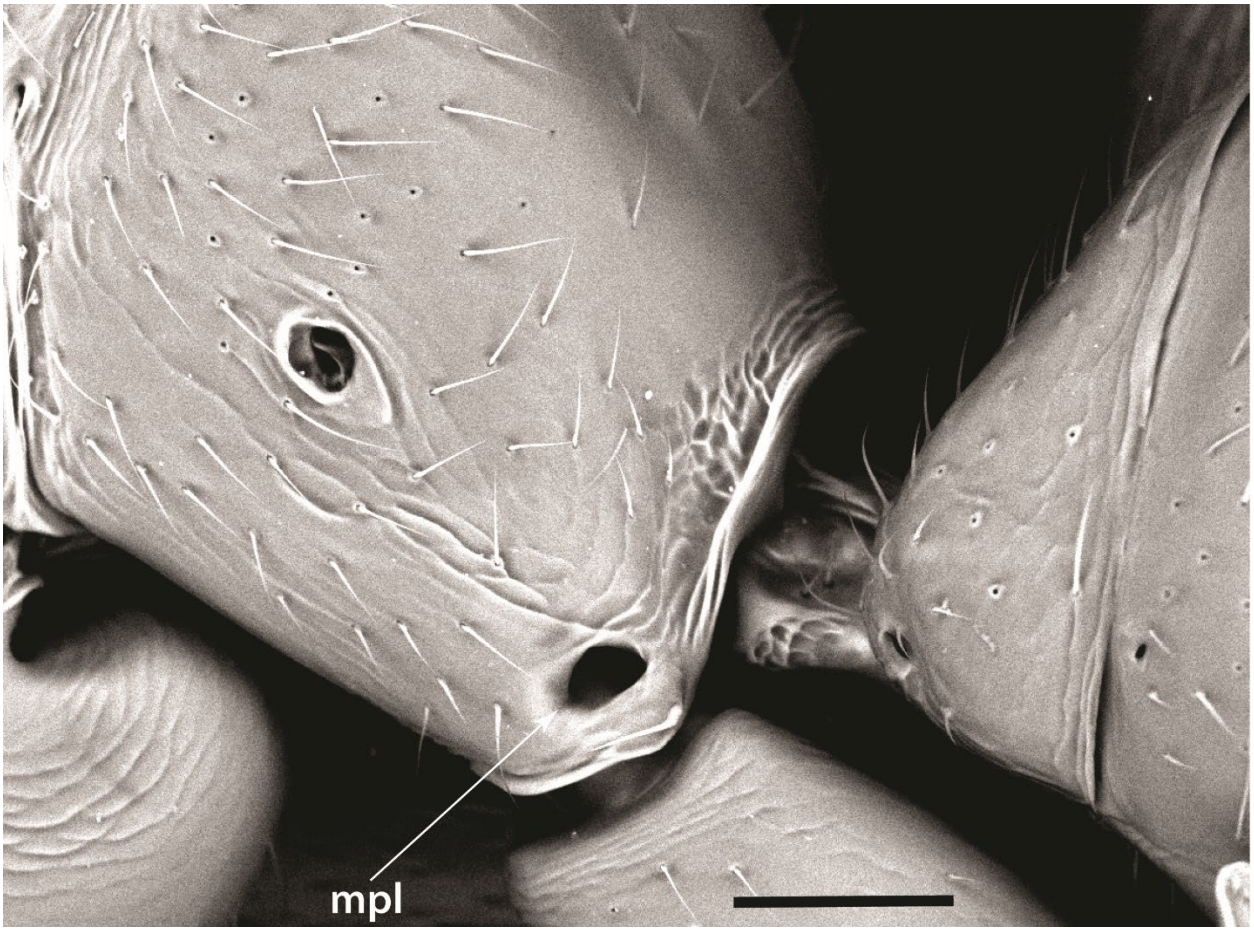

Figure 4.33. Metapleuron of *Leptanilla* zhg-th02. Abbreviation: mpl = metapleural gland orifice. Scale bar = 0.1 mm.

Larval diagnosis. Stenocephalous, with post-cranial soma moderately (i.e., habitus pogonomyrmecoid) to extremely (i.e., habitus leptanilloid) elongate. Mandibles typhlomyrmecoid or leptanilloid.

Included genera. Opamyrma Yamane, Bui and Eguchi; *Protanilla* Taylor in Bolton (= *Anomalomyrma* Taylor in Bolton **syn. nov.**; *Furcotanilla* Xu); *Leptanilla* Emery (= *Scyphodon* Brues **syn. nov.**; *Phaulomyrma* Wheeler and Wheeler; *Leptomesites* Kutter; *Noonilla* Petersen **syn. nov.**; *Yavnella* Kugler **syn. nov.**)

Opamyrmini Boudinot and Griebenow, **trib. nov.**

Worker diagnosis.

1. *Medial mandibular surface with single peg-like chaeta*.
2. *Mandible with one tooth and several preapical lobes*.
3. *Labrum with multiple ranks of peg-like chaetae (Yamada et al., 2020: fig. 2F).
4. Maxillary palp 4-merous.
5. Labial palp 2-merous.
6. Clypeus extending posteriorly between antennal toruli.
7. *Posteromedian epistomal sulcus not clearly discernible*.
8. *Occiput visible in full-face view*.
9. *Meso-metapleural suture absent*.
10. Propodeal lobe weakly present.
11. Subpetiolar process absent.
12. Abdominal postsclerites II without tergosternal fusion.
13. *Abdominal segment III not petiolate or narrower than posterad abdominal segments.
14. *Abdominal postsclerites IV subequal in length to abdominal postsclerites V-VI.
15. *Abdominal tergite VII hypertrophied, dome-like*.

Gyne diagnosis. As above, but alate, with compound eyes and three ocelli; occipital carina with short medioventral interruption. M + Cu complete, tubular; *cu-a* present; Rs + M, Cuf2 and -3, and *1m-cu* present and spectral; *2r-rs* + Rsf4 adjoined by Rsf3.

Male diagnosis. As for the Leptanillinae, but discal cell present, and abdominal segment II without tergosternal fusion. Lateropenite present, fully articulated to parossiculus, and malleate.

Larval diagnosis. Habitus pogonomyrmecoid. Cranium subelliptical in full-face view. Mandibles typhlomyrmecoid, without teeth, lateral surfaces smooth. Setae short, suberect. Ventral prothoracic process and hemolymph tap on abdominal segment IV absent.

Opamyrma Yamane, Bui and Eguchi

Type species. Opamyrma hungvuong Yamane, Bui and Eguchi, 2008: 56.

Included species. Opamyrma hungvuong Yamane, Bui and Eguchi.

Diagnosis. As for tribe.

Remarks. Opamyrma was described in the Amblyoponinae, based solely upon worker morphology (Yamane et al., 2008), and was subsequently found by Ward and Fisher (2016) to belong to the Leptanillinae based upon phylogenetic inference from 11 nuclear loci. All subsequent phylogenetic inference consistently recovers *Opamyrma* as sister to the remaining Leptanillinae (Borowiec et al., 2019; Griebenow, 2020, Chapter 5). Inclusion in the Leptanillinae is additionally supported by male morphology, namely the condition of the mandibles as edentate and nub-like, along with non-annularity of the cupula, which are synapomorphies of the Leptanillinae (Boudinot et al., 2022). All adult forms lack complete tergosternal fusion in abdominal segment II, a plesiomorphy unique among the Leptanillinae. The presence of weak propodeal lobes (Yamada et al., 2020: p. 34) is plesiomorphic relative to the Leptanillini, in which the propodeal lobes are absent in the worker caste. The lack of petiolation of abdominal segment III in the worker caste of *Opamyrma* is also unique among the Leptanillinae but this character state may not be plesiomorphic for the subfamily. The polarity of the proportions of abdominal postsclerites IV relative to V-VI within the Leptanillinae is also unclear.

Leptanillini Emery

Type genus. Leptanilla Emery, 1870.

Worker diagnosis.

1. *Medial mandibular surface with* or without peg-like chaetae.
2. Mandible with 0-4 teeth along medial margin.
3. *Labrum with (Fig. 4.34A-B) or without multiple ranks of peg- or pencil-like chaetae.
4. Maxillary palp 4- *or 1-merous*.
5. Labial palp 2- *or 1-merous*.
6. Clypeus extending posteriorly between antennal toruli (Fig. 4A) *or not* (Fig. 4B).
7. Posteromedian epistomal sulcus clearly discernible (Fig. 4A) *or not* (Fig. 4B).
8. Occiput not visible in full-face view.
9. Meso-metapleural suture present *or absent*.
10. *Propodeal lobes absent.*
11. *Subpetiolar process present* or absent.
12. *Abdominal postsclerites II-III with tergosternal fusion.*
13. *Abdominal segment III petiolate, narrower than posterad abdominal segments.
14. *Abdominal postsclerites IV subequal in length to, *or greater in length than*, abdominal postsclerites V-VI.
15. Abdominal tergite VII enlarged, not dome-like.

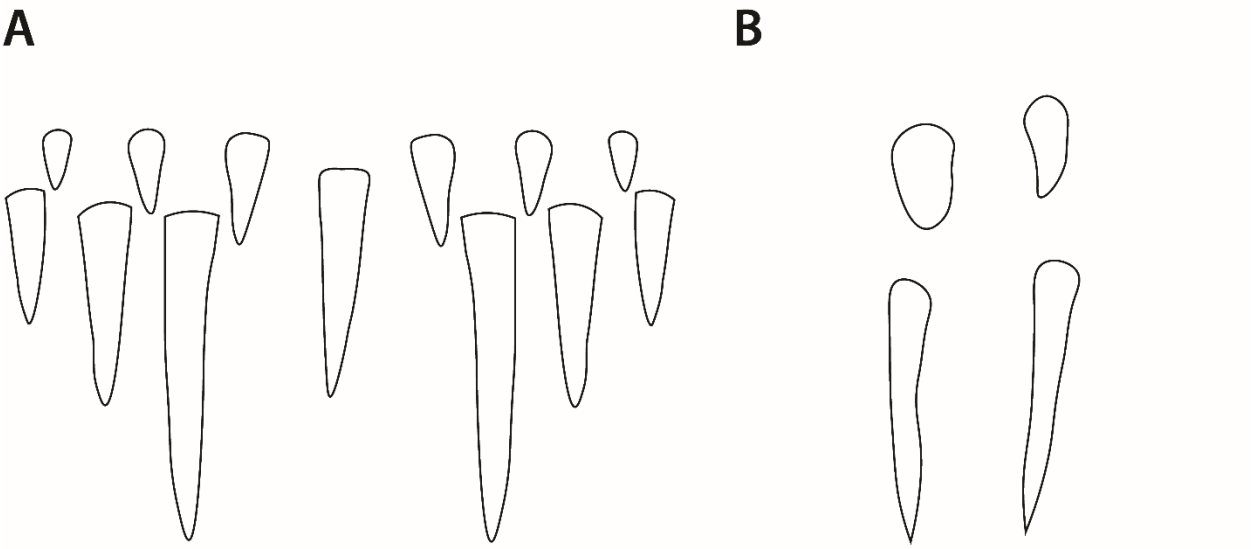

Figure 4.34. Labral chaetae in *Protanilla*, diagrammatic anterior view. **a** *Protanilla* id01, gyne **b** *Protanilla wallacei* (CASENT0842699), worker

Gyne diagnosis. See respective gyne-based diagnoses for *Protanilla* and *Leptanilla* below.

Male diagnosis. As for the Leptanillinae, but discal cell absent. Abdominal segment II with complete tergosternal fusion. Lateropenite present or absent; if present, then not articulated to parossiculus and never malleate.

Larval diagnosis. See respective larval diagnoses for *Protanilla* and *Leptanilla* below.

Included genera. Leptanilla Emery; *Protanilla* Taylor in Bolton.

Protanilla Taylor in Bolton (= *Anomalomyrma* Taylor in Bolton **syn. nov.**; *Furcotanilla* Xu)

Type species. Protanilla rafflesi Taylor in Bolton, 1990b: 279.

Worker diagnosis.

1. Medial mandibular surface with *or without* (*Protanilla taylori* species-group) multiple rows of peg-like chaetae.
2. *Medial mandibular margin with regularly spaced denticles.
3. *Medial mandibular margin without teeth.*

4. *Ventromedial mandibular margin with* or without subapical teeth.
5. Labrum with peg- or pencil-like chaetae (Fig. 4.34A-B).
6. Maxillary palp 4-merous.
7. Labial palp 2- *or 1-merous.*
8. Clypeus distinct, with epistomal sulcus present (Fig. 4A).
9. *Dorsal mandibular articulation apparent in full-face view* (Fig. 4.8A) or rarely not so (Fig. 4.8B) (*Protanilla concolor* Xu).
10. Meso-metapleural suture present, strongly impressed, scrobiculate.
11. Subpetiolar process present.
12. Abdominal segment III narrowly *or broadly* conjoined to abdominal segment IV.
13. *Length of abdominal postsclerites IV greater than that of abdominal postsclerites V-VI.

Gyne diagnosis. As in worker, but alate or rarely ergatoid; with compound eyes and 3 ocelli. If alate then venation Ogata Type IVb. M + Cu and Rsf3 absent; Rs + M, Cuf2-3, and *1m-cu* spectral or absent.

Male diagnosis.

1. Maxillary palp 4-merous.
2. Labial palp 2- *to 1-merous.*
3. Clypeus distinct.
4. Ocelli present, not set on tubercle.
5. Pronotum not anteroposteriorly prolonged.
6. Mesoscutum not anteroposteriorly prolonged.
7. Notauli present *or absent*.
8. Pterostigma present.

9. 1A in hindwing present *or absent*.
10. Upper metapleuron distinct from metapectal-propodeal complex.
11. Lower metapleuron indistinct from metapectal-propodeal complex.
12. Abdominal segment II petiolate.
13. *Abdominal segment III petiolate* or not.
14. Cupula present.
15. Volsellae present, parossiculus and lateropenite distinct.
16. Penial sclerites medially articulated.

Larval diagnosis. Habitus pogonomyrmecoid. Cranium subelliptical in full-face view. Mandibles typhlomyrmecoid, without teeth, lateral surfaces smooth. Setae short, suberect. Ventral prothoracic process absent; larval hemolymph tap apparently absent.

Included species. *Protanilla beijingensis* Man *et al.*; *Protanilla bicolor* Xu; *Protanilla boltoni* (Borowiec *et al.*) **comb. nov.**; *Protanilla concolor* Xu; *Protanilla flamma* Baidya and Bagchi; *Protanilla furcomandibula* Xu and Zhang; *Protanilla gengma* Xu; *Protanilla helenae* (Borowiec *et al.*) **comb. nov.**; *Protanilla izanagi* Terayama; *Protanilla jongi* Hsu *et al.*; *Protanilla lini* Terayama; *Protanilla rafflesi* Taylor in Bolton; *Protanilla schoedli* Baroni Urbani and de Andrade; *Protanilla taylori* (Taylor in Bolton) **comb. nov.**; *Protanilla tibeta* Xu; *Protanilla wallacei* Griebenow **sp. nov.**; *Protanilla wardi* Bharti and Akbar

Remarks. The tribe Anomalomyrmini was erected by Taylor in Bolton (1990b) to include *Anomalomyrma* and *Protanilla*, which were both monotypic when established. Boudinot et al. (2022) merged the tribe into Leptanillini, although the Anomalomyrmini and Leptanillini *sensu* Bolton are indubitably reciprocally monophyletic. All molecular phylogenetic inference (e.g., Borowiec et al., 2019; Griebenow 2020, Chapter 5) indicates the paraphyly of *Protanilla* relative

to *Anomalomyrma*, with statistical support of varying strength. *Anomalomyrma* is therefore here synonymized with *Protanilla* (see "*Protanilla taylori* species-group" for explanation of nomenclatural priority). The phylogeny of *Protanilla* remains debatable (Chapter 5), with morphological diagnoses formulated below for the major lineages revealed by these analyses, here treated as informal monophyletic species-groups. These lineages are recovered on deeply separated internal nodes (Chapter 5). *Protanilla izanagi* Terayama is left unplaced to species-group due to an absence of molecular data for this species and bizarrely modified mandibles which exclude it from the species-groups as diagnosed here. The position of *Protanilla* zhg-th02, known only from a single male specimen, is unstable across different phylogenomic analyses (Chapter 5), but is always situated on a long branch. This morphospecies does not conform to the male-based diagnoses of any of the species-groups here delimited for which male morphology is known, and does not represent the as-yet unknown male of the *Protanilla taylori* species-group. Based on this evidence, *Protanilla* zhg-th02 represents a major subclade of *Protanilla* for which workers remain to be discovered.

The *Protanilla rafflesi* species-group is further divided into three species-complexes, with two distinctive species left unplaced to species-complex. Species boundaries in *Protanilla* require further inquiry, with it being possible that the clade is over-split; each species-complex may respectively represent a widespread, geographically variable species. Both sexes are notably conservative in terms of morphology. Robust species delimitation, reciprocally illuminated by morphometric and molecular data, is impossible with material as scanty as is available for *Protanilla*, so no revisions to species-level taxonomy within this clade are made here.

***Protanilla rafflesi* species-group**

Worker diagnosis.

1. Medial mandibular surface armed with peg-like chaetae.
2. Mandible sublinear, not bowed along anteroposterior axis of cranium.
3. Vertical dorsal lamella absent from mandible (Fig. 4.35A).
4. Laterodorsal longitudinal groove present.
5. Clypeal surface flattened.
6. *Median clypeal ridge externally visible*.
7. Outline of clypeus in full-face view campaniform *to oblate-trapezoidal*.
8. Pronotal breadth subequal to propodeal breadth in dorsal view.
9. *Mesotibia without spurs.*
10. Petiole sessile.
11. *Subpetiolar process with fenestra.
12. Abdominal sternite III convex, *linear, or concave* in profile view.
13. Abdominal segments II-III without tergotergal or sternosternal fusion.
14. Abdominal segments III-IV narrowly *or broadly* conjoined.
15. Anterior margin of abdominal post-tergite IV linear *to strongly emarginate* in dorsal view.
16. Soma concolorous.

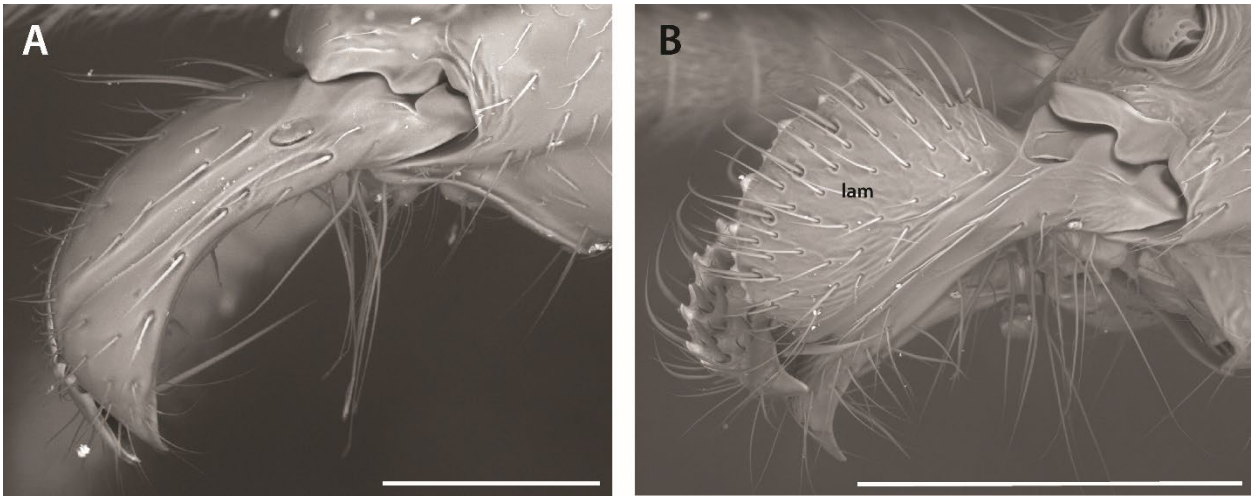

Figure 4.35. Mandibles in *Protanilla*, profile view. **a** *Protanilla wallacei* (CASENT0842699) **b** *Protanilla izanagi* (CASENT0842850). Abbreviations: lam = vertical dorsal lamella. Scale bars: A = 0.1 mm.; B = 0.2 mm.

Male diagnosis.

1. Distal 3 maxillary palpomeres of unequal lengths (Griebenow, 2020: fig. 10A).
2. Labial palp 2- *or 1-merous*.
3. Antennomere 3 shorter than scape.
4. Antero-admedian signum present *or absent.*
5. Notauli present *or absent*; if present, unsculptured.
6. Antero-admedian signum present *or absent*; if present, then unsculptured.
7. Parapsidal lines present *or absent*.
8. 1A present in hindwing.
9. Abdominal segment III not petiolate.
10. Length of abdominal segment IV subequal to, or less than, respective lengths of abdominal segments V-VII.

Larval diagnosis. As for genus.

Included species. Protanilla rafflesi Taylor in Bolton; *Protanilla concolor* Xu; *Protanilla furcomandibula* Xu and Zhang; *Protanilla schoedli* Baroni Urbani and de Andrade; *Protanilla lini* Terayama; *Protanilla tibeta* Xu; *Protanilla wardi* Bharti and Akbar; *Protanilla jongi* Hsu *et al.*; *Protanilla beijingensis* Man *et al.*; *Protanilla flamma* Baidya and Bagchi; *Protanilla wallacei* Griebenow **sp. nov.**

Remarks. For the most part, this clade shows striking morphological conservatism in the worker caste and males. *P. jongi* deviates from most of the clade in having broadly conjoined abdominal segments III-IV, and a ventral subapical mandibular tooth but is robustly confirmed to be nested well within the *Protanilla rafflesi* species-group by phylogenomic inference (Chapter 5). I therefore also place *Protanilla furcomandibula* Xu and Zhang in the *Protanilla rafflesi* species-group, as this species appears to be a close relative of *P. jongi* (Hsu et al., 2017), with the ventral subapical mandibular tooth being hypertrophied, and abdominal sternite II concave in profile view rather than linear to convex. The concavity of abdominal sternite II in profile view is homoplasious with the *Protanilla taylori* species-group, as is the broad connection of abdominal segments III-IV.

A 4,2 palpal formula was confirmed for the worker of *Protanilla lini* by examination with micro-CT (Richter et al., 2021), while the palpal formula of the conspecific male was tentatively interpreted as 4,1 by Griebenow (2020). The palpal formula of the worker in the *Protanilla rafflesi* species-group, and indeed *Protanilla* as a whole, has largely gone unreported, with this study being the first to confirm the palpal formula of any representative of the *Protanilla taylori* species-group. Palpal formula across the Formicidae shows sexual monomorphism, with few exceptions (Bolton, 2003; see sections on the *Protanilla bicolor* species-group and *Leptanilla*

thai species-group below), meaning that the interpretation by Griebenow (2020) of the male labial palp in *P. lini* as 1-merous was likely in error.

Three species-complexes are hereby recognized in the *Protanilla rafflesi* species-group: the *rafflesi*-complex (*P. rafflesi*, *schoedli*, and *wardi*); the *concolor*-complex (*P. concolor* and *tibeta*); and the *lini*-complex (*P. lini*, *beijingensis*, *flamma* and *wallacei*). Each of these complexes consist of species that are extremely similar, but for which material is too scarce to query interspecific boundaries. Only the *concolor*-complex is unrepresented in the sampling of Chapter 5. *P. furcomandibula* and *P. jongi* are presumably close relatives, but are readily distinguishable based on known specimens, and so are not consigned to a species-complex. Without phylogenomic inference, it is unclear if these species-complexes are reciprocally monophyletic. *Protanilla wallacei* **sp. nov.** based upon worker specimens is recovered as sister to *P. lini* (Chapter 5), as would be predicted based on observed worker phenotype.

A single specimen (CASENT0842639) of *Protanilla beijingensis* is herein reported from Khyber Pakhtunkhwa, Pakistan, in a remarkable range extension for a species heretofore known only from Beijing, China (Man et al., 2017). CASENT0842639 qualitatively differs from the type series in possessing a pair of peg-like chaetae on the labrum rather than a single median chaeta, but it is unknown whether this constitutes intra- or interspecific variation in *Protanilla*. This specimen is part of a series figured by Bolton (1990b: figs. 1-6), for which coordinates are unavailable. Despite this, it appears that the collection was made at an elevation of 2400-2700 meters, in a cold temperate climate resembling that of the type locality.

Dias et al. (2019: p. 164) described the worker of *Protanilla schoedli* from 10 specimens collected across Sri Lanka, based on "overall similarity in … general appearance" to the holotype gyne (CASENT0911228) and the implicit assumption that multiple *Protanilla* spp.

cannot not occur in sympatry. However, the putative worker *P. schoedli* display no more affinity to CASENT0911228 than to other members of the *Protanilla rafflesi* species-group, with the anterior margin of the petiolar node being straight (Dias et al., 2019: p. 164) rather than concave in profile view, as in CASENT0911228 (Baroni Urbani and de Andrade, 2006: p. 46). This excludes these worker specimens from the *Protanilla rafflesi* species-complex to which *P. schoedli* belongs. The putative workers of *P. schoedli* (Dias et al., 2019) more closely resemble *Protanilla flamma* (Baidya and Bagchi 2020), but the difference in reported ranges of CI, SI and PI between these two series supports their heterospecificity, if these morphometric differences reflect species boundaries. In this study, the putative *P. schoedli* (Dias et al., 2019) are regarded as an undescribed species belonging to the *Protanilla lini* species-complex. While neither *P. schoedli* nor *P. flamma* have been sequenced, other members of their respective species-complexes have (*P. wardi* vs. *P. lini* and *P. wallacei* **sp. nov.**), with phylogenomic inference therefrom supporting their heterospecificity (Chapter 5).

The *Protanilla rafflesi* species-group contains some of the only *Protanilla* spp. for which bionomic data are available, with micro-computed tomographic studies of cephalic skeletomusculature in *P. lini* demonstrating the existence of "trap-jaw" capabilities in that species (Richter et al., 2021). The existence of putative trigger hairs across *Protanilla* (Table 2.3) suggests that trap-jaw biology is a synapomorphy of the genus and paralleled in the Leptanillinae only by *Leptanilla laventa* **comb. nov**.

***Protanilla bicolor* species-group**

Worker diagnosis.

1. Medial mandibular margin armed with peg-like chaetae.

2. Mandible sublinear, not bowed along anteroposterior axis of cranium.
3. Vertical dorsal lamella absent from mandible.
4. *Laterodorsal longitudinal groove absent.*
5. *Clypeal surface concave*.
6. Median clypeal ridge not externally visible.
7. Outline of clypeus in full-face view campaniform.
8. Breadth of pronotum subequal to propodeum in dorsal view.
9. Mesotibia with 1 spur.
10. Petiole sessile.
11. Subpetiolar process with fenestra.
12. Abdominal sternite III convex in profile view.
13. Abdominal segments II-II without tergotergal and sternosternal fusion.
14. Abdominal segments III-IV narrowly joined.
15. Anterior margin of abdominal post-tergite IV linear to slightly emarginate in dorsal view.
16. Soma bicolored, rarely concolorous.

Male diagnosis.

1. *Distal 3 maxillary palpomeres subequal in length* (Griebenow, 2020: fig. 10B).
2. Labial palp 2-merous.
3. *Antennomere 3 longer than scape*.
4. *Antero-admedian signum absent*.
5. Notauli present, *scrobiculate*.
6. *Parapsidal lines absent*.
7. *1A absent from hindwing*.

8. *Abdominal segment III petiolate*.
9. *Abdominal segment IV equal in length to combined length of abdominal segments V-VIII*.

Larval diagnosis. Larva unknown.

Included species. Protanilla bicolor Xu; *Protanilla gengma* Xu.

Remarks. Phenotypic differentiation between the *Protanilla bicolor* and *Protanilla rafflesi* species-groups in the worker caste is comparatively slight, but the two clades are discretely distinguishable by tibial spur formula. The strong concavity of the anterior clypeal margin referred to in previous descriptive literature more correctly refers to the face of the clypeus: the anterior margin itself is in fact no more emarginate in this clade than in the *Protanilla rafflesi* species-group. The morphology of *Protanilla* TH03, a male singleton attributable to this clade by molecular data (e.g., Borowiec et al., 2019), differs from all other known males of *Protanilla* in multiple respects, most conspicuously in petiolation of abdominal segment III: this condition is unique among male Leptanillinae.

Workers of the *Protanilla bicolor* species-group are unique among examined *Protanilla* workers in exhibiting a mesotibial spur, an apparent symplesiomorphy of this clade. Palpal formula could not be assessed in the worker caste due to a lack of fresh specimens, but given sexual monomorphism of palpal formula across the Formicidae save for the Ponerini, *Typhlomyrmex* (Bolton, 2003), and probably the *Leptanilla thai* species-group as well (this study), it is sound to predict a 4,2 formula.

Species boundaries in the *Protanilla bicolor* species-group remain unclear. Specimens identified as *P. gengma* are known to vary in labral chaeta count according to geographical origin (Aswaj et al., 2020), but the relevance of this trait to species delimitation is unknown. *Protanilla* VN03

appears transitional in morphometric terms between *P. bicolor* and *P. gengma*, but PTL in *Protanilla* VN03 falls outside the range observed in either of these species.

***Protanilla taylori* species-group**

Worker diagnosis.

1. Medial mandibular surface with peg-like chaetae.
2. Mandible sublinear, not bowed along anteroposterior axis of cranium.
3. Vertical dorsal lamella absent *or present* (*Protanilla taylori*).
4. Laterodorsal longitudinal groove present.
5. *Clypeal surface concave*.
6. Median clypeal ridge not externally visible.
7. *Outline of clypeus in full-face view an oblate trapezoid*.
8. *Pronotal breadth greater than propodeal breadth in dorsal view*.
9. *Mesotibia without spurs*.
10. *Petiole subsessile.*
11. *Subpetiolar process with fenestra present.
12. Abdominal sternite II convex in profile view.
13. Abdominal segments II-III without tergotergal and sternosternal fusion.
14. Abdominal segment III narrowly joined to abdominal segment IV.
15. Anterior margin of abdominal tergite IV entire in dorsal view.
16. Soma concolorous.

Male diagnosis. Male unknown.

Larval diagnosis. Larva unknown.

Included species. Protanilla boltoni (Borowiec *et al.*) **comb. nov.**; *Protanilla helenae* (Borowiec *et al.*) **comb. nov.**; *Protanilla taylori* (Taylor in Bolton) **comb. nov.**

Remarks. Anomalomyrma was established for *Protanilla taylori* **comb. nov.** by Taylor in Bolton (1990b) on account of derived mandibular morphology and the tergotergal and sternosternal fusion of abdominal tergites II-III, a character state unique among the Formicidae (Bolton, 1990b; Borowiec et al., 2011). While *P. taylori* is known only from the gyne, Borowiec et al. (2011) described *P. boltoni* and *P. helenae* **combs. nov.** based on worker material, and refined the diagnosis of *Anomalomyrma*, demonstrating that the presence of a vertical mandibular lamella was of no diagnostic utility in the Anomalomyrmini at the genus level, and predicting that the resemblance between the mandibles of *Anomalomyrma* and the then-undescribed *Protanilla izanagi* (see below) was homoplasious. This hypothesis has not yet been tested with phylogenomic inference.

Given the paraphyly of *Protanilla* relative to *Anomalomyrma* under phylogenomic inference from several differently curated datasets (Chapter 5), the latter genus is synonymized under *Protanilla*. These names were established in the same publication (Bolton, 1990b), and the latter is here given precedence as permitted in Article 24.2 of the International Code of Zoological Nomenclature. The *Protanilla taylori* species-group is equivalent to the former genus *Anomalomyrma*.

The vertical dorsal lamella in *P. taylori* and *P. izanagi* have few parallels within the Formicoidea, being comparable to the morphology observed in both female and male beast ants (Camelomeciidae: *Camelosphecia*), which are known only from Cretaceous burmite (Boudinot et al., 2020). Among extant formicoids, the mandible of these two *Protanilla* spp. is most reminiscent of that observed in armadillo ants (Agroecomyrmecinae: Agroecomyrmecini:

Tatuidris tatusia Brown and Kempf), which is likewise bowed, but with the masticatory margin armed with a brush of robust feathery setae (Brown and Kempf, 1967: fig. 3) rather than peg-like chaetae, cuticular denticles, or both.

The feeding ecology of *P. taylori* and *P. izanagi* may therefore resemble that of the armadillo ants. Brown and Kempf (1967: p. 189) hypothesized that armadillo ants feed on "slippery or active arthropod prey", with William Brown speculating that these ants were specialist predators of oligochaetes (P. S. Ward, pers. comm.). Given that known ant specialists on oligochaete prey, such as *Psalidomyrmex procerus* Emery (Formicidae: Ponerinae: Ponerini) (Déjean et al., 1999; Lévieux, 1983), have mandibles quite unlike those of armadillo ants, this seems improbable. Food court experiments to determine the diet of these ants were unsuccessful, but isotopic analysis of armadillo ant tissue suggests that the unknown prey is itself predatory (Jacquemin et al., 2014: p. 5).

Protanilla taylori and *Protanilla* id01 differ notably from the species known only from workers in the presence of two and three ranks, respectively, of produced denticles on the mandible (Bolton, 1990b; this study), as opposed to the condition observed in most *Protanilla*; along with the presence of pencil-like chaetae on the mandible, which are absent in the worker-based species. The worker and queen caste remain unassociated in all three described species of the *Protanilla taylori* species-group, plus *Protanilla* id01. It does not appear that either *P. taylori* or *Protanilla* id01 represent the gyne of *P. boltoni* or *P. helenae* (Borowiec et al., 2011). Until the female castes respectively unknown from these species are discovered, we cannot determine whether observed mandibular differences are to be credited to allospecificity, or to caste dimorphism.

Incertae sedis

Protanilla izanagi Terayama

Worker diagnosis.

1. Medial mandibular surface with peg-like chaetae.
2. *Mandible bowed along anteroposterior axis of cranium* (Fig. 4.31B).
3. *Vertical dorsal lamella present* (Fig. 4.35B).
4. Laterodorsal longitudinal groove present.
5. Clypeal surface flattened.
6. Median clypeal ridge not externally visible.
7. *Outline of clypeus in full-face view an oblate trapezoid*.
8. *Pronotal breadth greater than propodeal breadth in dorsal view*.
9. *Mesotibia without spurs*.
10. Petiole sessile.
11. *Subpetiolar process with fenestra present.
12. Abdominal sternite II convex in profile view.
13. Abdominal segments II-III without tergotergal and sternosternal fusion.
14. Abdominal segment III narrowly joined to abdominal segment IV.
15. Anterior margin of abdominal tergite IV entire in dorsal view.
16. Soma concolorous.

Male diagnosis. Male unknown.

Larval diagnosis. Larva unknown.

Remarks. Prior to formal description, this peculiar species from southern Honshu was cited by Hölldobler and Wilson (1990) and Imai et al. (2003) as *Anomalomyrma* (the former authors

referring to it under the *nomen nudum Anomalomyrma kubotai*), due to the presence of an erect mandibular lamella. Borowiec et al. (2011) concluded that this character state alone was insufficient to place the morphospecies in *Anomalomyrma*, with its habitus being otherwise consistent with that of *Protanilla*. Terayama (2013) accordingly described *Protanilla izanagi* in that genus. The presence of distinct posterior faces on the dorsal petiolar and post-petiolar nodes, along with abdominal segments III-IV not being broadly conjoined, shows an affinity to the *Protanilla rafflesi* and *Protanilla bicolor* species-groups, but the phylogeny of *Protanilla* as inferred in Chapter 5 demonstrates that these character states are plesiomorphic for *Protanilla*. It is likely that the similar mandibular morphology of *P. izanagi* and the *Protanilla taylori* species-group reflects similar diet (see "Remarks" for the *Protanilla taylori* species-group above) and is therefore homoplasious (Borowiec et al., 2011). Terayama (2013) describes the compound eye as being absent in the worker, but the specimens that I examined are remarkable in the retention of two ommatidia (Fig. 4.31). The presence of any trace of the compound eye in the worker is unique among the Leptanillinae. No molecular data are available for *P. izanagi*, and so in the absence of compelling morphological evidence, this species must be left unplaced to species-group within *Protanilla*. I predict, however, that molecular data will demonstrate that *Protanilla izanagi* belongs within the *Protanilla rafflesi* species-group.

Leptanilla Emery (= *Scyphodon* Brues **syn. nov.**; *Phaulomyrma* Wheeler and Wheeler; *Leptomesites* Kutter; *Noonilla* Petersen **syn. nov.**; *Yavnella* **syn. nov.**)

Type species. Leptanilla revelierii Emery, 1870: 196.

Worker diagnosis.

1. *Medial mandibular margin without peg-like chaetae*.

2. *Medial mandibular margin with or without denticles, if present then irregularly spaced.
3. Medial mandibular margin with at least one subapical tooth.
4. Ventromedial mandibular margin without subapical teeth.
5. *Labrum without peg-like chaetae.*
6. *Maxillary palp 1- to 2-merous.*
7. *Labial palp 1-merous.*
8. *Clypeus indistinct*.
9. Dorsal mandibular articulation not visible in full-face view.
10. *Meso-metapleural suture usually vestigial to absent*, rarely present; if present then unsculptured.
11. Subpetiolar process present *or absent*.
12. Abdominal segment III narrowly joined to abdominal segment IV.
13. *Length of abdominal postsclerites IV longer than *or subequal to* that of abdominal postsclerites V-VI.

Gyne diagnosis. Dichthadiiform, and therefore lacking wings and axillary sclerites. Mandibles edentate or with three teeth (*Leptanilla kubotai*) (Terayama and Kinomura, 2015). Compound eyes repressed or present; *if* present *then* consisting of 1-2 ommatidia. Abdominal segment III never petiolate.

Male diagnosis.

1. *Maxillary palp 1- to 2-merous*.
2. Labial palp 1-merous.
3. Clypeus distinct *or indistinct*.

4. Ocelli present *or absent* (*Leptanilla* TH03, *Leptanilla* zhg-bt03); if present then *set on tubercle*.
5. *Pronotum anteroposteriorly prolonged*.
6. *Mesoscutum anteroposteriorly prolonged*.
7. *Notauli absent*.
8. *Pterostigma absent*.
9. *1A absent from hindwing*.
10. Upper metapleuron distinct from metapectal-propodeal complex (*Leptanilla thai* species-group, *Leptanilla bethyloides* **sp. nov.**, *Leptanilla* zhg-th01) *or indistinct*
11. *Lower metapleuron indistinct* or distinct from metapectal-propodeal complex (*Leptanilla havilandi* species-group, *Leptanilla bethyloides* **sp. nov.**, *Leptanilla* zhg-th01).
12. Abdominal segment II petiolate *or not* (e.g., *Leptanilla* TH02).
13. Abdominal segment III not petiolate.
14. *Cupula absent*.
15. Volsellae present *or absent* (*Leptanilla havilandi* species-group, *Leptanilla bethyloides* species-group), if present then *parossiculus and lateropenite indistinct* (Chapter 3).
16. *Penial sclerites medially fused* or articulated (*Leptanilla astylina* Petersen), rarely partly articulated (*Leptanilla* TH03).

Larval diagnosis. Habitus leptanilloid. Cranium subpyriform in full-face view. Mandibles leptanilloid, with teeth, lateral surface shagreened with spinules. Setae short and suberect or flexuous, elongated, and subdecumbent to erect. Ventral prothoracic process and hemolymph taps present.

Included species. Leptanilla acherontia **sp. nov.**; *Leptanilla africana* Baroni Urbani; *Leptanilla alexandri* Dlussky; *Leptanilla anomala* (Brues) **comb. nov.**; *Leptanilla argamani* (Kugler) **comb. nov.**; *Leptanilla astylina* Petersen; *Leptanilla australis* Baroni Urbani; *Leptanilla belantan* **sp. nov.**; *Leptanilla besucheti* Baroni Urbani; *Leptanilla bethyloides* **sp. nov.**; *Leptanilla bifurcata* Kugler; *Leptanilla boltoni* Baroni Urbani; *Leptanilla buddhista* Baroni Urbani; *Leptanilla butteli* Forel; *Leptanilla charonea* Barandica *et al.*; *Leptanilla clypeata* Yamane and Ito; *Leptanilla copiosa* (Petersen) **comb. nov.**; *Leptanilla doderoi* Emery; *Leptanilla escheri* (Kutter); *Leptanilla exigua* Santschi; *Leptanilla havilandi* Forel; *Leptanilla hunanensis* Tang *et al.*; *Leptanilla hypodracos* Wong and Guénard; *Leptanilla indica* (Kugler) **comb. nov.**; *Leptanilla islamica* Baroni Urbani; *Leptanilla israelis* Kugler; *Leptanilla japonica* Baroni Urbani; *Leptanilla javana* (Wheeler and Wheeler); *Leptanilla laventa* (Griebenow, *et al.*) **comb. nov.**; *Leptanilla kebunraya* Yamane and Ito; *Leptanilla kubotai* Baroni Urbani; *Leptanilla kunmingensis* Xu and Zhang; *Leptanilla lamellata* Bharti and Kumar; *Leptanilla laventa* (Griebenow, *et al.*) **comb. nov.**; *Leptanilla macauensis* Leong *et al.*; *Leptanilla minuscula* Santschi; *Leptanilla morimotoi* Yasumatsu; *Leptanilla najaphalla* **sp. nov.**; *Leptanilla nana* Santschi; *Leptanilla oceanica* Baroni Urbani; *Leptanilla okinawensis* Terayama; *Leptanilla ortunoi* López *et al.*; *Leptanilla palauensis* (M.R. Smith); *Leptanilla plutonia* López *et al.*; *Leptanilla poggii* Mei *et al.*; *Leptanilla revelierii* Emery; *Leptanilla santschii* Wheeler and Wheeler; *Leptanilla swani* Wheeler; *Leptanilla taiwanensis* Ogata *et al.*; *Leptanilla tanakai* Baroni Urbani; *Leptanilla tanit* Santschi; *Leptanilla tenuis* Santschi; *Leptanilla thai* Baroni Urbani; *Leptanilla theryi* Forel; *Leptanilla vaucheri* Emery; *Leptanilla ujjalai* Saroj *et al.*; *Leptanilla yunnanensis* Xu; *Leptanilla zaballosi* Barandica *et al.*

Remarks. The four genera known solely from males at the time of Bolton (1990b) were provisionally retained in the Leptanillini by that author, with the knowledge that at least some would prove to be satellite genera of *Leptanilla*. The phylogeny of the Leptanillini is now robustly resolved with phylogenomic and total-evidence approaches: *Leptanilla s. l.* (Griebenow, 2020, Chapter 1) includes *Scyphodon* and *Noonilla* (= *Scyphodon s. l.*), along with *Leptanilla s. str.*, with which *Phaulomyrma* was synonymized in Chapter 1; and is sister to a well-supported clade first recovered by Borowiec et al. (2019) and identified as *Yavnella* by Griebenow (2020) and Chapter 1.

The question of the formal rank of major subclades in the Leptanillini depends upon practical utility. For generic ranking of subclades to be useful, these clades must be distinguishable based upon the morphology of both the male sex and available female castes. *Yavnella* and *Leptanilla s. l.* are readily diagnosed based upon males, as are the subclades of *Leptanilla s. l.* (Chapter 5). The taxonomic problem then lies in whether these groups can be distinguished based upon worker morphology.

Using phylogenomic inference, Chapter 2 identified the worker of *Yavnella*, while Chapter 5 recovers *Leptanilla havilandi* Forel as sister to *Scyphodon s. l.* (in those analyses represented only by *Noonilla* spp.) and robustly recovers *Leptanilla thai* within *Yavnella* as well. The morphological similarities between *Leptanilla laventa* (Griebenow, *et al.*) **comb. nov.** and *L. thai* to the exclusion of *Leptanilla s. str.*, such as the emarginate frontoclypeal process, cannot be interpreted as synapomorphic. *L. havilandi* and *thai* are extremely close morphologically, as noted by Baroni Urbani (1977). In this study, I find that these two species are discriminated by areolate sculpturation of the torular rim in *L. thai* (no such sculpture is observed in *L. havilandi*; Fig. 4.11), different mandibular dentition, and a more elevated frontoclypeal process in *L.*

havilandi. Sculpturation requires scanning electron microscopy to be assessed, while elevation of the frontoclypeal process and mandibular dentition are difficult to accurately assess with light microscopy (as evidenced by the incorrect accounting of mandibular teeth in the description of *L. thai* [Baroni Urbani, 1977]), making these characters impractical for identification of leptanilline workers to genus. This impracticality, and lack of consistent morphological distinction between the worker castes across all *Yavnella* and *Leptanilla*, argues against maintaining the two as separate genera.

Therefore, the most conservative course of nomenclatural action is to synonymize *Scyphodon*, *Noonilla*, and *Yavnella* under *Leptanilla*. The diversity of *Leptanilla* is here organized in informal species-groups, for which diagnoses based upon all known castes are provided below. Wherever sampling of molecular data across *Leptanilla* is sufficient for phylogeny of these species-groups to be known, these are delimited to be monophyletic. Several aberrant species for which molecular data are unavailable are left unplaced to species-group.

***Leptanilla thai* species-group**

Worker diagnosis.

1. Mandible with 3-4 teeth.
2. Maxillary palp 1- to 2-merous.
3. *Frontoclypeal process present, apex emarginate.
4. Lateral clypeal teeth absent.
5. *Meso-metapleural groove absent or present (*Leptanilla kunmingensis*).
6. Mesotibia with two spurs.
7. Metatibia with 1-2 spurs.

8. Length of abdominal segment II subequal to width in dorsal view, or *length much greater than width* (*Leptanilla laventa*).
9. *Anterior of abdominal tergite IV lateromedially constricted in dorsal view* (*Leptanilla laventa*) or not so constricted.
10. *Length of abdominal tergite IV greater than combined length of posterior abdominal tergites in dorsal view.

Gyne diagnosis. As for genus, but petiole longer than broad in dorsal view, outline rectangular (*L. escheri*) to subpyriform (*L. belantan*). Placement of these two species in the *Leptanilla thai* species-group is provisional (see Remarks).

Male diagnosis.

1. Mandalus ≥0.5× length of that of the mandible.
2. *Mandible fused to cranium*, rarely articulated.
3. Anteromedian ocellus orthogonally dorsal to compound eye in profile view.
4. *LF2>SL*, rarely LF2≈SL.
5. Distal transverse carina absent from procoxa.
6. Protrochanter not elongated.
7. Profemur not enlarged, *sometimes proximally kurtotic*.
8. Arcuate medial carina absent from profemur.
9. Apicoventral hook absent from profemur.
10. Ventromedian carina absent from protibia.
11. Protibial comb absent.
12. Antero-admedian signum present *or absent*.
13. Pronotum and mesoscutum not anteroposteriorly prolonged.

14. Mesoscutellum without recurved posteroventral process.

15. Adventitious spectral M+Cu absent from forewing.

16. Upper metapleuron distinct from metapectal-propodeal complex *or indistinct*.

17. *Lower metapleuron indistinct* from metapectal-propodeal complex.

18. *Propodeal declivity concave in profile view.*

19. Petiole without distinct dorsal node.

20. Abdominal sternite II without ventral process.

21. Abdominal tergite VIII broader than long in posterodorsal view.

22. Abdominal sternite IX posteriorly separate from gonocoxites.

23. Mulceators absent.

24. *Gonopodites inarticulate*.

25. Gonocoxites with partial ventromedian fusion.

26. Gonocoxites without *or rarely with dorsomedian fusion* (*Leptanilla* TH03).

27. *Gonocoxites partly fused to penial sclerites* or unfused.

28. Gonostyli present *or rarely absent* (*Leptanilla* TH03).

29. Volsellae present.

30. Volsellae medially fused.

31. *Distivolsella furcated*, sometimes entire (*Leptanilla* TH03, *Leptanilla* zhg-bt03).

32. *Penial sclerites usually with complete median fusion, rarely with partial median fusion.

33. *Penial sclerites dorsoventrally compressed or not (*Leptanilla* TH03).

34. Phallotreme apical.

35. Phallotreme dorsal.

36. Dense phallotremal vestiture of setae absent.

Larval diagnosis. As for genus. Larva is known only in *Leptanilla escheri* and *Leptanilla judaica*, the placement of which in this species-group has not been confirmed by molecular phylogenetic inference.

Included species. Leptanilla argamani (Kugler) **comb. nov.**; *Leptanilla belantan* **comb. nov.**; *Leptanilla escheri* (Kutter); *Leptanilla indica* (Kugler) **comb. nov.**; *Leptanilla judaica* Kugler; *Leptanilla kunmingensis* Xu and Zhang; *Leptanilla lamellata* Bharti and Kumar; *Leptanilla laventa* (Griebenow, et al.) **comb. nov.**; *Leptanilla thai* Baroni Urbani; *Leptanilla ujjalai* Saroj *et al.*

Remarks. Leptanilla escheri, *L. judaica*, *L. kunmingensis*, *L. lamellata*, *L. ujjalai*, and *L. belantan* **sp. nov.** are placed in this species-group with some caution, given a lack of molecular data for these species. These four species bear some resemblance to *Leptanilla laventa* **comb. nov.** (e.g., in the palpal formula being 2,1), which differs from them only in the elongation of the appendicular sclerites. Since worker morphology in *Leptanilla* is often indecisive when inferring phylogeny, or downright misleading (Chapter 5), these species may belong elsewhere within *Leptanilla*. With only species included in phylogenomic analysis under consideration, the *Leptanilla thai* and *Leptanilla havilandi* species-groups are mutually indistinguishable based upon worker morphology without examination of cranial microsculpture. However, male specimens of the *Leptanilla havilandi* species-group are known only from the Sundan region, and so extralimital worker specimens that conform to the worker-based morphological diagnosis of that species-group presented here are instead referred to the *Leptanilla thai* species-group. These two clades are only definitively known in sympatry from peninsular Malaysia. Since phylogenomic inference confirms the position of *L. thai* within the former genus *Yavnella*, and

this is the oldest species name assigned to that clade for which that hypothesized placement can be confirmed with molecular data, this clade is informally exemplified by that species.

As noted in Chapter 2, the anatomical identity of the frontoclypeal process observed in the *Leptanilla thai* species-group, the *Leptanilla havilandi* species-group, *Leptanilla clypeata* Yamane and Ito, and *Leptanilla hypodracos* Wong and Guénard, is unclear. Prior authors assumed a clypeal origin, which may be in part correct, but this hypothesis cannot be tested with external examination due to the absence in worker *Leptanilla* of apparent anterior tentorial pits or an unequivocal epistomal sulcus. Elision of the boundaries between the frons and clypeus also occurs in *Discothyrea* (Proceratiinae) and *Aulacopone relicta* Arnol'di (Ectatomminae: Heteroponerini), likewise involved in an anteromedian projection from the cranium in full-face view (Taylor, 1979). Detailed micro-CT study of the shelf-like frontoclypeal process in the *Discothyrea oculata* and *traegordhi* species-complexes was able to confirm the identity of this process as a mosaic of the frons and clypeus (Hita-Garcia et al., 2019), and only similar data can possibly be used to clarify the anatomy of the frontoclypeal process in *Leptanilla*.

The palpal formula in the worker caste of *L. thai* and *L. laventa* is 2,1 (Chapter 2), which are the only species for which the worker is known that have been confirmed to belong to the *Leptanilla thai* species-group by phylogenomic inference. All known males of the *Leptanilla thai* species-group examined in this study possess a 1-merous palp (cf. Kugler, 1987), meaning that it is probable that the *Leptanilla thai* species-group shows sexual dimorphism in palpal formula. This would be only confirmed by definitive association of conspecific worker and male specimens belonging to this clade. If confirmed, the *Leptanilla thai* species-group would constitute only the third independent origin in the Formicidae of decoupled palpal formula between the sexes (Bolton, 2003). Curiously, this phenomenon would run opposite to the tendency in other cases of

decoupling, in which the palpomere counts of the worker are reduced relative to those in the male.

The *Leptanilla thai* species-group is broadly distributed across southern Asia (Fig. 2.20), with males being more diverse and abundant than any other leptanilline clade in Malaise trap residues from mainland Southeast Asia. An undescribed male morphospecies is recorded from Sana'a, Yemen (Collingwood and Agosti, 1996), meaning that the *Leptanilla thai* species-group extends at least to the extreme northeastern corner of the Afrotropics, but within that ecozone is perhaps restricted to the southern Arabian Peninsula. No specimens are yet known from the Eastern Palaearctic, with the nearest examples being *L. kunmingensis* and an undescribed worker specimen (CASENT0064302), both from Yunnan Province, China. This absence from the Eastern Palaearctic is notable given the thorough myrmecological sampling of Japan and to a lesser extent Taiwan. Better sampling of the Sundan region is needed, but members of the *Leptanilla thai* species-group are conspicuously rare in collections from this area compared to mainland Southeast Asia, with only two male morphospecies being known from a single locality south of the Pattani-Kangar Line (Whitmore, 1988), along with *Leptanilla belantan*, which may represent the worker of either of these. It may be surmised from the distribution of the *Leptanilla thai* species-group that this clade originated in subtropical seasonal forests of mainland Southeast Asia or the Indian subcontinent, explosively radiating in the former region, along with arid habitats in the Western Palaearctic and (marginally) the Afrotropics. The *Leptanilla thai* species-group appears to have been mostly unsuccessful in penetrating perhumid equatorial rainforests. I propose that preoccupation of ecological niche space in the Sundan region by the *Leptanilla havilandi* species-group is perhaps responsible, given the close functional similarities between

the worker phenotypes in these two clades to the exclusion of confirmed worker morphology in the *Leptanilla revelierii* species-group.

***Leptanilla havilandi* species-group**

Worker diagnosis.

1. Mandible with three teeth.
2. Maxillary palpomere 2-merous.
3. *Frontoclypeal process present, apex emarginate.
4. Lateral clypeal teeth absent.
5. *Meso-metapleural suture absent.
6. Mesotibia with two spurs.
7. Metatibia with two spurs.
8. Length of abdominal segment II subequal to width in dorsal view.
9. Anterior of abdominal tergite IV not lateromedially constricted in dorsal view.
10. *Length of abdominal tergite IV greater than combined length of posterior abdominal tergites in dorsal view.

Gyne diagnosis. Gyne unknown.

Male diagnosis.

1. Mandalus ≥0.5× length of the mandible; *or <0.5× length of mandible*.
2. Mandible never fused to cranium, fully articulated.
3. Anteromedian ocellus orthogonally dorsal to compound eye in profile view *or posterior to compound eye*.
4. LF2<SL, rarely LF2≈SL (*Leptanilla copiosa*).

5. *Distal transverse carina present on procoxa* (Fig. 4.18B).
6. Protrochanter not elongated.
7. Profemur not enlarged, *or moderately enlarged, sometimes proximally kurtotic*.
8. Arcuate medial carina absent from profemur.
9. Apicoventral hook absent from profemur.
10. *Ventromedian carina present on protibia*.
11. Protibial comb absent.
12. Antero-admedian signum present *or absent*.
13. *Pronotum and mesoscutum anteroposteriorly prolonged*.
14. Mesoscutellum without recurved posteroventral process.
15. Adventitious spectral M+Cu absent from forewing.
16. *Upper metapleuron indistinct from metapectal-propodeal complex*.
17. Lower metapleuron usually distinct from metapectal-propodeal complex, *rarely (*L. anomala*) indistinct*.
18. Propodeal declivity convex in profile view.
19. *Petiole reduced, without distinct dorsal node*.
20. *Abdominal sternite II without ventral process*.
21. *Abdominal tergite VIII distinctly longer than broad in posterodorsal view*.
22. *Abdominal sternite IX completely fused to gonocoxites*.
23. Mulceators absent.
24. Gonopodites articulate.
25. *Gonocoxites with complete ventromedian fusion*.
26. *Gonocoxites with complete dorsomedian fusion*.

27. Gonocoxites completely fused to penial sclerites.

28. Gonostyli present.

29. Volsellae absent.

30. ***Inapplicable***

31. ***Inapplicable***

32. *Penial sclerites with complete median fusion.

33. *Penial sclerites not dorsoventrally compressed.

34. *Phallotreme preapical*.

35. Phallotreme dorsal.

36. *Dense phallotremal vestiture of setae present.*

Larval diagnosis. Larva unknown.

Included species. Leptanilla anomala (Brues) **comb. nov.**; *Leptanilla copiosa* (Petersen) **comb. nov.**; *Leptanilla havilandi* Forel; + 6 undescribed morphospecies

Remarks. This clade is restricted to the Sundan region and the Philippines. Most known specimens are Bornean in origin. The bizarre males of the *Leptanilla havilandi* species-group were first described as the genera *Scyphodon* and *Noonilla*, with *Leptanilla anomala* being regarded as Hymenoptera *incertae sedis* (Brues, 1925). Male morphospecies attributable to *Noonilla* in addition to the type species (*Leptanilla copiosa* [Petersen]) were identified and sequenced by Griebenow (2020) and in Chapter 1. Chapter 3 treats this clade as *Scyphodon s. l.*, despite not yet having subjected the position of *Scyphodon* relative to *Noonilla* to phylogenetic analysis. Nonetheless, Bayesian total-evidence inference confirms the monophyly of *Scyphodon s. l.* inclusive of *L. havilandi* (Chapter 5), here formally synonymized with *Leptanilla*.

The worker of *L. havilandi* bears a striking resemblance to *L. thai*, including in the presence of an emarginate frontoclypeal process, but is distantly related, demonstrating the morphological conservatism of the worker caste in *Leptanilla*. *Leptanilla clypeata* and *L. hypodracos* are sympatric with the *Leptanilla havilandi* species-group, and morphologically alike *L. havilandi*, introducing the possibility that these are members of this clade. Given the lack of phylogenetic signal in leptanilline worker morphology, however, this hypothesis must be tested with molecular data.

The close affinity of *L. anomala* and *L. copiosa*, to the exclusion of other described Leptanillinae, was not suggested by previous authors who argued for the placement of *L. anomala* within the Leptanillinae (Boudinot, 2015; Petersen, 1968). This is in part due to the preservation in balsam of the type series of *L. anomala*, a status that conceals autapomorphies of the *Leptanilla havilandi* species-group, namely phallotremal setae and the distal transverse carina on the procoxa: examination of CASENT0106168 revealed these. In addition, the discovery of additional undescribed male morphospecies within the *Leptanilla havilandi* species-group (Griebenow, 2020; Chapters 1-2) revealed intermediates in morphospace, juxtaposing the dorsoventrally compressed head and mesosoma of *L. anomala* with the nub-like, non-spatulate mandibles of *L. copiosa*.

***Leptanilla bethyloides* species-group**

Worker diagnosis. Worker unknown.

Gyne diagnosis. Gyne unknown.

Male diagnosis.

1. Mandalus ≥0.5× length of the mandible.

2. Mandible never fused to cranium, fully articulated.
3. *Anteromedian ocellus posterior to compound eye.*
4. LF2<SL.
5. Distal transverse carina absent from procoxa.
6. Protrochanter not elongated.
7. Profemur not enlarged.
8. Arcuate medial carina absent from profemur.
9. Apicoventral hook absent from profemur.
10. Ventromedian carina absent from protibia.
11. Protibial comb absent.
12. *Antero-admedian signum absent.*
13. *Pronotum and mesoscutum anteroposteriorly prolonged.*
14. *Mesoscutellum with* or without recurved process.
15. Adventitious spectral M+Cu absent from forewing, *or present* (*Leptanilla* TH01).
16. Upper metapleuron distinct from metapectal-propodeal complex *or indistinct*.
17. Lower metapleuron distinct from metapectal-propodeal complex *or indistinct*.
18. Propodeal declivity convex in profile view.
19. Petiole well-developed, with *or rarely without distinct dorsal node* (*Leptanilla* TH07).
20. Abdominal sternite II with *or without ventral process*.
21. Abdominal tergite VIII broader than long in posterodorsal view.
22. Abdominal sternite IX posteriorly separate from gonocoxites.
23. Mulceators absent.
24. Gonopodites articulate.

25. Gonocoxites without ventromedian fusion.

26. Gonocoxites without complete dorsomedian fusion.

27. Gonocoxites unfused to penial sclerites.

28. Gonostyli present.

29. *Volsellae absent*.

30. ***Inapplicable***

31. ***Inapplicable***

32. *Penial sclerites with complete median fusion.

33. *Penial sclerites dorsoventrally compressed.

34. Phallotreme apical.

35. Dense phallotremal vestiture of setae absent.

Larval diagnosis. Larva unknown.

Included species. Leptanilla bethyloides sp. nov.; + ~6 undescribed morphospecies

Remarks. This species-group is restricted to mainland Southeast Asia north of the Pattani-Kangar Line, with the type locality of *L. bethyloides* being their northernmost extent. Like the *Leptanilla najaphalla* speces-group, the *Leptanilla bethyloides* species-group is known only from male specimens. These are never abundant in known collections, with it therefore appearing that this species-group exhibits genuine rather than artifactual rarity; no exemplars of this clade were featured in Chapter 3, meaning that the male genital skeletomusculature of the *Leptanilla bethyloides* species-group is more poorly understood than that of any other major leptanilline clade.

Unpublished micro-CT scans of *Leptanilla* zhg-mm03 (CASENT0842829) demonstrate that the volsellae are completely absent in this morphospecies, in an apparent homoplasy with the *Leptanilla havilandi* species-group. This condition applies to all males in this clade, although the total absence, as opposed to extreme reduction, of the volsellae cannot yet be definitively confirmed for any other representatives of the *Leptanilla bethyloides* species-group due to a lack of specimens for study.

The *Leptanilla bethyloides* species-group qualitatively possesses morphological diversity disproportionate to the depauperation of known lineages: the condition of the metapleuron varies from completely indiscernible (*Leptanilla* TH07) to both the upper and lower metapleuron being completely visible (e.g., *L. bethyloides*). However, the lower metapleuron is never distinct from the metapectal-propodeal complex in the absence of the same distinction for the upper metapleuron, as in most of the *Leptanilla havilandi* species-group. Other conditions unusual among *Leptanilla* that are sporadically observed in the *Leptanilla bethyloides* species-group include elongated antennomeres, a posteriorly recurved mesoscutellum (both only observed in *Leptanilla* zhg-th01), and a dorsomedian penial carina (*Leptanilla* TH01).

***Leptanilla najaphalla* species-group**

Worker diagnosis. Worker unknown.

Gyne diagnosis. Gyne unknown.

Male diagnosis.

1. Mandalus ≥0.5× length of the mandible.
2. Mandible never fused to cranium, fully articulated.
3. *Anteromedian ocellus posterior to compound eye.*

4. LF2<SL.
5. Distal transverse carina absent from procoxa.
6. Protrochanter not elongated.
7. *Profemur enlarged, sometimes markedly constricted proximally*.
8. Arcuate medial carina absent from profemur.
9. *Apicoventral hook present* or absent from profemur.
10. Ventromedian carina absent from protibia.
11. *Protibial comb present*.
12. *Antero-admedian signum absent*.
13. *Pronotum and mesoscutum anteroposteriorly prolonged*.
14. Mesoscutellum without recurved posterodorsal process.
15. *Adventitious spectral M+Cu present in forewing.*
16. *Upper metapleuron indistinct from metapectal-propodeal complex*.
17. *Lower metapleuron indistinct from metapectal-propodeal complex*.
18. Propodeal declivity convex in profile view, *with distinct dorsal and posterior faces, dorsal face parallel to craniocaudal axis*.
19. Petiole well-developed, with distinct dorsal node.
20. Abdominal sternite II with *or without ventral process*.
21. Abdominal tergite VIII broader than long in posterodorsal view.
22. *Abdominal sternite IX with narrow posteromedian fusion to gonocoxites*.
23. *Mulceators present*.
24. *Gonopodites inarticulate*.
25. *Gonocoxites with complete dorsomedian fusion*.

26. *Gonocoxites with complete ventromedian fusion*.
27. *Gonocoxites fused to penial sclerites* or unfused.
28. Gonostyli present *or absent*.
29. Volsellae present.
30. Volsellae medially fused.
31. Distivolsella never furcated, although paired, recurved cuticular processes may be present at apex.
32. *Penial sclerites with complete median fusion.
33. *Penial sclerites lateromedially compressed or subcircular in cross-section.
34. Phallotreme apical *or subapical*.
35. Phallotreme dorsal *or ventral*.
36. Dense phallotremal vestiture of setae absent.

Larval diagnosis. Larva unknown.

Included species. Leptanilla najaphalla **sp. nov.**; + 5 undescribed morphospecies

Remarks. This clade remains known only from males, necessitating the regrettable description of a species based solely upon male material (*L. najaphalla*) to provide the "Bornean morphospecies-group" (Griebenow, 2020; Chapter 1) with an informal species-group name. The males of the *Leptanilla najaphalla* species-group are unapologetically bizarre, defined by such autapomorphies as a protibial comb comprised of parallel-sided cuticular processes (previously misidentified as setae; Griebenow, 2020; Chapter 1), the complete median fusion of the volsellae at the base, and the presence of mulceators. It appears that the protibial comb is serially homologous with the probasitarsal comb, a structure synapomorphic for the Hymenoptera (Basibuyuk and Quicke, 1995). While the protibial comb and mulceators are unparalleled in the

Hymenoptera, the medial fusion of the volsellae is also observed in *Sceliphron caementarium* (Sphecidae: Sceliphrini) (Schulmeister, 2003: fig. 11C).

Micro-CT scans revealed that all 7 morphospecies sampled in that study (including *L. najaphalla*, as *Leptanilla* zhg-my02) show posteromedian fusion of abdominal sternite IX to the gonocoxites, an apomorphy apparently derived independently from the anatomical condition observed in the *Leptanilla havilandi* species-group (Chapter 5). This species-group is robustly supported as sister to the *Leptanilla havilandi* species-group (Griebenow, 2020; Chapters 1-2, 5), which likewise is restricted to the Sundan region. Despite this phylogenetic position, no unequivocal male morphological synapomorphies are known for the two clades, with the fusion of S9 to the gonocoxites, and medial fusion of the gonocoxites, being perhaps homoplasious between the two according, given a lack of the Remanean homology criterion of "special quality" (Chapter 3). Further Winkler and pitfall sampling in the Sundan region, particularly Borneo, will be required to collect the unknown female castes of the *Leptanilla najaphalla* species-group. It is also possible that *L. butteli* and *L. kebunraya*, the worker morphology of which is aberrant among *Leptanilla*, are representatives of this clade.

***Leptanilla revelierii* species-group**

Worker diagnosis.

1. Mandible with 3-4 teeth.
2. Maxillary palpomere 1-merous.
3. *Frontoclypeal process absent or present, never emarginate.
4. Lateral clypeal teeth absent.
5. *Meso-metapleural suture absent or present (*Leptanilla hunanensis*).

6. Mesotibia with 0-1 spurs.
7. Metatibia with two spurs.
8. Length of abdominal segment II subequal to width in dorsal view.
9. Anterior of abdominal tergite IV not lateromedially constricted in dorsal view.
10. Length of abdominal tergite IV equal or less than combined length of posterior abdominal tergites in dorsal view.

Gyne diagnosis. As for the genus, but petiole quadrate to distinctly broader than long in dorsal view.

Male diagnosis.

1. Mandalus ≥0.5× length of the mandible.
2. Mandible never fused to cranium, fully articulated.
3. *Anteromedian ocellus posterior to compound eye.*
4. LF2<SL.
5. Distal transverse carina absent from procoxa.
6. *Protrochanter rarely elongated* (*Leptanilla* ci01) (Fig. 4.36) or not elongated.
7. *Profemur enlarged* or not enlarged.
8. *Arcuate medial carina present on profemur* (*Leptanilla* ci01) or absent from profemur.
9. Apicoventral hook absent from profemur.
10. Ventromedian carina absent from protibia.
11. Protibial comb absent.
12. *Antero-admedian signum absent.*
13. *Pronotum and mesoscutum anteroposteriorly prolonged*.
14. Mesoscutellum without recurved posterodorsal process.

15. Adventitious spectral M+Cu absent from forewing.

16. *Upper metapleuron indistinct from metapectal-propodeal complex*.

17. *Lower metapleuron indistinct from metapectal-propodeal complex*.

18. Propodeal declivity convex in profile view.

19. Petiole well-developed, with *or without distinct dorsal node*.

20. Abdominal sternite II with *or without ventral process*.

21. Abdominal tergite VIII broader than long in posterodorsal view *or rarely longer than broad in posterodorsal view* (*Leptanilla* ci01).

22. Abdominal sternite IX posteriorly separate from gonocoxites.

23. Mulceators absent.

24. Gonopodites articulate, rarely *inarticulate* (*Leptanilla exigua*).

25. Gonocoxites with ventromedian fusion partial *to complete* (*L. astylina*).

26. Gonocoxites without complete dorsomedian fusion.

27. Gonocoxites unfused to penial sclerites.

28. Gonostyli present.

29. Volsellae present.

30. Volsellae medially separate.

31. Distivolsella entire.

32. *Penial sclerites with complete median fusion.

33. *Penial sclerites dorsoventrally compressed, rarely *lateromedially compressed* (*L. astylina*, *Leptanilla* zhg-na01).

34. Phallotreme apical *or subapical.*

35. Phallotreme dorsal.

36. Dense phallotremal vestiture of setae absent.

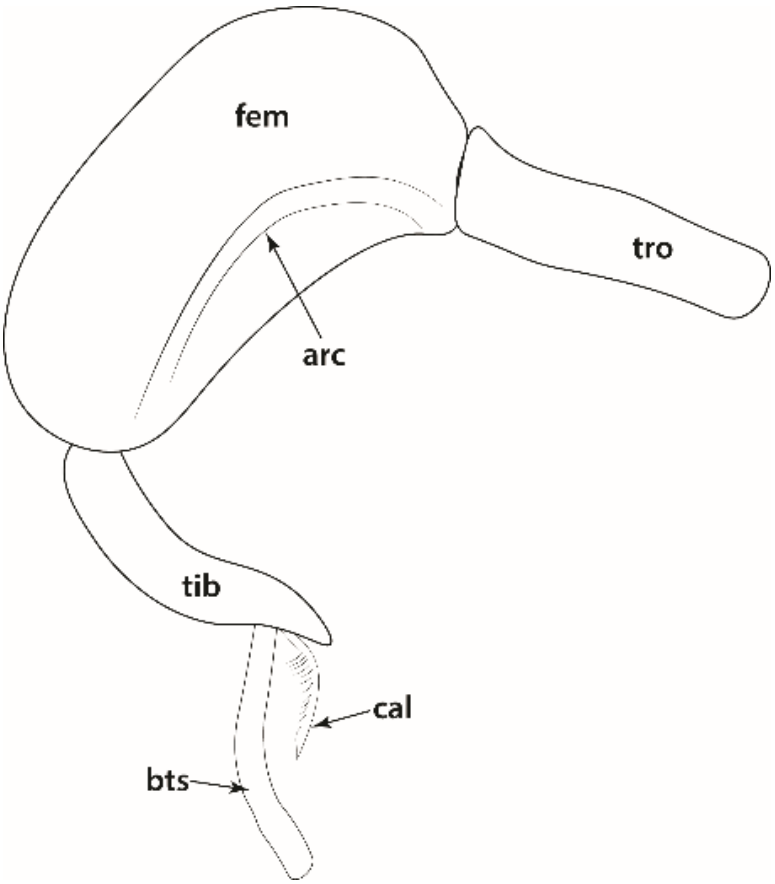

Figure 4.36. Foreleg of *Leptanilla* ci01, medial view, diagrammatic. Abbreviations: arc = arcuate medial carina; bts = probasitarsus; cal = calcar; fem = profemur; tib = protibia; tro = protrochanter

Larval diagnosis. As for genus.

Included species. Leptanilla acherontia **sp. nov.**; *Leptanilla africana* Baroni Urbani; *Leptanilla alexandri* Dlussky; *Leptanilla astylina* Petersen; *Leptanilla australis* Baroni Urbani; *Leptanilla besucheti* Baroni Urbani; *Leptanilla bifurcata* Kugler; *Leptanilla boltoni* Baroni Urbani; *Leptanilla buddhista* Baroni Urbani; *Leptanilla charonea* Barandica *et al.*; *Leptanilla doderoi* Emery; *Leptanilla exigua* Santschi; *Leptanilla hunanensis* Tang *et al.*; *Leptanilla islamica* Baroni Urbani; *Leptanilla israelis* Kugler; *Leptanilla japonica* Baroni Urbani; *Leptanilla javana* (Wheeler and Wheeler); *Leptanilla kubotai* Baroni Urbani; *Leptanilla macauensis* Leong *et al.*; *Leptanilla minuscula* Santschi; *Leptanilla morimotoi* Yasumatsu; *Leptanilla nana* Santschi;

Leptanilla oceanica Baroni Urbani; *Leptanilla okinawensis* Terayama; *Leptanilla ortunoi* López *et al.*; *Leptanilla plutonia* López *et al.*; *Leptanilla poggii* Mei *et al.*; *Leptanilla revelierii* Emery; *Leptanilla swani* Wheeler; *Leptanilla taiwanensis* Ogata *et al.*; *Leptanilla tanakai* Baroni Urbani; *Leptanilla tanit* Santschi; *Leptanilla tenuis* Santschi; *Leptanilla theryi* Forel; *Leptanilla vaucheri* Emery; *Leptanilla yunnanensis* Xu; *Leptanilla zaballosi* Barandica *et al.*

Remarks. The *Leptanilla revelierii* species-group is by far the most geographically widespread clade within the Leptanillinae and correspondingly is the most speciose. *Leptanilla revelierii* Emery was the first species within the Leptanillinae to be scientifically described, while *Leptanilla japonica* Baroni Urbani is the leptanilline species that has been subjected to the most bionomic study. This is the only leptanilline clade to have expanded its range west of the Arabian subcontinent, radiating extensively throughout the Afrotropics and the Mediterranean Basin. It does not appear that this species-group extends into temperate latitudes of the Western Palaearctic, but *Leptanilla alexandri* Dlussky is reported from Uzbekistan (Dlussky, 1969). The *Leptanilla revelierii* species-group, along with the *Protanilla rafflesi* species-group, are the sole leptanilline clades confirmed to range into the Eastern Palaearctic and occupy fully temperate climates. In addition, the *Leptanilla revelierii* species-group is so far the only clade within the Leptanillinae known to have traversed Wallace's Line. The apparent ease with which this clade has radiated across the Old World is striking when compared to its sister, which remains restricted to only a portion of the Indo-Malayan ecoregion. Collections of the *Leptanilla revelierii* species-group in the Indo-Malayan ecoregion remain scanty compared to sympatric members of other species-groups of *Leptanilla*.

There is a great undescribed diversity of the *Leptanilla revelierii* species-group in the Afrotropics, with no fewer than nine male morphospecies purportedly being collected at the

Brandberg Massif in Namibia (Robertson, 2000). *Leptanilla* ci01 is here provisionally considered to belong to the *Leptanilla revelierii* species-group, despite its extreme deviation from the male morphology observed in the rest of that clade, since (1) Bayesian total-evidence inference excludes this aberrant morphospecies from all other major *Leptanilla* clades with posterior probability greater than 0.95 (Chapter 5) and (2) no other clade of *Leptanilla* is known to exist in sub-Saharan Africa.

Using Bayesian total-evidence inference, Chapter 5 likewise excludes *Leptanilla astylina* from all clades within the Leptanillinae besides the *Leptanilla revelierii* species-group, with high posterior probability. What were interpreted as "medially fused volsellar plates" by Petersen (1968: p. 581) appear in fact to be the gonocoxites, with the "large, valve-like" sclerites interpreted as the gonocoxites (Petersen, 1968: p. 581) therefore corresponding to the gonostyli—the putative absence of gonostyli referred to by the specific epithet of *L. astylina* is therefore false. Even with this reinterpretation, the male genitalia in *L. astylina* deviate from what is observed in the remainder of the *Leptanilla revelierii* species-group, conspicuously in the complete ventromedian fusion of the gonocoxites and the medial separation of the penial sclerites shown in Petersen (1968: figs. 3, 4), which could not be confirmed by examination of the holotype. The medial concavity and ellipsoid outline of the gonostylus (Petersen 1968: fig. 3) is also aberrant among the *Leptanilla revelierii* species-group, as is the lateral concealment of the gonocoxite by the gonostylus (Petersen, 1968: fig. 5) and the exposure of the volsellae.

Leptanilla swani Wheeler is the sole species of *Leptanilla* to be described from Australia, although the undescribed species-level diversity of *Leptanilla* from that continent is conspicuous, with richness highest in Queensland. Specimens are known from as far south as the Australian Capital Territory. Contrary to the suggestion of Wheeler (1932) that *Leptanilla* are relict

elements of the Australian ant fauna, the *Leptanilla revelierii* species-group can be assumed to be recent arrivals to Australasia from the Indo-Malayan ecoregion.

Despite the variety and vast geographical range of the *Leptanilla revelierii* species-group, male morphology within the clade is quite homogeneous relative to the other major subclades of *Leptanilla* for which males are known, particularly relative to the species-poor *Leptanilla havilandi* and *najaphalla* species-groups. If not artifactual, this comparative depauperation is peculiar if we assume that the *Leptanilla revelierii* species-group originated in the Indo-Malayan ecoregion and radiated outwards. The dramatic innovation observed across the male phenotype of *Leptanilla* ci01 is striking when considered in this context.

Incertae sedis

Leptanilla butteli Forel; *Leptanilla palauensis* (Smith); *Leptanilla clypeata* Yamane and Ito; *Leptanilla kebunraya* Yamane and Ito; *Leptanilla hypodracos* Wong and Guénard.

Molecular data are unavailable for the species of *Leptanilla* listed here; even with the contextualization of leptanilline morphology onto a well-resolved phylogeny inferred from molecular data or jointly from those data and discretized male morphology (Chapters 1, 5), these species cannot be confidently placed to the species-groups delimited here, due to morphological evidence that is equivocal in phylogenetic signal or too aberrant to be of comparative use. *Leptanilla clypeata* is known from both the worker and queen; *Leptanilla palauensis* (Smith) from the male alone; and the remaining species only from the worker caste.

Leptanilla clypeata and *L. hypodracos* are very similar to one another, and closely conform to the worker-based diagnosis of the sympatric *Leptanilla havilandi* species-group and the parapatric *Leptanilla thai* species-group. The palpal formulae of these species would provide

further evidence as to their phylogenetic position, but have not been described, and I was not able to obtain specimens for study. These species differ from the *Leptanilla havilandi* and *thai* species-groups only in the emargination of the anterior petiolar margin in dorsal view. Worker morphology is quite invariable across *Leptanilla*, and so the phylogenetic significance of this character state cannot be extrapolated; given the relative morphological conformity of the worker caste between the phylogenetically distant *L. havilandi* and *L. thai*, even the phylogenetic affinity of *L. clypeata* and *L. hypodracos* with one another cannot be assumed without corroboration.

Leptanilla butteli resembles the *Leptanilla revelierii* species-group overall but differs from the members of that clade in having two mandibular teeth rather than 3-4, and abdominal sternite II projecting distinctly below the level of abdominal sternite III along the dorsoventral axis (Baroni Urbani 1977: fig. 25). *Leptanilla kebunraya* joins *L. butteli* in being one of the only two *Leptanilla* species in which the worker mandible has two teeth, but otherwise bears little apparent resemblance to *L. butteli* to the exclusion of other *Leptanilla*. *L. kebunraya* is unique among known *Leptanilla* in having anterolateral frontoclypeal processes, which invite comparison with the lateral clypeal teeth of *Feroponera ferox* Bolton and Fisher (Ponerinae: Ponerini). This is of no help in inferring the function of these structures in *L. kebunraya* since the biology of *F. ferox* is largely unknown (Bolton and Fisher, 2008).

Leptanilla palauensis (M. R. Smith) was described as the first known male of *Probolomyrmex* Mayr (Proceratiinae: Probolomyrmecini), without associated workers or gynes (Smith, 1953), and is still known only from the holotype. Taylor (1965) tentatively transferred the species to *Leptanilla*, with Petersen (1968) following this classification with some reservation, noting that William Brown and Edward O. Wilson doubted it was even an ant. Griebenow (2021) briefly mentioned *L. palauensis*, noting that examination of the holotype confirmed its placement within

Leptanilla s. l. (Griebenow, 2021: p. 628). This phylogenetic position is confirmed by Bayesian total-evidence inference; however, the exact phylogenetic position of this morphospecies within *Leptanilla* remains poorly resolved, and the combination of character states observed in in *L. palauensis* (Chapter 5) excludes the species from all species-groups of *Leptanilla* here delimited. The lateromedial compression of the penial sclerites, in conjunction with well-developed volsellae, perhaps implies a phylogenetic relation with the *Leptanilla najaphalla* species-group, or with *Leptanilla* zhg-my08 (for which molecular data are unavailable); both these lineages are known only from Borneo. *L. palauensis* is a striking biogeographical outlier among the Leptanillinae, being known only from the volcanic island of Babeldaob in Palau, and therefore the only known leptanilline from Oceania. All known *Leptanilla* gynes are flightless, limiting their dispersal capabilities, but the remote location of *L. palauensis* is paralleled by the presence of *Leptanilla oceanica* Baroni Urbani in the Ogasawara Islands (Baroni Urbani, 1977).

Almost nothing is known of the biology of *L. butteli*, *L. kebunraya*, and *L. hypodracos*. Among *Leptanilla*, our biological knowledge of *Leptanilla clypeata* Yamane and Ito is second in comprehensiveness only to that available for *L. japonica*, with Ito and Yamane (2020) providing observations of live colonies, including feeding and egg-laying behavior. Billen et al. (2022a, b) thoroughly described the exocrine glands of worker *L. clypeata*, with the dorsoproximal intramandibular gland discovered in this species being novel for the Formicidae.

Unplaced to species-group

Leptanilla santschii Wheeler and Wheeler.

Remarks. Molecular data are unavailable for *Leptanilla santschii*, which is known only from the male holotype. The club-like volsellae and absent gonostyli of *Leptanilla santschii* (Wheeler and

Wheeler, 1930: fig. 2D; Petersen, 1968) would exclude this species from the *Leptanilla revelierii* species-group, if the description of Wheeler and Wheeler (1930) is accurate, but with the holotype missing (Stefan Cover, pers. comm.), morphological data are too limited to permit Bayesian total-evidence inference to test this hypothesis.

Acknowledgements

I thank Jadranka Rota (MZLU), Debbie Jennings (ANIC), Masashi Yoshimura (OIST), Kevin Williams (CSCA), Jeremy Frank (BPBM), Crystal Maier (MCZC), Lars Vilhelmsen (ZMUC), Suzanne Ryder (BMNH), Bonnie Blaimer (ZMHB), Brian Fisher (CASC), Chris Darling (ROME), Benoit Guénard (HKUBM), Po-Wei Hsu (NCUE), Majid Moradmand (ZMUI), Alberto Tinaut, Yu Hisasue, and José María Gómez-Durán for loaning or donating material used in this study. This project was supported in part by NSF grant DEB-1932405 to P. S. Ward, UC Davis Jastro-Shields, the UC-Davis Dept. of Entomology, the Helmsley Charitable Trust, and SI Global Genome Initiative.

Supplementary Table, Chapter 4

Table 4.S1. Relevant collection data for specimens newly included in this study.

References

Ashmead, W.H., 1905. A skeleton of a new arrangement of the families, subfamilies, tribes and genera of the ants, or the superfamily Formicoidea. Canadian Entomologist 37, 381–384.

Aswaj, P., Anoop, K., Priyadarsanan, D.R., 2020. First record of the rarely collected ant *Protanilla gengma* Xu, 2012 (Hymenoptera, Formicidae, Leptanillinae) from the Indian subcontinent. CheckList 16, 1621–1625. https://doi.org/10.15560/16.6.1621

Barandica, J.M., López, F., Martínez, M.D., Ortuño, V.M., 1994. The larvae of *Leptanilla charonea* and *Leptanilla zaballosi* (Hymenoptera, Formicidae). Deutsche Entomologische Zeitschrift 41, 147–153. https://doi.org/10.1002/mmnd.19940410113

Baroni Urbani, C., 1989. Phytogeny [sic!] and behavioural evolution in ants, with a discussion of the role of behaviour in evolutionary processes. Ethology Ecology & Evolution 1, 137–168. https://doi.org/10.1080/08927014.1989.9525520

Baroni Urbani, C., 1977. Materiali per una revisione della sottofamiglia Leptanillinae Emery (Hymenoptera: Formicidae). Entomologica Basiliensia 2, 427–488.

Baroni Urbani, C., de Andrade, M.L., 2006. A new *Protanilla* Taylor, 1990 (Hymenoptera: Formicidae: Leptanillinae) from Sri Lanka. Myrmecologische Nachrichten 8, 45–47.

Barraclough, T.G., 2019. The evolutionary biology of species. Oxford University Press.

Basibuyuk, H.H., Quicke, D.L.J., 1995. Morphology of the antenna cleaner in the Hymenoptera with particular reference to non-aculeate families (Insecta). Zoologica Scripta 24, 157–177. https://doi.org/10.1111/j.1463-6409.1995.tb00397.x

Billen, J., Bauweleers, E., Hashim, R., Ito, F., 2013. Survey of the exocrine system in *Protanilla wallacei* (Hymenoptera, Formicidae). Arthropod Structure & Development 42, 173–183. https://doi.org/10.1016/j.asd.2013.01.001

Blaimer, B.B., Brady, S.G., Schultz, T.R., Lloyd, M.W., Fisher, B.L., Ward, P.S., 2015. Phylogenomic methods outperform traditional multi-locus approaches in resolving deep evolutionary history: a case study of formicine ants. BMC Evol Biol 15, 271. https://doi.org/10.1186/s12862-015-0552-5

Bolton, B., 2003. Synopsis and classification of the Formicidae, Memoirs of the American Entomological Institute. The American Entomological Institute, Gainesville, FL.

Bolton, B., 1990a. Army ants reassessed: the phylogeny and classification of the doryline section (Hymenoptera, Formicidae). Journal of Natural History 24, 1339–1364. https://doi.org/10.1080/00222939000770811

Bolton, B., 1990b. The higher classification of the ant subfamily Leptanillinae (Hymenoptera: Formicidae). Systematic Entomology 15, 267–282. https://doi.org/10.1111/j.1365-3113.1990.tb00063.x

Bolton, B., 1990c. Abdominal characters and status of the cerapachyine ants (Hymenoptera, Formicidae). Journal of Natural History 24, 53–68. https://doi.org/10.1080/00222939000770051

Bolton, B., Fisher, B.L., 2008. Afrotropical ants of the ponerine genera *Centromyrmex* Mayr, *Promyopias* Santschi gen. rev. and *Feroponera* gen. n., with a revised key to genera of African Ponerinae (Hymenoptera: Formicidae). Zootaxa 1929, 1–37. https://doi.org/10.11646/zootaxa.1929.1.1

Bond, J.E., Godwin, R.L., Colby, J.D., Newton, L.G., Zahnle, X.J., Agnarsson, I., Hamilton, C.A., Kuntner, M., 2022. Improving Taxonomic Practices and Enhancing Its Extensibility—An Example from Araneology. Diversity 14, 5. https://doi.org/10.3390/d14010005

Borgmeier, T., 1955. Die Wanderameisen der neotropischen Region. Studia Entomologica 3, 1–720.

Borowiec, M.L., Rabeling, C., Brady, S.G., Fisher, B.L., Schultz, T.R., Ward, P.S., 2019. Compositional heterogeneity and outgroup choice influence the internal phylogeny of the ants. Molecular Phylogenetics and Evolution 134, 111–121. https://doi.org/10.1016/j.ympev.2019.01.024

Borowiec, M.L., Schulz, A., Alpert, G.D., Baňař, P., 2011. Discovery of the worker caste and descriptions of two new species of *Anomalomyrma* (Hymenoptera: Formicidae: Leptanillinae) with unique abdominal morphology. Zootaxa 2810, 1. https://doi.org/10.11646/zootaxa.2810.1.1

Boudinot, B.E., 2015. Contributions to the knowledge of Formicidae (Hymenoptera, Aculeata): a new diagnosis of the family, the first global male-based key to subfamilies, and a treatment of early branching lineages. European Journal of Taxonomy. https://doi.org/10.5852/ejt.2015.120

Boudinot, B.E., Khouri, Z., Richter, A., Griebenow, Z.H., Kamp, T. van de, Perrichot, V., Barden, P., 2022. Evolution and systematics of the Aculeata and kin (Hymenoptera), with emphasis on the ants (Formicoidea: †@@@idae fam. nov., Formicidae). https://doi.org/10.1101/2022.02.20.480183

Boudinot, B.E., Moosdorf, O.T.D., Beutel, R.G., Richter, A., 2021. Anatomy and evolution of the head of *Dorylus helvolus* (Formicidae: Dorylinae): Patterns of sex- and caste-limited traits in

the sausagefly and the driver ant. Journal of Morphology 282, 1616–1658. https://doi.org/10.1002/jmor.21410

Boudinot, B.E., Perrichot, V., Chaul, J.C.M., 2020. †*Camelosphecia* gen. nov., lost ant-wasp intermediates from the mid-Cretaceous (Hymenoptera, Formicoidea). ZooKeys 1005, 21–55. https://doi.org/10.3897/zookeys.1005.57629

Brady, S.G., Fisher, B.L., Schultz, T.R., Ward, P.S., 2014. The rise of army ants and their relatives: diversification of specialized predatory doryline ants. BMC Evolutionary Biology 14, 93. https://doi.org/10.1186/1471-2148-14-93

Branstetter, M.G., Longino, J.T., Ward, P.S., Faircloth, B.C., 2017. Enriching the ant tree of life: enhanced UCE bait set for genome-scale phylogenetics of ants and other Hymenoptera. Methods in Ecology and Evolution 8, 768–776. https://doi.org/10.1111/2041-210X.12742

Brown, W.L., 1975. Contributions toward a reclassification of the Formicidae. V. Ponerinae, tribes Platythyreini, Cerapachyini, Cylindromyrmecini, Acanthostichini, and Aenictogitini. Agriculture (Ithaca, New York) 5, 1–115.

Brown, W.L., 1954. Remarks on the internal phylogeny and subfamily classification of the family Formicidae. Insectes Sociaux 1.

Brown, W.L., Kempf, W.W., 1968. *Tatuidris*, a remarkable new genus of Formicidae (Hymenoptera). Psyche 74, 183–190.

Brown, W.L., Nutting, W.L., 1949. Wing venation and the phylogeny of the Formicidae (Hymenoptera). Transactions of the American Entomological Society (1890-) 75, 113–132.

Brues, C., 1925. *Scyphodon*, an anomalous genus of Hymenoptera of doubtful affinities. Treubia 6, 93–96.

Camacho, G.P., Franco, W., Branstetter, M.G., Pie, M.R., Longino, J.T., Schultz, T.R., Feitosa, R.M., 2022. Uce phylogenomics resolves major relationships among ectaheteromorph ants (Hymenoptera: Formicidae: Ectatomminae, Heteroponerinae): a new classification for the subfamilies and the description of a new genus. Insect Systematics and Diversity 6, 5. https://doi.org/10.1093/isd/ixab026

Collingwood, C.A., Agosti, D., 1996. Formicidae (Insecta: Hymenoptera) of Saudi Arabia (part 2). Fauna of Saudi Arabia 15, 300–385.

Dalla Torre, K.W., 1893. Catalogus Hymenopterorum hucusque descriptorum systematicus et synonymicus. Vol. 7. Formicidae (Heterogyna). W. Engelmann, Leipzig.

Déjean, A., Schatz, B., Orivel, J., Beugnon, G., 1999. Prey capture behavior of *Psalidomyrmex procerus* (Formicidae: Ponerinae), a specialist predator of earthworms (Annelida). Sociobiology 34, 545–554.

Dias, R.K.S., Yamane, S., Akbar, S.A., Peiris, H.A.W.S., Wachkoo, A.A., 2019. Discovery of the worker caste of *Protanilla schoedli* Baroni Urbani & De Andrade (Formicidae: Leptanillinae) in Sri Lanka. Oriental Insects 53, 160–166. https://doi.org/10.1080/00305316.2018.1476273

Dlussky, G.M., 1969. First finding of an ant from the subfamily Leptanillinae (Hymenoptera, Formicidae) in the USSR. Zoologicheskii Zhurnal 48, 1666–1671.

Economo, E.P., Narula, N., Friedman, N.R., Weiser, M.D., Guénard, B., 2018. Macroecology and macroevolution of the latitudinal diversity gradient in ants. Nat Commun 9, 1778. https://doi.org/10.1038/s41467-018-04218-4

Emery, C., 1910. Hymenoptera. Fam. Formicidae. Subfam. Dorylinae. Genera Insectorum 102, 1–34.

Emery, C., 1904. Le affinità del genere Leptanilla e i limiti delle Dorylinae. Archivio Zoologico Italiano 2, 107–116.

Emery, C., 1870. Studi mirmecologici. Bullettino della Società Entomologica Italiana 2, 193–201.

Emery, C., Forel, A., 1879. Catalogue des Formicides d'Europe. Mitteilungen der Schweizerischen Entomologischen Gesellschaft 5, 441–481.

Griebenow, Z., 2020. Delimitation of tribes in the subfamily Leptanillinae (Hymenoptera: Formicidae), with a description of the male of *Protanilla lini* Terayama, 2009. Myrmecological News 30.

Griebenow, Z.H., Isaia, M., Moradmand, M., 2022. A remarkable troglomorphic ant, *Yavnella laventa* sp. nov. (Hymenoptera: Formicidae: Leptanillinae), identified as the first known worker of *Yavnella* Kugler by phylogenomic inference. Invert. Systematics 36, 1118–1138. https://doi.org/10.1071/IS22035

Harris, R.A., 1979. A glossary of surface sculpturing. Occasional Papers in Entomology 28, 1–31.

Hita-Garcia, F., Lieberman, Z., Audisio, T.L., Liu, C., Economo, E.P., 2019. Revision of the highly specialized ant genus *Discothyrea* (Hymenoptera: Formicidae) in the Afrotropics with X-ray microtomography and 3D cybertaxonomy. Insect Systematics and Diversity 3, 5. https://doi.org/10.1093/isd/ixz015

Hölldobler, B., Palmer, J.M., Masuko, K., Brown, W.L., 1989. New exocrine glands in the legionary ants of the genus *Leptanilla* (Hymenoptera, Formicidae, Leptanillinae). Zoomorphology 108, 255–261. https://doi.org/10.1007/BF00312158

Hölldobler, B., Wilson, E.O., 1990. The Ants. Harvard University Press.

Hsu, P.-W., Hsu, F.-C., Hsiao, Y., Lin, C.-C., 2017. Taxonomic notes on the genus *Protanilla* (Hymenoptera: Formicidae: Leptanillinae) from Taiwan. Zootaxa 4268, 117–130. https://doi.org/10.11646/zootaxa.4268.1.7

Imai, H.T., Kihara, A., Kondoh, M., Kubota, M., Kuribayashi, S., Ogata, K., Onoyama, K., Taylor, R.W., Terayama, M., Yoshimura, M., Ugawa, Y., 2003. Ants of Japan. Gakken, Tokyo.

Ito, F., Billen, J., 1998. Larval hemolymph feeding and oophagy: behavior of queen and workers in the primitive ponerine ant *Prionopelta kraepelini* (Hymenoptera, Formicidae) 128, 201–209.

Ito, F., Hashim, R., Mizuno, R., Billen, J., 2022. Notes on the biology of *Protanilla* sp. (Hymenoptera, Formicidae) collected in Ulu Gombak, Peninsular Malaysia. Insect. Soc. 69, 13–18. https://doi.org/10.1007/s00040-021-00839-z

Ito, F., Yamane, S., 2020. Behavior of the queen of *Leptanilla clypeata* Yamane et Ito collected in the Bogor Botanical Gardens, West Java, Indonesia (Hymenoptera; Formicidae), with a note

on colony composition and a description of the ergatoid queen. https://doi.org/10.20362/AM.012004

Jacquemin, J., Delsinne, T., Maraun, M., Leponce, M., 2014. Trophic ecology of the armadillo ant, *Tatuidris tatusia*, assessed by stable isotopes and behavioral observations. Journal of Insect Science 14, 108. https://doi.org/10.1093/jis/14.1.108

Katayama, M., Tsuji, K., 2011. Notes on prey menu of *Protanilla lini* in Okinawa Island. Ari 31, 17–20.

Kugler, J., 1987. The Leptanillinae (Hymenoptera: Formicidae) of Israel and a description of a new species from India. Israel Journal of Entomology 20, 45–57.

Kutter, H., 1948. Beitrag zur Kenntnis der Leptanillinae (Hym. Formicidae). Eine neue Ameisengattung aus Süd-Indien. Mitteilungen der Schweizerischen Entomologischen Gesellschaft 21, 286–295.

Lévieux, J., 1983. A comparison of the ground dwelling ant populations between a Guinea savanna and an evergreen rain forest of the Ivory Coast, in: The Biology Of Social Insects. CRC Press.

Lieberman, Z.E., Billen, J., van de Kamp, T., Boudinot, B.E., 2022. The ant abdomen: the skeletomuscular and soft tissue anatomy of *Amblyopone australis* workers (Hymenoptera: Formicidae). Journal of Morphology 283, 693–770. https://doi.org/10.1002/jmor.21471

Liu, S.-P., Richter, A., Stoessel, A., Beutel, R.G., 2019. The mesosomal anatomy of *Myrmecia nigrocincta* workers and evolutionary transformations in Formicidae (Hymenoptera). Arthropod Systematics & Phylogeny 77, 1–19.

López, F., Martinez, M.D., Barandica, J.M., 1994. Four new species of the genus *Leptanilla* (Hymenoptera: Formicidae) from Spain - relationships to other species and ecological issues 24, 179–212.

Man, P., Ran, H., Zhilin Chen, Zhenghui Xu, 2017. The northern-most record of Leptanillinae in China with description of *Protanilla beijingensis* sp. nov. (Hymenoptera: Formicidae). https://doi.org/10.20362/AM.009008

Mason, W.R.M., 1986. Standard drawing conventions and definitions for venational and other features of wings of Hymenoptera. Proceedings of the Entomological Society of Washington 88, 1–7.

Masuko, K., 2019. Larval hemolymph feeding and hemolymph taps in the ant *Proceratium itoi* (Hymenoptera: Formicidae). Myrmecological News 29.

Masuko, K., 1990. Behavior and ecology of the enigmatic ant *Leptanilla japonica* Baroni Urbani (Hymenoptera: Formicidae: Leptanillinae). Ins. Soc 37, 31–57. https://doi.org/10.1007/BF02223813

Masuko, K., 1989. Larval hemolymph feeding in the ant *Leptanilla japonica* by use of a specialized duct organ, the “larval hemolymph tap” (Hymenoptera: Formicidae). Behav Ecol Sociobiol 24, 127–132. https://doi.org/10.1007/BF00299644

Ogata, K., 1991. A generic synopsis of the poneroid complex of the family Formicidae (Hymenoptera). Part II. Subfamily Myrmicinae. Bulletin of the Institute of Tropical Agriculture Kyushu University 14, 61–149.

Ogata, K., Terayama, M., Masuko, K., 1995. The ant genus *Leptanilla*: discovery of the worker-associated male of L. japonica, and a description of a new species from Taiwan (Hymenoptera: Formicidae: Leptanillinae). Systematic Entomology 20, 27–34. https://doi.org/10.1111/j.1365-3113.1995.tb00081.x

Petersen, B., 1968. Some novelties in presumed males of the Leptanillinae (Hym., Formicidae). Entomologiske Meddelelser 36, 577–598.

Richter, A., Boudinot, B., Yamamoto, S., Katzke, J., Beutel, R.G., 2022. The first reconstruction of the head anatomy of a Cretaceous insect, †*Gerontoformica gracilis* (Hymenoptera: Formicidae), and the early evolution of ants. Insect Systematics and Diversity 6, 4. https://doi.org/10.1093/isd/ixac013

Richter, A., Garcia, F.H., Keller, R.A., Billen, J., Katzke, J., Boudinot, B.E., Economo, E.P., Beutel, R.G., 2021. The head anatomy of *Protanilla lini* (Hymenoptera: Formicidae: Leptanillinae), with a hypothesis of their mandibular movement. Myrmecological News 31, 85–114. https://doi.org/10.25849/myrmecol.news_031:085

Robertson, H.G., 2000. Formicidae (Hymenoptera: Vespoidea). Daures-biodiversity of the Brandberg Massif, Namibia. Cimbebasia Memoir 9, 371–382.

Romiguier, J., Borowiec, M.L., Weyna, A., Helleu, Q., Loire, E., La Mendola, C., Rabeling, C., Fisher, B.L., Ward, P.S., Keller, L., 2022. Ant phylogenomics reveals a natural selection hotspot preceding the origin of complex eusociality. Current Biology 32, 2942-2947.e4. https://doi.org/10.1016/j.cub.2022.05.001

Santschi, F., 1908. Nouvelles fourmis de l'Afrique du Nord (Égypte, Canaries, Tunisie). Annales de la Société Entomologique de France 77, 517–534.

Santschi, F., 1907. Fourmis de Tunisie capturées en 1906. Revue Suisse de Zoologie 15, 305–334.

Saroj, S., Arnab Mandi, Dubey, A.K., 2022. A new species of the rare ant genus, *Leptanilla* Emery (Hymenoptera: Formicidae) from Eastern Himalaya, India. https://doi.org/10.20362/AM.015005

Schmidt, C., 2013. Molecular phylogenetics of ponerine ants (Hymenoptera: Formicidae: Ponerinae). Zootaxa 3647, 201. https://doi.org/10.11646/zootaxa.3647.2.1

Schulmeister, S., 2003. Genitalia and terminal abdominal segments of male basal Hymenoptera (Insecta): morphology and evolution. Organisms Diversity & Evolution 3, 253–279. https://doi.org/10.1078/1439-6092-00078

Simpson, G.G., 1961. Principles of Animal Taxonomy. Columbia University Press, New York.

Smith, M.R., 1953. A new species of *Probolomyrmex*, and the first description of a *Probolomyrmex* male (Hymenoptera, Formicidae). Journal of the New York Entomological Society 61, 127–129.

Taylor, R.W., 1979. Notes on the Russian endemic ant genus *Aulacopone* Arnoldi (Hymenoptera: Formicidae). Psyche: A Journal of Entomology 86, 353–361. https://doi.org/10.1155/1979/65643

Taylor, R.W., 1965. A monographic revision of the rare tropicopolitan ant genus *Probolomyrmex*. Transactions of the Royal Entomological Society of London 117, 345–365.

Terayama, M., 2013. Additions to knowledge of the ant fauna of Japan (Hymenoptera; Formicidae). Memoirs of the Myrmecological Society of Japan 3, 1–24.

Terayama, M., Kinomura, K., 2015. Rediscovery of *Leptanilla kubotai* Baroni Urbani (Hymenoptera: Formicidae) from Kochi Prefecture, Japan, with a description of queen. Ari 37, 17–22.

Tobias, J.A., Seddon, N., Spottiswoode, C.N., Pilgrim, J.D., Fishpool, L.D.C., Collar, N.J., 2010. Quantitative criteria for species delimitation. Ibis 152, 724–746. https://doi.org/10.1111/j.1474-919X.2010.01051.x

Ward, P.S., 2007. Phylogeny, classification, and species-level taxonomy of ants (Hymenoptera: Formicidae). Zootaxa 1668, 549–563. https://doi.org/10.11646/zootaxa.1668.1.26

Ward, P.S., Boudinot, B.E., 2021. Grappling with homoplasy: taxonomic refinements and reassignments in the ant genera *Camponotus* and *Colobopsis* (Hymenoptera: Formicidae). Arthropod Systematics & Phylogeny 79. https://doi.org/10.3897/asp.79.e66978

Ward, P.S., Branstetter, M.G., 2022. Species paraphyly and social parasitism: phylogenomics, morphology, and geography clarify the evolution of the *Pseudomyrmex elongatulus* group (Hymenoptera: Formicidae), a Mesoamerican ant clade. Insect Systematics and Diversity 6, 4. https://doi.org/10.1093/isd/ixab025

Ward, P.S., Fisher, B.L., 2016. Tales of dracula ants: the evolutionary history of the ant subfamily Amblyoponinae (Hymenoptera: Formicidae). Systematic Entomology 41, 683–693. https://doi.org/10.1111/syen.12186

Wheeler, G.C., 1928. The larva of *Leptanilla*. Psyche 38, 85–91.

Wheeler, G.C., Wheeler, J., 1988. The larva of *Leptanilla japonica*, with notes on the genus (Hymenoptera: Formicidae: Leptanillinae) 95, 185–189.

Wheeler, G.C., Wheeler, J., 1986. Ten-year supplement to “Ant larvae: review and synthesis”. Proceedings of the Entomological Society of Washington 88, 684–702.

Wheeler, G.C., Wheeler, J., 1976. Ant larvae: review and synthesis. Proceedings of The Entomological Society of Washington 7, 1–108.

Wheeler, G.C., Wheeler, J., 1965. The ant larvae of the subfamily Leptanillinae (Hymenoptera, Formicidae). Psyche 72, 24–34.

Wheeler, G.C., Wheeler, J., 1930. Two new ants from Java. Psyche 37, 193–201.

Wheeler, W.M., 1932. An Australian *Leptanilla*. Psyche 39, 53–58.

Wheeler, W.M., 1923. Social life among the insects. Harcourt, Brace and Co., New York.

Wheeler, W.M., 1918. A study of some ant larvæ, with a consideration of the origin and meaning of the social habit among insects. Proceedings of the American Philosophical Society 57, 293–343.

Whitmore, T.C., 1988. Tropical rainforests of the Far East, 2nd ed. Clarendon Press, Oxford.

Xu, Z.-H., 2002. A systematic study on the ant subfamily Leptanillinae of China (Hymenoptera: Formicidae). Acta Entomologica Sinica 45, 115–120.

Yamada, A., Nguyen, D.D., Eguchi, K., 2020. Unveiling the morphology of the Oriental rare monotypic ant genus *Opamyrma* Yamane, Bui & Eguchi, 2008 (Hymenoptera: Formicidae: Leptanillinae) and its evolutionary implications, with first descriptions of the male, larva, tentorium, and sting apparatus. Myrmecological News 30, 111–124.

Yamamuro, K., 2018. Biological notes of *Protanilla lini* (Formicidae, Leptanillinae) in captivity. Tsunekibachi 32, 19–24.

Yamane, S., Bui, T.V., Eguchi, K., 2008. *Opamyrma hungvuong*, a new genus and species of ant related to *Apomyrma* (Hymenoptera: Formicidae: Amblyoponinae). Zootaxa 1767, 55. https://doi.org/10.11646/zootaxa.1767.1.3

Yoder, M.J., Mikó, I., Seltmann, K.C., Bertone, M.A., Deans, A.R., 2010. A gross anatomy ontology for Hymenoptera. PLOS ONE 5, e15991. https://doi.org/10.1371/journal.pone.0015991

Chapter 5. **Phylogenomics and Bayesian total-evidence inference reveal a robust phylogeny of the ant subfamily Leptanillinae (Hymenoptera: Formicidae)**

Abstract. Ants of the subfamily Leptanillinae (Hymenoptera: Formicidae) are minute and subterranean, with taxonomy impeded by the dissociation of disparate male and female forms. The advent of phylogenomic inference can remedy this dissociation while resolving leptanilline phylogeny with strong statistical support. However, the few phylogenomic studies so far to investigate the phylogeny of the Leptanillinae did not accommodate the risk of systematic bias in genome-scale molecular data, which may result in decisive statistical support for erroneous conclusions. Mitigation of these biases requires curation of genome-scale molecular data under a variety of different regimes. Here, I present the results of phylogenomic inference focused on the Leptanillinae from ultra-conserved elements (UCEs), using both Bayesian and frequentist methods, along with a coalescent-based approach. All analyses were replicated with several UCE alignments curated to compensate for potential systematic biases. In addition, I implemented Bayesian total-evidence inference from a reduced UCE alignment and male morphological data to resolve the phylogenetic position of the monotypic genus *Scyphodon* and three other terminals for which molecular data are unavailable: *Leptanilla palauensis* (Smith), *Leptanilla astylina* Petersen, and *Leptanilla* ci01. The phylogeny of the Leptanillinae here inferred is robust to compositional heterogeneity and gene-tree discordance. Previous concurrence on the basal topology of *Protanilla* with strong statistical support is here shown to probably be the result of systematic bias. The novel association in this phylogeny of *Leptanilla havilandi* Forel and *Leptanilla thai* Baroni Urbani with *Noonilla* and *Yavnella*, respectively, supports the synonymy

of those genera with *Leptanilla*; while Bayesian total-evidence inference places *Scyphodon* within *Noonilla*, and thus within *Leptanilla.*

1. Introduction

The subfamily Leptanillinae (Hymenoptera: Formicidae) consists of minute, rarely collected subterranean ants that are restricted to tropical and warm temperate regions of the Old World. All leptanillines for which behavior has been observed in the wild appear to be specialist predators of centipedes (Chilopoda: Geophilomorpha) (Hsu et al., 2017; Masuko, 1990) or forcepstails (Hexapoda: Diplura: Japygidae) (Ito et al., 2022), with larval morphology that is highly specialized (Barandica et al., 1994). The behavior of *Leptanilla* is derived in other respects, including cyclical brood production and adult feeding on larval hemolymph (Masuko, 1990). Seventy valid species are described in the Leptanillinae, in three genera (Chapter 4), but the spectacular variety of undescribed morphospecies known from male specimens across the Indo-Malayan ecoregion hints at considerable unknown species-richness.

The Leptanillinae were long regarded as akin to the legionary ants of the subfamily Dorylinae (e.g., Hölldobler and Wilson, 1990) or to *Apomyrma* (Apomyrminae) (Bolton 1990, 2003), due to behavioral and morphological resemblance. Both these hypothesized relationships were refuted by phylogenetic inference from molecular data, which consistently recovered the Leptanillinae as sister to most of the remaining Formicidae (Borowiec et al., 2019; Kück et al., 2011; Lucky et al., 2013; Moreau and Bell, 2013; Rabeling et al., 2008; Romiguier et al., 2022; Ward and Fisher, 2016). Comprehending the origins and evolution of the Leptanillinae may therefore inform our understanding of the evolution of the entire Antennoclypeata (Boudinot et al., 2022)—i.e., crown-group Formicidae, which was the only clade within the Formicoidea to

survive the K-Pg mass extinction. Of themselves, *Leptanilla* (i.e., the Leptanillini *sensu* Bolton) are remarkable for extreme derivation of male genital skeletomusculature, relative both to other leptanillines, and to the whole of the ants. Scleritic derivations in the male genitalia of *Leptanilla* are in some cases not only unique among the Formicidae, but without known parallels among the Hymenoptera: e.g., independent losses of the volsellae (the *Leptanilla najaphalla* species-group and *Leptanilla bethyloides* species-group); independent tergosternal fusions of abdominal segment IX (the *Leptanilla thai* species-group and *Leptanilla astylina* Petersen); and median fusion of the gonostyli (a single undescribed morphospecies in the *Leptanilla havilandi* species-group) (Chapters 3-4). This panoply is paralleled among other ant clades that show conspicuously diverse male genitalia (e.g., *Leptomyrmex*; Dolichoderinae: Leptomyrmecini) (Barden et al., 2017), but the sheer scale of innovation in male genital skeletomusculature in the Leptanillinae relative to those lineages is unexplained.

Understanding the evolution of the Leptanillinae requires a firm grasp of their phylogeny, and zoological nomenclature that reflects this phylogeny. All studies to infer the internal phylogeny of the Leptanillinae revealed a need to revise higher taxa towards conformity with actual evolutionary relationships among these ants, with taxonomy long suffering from artificiality due to the dissociation of the strongly divergent male and worker phenotypes, resulting in the description of multiple genera based only on male specimens (Bolton, 1990) and disconnected from knowledge of worker forms. These males are sometimes so derived as to be scarcely recognizable as ants (Petersen, 1968). Of those genera established solely based on male material, *Noonilla* Petersen and *Yavnella* Kugler were confirmed to be reciprocally monophyletic based on phylogenomic inference (Griebenow, 2020; Griebenow et al., 2022), but molecular data are unavailable for *Scyphodon* Brues. The assignment of this “strange hymenopteran” (Brues, 1925:

p. 93) to the Formicidae has in the past been controversial (Boudinot, 2015; Brues, 1925; Ogata et al., 1995; Petersen, 1968). *Phaulomyrma* Wheeler & Wheeler, monotypic and known only from male specimens, was confidently synonymized with *Leptanilla* based on the results of Bayesian total-evidence inference (Chapter 1). Molecular data are also unavailable for *Leptanilla palauensis* (Smith), which Petersen (1968) argued bore little resemblance to any other Leptanillinae and perhaps warranted assignment to its own genus, a contention so far unexamined.

A classification of the Leptanillinae that reflects evolutionary relationships must be informed by the disparate respective phenotypes of male and worker, with the aim of delimiting higher taxa that are both monophyletic and uniformly diagnosable based on both workers and males. The advent of an ultra-conserved element (UCE) probe set optimized for the Formicidae (Branstetter et al., 2017) enabled the incorporation of dissociated leptanilline ants into the same inferential schema with molecular data of an unprecedented scale, resulting in the first definitive identification of the male of a described *Protanilla* sp. (Griebenow, 2020) and the discovery of a worker referrable to *Yavnella* (Chapter 2). Phylogenomic inference in these two studies offered a strongly supported rendition of leptanilline phylogeny under both maximum-likelihood (ML) and Bayesian frameworks, and was congruent between the two studies despite differences in taxon sampling. This phylogeny was corroborated by Bayesian total-evidence inference involving an expanded version of the alignment from Borowiec et al. (2019) (Chapter 1), providing a seemingly strong scaffold on which to base systematic revision of the Leptanillinae.

The vast informational content of phylogenomic data obviates the risk of stochastic error for phylogenetic inference. However, this same vastness exacerbates systematic error due to model misfit (Philippe et al., 2005). Common assumptions of model-based phylogenetic inference

violated by empirical data include phylogenetic concordance among genes (Maddison, 1997; Mirarab et al., 2014); compositional homogeneity in the data (Jermiin et al., 2004; Romiguier et al., 2016, 2013); and lack of heterotachy in evolutionary rate. Heterogeneity in base composition is especially concerning for the Leptanillinae, which display pronounced differences in AT-richness according to subclade (Borowiec et al., 2019).

Violation of compositional heterogeneity and other model assumptions may co-occur in given data and are correlated with systematic error in phylogenomic inference—but that error is unacknowledged by prevalent measures of phylogenetic confidence. The decisive statistical support for phylogenies inferred from genome-scale data may therefore disguise falsehood (Thomson and Brown, 2022), especially in the case of non-parametric statistics (Vasilikopoulos et al., 2020) such as bootstrapping, which is commonly used in phylogenomic inference under a frequentist framework.

Even with the identification of optimal phylogenetic models for loci, phylogenomic inference cannot escape limitations to the informational content of those loci. Slow-evolving loci may contain little to no phylogenetic signal (Klopfstein et al., 2017); whereas substitution saturation by rapid evolution is problematic in also evacuating molecular data of phylogenetic signal (Duchêne et al., 2022). In theory, saturation is mitigated for protein-coding loci if one recodes the nucleotides in these loci to amino acids—but such recoding may result in inference incongruent with that from nucleotides if the customarily used amino acid substitution models fit poorly to the data (Gillung et al., 2018). Aside from misspecification of these substitution models, protein-coding loci may reveal phylogenetic signal discordant with that intrinsic to those that do not code for proteins (Blaimer et al., 2023; Chan et al., 2020; Kulkarni et al., 2021;

Reddy et al., 2017), and in theory, are less susceptible to incomplete lineage sorting (ILS), which produces conflicting phylogenetic signal among loci.

To ensure that inference of the phylogeny of the Leptanillinae is robust to these potential model violations, therefore revealing historical signal, I here undertake phylogenomic inference under both frequentist and Bayesian frameworks from a genome-scale dataset containing 75 leptanilline terminals, the most comprehensive sampling for the clade yet published, curating these data with different subsampling regimes to test for the effects of potential biases that could harm accurate phylogenetic inference. In addition, the effects of gene-tree discordance are accommodated by coalescent-based phylogenomic inference. I also implement Bayesian total-evidence inference from a small subset of UCEs jointly with 64 binary male morphological characters, to clarify the phylogenetic position of *Scyphodon* within the Leptanillinae, along with three other enigmatic terminals for which only male morphology is known. Of these, *L. astylina* unquestionably belongs to *Leptanilla s. l.* (Griebenow, 2021), but displays a male genital phenotype divergent from that of all other known members of this clade and thus is difficult to place within that clade. Conversely, the respective generic assignments of *L. palauensis* and *Leptanilla* ci01 are contentious (Smith, 1953; Taylor, 1965; Petersen, 1968; Bolton, 2003) and therefore in need of examination with Bayesian total-evidence inference.

2. Materials & Methods

2.1. Institutional deposition

The specimens newly included in this study are deposited at the following institutions:

MZLU = Lund University, Lund, Sweden

NCUE = National Changhua University of Education, Changhua, ROC

NHMUK = Natural History Museum, London, UK

ROME = Royal Ontario Museum, Toronto, ON, Canada

UCDC = R. M. Bohart Museum of Entomology, Davis, CA, USA

USNM = National Museum of Natural History, Washington, D.C., USA

ZMUC = Zoological Museum, University of Copenhagen, Copenhagen, Denmark

Refer to Griebenow (2020), Chapter 2 and Romiguier et al. (2022) for institutional deposition of specimens included in this study for which sequence data were previously published.

2.2. Taxon sampling

All seven leptanilline genera recognized as valid prior to Chapter 4 were sampled in the phylogenetic analyses presented in this study, whether in the form of molecular data only (as for *Anomalomyrma*), morphological data only (as for *Scyphodon*), or both. To ensure diagnostic utility across both worker and male specimens, and for intelligible communication of phylogenetic information by formal taxonomy, Chapter 4 synonymizes the Anomalomyrmini with the Leptanillini, while erecting the Opamyrmini for the monotypic sister genus to the remaining Leptanillini *sensu lato*. That classification conforms to the results presented here, with the monophyletic Anomalomyrmini being hereinafter prefixed with "former". Chapter 4 also synonymizes *Anomalomyrma* Taylor in Bolton with *Protanilla* Taylor in Bolton: *Protanilla s. str.* hereinafter refers to the *Protanilla rafflesi* species-group, the *Protanilla bicolor* species-group, and *Protanilla* zhg-th02, all together; while the *Protanilla taylori* species-group corresponds to the former genus *Anomalomyrma* (Chapter 4). Lastly, with consideration of the phylogenomic and total-evidence Bayesian results here presented and informed by taxonomic

utility, Chapter 4 synonymizes *Scyphodon*, *Noonilla*, and *Yavnella* with *Leptanilla*; that classification is followed in this study. Discrepancy in provisional morphospecies identifiers with those used in previous studies, along with alignments and raw output phylogenies presented here, are resolved by concordances in Table 5.1.

Current identifier	**Alignment identifier**
Protanilla boltoni	*Anomalomyrma boltoni*
Leptanilla acherontia	*Leptanilla* UG01
Leptanilla najaphalla	*Leptanilla* zhg-my02
Leptanilla cf. *copiosa*	*Noonilla* cf. *copiosa*
Leptanilla zhg-my10	*Noonilla* zhg-my01
Leptanilla zhg-my11	*Noonilla* zhg-my02
Leptanilla zhg-my14	*Noonilla* zhg-my06
Protanilla wallacei	*Protanilla* MY01
Leptanilla anomala	*Scyphodon anomalum*
Leptanilla argamani	*Yavnella argamani*
Leptanilla zhg-mm14	*Yavnella* indet.
Leptanilla laventa	*Yavnella laventa*
Leptanilla MM01	*Yavnella* MM01
Leptanilla nr. *indica*	*Yavnella* nr. *indica*
Leptanilla TH02	*Yavnella* TH02
Leptanilla TH03	*Yavnella* TH03
Leptanilla TH04	*Yavnella* TH04
Leptanilla TH06	*Yavnella* TH06
Leptanilla TH08	*Yavnella* TH08
Leptanilla zhg-bt03	*Yavnella* zhg-bt01
Leptanilla zhg-my16	*Yavnella* zhg-my01
Leptanilla zhg-th02	*Yavnella* zhg-th01
Leptanilla zhg-th04	*Yavnella* zhg-th03
Leptanilla zhg-th05	*Yavnella* zhg-th04

Table 5.1. Concordance of binomials and morphospecies identifiers for which there is a discrepancy between the name used in the text, figures, and tables ("Current identifier"), and that used in input alignments, raw output, and supplemental tables ("Alignment identifier").

Ultra-conserved elements (UCEs) were enriched for 75 exemplars of the Leptanillinae, representing all major clades recognized in Chapter 4. All these clades were represented by multiple exemplars, except for the *Protanilla taylori* species-group (the former *Anomalomyrma*),

which was represented only by *Protanilla boltoni* (Borowiec et al.). Given the multiple morphological synapomorphies of the rather depauperate *Protanilla taylori* species-group, there is no reason to doubt the monophyly of these ants, and so *P. boltoni* may serve as stand-in for the phylogenetic position of that clade.

All the major lineages of the Poneroformicines (Boudinot et al., 2022) except the Dorylinae are represented by the seven ant outgroups to the Leptanillinae; *Martialis heureka* Rabeling *et al.* (Martialinae), a lineage which together with the Leptanillinae comprises the Leptanillomorpha (Richter et al., 2021), is also included among those seven outgroups. Two outgroups are included from outside the Formicidae, representing the Apoidea (Ampulicidae: *Ampulex compressa* [Fab.]) and Thynnoidea (Chyphotidae: *Typhoctes peculiaris* [Cresson]). Collection data for all specimens for which UCEs are newly enriched in this study are provided in Tables 4.S1 and 5.S1.

For most putative species or morphospecies, sequence data for only a single exemplar are used here. Three exemplars are included each for *Protanilla lini* Terayama and *Protanilla* zhg-my01, representing as wide a geographical range for both putative species as possible. These were the only putative species in the Leptanillinae for which phylogenomic data from specimens collected across multiple and dispersed localities were used in this study.

Discretized male morphological data were coded for all outgroup terminals and for 61 leptanilline terminals. In some cases, it was necessary to acquire male morphological data from specimens other than those from which UCEs were enriched; collection data for these are included in Table 5.S2. Molecular data were unavailable for four of these: *Leptanilla anomala* (Brues), *L. palauensis*, *L. astylina*, and *Leptanilla* ci01. Morphological data for *L. anomala* were coded from CASENT0106168, a specimen treated as *Leptanilla* cf. *anomala* due to differences

from the type series in the shape of the mandible and the proportions of the metasoma to the genitalia; however, these differences do not affect the coding of discrete male morphological data, meaning that definitively ensuring the conspecificity of CASENT0106168 with *L. anomala* is impertinent to its appropriateness for morphological observations of that species.

2.3. Sequencing

Previously published sequence data are derived from Griebenow (2020), Chapter 2, or Romiguier et al. (2022). For the 25 terminals newly sequenced in this study, DNA was extracted non-destructively using a DNeasy Blood & Tissue Kit (Qiagen Inc., Valencia, CA) either according to manufacturer instructions, or with DNA eluted using buffer AE at 56°C (Cruaud et al*.,* 2019). Genomic concentrations were quantified for each sample with a Qubit 2.0 fluorometer (Life Technologies Inc., Carlsbad, CA). Input DNA was sheared to ~600 bp using either a QSonica Q800R3-110 (Qsonica Inc., Newtown, CT). Sheared product was used as input for the modified library preparation protocol of Branstetter et al. (2017) involving SPRI bead cleanup with a generic substitute (Rohland and Reich, 2012) and custom dual-indexing barcodes (Glenn et al., 2019), with phylogenomic data generated using the ant-specific version of the UCE probe set *hym-v2* (Branstetter et al., 2017). Enrichment success and size-adjusted DNA concentrations of pools were assessed using the SYBR FAST qPCR kit (Kapa Biosystems, Wilmington, MA), and all pools were combined into an equimolar final pool. For eight samples, libraries were prepared and enriched using similar protocols at RAPiD Genomics (Gainesville, FL). Final pools were sequenced on an Illumina HiSeq X at Novogene, Sacramento, CA or at Rapid Genomics LLC, Gainesville, FL. Sequencing protocols for the 59 terminals for which sequence data were published prior to this study can be found in Griebenow (2020), Chapter 2 and Romiguier et al. (2022).

2.4. Contig assembly and alignment

The FASTQ output was demultiplexed and cleansed of adapter contamination and low-quality reads using *illumiprocessor* (Faircloth, 2013) in the PHYLUCE package, v. 1.7.1. Raw reads were assembled with SPAdes v. 3.12.0 (Bankevich et al., 2012). UCEs for the eight terminals derived from Romiguier et al. (2022) were extracted from genomes published in that paper, using *phyluce_probe_slice_sequence_from_genomes* in PHYLUCE (Faircloth, 2016). All PHYLUCE commands hereinafter are cited from Faircloth (2016).

Species-specific contig assemblies were obtained with the ant-specific *hym-v2* probe set (Branstetter et al., 2017) using *phyluce_assembly_match_contigs_to_probes.py* (min_coverage = 80), with min_identity = 90 to minimize the influence of possible contamination; and a list of UCE loci shared across all taxa was generated using *phyluce_assembly_get_match_counts.py*, and separate FASTA files for each locus were created using these outputs. In this study, all loci are necessarily UCEs, and therefore the terms as used here are synonyms. Sequences were aligned separately by locus using MAFFT E-INS-i (Katoh and Toh, 2010) implemented with the command *phyluce_assembly_seqcap_align.py*. These sequences were then trimmed with Gblocks (Castresana, 2000) as implemented by the wrapper script *phyluce_assembly_get_gblocks_trimmed_alignment_from_untrimmed.py* (settings: b1 = 0.5, b2 = 0.5, b3 = 12, b4 = 7). Locus names were removed from taxon labels with *phyluce_align_remove_locus_name_from_files* and the final alignment created by *phyluce_align_get_only_loci_with_min_taxa* with the minimum percentage of taxa represented in each locus being 90%. Within *phyluce_assembly_match_contigs_to_probes.py*, min_identity = 80, resulting in an alignment 283,523 bp long and comprising 490 loci. By-taxon summary statistics for this alignment are provided in Table 5.S3.

2.5. Morphological data

Discrete male morphological data were coded for 70 terminals according to a binary non-additive regime (Pleijel, 1995), resulting in 64 characters, three of which are autapomorphic. This dataset is expanded from that published in Chapter 1, with some corrected observations for terminals that appeared both in Chapter 1 and in this study. Definitions for all male characters are provided below.

1. *Distal procoxal carina*. 0) "Apical prolongations beyond insertion of [pro]trochanters" (Petersen 1968: p. 583) absent, i.e., distal surface of procoxa rounded. 1) Produced transverse carina present on anterodistal margin of coxa, delimiting distinct anterior and distal procoxal faces. (1) is a synapomorphy of the *Leptanilla havilandi* species-group, but more extreme in *Leptanilla copiosa* (Petersen) than observed in other males of this clade.
2. *Protrochanteral length*. 0) Protrochanter sphenoid to subcylindrical, length <2× diameter. 1) Protrochanter an elongate tube, ≥2× diameter (Fig. 4.36) (1) is an autapomorphy of *Leptanilla* ci01.
3. *Ventromedial protibial margins carinate*. As in Griebenow (2021: pp. 606-607), "mesal protibial margin carinate".
4. *Profemoral medial surface*. 0) medial profemoral face convex to flattened. 1) Arcuate carina present on medial face. (1) is an autapomorphy of *Leptanilla* ci01 (Fig. 4.36).
5. *Profemoral venter.* 0) Without any processes. 1) With apicolateral cuticular hook.
6. *Protibial comb.* 0) protibia without ventromedial comb consisting of lamellate cuticular extensions. 1) ventromedial comb present on protibia. (1) is an autapomorphy of the

Leptanilla najaphalla species-group. Griebenow (2021: p. 607) misinterpreted modified setae as comprising the protibial comb.

7. *Head breadth*. 0) Head inclusive of compound eyes narrower than long. 1) Head inclusive of compound eyes broader than long.
8. *Clypeal length*. 0) medial anteroposterior length of clypeus equal to or less than diameter of torulus. 1) medial anteroposterior length of clypeus greater than diameter of torulus.
9. *Median clypeal condition*. 0) Clypeus anteroposteriorly compressed to the point of being indiscernible in full-face view, or distinct in full-face view but lacking median furrow. 1) Median clypeal furrow present, with indistinct margins, not intersecting the epistomal sulcus or anterior clypeal margin.
10. *Anterior tentorial pit.* 0) Anterior tentorial pit situated fully anterolaterad the antennal torulus. 1) Anterior tentorial pit situated directly anterad antennal torulus, in whole or in part.
11. *Medial mandibular margin*. 0) Only one apparent face on the medial mandibular margin (Richter et al. 2021: fig. 13B). 1) Basal and masticatory faces distinct on the medial mandibular margin (Richter et al. 2021: fig. 13A). (1) is a synapomorphy of the Poneroformicines (Boudinot et al., 2022).
12. *Mandalus length*. 1) proximodistal length of mandalus >0.5 length of mandible. 0) proximodistal length of mandalus ≤0.5 the length of the mandible.
13. *Mandible length.* 0) scape shorter than mandible. 1) scape longer than mandible, or scape and mandible length equal. (0) is symplesiomorphic for the Aculeata, with the alternative therefore being a derived condition of the Formicidae, with an autapomorphic secondary reversal in *Leptanilla anomala* (Brues, 1925: fig. 1A).

14. *Antennomere 3*. 0) length of antennomere 3 equal to, or less than, that of the scape. 1) length of antennomere 3 greater than that of the scape.
15. *Mandibular articulation*. 0) Mandible fused to gena. 1) Mandible articulated to gena.
16. *Cranial vertex*. 0) in dorsal view, cranial vertex entire to slightly emarginate. 1) in dorsal view, cranial vertex strongly emarginate.
17. *Mesosomal proportions.* 0) mesosoma not dorsoventrally compressed, length of pronotum in profile view ≤2× length of anepimeron measured anteroposteriorly across subalar area (Fig. 1.49A). 1) mesosoma usually dorsoventrally compressed, with the pronotum as measured in profile view from the anterior margin to pronotal-mesopectal suture extending >2× length of anepimeron measured anteroposteriorly across subalar area (Fig. 1.49B-C). This character undoubtedly represents a continuum across the Hymenoptera but is bimodal in the Leptanillinae.
18. *Mesoscutal profile*. 0) Mesoscutal outline planar or shallowly vaulted in profile view, with pronotum and mesoscutum therefore intersecting in profile view to form an anterior continuous curve or protruding angle (Fig. 1.10B). 1) Mesoscutal outline either vaulted in profile view or bulging anteriorly to overhang pronotum, in the latter case with intersection of pronotum and mesoscutum in profile view forming an excavated angle (Fig. 1.10A).
19. *Antero-admedian signum.* 0) no trace of a median impression on the anterior mesoscutum. 1) antero-admedian signum present as a sclerotized signum (Fig. 4.2B) or sculptured sulcus.
20. *Notauli*. 0) Notauli absent. 1) Notauli present.

21. *Parapsidal signa.* 0) Parapsidal signa absent. 1) Parapsidal signa present, distinctly impressed or not.
22. *Oblique mesopleural sulcus.* 0) oblique mesopleural sulcus absent, or present, but not adjoining metapectal-propodeal complex. 1) Oblique mesopleural sulcus adjoining metapectal-propodeal complex.
23. *Pterostigma.* 0) Pterostigma absent, sometimes with infuscation at confluence of Rf and *2s-rs*+Rs+4-6. 1) Pterostigma present.
24. 2s-rs+*Rsf4-6.* 0) *2s-rs*+Rsf4-6 absent (Baroni Urbani, 1977: fig. 44). 1) *2s-rs* and Rsf4-6 present, only delimited from one another if Rs+M or Rsf3 is present (Fig. 4.13A). In the Leptanillini, *2s-rs*+Rsf4-6 comprise an arc superficially resembling the so-called post-marginal vein observed in the Ceraphronoidea, Platygastroidea, and Chalcidoidea.
25. *M+Cu.* 0) M+Cu absent, with therefore no closed cells in the forewing (Fig. 4.20). 1) M+Cu present, unequivocally so when 1A occurs in conjunction with M+Cu (Fig. 4.12A-B), or a remnant abscissa of M+Cu demarcating the junction of *cu-a* and Mf1. In the former Anomalomyrmini and the *Leptanilla thai* species-group, there is only a single closed cell posterad Sc+R+Rs (Chapter 4.12D); the posterior vein delimiting that cell may be homologous with M+Cu, 1A, or both. Following Boudinot (2015: fig. 4F), I here consider the vein in these cases to be M+Cu.
26. *1A.* 0) 1A absent. If single closed cell posterad Sc+R+Rs (Fig. 4.12D), 1A is stipulated as absent (Boudinot 2015: fig. 4F). 1) 1A present. This is unequivocal when M+Cu occurs in conjunction with 1A.
27. *C.* 0) C absent. If single tubular vein is present along the costal margin, this is stipulated as Sc+R+Rs (Fig. 4.12D). 1) C present (Fig. 4.12A-C).

28. *Spectral M+Cu*. 0) No spectral extension of M+Cu distad *cu-a*, or distal disconnected fold thereof, is observed. 1) Isolated spectral longitudinal vein is present in distal remigium (Fig. 4.12C). This appears to be an adventitious extension of M+Cu given a lack of secondary homology (de Pinna 1991) with that vein.
29. *Rs+M*. 0) Rs+M spectral (Fig. 1.14B) to absent. 1) Rs+M tubular or nebulous.
30. 1m-cu. 0) *1m-cu* spectral to absent. 1) Tubular or nebulous.
31. *1A*. 0) 1A absent. 1) 1A present.
32. *Mesoscutellar vestiture.* 0) Mesoscutellum with sparse setae. 1) Mesoscutellum with dense, pubescent vestiture.
33. *Mesoscutellar profile*. 0) Mesoscutellar disc not projecting posteriorly in profile view. 1) Mesoscutellar disc projecting posteriorly as a process, either cuneiform or recurved.
34. *Upper metapleuron*. 0) Upper metapleuron indistinguishably fused to the propodeum. 1) 1) Upper metapectal-propodeal boundary distinct, either as suture or sulcus.
35. *Lower metapleuron.* 0) Lower metapleuron indistinguishably fused to the propodeum, although faint sulcus may appear ventrad the propodeal spiracle (e.g., *Leptanilla copiosa*). 1) Lower metapleuron with metapectal-propodeal boundary ventrad the propodeal spiracle marked as suture or sulcus.
36. *Propodeal dorsolateral carina.* 1) Posterodorsal face of propodeum laterally delimited from pleural propodeal surface by distinct carina. 0) Posterodorsal face of propodeum not distinct from pleural propodeal surface, or distinct but without delimitation by lateral carina.
37. *Propodeal profile.* 0) Propodeum convex in profile view (Fig. 1.17C) or produced into a right angle, with largely planar dorsal and posterior faces (Fig. 1.17B). 1) Propodeum

concave in profile view, sometimes only so immediately posteroventrad the metanotum (e.g., *Leptomyrmex ruficeps* Emery).

38. *Tergosternal condition of abdominal segment II.* 0) Abdominal segment II without tergosternal fusion or only partial tergosternal fusion. 1) Abdominal segment II with tergosternal fusion. Complete tergosternal fusion was observed in all Leptanillini and in *T. peculiaris*. Tergosternal condition in other exemplars was coded from the literature as follows: for the Poneroformicines, Bolton (2003); *A. compressa* Vilhelmsen et al. (2010); *M. heureka*, Boudinot (2015); and for *O. hungvuong*, Yamada et al. (2020).
39. *Lateral longitudinal carina of petiole.* 0) Petiolar venter not delimited by lateral longitudinal carina, and abdominal segment II with or without tergosternal fusion. 1) Lateral longitudinal carina laterally delimiting the petiolar venter. It is unclear based on existing taxon sampling if this lateral longitudinal carina corresponds to a tergosternal suture in any exemplar. If so, this would result in the logical dependence of this character on tergosternal fusion of abdominal segment II—diminishing severity of test (Brazeau, 2011).
40. *Abdominal tergite II.* 0) Abdominal tergite II without dorsal node. 1) Shallow to pronounced dorsal node present on abdominal tergite II.
41. *Abdominal sternite II*. 0) Abdominal sternite II without any ventral process. 1) Abdominal sternite II with ventral process, angular to rounded, with both distinct anterior and posterior faces.
42. *Dorsal outline of abdominal segment II.* 0) Breadth of petiolar node subequal to, or less than, length of petiole excluding presclerites. 1) Breadth of petiolar node exceeds length in dorsal view, excluding presclerites.

43. *Profile of abdominal segment II.* 0) Anteroposterior length of abdominal segment II including presclerites less than, or equal to, height of abdominal segment II measured in profile view. 1) Anteroposterior length of abdominal segment II including presclerites greater than height of abdominal segment II measured in profile view.
44. *Abdominal segment III.* 0) Abdominal segment III without cinctus. 1) Abdominal segment III with cinctus (i.e., abdominal segment III petiolate).
45. *Abdominal segment IV.* Abdominal segment IV without cinctus. 1) Abdominal segment IV with cinctus (i.e., abdominal segment IV petiolate).
46. *Posteromedian margin of abdominal sternite IX.* 0) Posteromedian margin of abdominal sternite IX entire or emarginate. 1) Posteromedian margin of abdominal sternite IX with subtriangular process. The filiform posteromedian process observed in *Leptanilla* TH03 at the ventral apex of the metasoma was coded in Chapter 1 as an extension of abdominal sternite IX, but this cannot be confirmed without dissection (Chapter 3). The condition of the posteromedian process of abdominal sternite IX in *Leptanilla* TH03 is therefore here coded as unknown.
47. *Posterolateral margins of abdominal sternite IX.* 0) Mulceators absent. 1) Mulceators present.
48. *Abdominal tergite VIII.* 0) Length of abdominal tergite VIII subequal to, or greater than, breadth of abdominal tergite VIII in dorsal view. 1) Length of abdominal tergite VIII less than breadth of abdominal tergite VIII in dorsal view.
49. *Abdominal tergites X-XI.* 0) Cerci absent. 1) Cerci present. Following Boudinot (2015), cerci are assumed to be absent (0) in the Leptanillomorpha even if not verified by dissection. This character state was confirmed in all exemplars of the Leptanillinae for

which volumetric reconstructions are provided in Chapter 3. Condition of the cerci in *O. hungvuong* was coded from Yamada et al. (2020). Presence of the cerci (1) was assessed by dissection in most outgroups to the Leptanillomorpha or, in the case of some Poneroformicine outgroups, derived from Bolton (2003).

50. *Gonocoxital venter*. 0) Gonocoxites with partial ventromedian fusion, or lacking any such fusion. 1) Gonocoxites with ventromedian fusion along entire length.
51. *Gonocoxites dorsum*. 0) Gonocoxites with partial dorsomedian fusion, or lacking any such fusion. 1) Gonocoxites with ventromedian fusion along entire length.
52. *Apicoventral gonocoxital margin*. 0) Ventrolateral gonocoxital surface convex, without process. 1) Gonocoxite with apicoventral laminae.
53. *Gonopodites.* 0) Gonopodite inarticulate. 1) Gonopodite articulate.
54. *Gonopodital vestiture.* 0) Gonopodital apex lacking vestiture. 1) Gonopodital apex with at least a few setae.
55. *Gonopodital apex.* 0) Gonopodital apex entire. 1) Gonopodital apex bifurcated, or with subapical tooth.
56. *Volsellae*. 0) Volsellae absent. 1) The absence of the volsellae (0) cannot be readily confirmed without dissection, which was not advisable in the case of several Leptanillinae in which the volsellae were not externally apparent, but no specimens were available for dissection: volsellar condition is therefore treated in these cases as unknown. Observations of the volsellae as absent in several members of the *Leptanilla havilandi* species-group follow Chapter 3.
57. *Penial dorsum.* 0) Base of penial sclerites not dorsally concealed by gonopodites. 1) Base of penial sclerites at least partly concealed dorsally by gonopodites.

58. *Penial angle in profile view.* 0) Penial sclerites subparallel to proximodistal axis of genital capsule in profile view, or curving ventrad proximodistal axis. 1) Penial sclerites dorsally recurved at base in profile view.
59. *Penial shape in cross-section.* 0) Penial sclerites lateromedially compressed or subcircular in cross-section, at least at apex. 1) Penial sclerites dorsoventrally compressed.
60. *Penial dorsum.* 0) Penial sclerites without dorsomedian carina if medially fused, or if not medially fused sometimes with dorsomedian margins carinate. 1) Penial sclerites with dorsomedian carina.
61. *Penial venter.* 0) Penial sclerites without ventromedian projection, venter sometimes carinate or serrate. 1) Penial sclerites with ventromedian projection.
62. *Phallotremal rim.* 0) Phallotreme either surrounded by cuticle or conjunctiva, without vestiture. 0) Phallotreme surrounded by cuticle bearing vestiture of decumbent setae.
63. *Margin of penial apex.* 0) Penial sclerites medially articulated, or if medially fused then with penial apex emarginate. 1) Penial sclerites medially fused, penial apex entire.
64. *Sculpture at penial apex.* 0) Penial apex without median recurved hook. 1) Penial apex with median recurved hook. (1) is an autapomorphy of *Leptanilla* zhg-id01 (Griebenow, 2020: fig. 13Ci).

These data are summarized in Table 5.S4.

2.6. Phylogenomic inference

2.6.1. Subsampling

Four different subsets of the 490 loci included in the full alignment (Matrix A) were selected using the following criteria.

1. Loci found to significantly deviate from the expectations of stationarity, compositional homogeneity, or both according to at least one of three separate matched-pair tests of symmetry (Jermiin et al., 2017) were identified and excluded with the --*symtest* option in IQ-Tree (Naser-Khdour et al., 2019). This resulted in an alignment of 287 loci, 166,662 bp long (Matrix B). Phylogenetic models in the general time-reversible (GTR) family assume by default that stationarity and compositional homogeneity (SH) are properties of the evolutionary process that gave rise to the observed data. Violation of these assumptions by the data therefore may result in systematic error with strong statistical support (Kubatko and Degnan, 2007).
2. To assess the inferential effects of data reduction relative to violation of SH assumptions, I retrieved the 203 loci from the full dataset that violate these assumptions as identified by the matches-pair tests of symmetry cited above. This alignment was 116,849 bp long (Matrix C).
3. Amino acids are putatively less susceptible to systematic biases than are nucleotides, and phylogenetic signal can differ among loci according to whether these code for amino acids. Therefore, I subsampled an alignment including only protein-coding UCEs. These UCEs were identified and extracted by *uce-to-protein.py* (Borowiec, 2019a). I used protein sequences from *Harpegnathos saltator* Jerdon, *Ooceraea biroi* (Forel), and *Acromyrmex echinatior* (Forel) as separate reference BLAST databases to identify protein-coding UCEs, formatted as unaligned FASTAs. Only those protein-coding loci retrieved that included ≥90% of all 84 UCE-enriched terminals were retained, resulting in

an alignment of 62 loci, 15,354 bp in length (Matrix D). Loci untrimmed by Spruceup were recoded to amino acids using AMAS (Borowiec, 2016), with stop codons and potentially misaligned sequences manually removed, resulting in an alignment 4,887 amino acids long (Matrix D†).

4. To produce an alignment brief enough to be computationally tractable for total-evidence Bayesian inference, I further subsampled the set of 287 loci found to fulfill SH assumptions by matched-pair tests of symmetry in IQ-Tree (as above), using *genesortR* (Mongiardino Koch, 2021). I inferred gene trees for each of these 287 loci, and a species tree from all of these loci concatenated, in IQ-Tree for 5,000 ultrafast bootstraps (UFBoot) (Hoang et al., 2018). I constrained the monophyly of the Leptanillomorpha, which following prior literature is preferred over alternative topologies (Borowiec et al., 2019; Romiguier et al., 2022). These gene trees were inferred from an alignment trimmed in Spruceup (Borowiec, 2019b) (Section 2.6.2) using a lognormal cutoff criterion of 0.9 (Section 2.6.2). These trees were then used as an input for *genesortR* (Mongiardino Koch, 2021), which ranks loci along a principal component axis derived from six calculated gene properties known to be correlated with artifactual phylogenetic inference, and corrected using Robinson-Foulds similarity. Gene properties were calculated only for the 75 ingroup terminals. Loci ranked in the top 80% of outliers by principal component analysis were discarded by *genesortR*, resulting in an alignment of 58 loci, 34,039 bp long (Matrix B′). Lastly, all terminals for which male morphological data are unavailable were omitted from Matrix B′, except for *Leptanilla havilandi* Forel, along with all but a single respective representative of *P. lini* and *Protanilla* zhg-my01. This left 68 terminals. Matrix B′ was used only in Bayesian total-evidence inference.

By-taxon summary statistics for these alignments are presented in Tables 5.S4-7.

2.6.2. Trimming of potentially misaligned sequences

To limit error in orthology inference, which may have a disproportionate effect on downstream phylogenomics (Brown and Thomson, 2017), Spruceup was used to trim potentially misaligned sequences across Matrices A-D. Genetic distances were calculated among sequences within alignment intervals of predefined length and overlap, with a log-normal curve being fitted to these distances; outliers along this distribution are then eliminated according to a predefined threshold. This process may therefore dispose of sequence data that are genuinely aberrant, rather than misaligned. Loss of these data, and causal excess stringency in threshold value, can only be revealed if a favored phylogeny is known *a priori*. Such a phylogeny is unavailable for the former tribe Anomalomyrmini, which constitutes the most controversial node within the internal phylogeny of the Leptanillinae. Therefore, to assess the effect of variation in cutoff, all ML analyses were replicated with alignments trimmed in Spruceup according to four arbitrary lognormal cutoff values—0.95, 0.90, 0.85, and 0.80, listed here from least to most strict—plus with said alignment untrimmed (i.e., lognormal cutoff value=1). Matrices are hereinafter prefixed with their respective cutoff values. Matrix B′ was trimmed with lognormal cutoff value=0.90.

2.6.3. Analytical frameworks and partitioning schemes

All substitution models in the GTR family were considered in inference of partitioning scheme for phylogenomic inference, including those that model among-site rate variation by both the proportion of invariable sites (+I) and gamma-distributed (+G) extensions in conjunction (i.e., I+G). IQ-Tree compensates for the statistical non-identifiability of substitution models with the

I+G extension (Nguyen et al., 2018; Yang, 1996). Matrix D was always partitioned by locus, while concatenation-based analyses using Matrices A-C were partitioned by-locus and within-locus. Within-locus partitioning SUBdivided UCEs according to site entropy (Tagliacollo and Lanfear, 2018). These subdivisions were inferred for each of Matrices 1A-C with the sliding-window site-characteristics (SWSC) algorithm in PartitionUCE (Tagliacollo and Lanfear, 2018), and used as input for inference of partitioning scheme and substitution model using ModelFinder (Kalyaanamoorthy et al., 2017) as implemented in IQ-Tree (v. 2.1.2 hereinafter) (Minh et al., 2020b), with the Bayesian Information Criterion (BIC) employed for model selection. All ML analyses in IQ-Tree were run for 5,000 ultrafast bootstraps (Hoang et al., 2018).

The within-locus partitioning schemes yielded by ML inference in IQ-Tree, from a version of each alignment trimmed with a lognormal value of 0.90 in Spruceup, were used for partitioned Bayesian phylogenomic inference from Matrices 0.9A-D with ExaBayes (Aberer et al., 2014). Four independent runs were implemented for each analysis for 1,000,000 generations, with a pair of Metropolis-coupled Markov-chain Monte Carlo (MCMC) being implemented for each run. Default prior probability distributions were used for continuous parameters, with branch lengths being treated as unlinked. Initial topology was inferred with maximum parsimony (MP). The initial 25% of output was discarded as burn-in.

To account for the potential effects of ILS, I used a gene tree summary approach with Accurate Species Tree ALgorithm, ASTRAL-III (Mirarab and Warnow, 2015; Zhang et al., 2018). This two-step approach is hereinafter referred to as “coalescent-based”, as ASTRAL is statistically consistent with the multi-species coalescent (MSC). The equivalence of this coalescent-based approach with the MSC allows modeling of the respective evolutionary histories of each locus—histories that are disregarded if loci are concatenated. Input for ASTRAL-III consisted of ML

gene trees inferred for each locus included in a given alignment using the -*S* option in IQ-Tree v. 2.1.2 (Minh et al., 2020b) along with inference of substitution model, selected by the BIC, run for 5,000 ultrafast bootstraps; for the randomized nearest-neighbor-interchange (NNI) tree search, perturbation strength=0.2. Summary of gene trees in ASTRAL-III was conducted with λ=0.5. Support for nodes was expressed as local posterior probability (localPP), computed from relative frequencies of gene tree quartets; branch length was expressed in coalescent units (Sayyari and Mirarab, 2016).

2.6.4. Concordance factors

For all untrimmed versions of Matrices A-C, using IQ-Tree 2.0.3 on an Ubuntu 22.04.1 LTS, both gene concordance factors (gCF) and site concordance factors (sCF) were calculated for unrooted species trees inferred in IQ-Tree under the within-locus partitioning scheme, as above; the same was employed for Matrix D, but with the by-locus partitioning scheme. gCF was calculated also using unrooted ML gene trees, inferred as above (Minh et al., 2020a). gCF and sCF respectively communicate the fraction of gene trees and alignment sites that decisively support a given node. gCF for given node *x* in the reference phylogeny is calculated using only those gene trees that could include node *x* (that is, are decisive for node *x*), and is expressed as the proportion of decisive gene trees that do in fact contain node *x*. In the interest of time, concordance factors were not calculated for all alignments trimmed in Spruceup, nor for Matrices A-D* (Section 2.6.5).

2.6.5. Perturbation of taxon sampling

All ML phylogenomic analyses were reproduced using alignments with *Protanilla* zhg-th02 omitted, to test the effect of the inclusion of this taxon on the inferred basal topology of the

former Anomalomyrmini. These alignments are suffixed with an asterisk. Due to the minimal differences in phylogeny as inferred from UCEs under ML as opposed to Bayesian methods, phylogeny was not inferred from Matrices A*-D* using a Bayesian framework. *Protanilla* zhg-th02 does not conform to the male-based diagnoses provided in Chapter 4 for the *Protanilla rafflesi* species-group or *Protanilla bicolor* species-group, and there is no prior morphological or biogeographical evidence to indicate that this morphospecies represents the as-yet unknown male of the *Protanilla taylori* species-group.

2.7. Total-evidence inference

Bayesian total-evidence phylogenetic inference was undertaken in RevBayes v. 1.1.1 (Höhna et al., 2017) on the CIPRES Science Gateway, with two independent runs for each analysis, and four MCMCs for each run. Metropolis coupling was not implemented. Four separate analyses were implemented in RevBayes to query the phylogenetic position of each terminal of interest—*L. anomala*, *L. palauensis*, *L. astylina*, and *Leptanilla* ci01; for each analysis, only the pertinent terminal among these four was included, plus the terminals selected for Matrix B′ as reported in Section 2.6.1.

Parsimony-informative and -uninformative morphological characters were partitioned (Rosa et al., 2019), whereas Matrix B′ was partitioned using PartitionUCE, followed by ModelFinder in IQ-Tree (Section 2.6.3). GTR+8Γ was stipulated as the substitution model for all partitions of Matrix B′ without assessment of absolute fit (by posterior predictive simulation) or relative fit (e.g., by Bayes Factors), because the parameters in this model are comparatively extensive, resulting in adequate model fit and inferential accuracy when applied to most data (Abadi et al., 2019); meanwhile, it avoids the non-identifiability of continuous parameters to which the still

more parameter-rich GTR+I+G model is susceptible (Yang, 1996). Morphological data were modeled with *mkv*+8Γ (Lewis, 2001), with stationary frequencies of character states allowed to vary (Felsenstein, 1981). Branch lengths were treated as unlinked across all partitions. All parameters of the phylogenetic model were allowed to vary among partitions. Each MCMC ran for 25,000 generations, preceded by an additional 1,000 burn-in generations in which proposal weights were optimized. Output phylogenies were summarized as a maximum *a posteriori* (MAP) tree.

3. Results

2.1. Phylogenomic inference

The phylogeny of the Leptanillinae as inferred by a phylogenomic approach is largely congruent across all analyses, resembling the phylogeny shown in Fig. 5.1. Major leptanilline subclades recognized and diagnosed according to the worker and male phenotype in Chapter 4, whether as genera (*Protanilla* and *Leptanilla*) or informal species-groups (three in *Protanilla*; five in *Leptanilla*), and are represented by more than a single terminal are recovered as reciprocally monophyletic with strong statistical support, regardless of dataset, partitioning scheme, or inferential framework; the exception lies in the phylogeny inferred by coalescent-based methods from Matrix D, for which the posterior probability of deeper nodes is often low. This degradation presumably arises from limited severity of test in a molecular dataset so brief. The rare cases in which the respective memberships of the major leptanilline subclades differ from consensus across all phylogenomic analyses occur only under coalescent-based inference. This phenomenon would be due to stochastic error in gene-tree inference, due to the brevity of protein-coding UCEs recovered by *uce-to-protein.py* ($\bar{x} = 248\ bp;\ \sigma = 103$) relative to the loci in Matrices A-C ($\bar{x} = 577\ bp;\ \sigma = 135$). Indeed, the comparative lack of available information

in individual protein-coding loci, coded as amino acids, means that coalescent-based inference of Matrices D† and D†* yields a phylogeny largely comprised of polytomies, and so these results are not presented here.

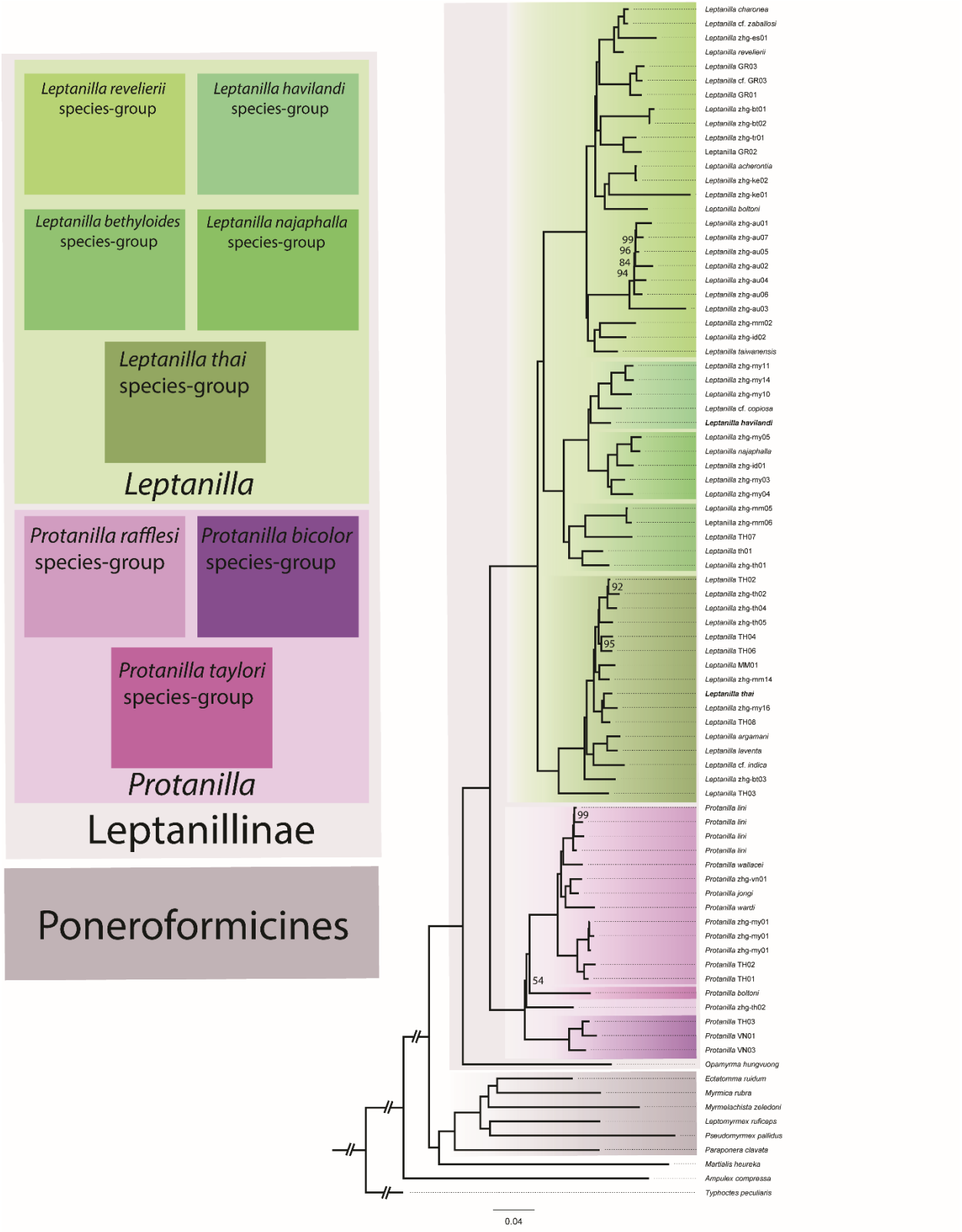

Figure 5.1. ML phylogeny of the Leptanillinae and nine outgroups, inferred from Matrix 0.90A with IQ-Tree for 5,000 ultrafast bootstraps. *Leptanilla havilandi* and *Leptanilla thai* are written in bold. UFBoot values are noted for nodes when <100.

The relationships among the principal leptanilline subclades are congruent and strongly supported among different phylogenomic analyses, with the major lineages of the former Anomalomyrmini being a notable exception (Section 3.3). This phylogeny is also largely robust to by-locus versus within-locus partitioning. There are also no conspicuous differences in the backbone of leptanilline phylogeny as inferred using ML versus a Bayesian approach, except with respect to the topology of the former Anomalomyrmini. All results are congruent with those of previous studies that addressed the phylogeny of the Leptanillinae (Borowiec et al., 2019; Griebenow, 2020, 2021; Chapter 2), except for the internal topology of the former Anomalomyrmini, which is conflicted according to dataset.

Leptanilla thai Baroni Urbani unequivocally belongs to the former *Yavnella* (equivalent to the *Leptanilla thai* species-group; Chapter 4), along with *Leptanilla laventa* (Griebenow *et al.*) one of only two species definitively placed in that clade by phylogenomic inference for which the worker caste is known. *Leptanilla havilandi*, which is distinguishable from *L. thai* by mandibular dentition, cranial sculpture, and continuous differences in the elevation of the frontoclypeal process (Chapter 4), is robustly recovered distant to *L. thai* (Baroni Urbani, 1977) as sister to the clade corresponding to the genus *Noonilla*, known only from male specimens.

The placement of the *Leptanilla thai* species-group as sister to the rest of *Leptanilla sensu* Chapter 4 is recovered with weakened support values (UFBoot=70-99) by concatenation-based inference from Matrix D and is weakly contradicted (localPP=0.44-0.68) by most coalescent-based analyses from that same dataset (Figs. 5.S45-54). In concatenation-based analyses, support values for a position of the *Leptanilla thai* species-group as sister to the remainder of *Leptanilla* increase in tandem with the stringency of the lognormal cutoff value implemented in Spruceup. Only a small fraction of protein-coding loci (untrimmed) support this phylogeny (gCF=4.84)

(Fig. 5.S123). Depending on lognormal cutoff value implemented in Spruceup, this relationship is either recovered with negligible support (localPP=0.40) or the *Leptanilla revelierii* species-group is weakly supported as sister to the remainder of *Leptanilla*, exchanging inferred phylogenetic position with the *Leptanilla thai* species-group. A phylogenetic position for *Leptanilla* zhg-ke01 outside of the *Leptanilla revelierii* species-group, recovered only by coalescent-based inference from Matrix 0.85D [Fig. 5.S48], is certainly the result of gene-tree error. Otherwise, the relationships among the four monophyletic species-groups delimited within *Leptanilla* in Chapter 4 are robustly supported by phylogenomic inference.

The paraphyly of *Protanilla s. str.* relative to the former *Anomalomyrma* received strong statistical support in previous studies (Borowiec et al., 2019; Griebenow, 2020; Chapter 2). Despite conflict among analyses regarding the topology of the former Anomalomyrmini, *Protanilla boltoni*, the sole sampled representative of the former *Anomalomyrma*, renders *Protanilla s. str.* paraphyletic in all analyses, save for coalescent-based inference from Matrices 0.95A-0.95B (Figs. 5.S12, 5.S27) and Matrix 0.85D (Fig. 5.S48). The monophyly of *Protanilla s. str.* was recovered in these cases with negligible support (localPP=0.57, 0.58). A favored phylogeny for the major lineages of the former Anomalomyrmini could not be resolved in this study.

Only rarely is the monophyly of the Leptanillomorpha recovered. Most analyses instead recover the Leptanillinae as sister to the remainder of the Formicidae, usually with high support. Most phylogenies that contradict the placement of the Leptanillinae as sister to the remainder of the Formicidae were inferred from Matrix D and recover the two alternative basal topologies for the crown-group Formicidae with statistical support that is often negligible to weak. For example, Bayesian inference from Matrix 0.9D weakly recovers *M. heureka* as sister to all other

Formicidae (BPP=0.79) (Fig. 5.S59)—whereas Bayesian inference from Matrices 0.9A-C recovers *M. heureka* sister to the Poneroformicines with high posterior probability (BPP=0.99-1) (Figs. 5.S56-58). Coalescent-based inference from Matrices 0.95-1B also recovers this phylogeny with respectively strong (localPP=1) or weak (localPP=0.75) posterior probability, but all other inferences from Matrix B recover the Leptanillinae as sister to the remaining Formicidae (UFBoot=94-100; localPP=0.65-0.99; BPP=1) (Figs. 5.S16-S30, 5.S57). Phylogenomic inferences from matrices D† and D†* are unique in that the monophyly of the Poneroformicines is not decisively recovered, with *Paraponera clavata* (Fab.)—the sole sampled representative of Poneria (Boudinot et al., 2022)—forming a polytomy with the Leptanillinae, *M. heureka*, and the Formicae (Boudinot et al., 2022) (Fig. 5.S55, 5.S119). Concordance factors show that phylogenetic signal for Matrix 1D is highly conflicted regarding the placement of *M. heureka* relative to the Leptanillinae (gCF=10, sCF=30.5) (Fig. 5.S123). The phylogenetic position of the Leptanillinae as sister to the remainder of the Formicidae is in this study therefore largely robust to compensation for within-locus compositional heterogeneity.

2.2. Total-evidence Bayesian inference

The phylogeny of the Leptanillinae as inferred by Bayesian methods from Matrix B′ and 64 binary male morphological characters is congruent with that phylogeny as inferred from Matrices A-D (Figs. 5.S1-55), but in three out of the four analyses, the inclusion of even a single terminal for which molecular data are unavailable—*L. palauensis*, *L. astylina*, and *Leptanilla* ci01—severely degrades posterior probability along the backbone of leptanilline phylogeny as a whole, with the respective monophyly of the Leptanillinae, Leptanillini, *Protanilla*, and *Leptanilla* being recovered with negligible support (BPP=0.5) (Figs. 5.S61-63). The Bayesian total-evidence analysis including *L. astylina* recovers the monophyly of the Formicidae with low posterior

probability (BPP=0.5), as for the Poneroformicines (BPP=0.5) in the case of Bayesian total-evidence inference including *L. palauensis*. An exception in these three analyses is the strong support (BPP=0.97-0.99) for the monophyly of the Indo-Malayan clade sister to the *Leptanilla revelierii* species-group (Figs. 5.S61-63).

Leptanilla palauensis, *L. astylina*, and *Leptanilla* ci01 are all recovered within the *Leptanilla revelierii* species-group with low support (BPP=0.45-0.49) but are decisively excluded from all other major clades within the Leptanillinae (Figs. 5.S61-63). Conversely, *L. anomala* is recovered within the *Leptanilla havilandi* species-group with high posterior probability (BPP=0.99) (Fig. 5.2). Bayesian total-evidence inference of the phylogenetic position of *L. anomala* also shows high posterior probability for the Leptanillinae and all major clades therein (BPP=0.99-1), with this phylogeny being congruent with phylogenomic results (Fig. 5.S60).

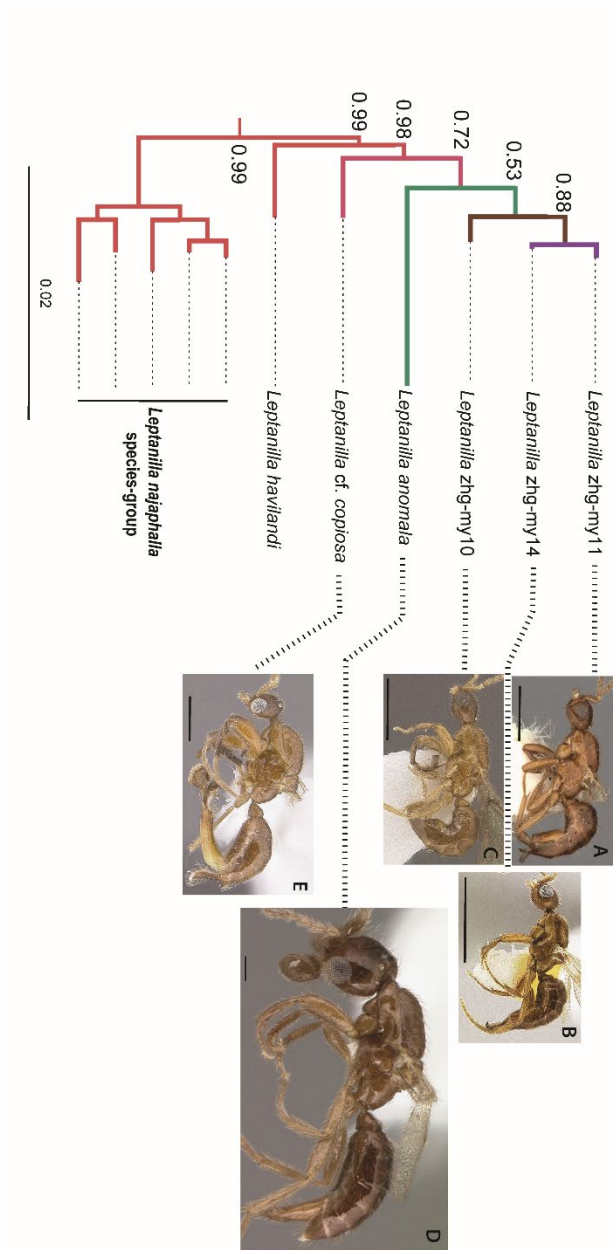

Figure 5.2. Phylogeny of the *Leptanilla havilandi* species-group and sister clade, the *Leptanilla najaphalla* species-group, as inferred under Bayesian total-evidence inference from Matrix B′ and 64 binary male morphological characters. Clades outside the *Leptanilla havilandi* species-group and *Leptanilla najaphalla* species-group are omitted. Phylogeny colored according to Bayesian posterior probability (BPP) of internal nodes; BPP noted only where <1. Branch length expressed in number of expected substitutions per site. Scale bars: A, C, E = 0.5 mm.; B = 1 mm.; D = 0.1 mm.

2.3. Conflicted phylogeny of the former Anomalomyrmini

Although the respective phylogenies of the sampled exemplars of the *Protanilla rafflesi* species-group and *Protanilla bicolor* species-group are robust across all phylogenomic analyses, the internal relationships among the four major lineages of the former Anomalomyrmini are far from robust. These are almost always recovered with weak statistical support and are largely incongruent with one another (Figs. 5.3-4).

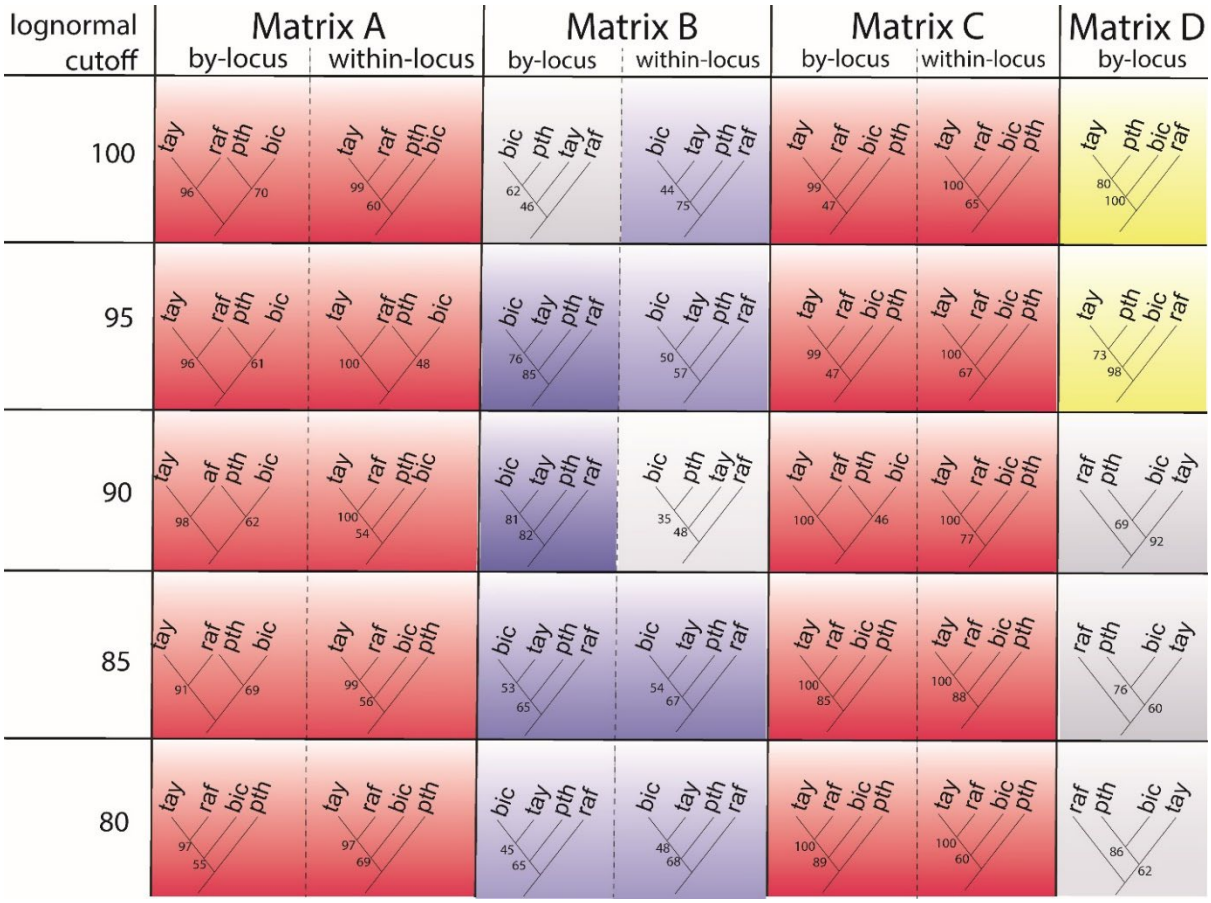

Figure 5.3. Matrix of the topology of the former Anomalomyrmini as recovered across all ML phylogenomic analyses, except for those from Matrix D†. Coloration refers to phylogenetic hypothesis concerning the *Protanilla taylori* species-group, with shade corresponding to relative strength of statistical support under pertinent inferential framework. Red=*Protanilla taylori* species-group + *Protanilla rafflesi* species-group; blue=*Protanilla taylori* species-group + *Protanilla bicolor* species-group; yellow=*Protanilla taylori* species-group + *Protanilla* zhg-th02. Gray corresponds to other phylogenetic hypotheses regarding the *Protanilla taylori* species-group. Abbreviations: bic = *Protanilla bicolor* species-group; pth = *Protanilla* zhg-th02; raf = *Protanilla rafflesi* species-group; tay = *Protanilla taylori* species-group.

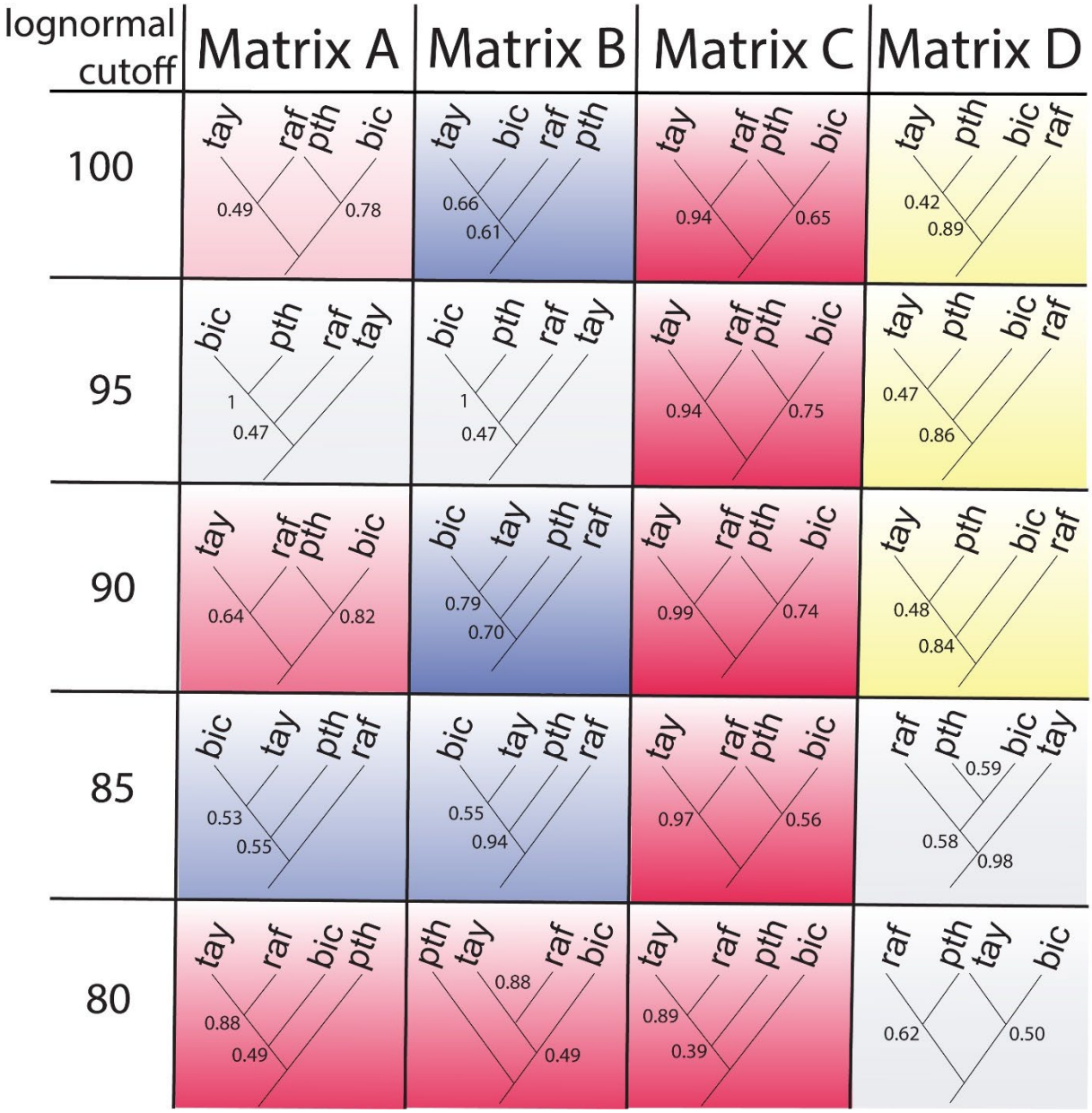

Figure 5.4. Matrix of the topology of the former Anomalomyrmini as recovered across all coalescent-based phylogenomic analyses, except for those from Matrix D†. Coloration refers to phylogenetic hypothesis concerning the *Protanilla taylori* species-group, with shade corresponding to relative strength of statistical support under pertinent inferential framework. Red=*Protanilla taylori* species-group + *Protanilla rafflesi* species-group; blue=*Protanilla taylori* species-group + *Protanilla bicolor* species-group; yellow=*Protanilla taylori* species-group + *Protanilla* zhg-th02. Gray corresponds to other phylogenetic hypotheses regarding the *Protanilla taylori* species-group. Abbreviations: bic = *Protanilla bicolor* species-group; pth = *Protanilla* zhg-th02; raf = *Protanilla rafflesi* species-group; tay = *Protanilla taylori* species-group.

2.3.1. Concatenation-based analyses

Relationships among the major subclades of the former Anomalomyrmini are robust to partitioning scheme used in phylogenomic inference but are affected by differences in inferential framework and choice of matrix. The plurality of concatenation-based analyses favors a sister-group relationship between *Protanilla boltoni* (the sole sampled representative of the *Protanilla taylori* species-group) and the *Protanilla rafflesi* species-group. This relationship is recovered with strong support (UFBoot=91-100; BPP=1) from Matrix A, and even more strongly from Matrix C (UFBoot=99-100; BPP=1) (Fig. 5.3). The relationship between the *Protanilla bicolor* species-group and *Protanilla* zhg-th02 is unresolved by ML inference from these alignments. Conversely, Bayesian phylogenomic inference from Matrices 0.9A-C displays high posterior probability for all internal nodes of the former Anomalomyrmini (BPP=0.96-1) (Figs. 5.S56-58), with degradation in posterior probability under inference from Matrix D (Fig. 5.S59). Bayesian phylogenomic inference from all matrices except Matrix 0.9C (Fig. 5.S58) contradicts the basal topology inferred for the former Anomalomyrmini under ML with respect to nodes that received only weak support under ML. Concatenation-based phylogenomic inference from Matrix B under ML contradicts a sister-group relationship between the *Protanilla rafflesi* species-group and *Protanilla taylori* species-group, instead usually recovering *P. boltoni* as sister to the *Protanilla bicolor* species-group (Fig. 5.3): inference under within-locus partitioning from Matrix 0.9B reveals a polytomy (UFBoot=48-35) (Fig. 5.3; Fig. 5.S23). Statistical support for relationships among all four principal subclades of the former Anomalomyrmini is negligible to weak when inferred from Matrix B. Concatenation-based phylogenomic inference applied to Matrices 0.95-1D recovers the *Protanilla rafflesi* species-group as sister to the remainder of the former Anomalomyrmini with strong bootstrap support, an inference that is contradicted with

weak to moderate bootstrap support (UFBoot=60-92) from concatenation-based inference from Matrix D as trimmed in Spruceup under less stringent lognormal cutoffs (Fig. 5.3).

2.3.2. Coalescent-based analyses

Coalescent-based phylogenomic inference from Matrices A-D is inconsistent with respect to the phylogenetic relationships of the four main lineages of the former Anomalomyrmini (Fig. 5.4). Conclusions differ across Spruceup trimming stringencies, with statistical support for any internal nodes among these four lineages being negligible to moderate (localPP=0.57-0.88) except for the sister-group relationship of *Protanilla* zhg-th02 + the *Protanilla bicolor* species-group recovered by coalescent-based inference from Matrix 0.95A (Fig. 5.S12). Despite this inconsistency, coalescent-based inference from a given matrix tends to recapitulate the topological hypothesis most frequently retrieved by concatenation-based inference from that same matrix. Coalescent-based inference from Matrix 0.8D contradicts the phylogenetic position for the *Protanilla rafflesi* species-group recovered by concatenation-based inference from that same alignment, but with low posterior probability (localPP=0.62) (Fig. 5.4, 5.S46). Coalescent-based inference from Matrix C is more consistent in recovered phylogeny than that from other matrices, and always conforms to the conclusions of concatenation-based inference from the same matrix, recovering *P. boltoni* as sister to the *Protanilla rafflesi* species-group with high posterior probability (localPP=0.89-0.99) (Fig. 5.4).

2.3.3. Results of omission of Protanilla *zhg-th02*

Omission of *Protanilla* zhg-th02 in Matrices A*-D* results in some improvement to support values for the basal topology of the remaining three principal subclades of the former Anomalomyrmini, but this node is nonetheless often recovered as polytomy. For each matrix,

conclusions corroborate most phylogenies inferred from that same matrix inclusive of *Protanilla* zhg-th02. To wit, concatenation-based phylogenomic inference from Matrix A* weakly to strongly supports *Protanilla boltoni* as sister to the *Protanilla rafflesi* species-group (UFBoot=78-99) (Figs. 5.S64-78), a conclusion also supported by inference from Matrix C* (UFBoot=89-100; localPP=0.52-0.99) (Figs. 5.S94-108). Coalescent-based inference from Matrix A* is indecisive, either weakly to strongly supporting *P. boltoni* + the *Protanilla rafflesi* species-group (Matrices 0.80A*, 0.90A*: localPP=0.76, 0.92) or weakly supporting the alternative topology (Matrices 0.85A*, 0.95-1*: localPP=0.82-0.84) (Figs. 5.S64-78). Matrix B* supports *P. boltoni* as sister to *Protanilla bicolor* species-group strongly under coalescent-based inference (localPP=0.90-0.99) but with comparatively weakened statistical support under concatenation-based inference (UFBoot=63-91) (Figs. 5.S79-93). With phylogenomic inference from Matrix D*, *Protanilla boltoni* + the *Protanilla bicolor* species-group is negligibly to strongly supported (UFBoot=56-88; localPP=0.91-0.95), except for concatenation-based phylogenomic inference from Matrices D* and D*†, and coalescent-based phylogenomic inference from Matrix 0.85D* (Fig. 5.S112). These latter analyses instead retrieve polytomies for the former Anomalomyrmini (UFBoot=47, 62; localPP=0.44).

3. Discussion

3.1. Internal phylogeny of the Leptanillinae

The phylogeny of the Leptanillinae, including multiple representatives of all but one of the major clades, is largely robust to compositional heterogeneity, gene-tree discordance, and conflicting signal between protein-coding and non-protein-coding loci. Differences in partitioning scheme and inferential framework also have little effect on inferred phylogeny. As such, there is no evidence in this study to indicate that the high bootstrap support and posterior probabilities

recovered for the phylogeny of the Leptanillinae by previous phylogenomic analyses are spurious—with the basal topology of the former tribe Anomalomyrmini being a notable exception. Coalescent-based inference from protein-coding loci alone (Matrix D) contrasts with other analyses by the poor posterior probability of several deep nodes within the Leptanillinae: given that support values are generally high in coalescent-based analyses using other alignments, I conclude that this phenomenon results from stochastic error in the inference of respective gene trees, rather than gene-tree discordance due to historical signal. The phylogenomic results presented here are largely congruent with previous studies.

Posterior probability for the phylogeny of the Leptanillinae as inferred jointly from male morphology and molecular data, with the inclusion of lone terminals for which male morphology alone is available, is equivocal for most deeper nodes in all Bayesian analyses—except for that including *L. anomala*. This demonstrates that joint inference from a matrix of 64 binary male morphological characters and a 34,039-bp UCE alignment, with 67 out of 68 terminals being represented by both forms of data, is insufficient to decisively resolve the phylogenetic position of *L. palauensis*, *L. astylina*, or *Leptanilla* ci01 (Section 3.2).

As noted in Chapter 4, specimens of most leptanilline morphospecies are too sparse for species delimitation with statistical power. Species boundaries in the *Protanilla rafflesi* species-group, in which both the worker caste and males show strong phenotypic conservatism, are therefore questionable. This study is unable to test the validity of *Protanilla wallacei* Griebenow as a species relative to *P. lini* due to geographically intermediate forms remaining unsampled in phylogenomic inference. Phylogenetic inference here does definitively indicate that *Protanilla* zhg-my01 is not the male of *P. wallacei*: thus, there are at least two sympatric species of the *Protanilla rafflesi* species-group present in the Sundan region.

Given the phylogenetic positions of *L. havilandi* and *L. thai* as inferred here from genome-scale data, Chapter 4 synonymizes *Noonilla* and *Yavnella* with *Leptanilla*. Total-evidence inference recovers the monophyly of *Scyphodon* and the former *Noonilla* (i.e., *Scyphodon s. l.*; Chapter 3) with high posterior probability (Section 3.2), justifying the synonymy of *Scyphodon* with *Leptanilla* by the same rationale as given for the synonymy of *Noonilla* with *Leptanilla*. Due to the impracticality of uniformly discriminating the worker caste of *Yavnella* from its sister clade, which includes *Scyphodon*, *Noonilla*, and *Leptanilla sensu stricto*, among other morphotaxa (Chapter 1), Chapter 4 synonymizes *Scyphodon*, *Noonilla*, and *Yavnella* with *Leptanilla*. The complete robustness of the inferred positions of *L. thai* and *L. havilandi* to analytical perturbations in this study, respectively within clades corresponding to the former *Yavnella* and *Scyphodon s. l.*, and the strongly supported placement of *L. anomala*, provides a firm phylogenetic foundation for the taxonomic actions of Chapter 4 concerning the limits of the genus *Leptanilla*.

Given the phenotypic affinity of *Protanilla jongi* Hsu *et al.* to *Protanilla furcomandibula* Xu & Zhang, I presume that the two are closely related, although *P. furcomandibula* was not sequenced in this study. If this assumption is correct, the results presented here also provide decisive phylogenomic support for the synonymy of *Furcotanilla* Xu, established by monotypy for *P. furcomandibula* (Xu, 2012), with *Protanilla* (Hsu et al., 2017): *P. jongi* is robustly recovered within the *Protanilla rafflesi* species-group. However, phylogenomic support for the synonymy of *Anomalomyrma* with *Protanilla* (Chapter 4) is not so straightforward.

Previous phylogenetic analysis of the former Anomalomyrmini prefigured the conflicting topologies for that clade recovered in this study. Majority-rule consensus phylogenies inferred from 10 protein-coding loci and 28S rDNA concurred in recovering *P. boltoni* as sister to the

Protanilla bicolor species-group with strong to maximal support (Borowiec et al., 2019). Whether in the form of phylogenomic inference (Chapter 2) or total-evidence inference using discretized male morphology jointly with the molecular dataset of Borowiec et al. (2019) (Chapter 1), subsequent analyses contradicted the topology of the former Anomalomyrmini as recovered by Borowiec et al. (2019) with strong to maximal statistical support, instead recovering *P. boltoni* as sister to the *Protanilla rafflesi* species-group. Only three exemplars of the *Protanilla rafflesi* species-group were included in Borowiec et al. (2019), and subsequent phylogenetic inference focusing on the Leptanillinae did not improve much upon the sampling of the former Anomalomyrmini (Griebenow, 2020) (Chapters 1-2). Expanded phylogenomic sampling within the *Protanilla rafflesi* species-group herein does not further resolve phylogenetic relationships among the major lineages of the former Anomalomyrmini beyond what was reported in previous studies. The inclusion of *Protanilla* zhg-th02, an undescribed male morphospecies belonging to the former Anomalomyrmini, exacerbates the lack of resolution at the base of that clade. The effect induced on phylogenetic inference by the inclusion of *Protanilla* zhg-th02 is not an artifact resulting from incompleteness of the phylogenomic data, which is merely ≤21% with respect to *Protanilla* zhg-th02 in Matrices A-D (Table 5.2), but rather signal intrinsic to those data themselves.

UCE subsampling in this study under different analytical conditions and accommodation of gene-tree discordance does not reveal a favored topology for the major subclades of the former Anomalomyrmini, or placement for *Protanilla* zhg-th02, which is here always recovered on a long branch and never within the *Protanilla rafflesi* species-group or the *Protanilla bicolor* species-group. I attribute the intractability of this node to gene-tree discordance. Alternatively, the polytomy at the base of the Anomalomyrmini may reflect historical signal if cladogenesis

was so rapid as to now be unresolvable. In either scenario, improved sampling of *Protanilla* outside the *Protanilla rafflesi* species-group will not produce a decisive result, given the testament of phylogenomic literature on recalcitrant nodes elsewhere across the Tree of Life (e.g., Betancur-R. et al., 2019).

The moderate to strong support for *P. boltoni* as sister to the *Protanilla rafflesi* species-group reported in previous phylogenomic studies (Griebenow, 2020; Chapter 2) is here supported mostly by phylogenomic inference from Matrices A and C. This relationship is not robust to exclusion of loci that do not conform to SH assumptions (Matrix B), or reduction to protein-coding loci alone (Matrix D). That this relationship only receives strong statistical support in phylogenomic inference from alignments including, or exclusively consisting, of loci that deviate from SH assumptions suggests that the inferred sister-group relationship of *P. boltoni* to the *Protanilla rafflesi* species-group is an artifact of model misfit, resulting from violation by the data of the assumptions of stationarity, compositional homogeneity, or both. This conclusion is further argued for by the increase in statistical support for this relationship under both concatenation- and coalescent-based phylogenomic inference from SH-violating UCEs alone (Matrix C) versus a mixture of SH-violating and SH-conforming UCEs (Matrix A). Loss of mesotibial spurs (Chapter 4) therefore cannot be adduced as a synapomorphy of the *Protanilla taylori* species-group and the *Protanilla rafflesi* species-group.

In conclusion, the relationships of the major subclades of the former Anomalomyrmini are still debatable. However, *Protanilla boltoni* is almost never inferred to be sister to the remainder of the former Anomalomyrmini (i.e., *Protanilla s. str.*): by Hennigian reasoning, this is the only phylogeny that would justify the retention of *Anomalomyrma* and *Protanilla s. str.* as distinct genera. The monophyly of *Protanilla s. str.* was never recovered by previous phylogenetic

inference (Borowiec et al., 2019; Griebenow, 2020) (Chapter 2) from datasets with less extensive taxon coverage of the former Anomalomyrmini. Thus, there is no decisive indication that *Protanilla s. str.* is monophyletic, meaning that the synonymy of *Anomalomyrma* with *Protanilla* remains a justified taxonomic course of action (Chapter 4).

3.2. Placement of aberrant Leptanilla

There are four species included in this study for which molecular data are unavailable but male morphology is so aberrant as to render qualitative taxonomy doubtful, necessitating Bayesian total-evidence inference in hopes of revealing their respective phylogenetic positions, as proved decisive when applied to *Leptanilla javana* (Wheeler & Wheeler) (Chapter 1). I here find that 64 discrete binary male morphological characters in conjunction with Matrix B′ do yield some phylogenetic signal, but only compellingly so in the case of *L. anomala*, which is strongly supported as belonging to a clade comprising *Leptanilla* zhg-my10, -11 and -14 (BPP=0.97), although the phylogenetic relationships among these terminals are poorly resolved (BPP=0.71) (Fig. 5.2). The qualitative supposition that the former *Scyphodon* and *Noonilla* are close kin, supported by multiple putative male synapomorphies of the *Leptanilla havilandi* species-group, is therefore corroborated by probabilistic means; in conjunction with other information from across the diversity of the Leptanillinae, this supports the synonymy of *Scyphodon* with *Leptanilla* (Chapter 4).

Bolton (2003: p. 40) cited a “single Afrotropical male” of the Leptanillinae as being akin to the former *Noonilla*: this was presumably CASENT0102373, the only known specimen of *Leptanilla* ci01, which was collected along the course of the Komoé River through Côte d’Ivoire, with further locality data being unavailable. The hypothesis that *Leptanilla* ci01 has any phylogenetic

affiliation with the *Leptanilla havilandi* species-group (i.e., *L. havilandi* + *Scyphodon* + *Noonilla*) is here refuted with high posterior probability, as predicted given the biogeographical remoteness of this morphospecies from the exclusively Sundan *Leptanilla havilandi* species-group. Likewise, the results of Bayesian total-evidence inference presented here exclude *Leptanilla* ci01 from all other subclades of *Leptanilla* save the *Leptanilla revelierii* species-group with high posterior probability, although positive support for the placement of *Leptanilla* ci01 within that clade is lacking (BPP=0.45). The male genitalia of this morphospecies resemble those of the *Leptanilla revelierii* species-group to a greater extent than do those of any other *Leptanilla* by the conjunction of articulated gonopodites and dorsoventrally compressed penial sclerites. It is doubtful that any other major lineages of *Leptanilla* exist in sub-Saharan Africa aside from the *Leptanilla revelierii* species-group: *Leptanilla* ci01 therefore must be regarded as an aberrant member of that clade for the time being.

Unlike *L. anomala* or *Leptanilla* ci01, the assignment of *L. astylina* to *Leptanilla* has never been in question (Petersen, 1968). Here, the phylogenetic signal is insufficient to support this identification (BPP=0.5), but *L. astylina* is at least strongly excluded (BPP=1) from the remaining Formicidae included in this analysis, and there is no prior evidence to doubt the inclusion of this species within *Leptanilla*. The peculiar male genital morphology of *L. astylina*—known only from the holotype, collected on Palawan, Philippines—excludes it from the existing logical definition of the *Leptanilla revelierii* species-group (Chapter 4). Bayesian total-evidence inference excludes *L. astylina* from all other clades of *Leptanilla*, as well as *Protanilla*, with high posterior probability, arguing for the placement of this species within the *Leptanilla revelierii* species-group. Given the confirmed existence of almost all major leptanilline lineages in the Sundan region (except *Opamyrma*, for which the male is already

known; Yamada et al., 2020), biogeography cannot be invoked to exclude *L. astylina* from any of those lineages, as is possible for the case of *Leptanilla* ci01.

Leptanilla palauensis is likewise strongly excluded by Bayesian total-evidence inference from all major clades within the Leptanillinae save for the *Leptanilla revelierii* species-group, and as is the case for *L. astylina*, this hypothesis cannot be falsified by biogeographical evidence. This is because the type locality of Babeldaob, Palau, is adjacent to the Sundan region, and therefore the arrival in Babeldaob of any leptanilline clade also present in the Malay Archipelago is plausible; the winglessness of all known *Leptanilla* gynes has not prevented the occupation of remote volcanic islands by *Leptanilla* (Baroni Urbani, 1977). The equivocal support for the placement of *L. palauensis* within the Leptanillinae (BPP=0.5) and its exclusion from the Poneroformicines (BPP=0.5) do not necessarily exclude this species from that subfamily, as *L. palauensis* fully conforms to the male-based diagnosis for the Leptanillinae provided in Chapter 4. Rather, I interpret this result as attesting to indecisiveness in the molecular and morphological data from which the phylogenetic position of *L. palauensis* was here inferred.

3.3. Rooting of the Formicidae

The results of phylogenomic analyses presented here further obfuscate the position of the Leptanillinae relative to other extant Formicidae. The phylogenetic position of the Leptanillinae and Martialinae relative to the Poneroformicines was controversial as inferred from handfuls of loci (Borowiec et al., 2019; Kück et al., 2011; Rabeling et al., 2008). Compensation for compositional bias in chosen outgroups to the Formicidae resulted in the monophyly of Martialinae + Leptanillinae (i.e., the Leptanillomorpha *sensu* Richter et al. [2021]) (Borowiec et

al., 2019). The Leptanillomorpha were robustly supported by phylogenomic inference regardless of outgroup composition (Romiguier et al., 2022).

The Leptanillinae are here retrieved as sister to the rest of the Antennoclypeata with high support, contradicting the only previous phylogenomic study with sufficient taxon sampling to test the monophyly of the Leptanillomorpha (Romiguier et al., 2022). Concordance factors demonstrate that although the position of the Leptanillinae as sister to the rest of crown group Formicidae may, in this study, be robustly supported by ML and Bayesian inference from most alignments, only a small minority of gene trees in any (untrimmed) alignment support this conclusion (gCF=20-27.7) (Figs. 5.S120-22); or, as in the case of Matrix D, support the monophyly of the Leptanillomorpha, but with an even lower fraction of gene trees concurring with that node (gCF=10) (Fig. 5.S123).

Recovery of the Leptanillinae as sister to the remainder of the extant Formicidae was found by Borowiec et al. (2019) to be an artifact of compositional biases within the Formicidae relative to outgroups, with the Leptanillinae on average having higher AT content than most of the Formicidae, including *Martialis*. By-terminal compositional bias here measured for UCEs recapitulates that previously reported across the Leptanillomorpha for 11 nuclear loci (Borowiec et al., 2019): depending on alignment, AT content of *M. heureka* ranks at 2nd- or third-lowest among the 84 UCE-enriched terminals, contrasting with the Leptanillinae (Table 5.S9). Outgroup choice is known to exert strong influence on the inferred basal topology of the Formicidae, but I included merely two outgroups beyond the limits of the Formicidae, as opposed to 13 (Borowiec et al., 2019) or 115 (Romiguier et al., 2022). I did not test the effects of altering outgroup choice. I therefore can draw no definitive conclusions concerning the monophyly of the Leptanillomorpha based on the results presented herein.

4. Conclusions

The taxonomy of the Leptanillinae has historically been impeded by the dissociation of male and female forms, which are always strikingly divergent in habitus, resulting in an artificial classification. This study presents phylogenomic inference focused on the internal phylogeny of the Leptanillinae from an array of datasets that correct for multiple potential sources of systematic bias and associated inferential error. The results provide a robust view of leptanilline phylogeny, with the only remaining point of uncertainty being relationships among the major clades of *Protanilla*. The high statistical support consistently recovered for a given basal topology of *Protanilla* by previous phylogenomic inference is here revealed to be spurious, disguising discordant phylogenetic signal. I attribute this uncertainty to gene-tree discordance. Further examination of the origins of gene-tree discordance among the major clades of *Protanilla* is in order, and in particular comparison of inferential error in gene tree estimation under ML (as in this study) and that under a Bayesian framework (Bossert et al., 2021).

In addition, Bayesian total-evidence inference provides a probabilistic resolution of the phylogenetic placement of several enigmatic leptanilline species for which molecular data are unavailable, most notably the bizarre *Leptanilla anomala*, supporting the placement of this morphospecies within the *Leptanilla havilandi* species-group, and the concomitant synonymy of *Scyphodon* with *Leptanilla*. However, Bayesian total-evidence inference from these data is insufficient to resolve the respective phylogenetic positions of three other enigmatic lineages of *Leptanilla* for which male morphology is insufficient for qualitative placement.

The sensitivity of the basal topology of the Formicidae to outgroup sampling was not queried in this study. Future work on this subject should incorporate both the extensive phylogenomic dataset for the Leptanillinae published here and greater sampling of the Apoidea and Scolioidea,

which are the first and second closest kin to the Formicoidea, respectively (Blaimer et al., 2023; Peters et al., 2017). This will test the monophyly of the Leptanillomorpha with comprehensive sampling of the Leptanillinae, addressing the problem of the basal topology of the Formicidae with a dataset that includes unprecedented taxon sampling within the Leptanillomorpha.

5. Acknowledgements

I thank Ziad Khouri, Mark Miller, and Wayne Pfeiffer for their analytical help at various stages of this project, and Michael Branstetter for assembly of the new phylogenomic data here published. I thank Bonnie Blaimer (ZMHB), Chris Darling (ROME), Brennen Dyer (UCDC), Brian Fisher (CASC), José María Gómez-Durán, Benoit Guénard (HKUBM), Po-Wei Hsu (NCUE), Debbie Jennings (ANIC), Eugenia Okonski (USNM), Jadranka Rota (MZLU), Suzanne Ryder (NHMUK), Lars Vilhelmsen (ZMUC), Kevin Williams (CSCA) and Masashi Yoshimura (OIST) for loans or gifts of material used in this study. I also thank Bui Tuan Viet, Katsuyuki Eguchi, Michael Ohl, Christian Rabeling and Michael Sharkey for material sequenced by Borowiec et al. (2019) that was also included in this study. This project was supported in part by NSF grant DEB-1932405 to P. S. Ward, the UC-Davis Dept. of Entomology, the Helmsley Charitable Trust, and SI Global Genome Initiative.

Supplementary Tables, Chapter 5

Table 5.S1. Relevant collection data for specimens included in this study for which UCEs were newly enriched.

Table 5.S2. Summary statistics for 283,523-bp, 490-locus UCE alignment (Matrix A).

Table 5.S3. Relevant collection data for specimens included in this study for which UCEs were not enriched.

Table 5.S4. Matrix of 64 binary male morphological characters used for Bayesian total-evidence inference in this study.

Table 5.S5. Summary statistics for untrimmed 166,662-bp, 287-locus UCE alignment (Matrix B).

Table 5.S6. Summary statistics for untrimmed 116,849-bp, 203-locus alignment (Matrix C).

Table 5.S7. Summary statistics for untrimmed 15,354-bp, 62-locus alignment (Matrix D).

Table 5.S8. Summary statistics for untrimmed 34,039-bp, 58-locus alignment (Matrix B′).

Table 5.S9. Ranking of relative AT-content, and respective AT percentages, for all UCE-enriched terminals across Matrices A-D and B′.

Abadi, S., Azouri, D., Pupko, T., Mayrose, I., 2019. Model selection may not be a mandatory step for phylogeny reconstruction. Nat. Commun. 10, 934. https://doi.org/10.1038/s41467-019-08822-w

Aberer, A.J., Kobert, K., Stamatakis, A., 2014. ExaBayes: massively parallel Bayesian tree inference for the whole-genome era. Mol. Biol. Evol. 31, 2553–2556. https://doi.org/10.1093/molbev/msu236

Bankevich, A., Nurk, S., Antipov, D., Gurevich, A.A., Dvorkin, M., Kulikov, A.S., Lesin, V.M., Nikolenko, S.I., Pham, S., Prjibelski, A.D., Pyshkin, A.V., Sirotkin, A.V., Vyahhi, N., Tesler, G., Alekseyev, M.A., Pevzner, P.A., 2012. Spades: a new genome assembly algorithm and its applications to single-cell sequencing. J. Comput. Biol. 19, 455–477. https://doi.org/10.1089/cmb.2012.0021

Barandica, J.M., López, F., Martínez, M.D., Ortuño, V.M., 1994. The larvae of *Leptanilla charonea* and *Leptanilla zaballosi* (Hymenoptera, Formicidae). Dtsch. Entomol. Z. 41, 147–153. https://doi.org/10.1002/mmnd.19940410113

Barden, P., Boudinot, B., Lucky, A., Barden, P., Boudinot, B., Lucky, A., 2017. Where Fossils Dare and Males Matter: combined morphological and molecular analysis untangles the evolutionary history of the spider ant genus <i>Leptomyrmex<i/> Mayr (Hymenoptera : Dolichoderinae). Invertebr. Syst. 31, 765–780. https://doi.org/10.1071/IS16067

Baroni Urbani, C., 1977. Materiali per una revisione della sottofamiglia Leptanillinae Emery (Hymenoptera: Formicidae). Entomol. Basiliensia 2, 427–488.

Betancur-R., R., Arcila, D., Vari, R.P., Hughes, L.C., Oliveira, C., Sabaj, M.H., Ortí, G., 2019. Phylogenomic incongruence, hypothesis testing, and taxonomic sampling: The monophyly of characiform fishes*. Evolution 73, 329–345. https://doi.org/10.1111/evo.13649

Blaimer, B.B., Santos, B.F., Cruaud, A., Gates, M.W., Kula, R.R., Mikó, I., Rasplus, J.-Y., Smith, D.R., Talamas, E.J., Brady, S.G., Buffington, M.L., 2023. Key innovations and the diversification of Hymenoptera. Nat. Commun. 14, 1212. https://doi.org/10.1038/s41467-023-36868-4

Bolton, B., 1990. The higher classification of the ant subfamily Leptanillinae (Hymenoptera: Formicidae). Syst. Entomol. 15, 267–282. https://doi.org/10.1111/j.1365-3113.1990.tb00063.x

Borowiec, M.L., 2019a. Convergent evolution of the army ant syndrome and congruence in big-data phylogenetics. Syst. Biol. 68, 642–656. https://doi.org/10.1093/sysbio/syy088

Borowiec, M.L., 2019b. Spruceup: fast and flexible identification, visualization, and removal of outliers from large multiple sequence alignments. J. Open Source Softw. 4, 1635. https://doi.org/10.21105/joss.01635

Borowiec, M.L., 2016. AMAS: a fast tool for alignment manipulation and computing of summary statistics. PeerJ 4, e1660. https://doi.org/10.7717/peerj.1660

Borowiec, M.L., Rabeling, C., Brady, S.G., Fisher, B.L., Schultz, T.R., Ward, P.S., 2019. Compositional heterogeneity and outgroup choice influence the internal phylogeny of the ants. Mol. Phylogenet. Evol. 134, 111–121. https://doi.org/10.1016/j.ympev.2019.01.024

Bossert, S., Murray, E.A., Pauly, A., Chernyshov, K., Brady, S.G., Danforth, B.N., 2021. Gene Tree Estimation Error with Ultraconserved Elements: An Empirical Study on *Pseudapis* Bees. Syst. Biol. 70, 803–821. https://doi.org/10.1093/sysbio/syaa097

Boudinot, B.E., 2015. Contributions to the knowledge of Formicidae (Hymenoptera, Aculeata): a new diagnosis of the family, the first global male-based key to subfamilies, and a treatment of early branching lineages. Eur. J. Taxon. https://doi.org/10.5852/ejt.2015.120

Boudinot, B.E., Khouri, Z., Richter, A., Griebenow, Z.H., Kamp, T. van de, Perrichot, V., Barden, P., 2022. Evolution and systematics of the Aculeata and kin (Hymenoptera), with emphasis on the ants (Formicoidea: †@@@idae fam. nov., Formicidae). https://doi.org/10.1101/2022.02.20.480183

Branstetter, M.G., Longino, J.T., Ward, P.S., Faircloth, B.C., 2017. Enriching the ant tree of life: enhanced UCE bait set for genome-scale phylogenetics of ants and other Hymenoptera. Methods Ecol. Evol. 8, 768–776. https://doi.org/10.1111/2041-210X.12742

Brazeau, M.D., 2011. Problematic character coding methods in morphology and their effects. Biol. J. Linn. Soc. 104, 489–498. https://doi.org/10.1111/j.1095-8312.2011.01755.x

Brown, J.M., Thomson, R.C., 2017. Bayes factors unmask highly variable information content, bias, and extreme influence in phylogenomic analyses. Syst. Biol. 66, 517–530. https://doi.org/10.1093/sysbio/syw101

Brues, C., 1925. *Scyphodon*, an anomalous genus of Hymenoptera of doubtful affinities. Treubia 6, 93–96.

Castresana, J., 2000. Selection of conserved blocks from multiple alignments for their use in phylogenetic analysis. Mol. Biol. Evol. 17, 540–552. https://doi.org/10.1093/oxfordjournals.molbev.a026334

Chan, K.O., Hutter, C.R., Wood, P.L., Grismer, L.L., Brown, R.M., 2020. Larger, unfiltered datasets are more effective at resolving phylogenetic conflict: Introns, exons, and UCEs resolve ambiguities in Golden-backed frogs (Anura: Ranidae; genus Hylarana). Mol. Phylogenet. Evol. 151, 106899. https://doi.org/10.1016/j.ympev.2020.106899

Duchêne, D.A., Mather, N., Van Der Wal, C., Ho, S.Y.W., 2022. Excluding loci with substitution saturation improves inferences from phylogenomic data. Syst. Biol. 71, 676–689. https://doi.org/10.1093/sysbio/syab075

Faircloth, B.C., 2016. PHYLUCE is a software package for the analysis of conserved genomic loci. Bioinformatics 32, 786–788. https://doi.org/10.1093/bioinformatics/btv646

Felsenstein, J., 1981. Evolutionary trees from DNA sequences: A maximum likelihood approach. J. Mol. Evol. 17, 368–376. https://doi.org/10.1007/BF01734359

Gillung, J.P., Winterton, S.L., Bayless, K.M., Khouri, Z., Borowiec, M.L., Yeates, D., Kimsey, L.S., Misof, B., Shin, S., Zhou, X., Mayer, C., Petersen, M., Wiegmann, B.M., 2018. Anchored phylogenomics unravels the evolution of spider flies (Diptera, Acroceridae) and reveals discordance between nucleotides and amino acids. Mol. Phylogenet. Evol. 128, 233–245. https://doi.org/10.1016/j.ympev.2018.08.007

Glenn, T.C., Nilsen, R.A., Kieran, T.J., Sanders, J.G., Bayona-Vásquez, N.J., Finger, J.W., Pierson, T.W., Bentley, K.E., Hoffberg, S.L., Louha, S., Leon, F.J.G.-D., Portilla, M.A. del R., Reed, K.D., Anderson, J.L., Meece, J.K., Aggrey, S.E., Rekaya, R., Alabady, M., Belanger, M.,

Winker, K., Faircloth, B.C., 2019. Adapterama I: universal stubs and primers for 384 unique dual-indexed or 147,456 combinatorially-indexed Illumina libraries (iTru & iNext). PeerJ 7, e7755. https://doi.org/10.7717/peerj.7755

Griebenow, Z., 2020. Delimitation of tribes in the subfamily Leptanillinae (Hymenoptera: Formicidae), with a description of the male of *Protanilla lini* Terayama, 2009. Myrmecol. News 30.

Griebenow, Z.H., 2021. Synonymisation of the male-based ant genus *Phaulomyrma* (Hymenoptera: Formicidae) with Leptanilla based upon Bayesian total-evidence phylogenetic inference. Invertebr. Syst. https://doi.org/10.1071/IS20059

Griebenow, Z.H., Isaia, M., Moradmand, M., 2022. A remarkable troglomorphic ant, *Yavnella laventa* sp. nov. (Hymenoptera: Formicidae: Leptanillinae), identified as the first known worker of *Yavnella* Kugler by phylogenomic inference. Invertebr. Syst. 36, 1118–1138. https://doi.org/10.1071/IS22035

Hoang, D.T., Chernomor, O., von Haeseler, A., Minh, B.Q., Vinh, L.S., 2018. UFBoot2: improving the ultrafast bootstrap approximation. Mol. Biol. Evol. 35, 518–522. https://doi.org/10.1093/molbev/msx281

Höhna, S., Landis, M.J., Heath, T.A., 2017. Phylogenetic inference using RevBayes. Curr. Protoc. Bioinforma. 57, 6.16.1-6.16.34. https://doi.org/10.1002/cpbi.22

Hsu, P.-W., Hsu, F.-C., Hsiao, Y., Lin, C.-C., 2017. Taxonomic notes on the genus *Protanilla* (Hymenoptera: Formicidae: Leptanillinae) from Taiwan. Zootaxa 4268, 117–130. https://doi.org/10.11646/zootaxa.4268.1.7

Ito, F., Hashim, R., Mizuno, R., Billen, J., 2022. Notes on the biology of *Protanilla* sp. (Hymenoptera, Formicidae) collected in Ulu Gombak, Peninsular Malaysia. Insectes Sociaux 69, 13–18. https://doi.org/10.1007/s00040-021-00839-z

Jermiin, L.S., Ho, S.Y.W., Ababneh, F., Robinson, J., Larkum, A.W.D., 2004. The biasing effect of compositional heterogeneity on phylogenetic estimates may be underestimated. Syst. Biol. 53, 638–643. https://doi.org/10.1080/10635150490468648

Kalyaanamoorthy, S., Minh, B.Q., Wong, T.K.F., von Haeseler, A., Jermiin, L.S., 2017. ModelFinder: fast model selection for accurate phylogenetic estimates. Nat. Methods 14, 587–589. https://doi.org/10.1038/nmeth.4285

Katoh, K., Toh, H., 2010. Parallelization of the MAFFT multiple sequence alignment program. Bioinformatics 26, 1899–1900. https://doi.org/10.1093/bioinformatics/btq224

Klopfstein, S., Massingham, T., Goldman, N., 2017. More on the best evolutionary rate for phylogenetic analysis. Syst. Biol. 66, 769–785. https://doi.org/10.1093/sysbio/syx051

Kubatko, L.S., Degnan, J.H., 2007. Inconsistency of phylogenetic estimates from concatenated data under coalescence. Syst. Biol. 56, 17–24. https://doi.org/10.1080/10635150601146041

Kück, P., Garcia, F.H., Misof, B., Meusemann, K., 2011. Improved phylogenetic analyses corroborate a plausible position of *Martialis heureka* in the ant tree of life. PLOS ONE 6, e21031. https://doi.org/10.1371/journal.pone.0021031

Kulkarni, S., Kallal, R.J., Wood, H., Dimitrov, D., Giribet, G., Hormiga, G., 2021. Interrogating genomic-scale data to resolve recalcitrant nodes in the spider tree of life. Mol. Biol. Evol. 38, 891–903. https://doi.org/10.1093/molbev/msaa251

Lewis, P.O., 2001. A likelihood approach to estimating phylogeny from discrete morphological character data. Syst. Biol. 50, 913–925. https://doi.org/10.1080/106351501753462876

Lucky, A., Trautwein, M.D., Guénard, B.S., Weiser, M.D., Dunn, R.R., 2013. Tracing the rise of ants - out of the ground. PLOS ONE 8, e84012. https://doi.org/10.1371/journal.pone.0084012

Maddison, W.P., 1997. Gene trees in species trees. Syst. Biol. 46, 523–536. https://doi.org/10.1093/sysbio/46.3.523

Masuko, K., 1990. Behavior and ecology of the enigmatic ant *Leptanilla japonica* Baroni Urbani (Hymenoptera: Formicidae: Leptanillinae). Insectes Sociaux 37, 31–57. https://doi.org/10.1007/BF02223813

Minh, B.Q., Hahn, M.W., Lanfear, R., 2020a. New methods to calculate concordance factors for phylogenomic datasets. Mol. Biol. Evol. 37, 2727–2733. https://doi.org/10.1093/molbev/msaa106

Minh, B.Q., Schmidt, H.A., Chernomor, O., Schrempf, D., Woodhams, M.D., von Haeseler, A., Lanfear, R., 2020b. IQ-TREE 2: new models and efficient methods for phylogenetic inference in the genomic era. Mol. Biol. Evol. 37, 1530–1534. https://doi.org/10.1093/molbev/msaa015

Mirarab, S., Reaz, R., Bayzid, Md.S., Zimmermann, T., Swenson, M.S., Warnow, T., 2014. ASTRAL: genome-scale coalescent-based species tree estimation. Bioinformatics 30, i541–i548. https://doi.org/10.1093/bioinformatics/btu462

Mirarab, S., Warnow, T., 2015. ASTRAL-II: coalescent-based species tree estimation with many hundreds of taxa and thousands of genes. Bioinformatics 31, i44–i52. https://doi.org/10.1093/bioinformatics/btv234

Mongiardino Koch, N., 2021. Phylogenomic subsampling and the search for phylogenetically reliable loci. Mol. Biol. Evol. 38, 4025–4038. https://doi.org/10.1093/molbev/msab151

Moreau, C.S., Bell, C.D., 2013. Testing the museum versus cradle tropical biological diversity hypothesis: phylogeny, diversification, and ancestral biogeographic range evolution of the ants. Evolution 67, 2240–2257. https://doi.org/10.1111/evo.12105

Naser-Khdour, S., Minh, B.Q., Zhang, W., Stone, E.A., Lanfear, R., 2019. The prevalence and impact of model violations in phylogenetic analysis. Genome Biol. Evol. 11, 3341–3352. https://doi.org/10.1093/gbe/evz193

Nguyen, L.-T., von Haeseler, A., Minh, B.Q., 2018. Complex models of sequence evolution require accurate estimators as exemplified with the invariable site plus gamma model. Syst. Biol. 67, 552–558. https://doi.org/10.1093/sysbio/syx092

Ogata, K., Terayama, M., Masuko, K., 1995. The ant genus *Leptanilla*: discovery of the worker-associated male of L. japonica, and a description of a new species from Taiwan (Hymenoptera: Formicidae: Leptanillinae). Syst. Entomol. 20, 27–34. https://doi.org/10.1111/j.1365-3113.1995.tb00081.x

Peters, R.S., Krogmann, L., Mayer, C., Donath, A., Gunkel, S., Meusemann, K., Kozlov, A., Podsiadlowski, L., Petersen, M., Lanfear, R., Diez, P.A., Heraty, J., Kjer, K.M., Klopfstein, S., Meier, R., Polidori, C., Schmitt, T., Liu, S., Zhou, X., Wappler, T., Rust, J., Misof, B., Niehuis, O., 2017. Evolutionary history of the Hymenoptera. Curr. Biol. 27, 1013–1018. https://doi.org/10.1016/j.cub.2017.01.027

Petersen, B., 1968. Some novelties in presumed males of the Leptanillinae (Hym., Formicidae). Entomol. Meddelelser 36, 577–598.

Philippe, H., Delsuc, F., Brinkmann, H., Lartillot, N., 2005. Phylogenomics. Annu. Rev. Ecol. Evol. Syst. 36, 541–562. https://doi.org/10.1146/annurev.ecolsys.35.112202.130205

Pleijel, F., 1995. On character coding for phylogeny reconstruction. Cladistics 11, 309–315. https://doi.org/10.1016/0748-3007(95)90018-7

Rabeling, C., Brown, J.M., Verhaagh, M., 2008. Newly discovered sister lineage sheds light on early ant evolution. Proc. Natl. Acad. Sci. 105, 14913–14917. https://doi.org/10.1073/pnas.0806187105

Reddy, S., Kimball, R.T., Pandey, A., Hosner, P.A., Braun, M.J., Hackett, S.J., Han, K.-L., Harshman, J., Huddleston, C.J., Kingston, S., Marks, B.D., Miglia, K.J., Moore, W.S., Sheldon, F.H., Witt, C.C., Yuri, T., Braun, E.L., 2017. Why do phylogenomic data sets yield conflicting trees? Data type influences the avian tree of life more than taxon sampling. Syst. Biol. 66, 857–879. https://doi.org/10.1093/sysbio/syx041

Rohland, N., Reich, D., 2012. Cost-effective, high-throughput DNA sequencing libraries for multiplexed target capture. Genome Res. 22, 939–946. https://doi.org/10.1101/gr.128124.111

Romiguier, J., Borowiec, M.L., Weyna, A., Helleu, Q., Loire, E., La Mendola, C., Rabeling, C., Fisher, B.L., Ward, P.S., Keller, L., 2022. Ant phylogenomics reveals a natural selection hotspot preceding the origin of complex eusociality. Curr. Biol. 32, 2942-2947.e4. https://doi.org/10.1016/j.cub.2022.05.001

Romiguier, J., Cameron, S.A., Woodard, S.H., Fischman, B.J., Keller, L., Praz, C.J., 2016. Phylogenomics controlling for base compositional bias reveals a single origin of eusociality in corbiculate bees. Mol. Biol. Evol. 33, 670–678. https://doi.org/10.1093/molbev/msv258

Romiguier, J., Ranwez, V., Delsuc, F., Galtier, N., Douzery, E.J.P., 2013. Less is more in mammalian phylogenomics: AT-rich genes minimize tree conflicts and unravel the root of placental mammals. Mol. Biol. Evol. 30, 2134–2144. https://doi.org/10.1093/molbev/mst116

Rosa, B.B., Melo, G.A.R., Barbeitos, M.S., 2019. Homoplasy-based partitioning outperforms alternatives in Bayesian analysis of discrete morphological data. Syst. Biol. 68, 657–671. https://doi.org/10.1093/sysbio/syz001

Sayyari, E., Mirarab, S., 2016. Fast coalescent-based computation of local branch support from quartet frequencies. Mol. Biol. Evol. 33, 1654–1668. https://doi.org/10.1093/molbev/msw079

Tagliacollo, V.A., Lanfear, R., 2018. Estimating improved partitioning schemes for ultraconserved elements. Mol. Biol. Evol. 35, 1798–1811. https://doi.org/10.1093/molbev/msy069

Thomson, R.C., Brown, J.M., 2022. On the need for new measures of phylogenomic support. Syst. Biol. 71, 917–920. https://doi.org/10.1093/sysbio/syac002

Vasilikopoulos, A., Misof, B., Meusemann, K., Lieberz, D., Flouri, T., Beutel, R.G., Niehuis, O., Wappler, T., Rust, J., Peters, R.S., Donath, A., Podsiadlowski, L., Mayer, C., Bartel, D., Böhm, A., Liu, S., Kapli, P., Greve, C., Jepson, J.E., Liu, X., Zhou, X., Aspöck, H., Aspöck, U., 2020. An integrative phylogenomic approach to elucidate the evolutionary history and divergence times of Neuropterida (Insecta: Holometabola). BMC Evol. Biol. 20, 64. https://doi.org/10.1186/s12862-020-01631-6

Vilhelmsen, L., Miko, I., Krogmann, L., 2010. Beyond the wasp-waist: structural diversity and phylogenetic significance of the mesosoma in apocritan wasps (Insecta: Hymenoptera). Zool. J. Linn. Soc. 159, 22–194. https://doi.org/10.1111/j.1096-3642.2009.00576.x

Ward, P.S., Fisher, B.L., 2016. Tales of dracula ants: the evolutionary history of the ant subfamily Amblyoponinae (Hymenoptera: Formicidae). Syst. Entomol. 41, 683–693. https://doi.org/10.1111/syen.12186

Xu, Z.-H., 2012. *Furcotanilla*, a new genus of the ant subfamily Leptanillinae from China with descriptions of two new species of *Protanilla* and *P. rafflesi* Taylor (Hymenoptera: Formicidae). Sociobiology 59, 477–491. https://doi.org/10.13102/sociobiology.v59i2.612

Yang, Z., 1996. Among-site rate variation and its impact on phylogenetic analyses. Trends Ecol. Evol. 11, 367–372. https://doi.org/10.1016/0169-5347(96)10041-0

Zhang, C., Rabiee, M., Sayyari, E., Mirarab, S., 2018. ASTRAL-III: polynomial time species tree reconstruction from partially resolved gene trees. BMC Bioinformatics 19, 153. https://doi.org/10.1186/s12859-018-2129-y

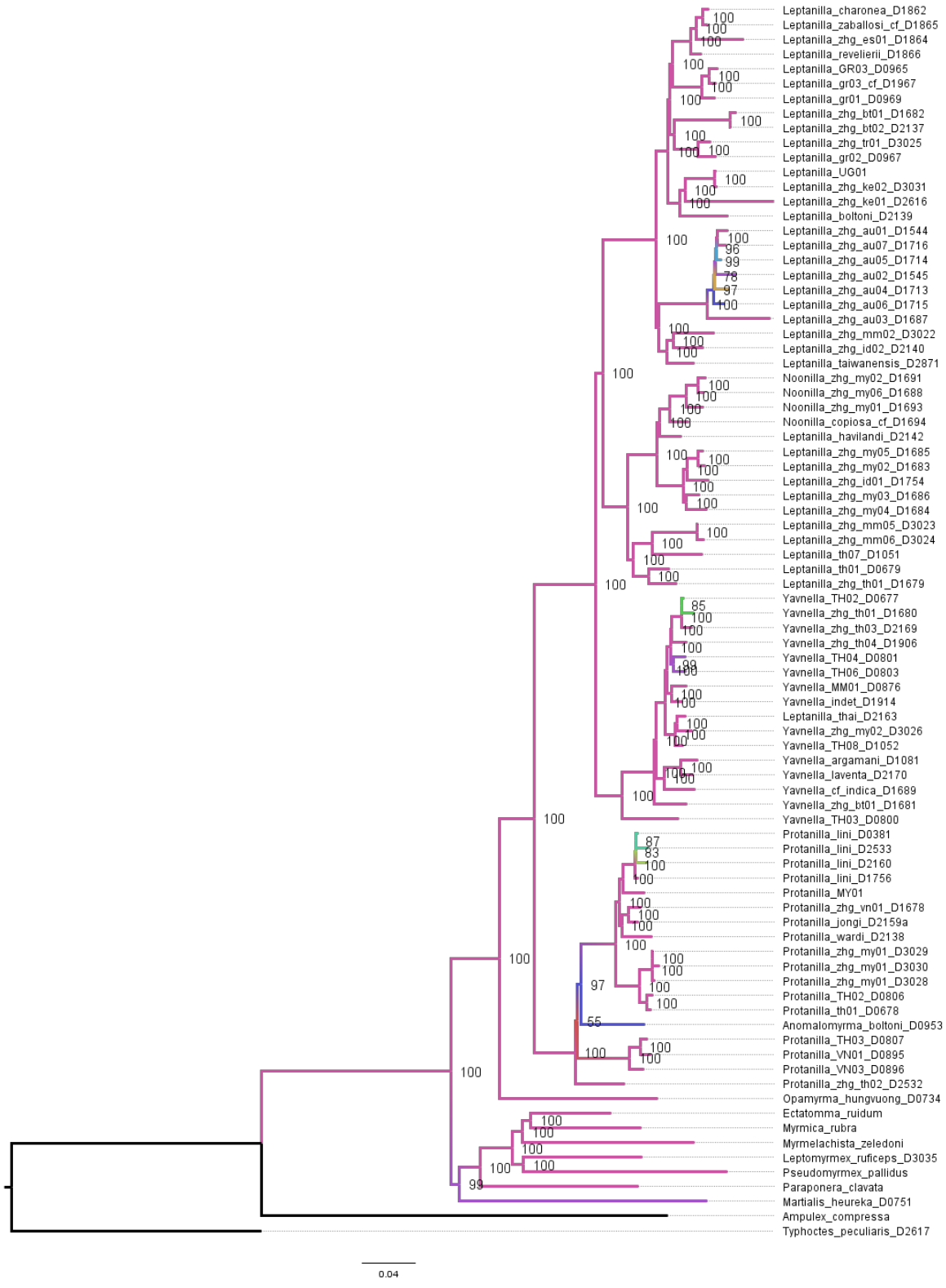
Leptanilla_charonea_D1862
Leptanilla_zaballosi_cf_D1865
Leptanilla_zhg_es01_D1864
Leptanilla_revelierii_D1866
Leptanilla_GR03_D0965
Leptanilla_gr03_cf_D1967
Leptanilla_gr01_D0969
Leptanilla_zhg_bt01_D1682
Leptanilla_zhg_bt02_D2137
Leptanilla_zhg_tr01_D3025
Leptanilla_gr02_D0967
Leptanilla_UG01
Leptanilla_zhg_ke02_D3031
Leptanilla_zhg_ke01_D2616
Leptanilla_boltoni_D2139
Leptanilla_zhg_au01_D1544
Leptanilla_zhg_au07_D1716
Leptanilla_zhg_au05_D1714
Leptanilla_zhg_au02_D1545
Leptanilla_zhg_au04_D1713
Leptanilla_zhg_au06_D1715
Leptanilla_zhg_au03_D1687
Leptanilla_zhg_mm02_D3022
Leptanilla_zhg_id02_D2140
Leptanilla_taiwanensis_D2871
Noonilla_zhg_my02_D1691
Noonilla_zhg_my06_D1688
Noonilla_zhg_my01_D1693
Noonilla_copiosa_cf_D1694
Leptanilla_havilandi_D2142
Leptanilla_zhg_my05_D1685
Leptanilla_zhg_my02_D1683
Leptanilla_zhg_id01_D1754
Leptanilla_zhg_my03_D1686
Leptanilla_zhg_my04_D1684
Leptanilla_zhg_mm05_D3023
Leptanilla_zhg_mm06_D3024
Leptanilla_th07_D1051
Leptanilla_th01_D0679
Leptanilla_zhg_th01_D1679
Yavnella_TH02_D0677
Yavnella_zhg_th01_D1680
Yavnella_zhg_th03_D2169
Yavnella_zhg_th04_D1906
Yavnella_TH04_D0801
Yavnella_TH06_D0803
Yavnella_MM01_D0876
Yavnella_indet_D1914
Leptanilla_thai_D2163
Yavnella_zhg_my02_D3026
Yavnella_TH08_D1052
Yavnella_argamani_D1081
Yavnella_laventa_D2170
Yavnella_cf_indica_D1689
Yavnella_zhg_bt01_D1681
Yavnella_TH03_D0800
Protanilla_lini_D0381
Protanilla_lini_D2533
Protanilla_lini_D2160
Protanilla_lini_D1756
Protanilla_MY01
Protanilla_zhg_vn01_D1678
Protanilla_jongi_D2159a
Protanilla_wardi_D2138
Protanilla_zhg_my01_D3029
Protanilla_zhg_my01_D3030
Protanilla_zhg_my01_D3028
Protanilla_TH02_D0806
Protanilla_th01_D0678
Anomalomyrma_boltoni_D0953
Protanilla_TH03_D0807
Protanilla_VN01_D0895
Protanilla_VN03_D0896
Protanilla_zhg_th02_D2532
Opamyrma_hungvuong_D0734
Ectatomma_ruidum
Myrmica_rubra
Myrmelachista_zeledoni
Leptomyrmex_ruficeps_D3035
Pseudomyrmex_pallidus
Paraponera_clavata
Martialis_heureka_D0751
Ampulex_compressa
Typhoctes_peculiaris_D2617
0.04

Fig. 5.S1. Phylogeny of the Leptanillinae and nine outgroup terminals, as inferred under ML with by-locus partitioning from Matrix 0.8A.

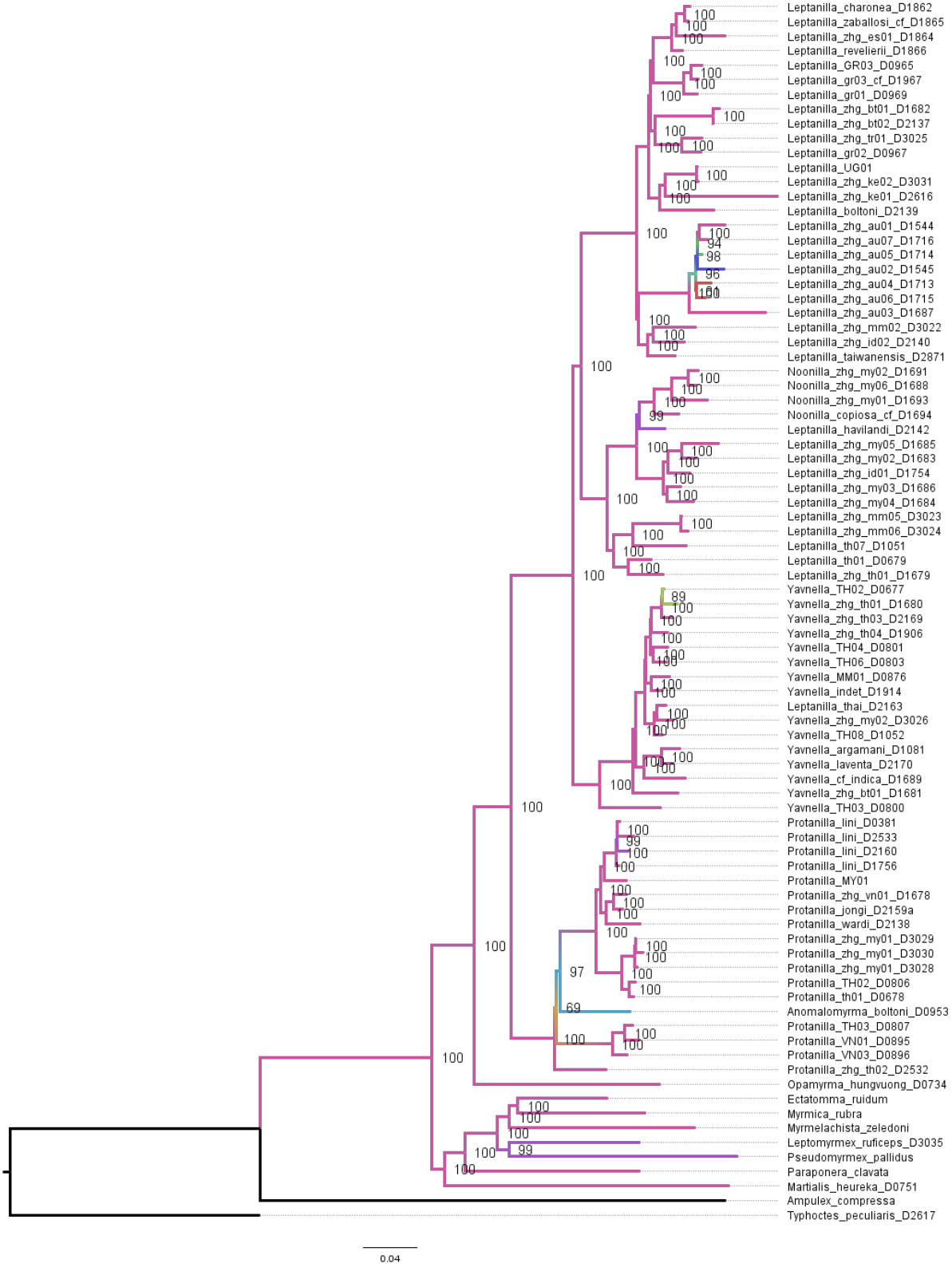

Fig. 5.S2. Phylogeny of the Leptanillinae and nine outgroup terminals, as inferred under ML with within-locus partitioning from Matrix 0.8A.

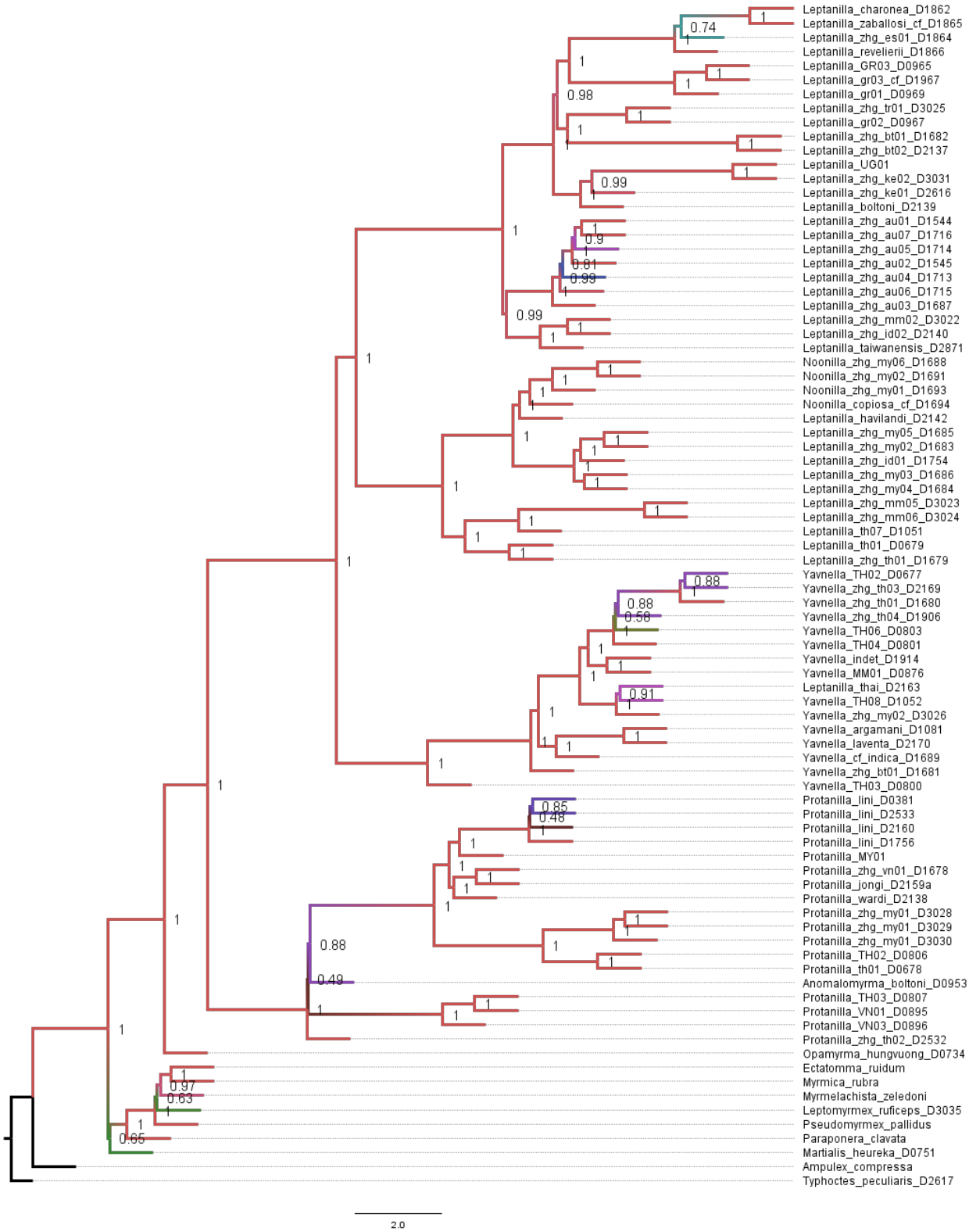

Fig. 5.S3. Phylogeny of the Leptanillinae and nine outgroup terminals, as inferred under a coalescent-based approach from Matrix 0.8A.

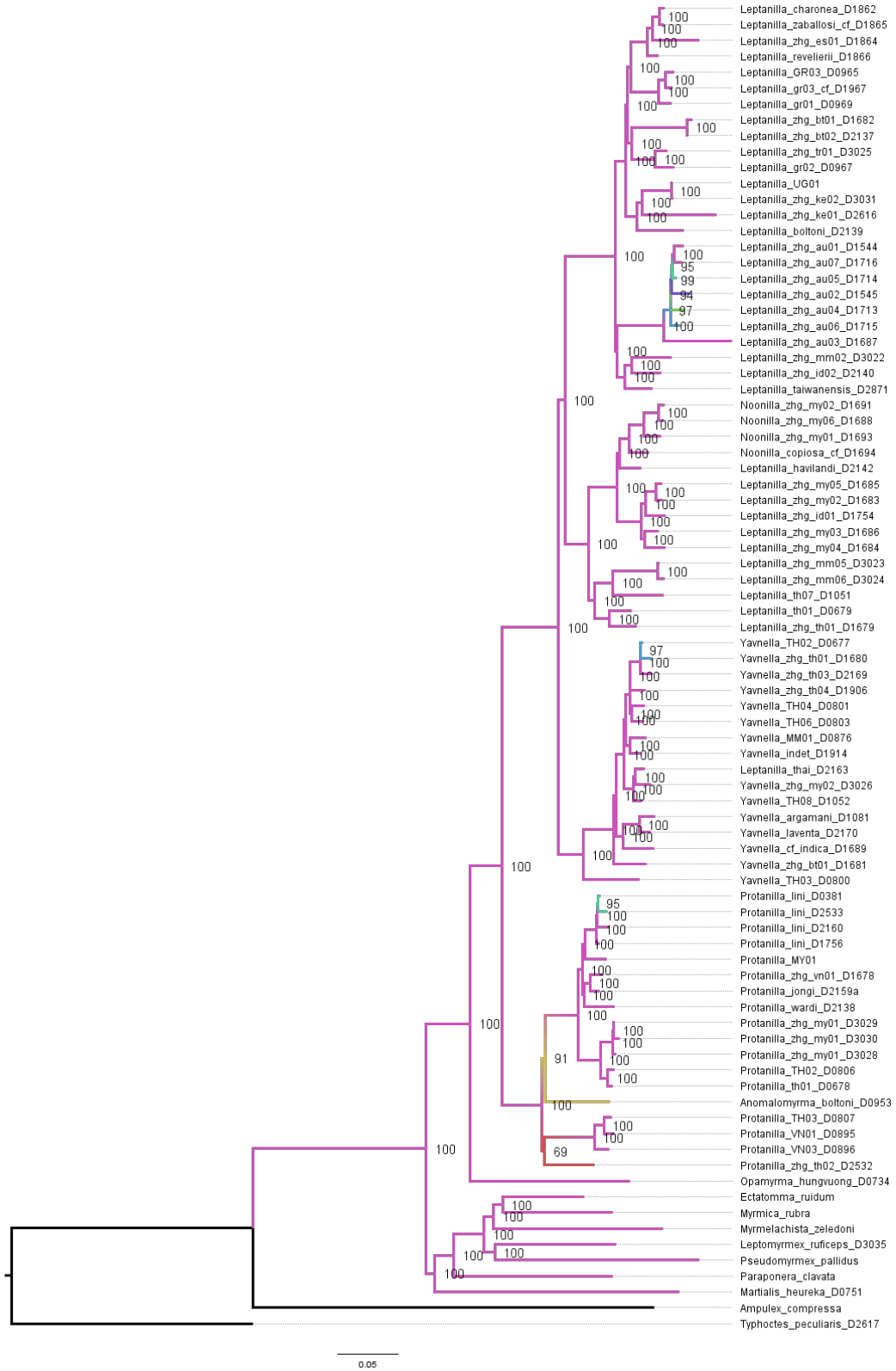

Fig. 5.S4. Phylogeny of the Leptanillinae and nine outgroup terminals, as inferred under ML with by-locus partitioning from Matrix 0.85A.

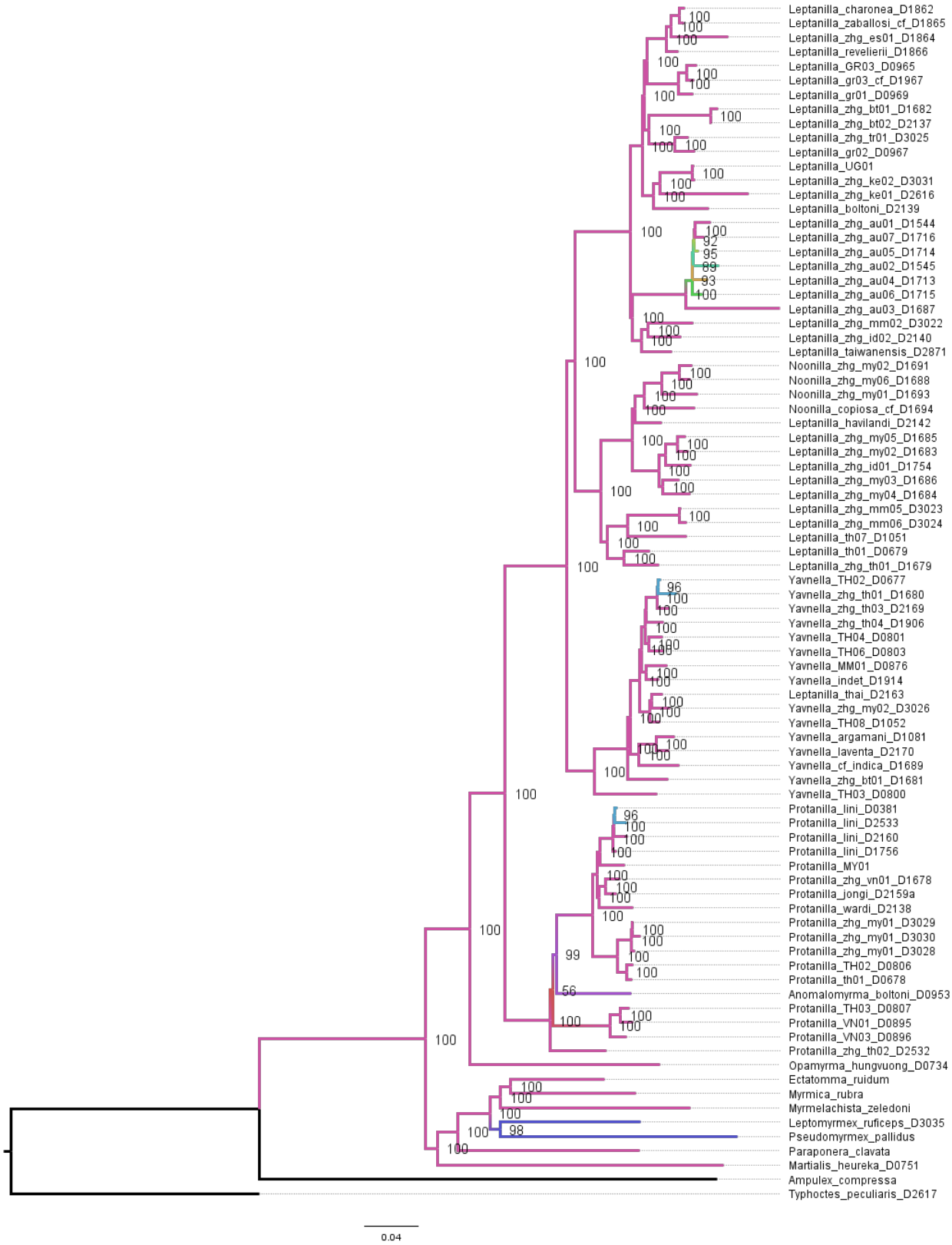

Fig. 5.S5. Phylogeny of the Leptanillinae and nine outgroup terminals, as inferred under ML with within-locus partitioning from Matrix 0.85A.

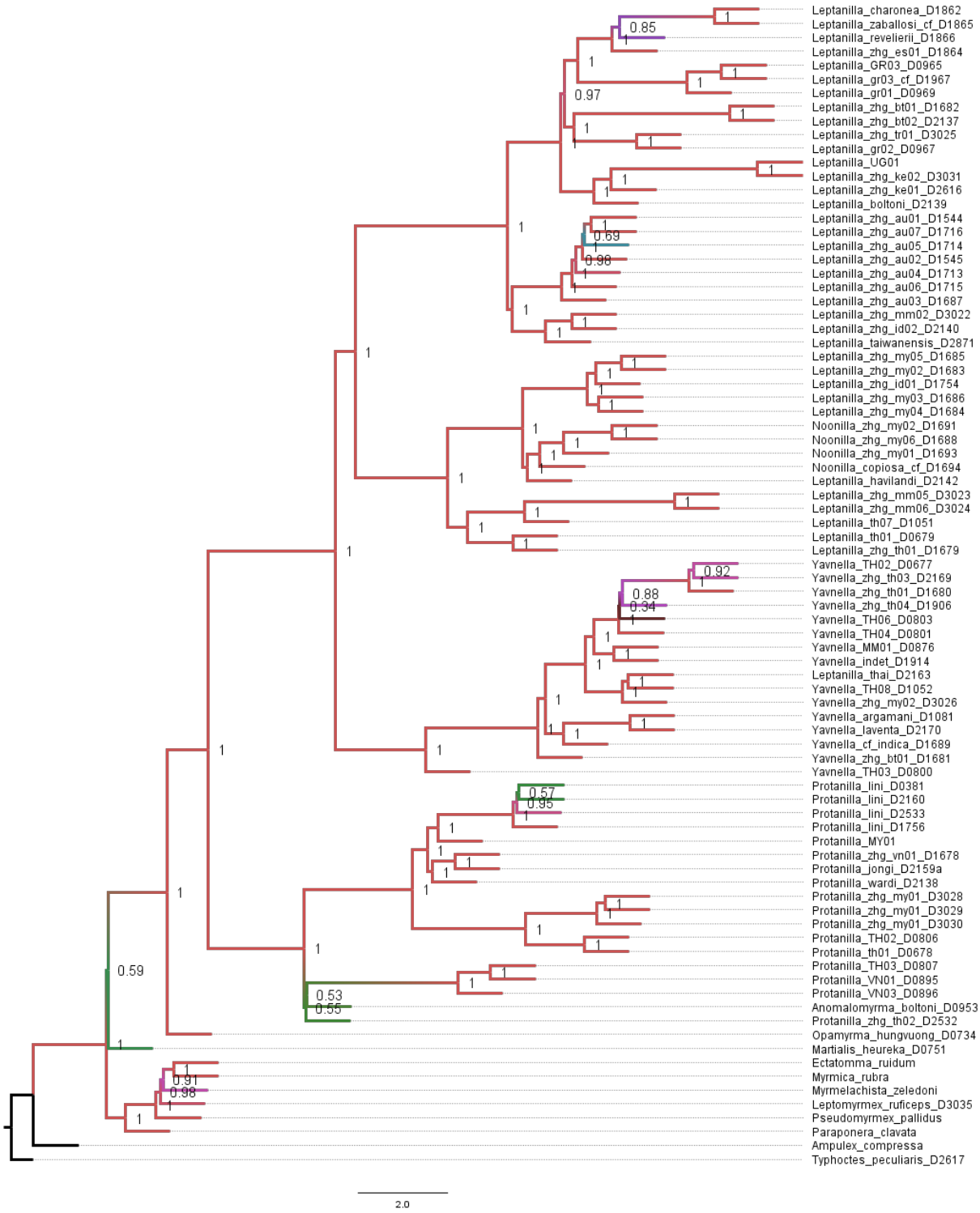

Fig. 5.S6. Phylogeny of the Leptanillinae and nine outgroup terminals, as inferred under a coalescent-based approach from Matrix 0.85A.

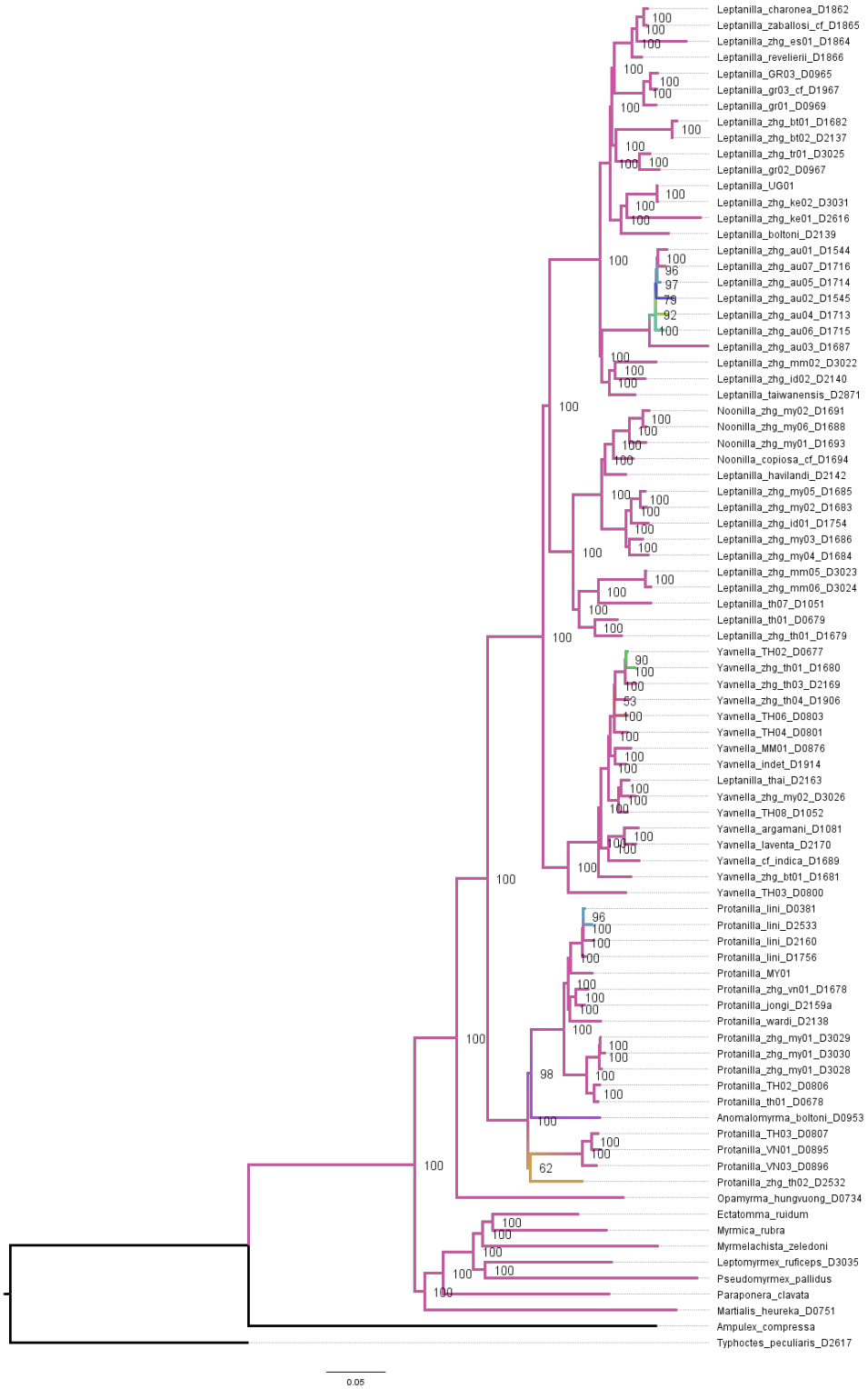

Fig. 5.S7. Phylogeny of the Leptanillinae and nine outgroup terminals, as inferred under ML with by-locus partitioning from Matrix 0.9A.

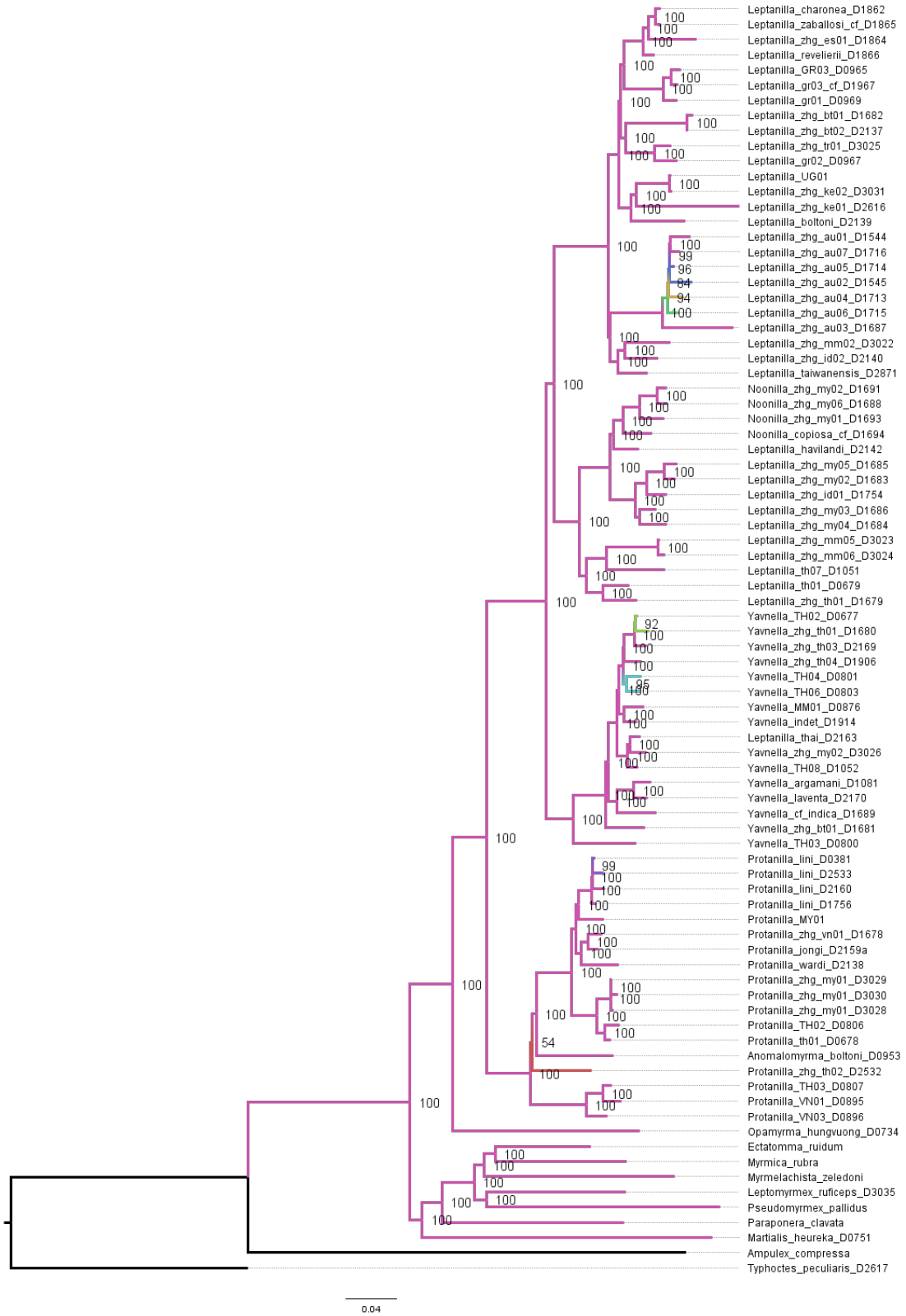

Fig. 5.S8. Phylogeny of the Leptanillinae and nine outgroup terminals, as inferred under ML with within-locus partitioning from Matrix 0.9A.

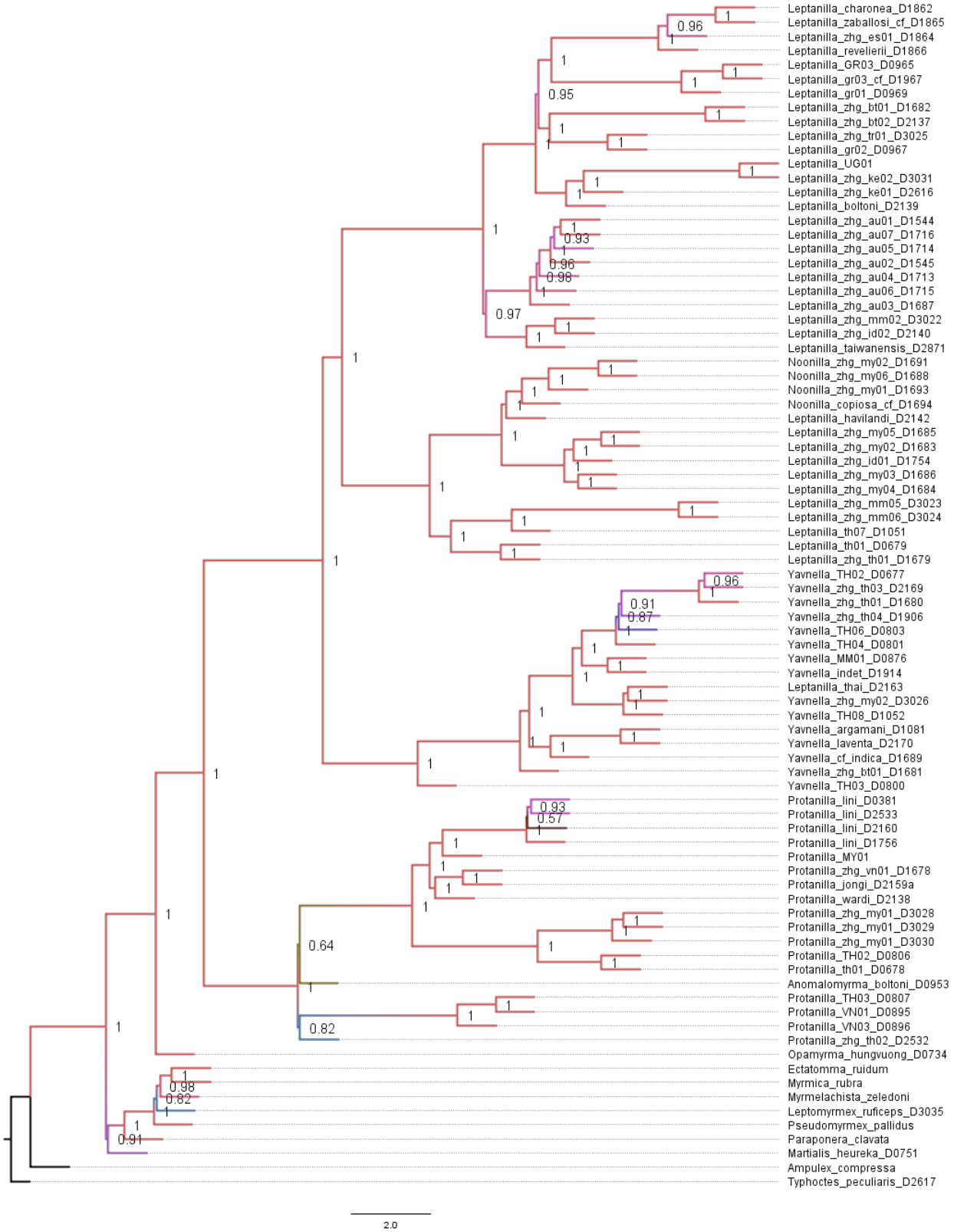

Fig. 5.S9. Phylogeny of the Leptanillinae and nine outgroup terminals, as inferred under a coalescent-based approach from Matrix 0.9A.

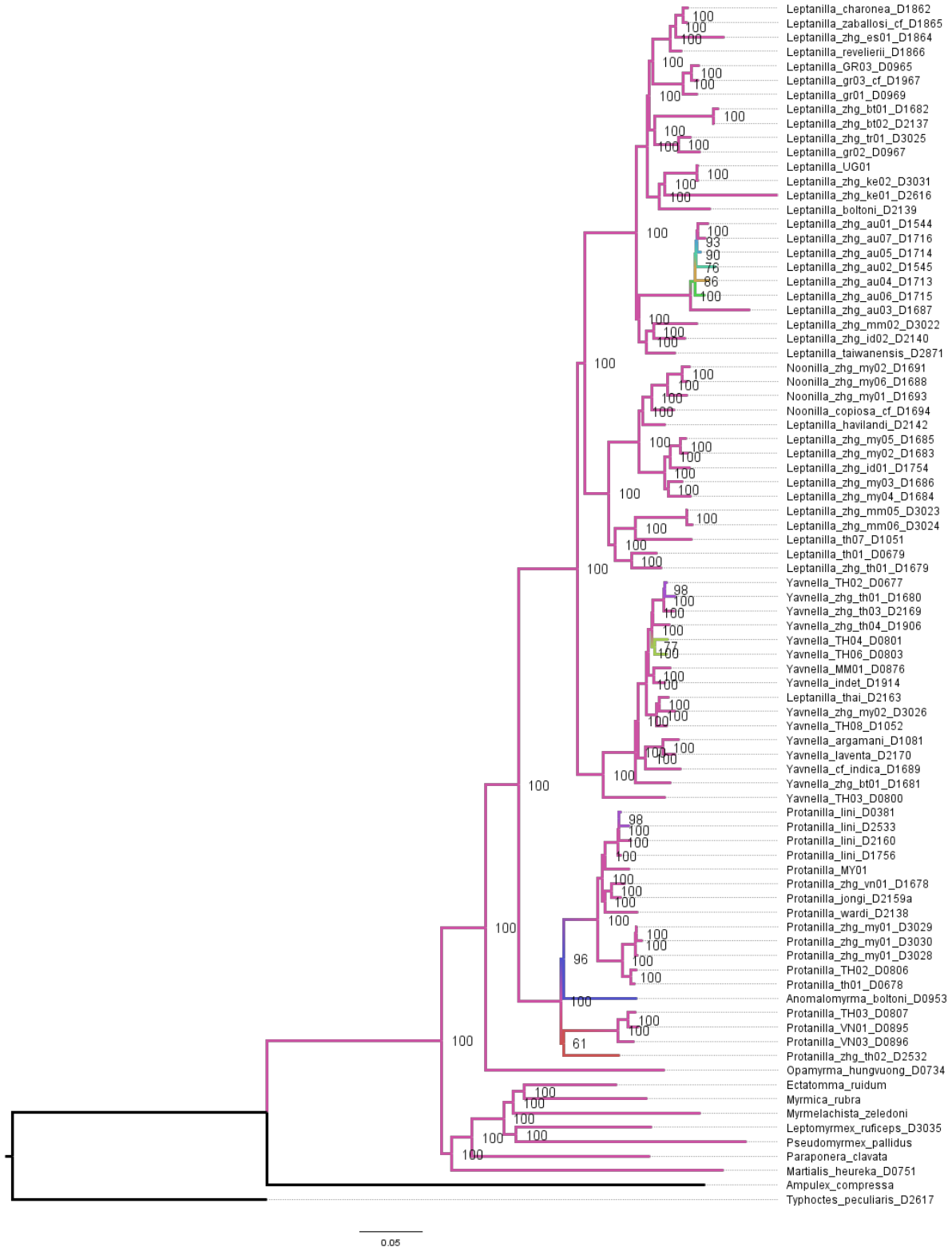

Fig. 5.S10. Phylogeny of the Leptanillinae and nine outgroup terminals, as inferred under ML with by-locus partitioning from Matrix 0.95A.

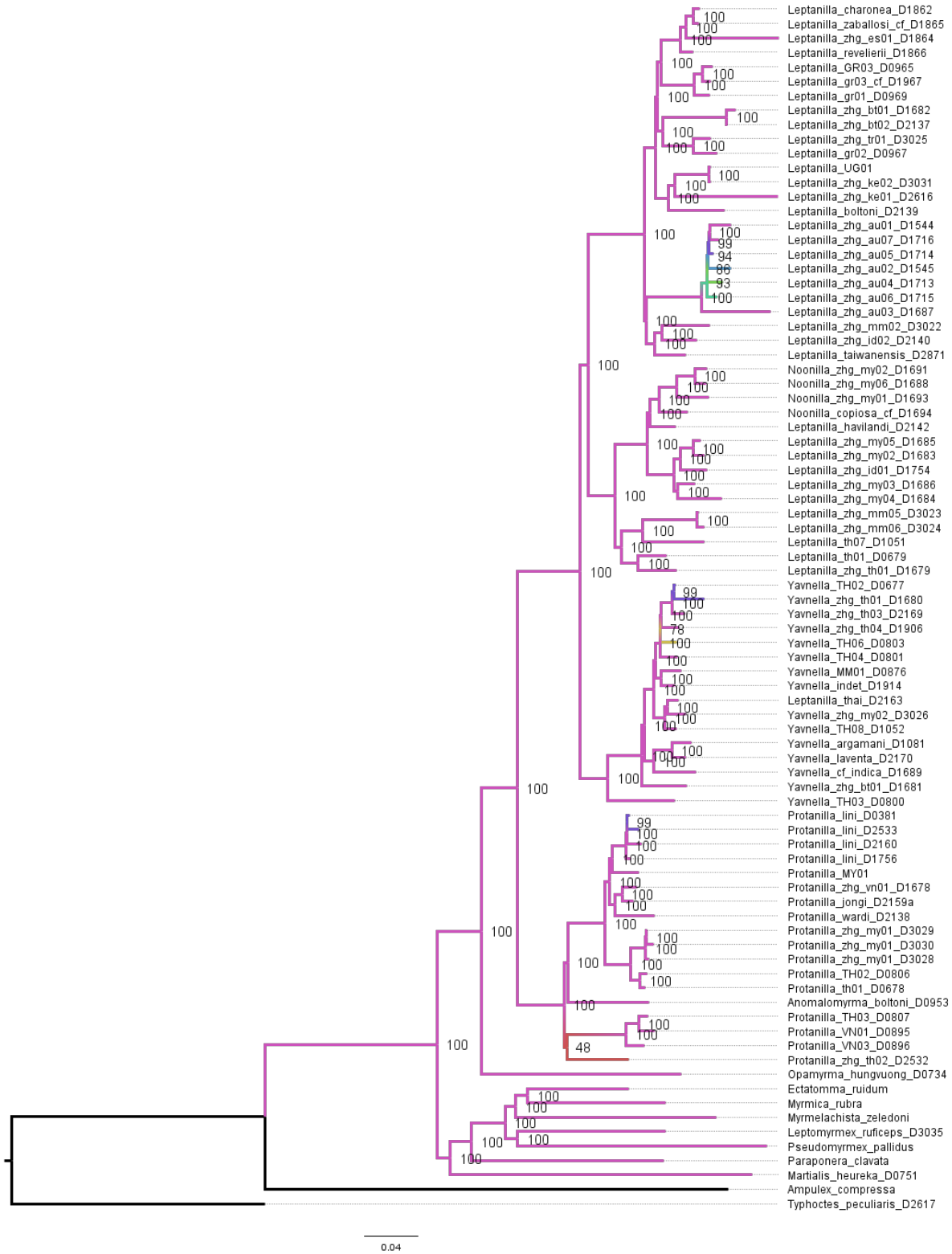

Fig. 5.S11. Phylogeny of the Leptanillinae and nine outgroup terminals, as inferred under ML with within-locus partitioning from Matrix 0.95A.

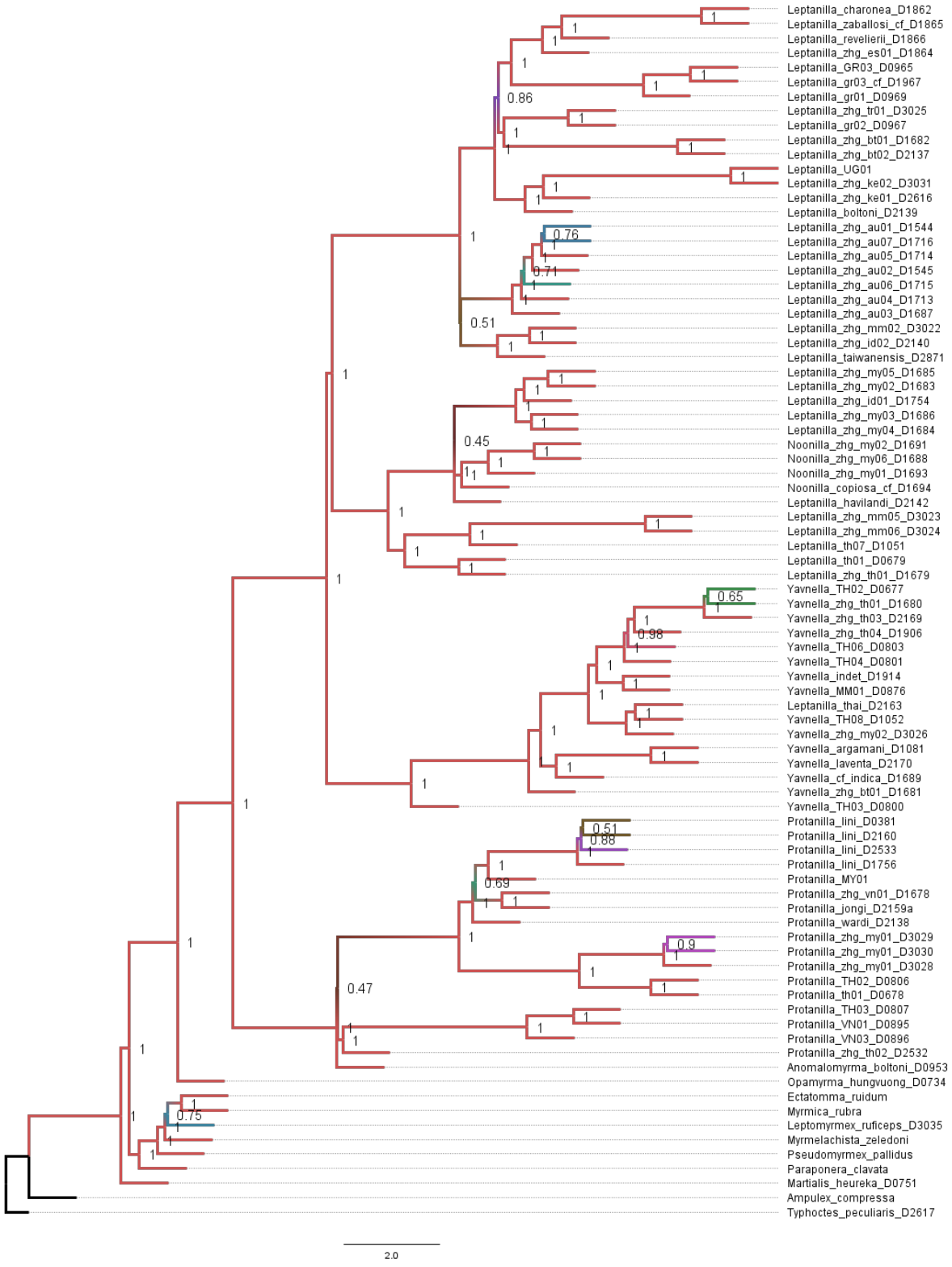

Fig. 5.S12. Phylogeny of the Leptanillinae and nine outgroup terminals, as inferred under a coalescent-based approach from Matrix 0.95A.

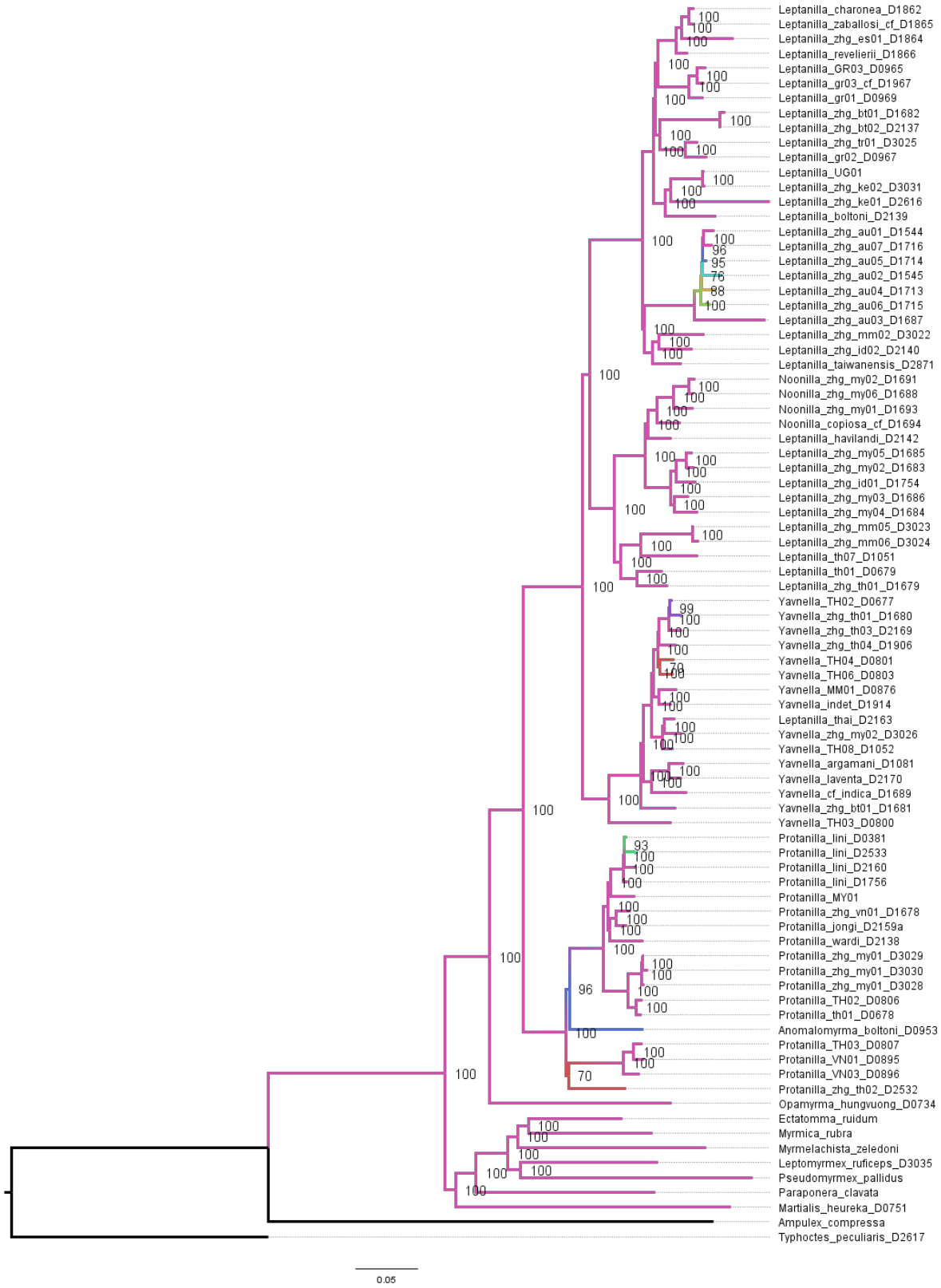

Fig. 5.S13. Phylogeny of the Leptanillinae and nine outgroup terminals, as inferred under ML with by-locus partitioning from Matrix 1A.

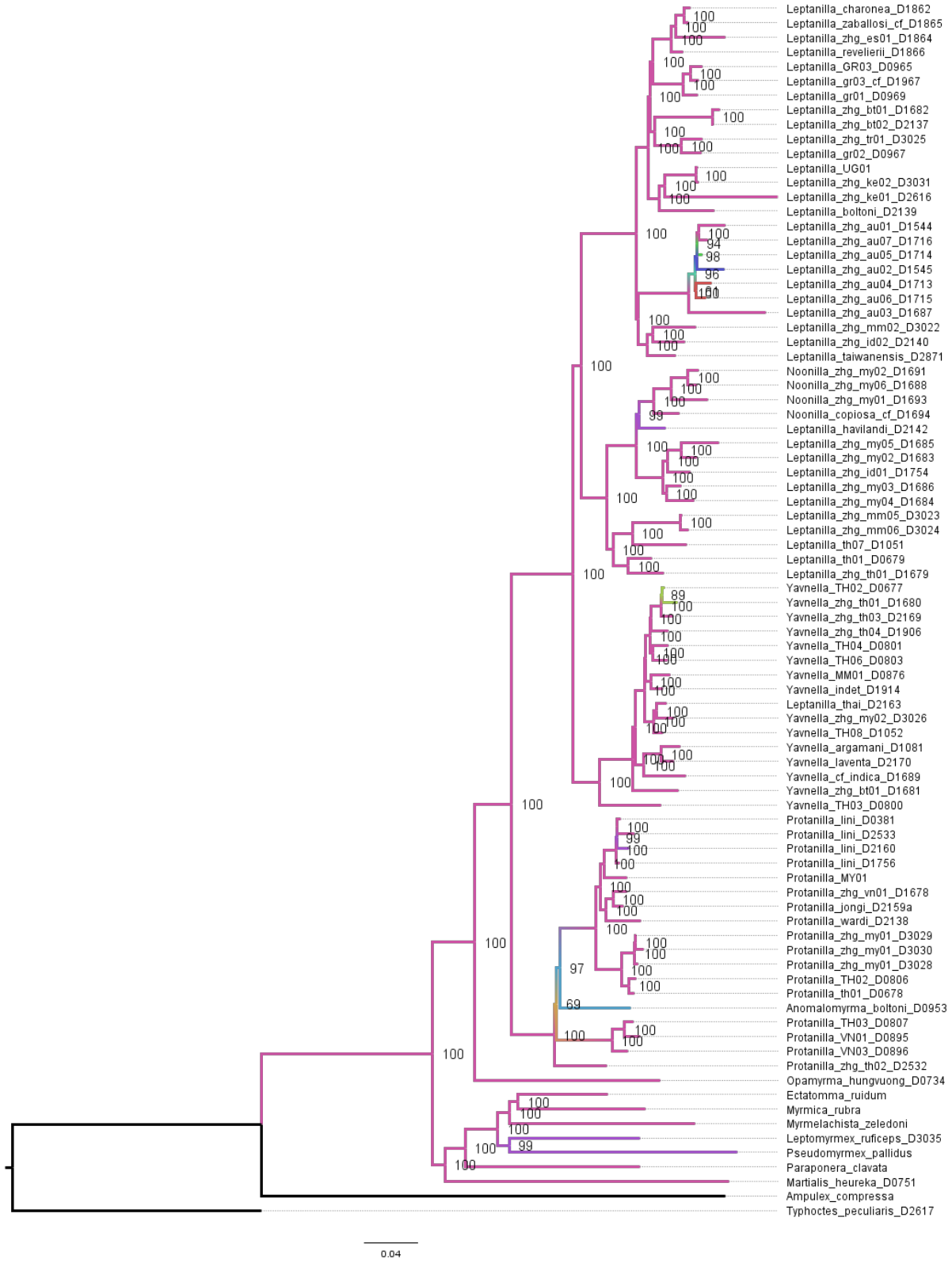

Fig. 5.S14. Phylogeny of the Leptanillinae and nine outgroup terminals, as inferred under ML with within-locus partitioning from Matrix 1A.

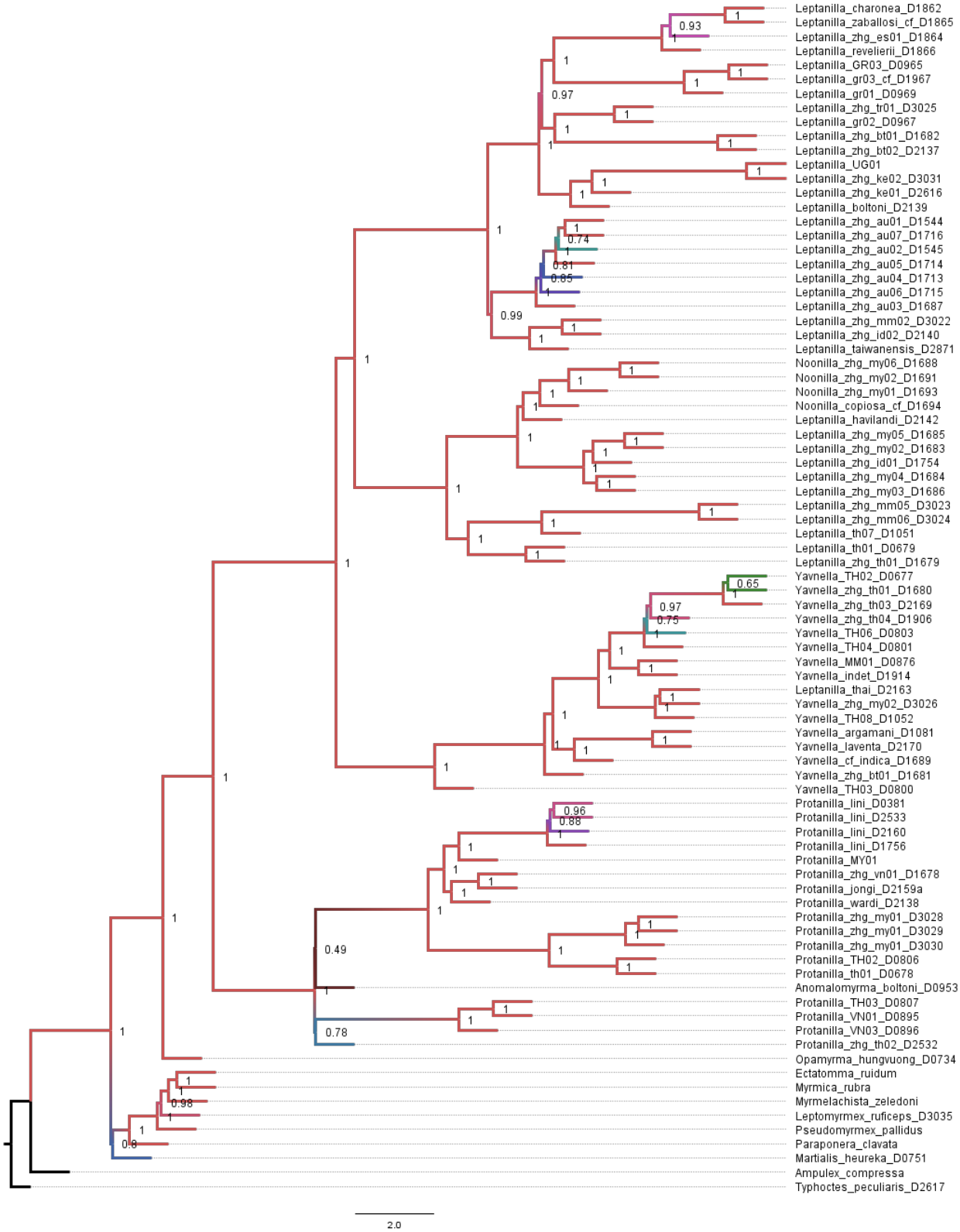

Fig. 5.S15. Phylogeny of the Leptanillinae and nine outgroup terminals, as inferred under a coalescent-based approach from Matrix 1A.

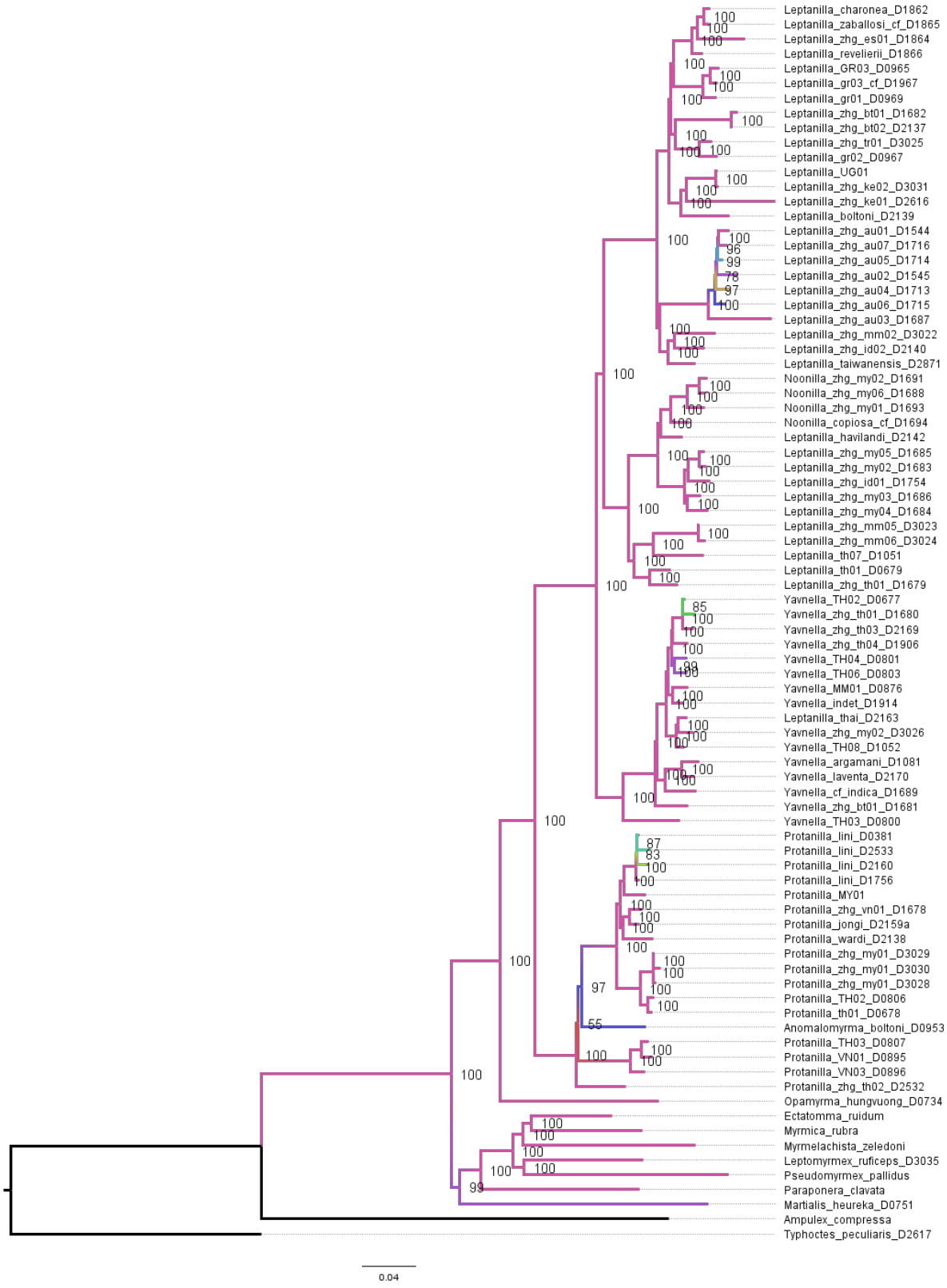

Fig. 5.S16. Phylogeny of the Leptanillinae and nine outgroup terminals, as inferred under ML with by-locus partitioning from Matrix 0.8B.

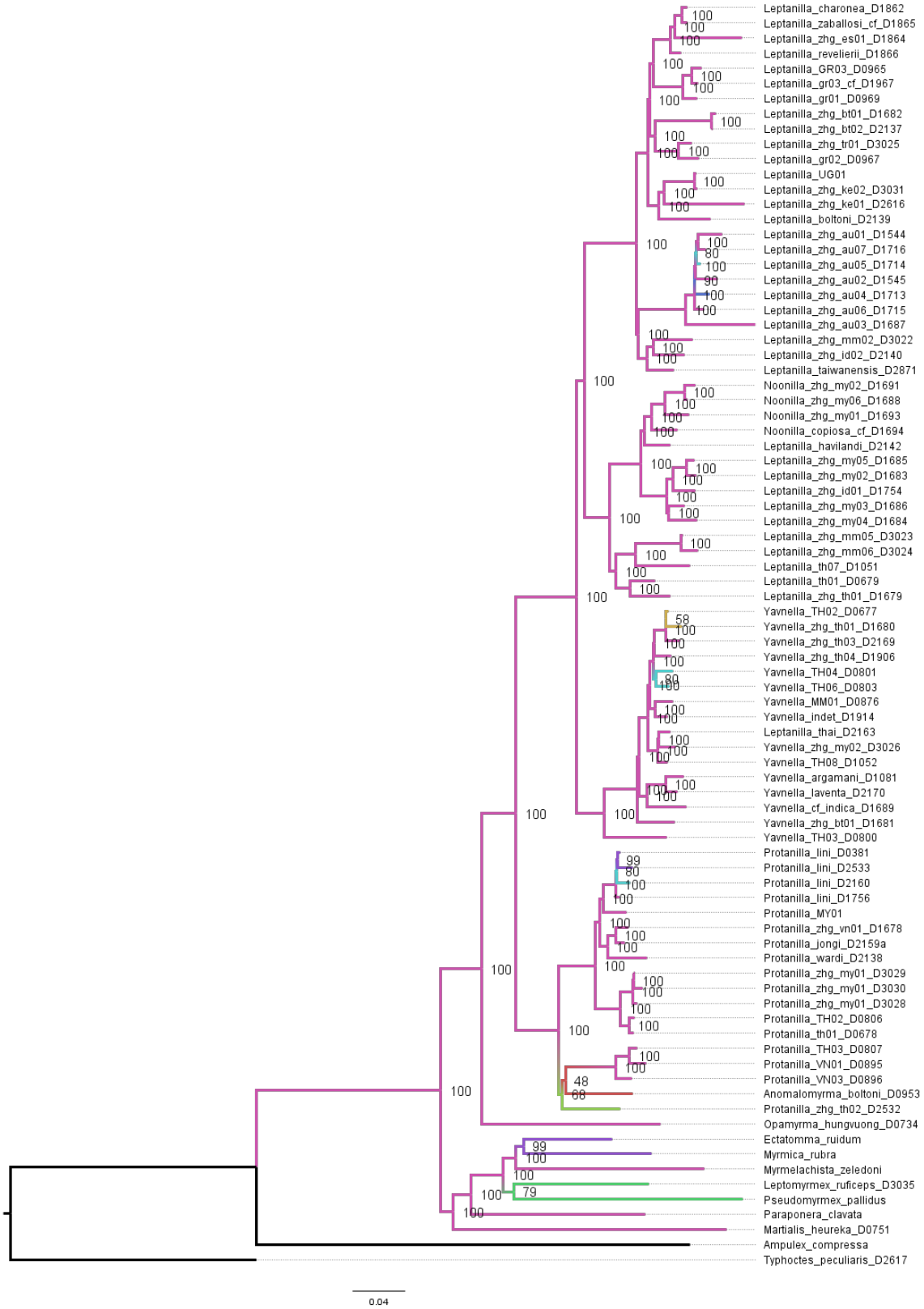

Fig. 5.S17. Phylogeny of the Leptanillinae and nine outgroup terminals, as inferred under ML with within-locus partitioning from Matrix 0.8B.

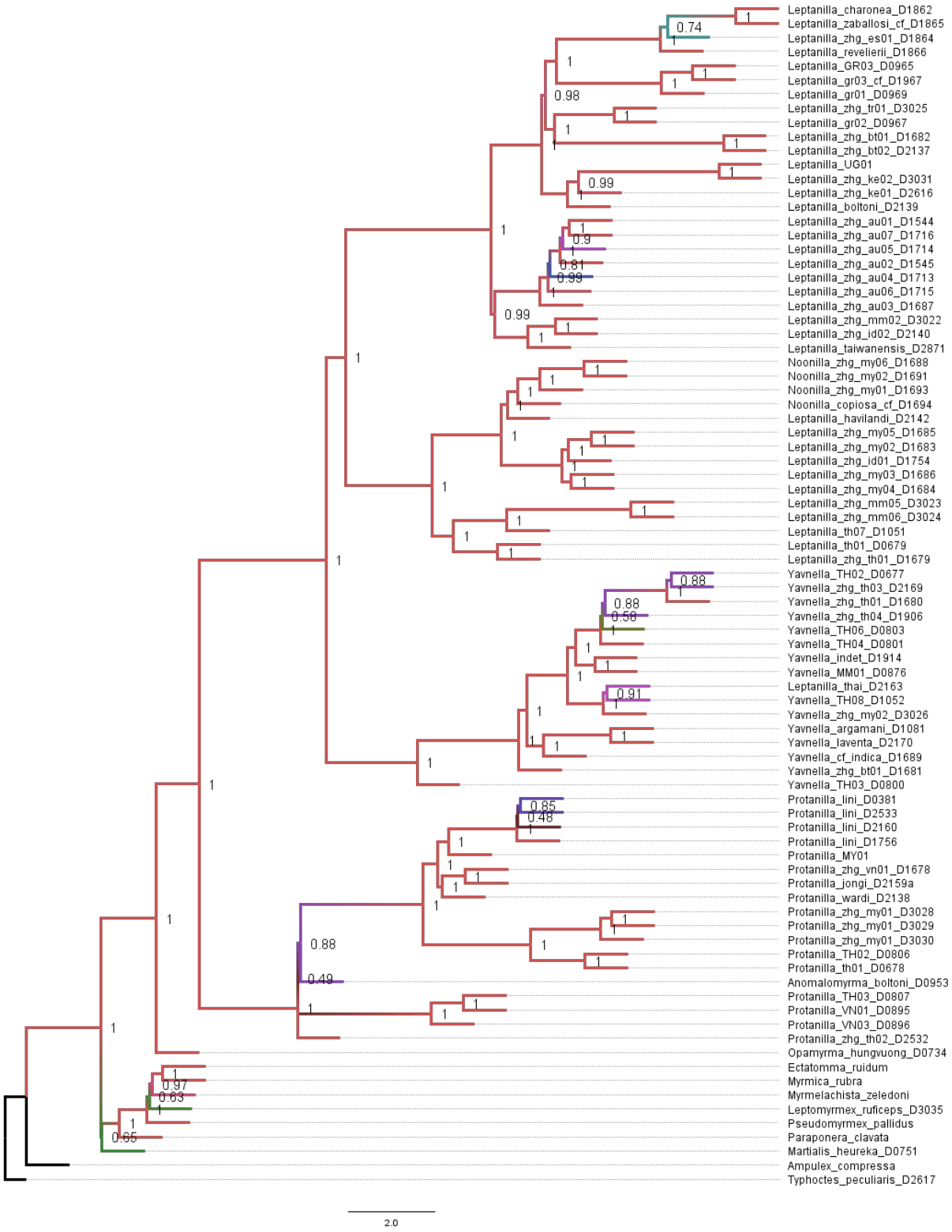

Fig. 5.S18. Phylogeny of the Leptanillinae and nine outgroup terminals, as inferred under a coalescent-based approach from Matrix 0.8B.

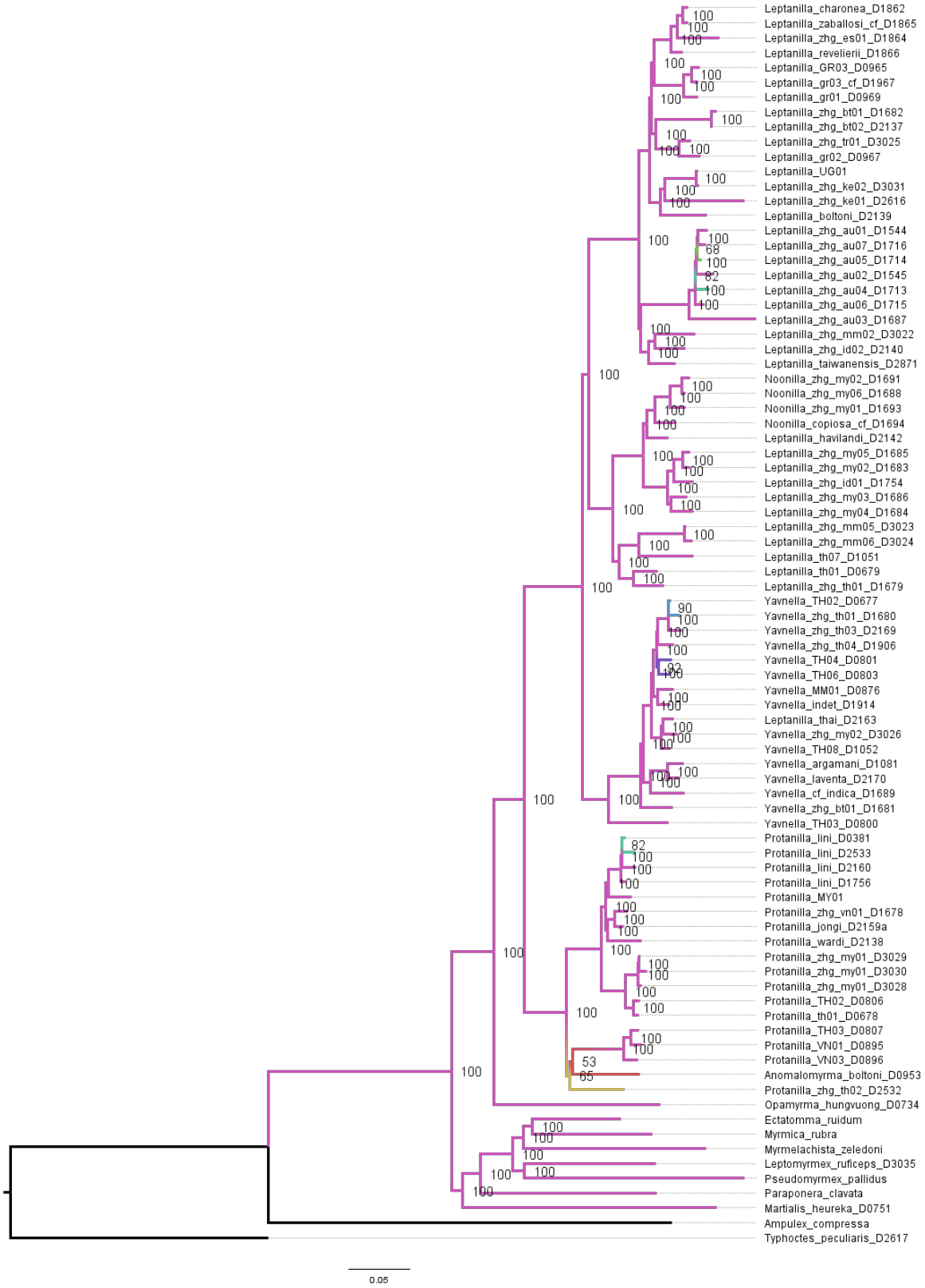

Fig. 5.S19. Phylogeny of the Leptanillinae and nine outgroup terminals, as inferred under ML by-locus partitioning from Matrix 0.85B.

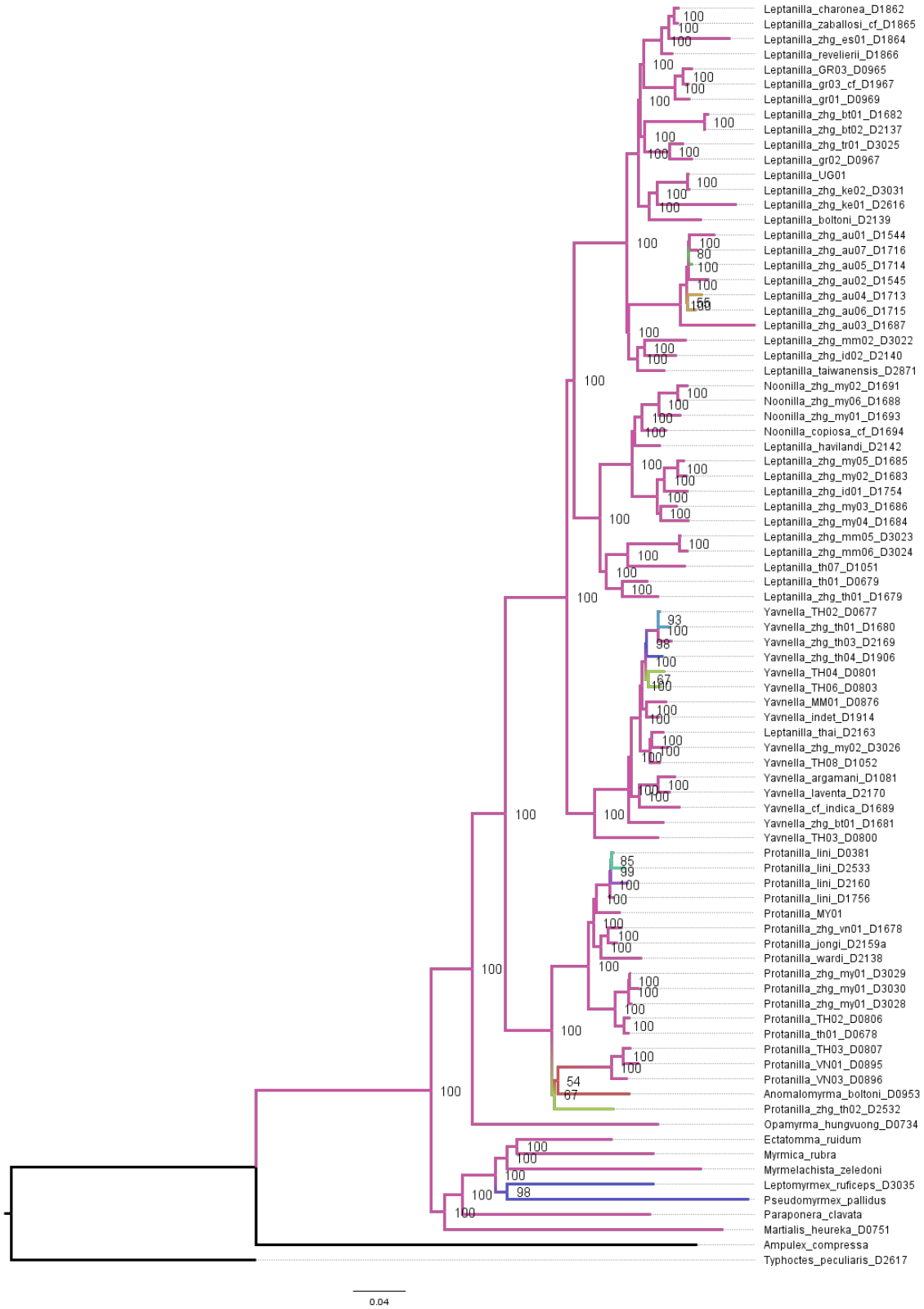

Fig. 5.S20. Phylogeny of the Leptanillinae and nine outgroup terminals, as inferred under ML with within-locus partitioning from Matrix 0.85B.

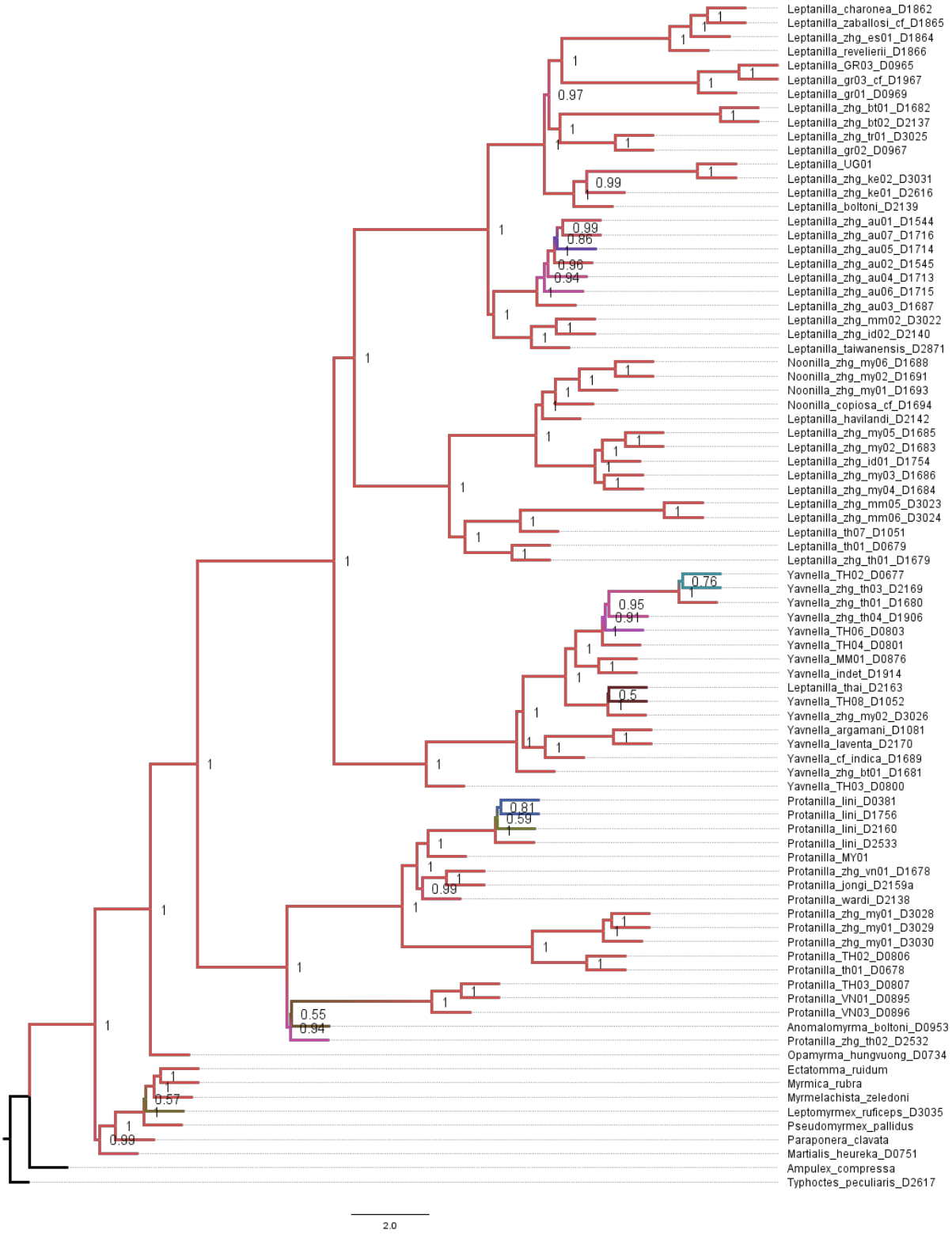

Fig. 5.S21. Phylogeny of the Leptanillinae and nine outgroup terminals, as inferred under a coalescent-based approach from Matrix 0.85B.

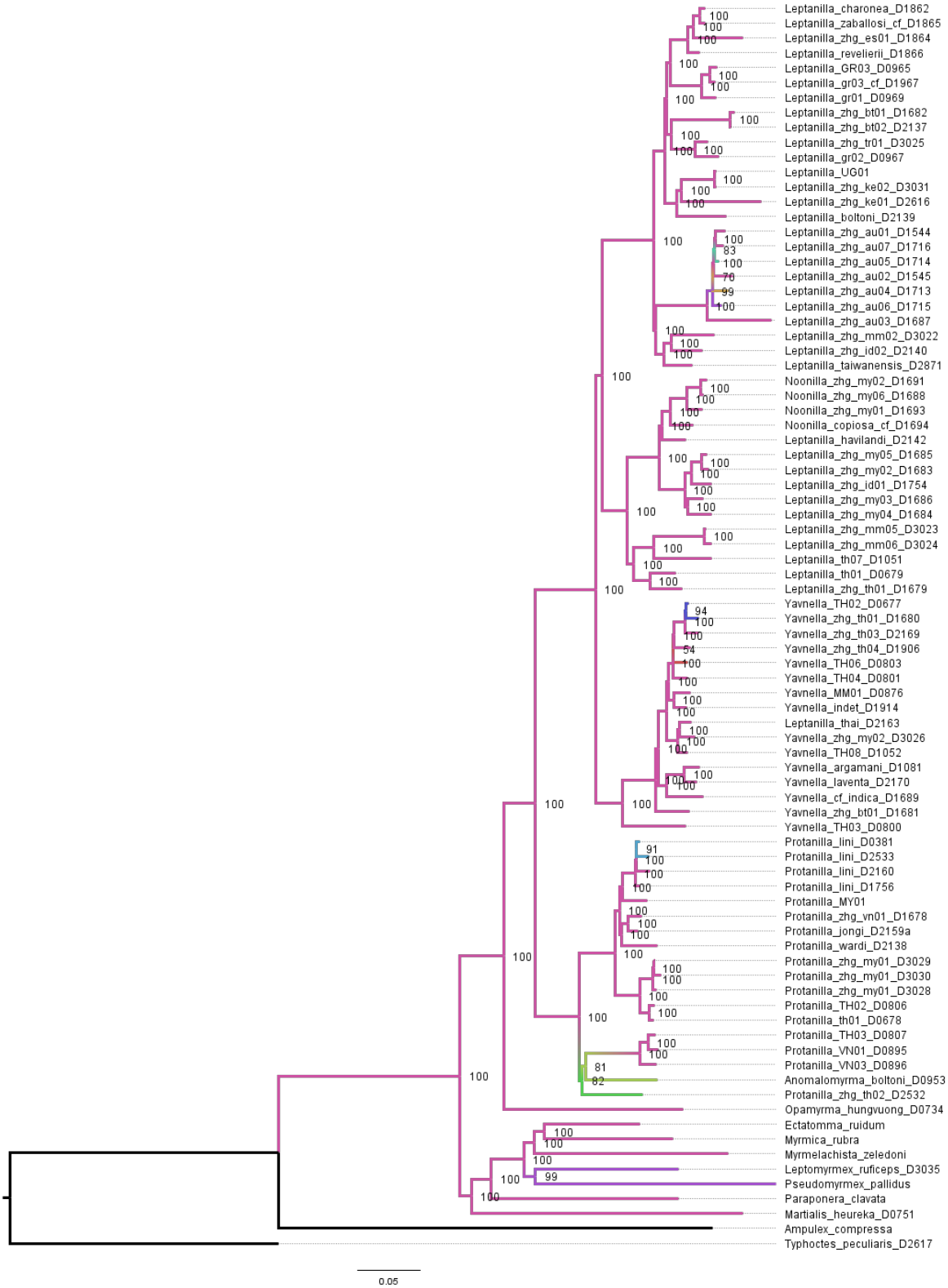

Fig. 5.S22. Phylogeny of the Leptanillinae and nine outgroup terminals, as inferred under by-locus partitioning from Matrix 0.9B.

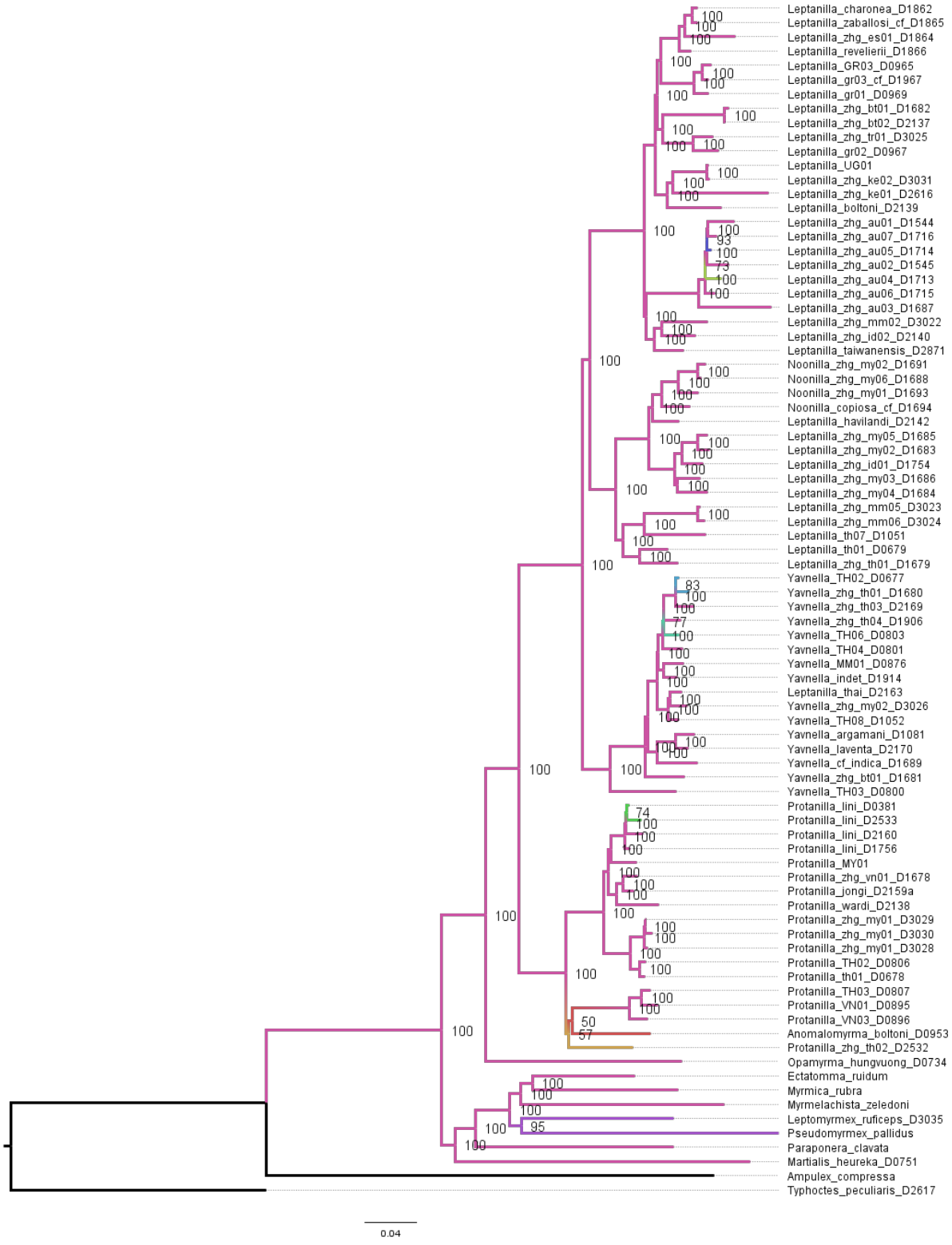

Fig. 5.S23. Phylogeny of the Leptanillinae and nine outgroup terminals, as inferred under within-locus partitioning from Matrix 0.9B.

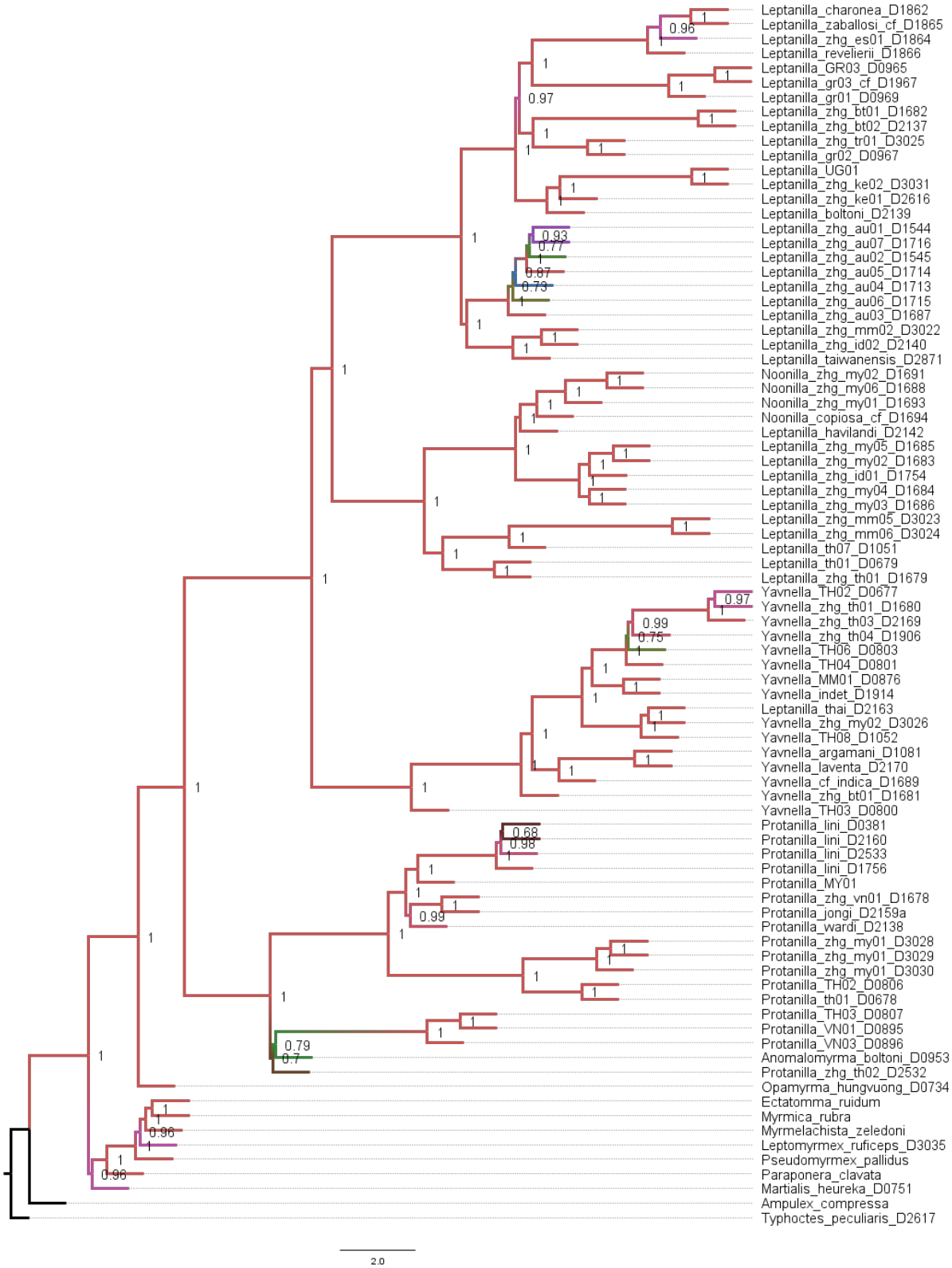

Fig. 5.S24. Phylogeny of the Leptanillinae and nine outgroup terminals, as inferred under a coalescent-based approach from Matrix 0.9B.

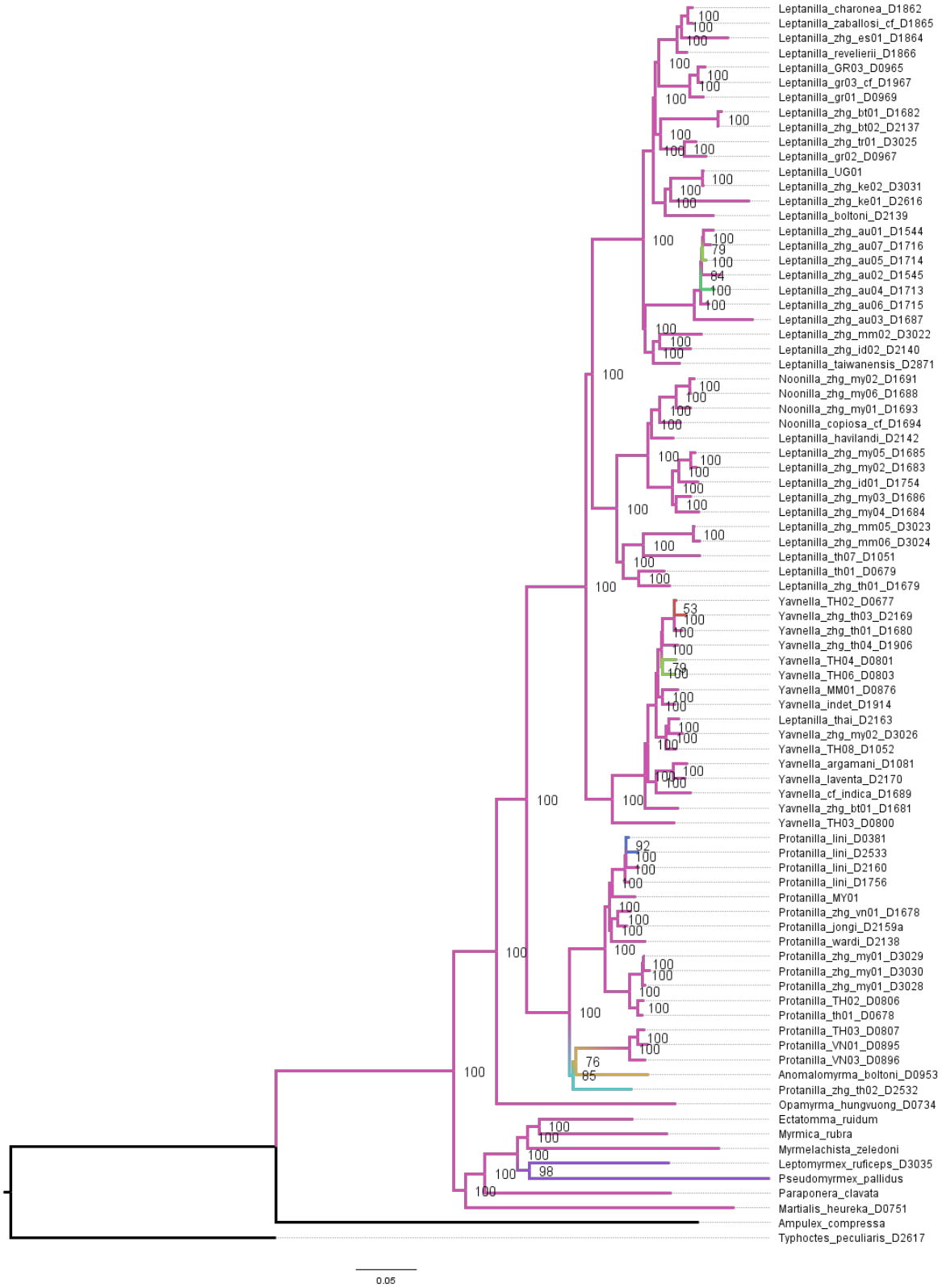

Fig. 5.S25. Phylogeny of the Leptanillinae and nine outgroup terminals, as inferred under ML with by-locus partitioning from Matrix 0.95B.

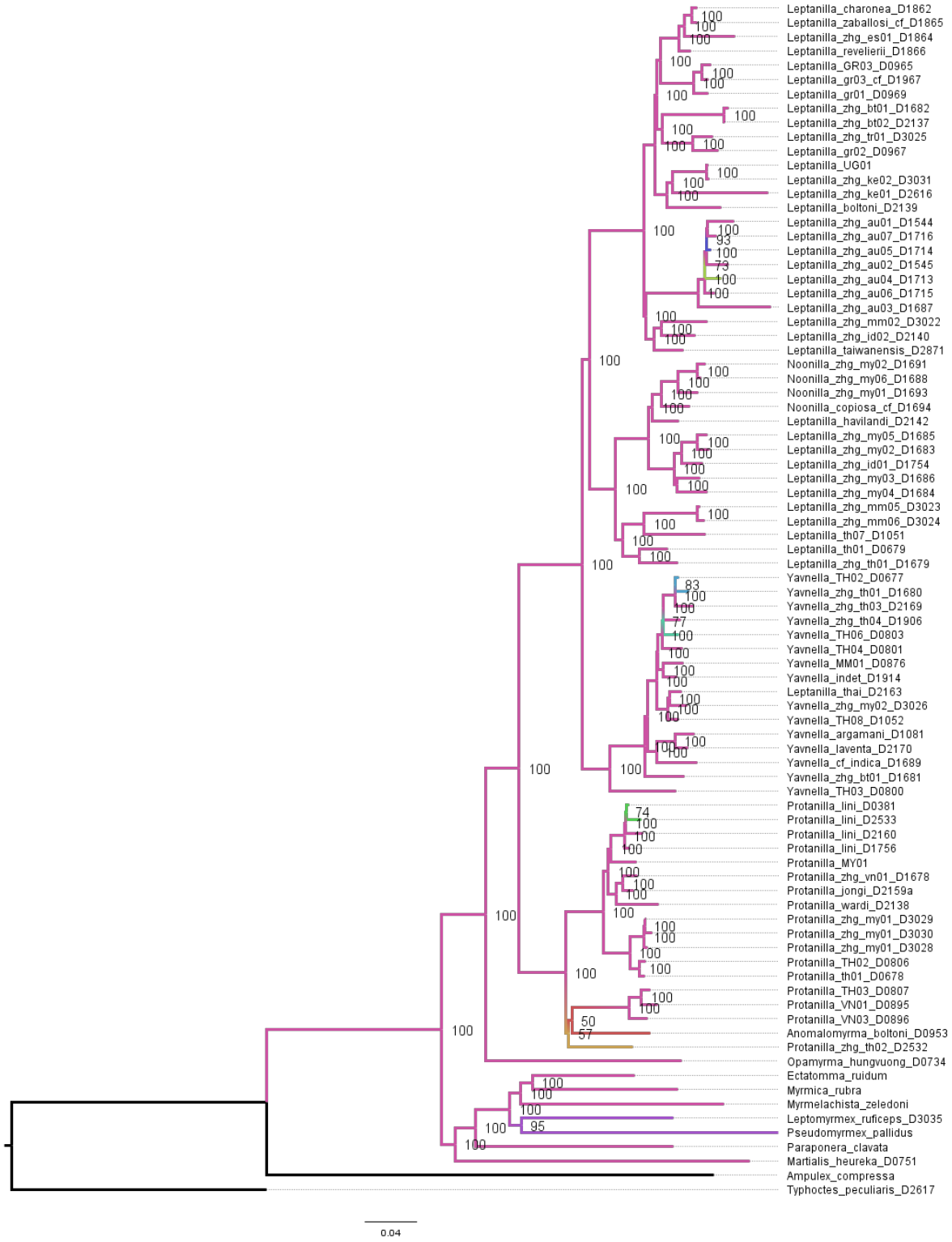

Fig. 5.S26. Phylogeny of the Leptanillinae and nine outgroup terminals, as inferred under ML with within-locus partitioning from Matrix 0.95B.

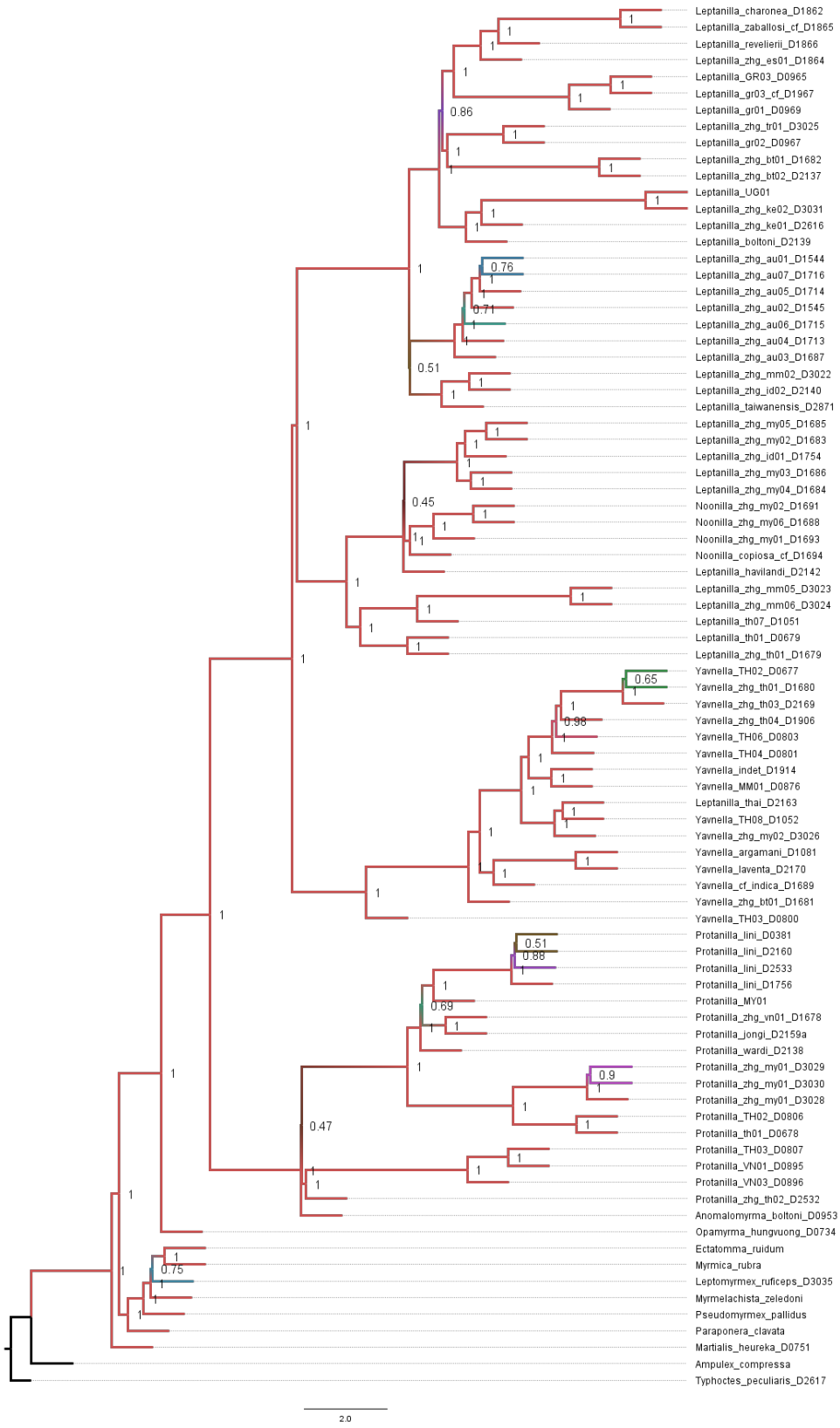

Fig. 5.S27. Phylogeny of the Leptanillinae and nine outgroup terminals, as inferred under coalescent-based inference from Matrix 0.95B.

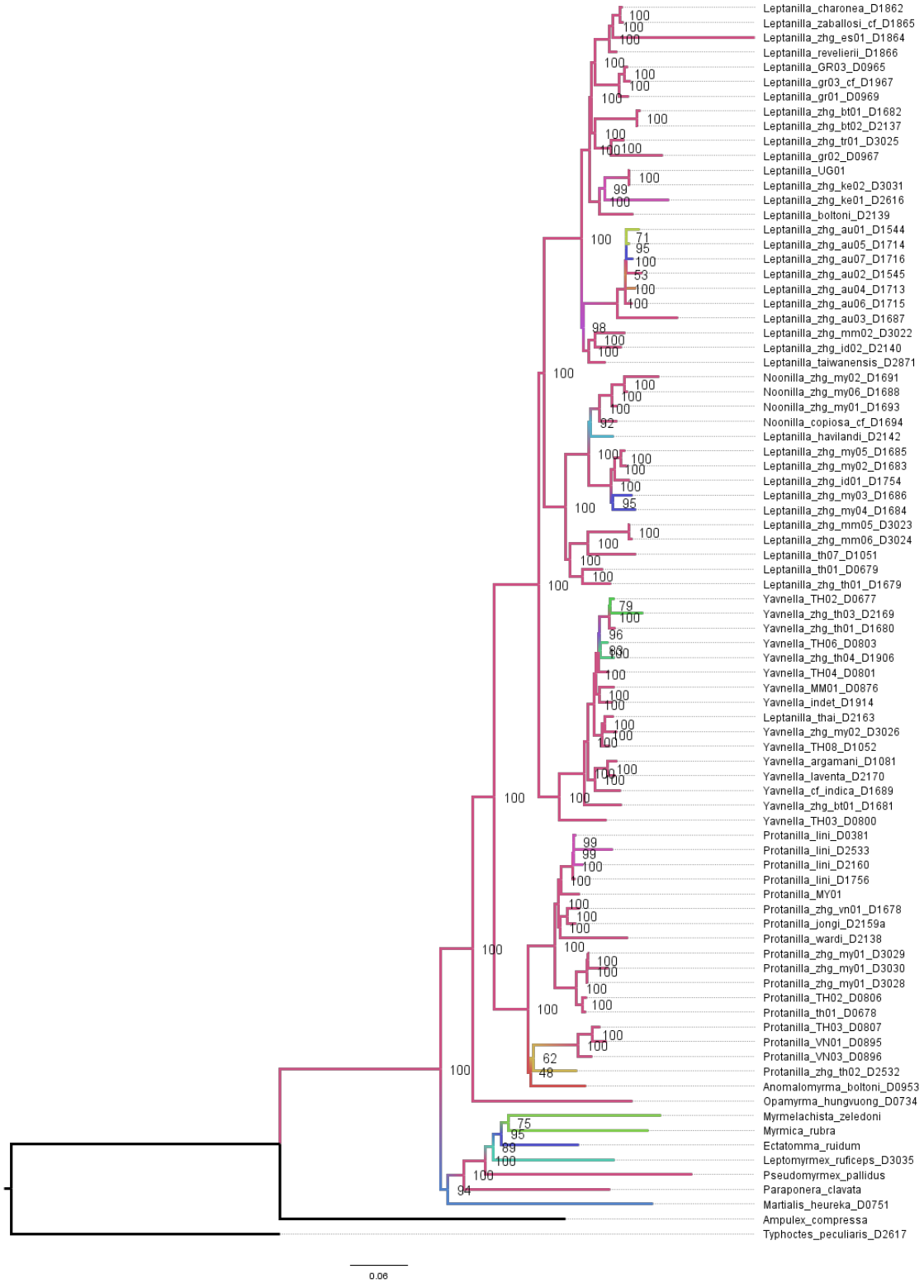

Fig. 5.S28. Phylogeny of the Leptanillinae and nine outgroup terminals, as inferred under ML with by-locus partitioning from Matrix 1B.

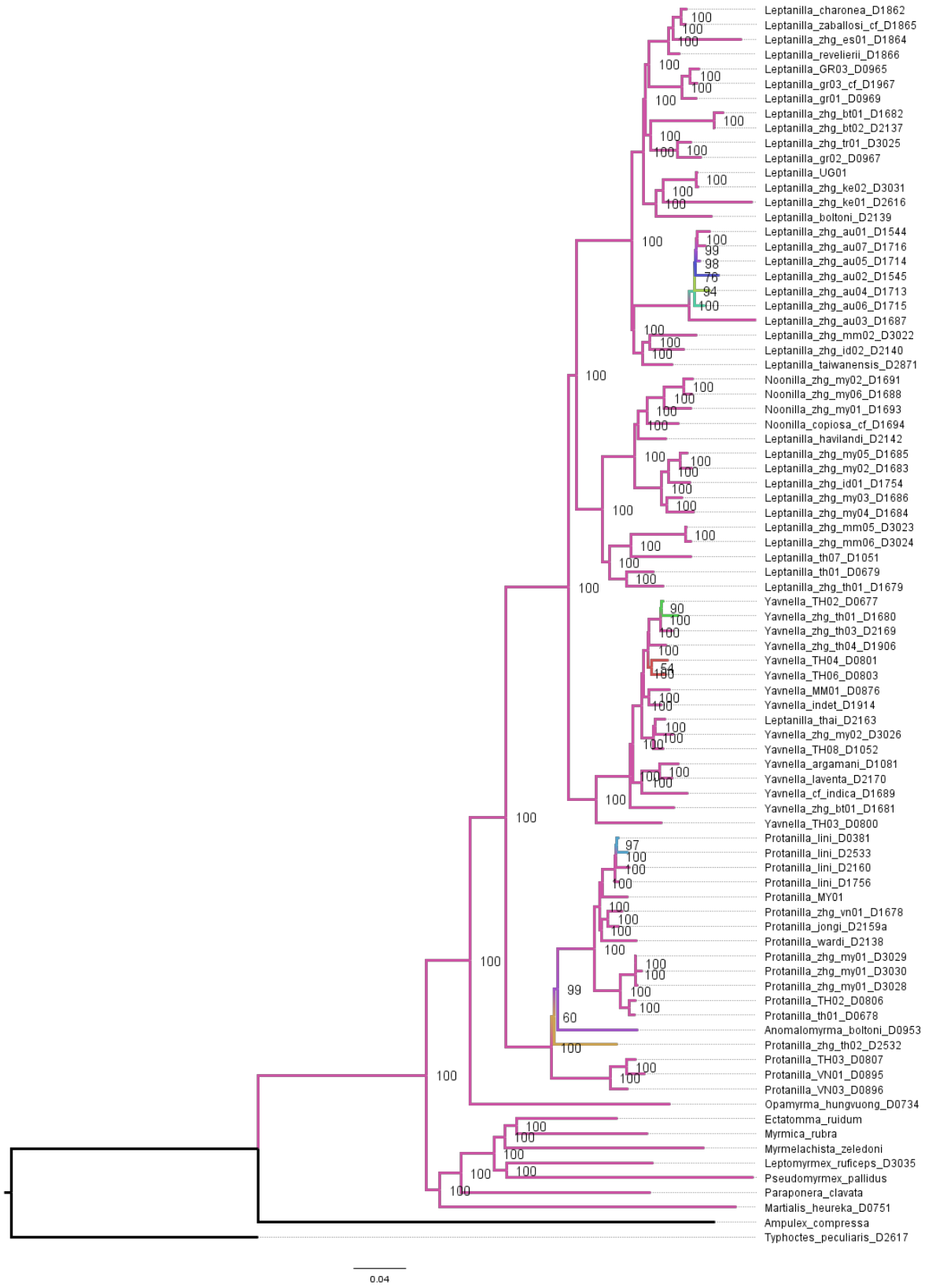

Fig. 5.S29. Phylogeny of the Leptanillinae and nine outgroup terminals, as inferred under ML with within-locus partitioning from Matrix 1B.

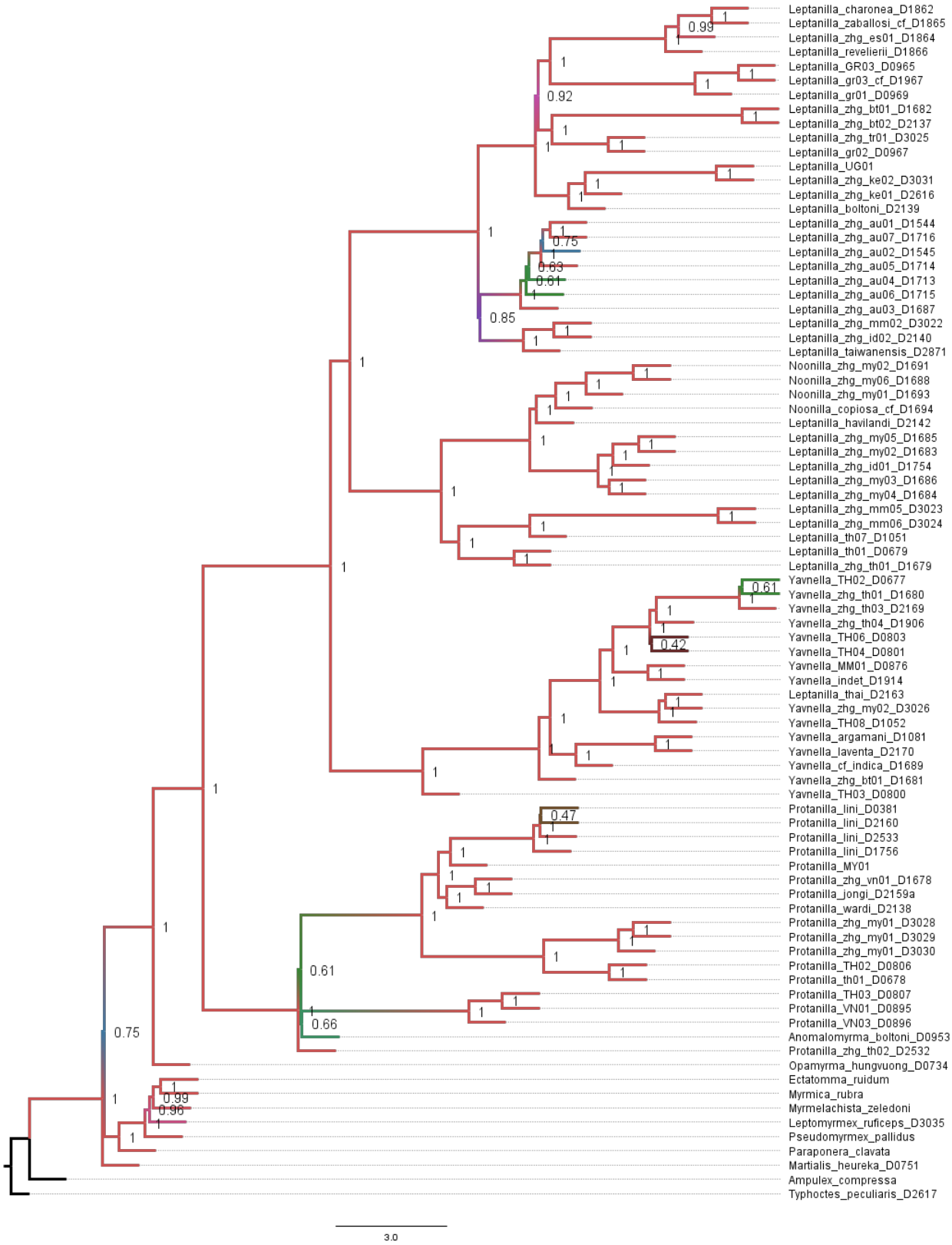

Fig. 5.S30. Phylogeny of the Leptanillinae and nine outgroup terminals, as inferred under coalescent-based inference from Matrix 1B.

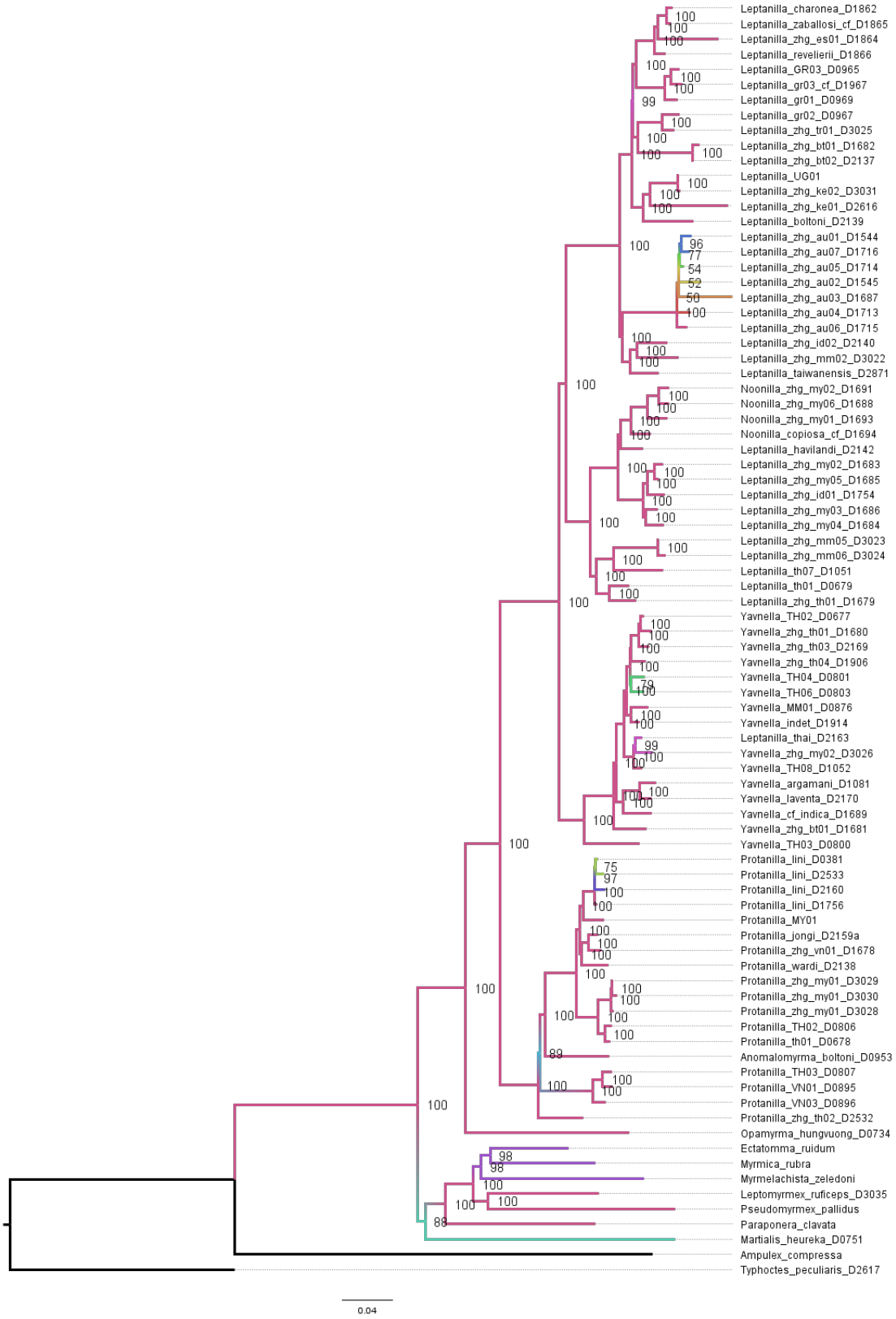

Fig. 5.S31. Phylogeny of the Leptanillinae and nine outgroup terminals, as inferred under ML with by-locus partitioning from Matrix 0.8C.

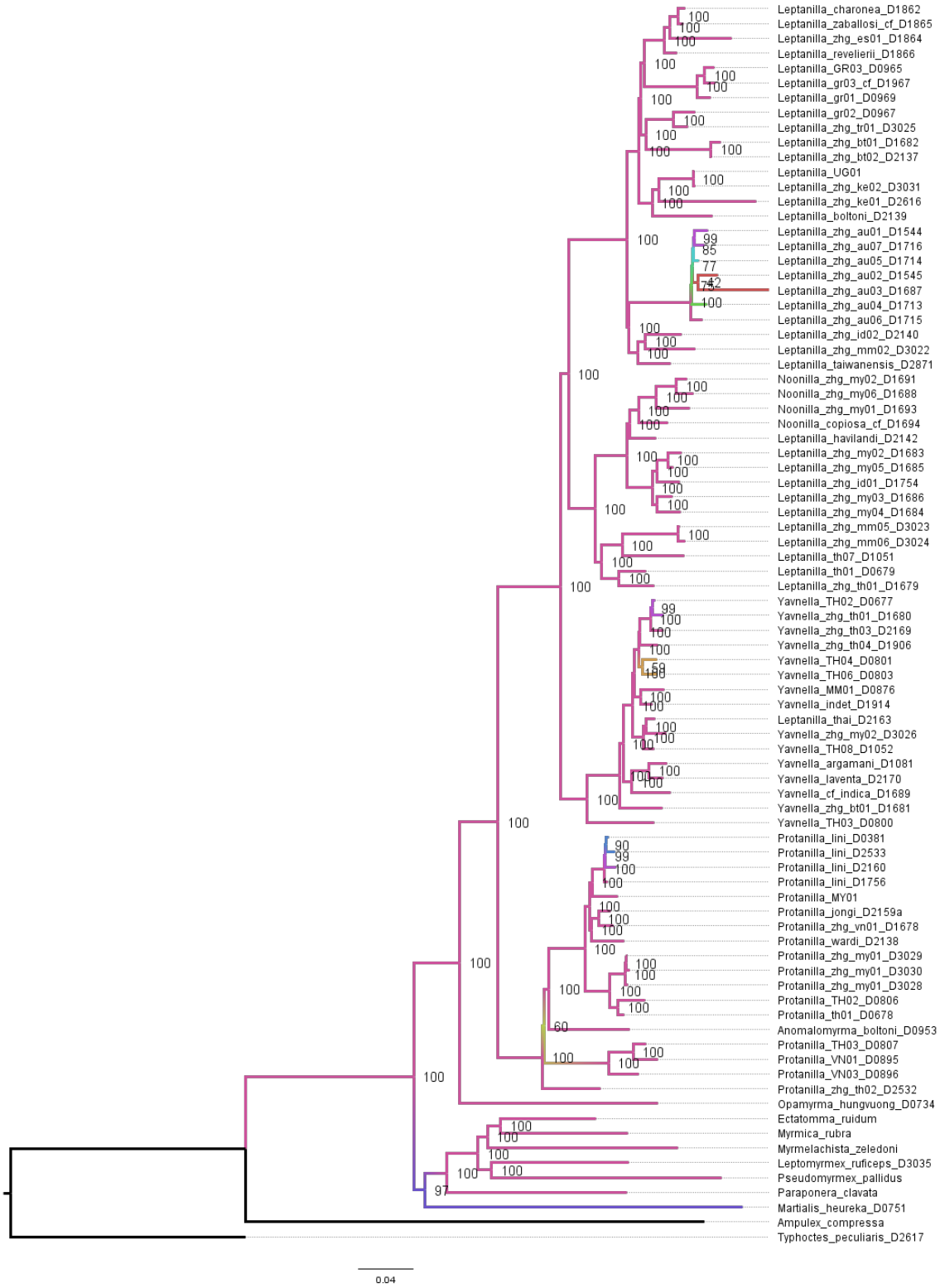

Fig. 5.S32. Phylogeny of the Leptanillinae and nine outgroup terminals, as inferred under ML with within-locus partitioning from Matrix 0.8C.

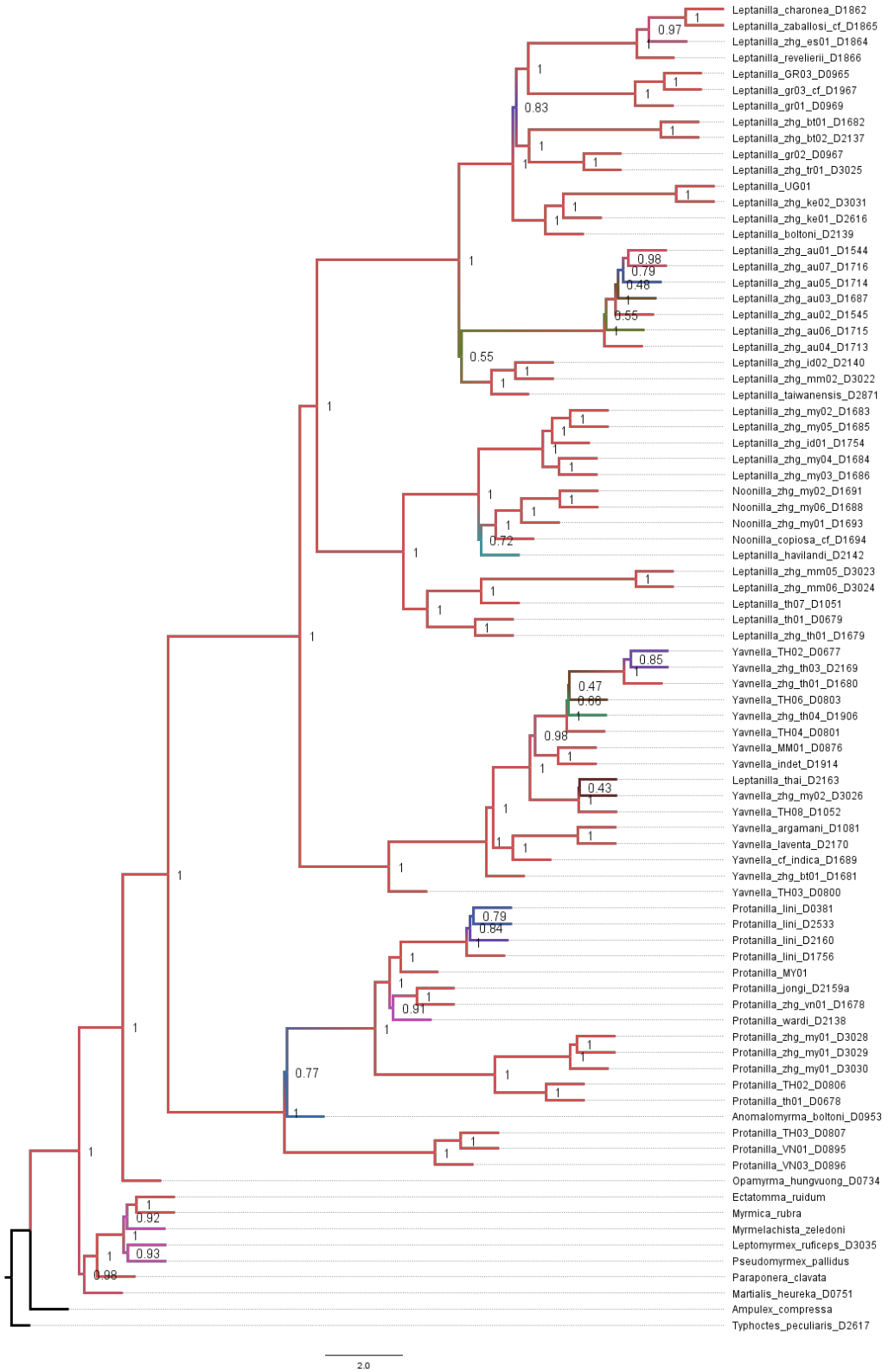

Fig. 5.S33. Phylogeny of the Leptanillinae and nine outgroup terminals, as inferred under ML with by-locus partitioning from Matrix 0.85C.

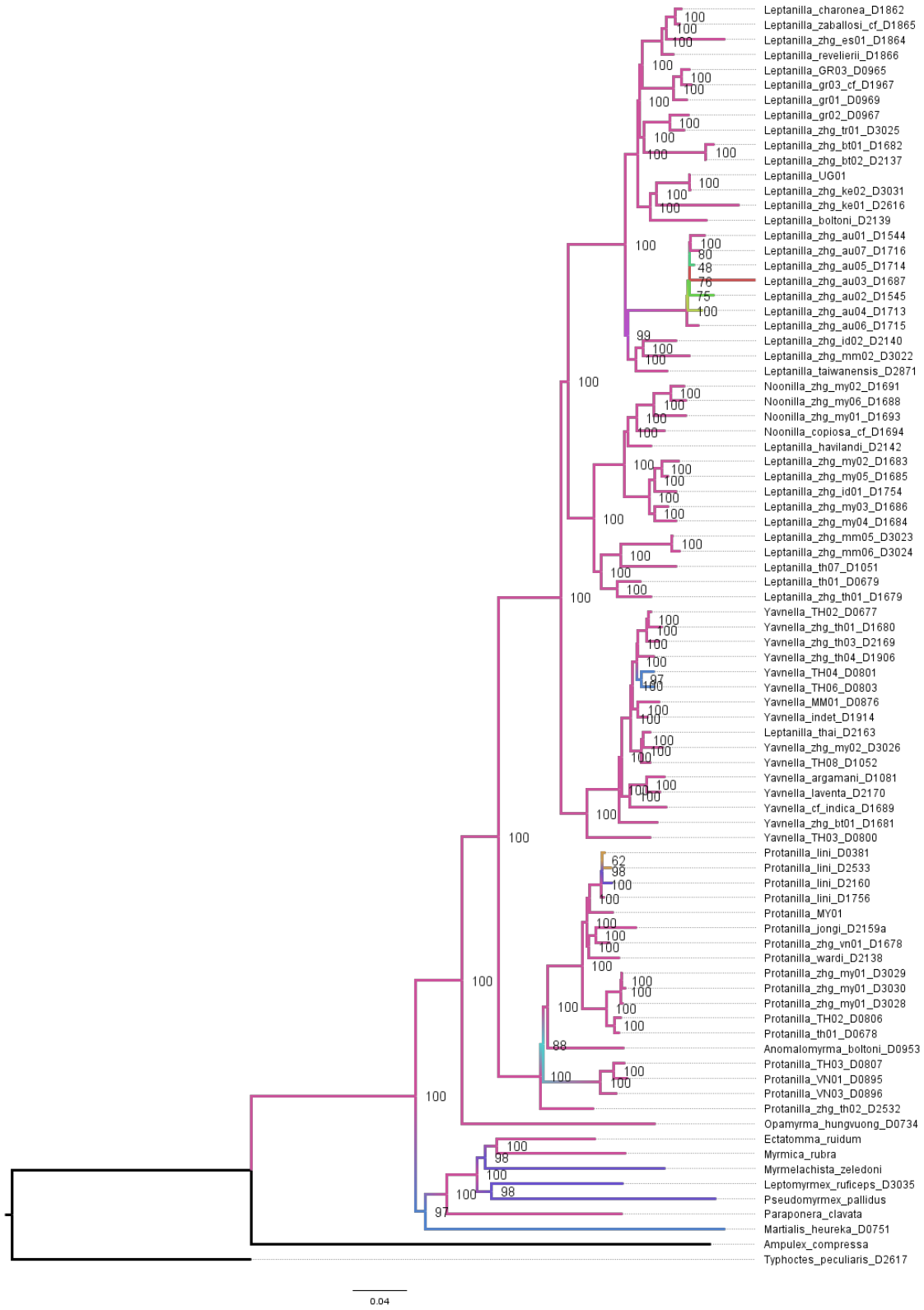

Fig. 5.S34. Phylogeny of the Leptanillinae and nine outgroup terminals, as inferred under ML with within-locus partitioning from Matrix 0.85C.

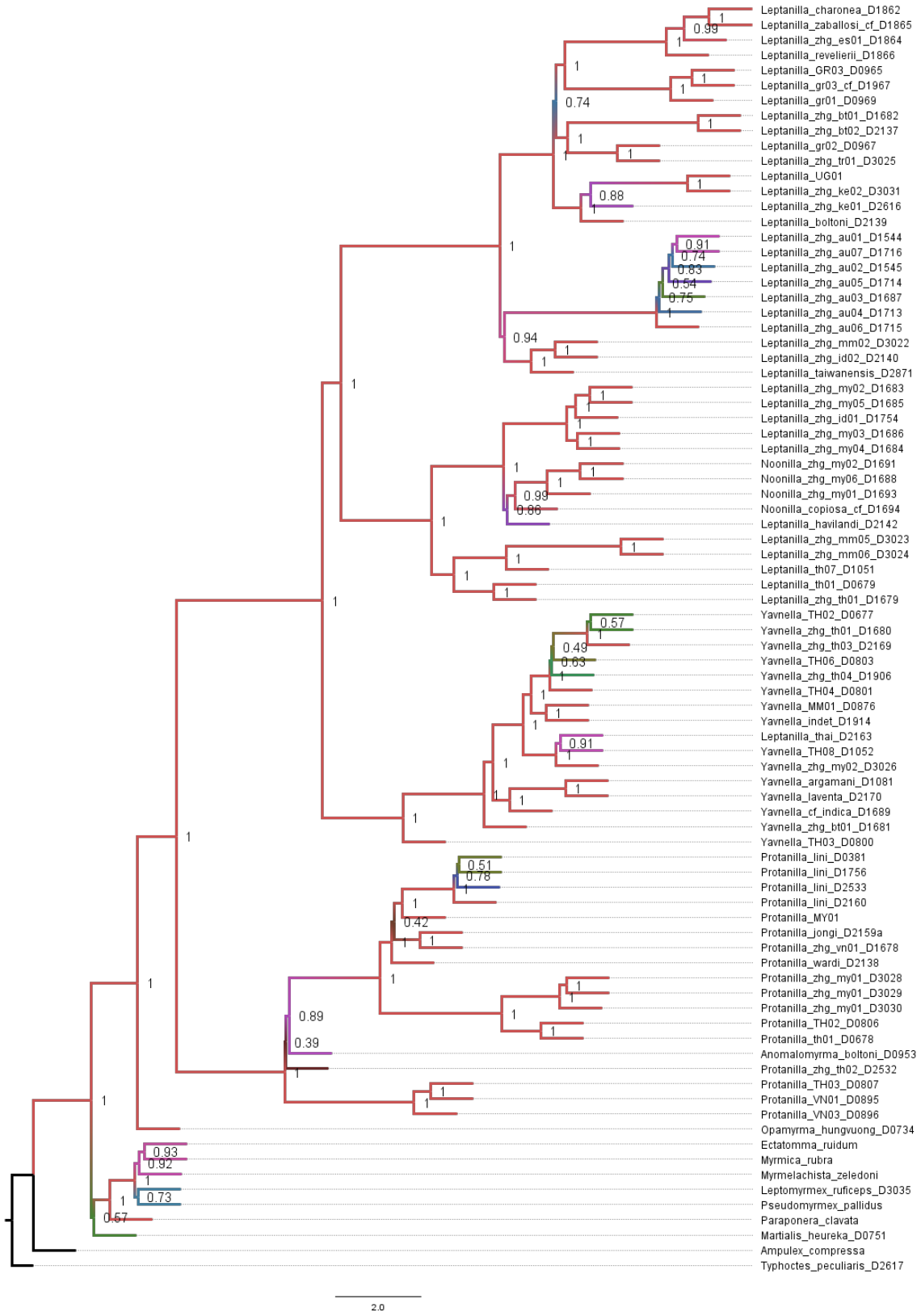

Fig. 5.S35. Phylogeny of the Leptanillinae and nine outgroup terminals, as inferred under coalescent-based inference from Matrix 0.85C.

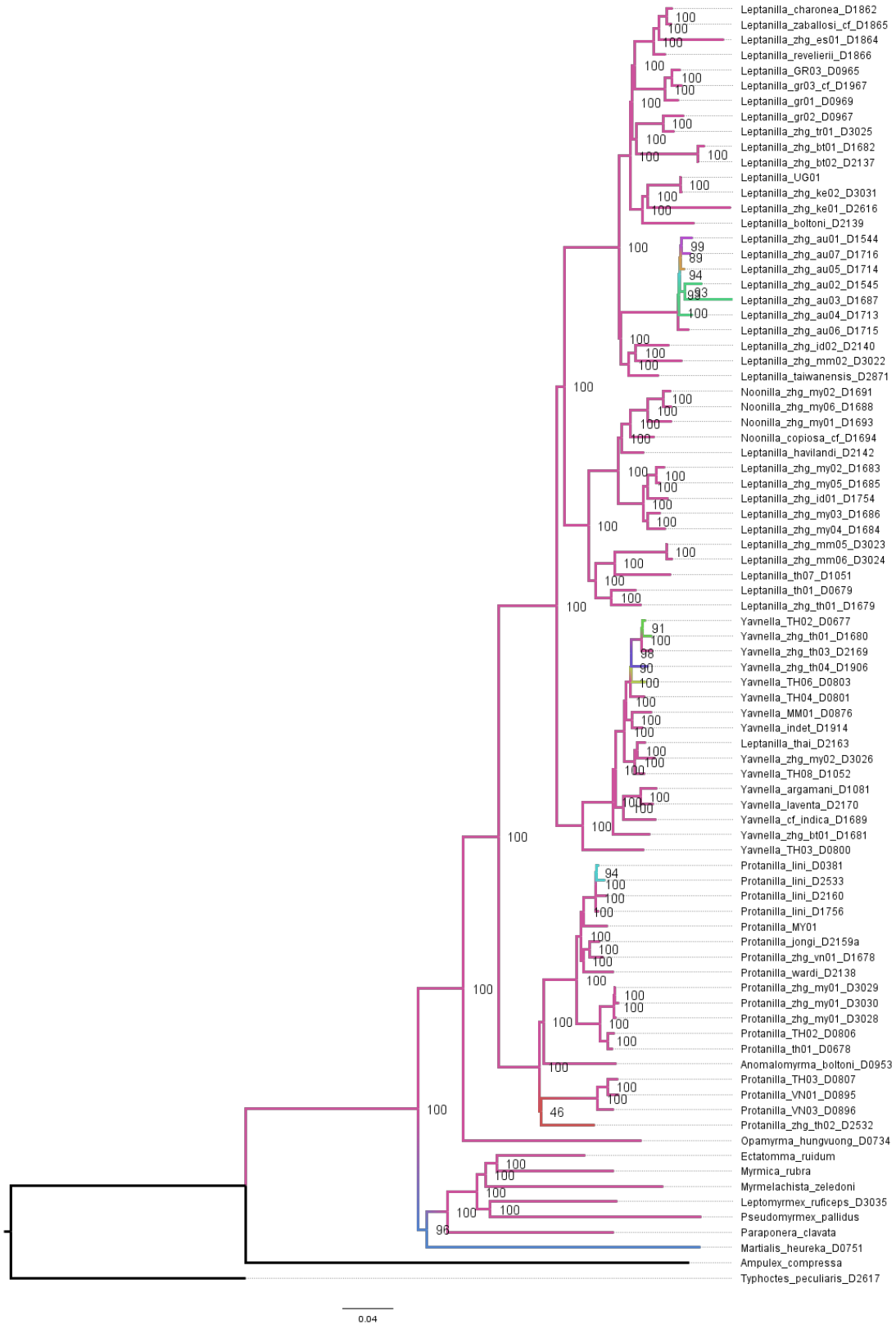

Fig. 5.S36. Phylogeny of the Leptanillinae and nine outgroup terminals, as inferred under ML with by-locus partitioning from Matrix 0.9C.

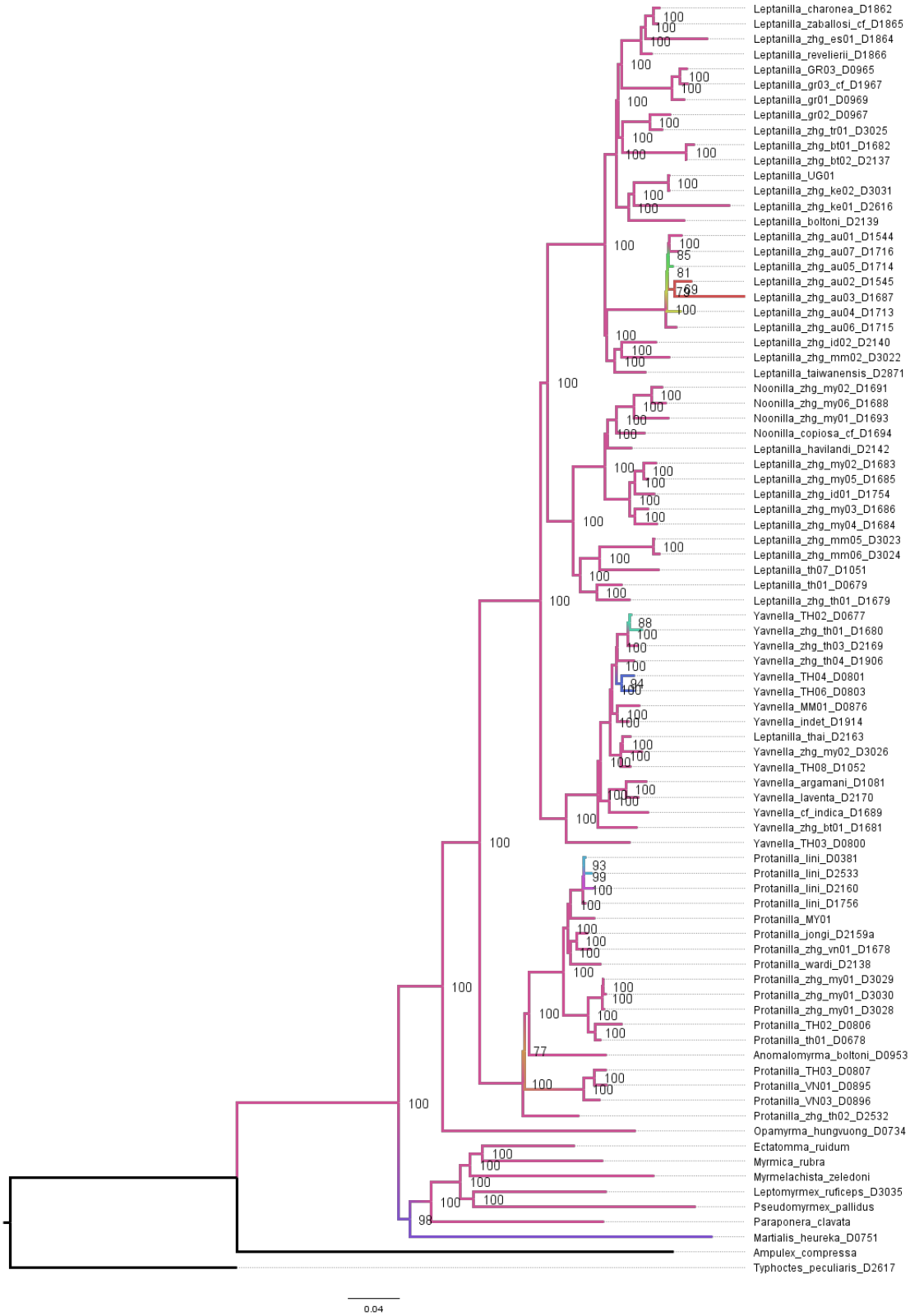

Fig. 5.S37. Phylogeny of the Leptanillinae and nine outgroup terminals, as inferred under ML with within-locus partitioning from Matrix 0.9C.

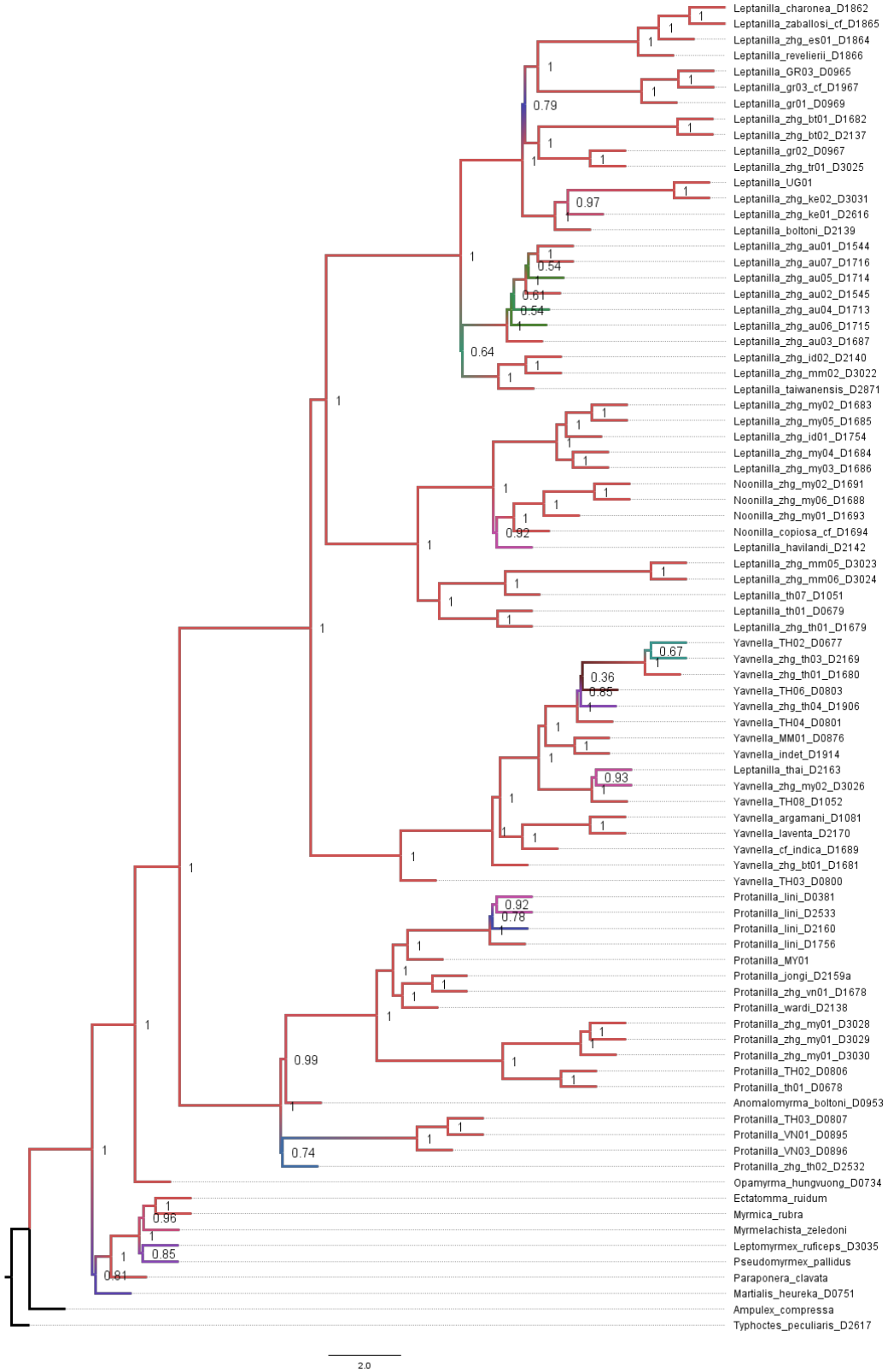

Fig. 5.S38. Phylogeny of the Leptanillinae and nine outgroup terminals, as inferred under coalescent-based inference from Matrix 0.9C.

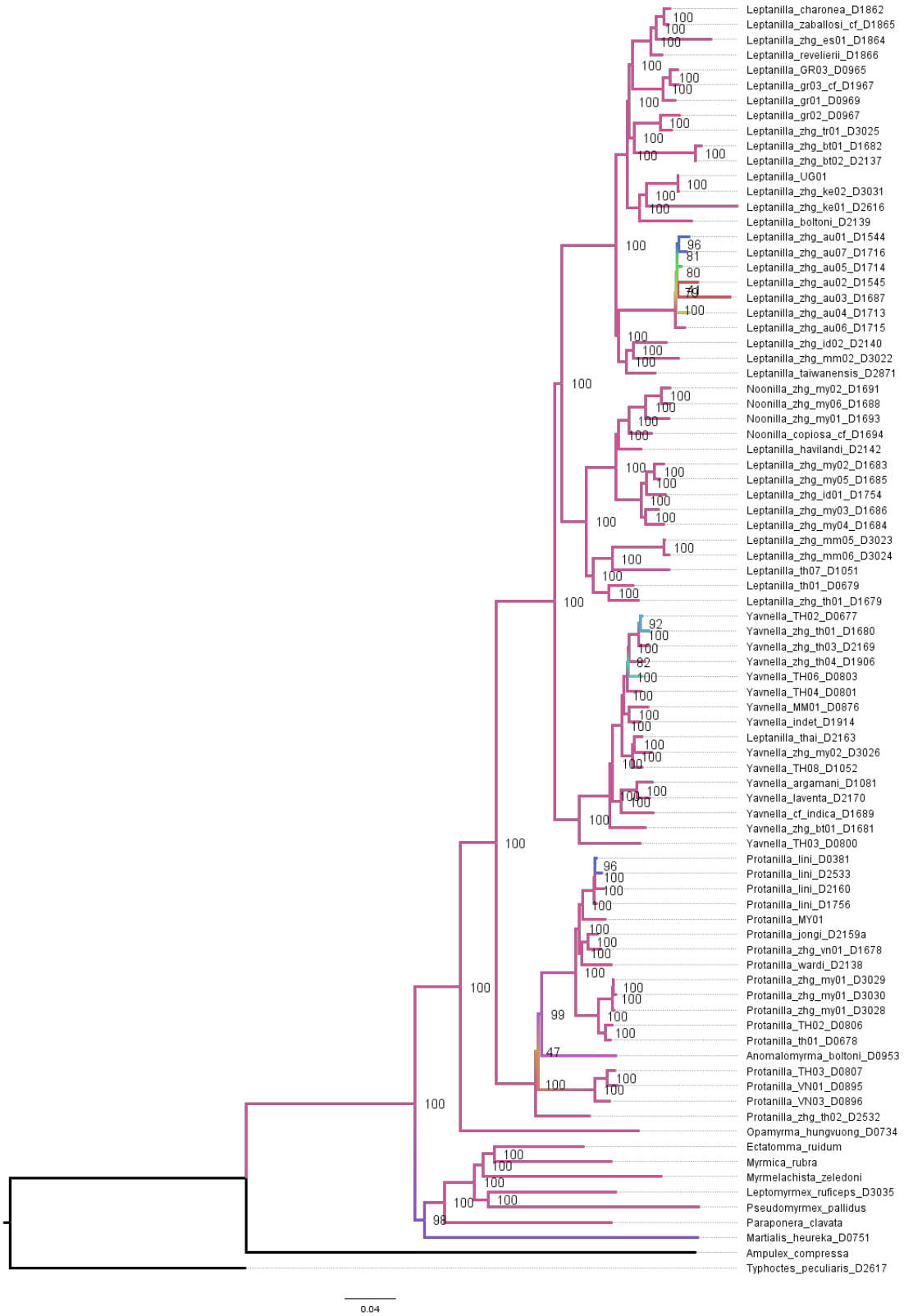

Fig. 5.S39. Phylogeny of the Leptanillinae and nine outgroup terminals, as inferred under ML with by-locus partitioning from Matrix 0.95C.

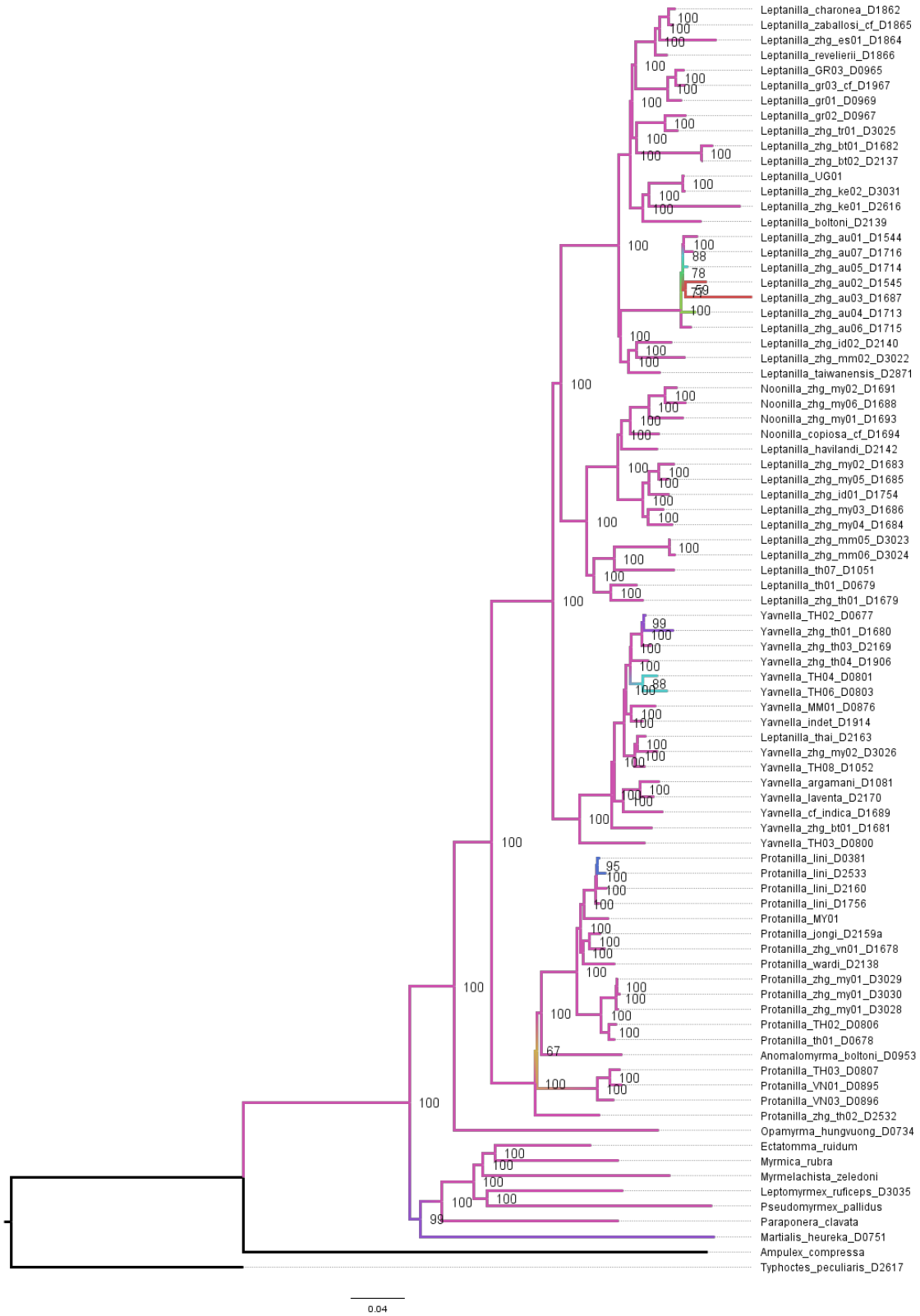

Fig. 5.S40. Phylogeny of the Leptanillinae and nine outgroup terminals, as inferred under ML with within-locus partitioning from Matrix 0.95C.

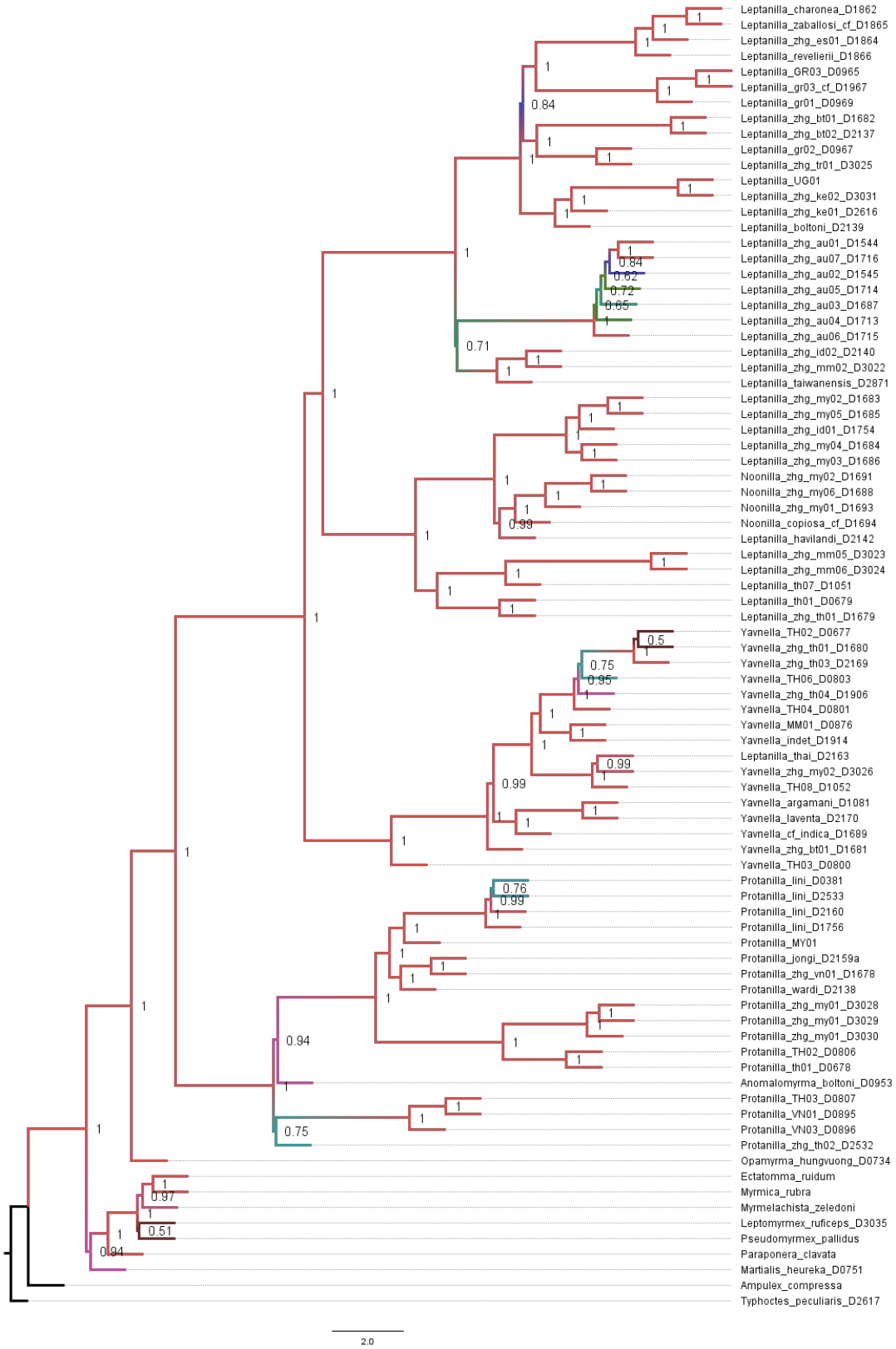

Fig. 5.S41. Phylogeny of the Leptanillinae and nine outgroup terminals, as inferred under coalescent-based inference from Matrix 0.95C.

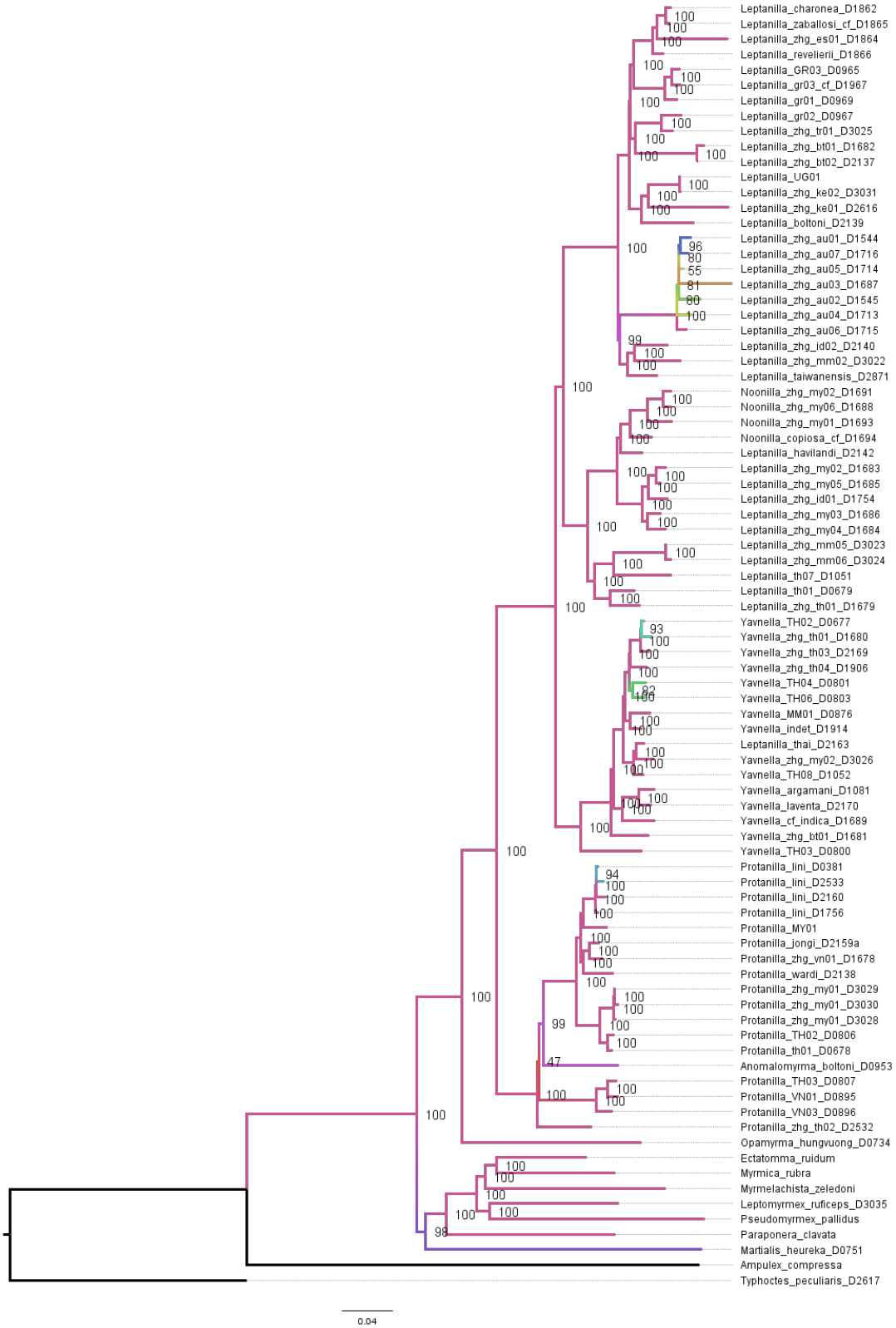

Fig. 5.S42. Phylogeny of the Leptanillinae and nine outgroup terminals, as inferred under ML with by-locus partitioning from Matrix 1C.

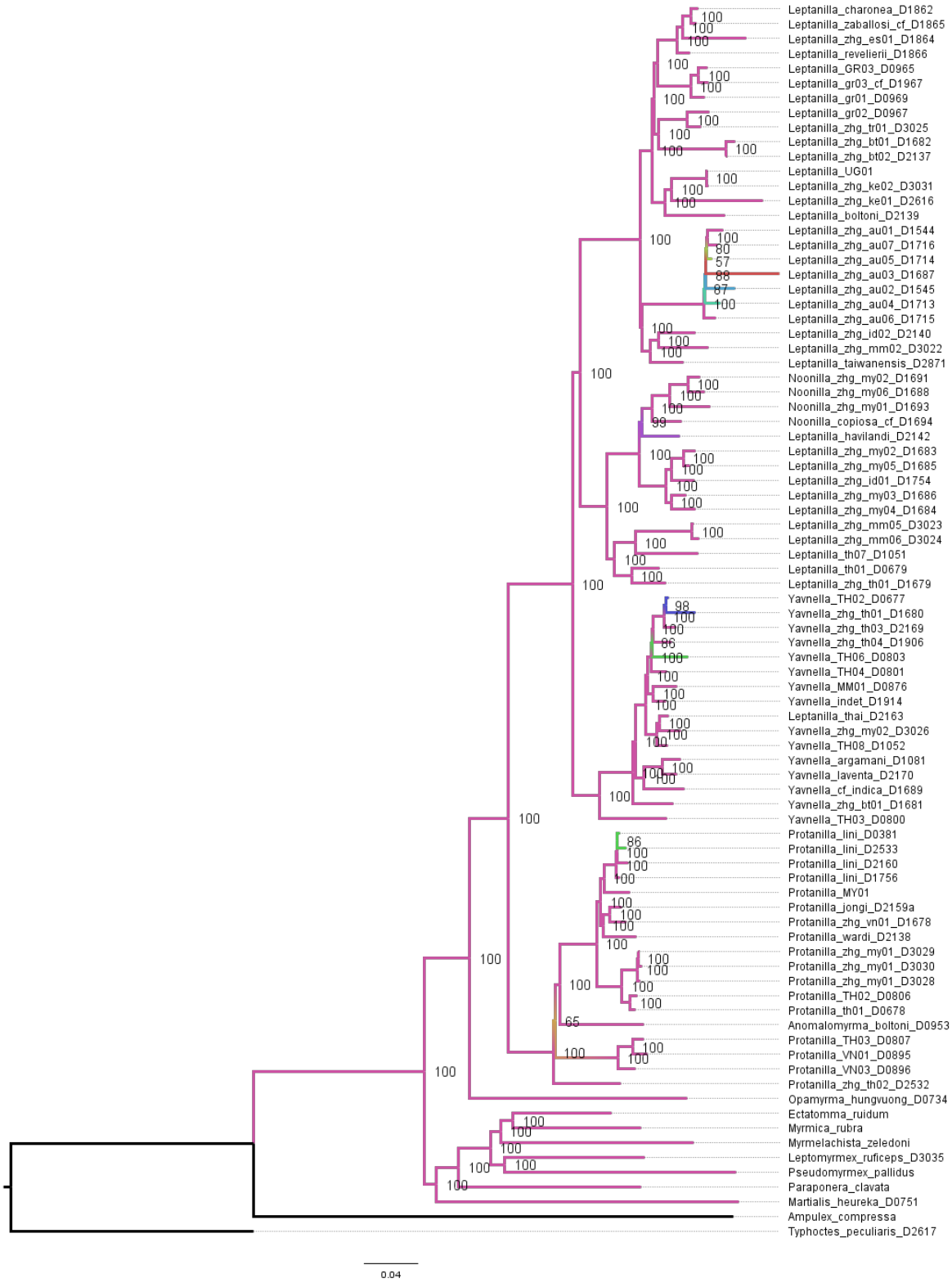

Fig. 5.S43. Phylogeny of the Leptanillinae and nine outgroup terminals, as inferred under ML with within-locus partitioning from Matrix 1C.

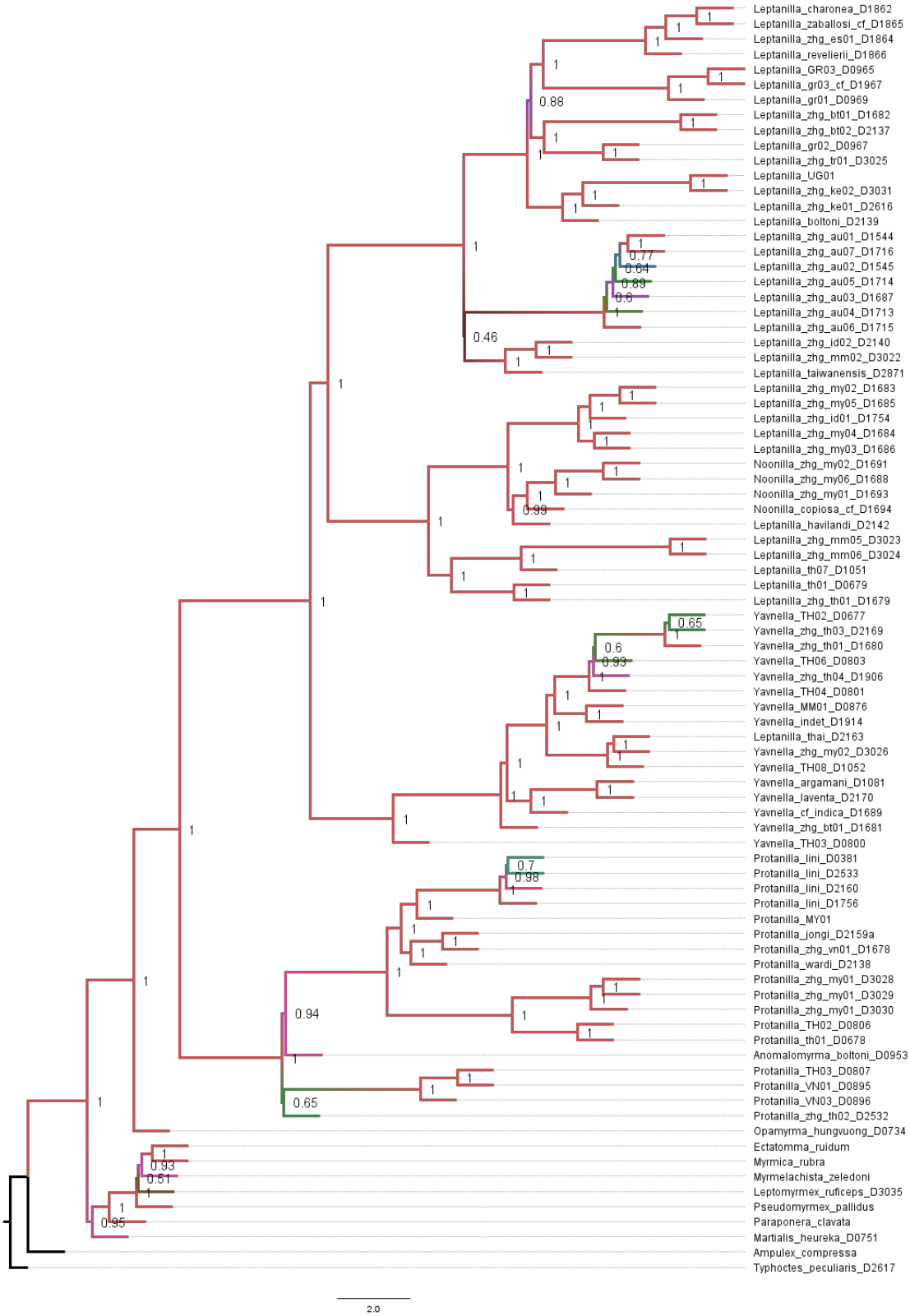

Fig. 5.S44. Phylogeny of the Leptanillinae and nine outgroup terminals, as inferred under coalescent-based inference from Matrix 1C.

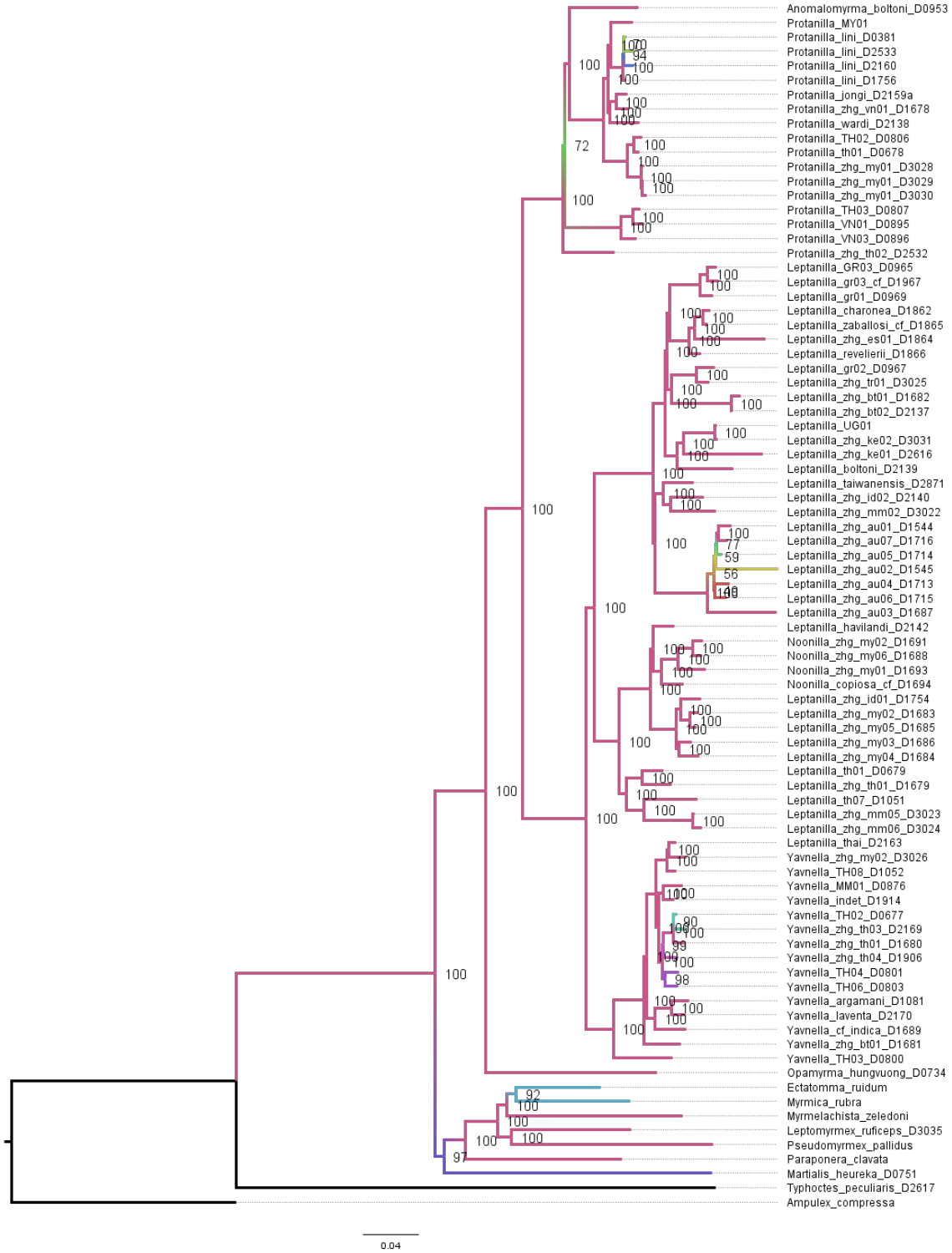

Fig. 5.S45. Phylogeny of the Leptanillinae and nine outgroup terminals, as inferred under ML with by-locus partitioning from Matrix 0.8D.

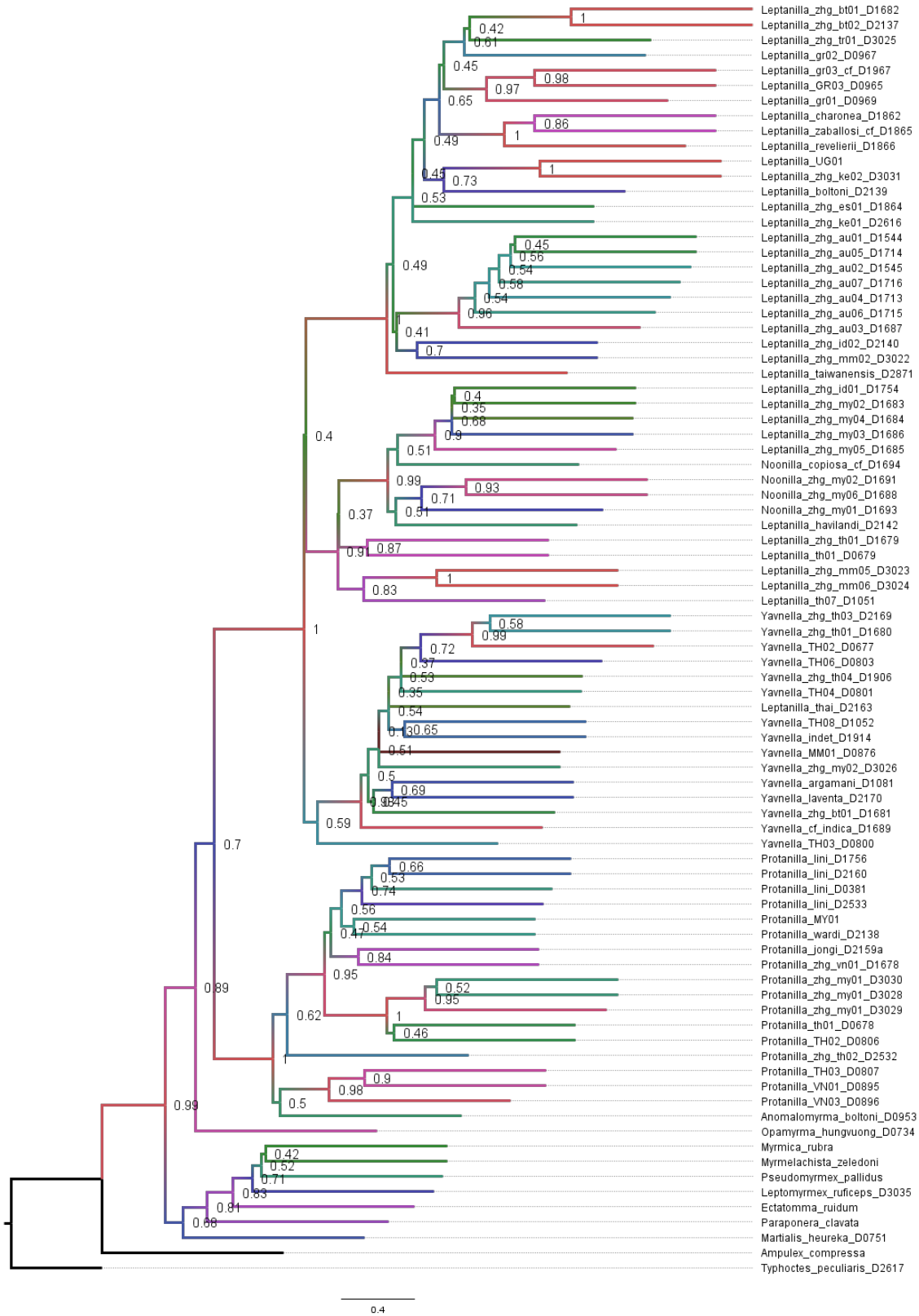

Fig. 5.S46. Phylogeny of the Leptanillinae and nine outgroup terminals, as inferred under coalescent-based inference from Matrix 0.8D.

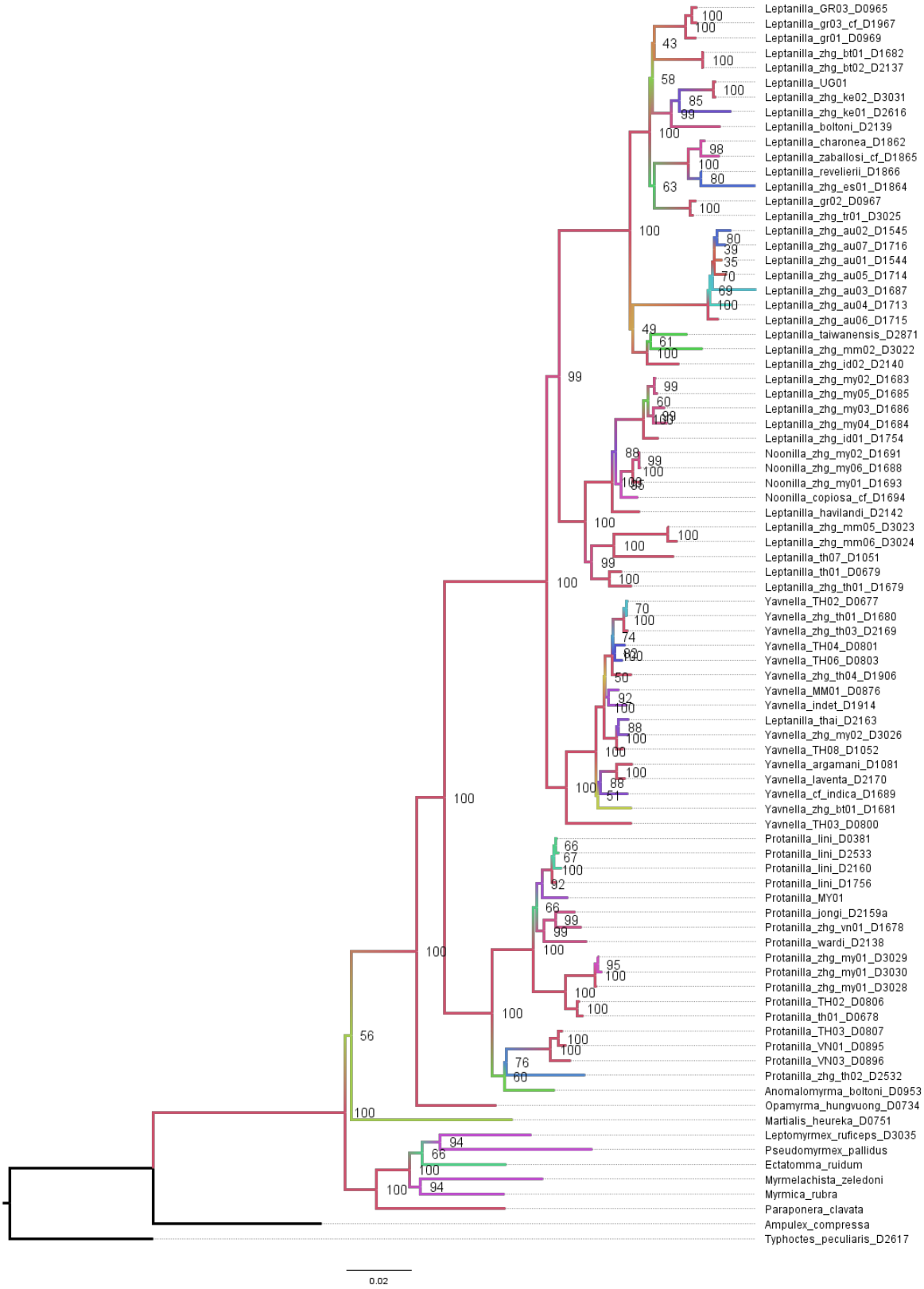

Fig. 5.S47. Phylogeny of the Leptanillinae and nine outgroup terminals, as inferred under ML with by-locus partitioning from Matrix 0.85D.

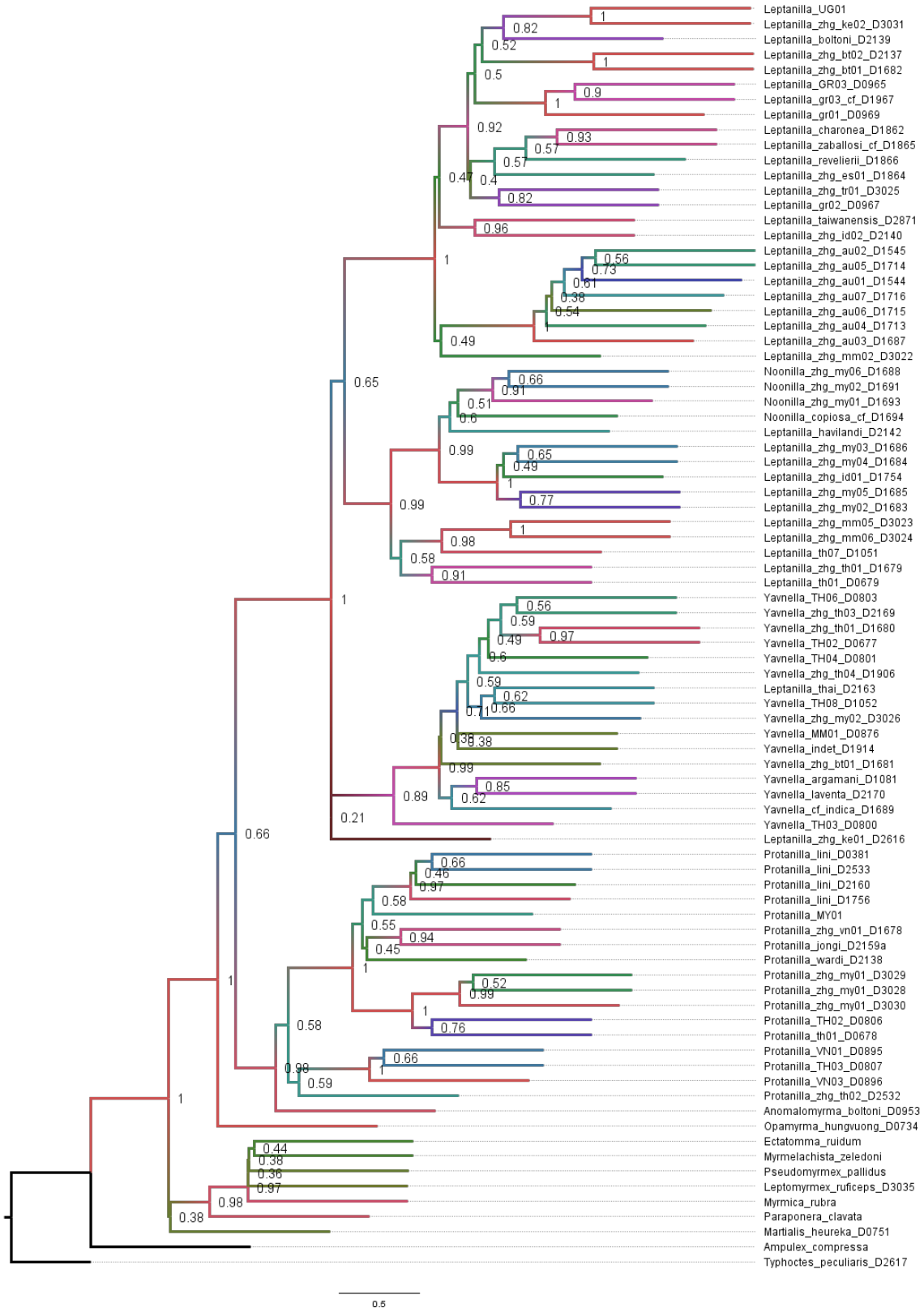

Fig. 5.S48. Phylogeny of the Leptanillinae and nine outgroup terminals, as inferred under coalescent-based inference from Matrix 0.85D.

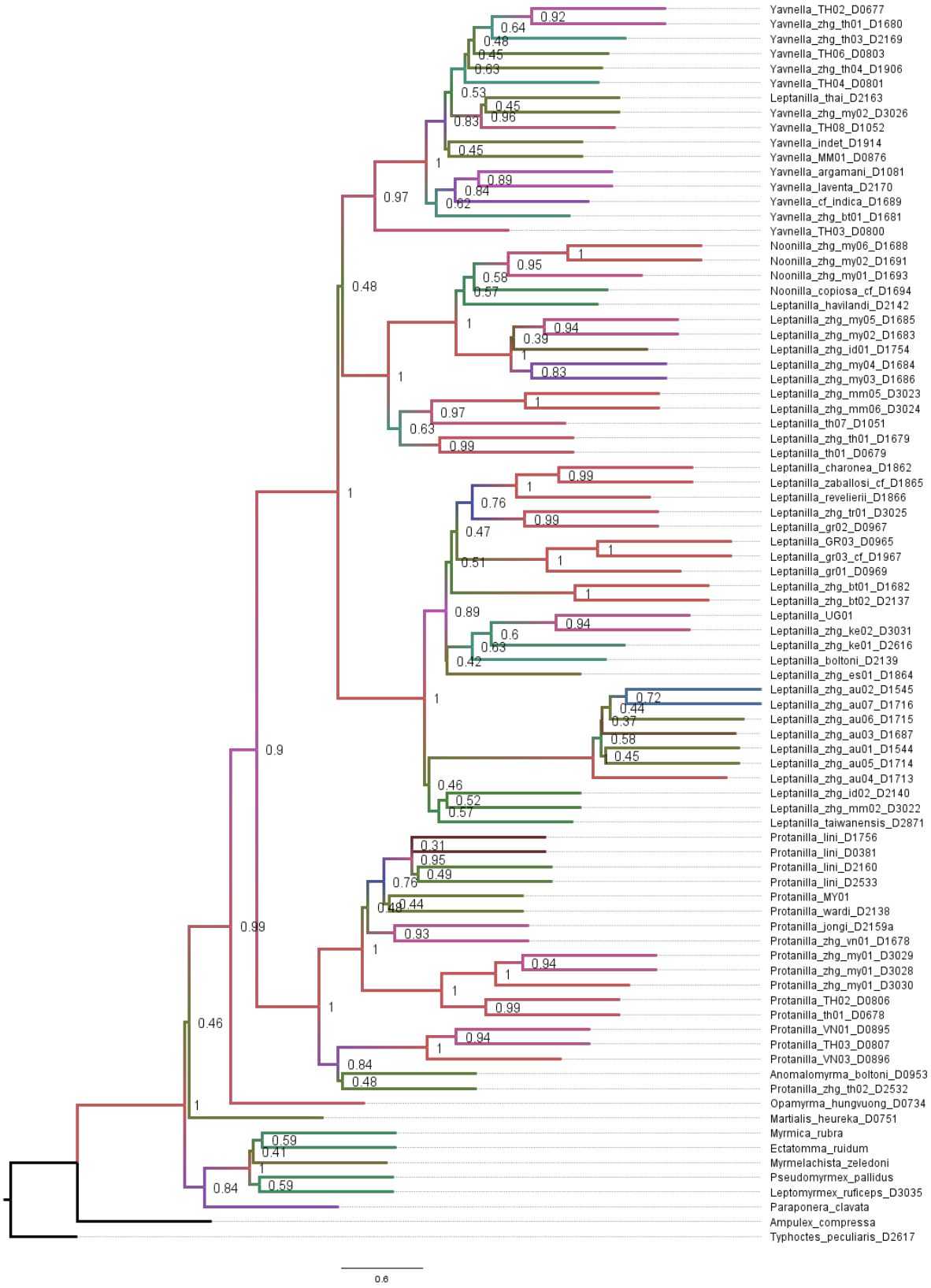

Fig. 5.S49. Phylogeny of the Leptanillinae and nine outgroup terminals, as inferred under ML with by-locus partitioning from Matrix 0.9D.

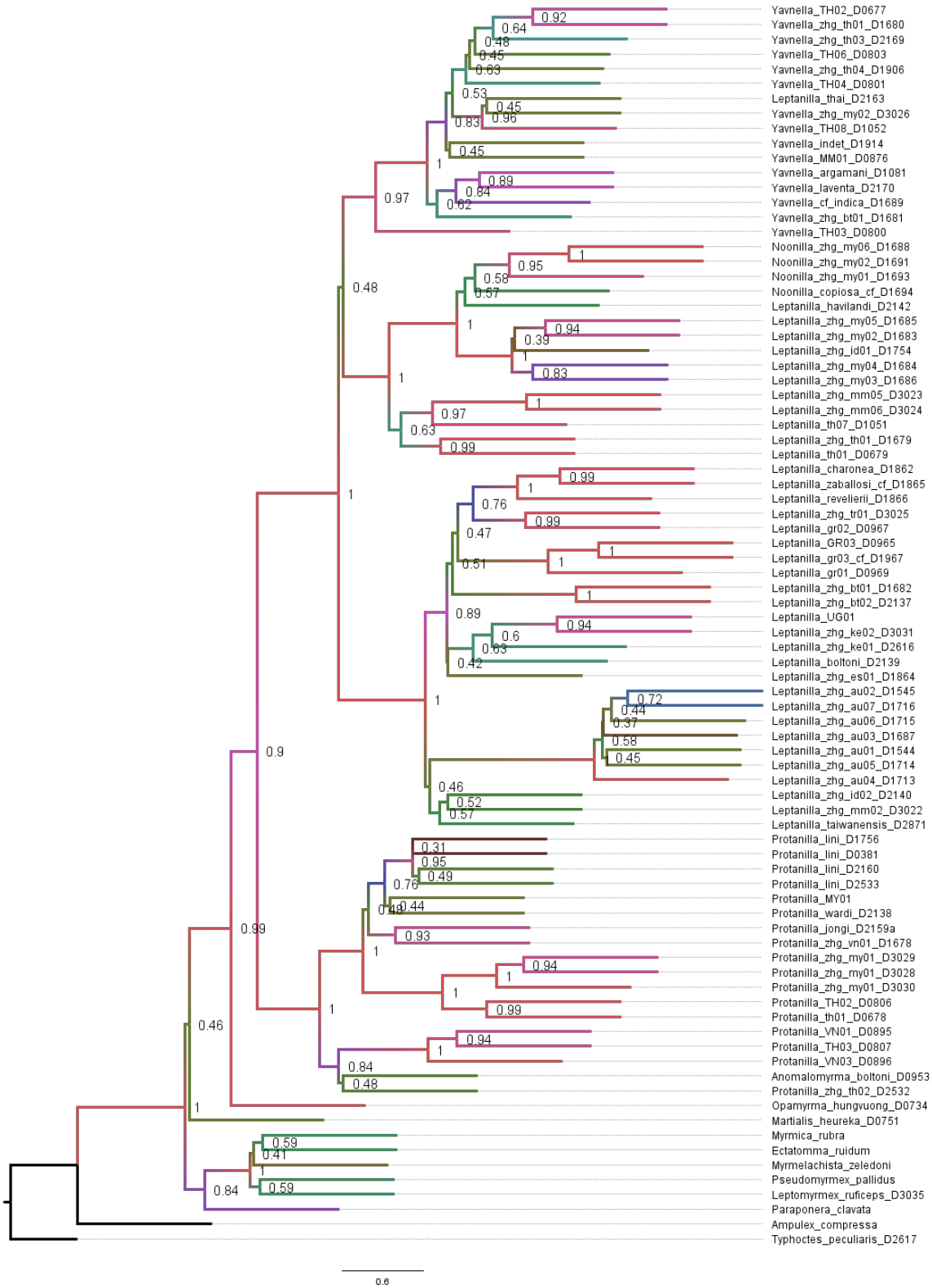

Fig. 5.S50. Phylogeny of the Leptanillinae and nine outgroup terminals, as inferred under coalescent-based inference with by-locus partitioning from Matrix 0.9D.

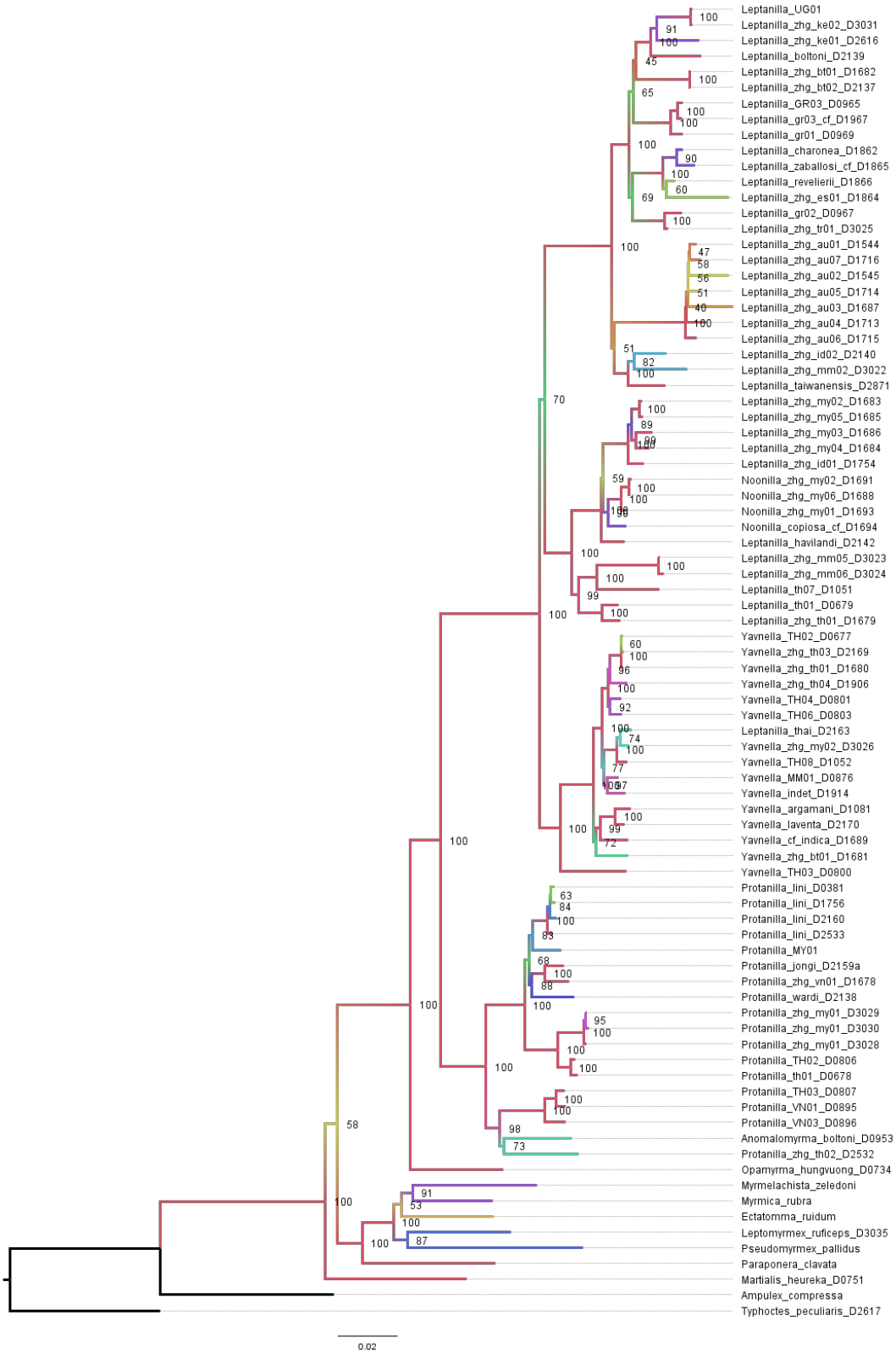

Fig. 5.S51. Phylogeny of the Leptanillinae and nine outgroup terminals, as inferred under ML with by-locus partitioning from Matrix 0.95D.

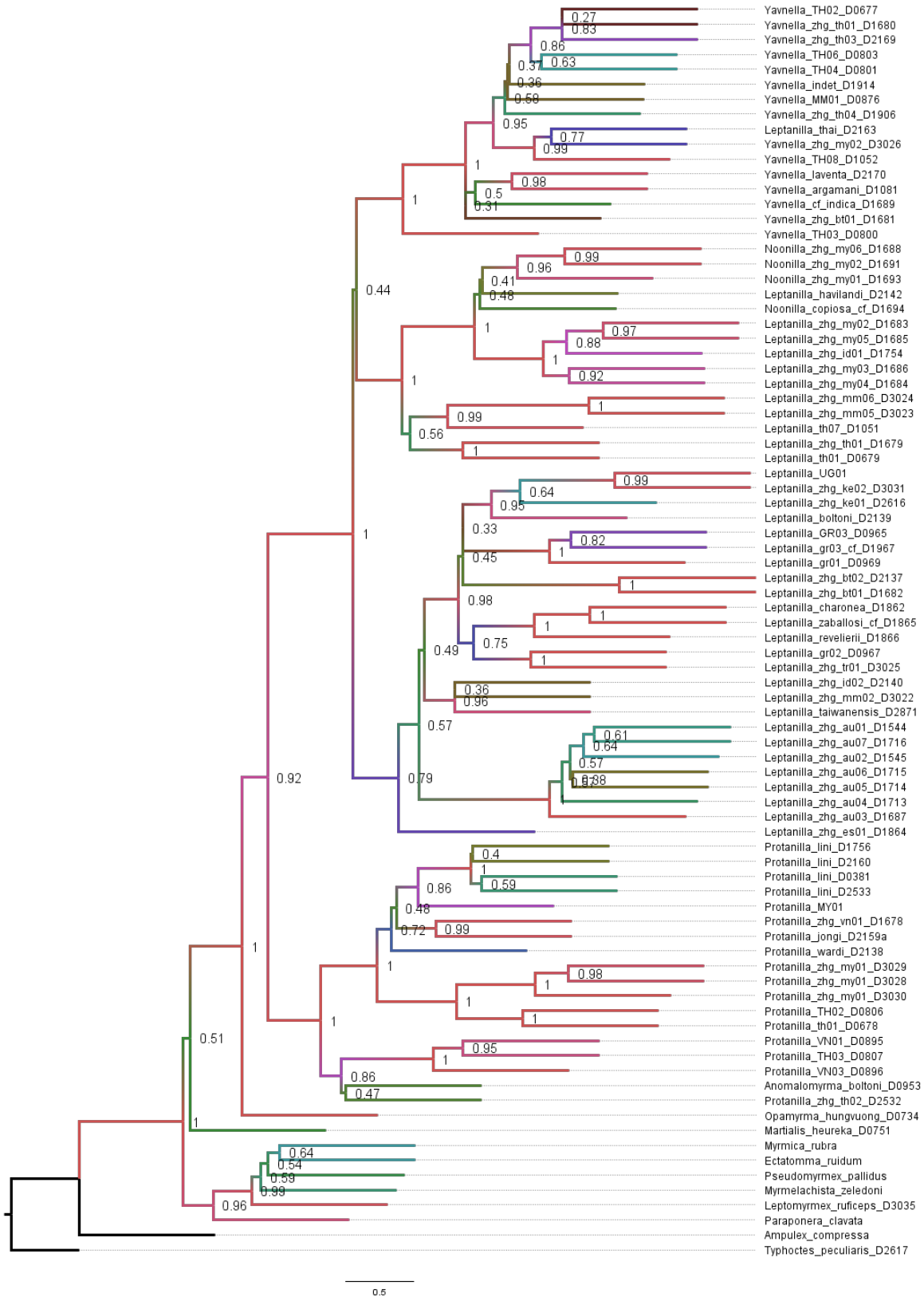

Fig. 5.S52. Phylogeny of the Leptanillinae and nine outgroup terminals, as inferred under coalescent-based inference from Matrix 0.95D.

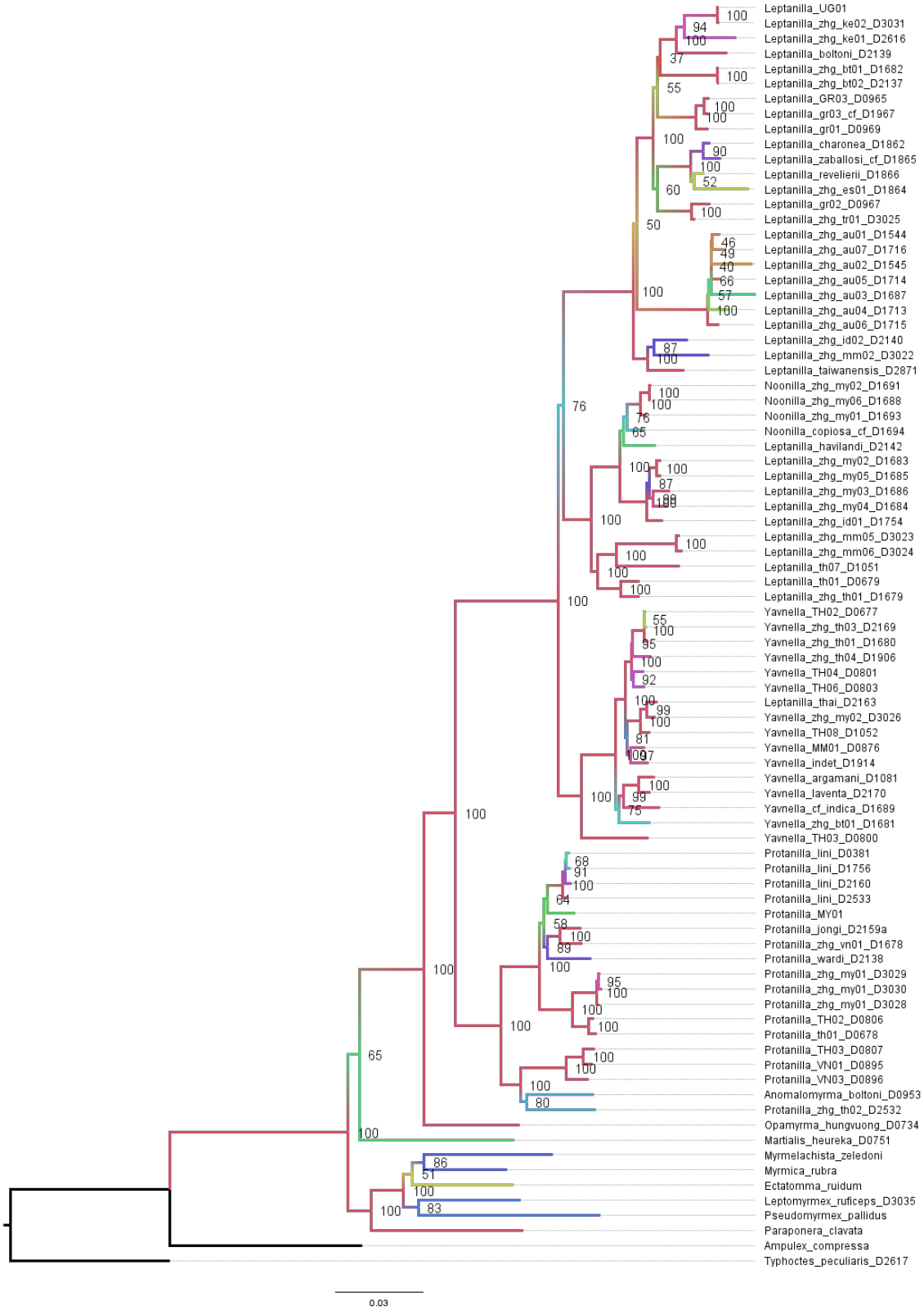

Fig. 5.S53. Phylogeny of the Leptanillinae and nine outgroup terminals, as inferred under ML with by-locus partitioning from Matrix 1D.

Fig. 5.S54. Phylogeny of the Leptanillinae and nine outgroup terminals, as inferred under coalescent-based inference from Matrix 1D.

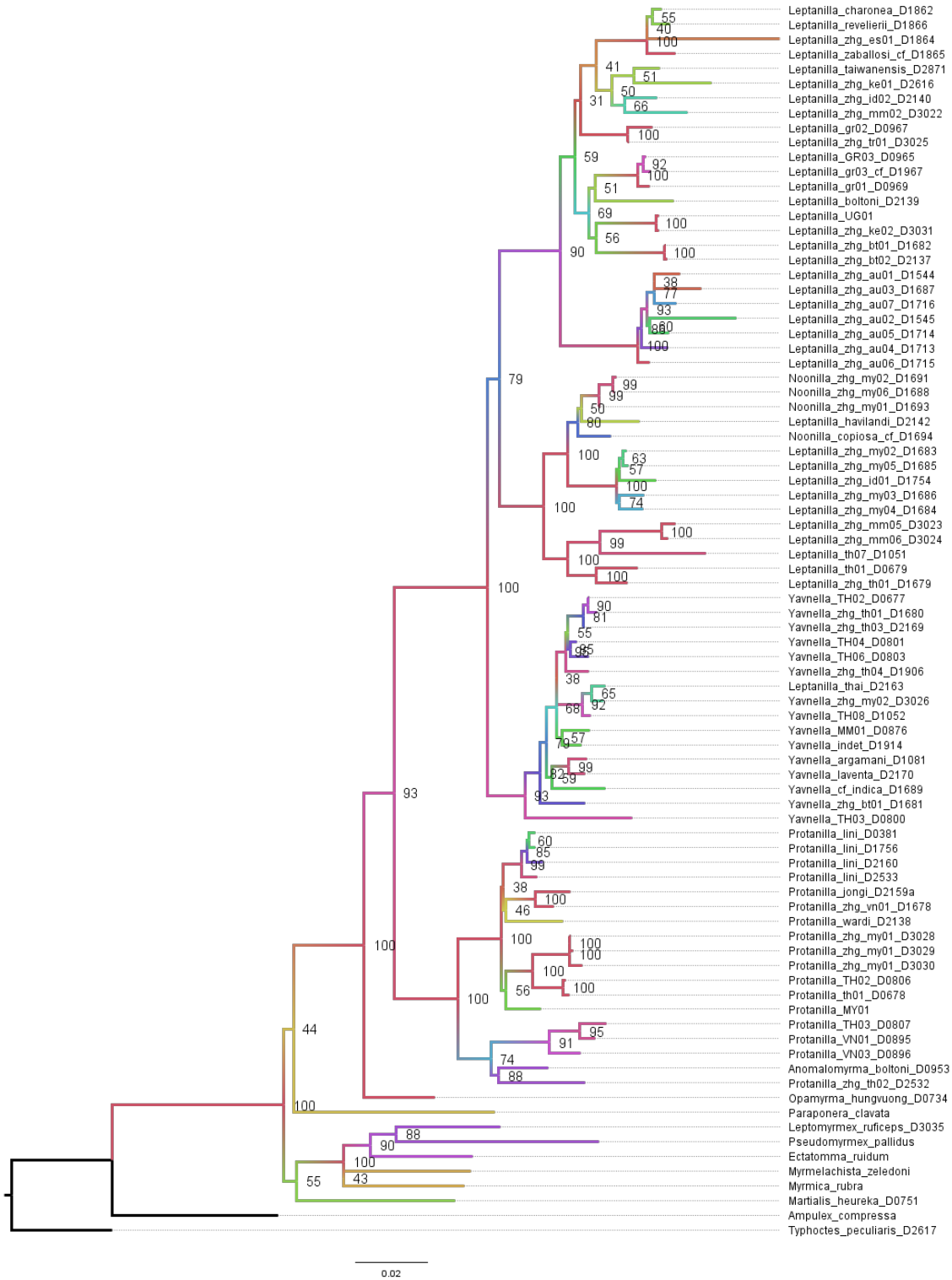

Fig. 5.S55. Phylogeny of the Leptanillinae and nine outgroup terminals, as inferred under ML with by-locus partitioning from Matrix 1D†.

Fig. 5.S56. Phylogeny of the Leptanillinae and nine outgroup terminals, as inferred under a Bayesian framework from Matrix 0.9A.

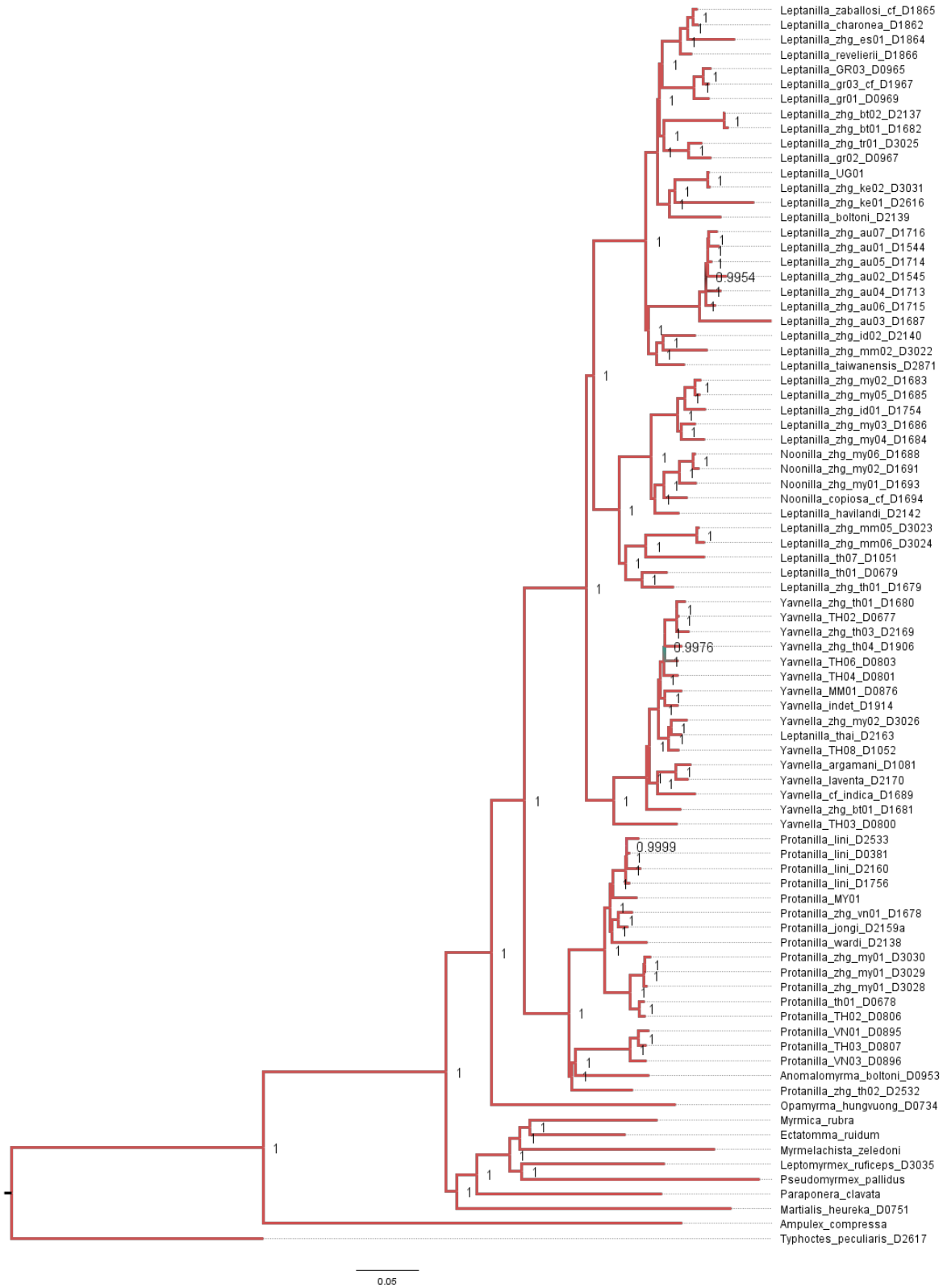

Fig. 5.S57. Phylogeny of the Leptanillinae and nine outgroup terminals, as inferred under a Bayesian framework from Matrix 0.9B.

Fig. 5.S58. Phylogeny of the Leptanillinae and nine outgroup terminals, as inferred under a Bayesian framework from Matrix 0.9C.

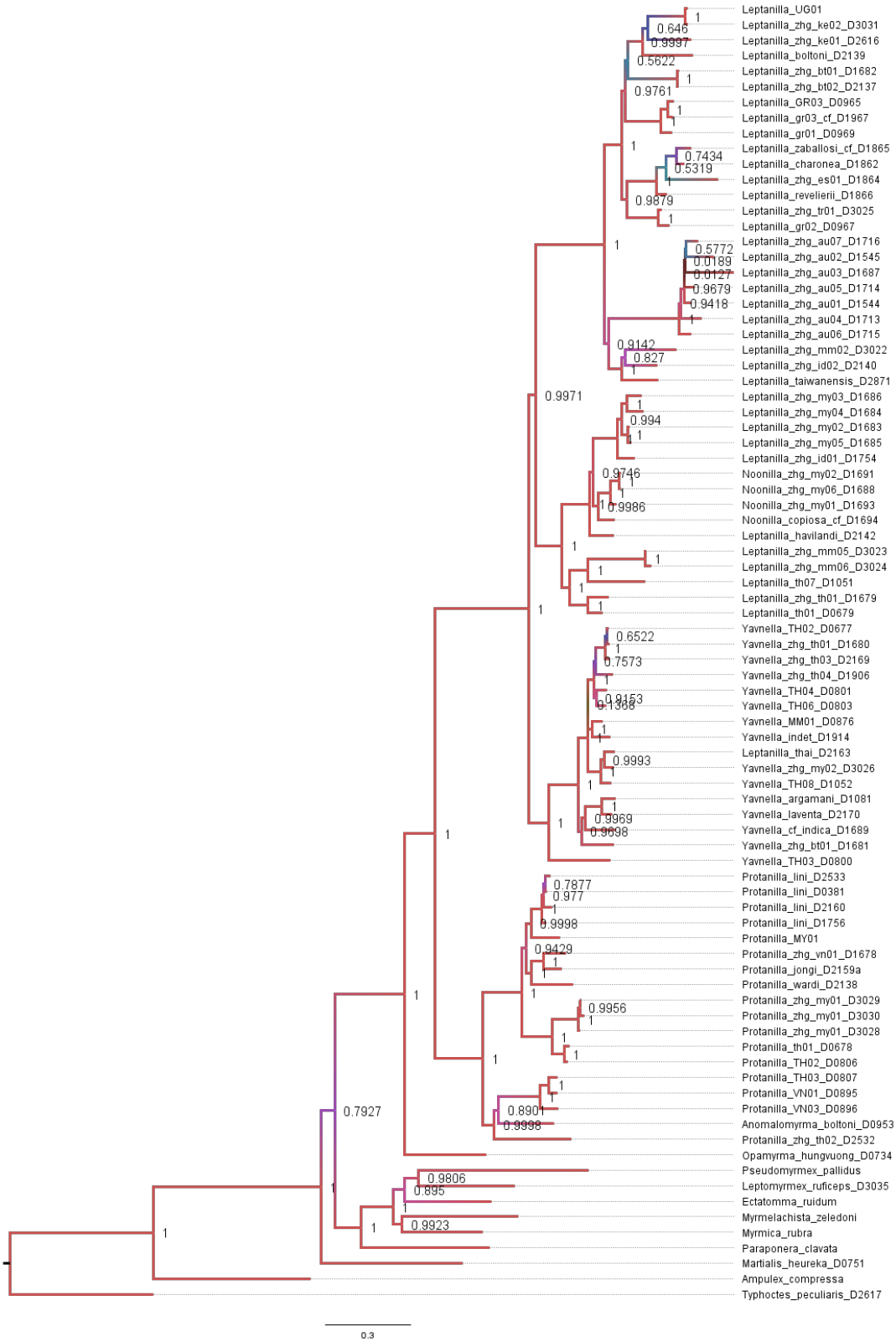

Fig. 5.S59. Phylogeny of the Leptanillinae and nine outgroup terminals, as inferred under a Bayesian framework from Matrix 0.9D.

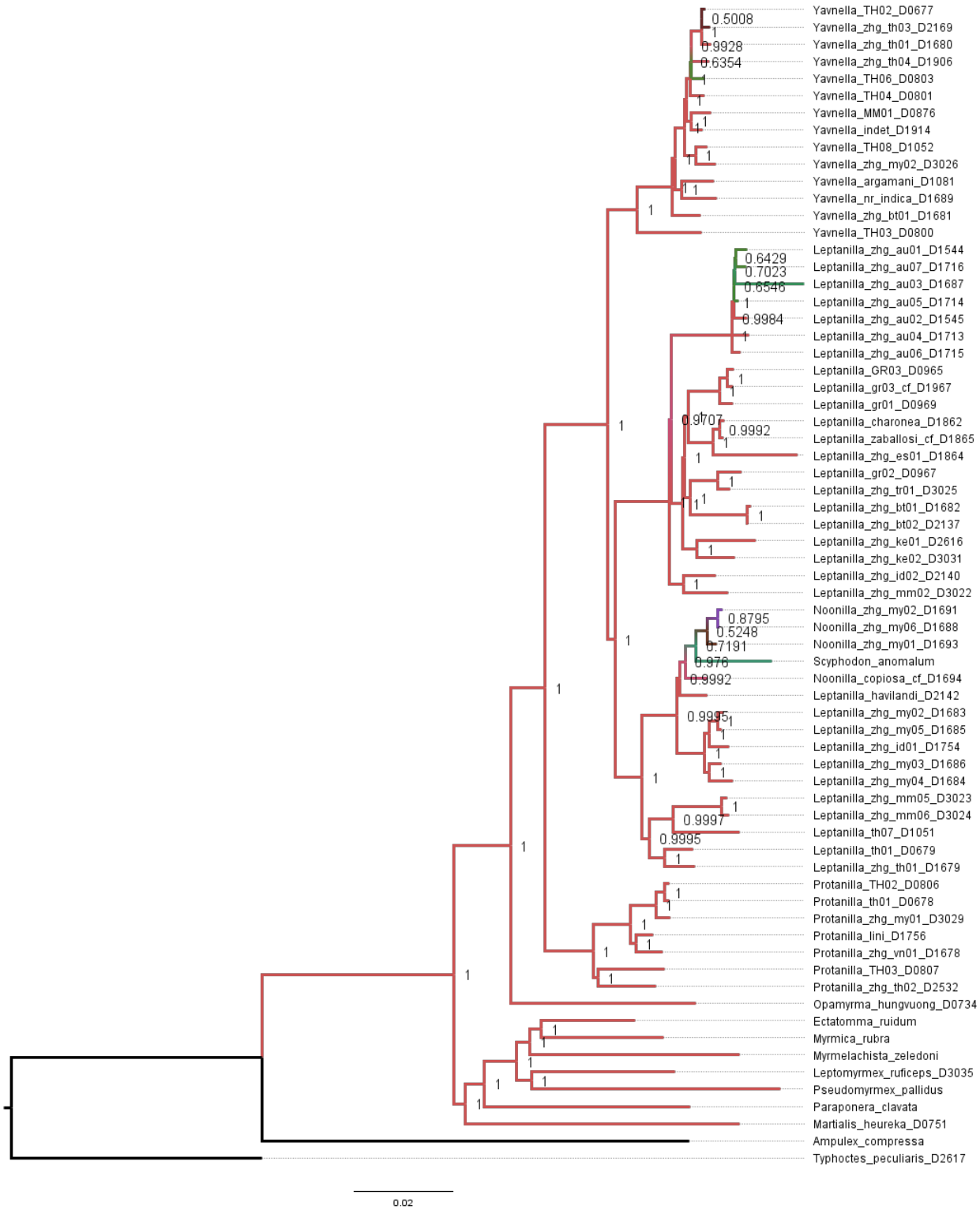

Fig. 5.S60. Bayesian total-evidence phylogeny of the Leptanillinae and nine outgroup terminals, inferred from Matrix B′ and a matrix of 62 binary male morphological characters, including *Leptanilla anomala* (Brues).

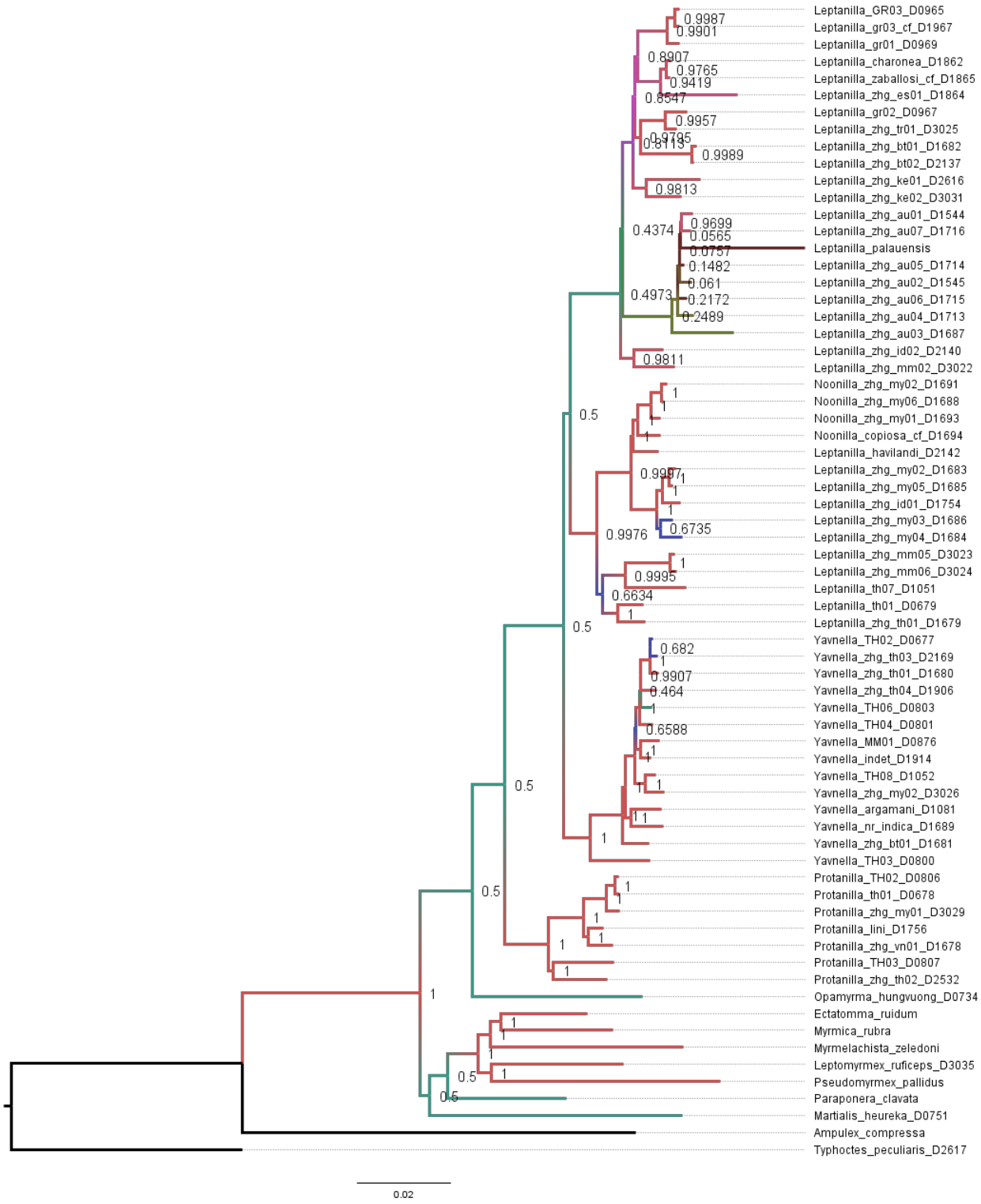

Fig. 5.S61. Bayesian total-evidence phylogeny of the Leptanillinae and nine outgroup terminals, inferred from Matrix B′ and a matrix of 62 binary male morphological characters, including *Leptanilla palauensis* (Smith).

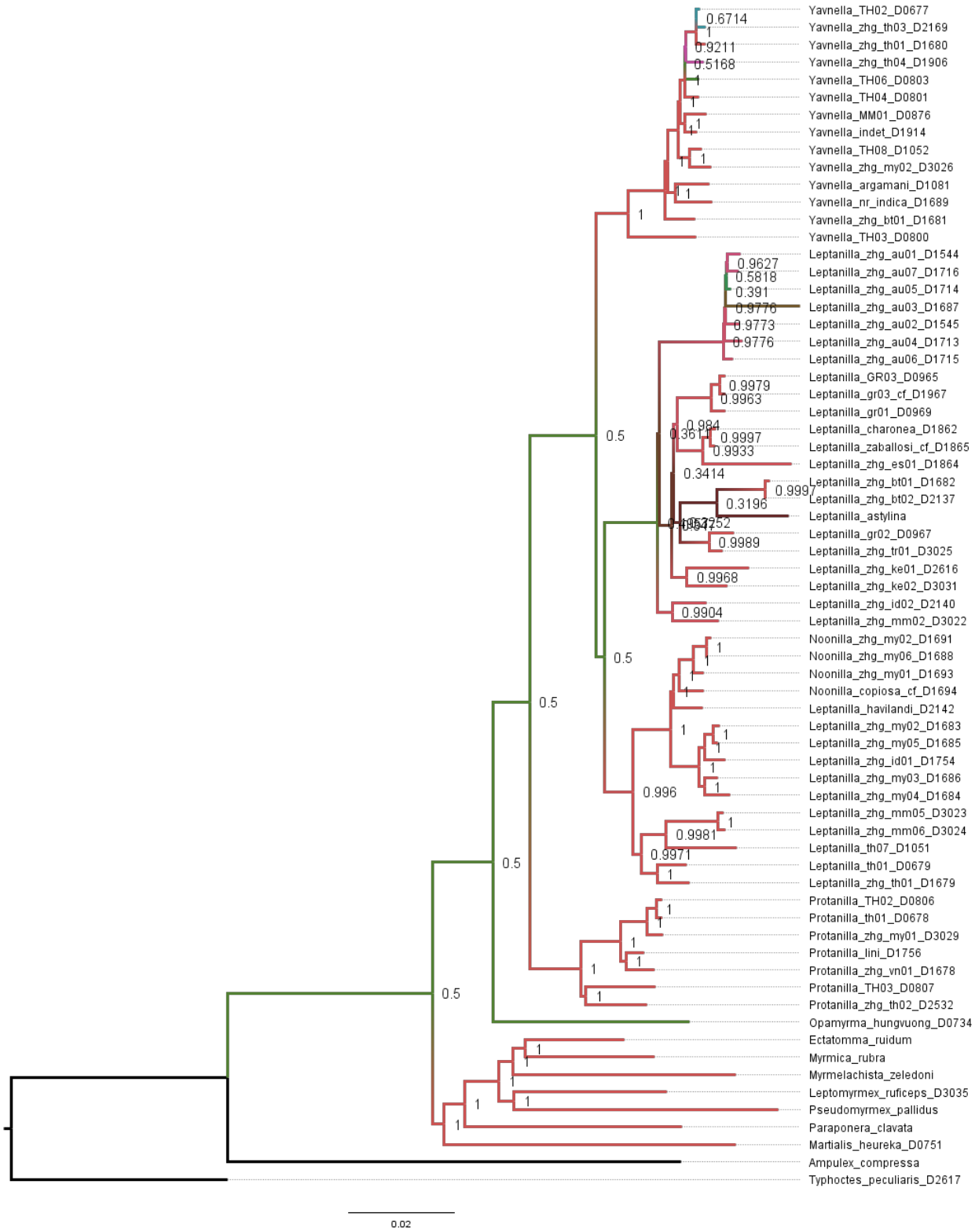

Fig. 5.S62. Bayesian total-evidence phylogeny of the Leptanillinae and nine outgroup terminals, inferred from Matrix B′ and a matrix of 62 binary male morphological characters, including *Leptanilla astylina* Petersen.

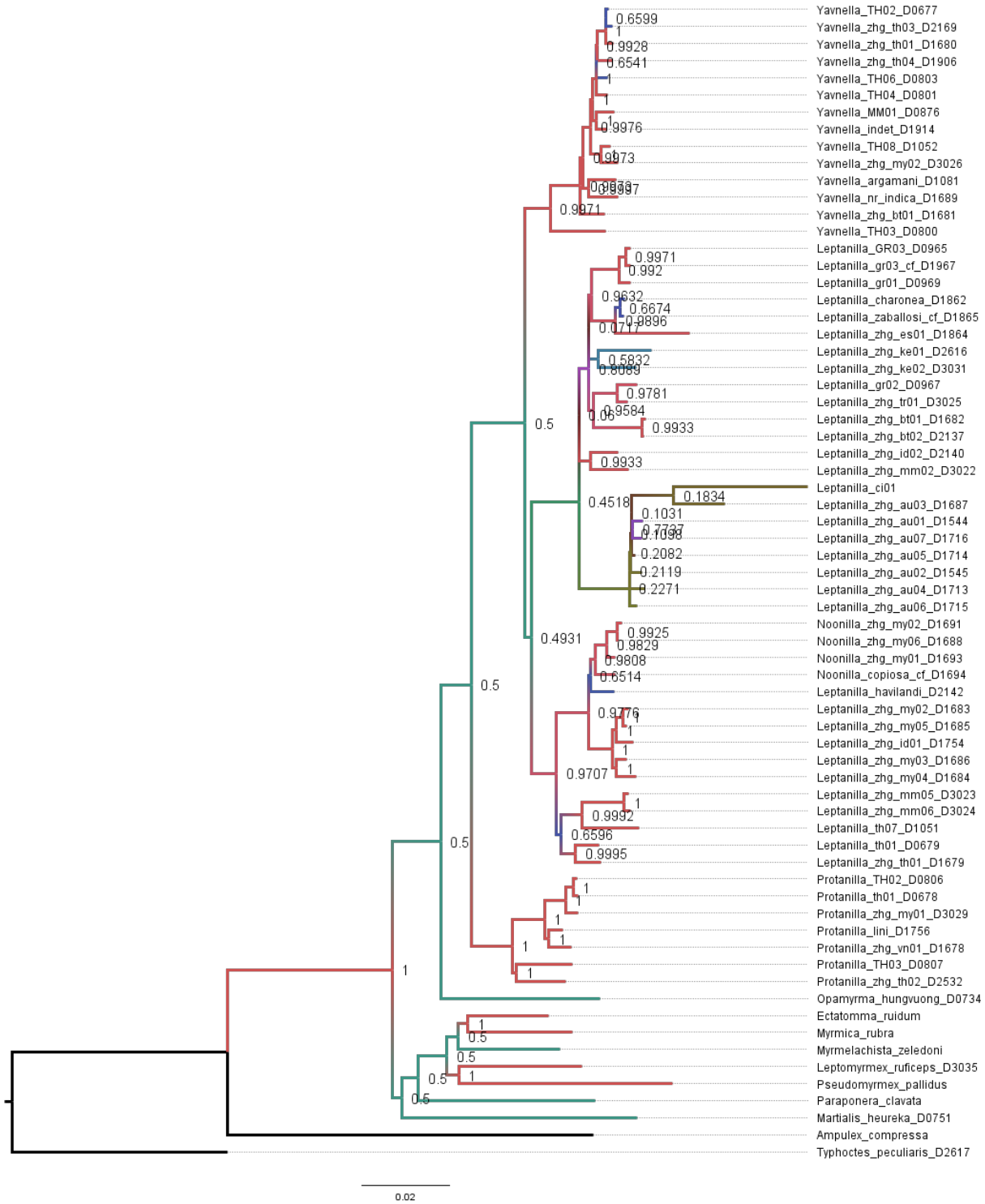

Fig. 5.S63. Bayesian total-evidence phylogeny of the Leptanillinae and nine outgroup terminals, inferred from Matrix B′ and a matrix of 62 binary male morphological characters, including *Leptanilla* ci01.

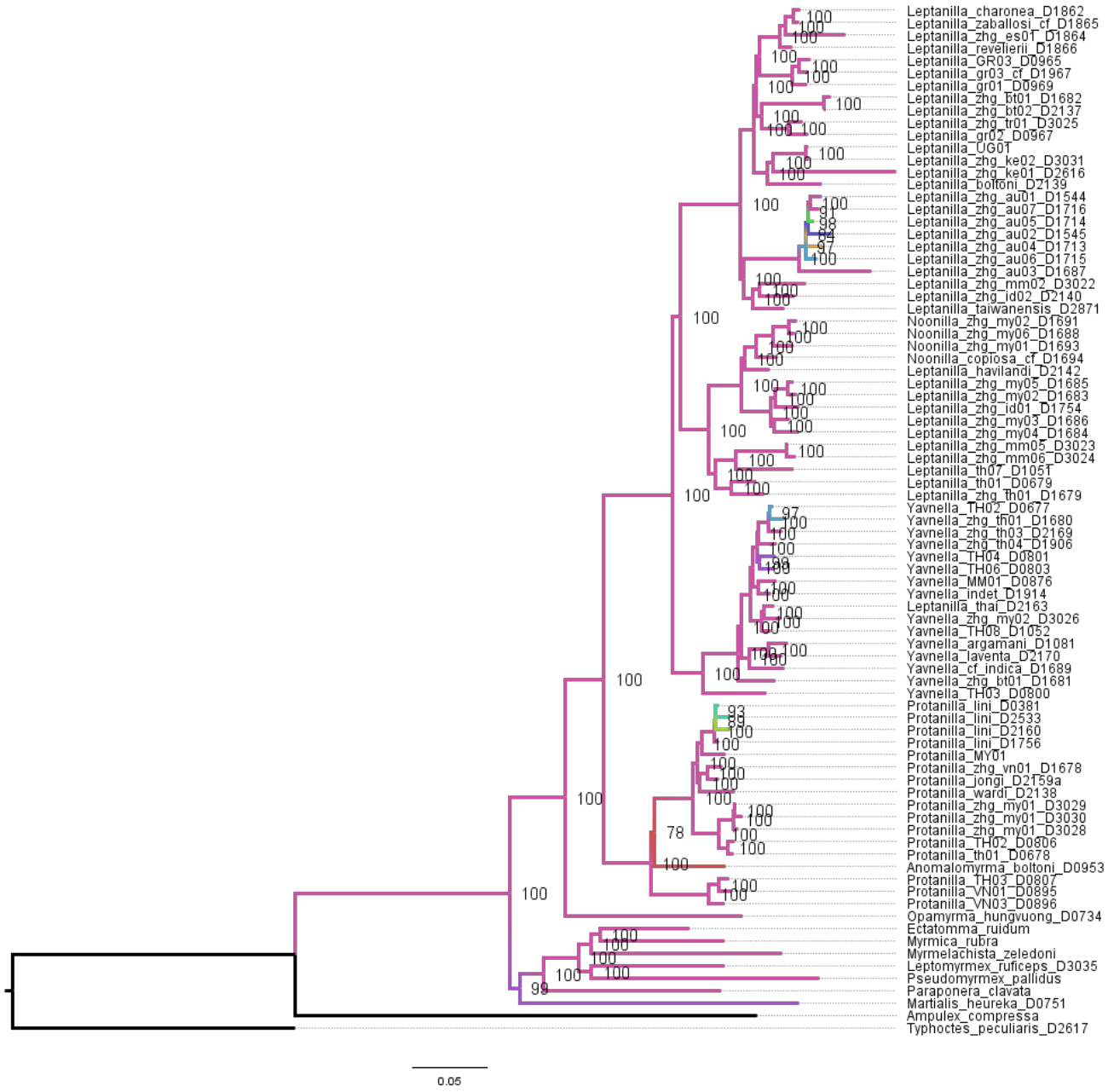

Fig. 5.S64. Phylogeny of the Leptanillinae and nine outgroup terminals, as inferred under ML with by-locus partitioning from Matrix 0.8A*.

Fig. 5.S65. Phylogeny of the Leptanillinae and nine outgroup terminals, as inferred under ML with within-locus partitioning from Matrix 0.8A*.

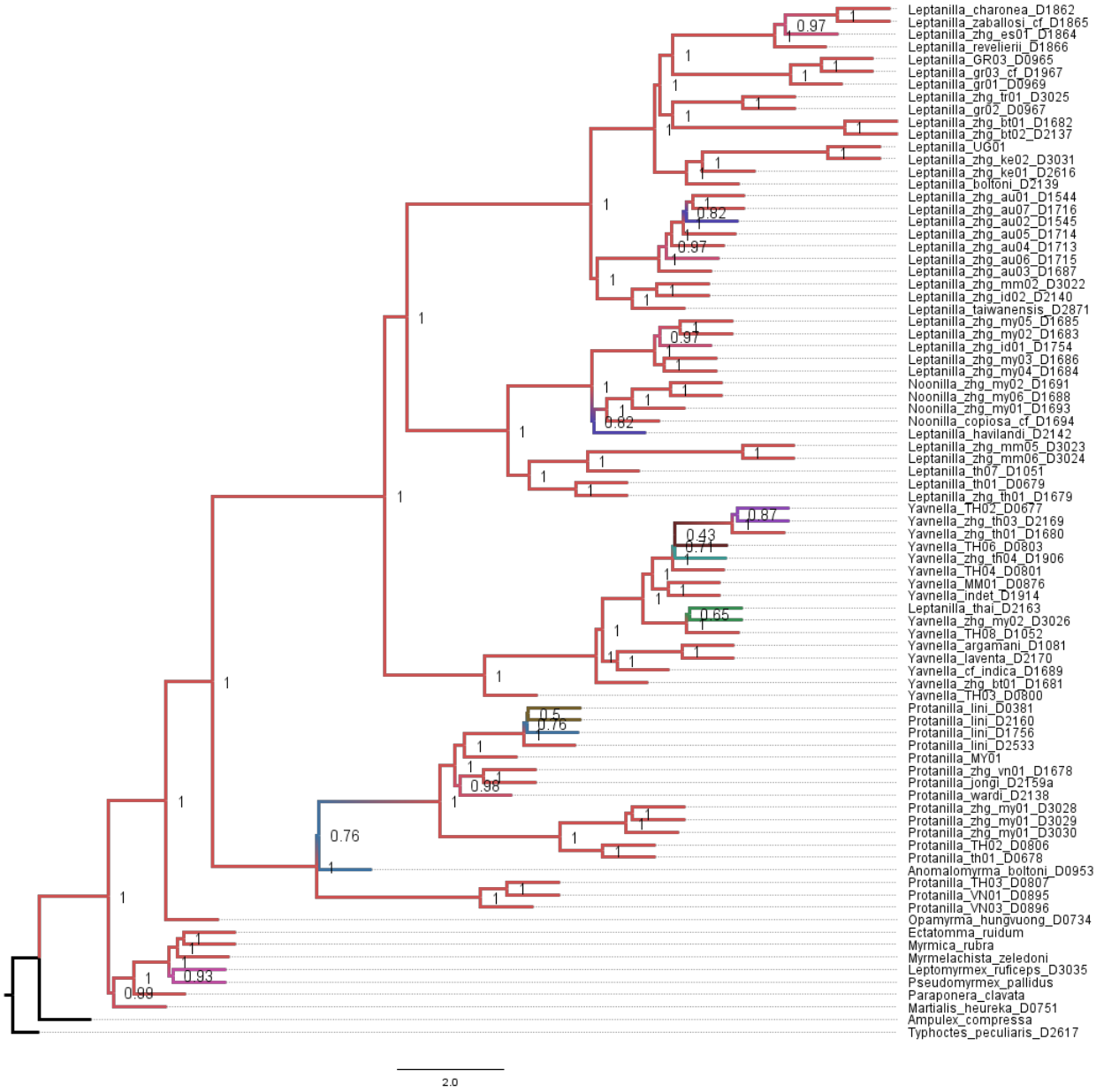

Fig. 5.S66. Phylogeny of the Leptanillinae and nine outgroup terminals, as inferred under coalescent-based inference with by-locus partitioning from Matrix 0.8A*.

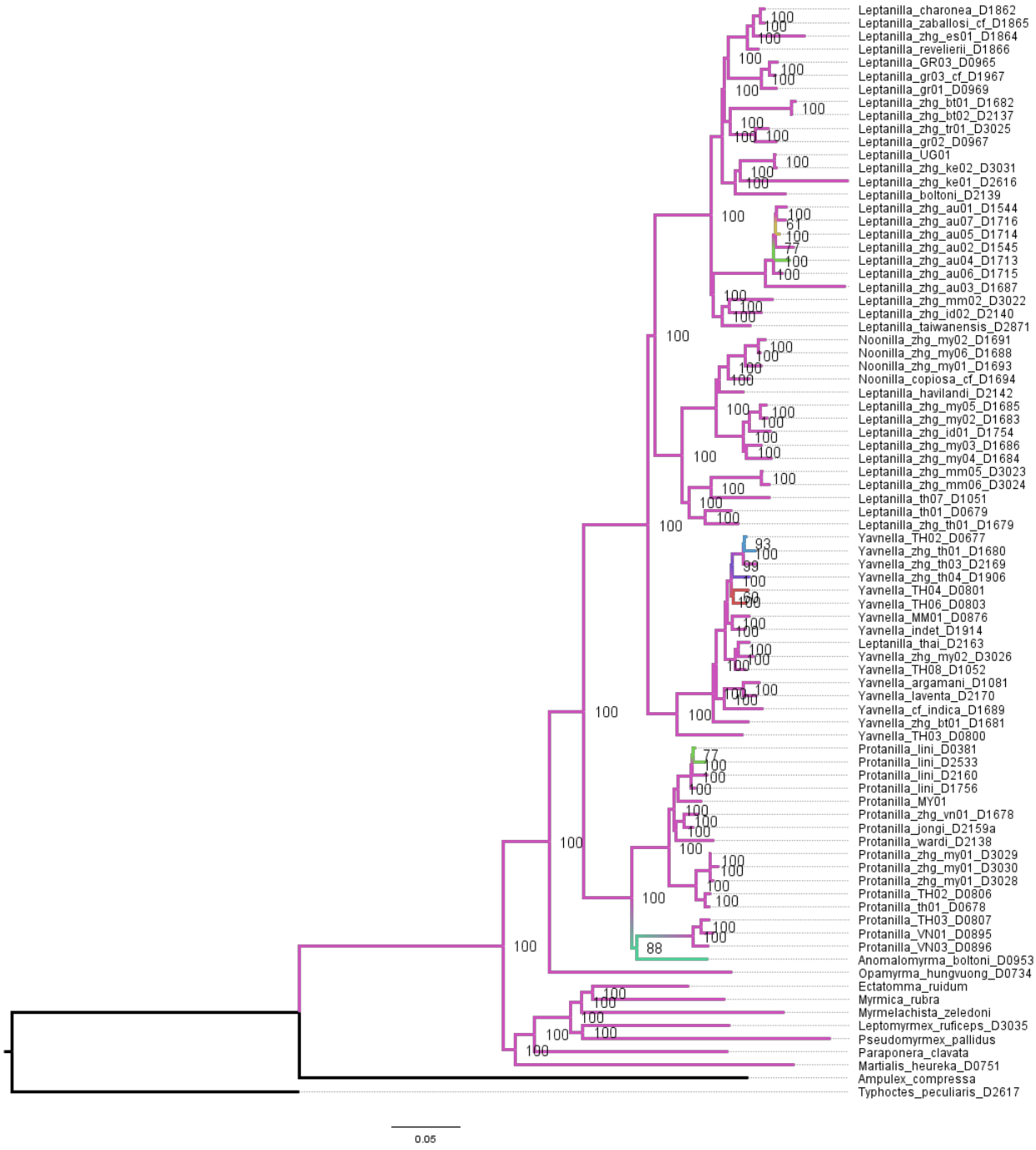

Fig. 5S67. Phylogeny of the Leptanillinae and nine outgroup terminals, as inferred under ML with by-locus partitioning from Matrix 0.85A*.

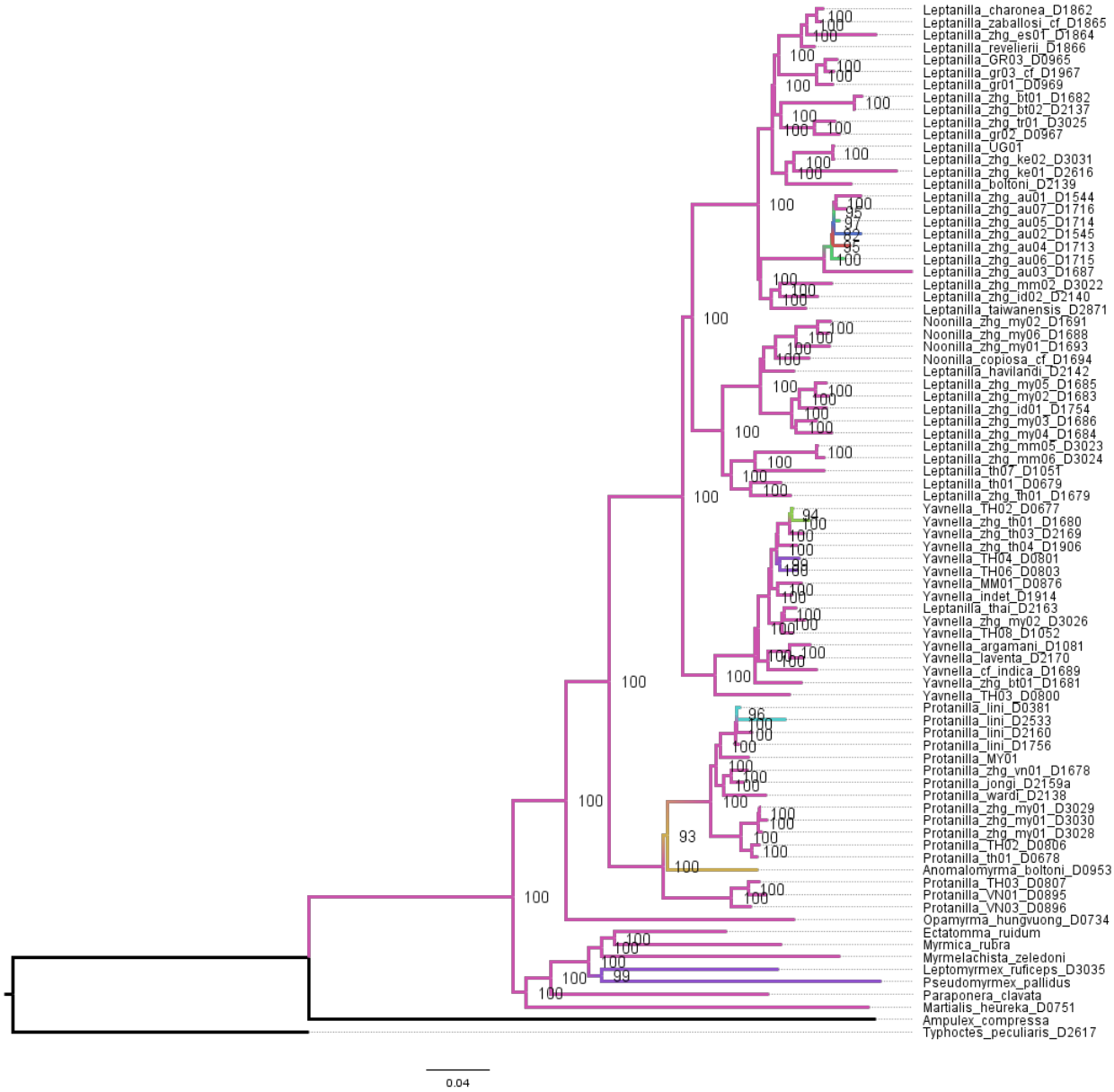

Fig. 5.S68. Phylogeny of the Leptanillinae and nine outgroup terminals, as inferred under ML with within-locus partitioning from Matrix 0.85A*.

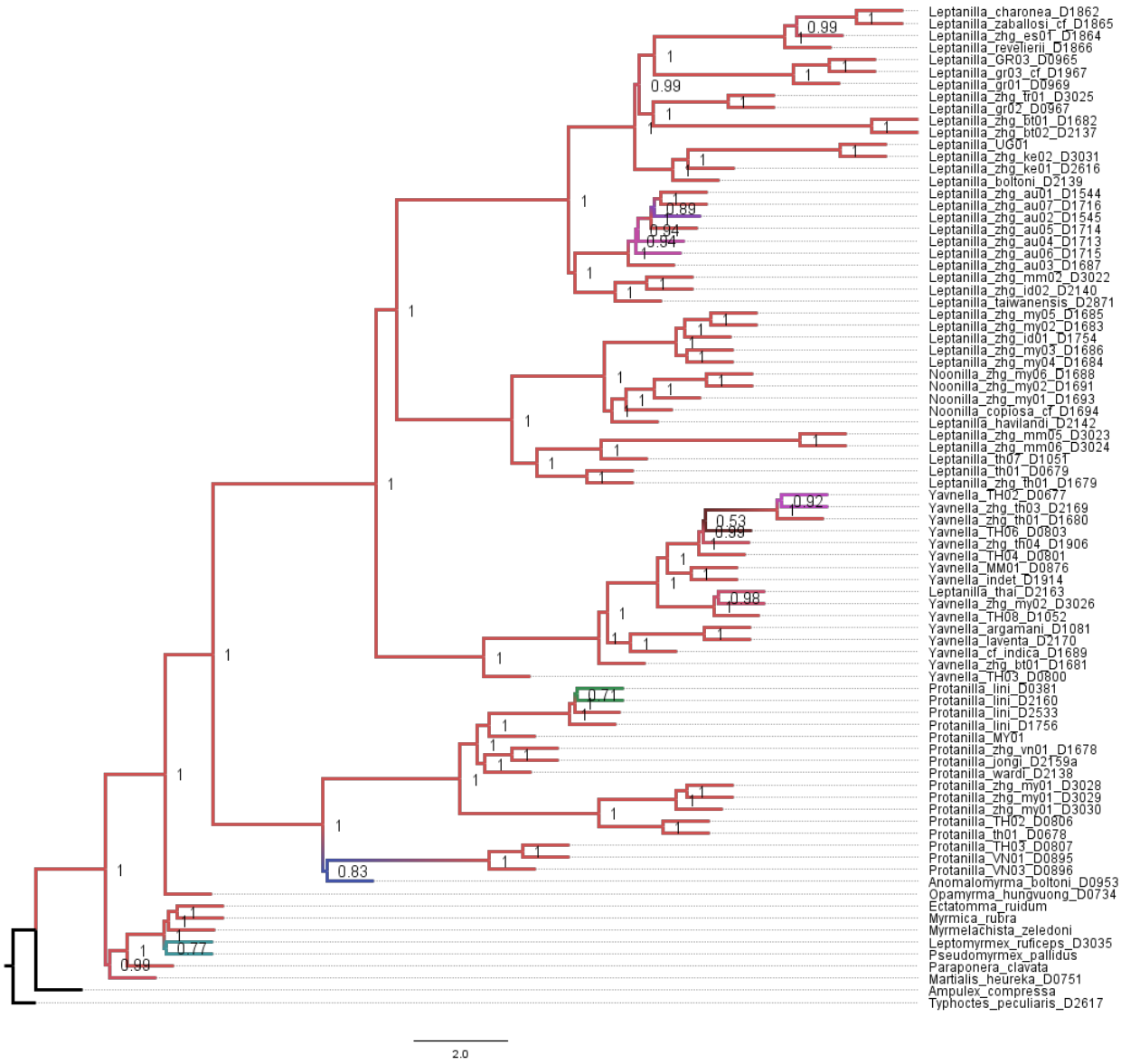

Fig. 5.S69. Phylogeny of the Leptanillinae and nine outgroup terminals, as inferred under coalescent-based inference with by-locus partitioning from Matrix 0.85A*.

Fig. 5.S70. Phylogeny of the Leptanillinae and nine outgroup terminals, as inferred under ML with by-locus partitioning from Matrix 0.9A*.

Fig. 5.S71. Phylogeny of the Leptanillinae and nine outgroup terminals, as inferred under ML with within-locus partitioning from Matrix 0.9A*.

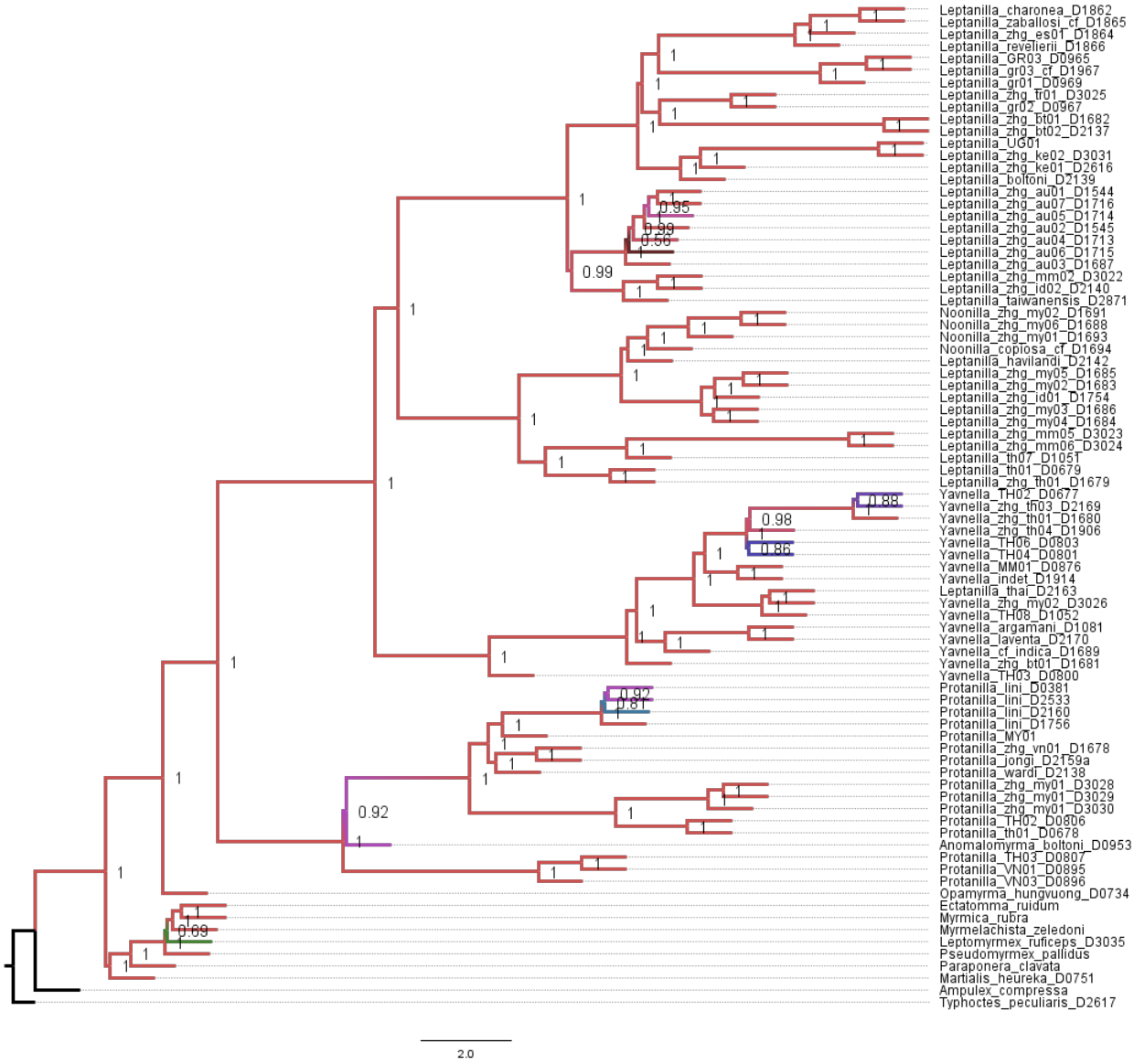

Fig. 5.S72. Phylogeny of the Leptanillinae and nine outgroup terminals, as inferred under coalescent-based inference with by-locus partitioning from Matrix 0.9A*.

Fig. 5.S73. Phylogeny of the Leptanillinae and nine outgroup terminals, as inferred under ML with by-locus partitioning from Matrix 0.95A*.

Fig. 5.S74. Phylogeny of the Leptanillinae and nine outgroup terminals, as inferred under ML with within-locus partitioning from Matrix 0.95A*.

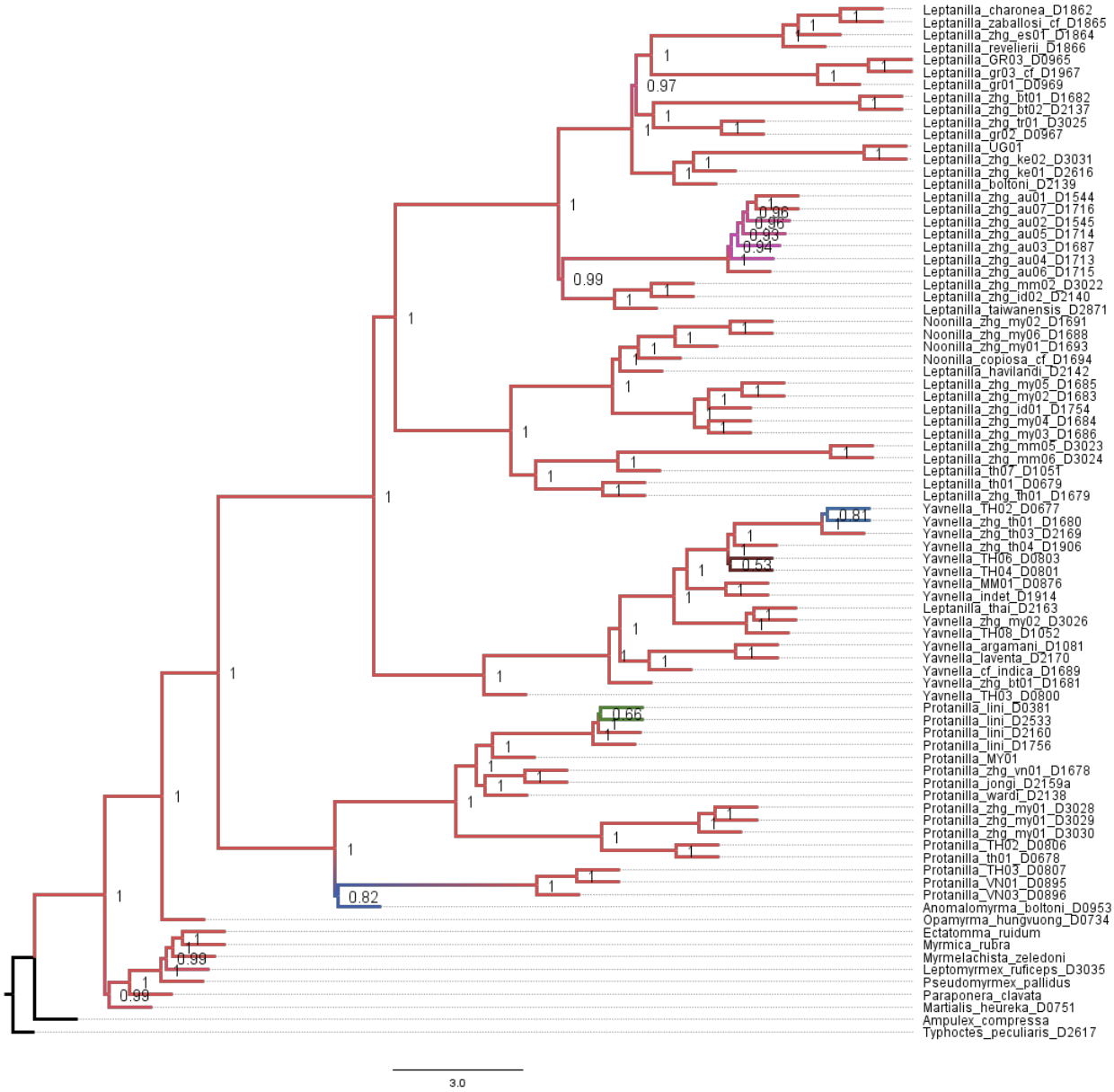

Fig. 5.S75. Phylogeny of the Leptanillinae and nine outgroup terminals, as inferred under coalescent-based inference with by-locus partitioning from Matrix 0.95A*.

Fig. 5.S76. Phylogeny of the Leptanillinae and nine outgroup terminals, as inferred under ML with by-locus partitioning from Matrix 1A*.

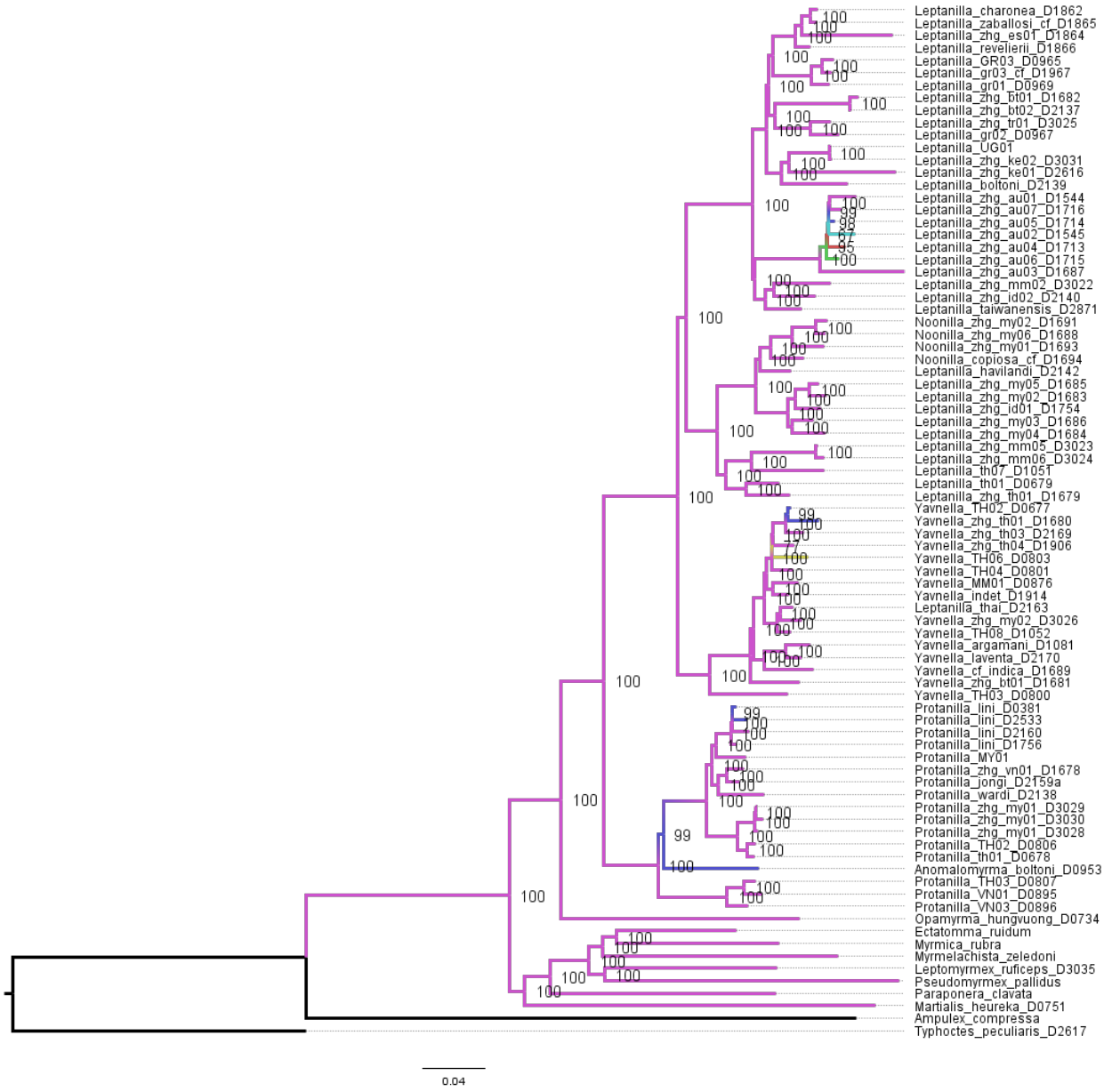

Fig. 5.S77. Phylogeny of the Leptanillinae and nine outgroup terminals, as inferred under ML with within-locus partitioning from Matrix 1A*.

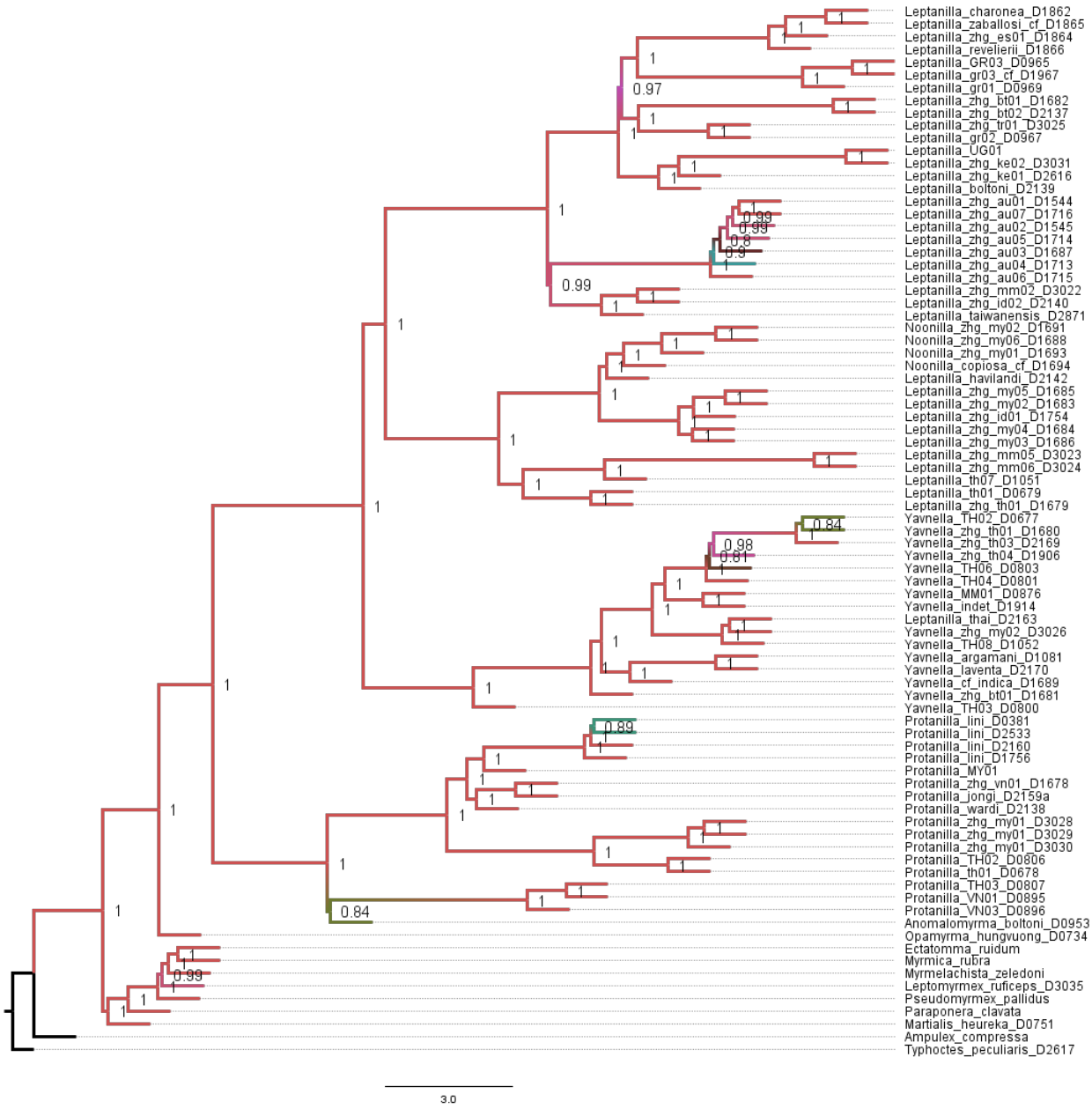

Fig. 5.S78. Phylogeny of the Leptanillinae and nine outgroup terminals, as inferred under coalescent-based inference with by-locus partitioning from Matrix 1A*.

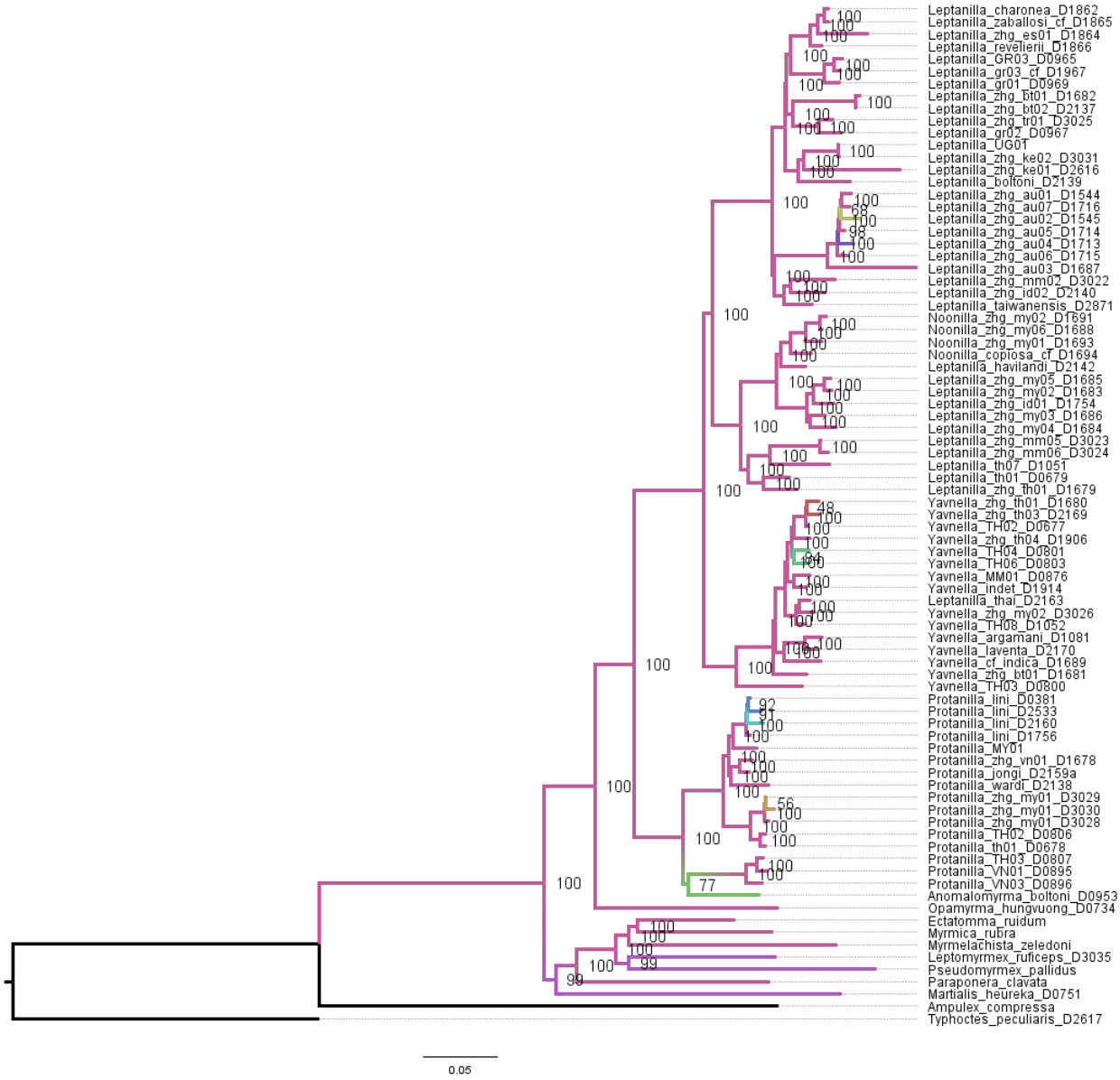

Fig. 5.S79. Phylogeny of the Leptanillinae and nine outgroup terminals, as inferred under ML with by-locus partitioning from Matrix 0.8B*.

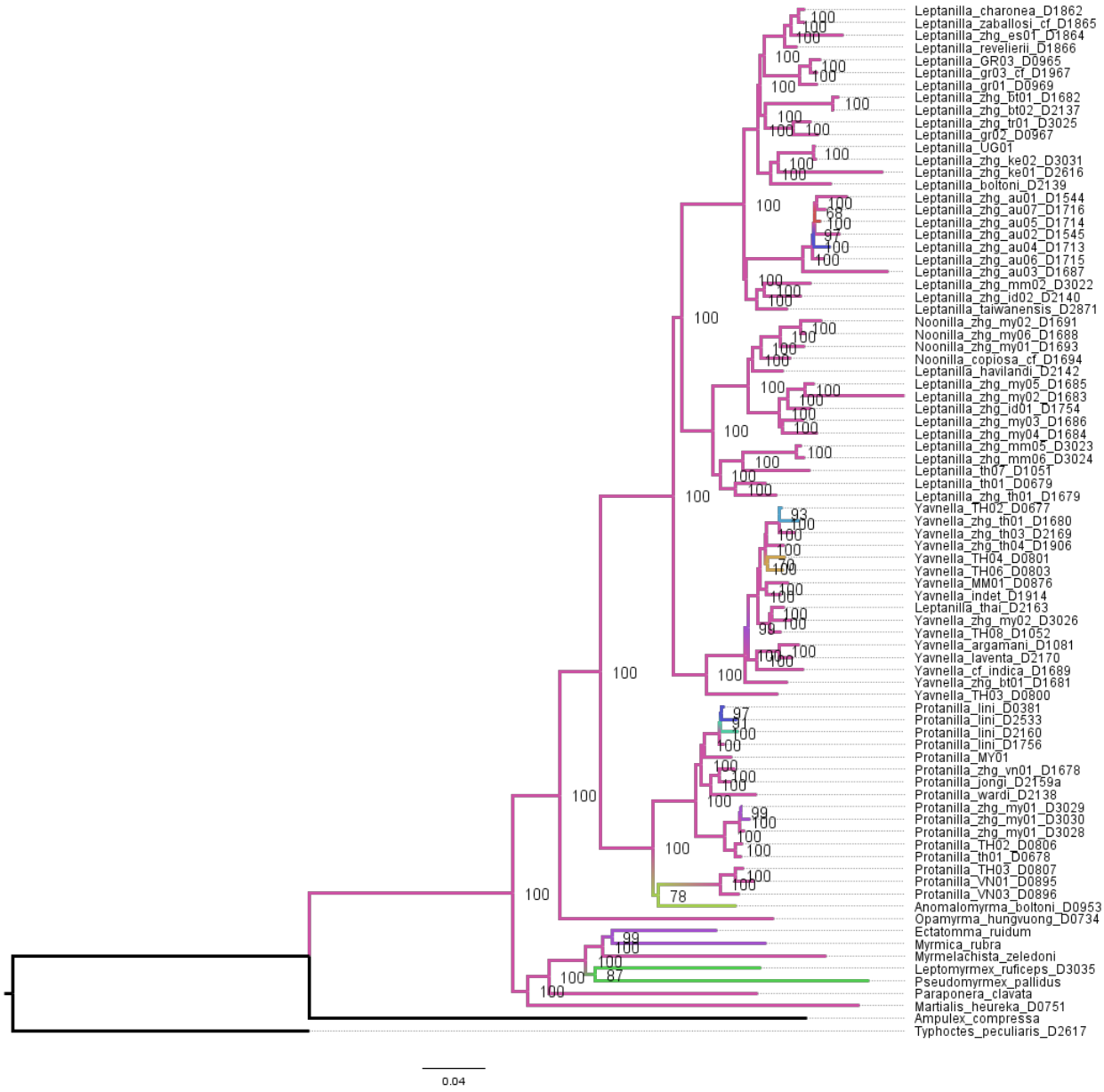

Fig. 5.S80. Phylogeny of the Leptanillinae and nine outgroup terminals, as inferred under ML with within-locus partitioning from Matrix 0.8B*.

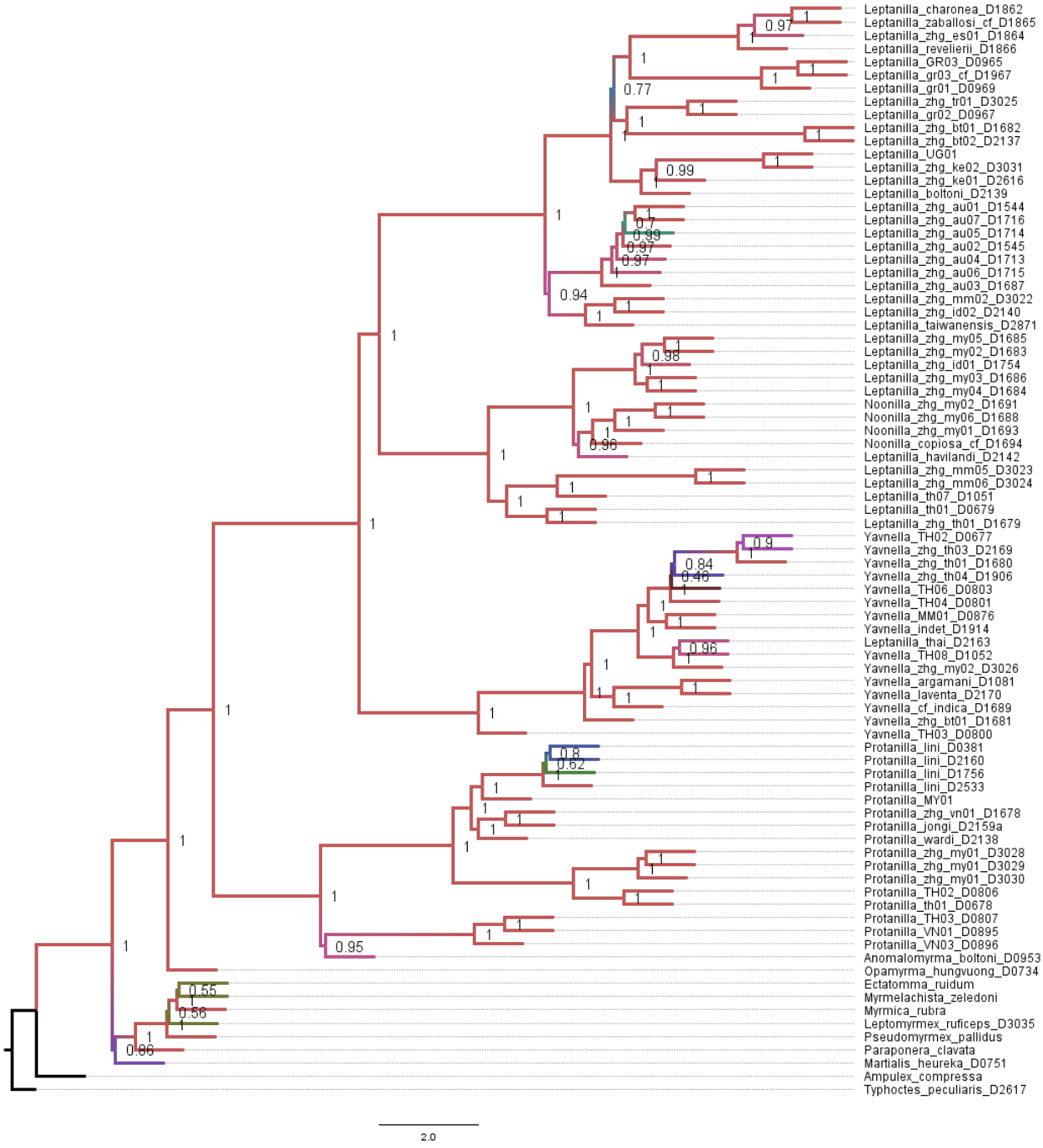

Fig. 5.S81. Phylogeny of the Leptanillinae and nine outgroup terminals, as inferred under coalescent-based inference with by-locus partitioning from Matrix 0.8B*.

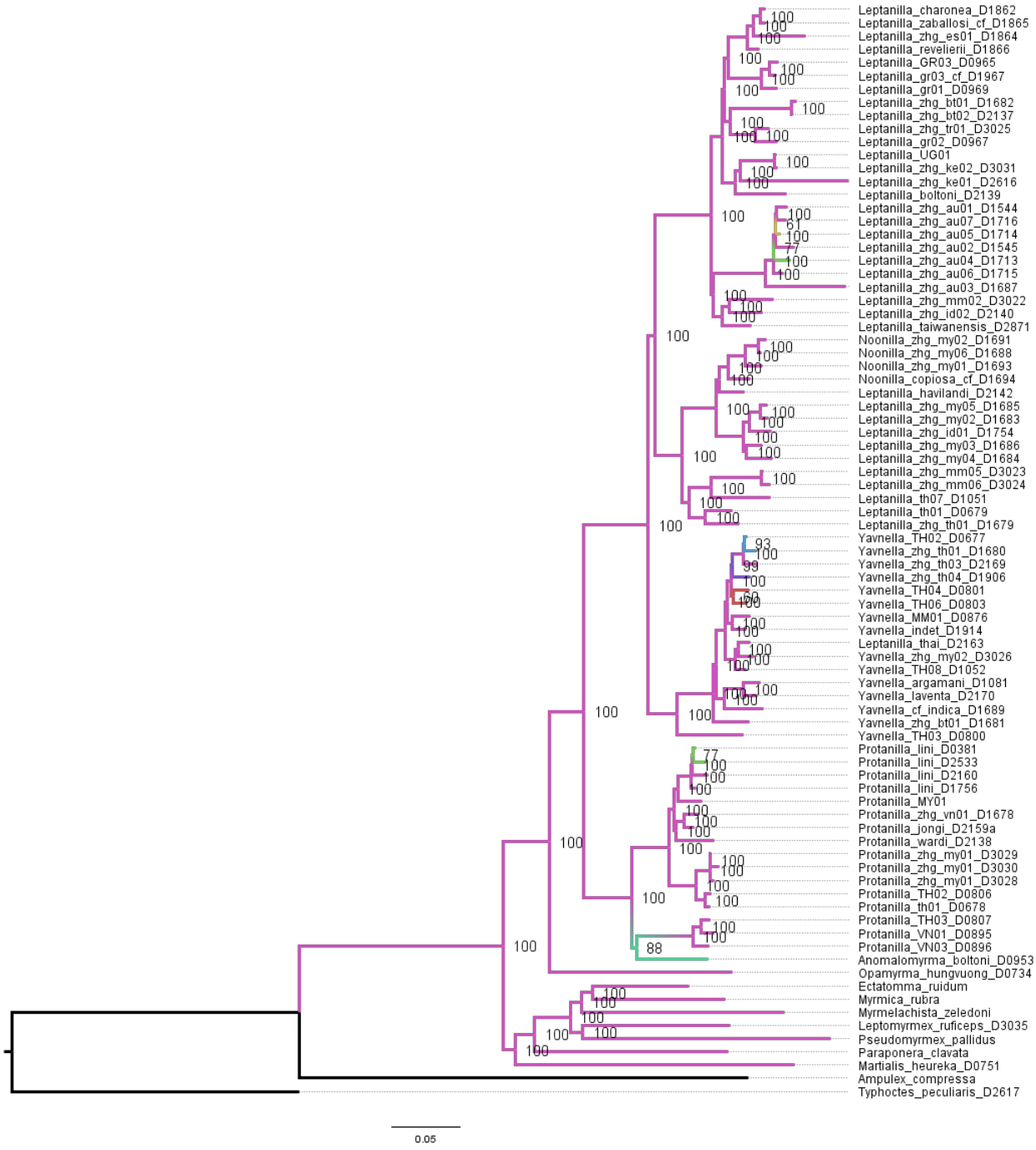

Fig. 5.S82. Phylogeny of the Leptanillinae and nine outgroup terminals, as inferred under ML with by-locus partitioning from Matrix 0.85B*.

Fig. 5.S83. Phylogeny of the Leptanillinae and nine outgroup terminals, as inferred under ML with within-locus partitioning from Matrix 0.85B*.

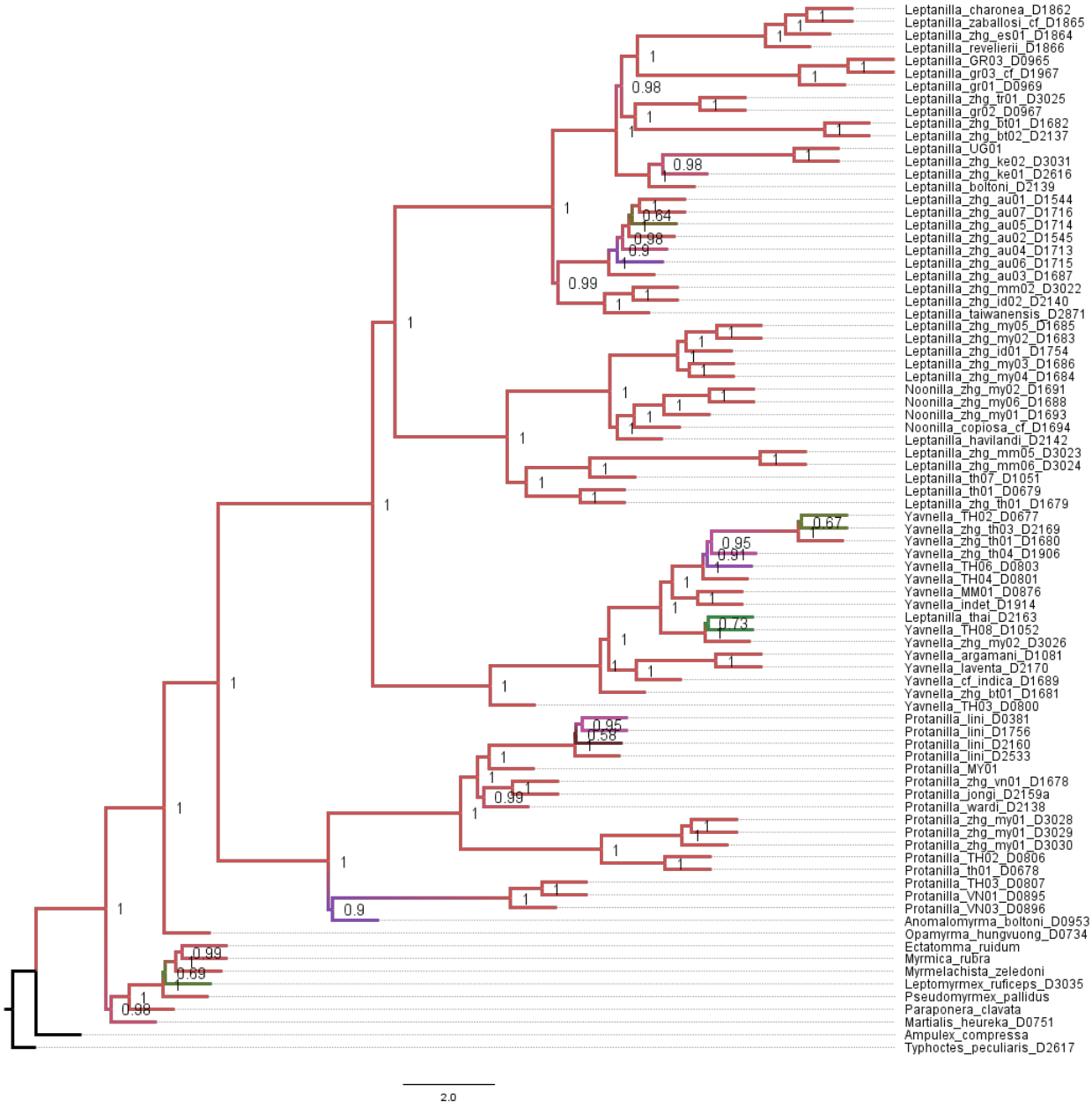

Fig. 5.S84. Phylogeny of the Leptanillinae and nine outgroup terminals, as inferred under coalescent-based with by-locus partitioning from Matrix 0.85B*.

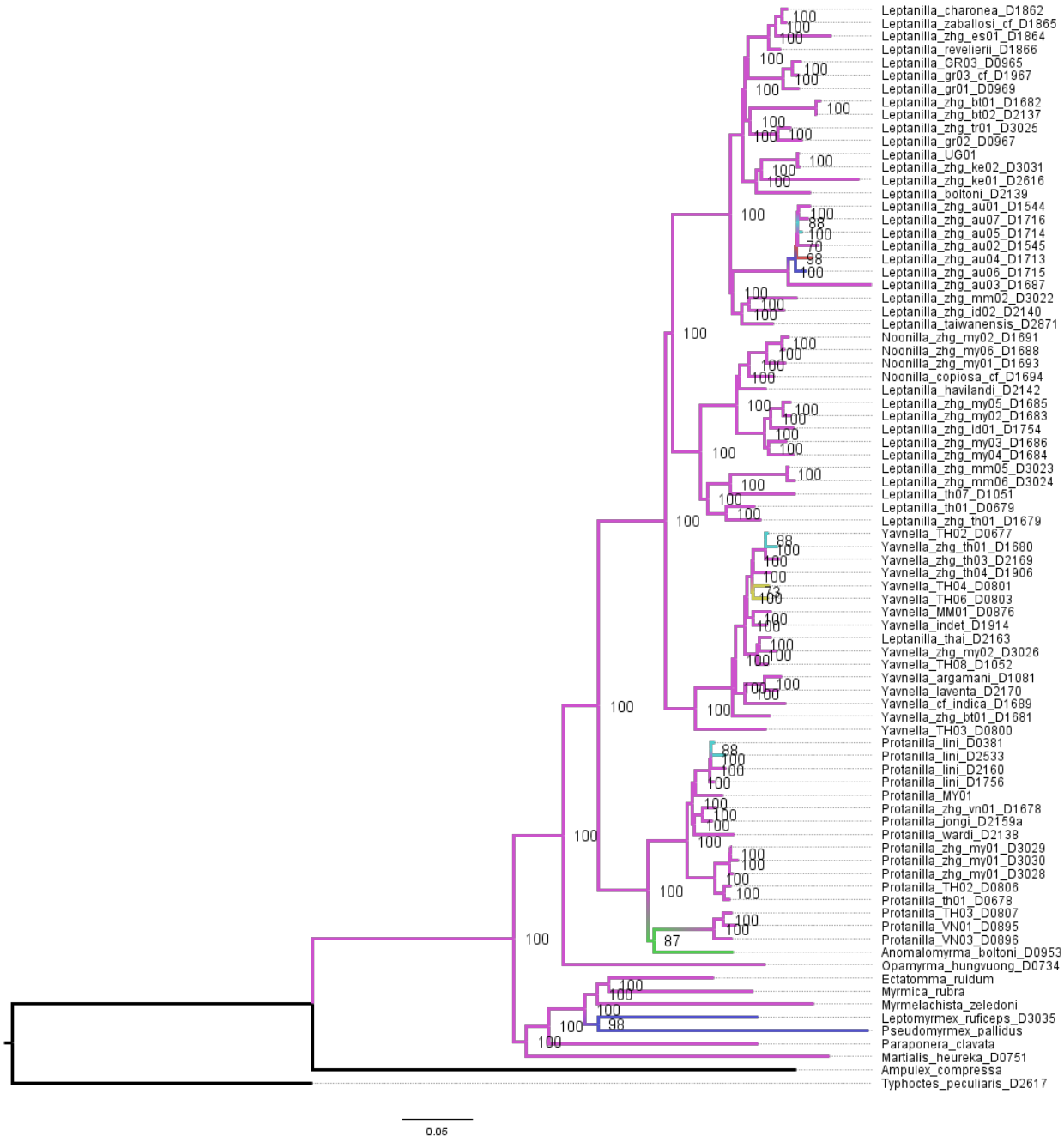

Fig. 5.S85. Phylogeny of the Leptanillinae and nine outgroup terminals, as inferred under ML with by-locus partitioning from Matrix 0.9B*.

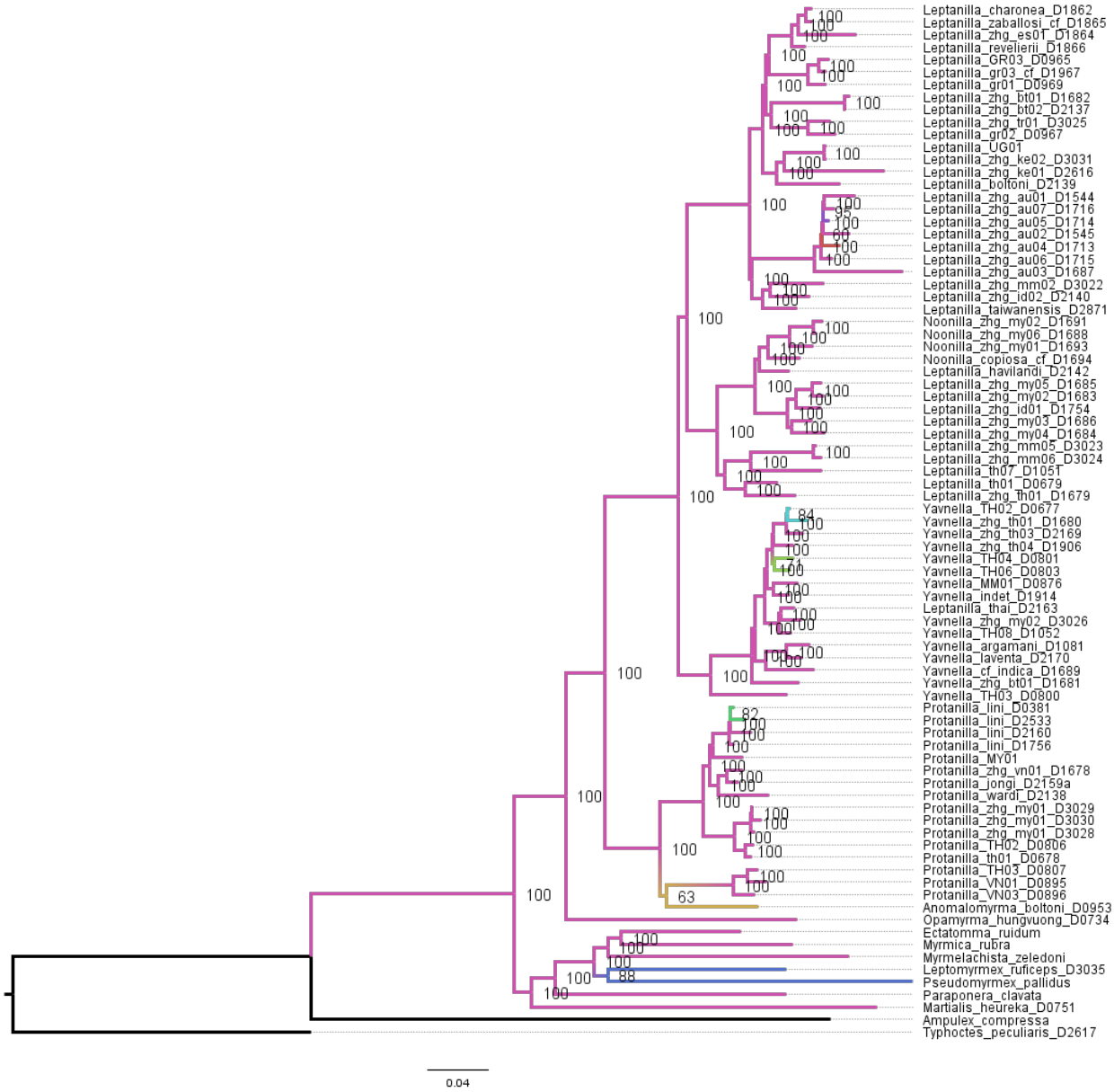

Fig. 5.S86. Phylogeny of the Leptanillinae and nine outgroup terminals, as inferred under ML with within-locus partitioning from Matrix 0.9B*.

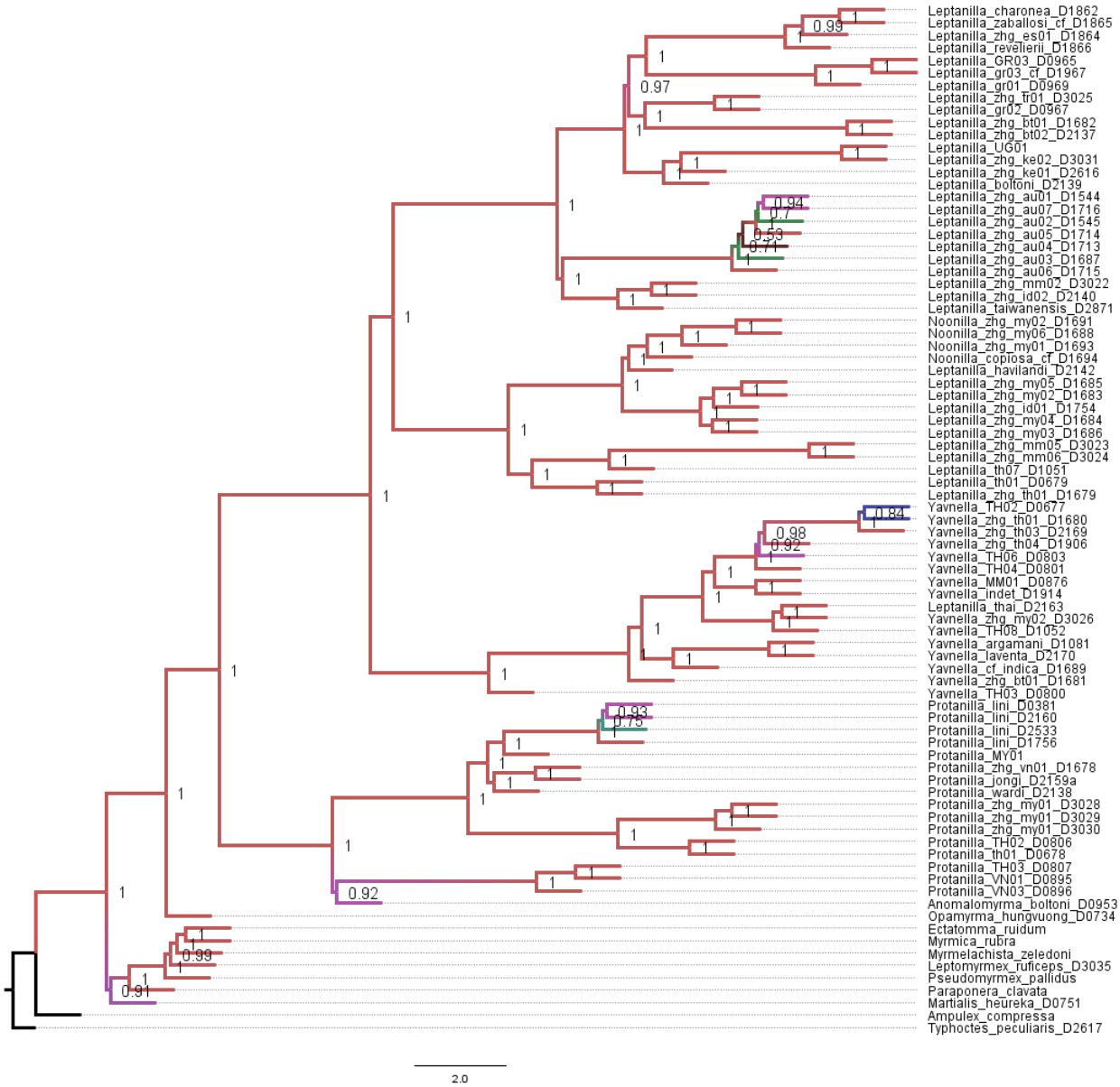

Fig. 5.S87. Phylogeny of the Leptanillinae and nine outgroup terminals, as inferred under coalescent-based inference with by-locus partitioning from Matrix 0.85B*.

Fig. 5.S88. Phylogeny of the Leptanillinae and nine outgroup terminals, as inferred under ML with by-locus partitioning from Matrix 0.95B*.

Fig. 5.S89. Phylogeny of the Leptanillinae and nine outgroup terminals, as inferred under ML with within-locus partitioning from Matrix 0.95B*.

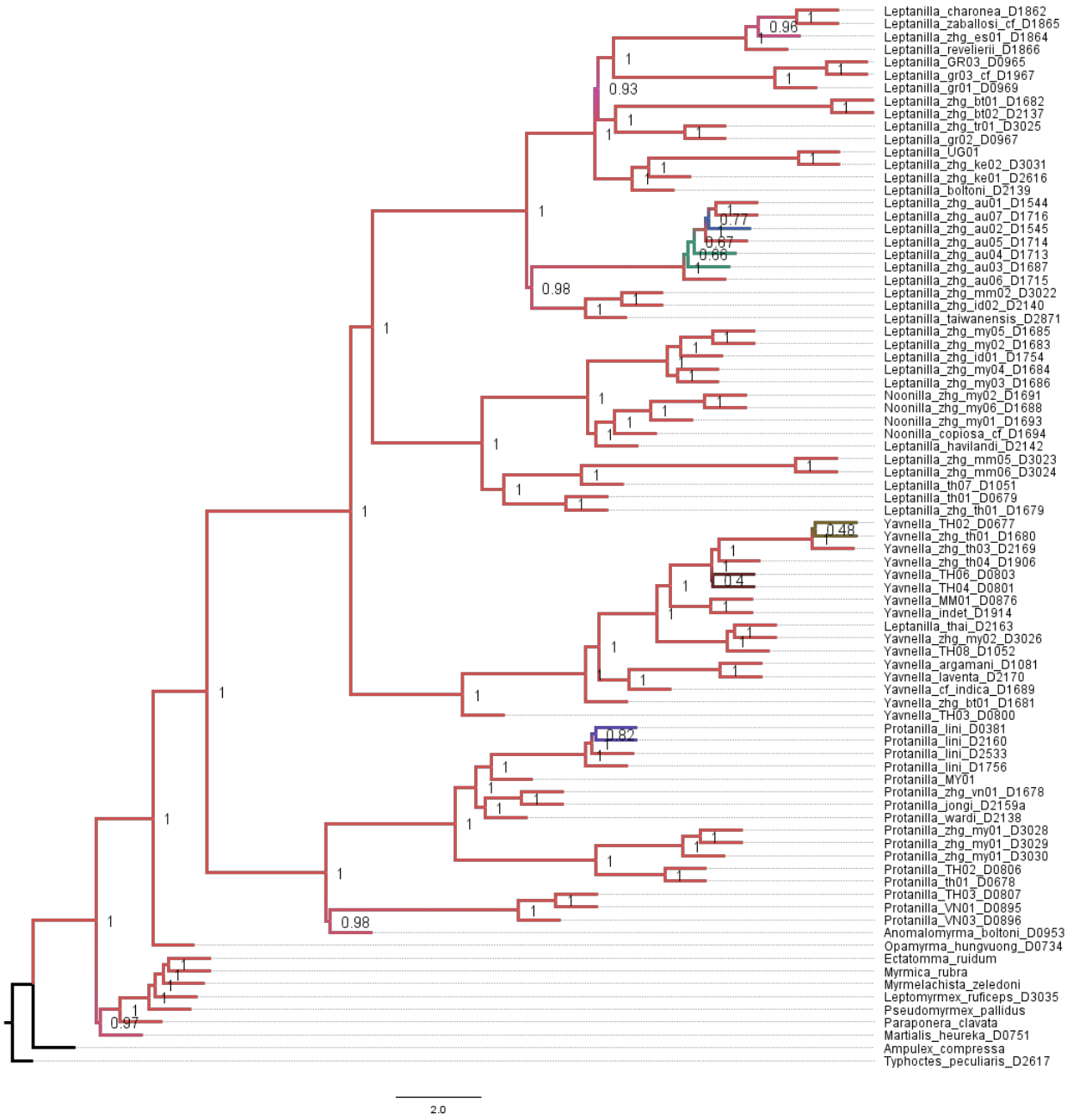

Fig. 5.S90. Phylogeny of the Leptanillinae and nine outgroup terminals, as inferred under coalescent-based inference with by-locus partitioning from Matrix 0.95B*.

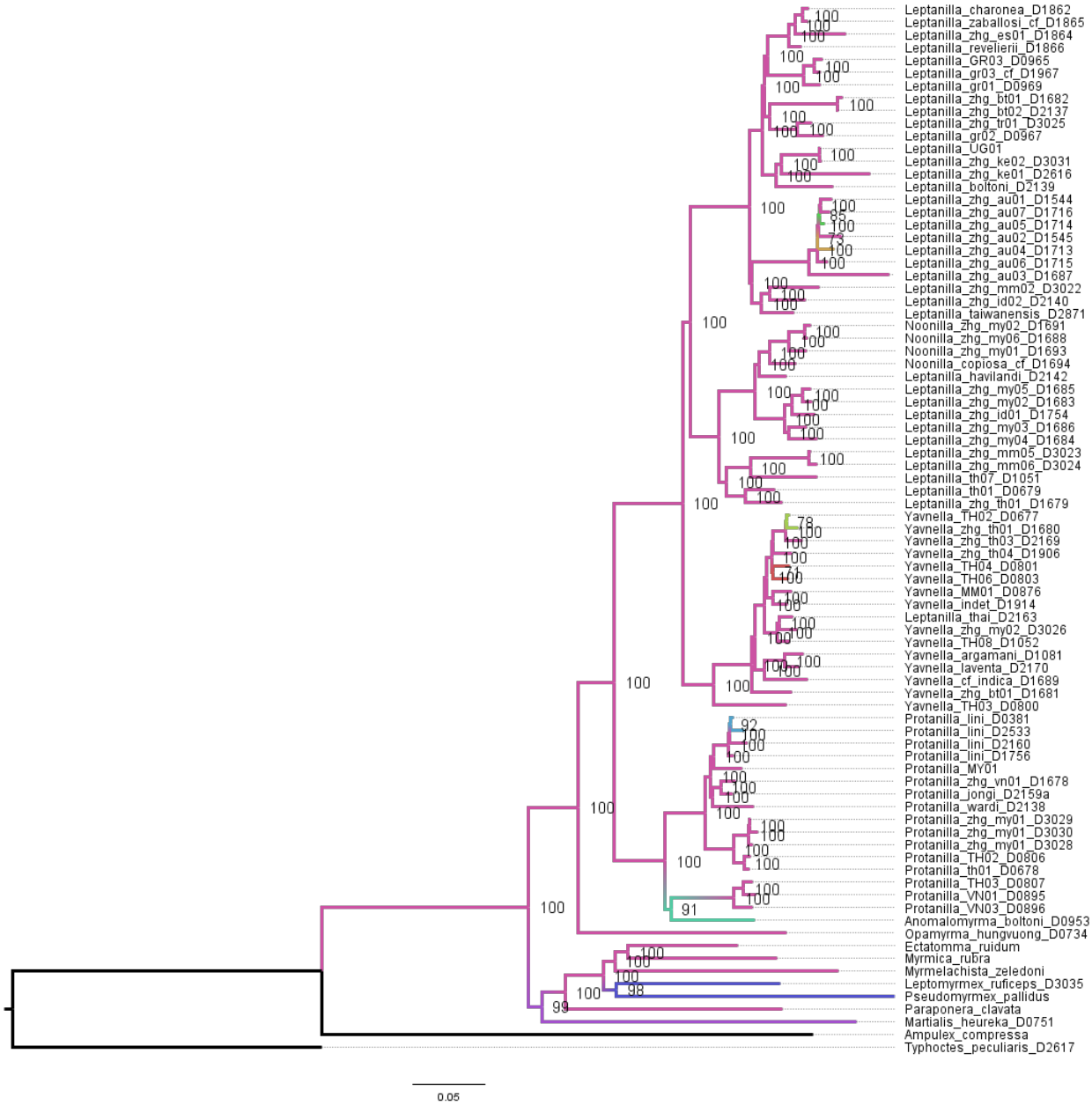

Fig. 5.S91. Phylogeny of the Leptanillinae and nine outgroup terminals, as inferred under ML with by-locus partitioning from Matrix 1B*.

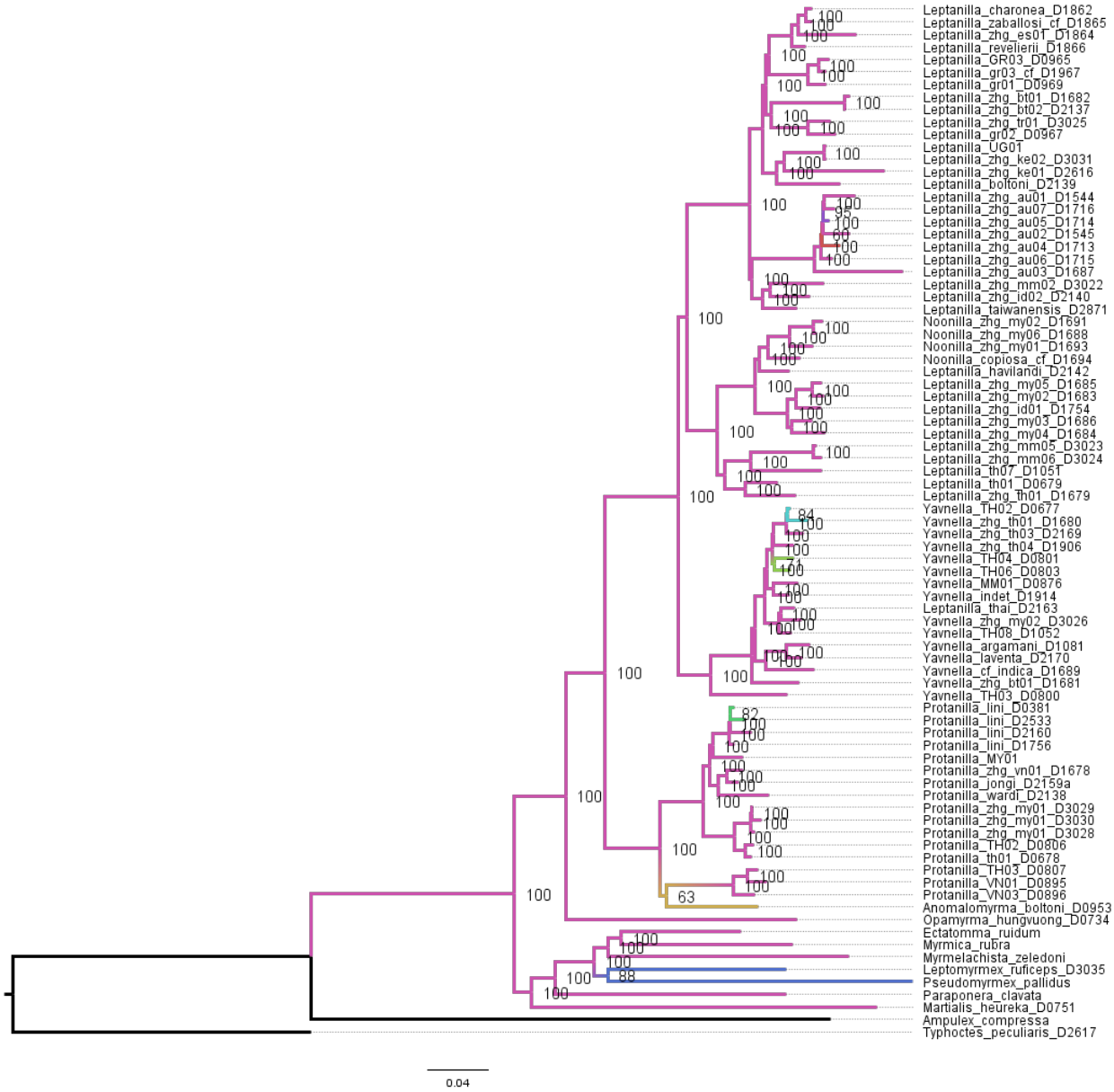

Fig. 5.S92. Phylogeny of the Leptanillinae and nine outgroup terminals, as inferred under ML with within-locus partitioning from Matrix 1B*.

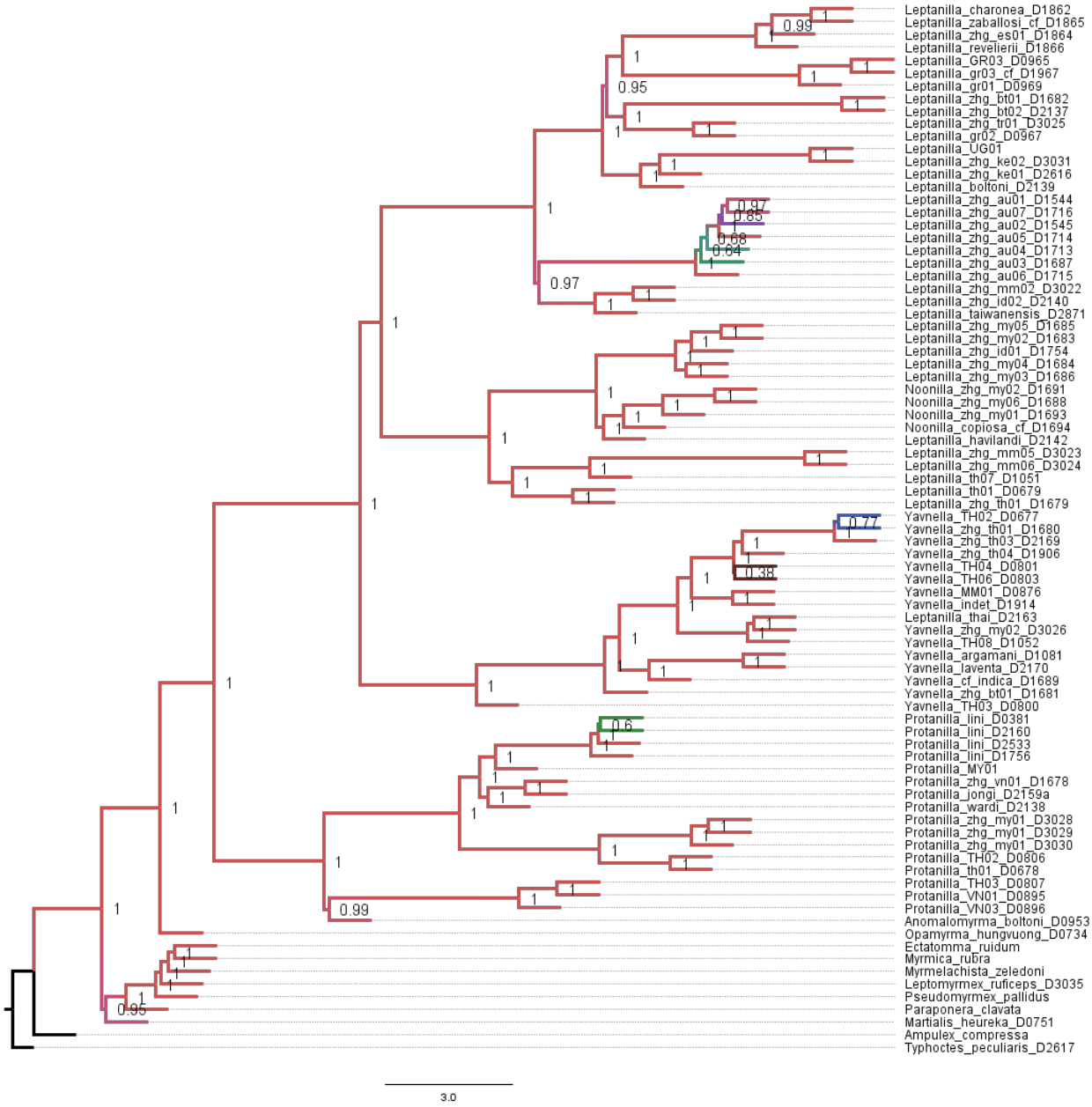

Fig. 5.S93. Phylogeny of the Leptanillinae and nine outgroup terminals, as inferred under coalescent-based inference with by-locus partitioning from Matrix 1B*.

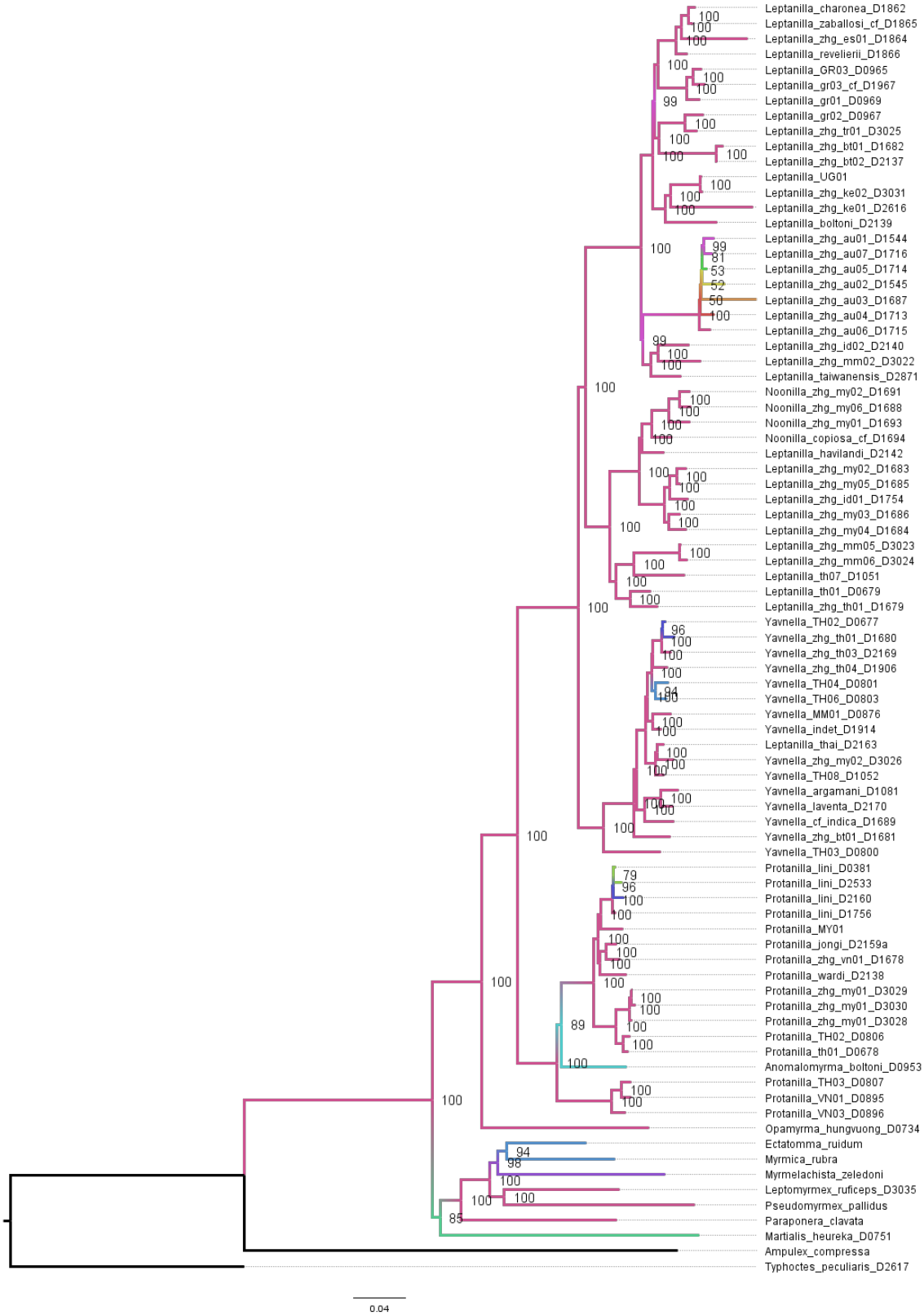

Fig. 5.S94. Phylogeny of the Leptanillinae and nine outgroup terminals, as inferred under ML with by-locus partitioning from Matrix 0.8C*.

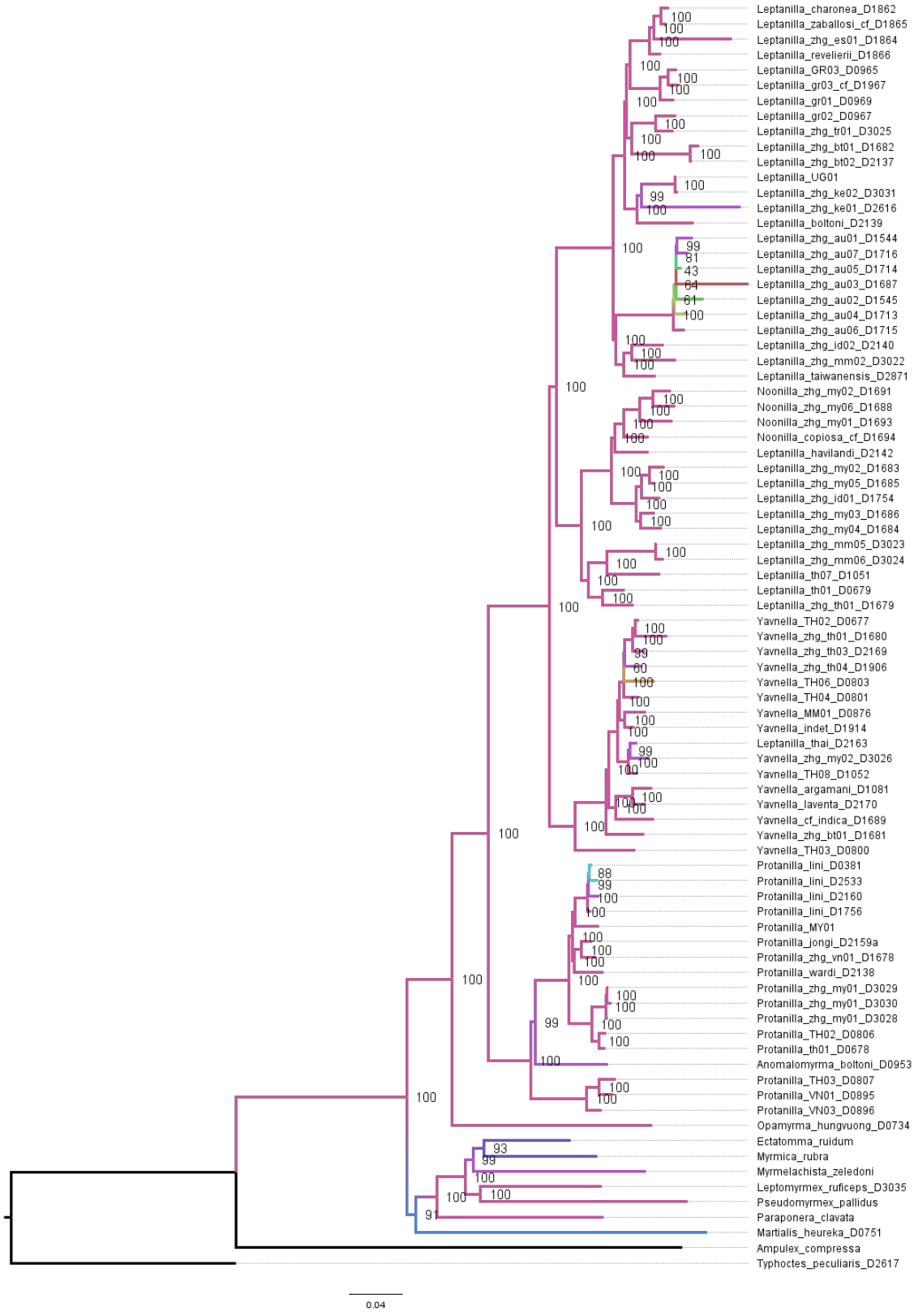

Fig. 5.S95. Phylogeny of the Leptanillinae and nine outgroup terminals, as inferred under ML with within-locus partitioning from Matrix 0.8C*.

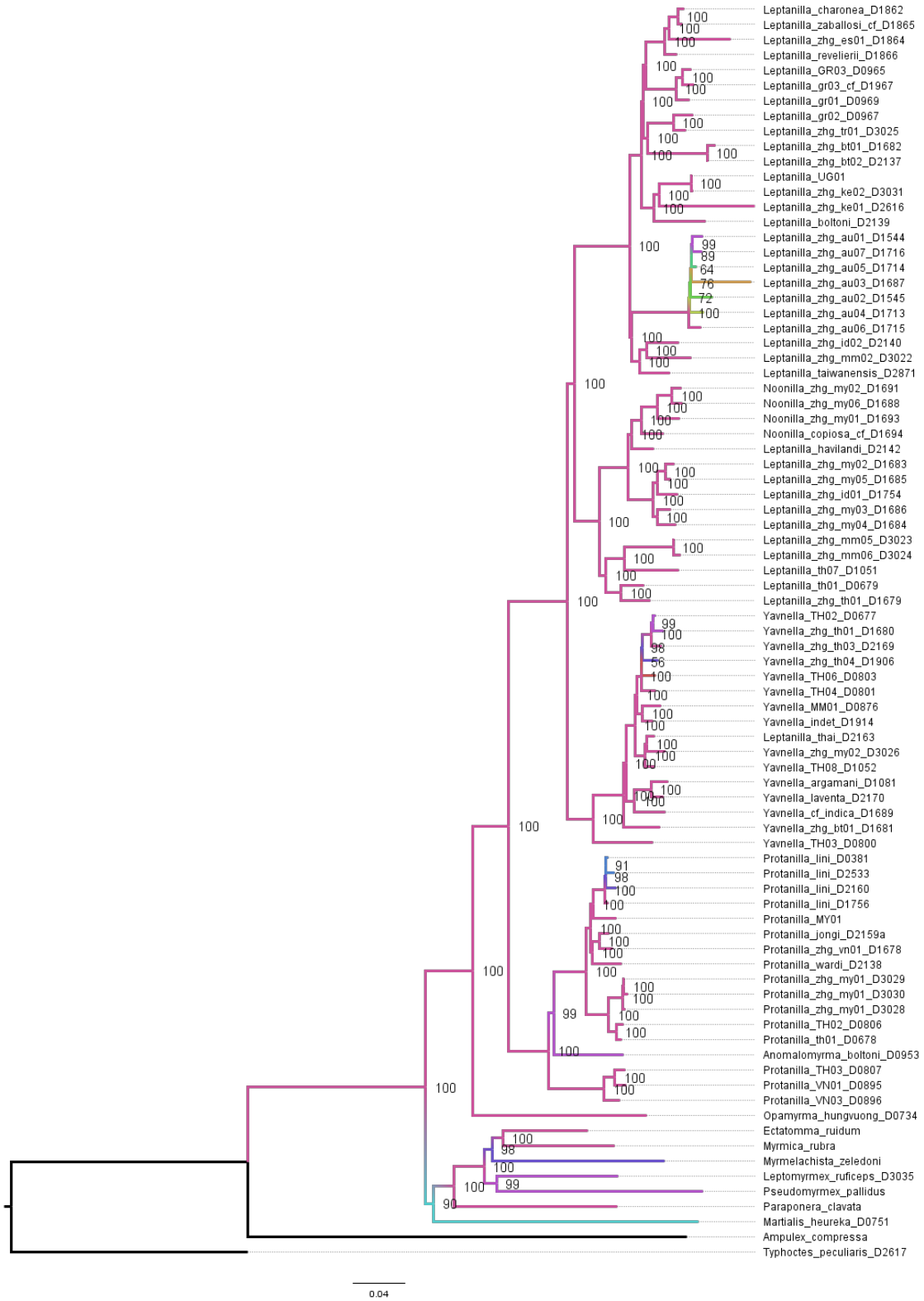

Fig. 5.S96. Phylogeny of the Leptanillinae and nine outgroup terminals, as inferred under coalescent-based inference with by-locus partitioning from Matrix 0.85C*.

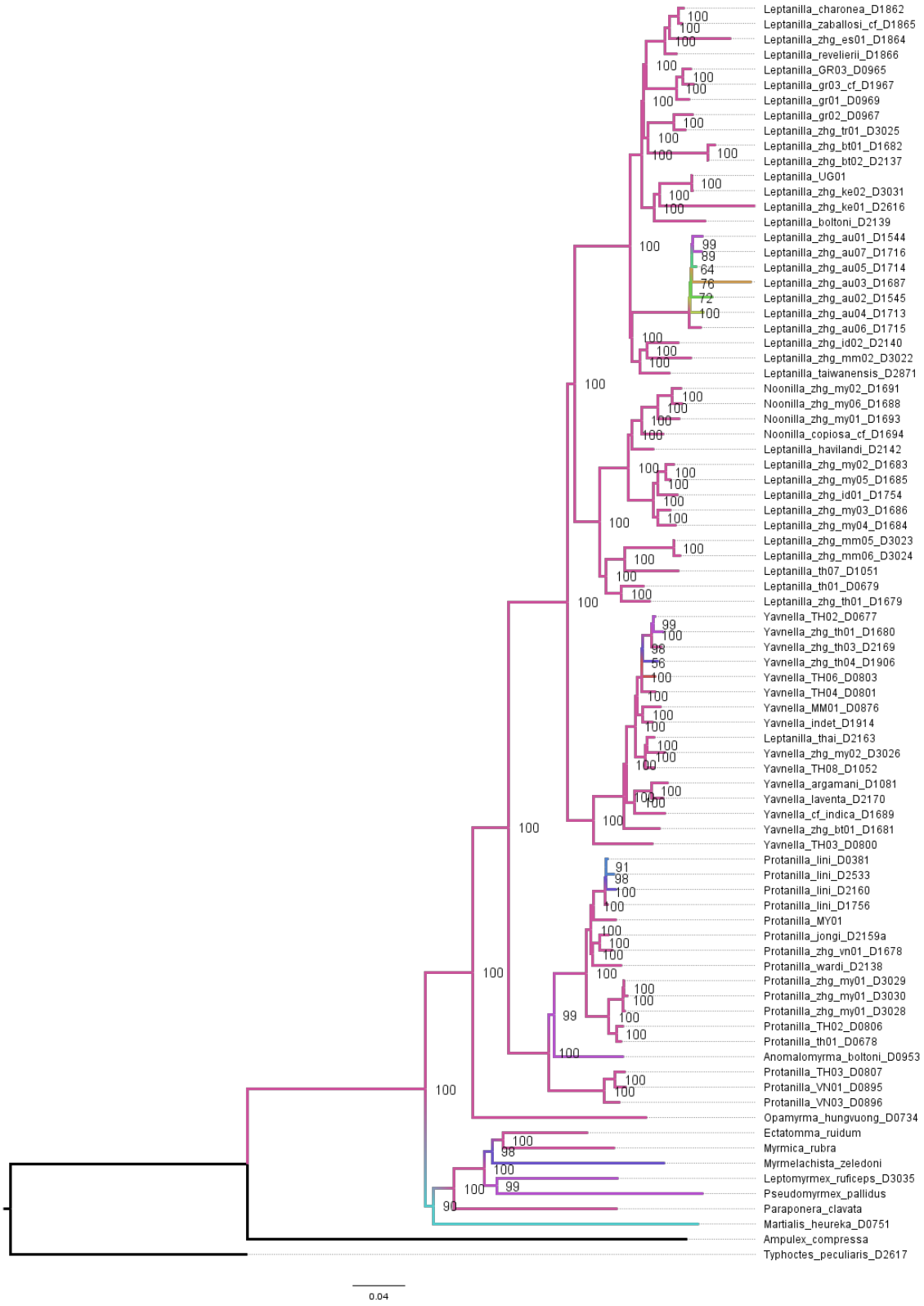

Fig. 5.S97. Phylogeny of the Leptanillinae and nine outgroup terminals, as inferred under ML with by-locus partitioning from Matrix 0.85C*.

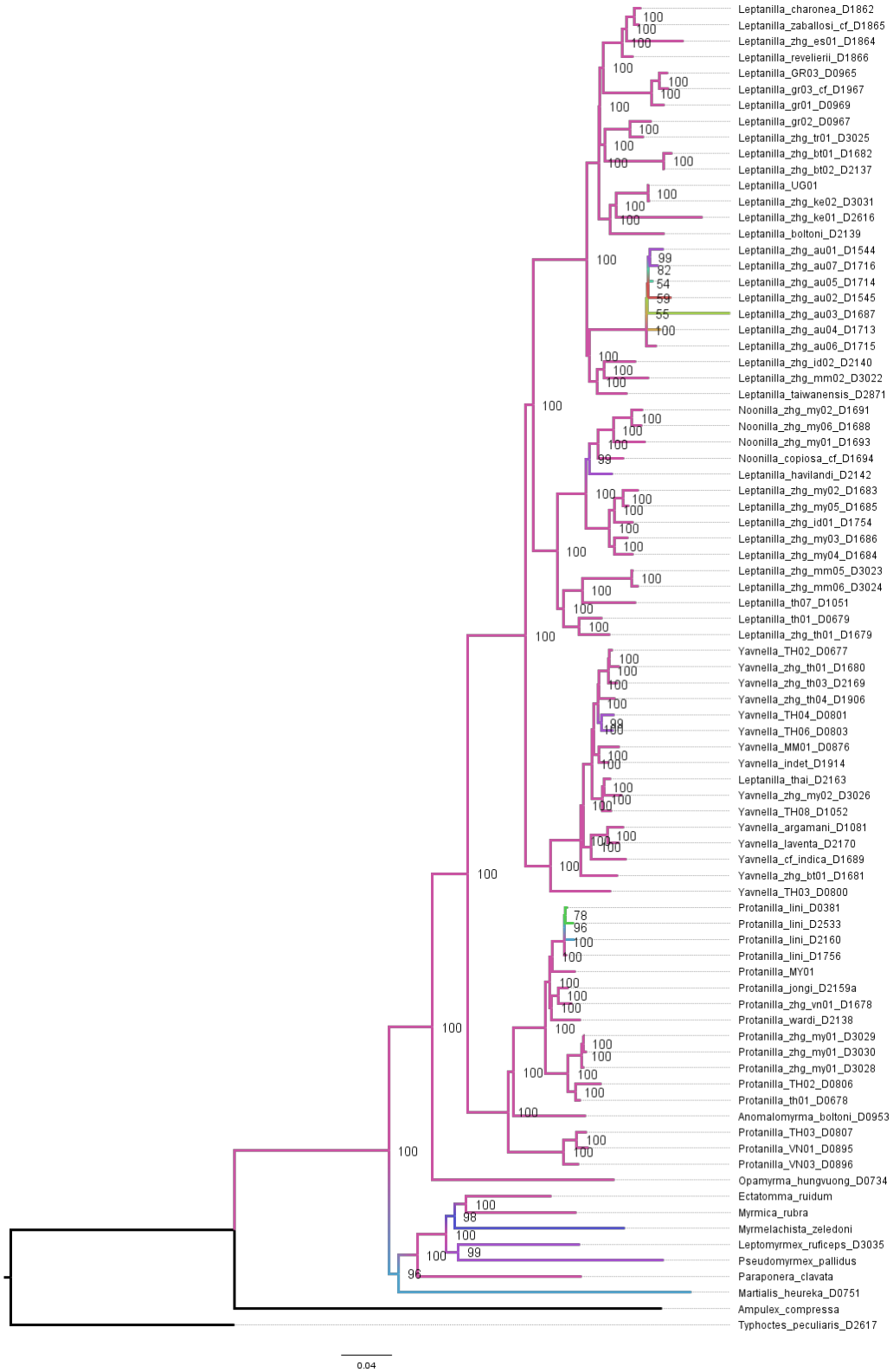

Fig. 5.S98. Phylogeny of the Leptanillinae and nine outgroup terminals, as inferred under ML with within-locus partitioning from Matrix 0.85C*.

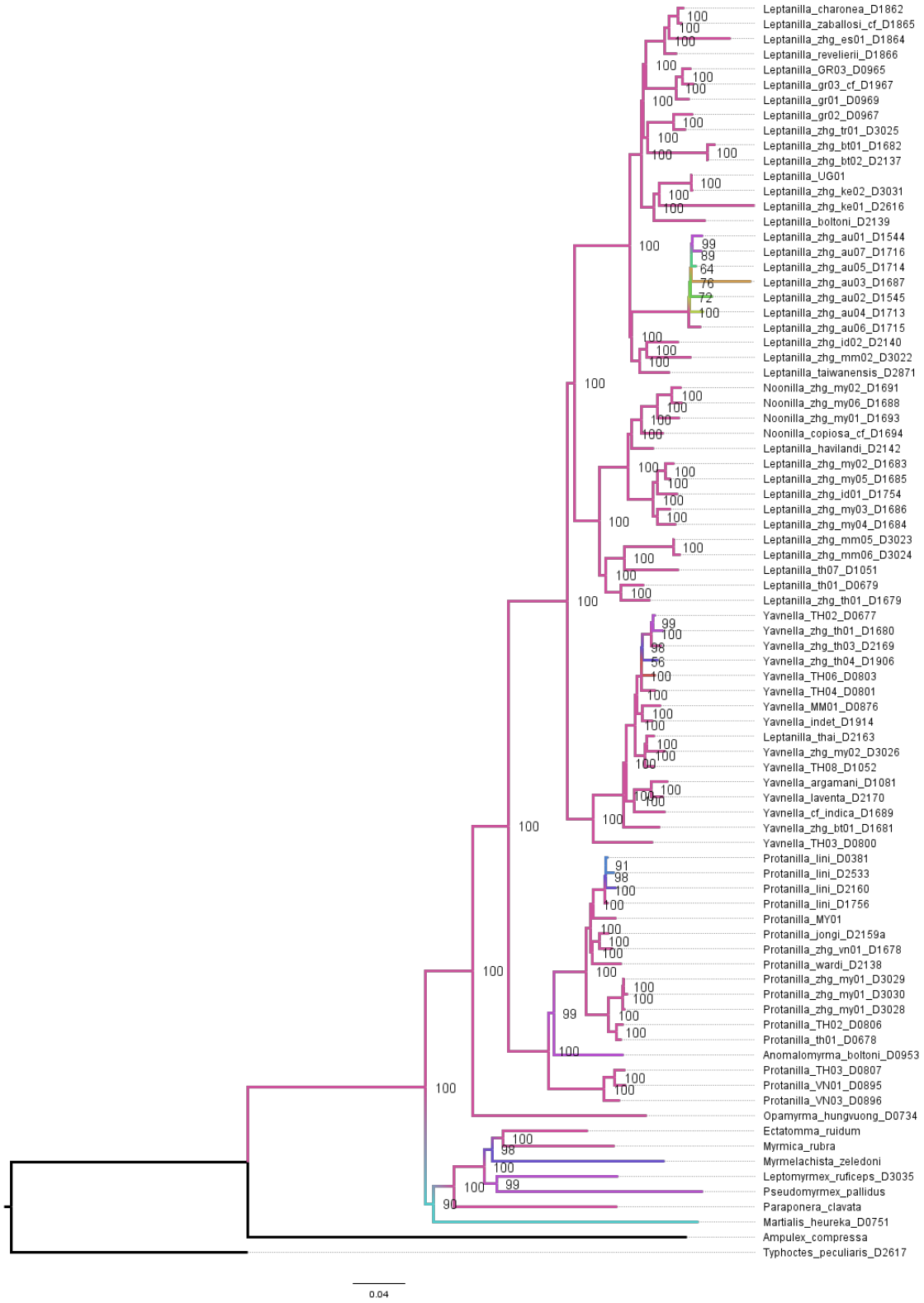

Fig. 5.S99. Phylogeny of the Leptanillinae and nine outgroup terminals, as inferred under coalescent-based inference with by-locus partitioning from Matrix 0.85C*.

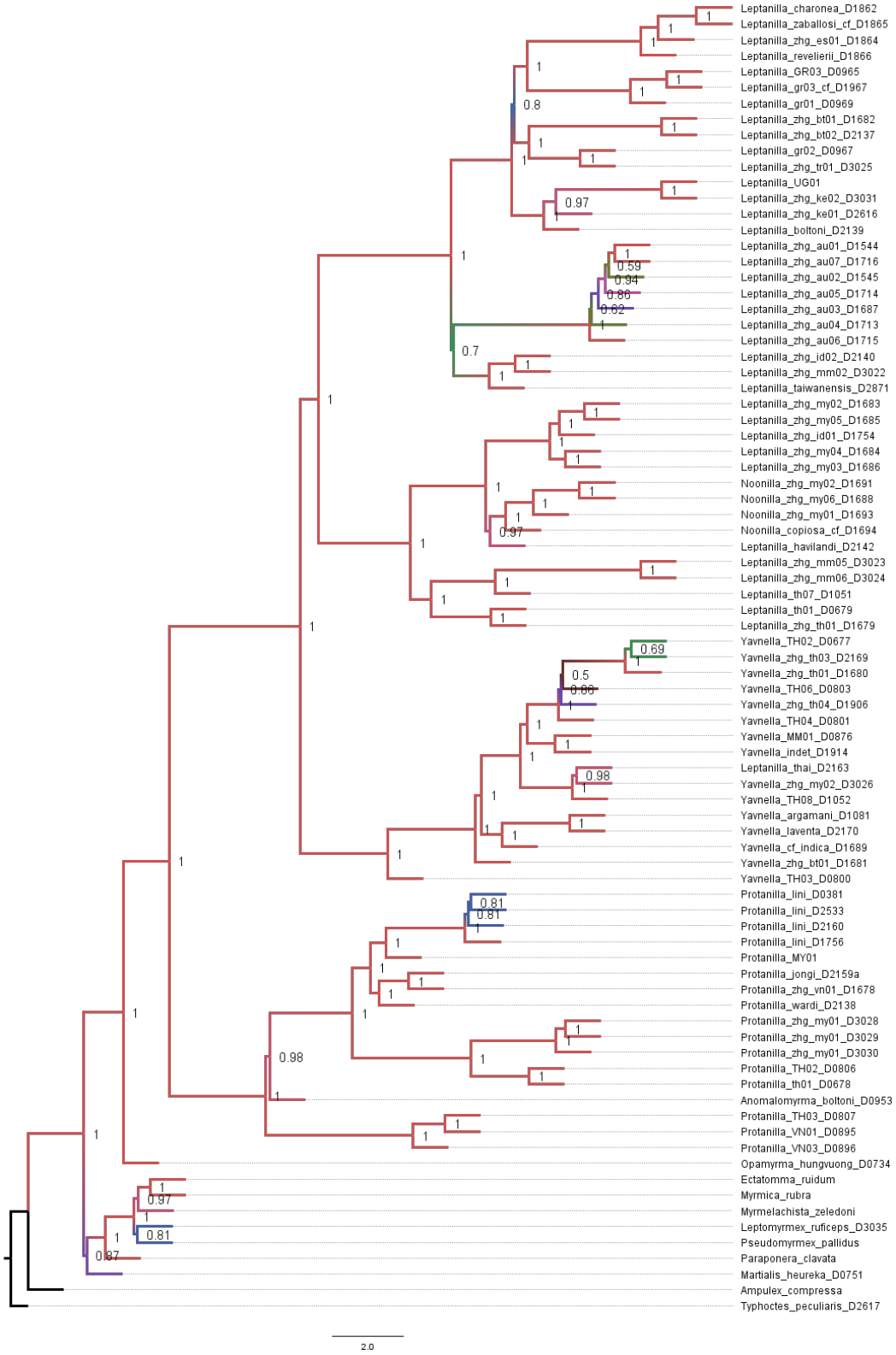

Fig. 5.S100. Phylogeny of the Leptanillinae and nine outgroup terminals, as inferred under ML with by-locus partitioning from Matrix 0.9C*.

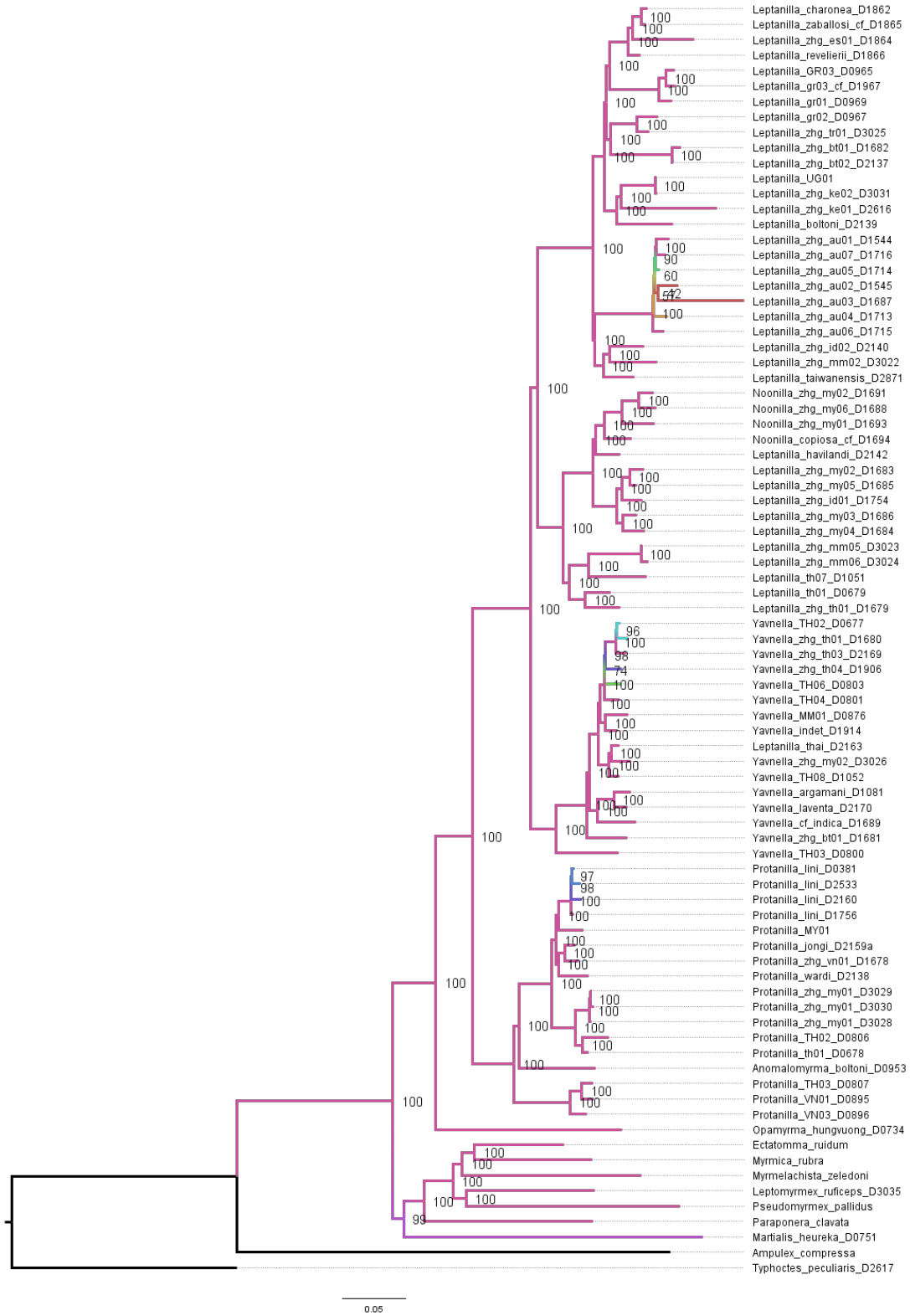

Fig. 5.S101. Phylogeny of the Leptanillinae and nine outgroup terminals, as inferred under ML with within-locus partitioning from Matrix 0.9C*.

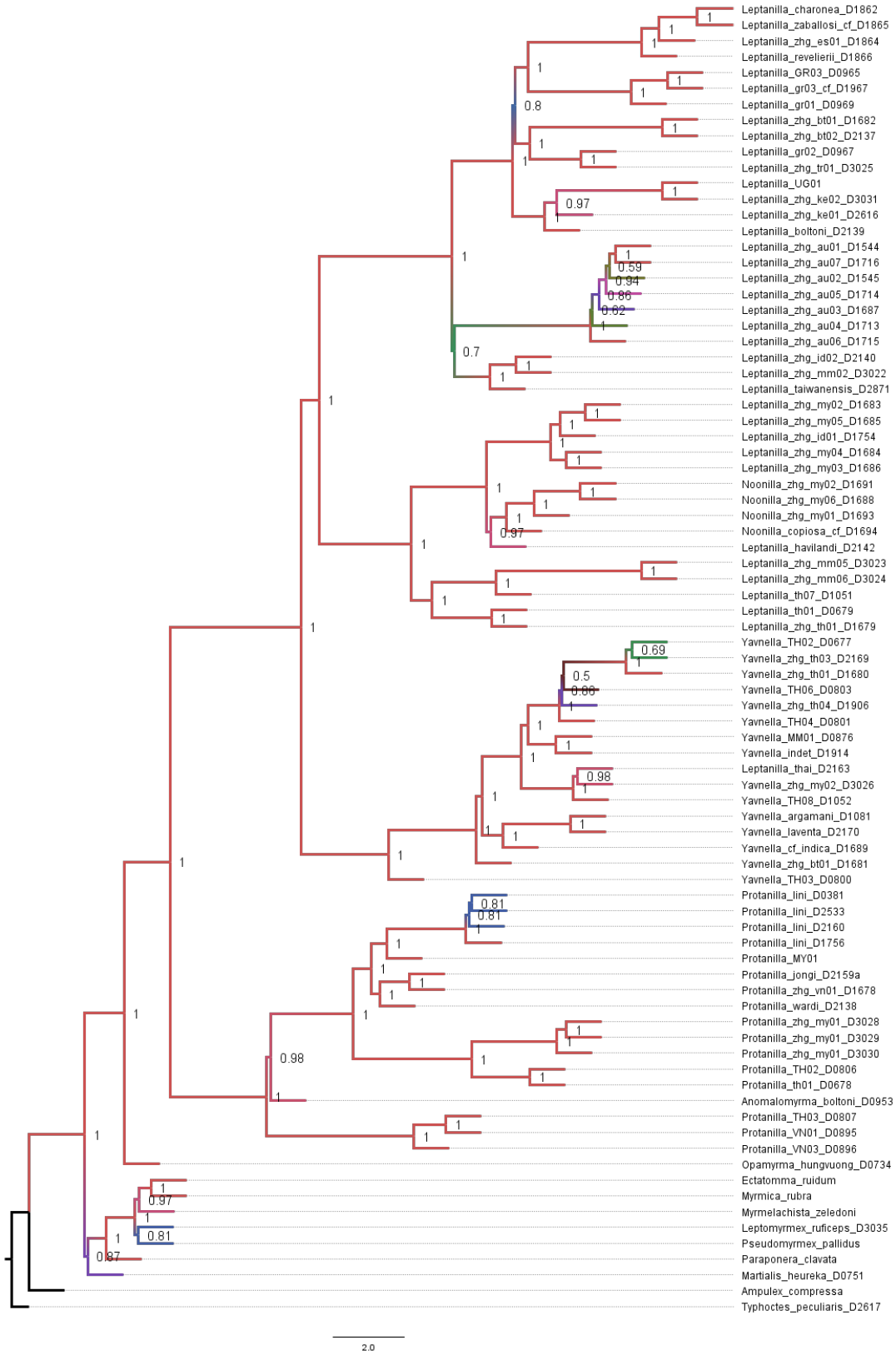

Fig. 5.S102. Phylogeny of the Leptanillinae and nine outgroup terminals, as inferred under coalescent-based partitioning with by-locus partitioning from Matrix 0.9C*.

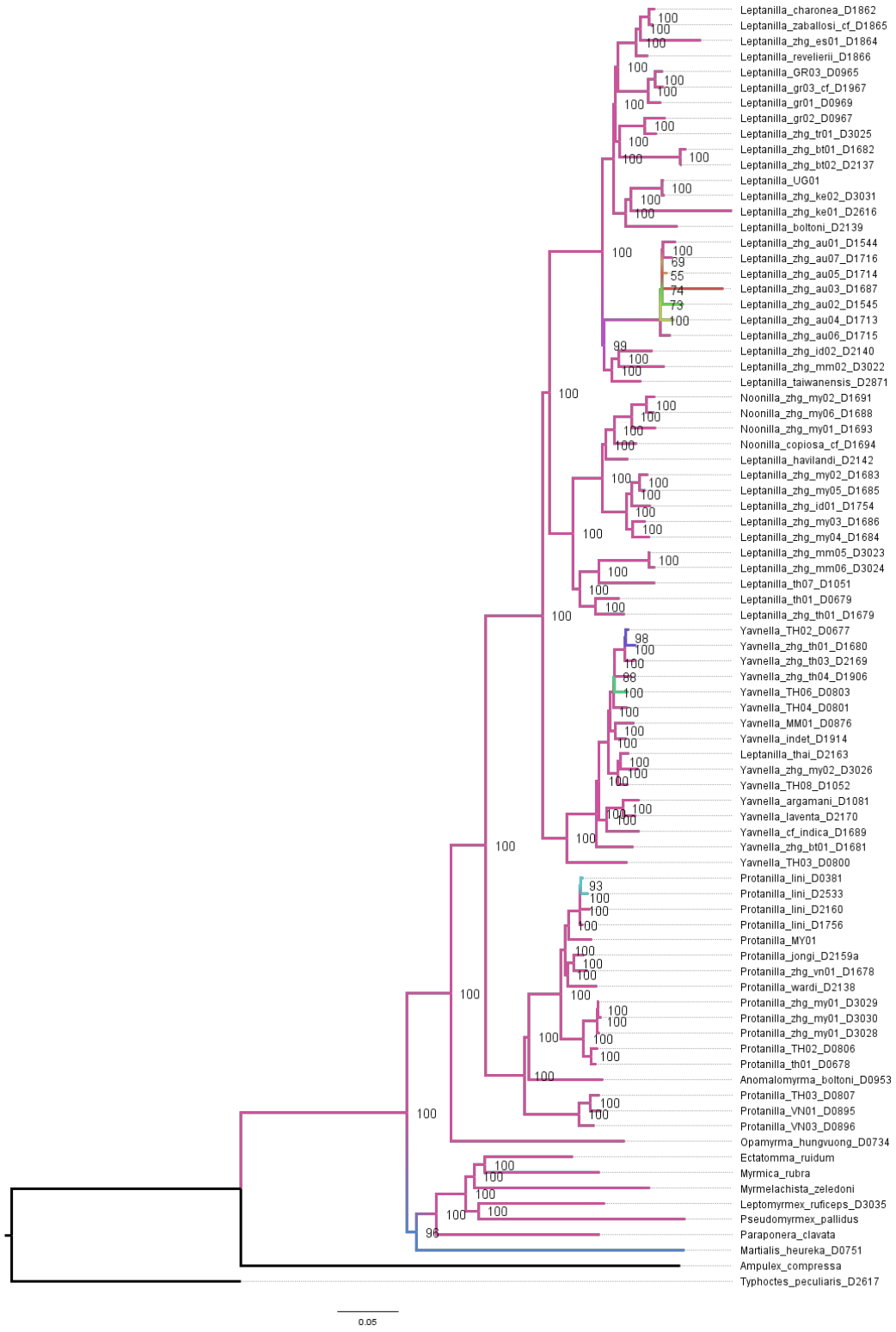

Fig. 5.S103. Phylogeny of the Leptanillinae and nine outgroup terminals, as inferred under ML with by-locus partitioning from Matrix 0.95C*.

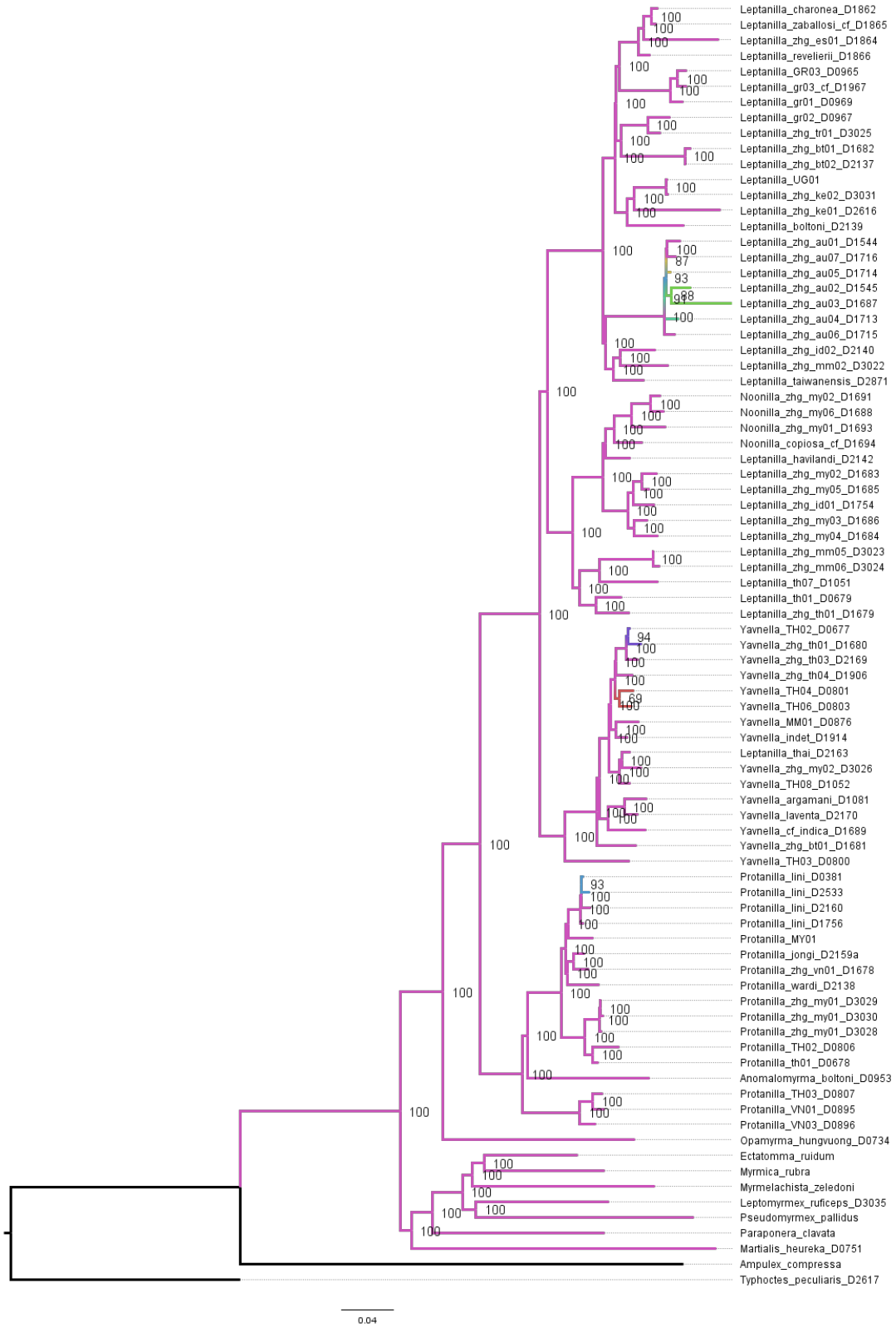

Fig. 5.S104. Phylogeny of the Leptanillinae and nine outgroup terminals, as inferred under ML with within-locus partitioning from Matrix 0.95C*.

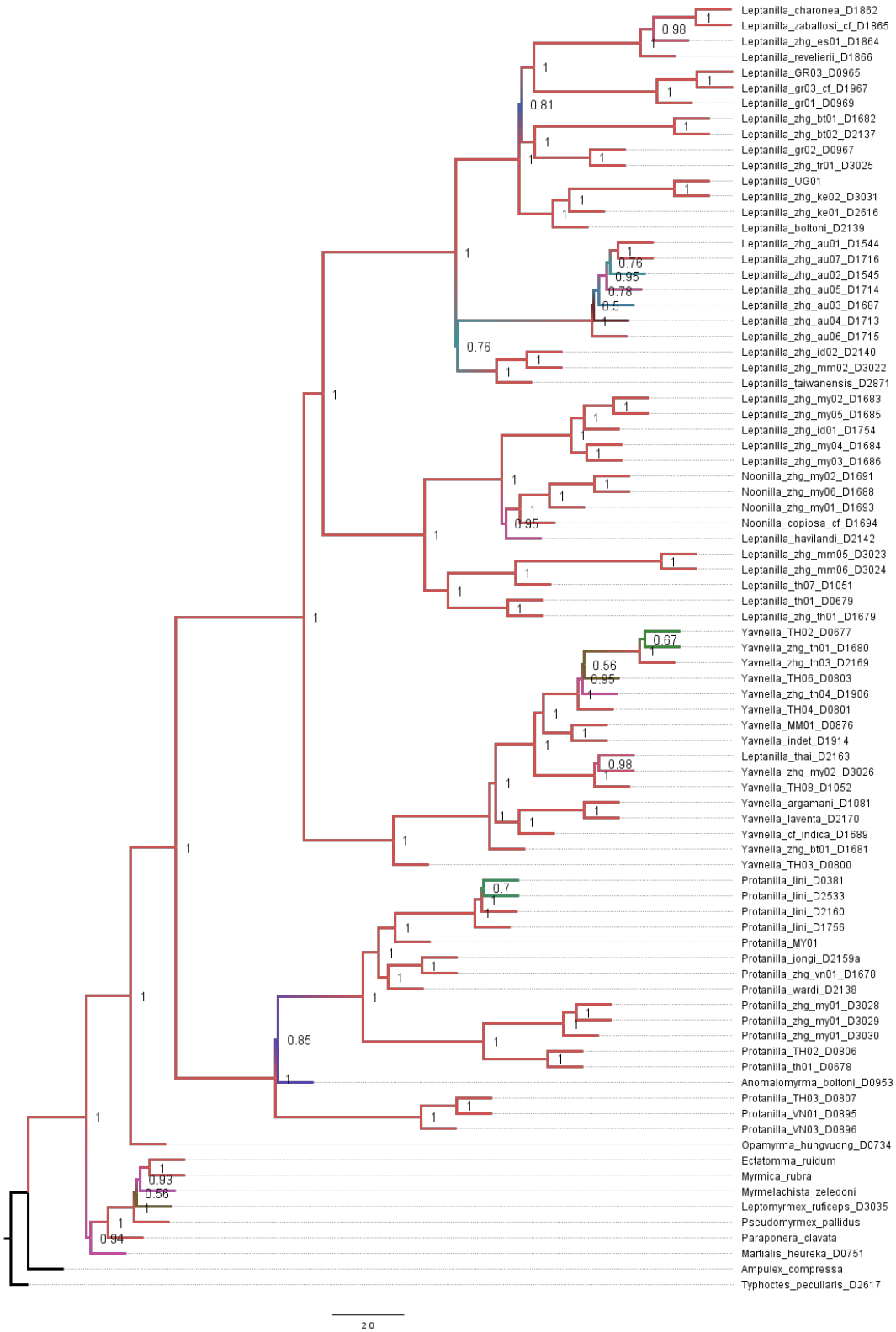

Fig. 5.S105. Phylogeny of the Leptanillinae and nine outgroup terminals, as inferred under coalescent-based inference with by-locus partitioning from Matrix 0.95C*.

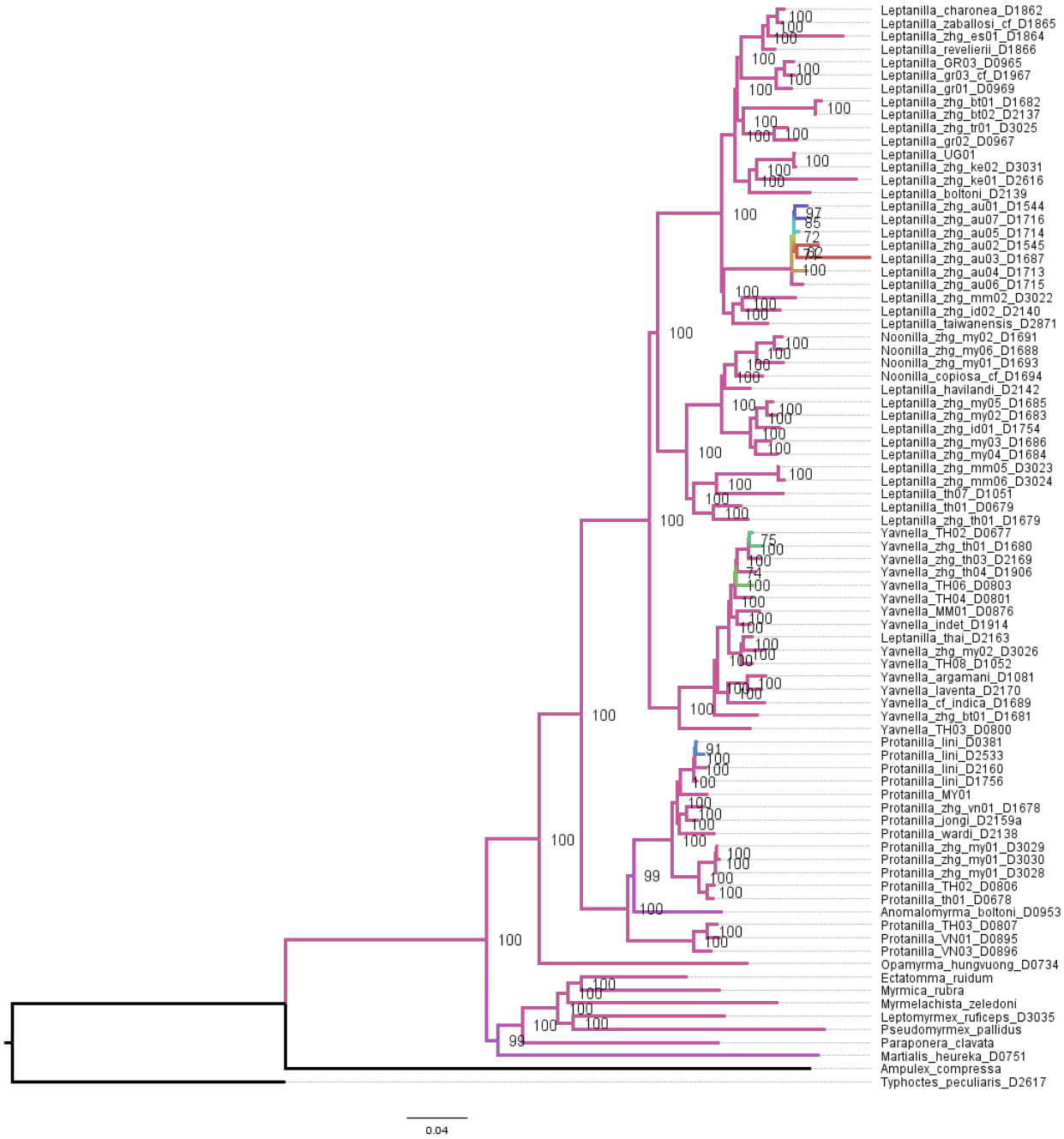

Fig. 5.S106. Phylogeny of the Leptanillinae and nine outgroup terminals, as inferred under ML with by-locus partitioning from Matrix 1C*.

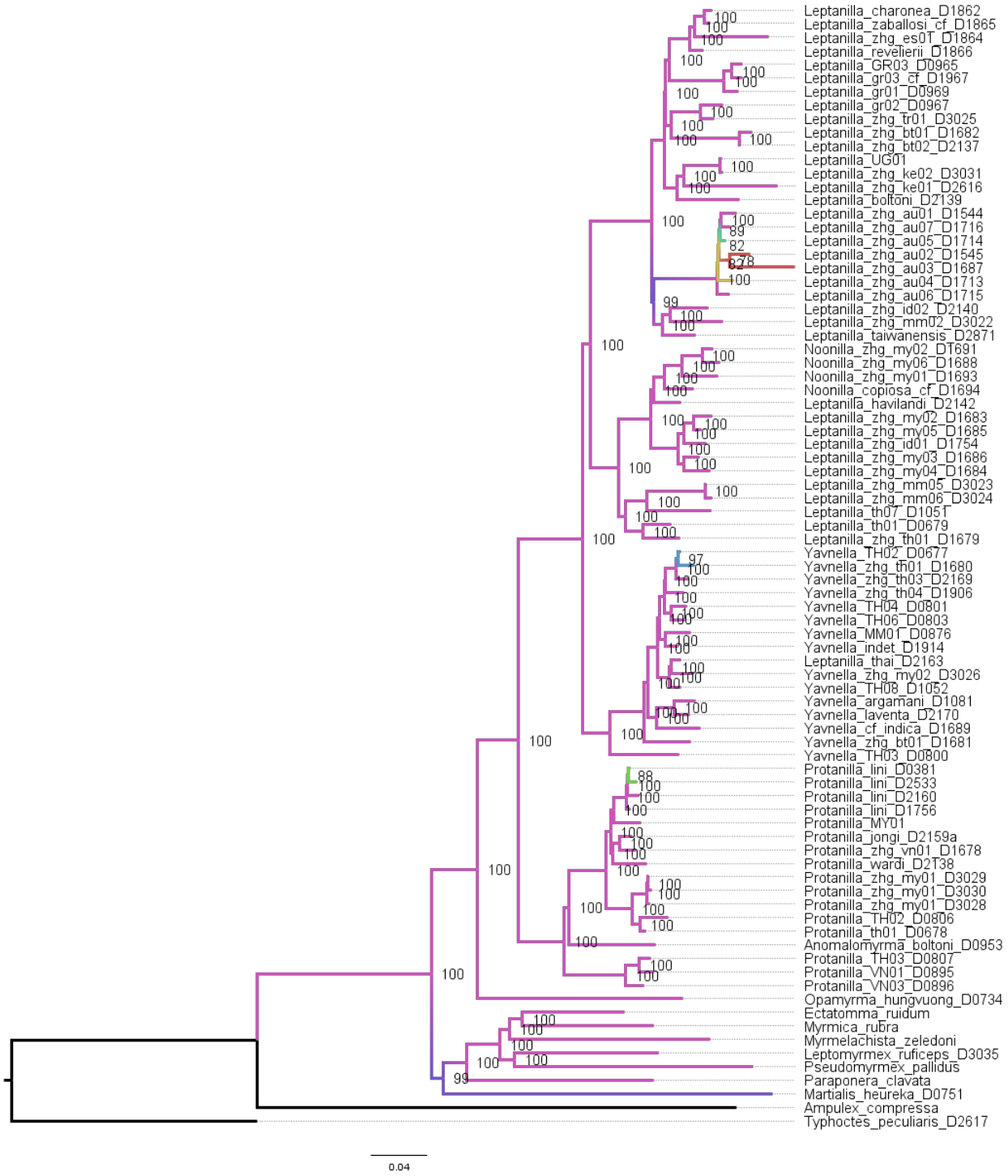

Fig. 5S107. Phylogeny of the Leptanillinae and nine outgroup terminals, as inferred under ML with within-locus partitioning from Matrix 1C*.

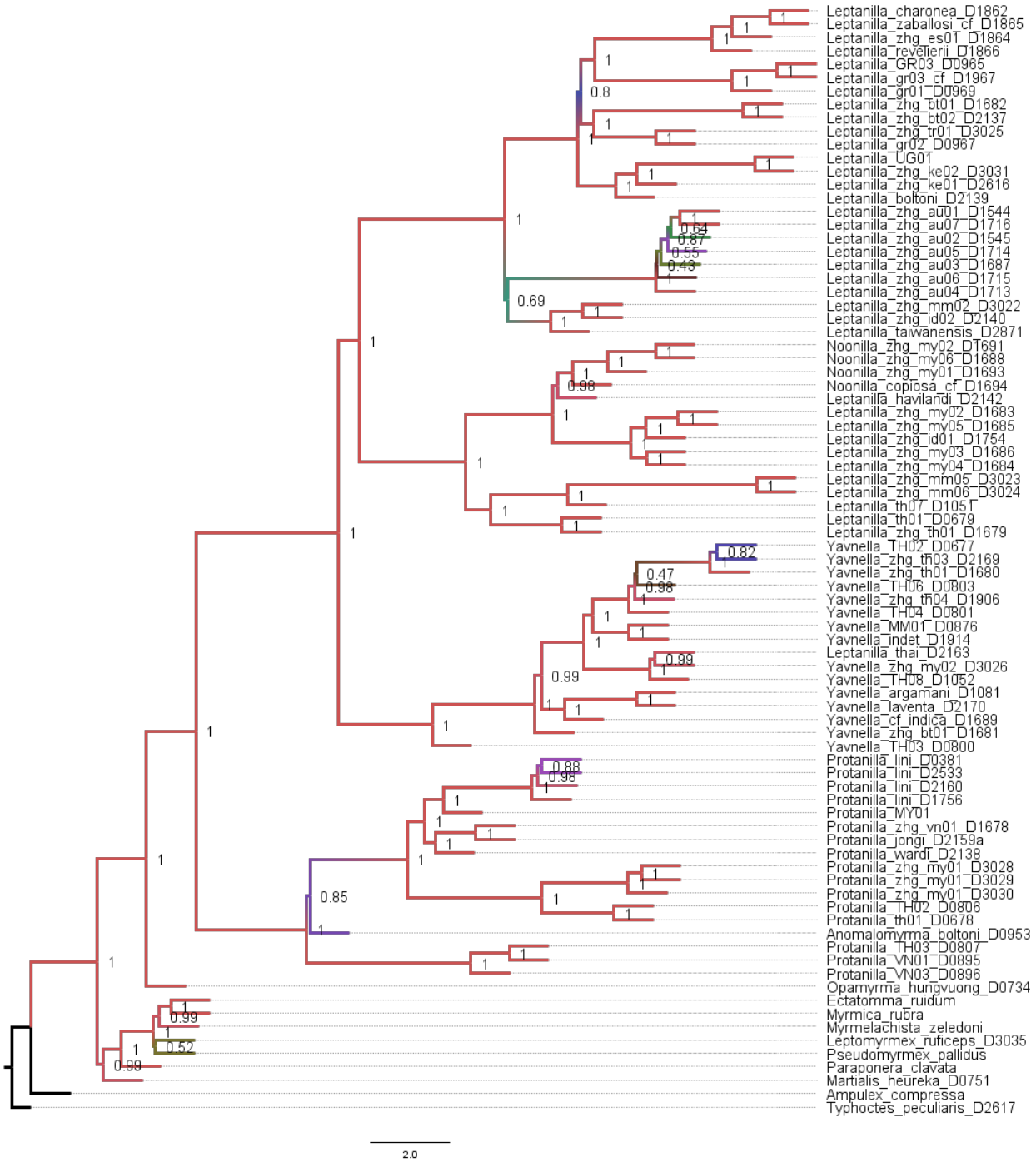

Fig. 5.S108. Phylogeny of the Leptanillinae and nine outgroup terminals, as inferred under coalescent-based inference with by-locus partitioning from Matrix 1C*.

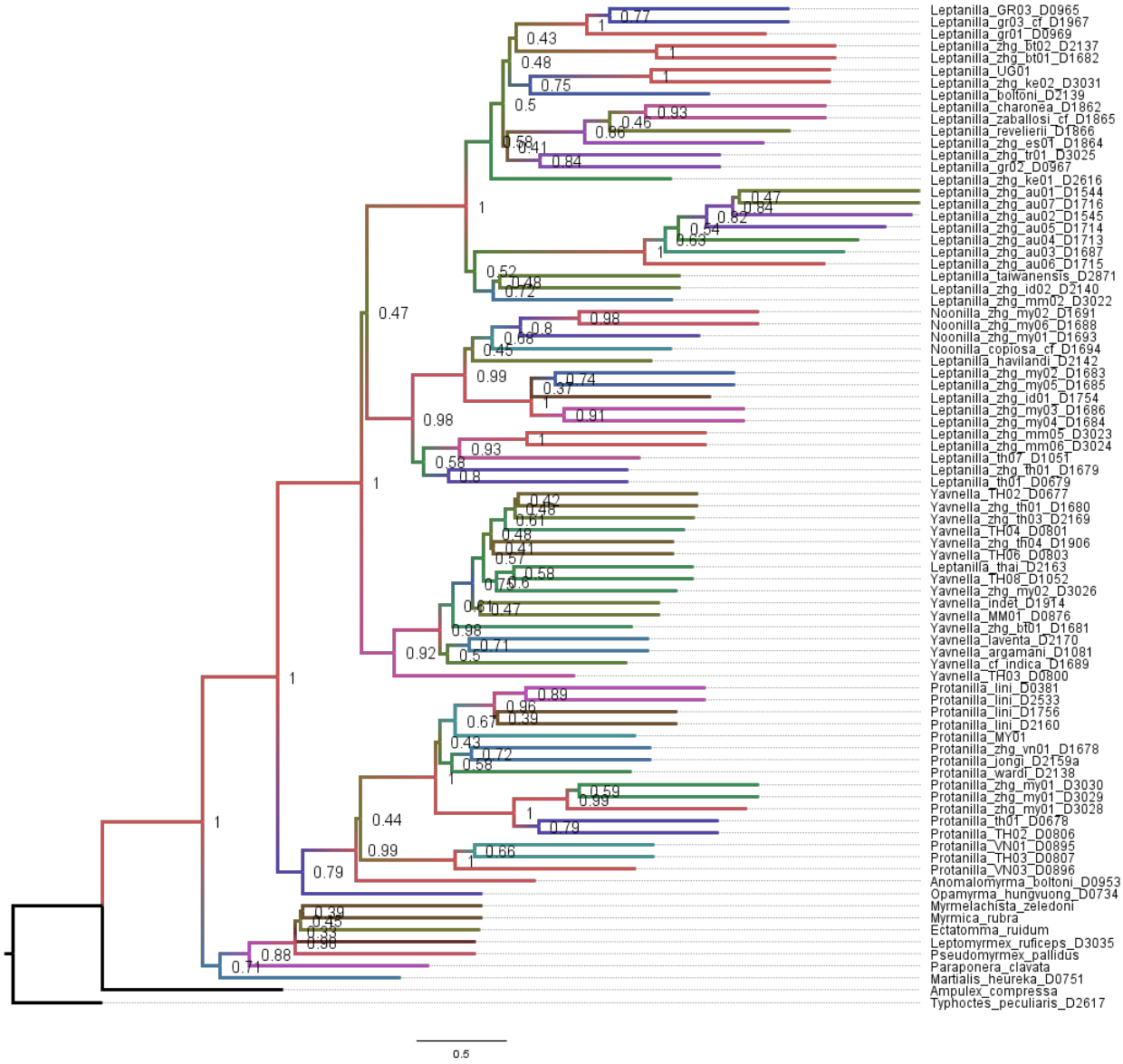

Fig. 5.S109. Phylogeny of the Leptanillinae and nine outgroup terminals, as inferred under ML with by-locus partitioning from Matrix 0.8D*.

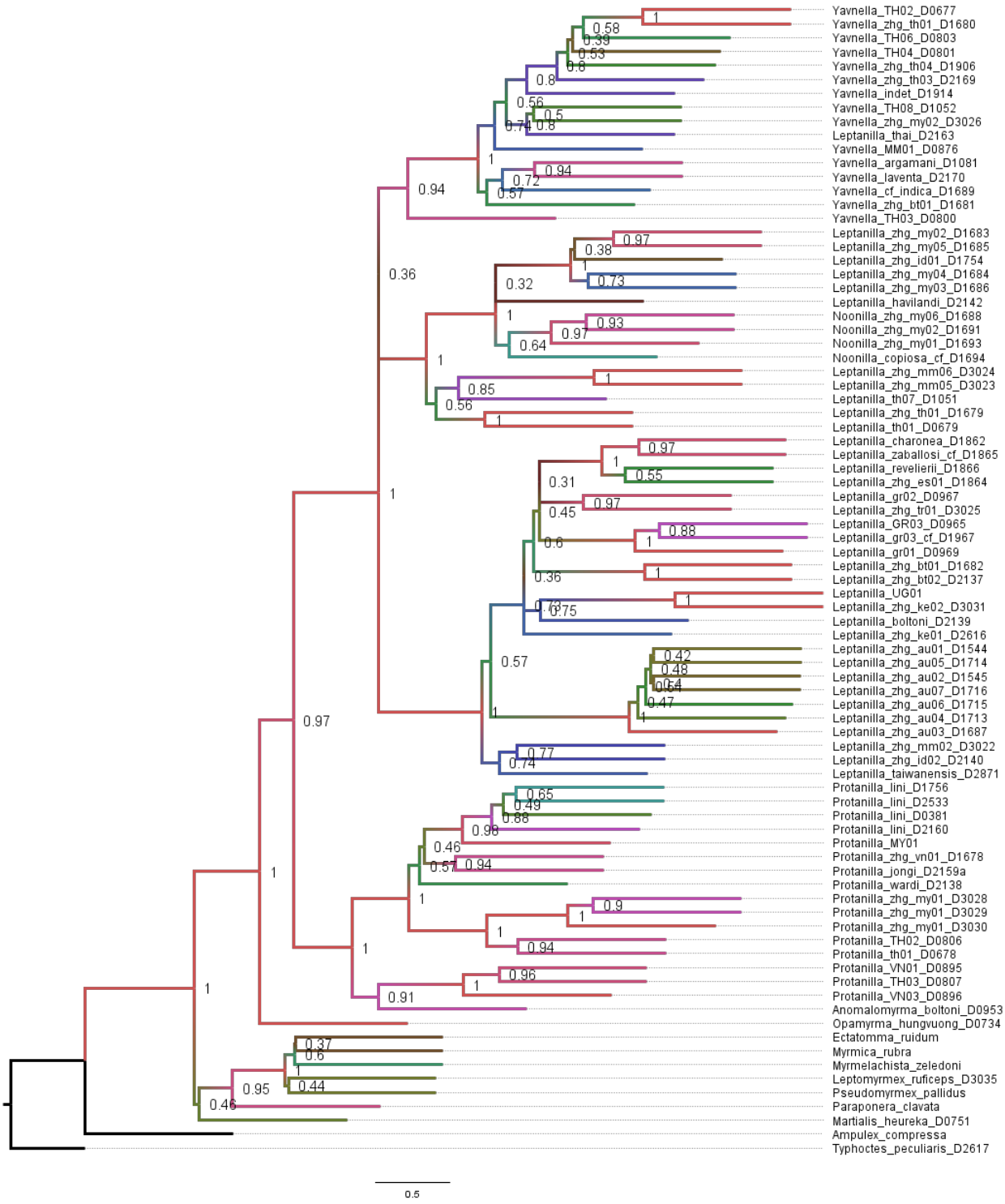

Fig. 5.S110. Phylogeny of the Leptanillinae and nine outgroup terminals, as inferred under coalescent-based inference with by-locus partitioning from Matrix 0.8D*.

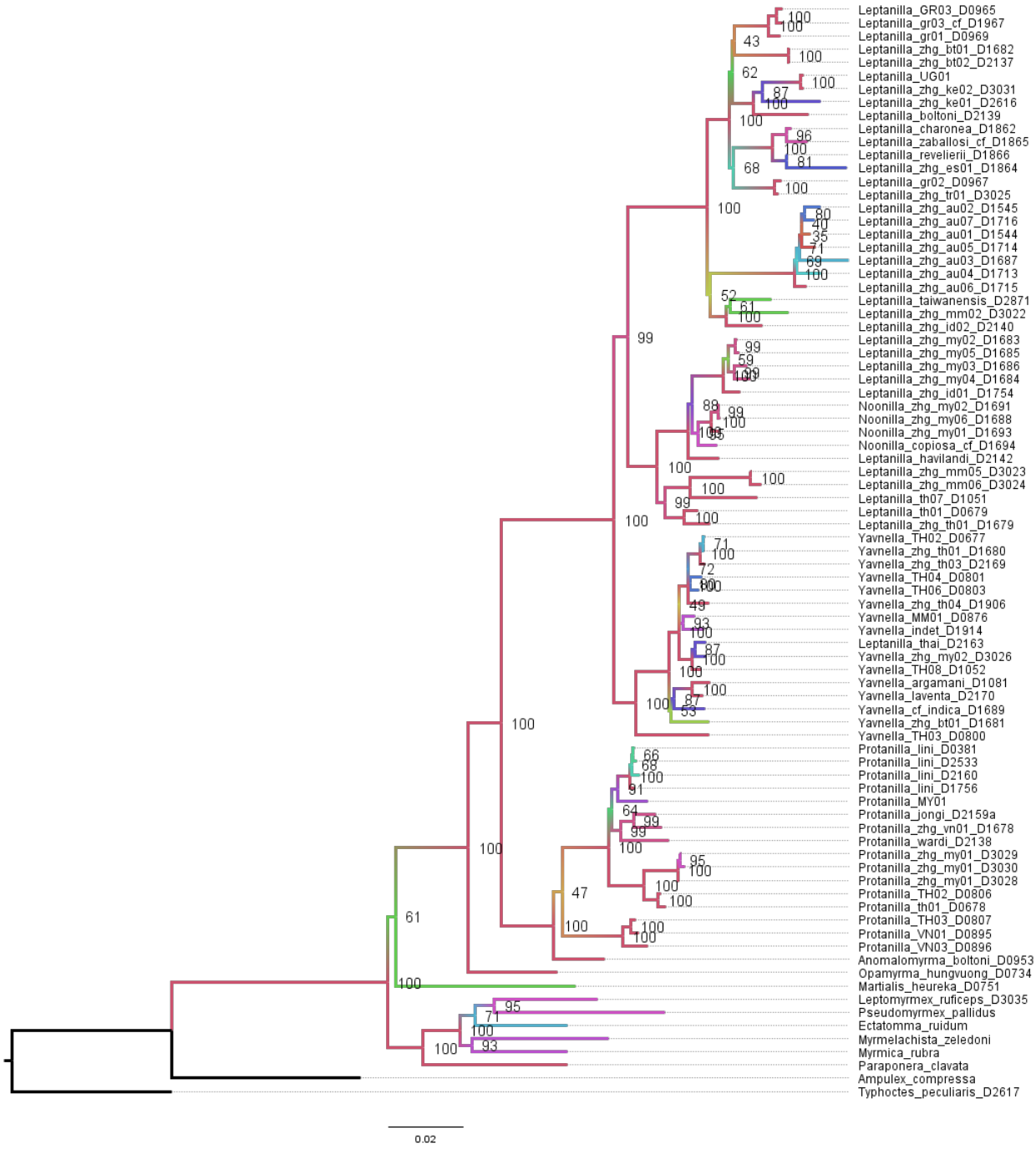

Fig. 5.S111. Phylogeny of the Leptanillinae and nine outgroup terminals, as inferred under ML with by-locus partitioning from Matrix 0.85D*.

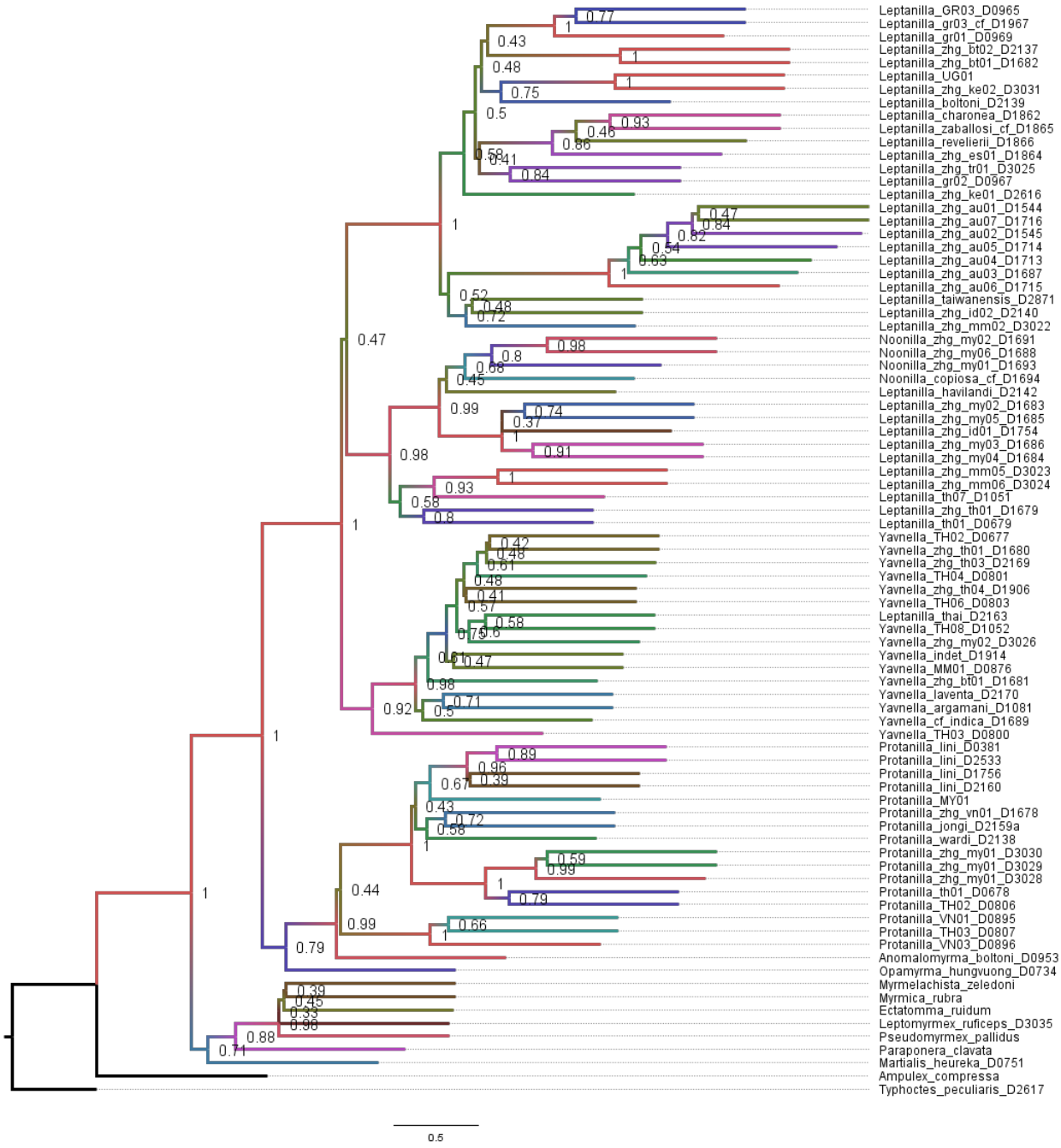

Fig. 5.S112. Phylogeny of the Leptanillinae and nine outgroup terminals, as inferred under coalescent-based inference with by-locus partitioning from Matrix 0.85D*.

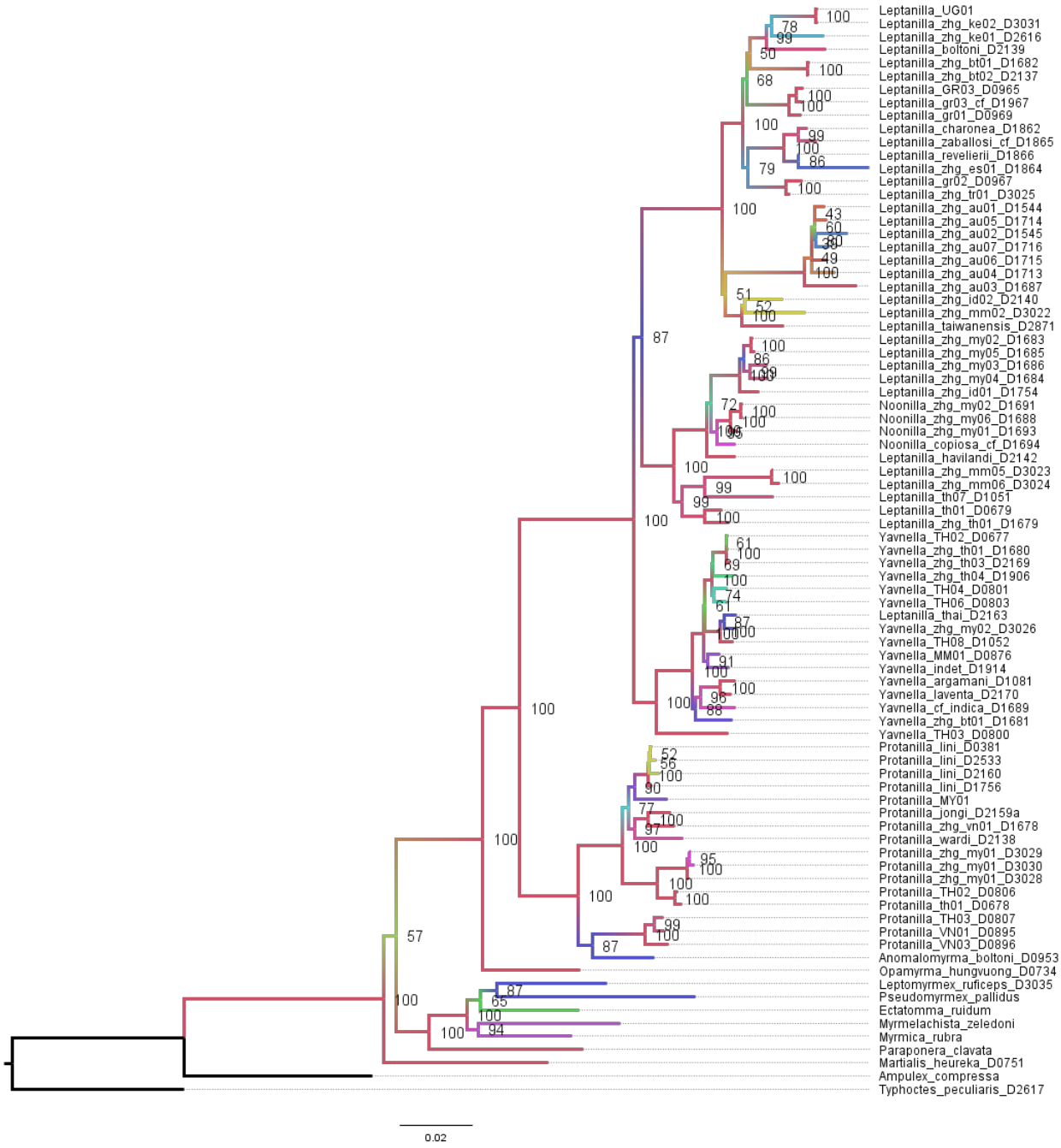

Fig. 5.S113. Phylogeny of the Leptanillinae and nine outgroup terminals, as inferred under ML with by-locus partitioning from Matrix 0.9D*.

Fig. 5.S114. Phylogeny of the Leptanillinae and nine outgroup terminals, as inferred under coalescent-based inference with by-locus partitioning from Matrix 0.9D*.

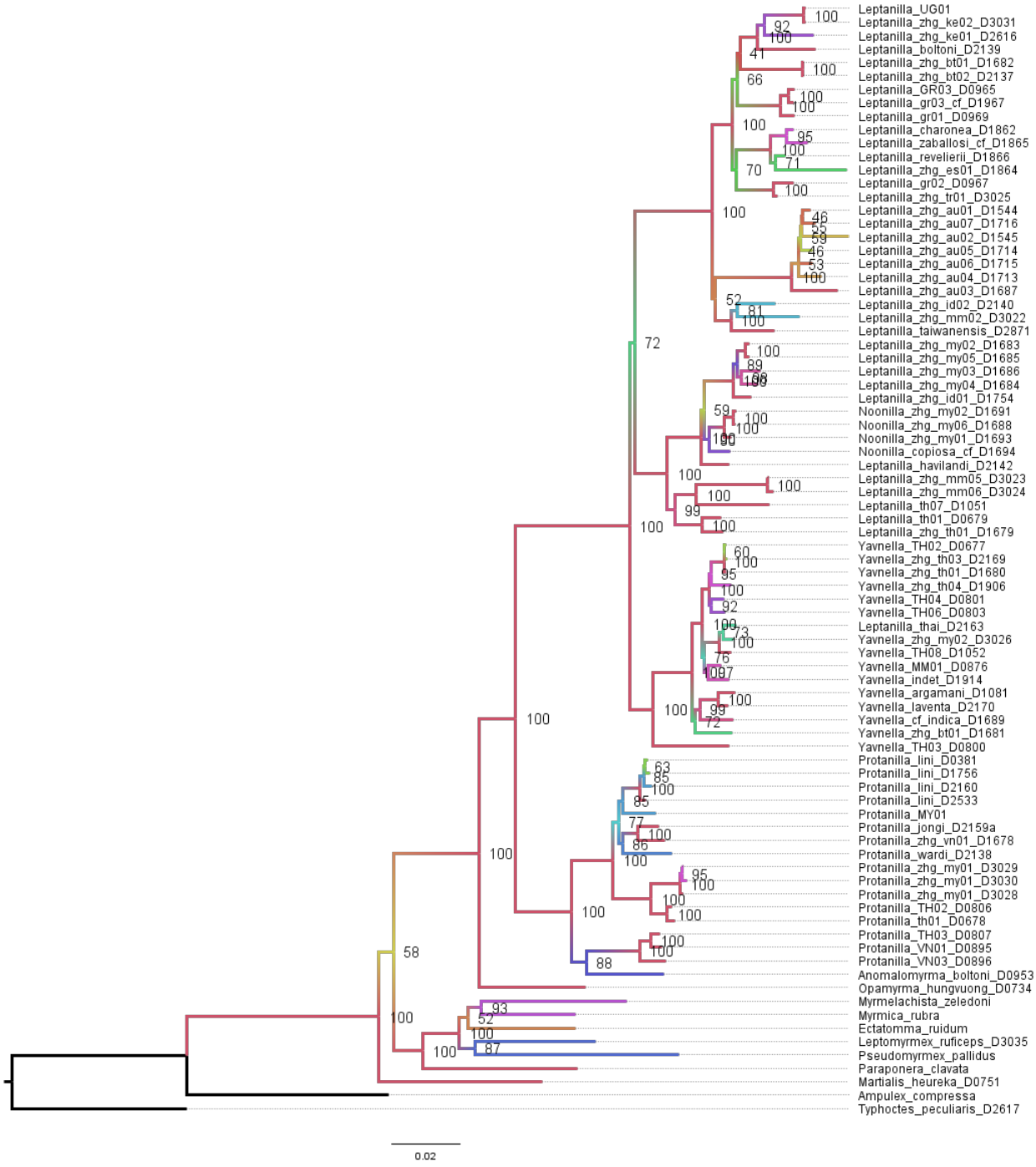

Fig. 5.S115. Phylogeny of the Leptanillinae and nine outgroup terminals, as inferred under ML with by-locus partitioning from Matrix 0.95D*.

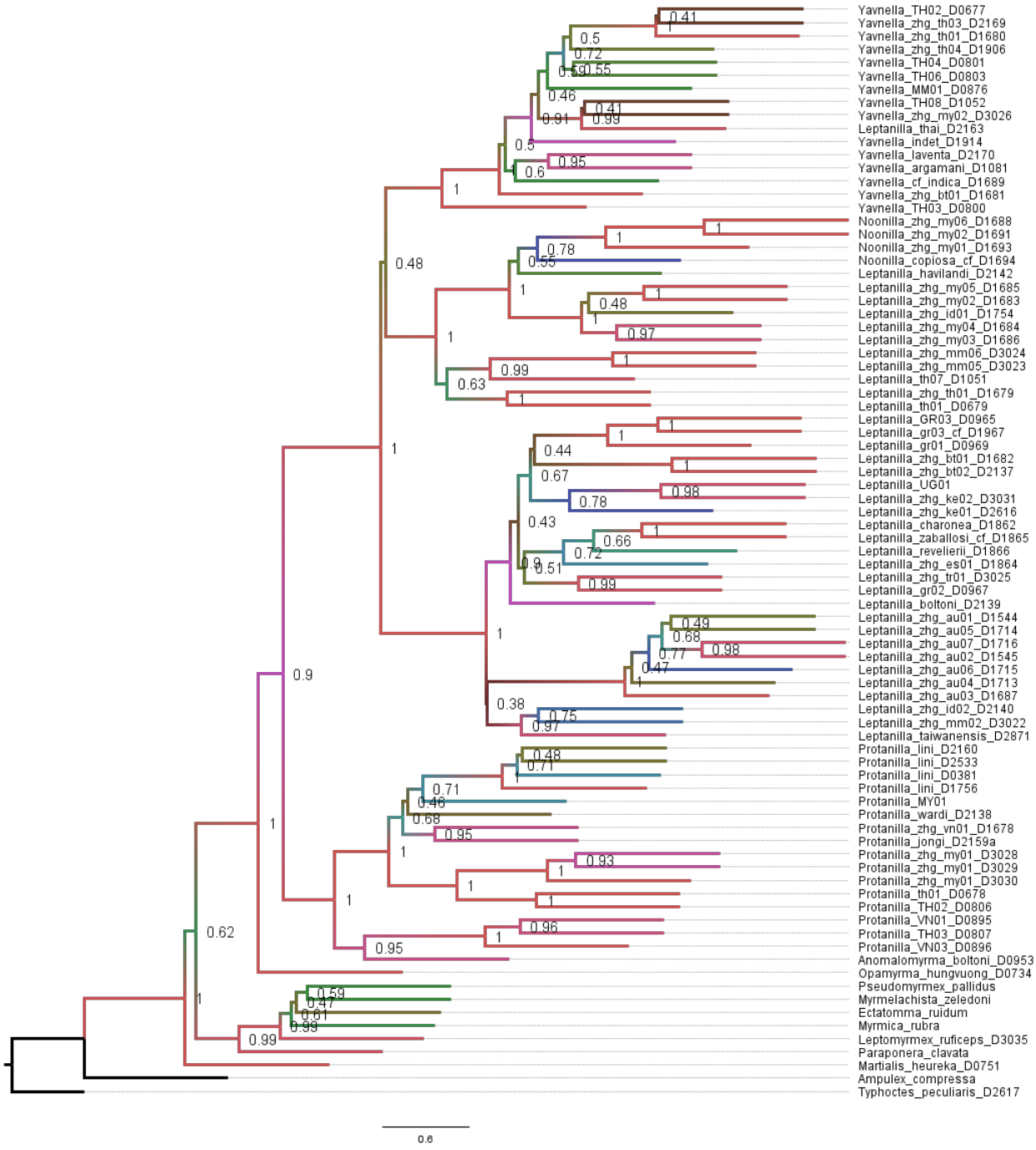

Fig. 5.S116. Phylogeny of the Leptanillinae and nine outgroup terminals, as inferred under coalescent-based inference with by-locus partitioning from Matrix 0.95D*.

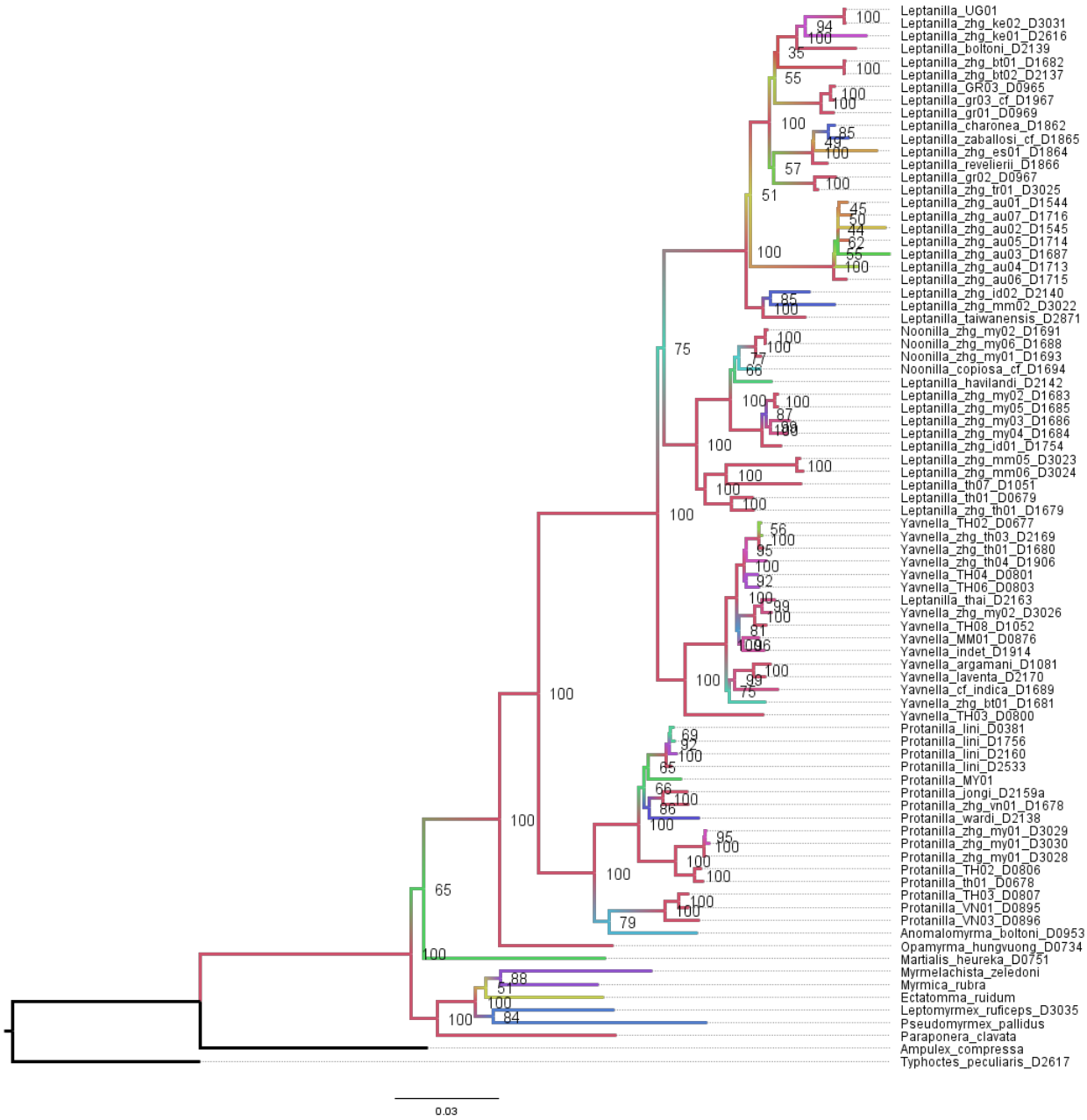

Fig. 5.S117. Phylogeny of the Leptanillinae and nine outgroup terminals, as inferred under ML with by-locus partitioning from Matrix 1D*.

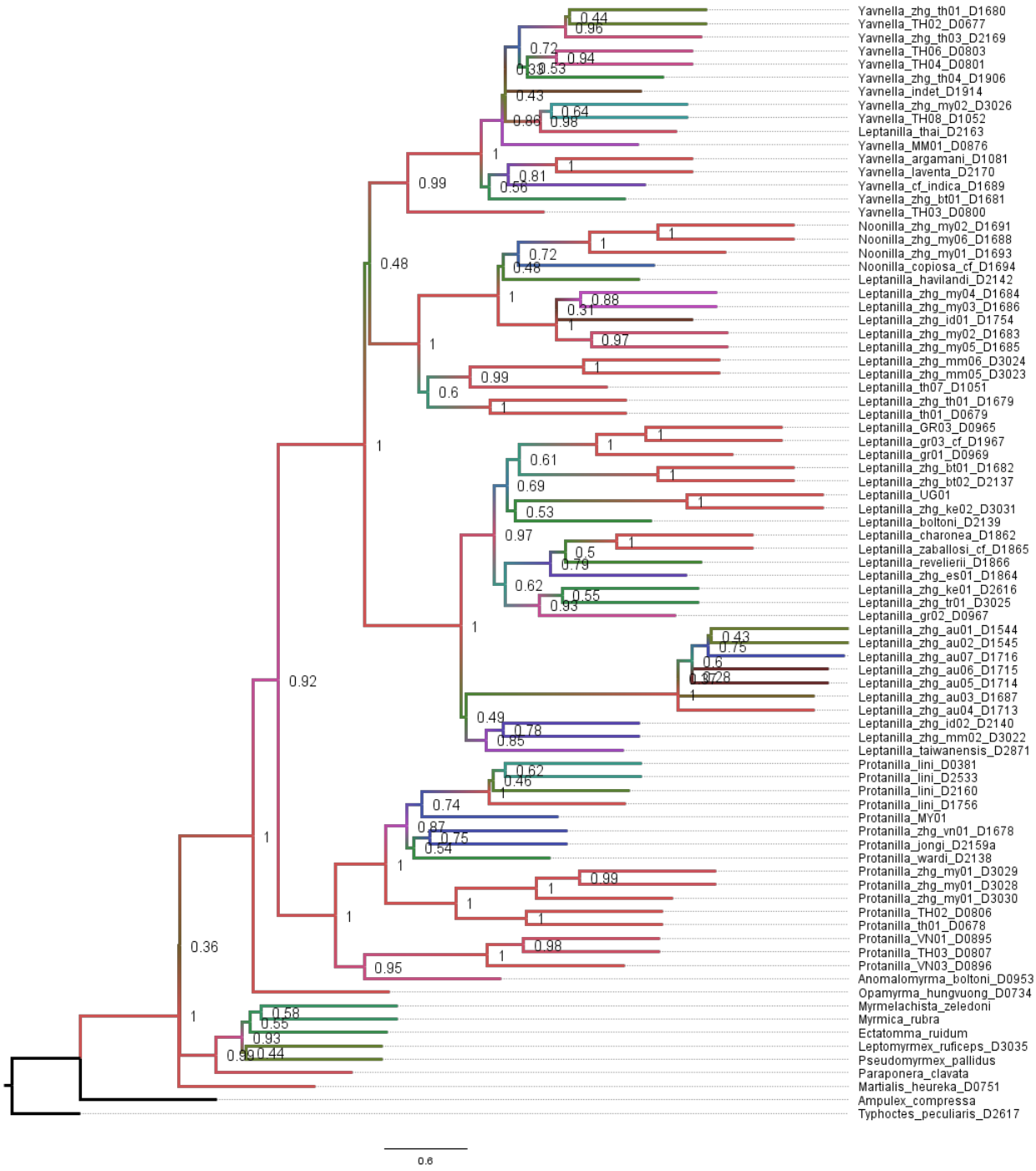

Fig. 5.S118. Phylogeny of the Leptanillinae and nine outgroup terminals, as inferred under coalescent-based inference with by-locus partitioning from Matrix 1D*.

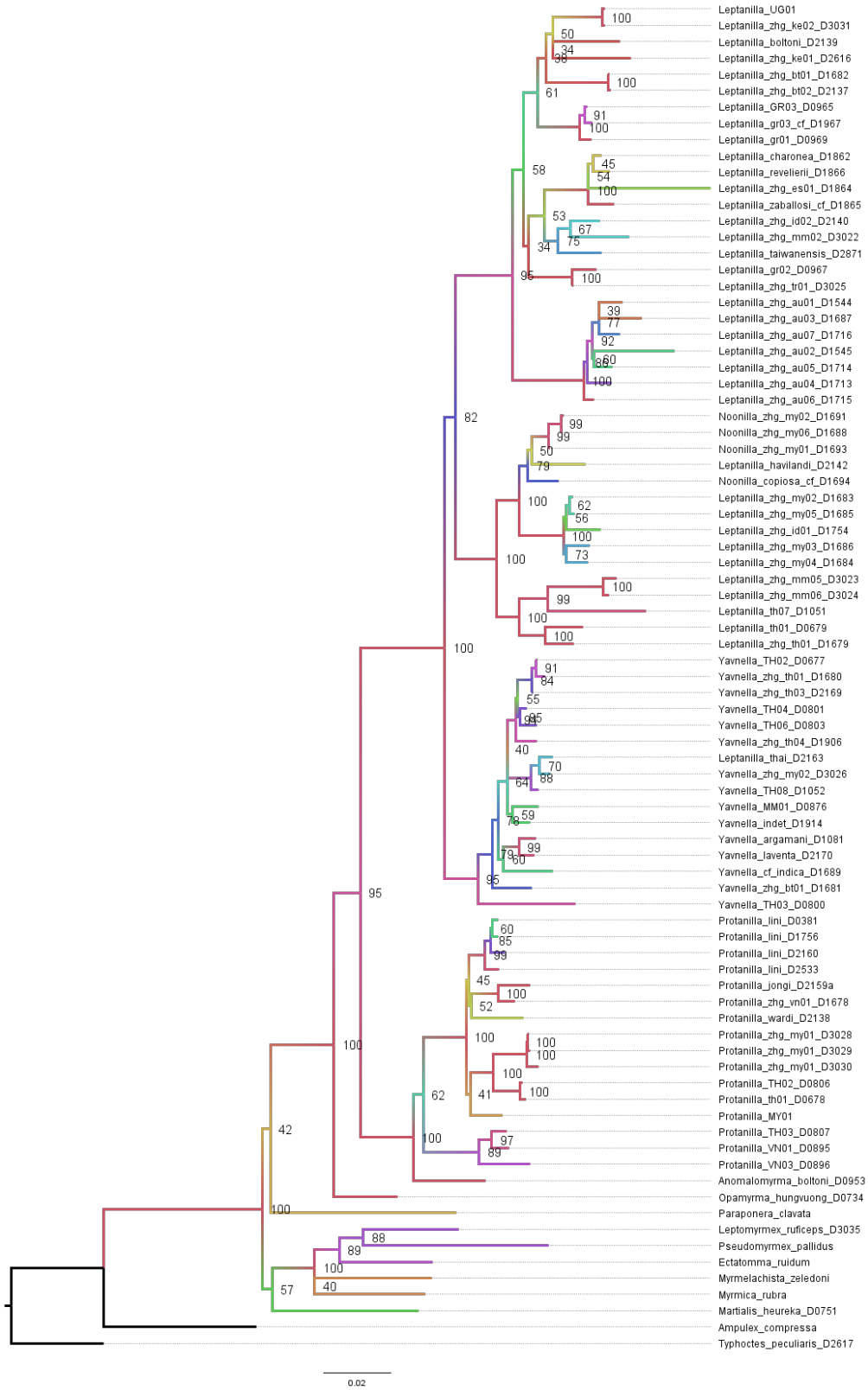

Fig. 5.S119. Phylogeny of the Leptanillinae and nine outgroup terminals, as inferred under ML with by-locus partitioning from Matrix 1D†*.

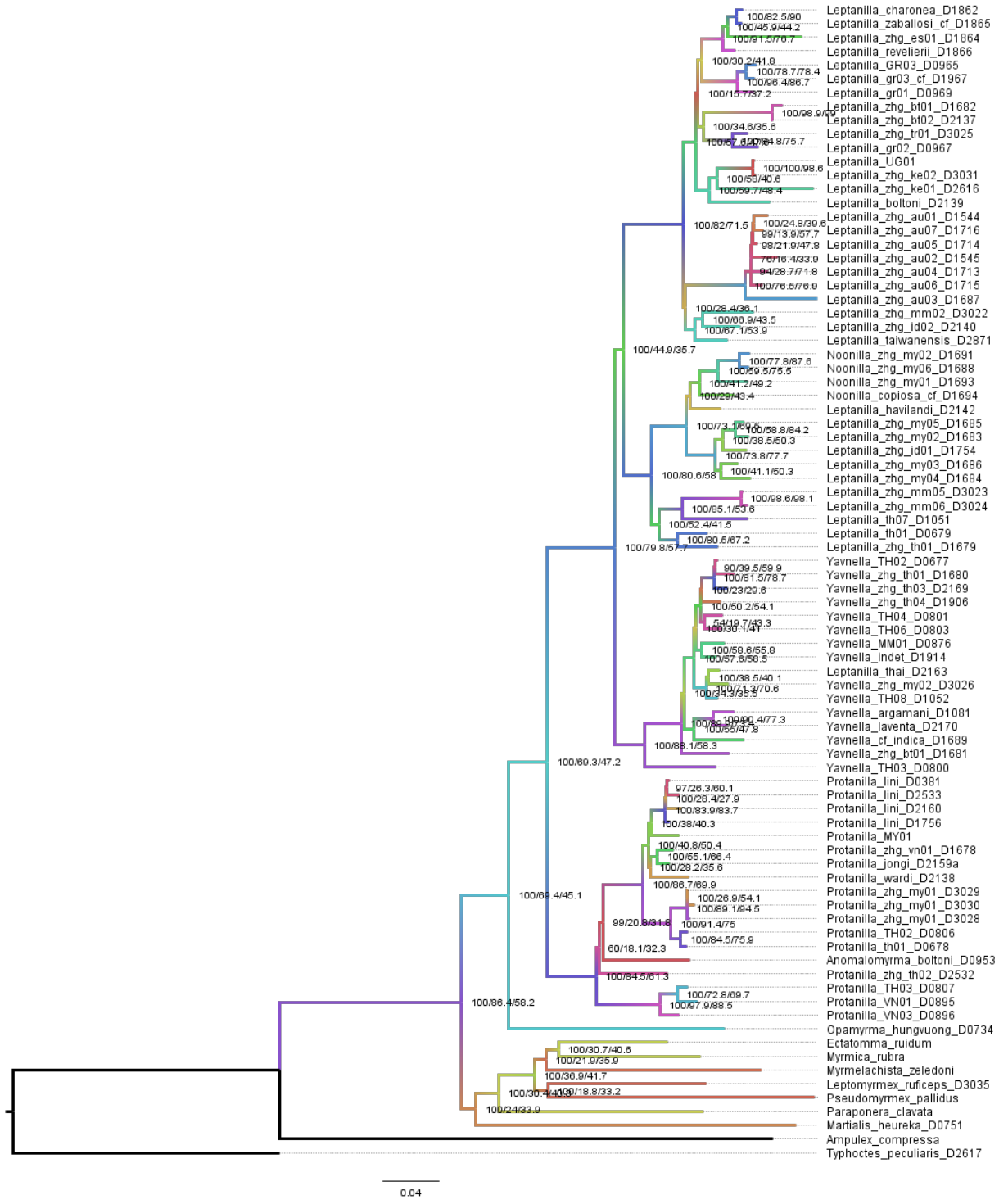

Fig. 5.S120. Phylogeny of the Leptanillinae and nine outgroup terminals, as inferred under ML with within-locus partitioning from Matrix 1A. Nodes denoted with bootstrap support/gCF/sCF.

Fig. 5.S121. Phylogeny of the Leptanillinae and nine outgroup terminals, as inferred under ML with within-locus partitioning from Matrix 1B. Nodes denoted with bootstrap support/gCF/sCF.

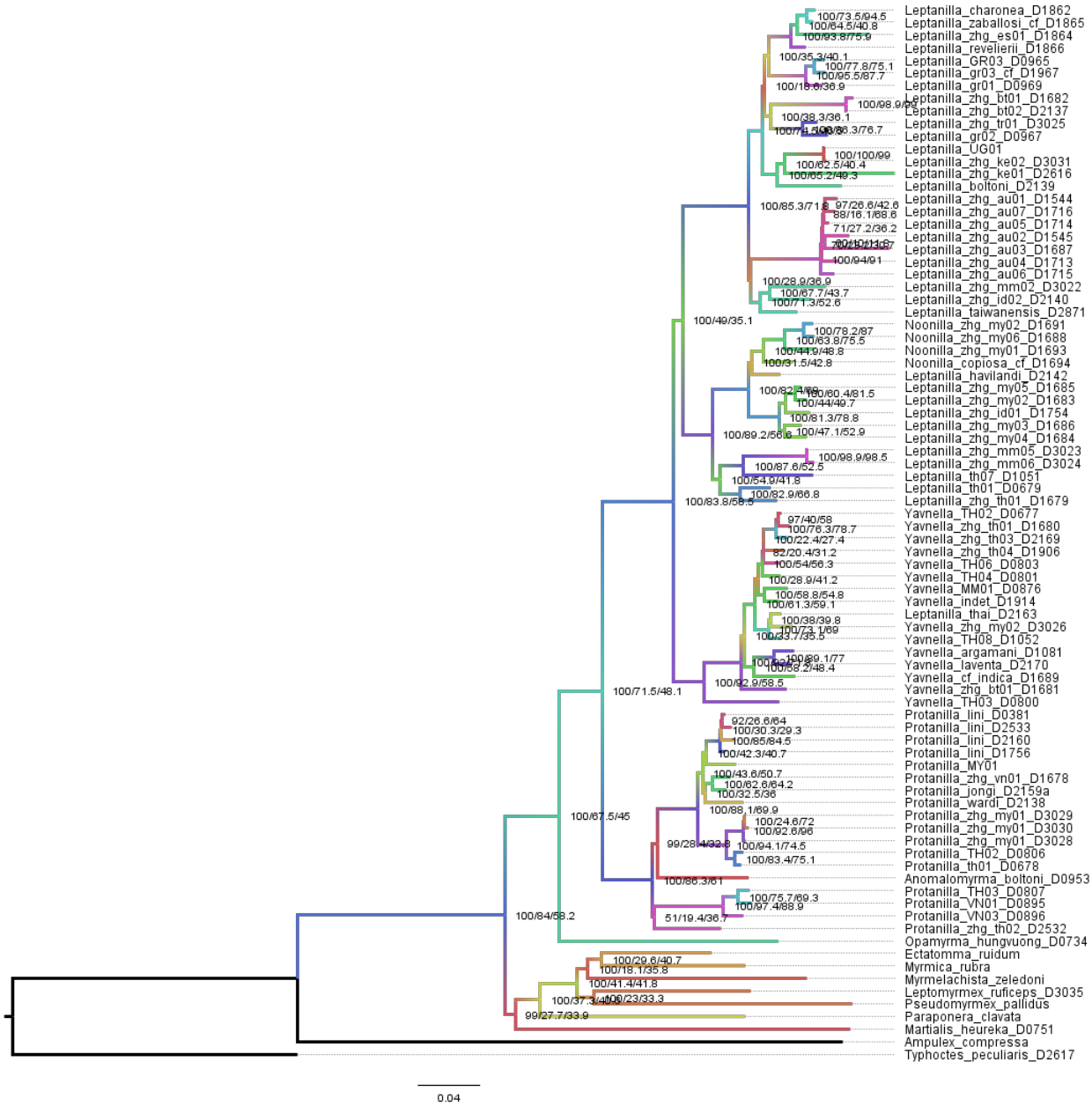

Fig. 5.S122. Phylogeny of the Leptanillinae and nine outgroup terminals, as inferred under ML with within-locus partitioning from Matrix 1C. Nodes denoted with bootstrap support/gCF/sCF.

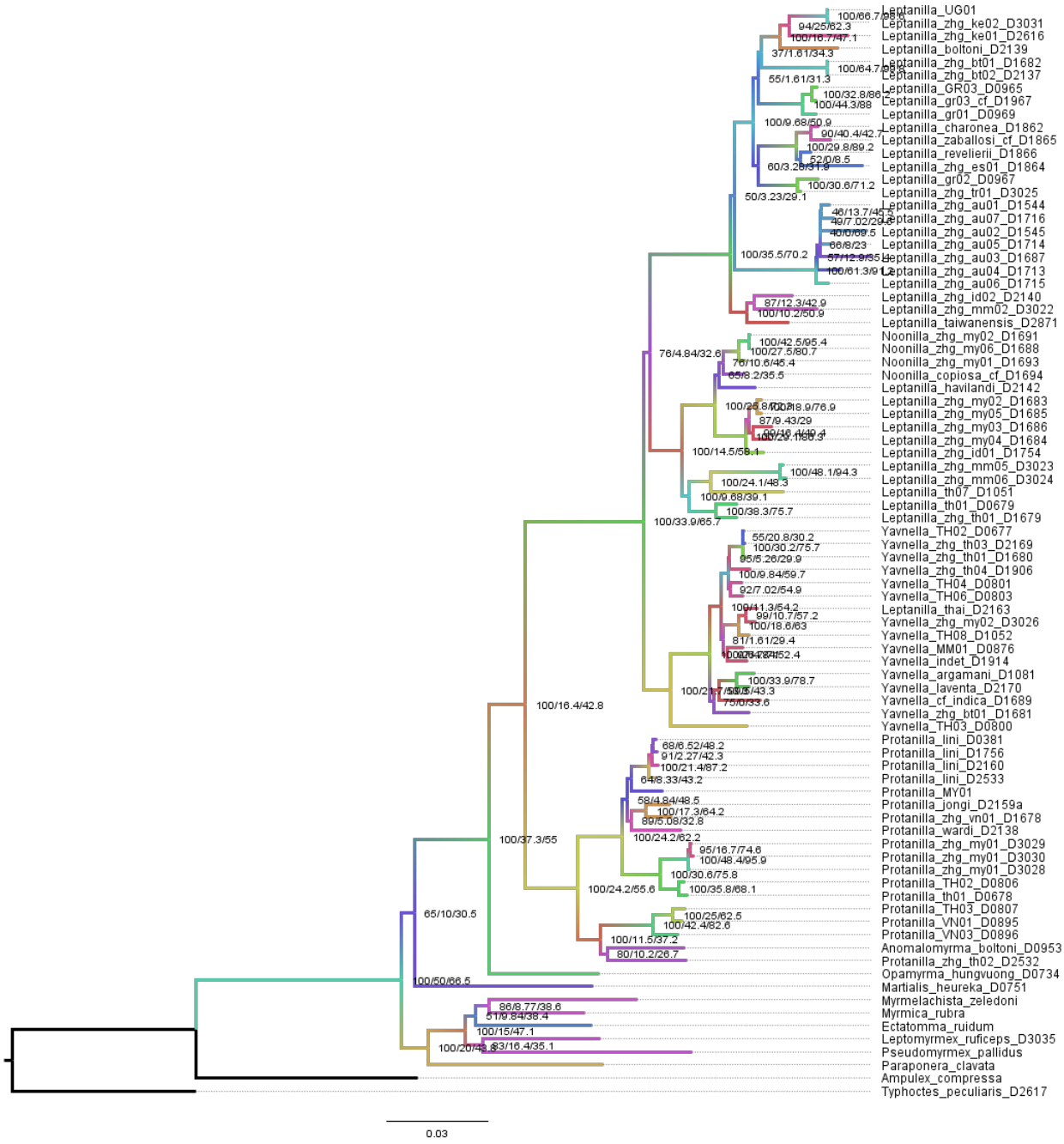

Fig. 5.S123. Phylogeny of the Leptanillinae and nine outgroup terminals, as inferred under ML with within-locus partitioning from Matrix 1D. Nodes denoted with bootstrap support/gCF/sCF.

Abadi, S., Azouri, D., Pupko, T., Mayrose, I., 2019. Model selection may not be a mandatory step for phylogeny reconstruction. Nat. Commun. 10, 934. https://doi.org/10.1038/s41467-019-08822-w

Aberer, A.J., Kobert, K., Stamatakis, A., 2014. ExaBayes: massively parallel Bayesian tree inference for the whole-genome era. Mol. Biol. Evol. 31, 2553–2556. https://doi.org/10.1093/molbev/msu236

Bankevich, A., Nurk, S., Antipov, D., Gurevich, A.A., Dvorkin, M., Kulikov, A.S., Lesin, V.M., Nikolenko, S.I., Pham, S., Prjibelski, A.D., Pyshkin, A.V., Sirotkin, A.V., Vyahhi, N., Tesler, G., Alekseyev, M.A., Pevzner, P.A., 2012. Spades: a new genome assembly algorithm and its applications to single-cell sequencing. J. Comput. Biol. 19, 455–477. https://doi.org/10.1089/cmb.2012.0021

Barandica, J.M., López, F., Martínez, M.D., Ortuño, V.M., 1994. The larvae of *Leptanilla charonea* and *Leptanilla zaballosi* (Hymenoptera, Formicidae). Dtsch. Entomol. Z. 41, 147–153. https://doi.org/10.1002/mmnd.19940410113

Barden, P., Boudinot, B., Lucky, A., Barden, P., Boudinot, B., Lucky, A., 2017. Where Fossils Dare and Males Matter: combined morphological and molecular analysis untangles the evolutionary history of the spider ant genus <i>Leptomyrmex<i/> Mayr (Hymenoptera : Dolichoderinae). Invertebr. Syst. 31, 765–780. https://doi.org/10.1071/IS16067

Baroni Urbani, C., 1977. Materiali per una revisione della sottofamiglia Leptanillinae Emery (Hymenoptera: Formicidae). Entomol. Basiliensia 2, 427–488.

Betancur-R., R., Arcila, D., Vari, R.P., Hughes, L.C., Oliveira, C., Sabaj, M.H., Ortí, G., 2019. Phylogenomic incongruence, hypothesis testing, and taxonomic sampling: The monophyly of characiform fishes*. Evolution 73, 329–345. https://doi.org/10.1111/evo.13649

Blaimer, B.B., Santos, B.F., Cruaud, A., Gates, M.W., Kula, R.R., Mikó, I., Rasplus, J.-Y., Smith, D.R., Talamas, E.J., Brady, S.G., Buffington, M.L., 2023. Key innovations and the diversification of Hymenoptera. Nat. Commun. 14, 1212. https://doi.org/10.1038/s41467-023-36868-4

Bolton, B., 1990. The higher classification of the ant subfamily Leptanillinae (Hymenoptera: Formicidae). Syst. Entomol. 15, 267–282. https://doi.org/10.1111/j.1365-3113.1990.tb00063.x

Borowiec, M.L., 2019a. Convergent evolution of the army ant syndrome and congruence in big-data phylogenetics. Syst. Biol. 68, 642–656. https://doi.org/10.1093/sysbio/syy088

Borowiec, M.L., 2019b. Spruceup: fast and flexible identification, visualization, and removal of outliers from large multiple sequence alignments. J. Open Source Softw. 4, 1635. https://doi.org/10.21105/joss.01635

Borowiec, M.L., 2016. AMAS: a fast tool for alignment manipulation and computing of summary statistics. PeerJ 4, e1660. https://doi.org/10.7717/peerj.1660

Borowiec, M.L., Rabeling, C., Brady, S.G., Fisher, B.L., Schultz, T.R., Ward, P.S., 2019. Compositional heterogeneity and outgroup choice influence the internal phylogeny of the ants. Mol. Phylogenet. Evol. 134, 111–121. https://doi.org/10.1016/j.ympev.2019.01.024

Bossert, S., Murray, E.A., Pauly, A., Chernyshov, K., Brady, S.G., Danforth, B.N., 2021. Gene Tree Estimation Error with Ultraconserved Elements: An Empirical Study on *Pseudapis* Bees. Syst. Biol. 70, 803–821. https://doi.org/10.1093/sysbio/syaa097

Boudinot, B.E., 2015. Contributions to the knowledge of Formicidae (Hymenoptera, Aculeata): a new diagnosis of the family, the first global male-based key to subfamilies, and a treatment of early branching lineages. Eur. J. Taxon. https://doi.org/10.5852/ejt.2015.120

Boudinot, B.E., Khouri, Z., Richter, A., Griebenow, Z.H., Kamp, T. van de, Perrichot, V., Barden, P., 2022. Evolution and systematics of the Aculeata and kin (Hymenoptera), with emphasis on the ants (Formicoidea: †@@@idae fam. nov., Formicidae). https://doi.org/10.1101/2022.02.20.480183

Branstetter, M.G., Longino, J.T., Ward, P.S., Faircloth, B.C., 2017. Enriching the ant tree of life: enhanced UCE bait set for genome-scale phylogenetics of ants and other Hymenoptera. Methods Ecol. Evol. 8, 768–776. https://doi.org/10.1111/2041-210X.12742

Brazeau, M.D., 2011. Problematic character coding methods in morphology and their effects. Biol. J. Linn. Soc. 104, 489–498. https://doi.org/10.1111/j.1095-8312.2011.01755.x

Brown, J.M., Thomson, R.C., 2017. Bayes factors unmask highly variable information content, bias, and extreme influence in phylogenomic analyses. Syst. Biol. 66, 517–530. https://doi.org/10.1093/sysbio/syw101

Brues, C., 1925. *Scyphodon*, an anomalous genus of Hymenoptera of doubtful affinities. Treubia 6, 93–96.

Castresana, J., 2000. Selection of conserved blocks from multiple alignments for their use in phylogenetic analysis. Mol. Biol. Evol. 17, 540–552. https://doi.org/10.1093/oxfordjournals.molbev.a026334

Chan, K.O., Hutter, C.R., Wood, P.L., Grismer, L.L., Brown, R.M., 2020. Larger, unfiltered datasets are more effective at resolving phylogenetic conflict: Introns, exons, and UCEs resolve ambiguities in Golden-backed frogs (Anura: Ranidae; genus Hylarana). Mol. Phylogenet. Evol. 151, 106899. https://doi.org/10.1016/j.ympev.2020.106899

Duchêne, D.A., Mather, N., Van Der Wal, C., Ho, S.Y.W., 2022. Excluding loci with substitution saturation improves inferences from phylogenomic data. Syst. Biol. 71, 676–689. https://doi.org/10.1093/sysbio/syab075

Faircloth, B.C., 2016. PHYLUCE is a software package for the analysis of conserved genomic loci. Bioinformatics 32, 786–788. https://doi.org/10.1093/bioinformatics/btv646

Felsenstein, J., 1981. Evolutionary trees from DNA sequences: A maximum likelihood approach. J. Mol. Evol. 17, 368–376. https://doi.org/10.1007/BF01734359

Gillung, J.P., Winterton, S.L., Bayless, K.M., Khouri, Z., Borowiec, M.L., Yeates, D., Kimsey, L.S., Misof, B., Shin, S., Zhou, X., Mayer, C., Petersen, M., Wiegmann, B.M., 2018. Anchored phylogenomics unravels the evolution of spider flies (Diptera, Acroceridae) and reveals discordance between nucleotides and amino acids. Mol. Phylogenet. Evol. 128, 233–245. https://doi.org/10.1016/j.ympev.2018.08.007

Glenn, T.C., Nilsen, R.A., Kieran, T.J., Sanders, J.G., Bayona-Vásquez, N.J., Finger, J.W., Pierson, T.W., Bentley, K.E., Hoffberg, S.L., Louha, S., Leon, F.J.G.-D., Portilla, M.A. del R., Reed, K.D., Anderson, J.L., Meece, J.K., Aggrey, S.E., Rekaya, R., Alabady, M., Belanger, M.,

Winker, K., Faircloth, B.C., 2019. Adapterama I: universal stubs and primers for 384 unique dual-indexed or 147,456 combinatorially-indexed Illumina libraries (iTru & iNext). PeerJ 7, e7755. https://doi.org/10.7717/peerj.7755

Griebenow, Z., 2020. Delimitation of tribes in the subfamily Leptanillinae (Hymenoptera: Formicidae), with a description of the male of *Protanilla lini* Terayama, 2009. Myrmecol. News 30.

Griebenow, Z.H., 2021. Synonymisation of the male-based ant genus *Phaulomyrma* (Hymenoptera: Formicidae) with Leptanilla based upon Bayesian total-evidence phylogenetic inference. Invertebr. Syst. https://doi.org/10.1071/IS20059

Griebenow, Z.H., Isaia, M., Moradmand, M., 2022. A remarkable troglomorphic ant, *Yavnella laventa* sp. nov. (Hymenoptera: Formicidae: Leptanillinae), identified as the first known worker of *Yavnella* Kugler by phylogenomic inference. Invertebr. Syst. 36, 1118–1138. https://doi.org/10.1071/IS22035

Hoang, D.T., Chernomor, O., von Haeseler, A., Minh, B.Q., Vinh, L.S., 2018. UFBoot2: improving the ultrafast bootstrap approximation. Mol. Biol. Evol. 35, 518–522. https://doi.org/10.1093/molbev/msx281

Höhna, S., Landis, M.J., Heath, T.A., 2017. Phylogenetic inference using RevBayes. Curr. Protoc. Bioinforma. 57, 6.16.1-6.16.34. https://doi.org/10.1002/cpbi.22

Hsu, P.-W., Hsu, F.-C., Hsiao, Y., Lin, C.-C., 2017. Taxonomic notes on the genus *Protanilla* (Hymenoptera: Formicidae: Leptanillinae) from Taiwan. Zootaxa 4268, 117–130. https://doi.org/10.11646/zootaxa.4268.1.7

Ito, F., Hashim, R., Mizuno, R., Billen, J., 2022. Notes on the biology of *Protanilla* sp. (Hymenoptera, Formicidae) collected in Ulu Gombak, Peninsular Malaysia. Insectes Sociaux 69, 13–18. https://doi.org/10.1007/s00040-021-00839-z

Jermiin, L.S., Ho, S.Y.W., Ababneh, F., Robinson, J., Larkum, A.W.D., 2004. The biasing effect of compositional heterogeneity on phylogenetic estimates may be underestimated. Syst. Biol. 53, 638–643. https://doi.org/10.1080/10635150490468648

Kalyaanamoorthy, S., Minh, B.Q., Wong, T.K.F., von Haeseler, A., Jermiin, L.S., 2017. ModelFinder: fast model selection for accurate phylogenetic estimates. Nat. Methods 14, 587–589. https://doi.org/10.1038/nmeth.4285

Katoh, K., Toh, H., 2010. Parallelization of the MAFFT multiple sequence alignment program. Bioinformatics 26, 1899–1900. https://doi.org/10.1093/bioinformatics/btq224

Klopfstein, S., Massingham, T., Goldman, N., 2017. More on the best evolutionary rate for phylogenetic analysis. Syst. Biol. 66, 769–785. https://doi.org/10.1093/sysbio/syx051

Kubatko, L.S., Degnan, J.H., 2007. Inconsistency of phylogenetic estimates from concatenated data under coalescence. Syst. Biol. 56, 17–24. https://doi.org/10.1080/10635150601146041

Kück, P., Garcia, F.H., Misof, B., Meusemann, K., 2011. Improved phylogenetic analyses corroborate a plausible position of *Martialis heureka* in the ant tree of life. PLOS ONE 6, e21031. https://doi.org/10.1371/journal.pone.0021031

Kulkarni, S., Kallal, R.J., Wood, H., Dimitrov, D., Giribet, G., Hormiga, G., 2021. Interrogating genomic-scale data to resolve recalcitrant nodes in the spider tree of life. Mol. Biol. Evol. 38, 891–903. https://doi.org/10.1093/molbev/msaa251

Lewis, P.O., 2001. A likelihood approach to estimating phylogeny from discrete morphological character data. Syst. Biol. 50, 913–925. https://doi.org/10.1080/106351501753462876

Lucky, A., Trautwein, M.D., Guénard, B.S., Weiser, M.D., Dunn, R.R., 2013. Tracing the rise of ants - out of the ground. PLOS ONE 8, e84012. https://doi.org/10.1371/journal.pone.0084012

Maddison, W.P., 1997. Gene trees in species trees. Syst. Biol. 46, 523–536. https://doi.org/10.1093/sysbio/46.3.523

Masuko, K., 1990. Behavior and ecology of the enigmatic ant *Leptanilla japonica* Baroni Urbani (Hymenoptera: Formicidae: Leptanillinae). Insectes Sociaux 37, 31–57. https://doi.org/10.1007/BF02223813

Minh, B.Q., Hahn, M.W., Lanfear, R., 2020a. New methods to calculate concordance factors for phylogenomic datasets. Mol. Biol. Evol. 37, 2727–2733. https://doi.org/10.1093/molbev/msaa106

Minh, B.Q., Schmidt, H.A., Chernomor, O., Schrempf, D., Woodhams, M.D., von Haeseler, A., Lanfear, R., 2020b. IQ-TREE 2: new models and efficient methods for phylogenetic inference in the genomic era. Mol. Biol. Evol. 37, 1530–1534. https://doi.org/10.1093/molbev/msaa015

Mirarab, S., Reaz, R., Bayzid, Md.S., Zimmermann, T., Swenson, M.S., Warnow, T., 2014. ASTRAL: genome-scale coalescent-based species tree estimation. Bioinformatics 30, i541–i548. https://doi.org/10.1093/bioinformatics/btu462

Mirarab, S., Warnow, T., 2015. ASTRAL-II: coalescent-based species tree estimation with many hundreds of taxa and thousands of genes. Bioinformatics 31, i44–i52. https://doi.org/10.1093/bioinformatics/btv234

Mongiardino Koch, N., 2021. Phylogenomic subsampling and the search for phylogenetically reliable loci. Mol. Biol. Evol. 38, 4025–4038. https://doi.org/10.1093/molbev/msab151

Moreau, C.S., Bell, C.D., 2013. Testing the museum versus cradle tropical biological diversity hypothesis: phylogeny, diversification, and ancestral biogeographic range evolution of the ants. Evolution 67, 2240–2257. https://doi.org/10.1111/evo.12105

Naser-Khdour, S., Minh, B.Q., Zhang, W., Stone, E.A., Lanfear, R., 2019. The prevalence and impact of model violations in phylogenetic analysis. Genome Biol. Evol. 11, 3341–3352. https://doi.org/10.1093/gbe/evz193

Nguyen, L.-T., von Haeseler, A., Minh, B.Q., 2018. Complex models of sequence evolution require accurate estimators as exemplified with the invariable site plus gamma model. Syst. Biol. 67, 552–558. https://doi.org/10.1093/sysbio/syx092

Ogata, K., Terayama, M., Masuko, K., 1995. The ant genus *Leptanilla*: discovery of the worker-associated male of *L. japonica*, and a description of a new species from Taiwan (Hymenoptera: Formicidae: Leptanillinae). Syst. Entomol. 20, 27–34. https://doi.org/10.1111/j.1365-3113.1995.tb00081.x

Peters, R.S., Krogmann, L., Mayer, C., Donath, A., Gunkel, S., Meusemann, K., Kozlov, A., Podsiadlowski, L., Petersen, M., Lanfear, R., Diez, P.A., Heraty, J., Kjer, K.M., Klopfstein, S., Meier, R., Polidori, C., Schmitt, T., Liu, S., Zhou, X., Wappler, T., Rust, J., Misof, B., Niehuis, O., 2017. Evolutionary history of the Hymenoptera. Curr. Biol. 27, 1013–1018. https://doi.org/10.1016/j.cub.2017.01.027

Petersen, B., 1968. Some novelties in presumed males of the Leptanillinae (Hym., Formicidae). Entomol. Meddelelser 36, 577–598.

Philippe, H., Delsuc, F., Brinkmann, H., Lartillot, N., 2005. Phylogenomics. Annu. Rev. Ecol. Evol. Syst. 36, 541–562. https://doi.org/10.1146/annurev.ecolsys.35.112202.130205

Pleijel, F., 1995. On character coding for phylogeny reconstruction. Cladistics 11, 309–315. https://doi.org/10.1016/0748-3007(95)90018-7

Rabeling, C., Brown, J.M., Verhaagh, M., 2008. Newly discovered sister lineage sheds light on early ant evolution. Proc. Natl. Acad. Sci. 105, 14913–14917. https://doi.org/10.1073/pnas.0806187105

Reddy, S., Kimball, R.T., Pandey, A., Hosner, P.A., Braun, M.J., Hackett, S.J., Han, K.-L., Harshman, J., Huddleston, C.J., Kingston, S., Marks, B.D., Miglia, K.J., Moore, W.S., Sheldon, F.H., Witt, C.C., Yuri, T., Braun, E.L., 2017. Why do phylogenomic data sets yield conflicting trees? Data type influences the avian tree of life more than taxon sampling. Syst. Biol. 66, 857–879. https://doi.org/10.1093/sysbio/syx041

Rohland, N., Reich, D., 2012. Cost-effective, high-throughput DNA sequencing libraries for multiplexed target capture. Genome Res. 22, 939–946. https://doi.org/10.1101/gr.128124.111

Romiguier, J., Borowiec, M.L., Weyna, A., Helleu, Q., Loire, E., La Mendola, C., Rabeling, C., Fisher, B.L., Ward, P.S., Keller, L., 2022. Ant phylogenomics reveals a natural selection hotspot preceding the origin of complex eusociality. Curr. Biol. 32, 2942-2947.e4. https://doi.org/10.1016/j.cub.2022.05.001

Romiguier, J., Cameron, S.A., Woodard, S.H., Fischman, B.J., Keller, L., Praz, C.J., 2016. Phylogenomics controlling for base compositional bias reveals a single origin of eusociality in corbiculate bees. Mol. Biol. Evol. 33, 670–678. https://doi.org/10.1093/molbev/msv258

Romiguier, J., Ranwez, V., Delsuc, F., Galtier, N., Douzery, E.J.P., 2013. Less is more in mammalian phylogenomics: AT-rich genes minimize tree conflicts and unravel the root of placental mammals. Mol. Biol. Evol. 30, 2134–2144. https://doi.org/10.1093/molbev/mst116

Rosa, B.B., Melo, G.A.R., Barbeitos, M.S., 2019. Homoplasy-based partitioning outperforms alternatives in Bayesian analysis of discrete morphological data. Syst. Biol. 68, 657–671. https://doi.org/10.1093/sysbio/syz001

Sayyari, E., Mirarab, S., 2016. Fast coalescent-based computation of local branch support from quartet frequencies. Mol. Biol. Evol. 33, 1654–1668. https://doi.org/10.1093/molbev/msw079

Tagliacollo, V.A., Lanfear, R., 2018. Estimating improved partitioning schemes for ultraconserved elements. Mol. Biol. Evol. 35, 1798–1811. https://doi.org/10.1093/molbev/msy069

Thomson, R.C., Brown, J.M., 2022. On the need for new measures of phylogenomic support. Syst. Biol. 71, 917–920. https://doi.org/10.1093/sysbio/syac002

Vasilikopoulos, A., Misof, B., Meusemann, K., Lieberz, D., Flouri, T., Beutel, R.G., Niehuis, O., Wappler, T., Rust, J., Peters, R.S., Donath, A., Podsiadlowski, L., Mayer, C., Bartel, D., Böhm, A., Liu, S., Kapli, P., Greve, C., Jepson, J.E., Liu, X., Zhou, X., Aspöck, H., Aspöck, U., 2020. An integrative phylogenomic approach to elucidate the evolutionary history and divergence times of Neuropterida (Insecta: Holometabola). BMC Evol. Biol. 20, 64. https://doi.org/10.1186/s12862-020-01631-6

Vilhelmsen, L., Miko, I., Krogmann, L., 2010. Beyond the wasp-waist: structural diversity and phylogenetic significance of the mesosoma in apocritan wasps (Insecta: Hymenoptera). Zool. J. Linn. Soc. 159, 22–194. https://doi.org/10.1111/j.1096-3642.2009.00576.x

Ward, P.S., Fisher, B.L., 2016. Tales of dracula ants: the evolutionary history of the ant subfamily Amblyoponinae (Hymenoptera: Formicidae). Syst. Entomol. 41, 683–693. https://doi.org/10.1111/syen.12186

Xu, Z.-H., 2012. *Furcotanilla*, a new genus of the ant subfamily Leptanillinae from China with descriptions of two new species of *Protanilla* and *P. rafflesi* Taylor (Hymenoptera: Formicidae). Sociobiology 59, 477–491. https://doi.org/10.13102/sociobiology.v59i2.612

Yang, Z., 1996. Among-site rate variation and its impact on phylogenetic analyses. Trends Ecol. Evol. 11, 367–372. https://doi.org/10.1016/0169-5347(96)10041-0

Zhang, C., Rabiee, M., Sayyari, E., Mirarab, S., 2018. ASTRAL-III: polynomial time species tree reconstruction from partially resolved gene trees. BMC Bioinformatics 19, 153. https://doi.org/10.1186/s12859-018-2129-y